The Hydrogenation of Pyrolysis Gasoline (PyGas) Over Nickel and Palladium Catalysts

Javed Ali

VIA VERITAS VITA

School of Chemistry
University of Glasgow

A thesis submitted in fulfilment of the requirements for the degree of Doctor of Philosophy

July 2012

Abstract

Pyrolysis gasoline (PyGas) is a by-product of high temperature naphtha cracking during ethylene and propylene production. It is a high octane number mixture which contains aromatics, olefins and paraffins ranging from C_5s to C_{12}s. PyGas has high potential for use as a gasoline blending mixture and/or as a source of aromatics. Currently, PyGas is generally used as a gasoline blending mixture due to its high octane number, but global production of PyGas is very high and further increases are anticipated in the future due to higher demands for ethylene and propylene. However, current strict fuel regulations for aromatic content make PyGas utilisation as a blending mixture more difficult, therefore a useful avenue for PyGas consumption is desired.

Catalytic hydrogenation of PyGas is an important industrial and academic research area for the stabilisation, upgrading and utilisation of PyGas. Limited work has been performed on the hydrogenation of PyGas and an incomplete picture of the process has been obtained. The composition of PyGas is very complex and therefore most of the studies have been carried out with single compounds or a mixture of a few model compounds for simplicity and generality. However, the single model compound cannot be representative of the entire PyGas hydrogenation process. Furthermore, the behaviour of these compounds is generally different in mixtures than as individual compounds. Hence, the hydrogenation of a PyGas, which contained styrene, toluene, 1-octene, cyclopentene, heptane, decane and 1,3-pentadiene/1-pentene, was investigated over alumina supported nickel and palladium catalysts. This is a comprehensive model for the broader groups of hydrocarbons present in PyGas. The aim of the work was to investigate the effect of reaction parameters such as reaction temperature, total reaction pressure, hydrogen partial pressure and WHSV of PyGas on the hydrogenation of PyGas.

Different strategies were proposed for PyGas consumption to obtain; (i) a high octane number gasoline blend, (ii) an aromatic source mixture and (iii) hydrogenation of surplus aromatics present in PyGas.

These desired products were achieved during PyGas hydrogenation over both the nickel and palladium catalysts by using different reaction conditions. However,

the palladium catalyst was found to be preferable for the selective hydrogenation of reactive species such as styrene, diolefins and for the isomerisation of olefins, without the hydrogenation of aromatics during PyGas hydrogenation at mild reaction temperatures. However, surplus aromatics hydrogenation can be achieved over the palladium catalyst with an increase in reaction temperature. Conversely, a greater amount of aromatics saturation was observed during PyGas hydrogenation over the nickel catalyst. Therefore the nickel catalyst was found to be preferable when aromatic ring saturation is desired during PyGas hydrogenation. The selective hydrogenation of PyGas without aromatics saturation was achieved over a nickel catalyst when using a low hydrogen partial pressure.

The kinetics of PyGas hydrogenation were also investigated for a better understanding of the process. The apparent orders for hydrogenation /isomerisation of the PyGas components were investigated by using an empirical rate equation. During PyGas hydrogenation, first order (1.1 to 1.6) kinetics were observed for the hydrogenation of olefins to their respective paraffins over both the nickel and palladium catalysts with an increase in hydrogen partial pressure, which became zero or negative order kinetics when sufficient amounts of hydrogen were available on the surface of the catalyst. Negative order kinetics were observed for olefin isomerisation to internal olefin with an increase in hydrogen partial pressure. Meanwhile the hydrogenation of styrene to ethylbenzene followed zero order kinetics with respect to hydrogen over both catalysts due to the strong adsorption of styrene onto the catalyst. Third order kinetics were observed for aromatics hydrogenation over both catalysts. On the other hand, the hydrogenation of olefins to paraffins followed zero to negative order (0 to -0.7) kinetics, whilst positive order (1.6 to 3.6) kinetics were observed for isomerisation of olefins to internal olefins with respect to PyGas. Moreover, positive order (0.7 to 1.0) kinetics were observed for styrene hydrogenation to ethylbenzene with respect to PyGas. The hydrogenation of aromatics followed negative orders kinetics with respect to PyGas over both catalysts due to competitive hydrogenation of the olefinic and aromatic components.

Coke deposition is believed to be the main reason for catalyst deactivation during the PyGas hydrogenation reaction. The amount and nature of the coke

deposited was investigated by *in-situ* temperature programmed oxidation (TPO). The increase in reaction temperature not only increased the amount of coke deposition but also produced more condensed hydrogen deficient type coke. Conversely, the carbon laydown decreased with an increase in hydrogen partial pressure. Larger amounts of coke deposition took place over the nickel catalyst when compared to the coke deposited over the palladium catalyst under identical reaction conditions. Moreover, a soft type coke (with lower C/H ratio) was deposited over the palladium catalyst, while a comparatively hard type coke (with higher C/H ratio) was deposited over the nickel catalyst. Both the nickel and palladium catalysts used during PyGas hydrogenation were effectively regenerated by *in-situ* TPO with no significant loss to their catalytic properties.

Table of Contents

Acknowledgment

First and foremost thanks must go to my supervisor David Jackson for all his help and advice throughout through out my PhD studies. Most important of all, he provided me with unflinching encouragement and support in various ways. I would have been lost without him. I would also like to thank my second supervisor Dr Justin Hargreaves for continuous support throughout my studies.

I would like to give special thanks to Ron Spence for help and support during the entire period of my studies. Always asking, "Excuse me Ron" there is problem in ….. , with reply "Nae chance" and then fixing every problem for me, thanks Ron. A big thank to Andy Monaghan for always helping no matter what the problem and providing great company. That was an unforgettable time with you Andy.

I would like to thank Fiona Wigzell for helping me from my first day in the University of Glasgow when I didn't know anything or anyone here. Thanks goes to Stuart Blain for helping me a lot in everything and providing a good company for a few years. Thank you very much Lynsey Pugh for helping me throughout my PhD studies. Special thanks to Ailsa lynch for helping me a lot, especially in the nonstop proof reading of my thesis. My thesis is readable due to the continuous help of Ailsa Lynch, Andy Monaghan, Kathryn Girling, Dr Majid, Stuart Blain and Alexander Munnoch in proof reading and checking my thesis again and again, thank you very much guys, I cannot explain how much it helped me. I would like to thank all other members of my group. And last but not least, I would like to thank Muhammad Bilal for helping and being with me during the entire period of my studies, from start to finish each and every day.

A huge thanks to my mates in Glasgow, Sardar, Jehan, Fawad, Sajjad, Musadiq, Shahid and Dr. Javid for moral support and making ever day an interesting and memorable one. I will remember each and ever day with you guys.

Finally, thanks to my grandparents, parents and other family member for your love and emotional support over the years, I hope it will make you proud.

I would like to acknowledge, Kohat University of Science and Technology (KUST), Pakistan for giving me this opportunities and financial support.

Declaration

The work contained in this thesis, submitted for the degree of Doctor of Philosophy, is my own original work, except where due reference is made to other authors. No material within has been previously submitted for a degree at this or any other university.

…………………………………..

Javed Ali

1. Introduction

1.1 Introduction of pyrolysis gasoline

Pyrolysis gasoline (PyGas) is a by-product of high temperature naphtha cracking during ethylene and propylene production [1, 2]. It is a mixture of highly unsaturated hydrocarbons ranging from C_{5s} to C_{12s}. PyGas contains considerable amounts of aromatics, normally 40-80% (benzene, toluene and xylene), together with paraffins, olefins and diolefins [3]. Composition of the PyGas produced depends on the feedstock and operating conditions and varies from plant to plant. A typical PyGas composition is given in Table 1.1 [4].

PyGas Components	Weight percent (wt %)
Benzene, toluene and xylenes	50
Olefins and dienes	25
Styrene and other aromatics	15
Paraffins and naphthenics	10

Table 1.1 Typical composition of Pyrolysis Gasoline [4]

Ethylene and propylene are produced commercially by steam cracking of a wide range of hydrocarbon feedstocks. The world wide production of ethylene and propylene is more than 130 million and 48 million tonnes per annum respectively [5]. Consequently, a significant amount of PyGas is produced, as it is a major by-product of these plants [6]. The amount of PyGas production mainly depends on the type of feedstock used in the olefins plant. Highly saturated and less aromatic feedstocks produce high amounts of olefins with less PyGas. Naphtha is the main commercial source for olefins *i.e.* ethylene and propylene production. The production of PyGas is generally about 20-30% when naphtha is used as a feedstock [1, 7]. At least 50% of olefins plants worldwide use naphtha as their feed stock. This figure is even greater in some regions of the world e.g. Western Europe and Japan, as shown in Table 1.2 [8].

Raw materials	USA		W.Europe		Japan		World	
	1979	1991	1981	1991	1981	1991	1981	1991
Refinery gas	1	3	–	2	-	-	-	17
LPG, NGL	65	73	4	14	10	2	31	27
Naphtha	14	18	80	72	90	98	58	48
Gas oil	20	6	16	12	-	-	11	8

Table 1.2 Raw materials for ethylene production [8]

Continuing high demand for ethylene and propylene is anticipated for the near future [9]. Ethylene production is expected to reach about 177 million tonnes per annum and propylene to 116 million tonnes per annum in 2020 [10]. Therefore, a considerable increase is also expected in the production of PyGas. There are two main routes to utilise the PyGas produced to provide useful products [11-16]:

- PyGas contains a large quantity of aromatic (BTX) and aliphatic hydrocarbons and therefore can be used as a gasoline pool due its high octane number

- The high content of aromatics present in PyGas makes it a good potential feedstock for aromatics extraction

However PyGas is unstable and contains a large amount of active species such as styrene and diolefins which must be stabilised before utilisation, as these species can form coke and gum [11, 17, 18]. In addition, PyGas also contains small amounts of undesirable heteroatom containing hydrocarbons such as sulphur and nitrogen containing compounds [19]. Different hydrotreatments of PyGas are essential prior to its utilisation, which depend on the composition of the PyGas and the objective of its utilisation.

1.2 Hydrotreatments of pyrolysis gasoline

Commercially, catalytic hydrogenation is an important process for the upgrading and utilisation of PyGas to valuable products. However, due to the complex composition of PyGas, the hydrogenation process is not straightforward and a variety of strategies have been proposed and applied. Generally, PyGas

hydrogenation is carried out in more than one stage or alternatively PyGas is separated into various fractions e.g. light naphtha (C_5s) and heavy naphtha (C_6s-C_8s) and each fraction is individually treated to convert it into useful products [20, 21]. Most commonly, PyGas is hydrogenated in two stages. Generally, the selective hydrogenation of reactive species such as styrene and diolefins is performed under mild reaction conditions in the first stage to prevent coke and gum formation. Meanwhile, the isomerisation of olefins to internal olefins is desirable for high octane number mixture. The products of the first stage are stable, have a high octane number and are suitable for addition to the gasoline pool or for further processing [22]. Second stage treatment depends on the objective of the process and feed composition from the first stage. Commonly, the olefins and impurities, like sulfur containing compounds are eliminated in the second stage hydrogenation when PyGas is used for aromatic extraction [16, 23, 24]. However, when high octane gasoline blending is the desired product, then second stage hydrogenation can be by-passed or other required treatments can be performed, such as removal of sulfur containing compounds and to achieve the desired aromatic specification [24].

Hydrogenation of the aromatic components has not been investigated in detail within PyGas. However, with the introduction of new fuel regulations the reduction of aromatics in gasoline has gained attention [7, 25-28]. In recent years, strengthened fuel regulations have reduced the maximum allowable aromatics content in gasoline to less than 35% according to European union gasoline specification as shown in Table 1.3 [7, 26, 27].

Maximum content of	Unit	Before 2000	From 2000	From 2005
Olefins	vol.%	–	18	18
Aromatics	vol.%	45	42	35
Benzene	vol.%	5	1	1

Table 1.3 Gasoline specifications in the European Union [7, 26, 27]

Some parts of the world have even tighter gasoline regulations, for example in California only 22 vol.% aromatics are allowed in gasoline [28]. Therefore, only small amounts of PyGas can be utilised by the gasoline pool, or alternatively

severe hydrotreatments are required to achieve the gasoline specification. Consequently, the extraction and/or hydrogenation of aromatic compounds gained attention with respect to utilising the excess of aromatics present in PyGas [7, 29-31]. Alternatively to aromatics extraction, the hydrogenation and hydrocracking of aromatics is an important route to utilise the surplus aromatics present in PyGas. For this purpose, generally the aromatics are first hydrogenated to saturated compounds. Subsequently, the saturated compounds can be converted to valuable products by the ring opening/hydrocracking. The surplus aromatics present in PyGas can be hydrocracked to the following valuable products [7, 13, 31-36]:

- High-octane components (iso-alkanes) for gasoline pool mixture

- High quality synthetic cracker feed stock

The treatment and main utilisation of PyGas is summarised in Figure 1.1.

Feedstocks (Naphthas)

→ **Stream cracker plant**

→ **Olefins (Ethene , Propene etc)**

Stream cracker plant → **PyGas**

PyGas → **1st stage Hydrogenation**

1st stage Hydrogenation → **2nd stage Hydrogenation**

2nd stage Hydrogenation → **Aromatic Extraction**

2nd stage Hydrogenation → **Gasoline blending**

Aromatic Extraction → **Aromatics (Benzene, Toluene, Xylenes)**

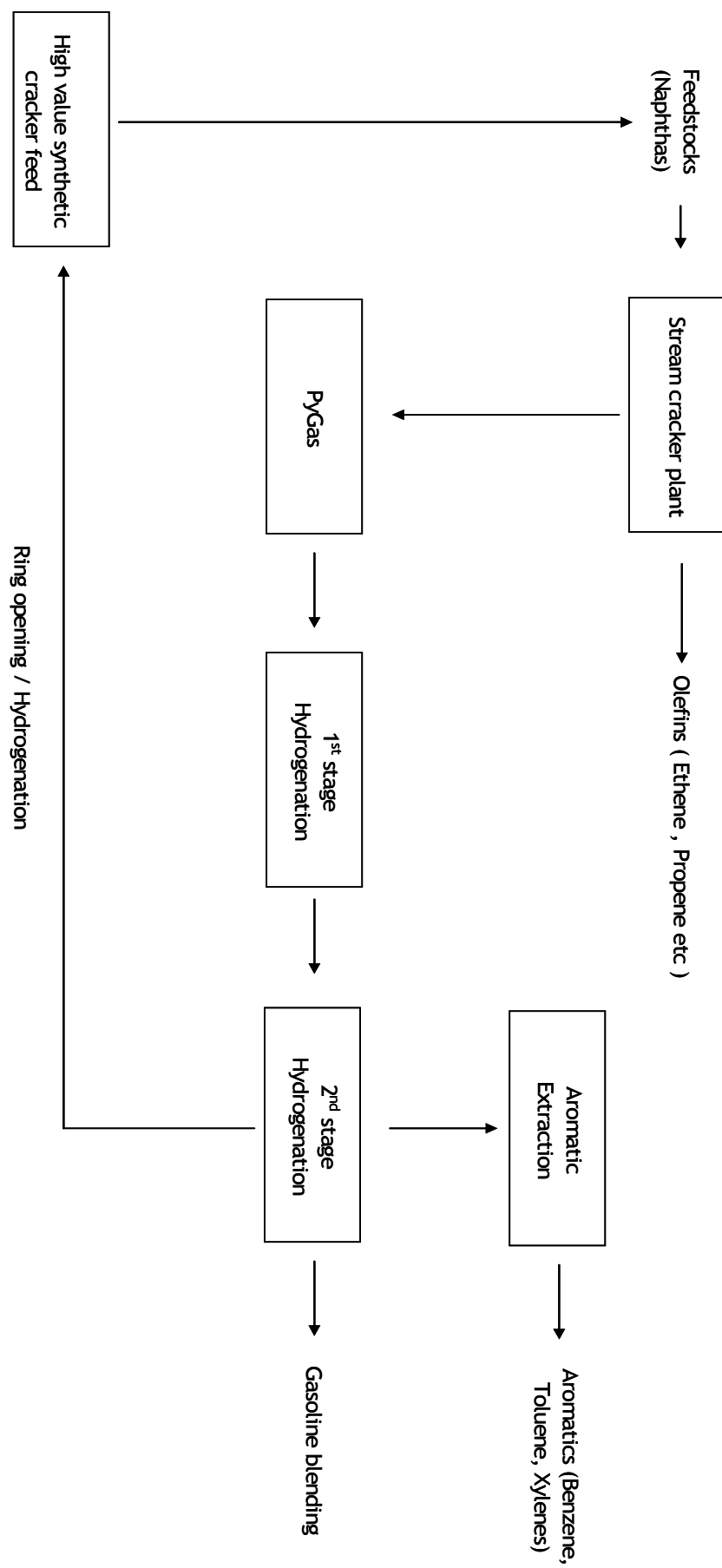**2nd stage Hydrogenation** → (Ring opening / Hydrogenation) → **High value synthetic cracker feed**

Figure 1.1 Simplified flow diagram of PyGas treatment and utilisation

1.3 Hydrogenation of pyrolysis gasoline

Pyrolysis gasoline hydrogenation can be performed as either a single or multi stage process. However, the first stage/treatment of PyGas hydrogenation is of significant importance for its role in stabilisation and useful utilisation of PyGas. The desired reactions during the PyGas hydrogenation are dependant on the PyGas composition and its desired use. The main reactions during PyGas hydrogenation are shown in Figure 1.2.
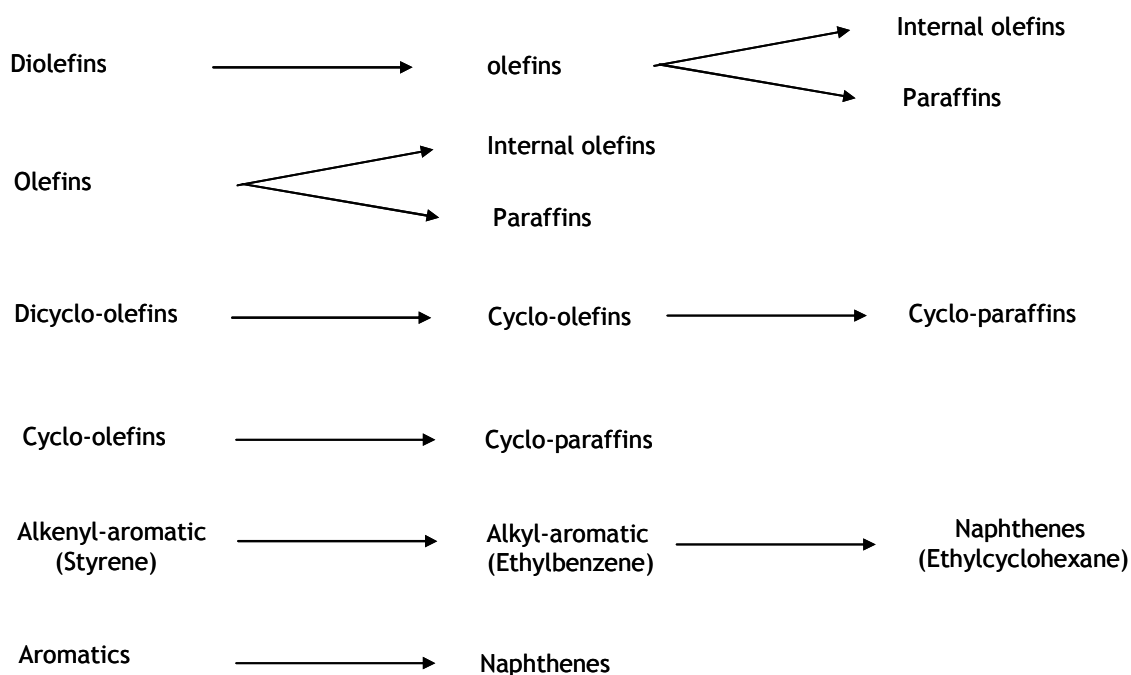
Diolefins $\longrightarrow$ olefins $\begin{cases} \text{Internal olefins} \\ \text{Paraffins} \end{cases}$

Olefins $\begin{cases} \text{Internal olefins} \\ \text{Paraffins} \end{cases}$

Dicyclo-olefins $\longrightarrow$ Cyclo-olefins $\longrightarrow$ Cyclo-paraffins

Cyclo-olefins $\longrightarrow$ Cyclo-paraffins

Alkenyl-aromatic (Styrene) $\longrightarrow$ Alkyl-aromatic (Ethylbenzene) $\longrightarrow$ Naphthenes (Ethylcyclohexane)

Aromatics $\longrightarrow$ Naphthenes

Figure 1.2 Main reactions during PyGas hydrogenation

Ni and Pd, with or without promoters, over supported alumina are widely used as catalysts for the first stage PyGas hydrogenation [2, 11, 37-45]. The first stage of hydrogenation is generally performed at mild reaction temperatures (T ≤ 200°C) due to high coke deposition on the catalyst caused by reactive species such as styrene and diolefins at higher temperatures [11]. The rates of hydrogenation of olefins and aromatic compounds generally increase with a rise in the reaction temperature and hydrogen partial pressure.

Styrene and diolefins can be selectively hydrogenated at mild reaction conditions. Meanwhile higher amounts of olefins isomerise to internal olefins at low reaction temperatures and low hydrogen partial pressure [46]. Therefore, low reaction temperature and low hydrogen partial pressure is preferable for selective hydrogenation of PyGas for use in a high octane gasoline mixture.

However, with much lower temperature, the flow rate of PyGas feed decreases and the hydrogenation process become expensive which is not desirable for a commercial process [47].

However, when PyGas is treated as a source of aromatics, then the olefins present in the PyGas must be also hydrogenated to saturated paraffins because olefins can form gum and cause problems during the aromatic extraction process. Therefore, moderate reaction temperatures and hydrogen partial pressures are necessary.

The aromatic compounds present in PyGas are mainly used in gasoline blending mixtures and/or as an aromatic source. However, to fulfil current tight fuel regulations and utilise the surplus aromatic compounds, the hydrogenation of the aromatics is desirable which can be achieved by implementing severe reaction conditions. However, the reaction temperature is required to be low ($\leq$ 200°C) in the first stage of hydrogenation because large amounts of coke/gum can be deposited on the catalyst at higher reaction conditions [11]. Catalyst deactivation by sulfur poisoning is also very small with reaction temperatures up to 180°C [45]. Thus PyGas hydrogenation must be performed in more than one stage when desired products require very high reaction temperatures. In conclusion, the reaction temperature and hydrogen partial pressure should be optimised according to the desired products and the viability of unit operating process [2]. General reaction conditions used for first stage of hydrogenation are summarised in Table 1.4 [11, 12, 22, 48, 49].

Reaction variable	Variable value
Reaction temperature	50-200°C
Total reaction pressure	20-80 barg
Hydrogen partial pressure	5-60 barg
WHSV	1-10 h^{-1}

Table 1.4 PyGas hydrogenation reaction conditions

The reaction for the PyGas hydrogenation is very exothermic. The heats of hydrogenation for the PyGas components are given in Table 1.5.

PyGas components	ΔH^o (kJ mol^{-1})
Mono-olefins	-110 to -125
Di-olefins to mono-olefins	-100 to -125
Di-olefins to paraffins	-220 to -250
Mono-aromatics	-200 to -220
Styrene to ethylbenzene	-117
Styrene to ethylcyclohexane	-320

Table 1.5 Heat of hydrogenation of PyGas components

Consequently, large amounts of heat can be produced during PyGas hydrogenation. Therefore, a refined heat exchange system and control operation conditions are required to prevent an increase in the temperature of the catalyst bed and reactor runaway [50, 51]. In addition, a uniform feed of PyGas to the catalyst bed is required because maldistribution in a trickle bed reactor of liquid could result in the formation of a hot spot on the catalyst. In such a case it is possible for a large amount of heat to be produced, which could cause a sudden increase in reactor temperature and pressure leading to a reactor runaway and potential rupture of the reactor [50, 51]. As the commercial process for the hydrogenation of PyGas is commonly operating as a trickle bed, the PyGas feed is diluted with recycled hydrogenated PyGas to control any temperature rise in the reactor due to the exothermic reactions.

1.4 Kinetics and mechanism

The main species present in PyGas are olefins (mono-olefins, cyclo-olefins, diolefins, etc.) and aromatic components (benzene, toluene, xylene, styrene, etc.). Two different mechanisms have been proposed for the hydrogenation of these unsaturated hydrocarbons; the Langmuir-Hinshelwood and the Eley-Rideal mechanisms [52-55]. A mechanism for surface catalysis in which the reaction occurs between species that are both adsorbed on the surface is known as a Langmuir-Hinshelwood, whilst the Eley-Rideal mechanism describes a process where one of the molecules adsorbs and another reacts with it directly from the gas phase, without adsorbing [53].
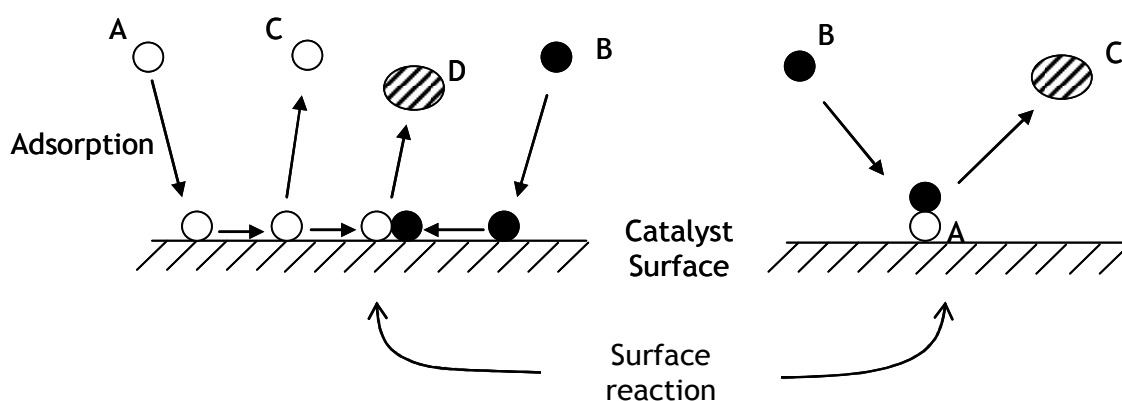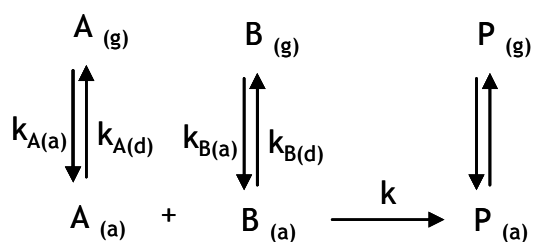

Figure 1.3 Langmuir-Hinshelwood mechanism (left) and Eley-Rideal mechanism (right)

Langmuir-Hinshelwood Mechanism

The reaction between adsorbed molecules on the surface of the catalyst can be presented as:

The rate of reaction is dependant on the amount of adsorbed species on the surface of the catalyst. The equation for the rate of reaction is shown below:

$$\text{Rate} = k\,\theta_A\,\theta_B \qquad\qquad (1.1)$$

Where θ_A and θ_B are fractions of available sites covered with components A and B respectively and k = rate constant.

Two different scenarios may occur when the reaction is competitive on the same sites, or it is non-competitive on the different sites.

To consider the reaction on the same site, the equation at equilibrium can be assumed.

$$k_{A(d)}\, \theta_A = k_{A(a)}\, (1 - \theta_A - \theta_B)P_A \qquad (1.2)$$

$$k_{B(d)}\, \theta_B = k_{B(a)}\, (1 - \theta_A - \theta_B)P_B \qquad (1.3)$$

Where $k_{(a)}$ and $k_{(d)}$ are rate constants for adsorption and desorption respectively, and P_A and P_B are partial pressure of component A and B.

The equation (1.4) can be derived by putting the θ_A and θ_B values from equations (1.2) and (1.3) into equation (1.1);

$$\text{Rate} = \frac{k\, K_A\, K_B\, P_A\, P_B}{(1 + K_A\, P_A + K_B\, P_B)^2} \qquad (1.4)$$

Where $K_A = k_{A(a)}/k_{A(d)}$, $K_B = k_{B(a)}/k_{B(d)}$.

If one component is dissociativily adsorbed e.g. ($B_{2(g)} \rightarrow 2B_{(a)}$) then equation (1.3) becomes equation (1.5) [53];

$$\theta_B = (1 - \theta_A - \theta_B)\sqrt{k_B\, P_{B2}} \qquad (1.5)$$

Then the Langmuir-Hinshelwood becomes equation (1.6);

$$\text{Rate} = \frac{k\, K_A\, P_A\, \sqrt{K_B\, P_{B2}}}{(1 + K_A\, P_A + \sqrt{K_B\, P_{B2}})^2} \qquad (1.6)$$

If the adsorption occurs at different sites, then the adsorption equation for the component can be presented as;

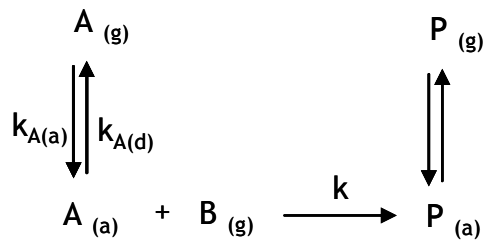$$\theta_A = \frac{K_A\, P_A}{1 + K_A\, P_A} \qquad (1.7)$$

$$\theta_B = \frac{K_B\, P_B}{1 + K_B\, P_B} \qquad (1.8)$$

The rate equation can be derived by inserting the θ_A and θ_B values from equations (1.7) and (1.8) into equation (1.1).

$$\text{Rate} = \frac{k\,K_A\,K_B\,P_A\,P_B}{(1+K_A\,P_A)\,(1+K_B\,P_B)} \qquad (1.9)$$

Eley-Rideal Mechanism

The Eley-Rideal mechanism for the reaction on the surface of catalyst is summarised below:

The rate of reaction is: **Rate = k $\theta_A P_B$**   (1.1)

The surface coverage of A can be described by equation (1.7):

$$\theta_A = \frac{K_A\,P_A}{1+K_A\,P_A} \qquad (1.7)$$

The rate equation (1.10) can be obtained by inserting equation (1.7) in equation (1.1):

$$\text{Rate} = \frac{k\,K_A\,P_A\,P_B}{(1+K_A\,P_A)} \qquad (1.10)$$

In the vast majority, the Langmuir-Hinshelwood mechanism is generally accepted for the hydrogenation of unsaturated hydrocarbons [56].

1.4.1 Kinetics and mechanism of olefins hydrogenation

Olefins are mostly hydrogenated in the presence of heterogeneous catalysts such as palladium, nickel and platinum supported catalyst. The hydrogenation of olefins depends on the nature and number of groups attached to the olefin, and the reaction conditions. Generally, reactivity of olefins hydrogenation is decreased with increasing the number of substitutions and their bulkiness. The rate of hydrogenation of olefins follows the order below [46, 57]:

$$RCH=CH_2 > R_2C=CH_2 > RCH=CHR > R_2C=CHR > R_2C=CR_2$$
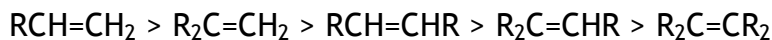
The Horiuti-Polanyi mechanism is the generally agreed mechanism for olefin hydrogenation and isomerisation, and is shown in Figure 1.4 [57].
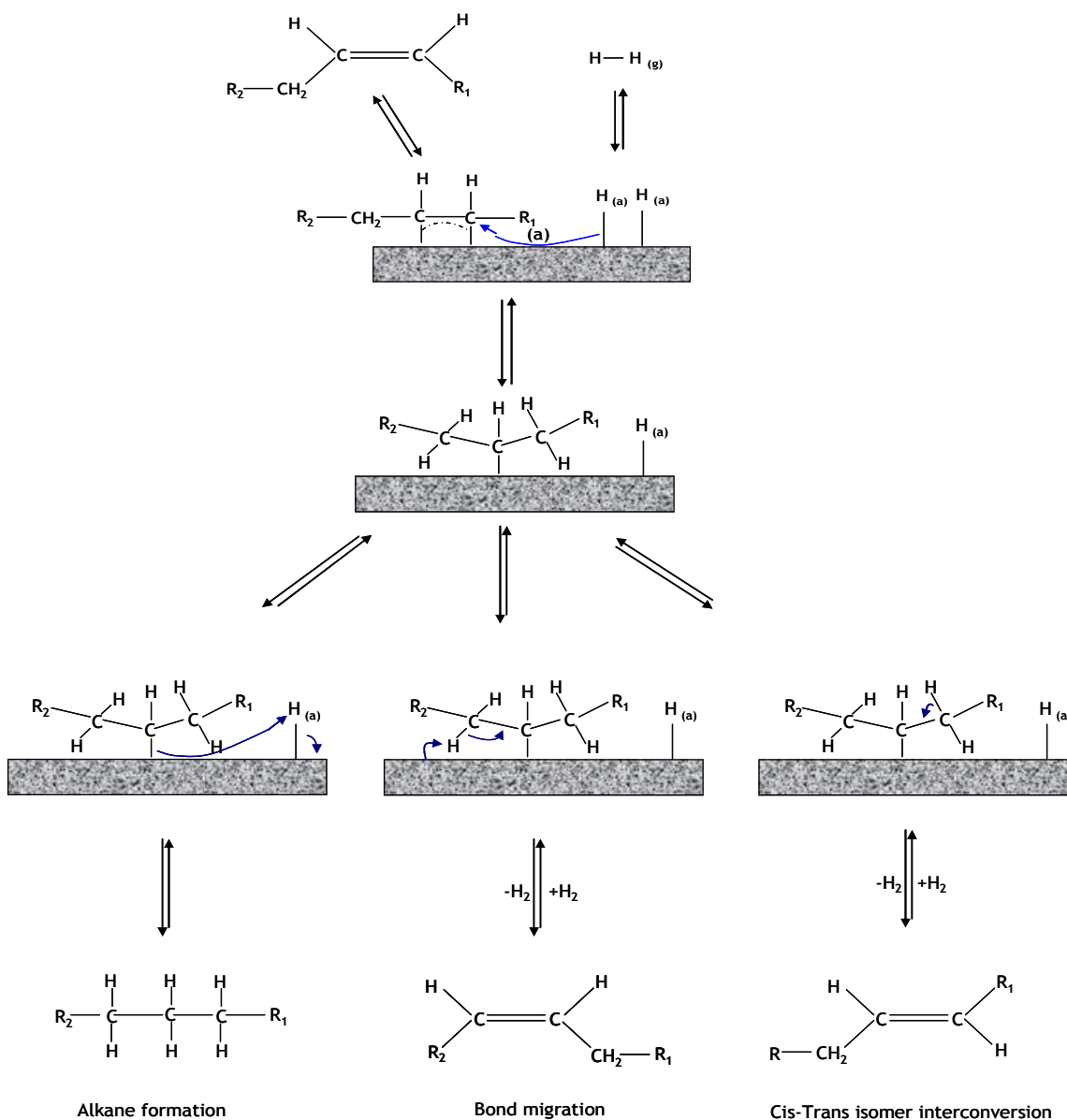

Figure 1.4 Mechanism of catalytic hydrogenation and isomerisation of olefins over group VIII metals catalyst [R$_1$ and R$_2$ representing hydrogen atom or hydrocarbon chain] [57]

Similarly, the cyclo-olefins and diolefins also hydrogenated in the same way in the presence of a heterogeneous catalyst (Ni, Pt, and Pd). The complete hydrogenation of diolefins produces paraffins, whilst selective hydrogenation of diolefins, depends on the experimental conditions and catalyst. Lower hydrogen partial pressures are more favourable for the selective hydrogenation of diolefins to mono-olefins. Moreover, the rate of isomerisation of olefins to internal olefins is also high at a low hydrogen partial pressure. Selectivity

towards olefins decreases and the formation of saturated paraffins increases with a rise in hydrogen partial pressure. Similarly, the hydrogenation of olefins *i.e.* diolefins and mono-olefins generally increases with an increase in reaction temperature.

Platinum, palladium and nickel supported catalysts are most widely used for olefin hydrogenation. Platinum metal catalysts are normally extremely active for hydrogenation reactions. Whilst nickel and palladium metal catalysts exhibit good activity and selectivity, they also show a high potential to migrate double bonds within hydrocarbons [46, 57], which will be discussed in detail in section 1.5.1. Different olefins are mainly adsorbed onto the same active sites on the catalyst, therefore competitive hydrogenation is observed when the hydrogenation of olefin mixtures is carried out [58-60]. Kinetic studies of olefin hydrogenation are almost always expressed by the Power Rate equation and only rarely have been interpreted using Langmuir-Hinshelwood formalisms [46]. Reaction kinetics are highly dependent on the reaction conditions. Generally, positive order (~ first order) kinetics of olefin hydrogenation to saturated paraffin is observed with respect to hydrogen, and zero or slight negative, order kinetics have been observed with respect to the olefins. This shows that olefins are more strongly adsorbed onto the surface of the catalyst [46]. Similarly, the selective hydrogenation of diolefins to mono-olefins shows a positive order with respect to hydrogen and zero or slightly negative order kinetics with respect to diolefins. However, reaction kinetics of diolefins hydrogenation are highly dependent upon the reaction conditions and very inconsistent results have been reported in the literature [46].

1.4.2 Kinetics and mechanism of aromatics hydrogenation

The hydrogenation of aromatics has been widely studied on supported group VIII metal catalysts (Ni, Pd and Pt) [46, 57, 61-65]. The hydrogenation of mono-aromatics (benzene and toluene) have been investigated in more detail compared to the di- and polyaromatic compounds [46, 57, 63, 64]. The generally agreed mechanism for the hydrogenation of aromatics is a step wise reaction between adsorbed aromatics (benzene, toluene) and adsorbed hydrogen gas [63, 66-73].
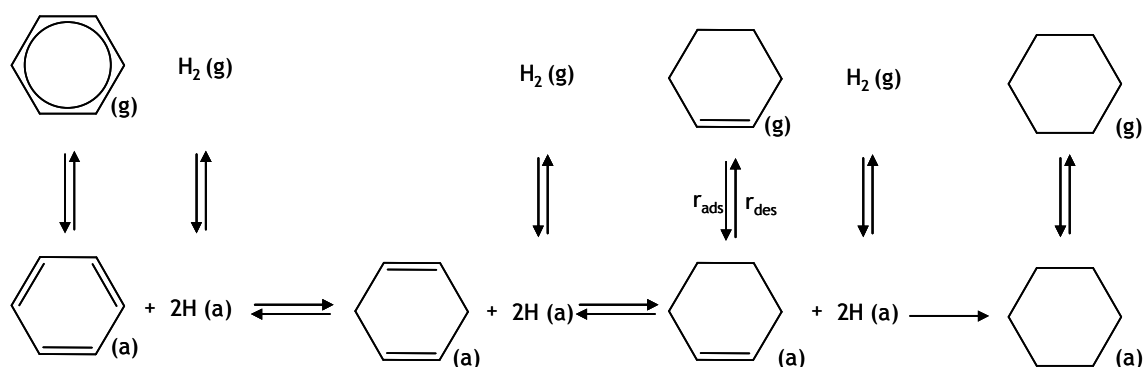
Figure 1.5 Mechanism of catalytic hydrogenation of aromatic over group VIII metals

The monoaromatic compounds hydrogenate in a stepwise manner to cycloalkane. However, the intermediates are highly reactive and are generally not observed during a reaction. Cyclohexadiene is strongly adsorbed onto the surface of the catalyst and reacts much faster than benzene, although intermediate cyclohexene has been observed in some studies [70, 71]. The hydrogenation of di and polyaromatic species is more complicated and most of the studies in the literature deal with only the reaction pathway and activities rather than actual kinetics [46, 63]. However, the hydrogenation of polyaromatic species is comparatively easier than that of the mono-aromatics [63, 64]. The rates of hydrogenation of mono-aromatics generally decrease with alkyl-substitutions, and follow the order [57, 46, 65];

<div align="center">Benzene ≥ Toluene > o-Xylene</div>

The reaction order of aromatic hydrogenations e.g. toluene, benzene over supported Ni, Pd and Pt are found in literature with a wide range of reaction kinetic orders from 0.5 to 0.7 below 100°C and from 0.7 to 4 above 100°C with respect to hydrogenation [63, 65-67, 74-77]. Zero order kinetics are generally observed for the hydrogenation of aromatic compounds with respect to aromatic concentration/partial pressure [46, 65, 77-79]. However slightly higher orders up to 0.5 have also been reported in some studies [46].

1.4.3 Kinetics and mechanism of pyrolysis gasoline hydrogenation

Limited work has been performed on the hydrogenation of PyGas and an incomplete picture of the process kinetics and mechanism has been obtained. Most of the studies on the kinetics of PyGas hydrogenation have been carried out

with single compounds or a few model compounds mixtures for simplicity and generality. Kinetic studies of styrene hydrogenation are the most widely reported as model Pyrolysis Gasoline [2, 18, 80, 81]. Nijhuis *et al.* [18] observed first order kinetics for styrene hydrogenation with respect to hydrogen up to 20 barg hydrogen pressure which decreased to zero order kinetics with further increase in hydrogen pressure. Moreover, zero order reaction kinetics was observed for styrene hydrogenation with respect to styrene and Langmuir-Hinshelwood kinetics were proposed [18]. Some studies have also been performed over a mixture of a few model components. Zhou *et al.* [82] conducted a study on the hydrogenation of a model PyGas containing styrene, cyclopentadiene, 1-hexene and n-heptane over a Pd/Al_2O_3 catalyst. The competitive hydrogenation of styrene, diolefins and monoolefins was emphasised and the Langmuir-Hinshelwood type model was proposed for the selective hydrogenation of the model PyGas [82]. The competitive hydrogenation of styrene, diolefins and olefins was also reported by Hoffer *et al.* [40]. They found that the hydrogenation of 1-octene was depressed in the presence of styrene due to strong adsorption of styrene on the surface of the catalyst. Similar behaviour was observed by Nijhuis *et al.* [18] and Smites *et al.* [83] in their studies performed over palladium catalysts. This type of behaviour can be appropriately explained by the Langmuir-Hinshelwood kinetic model [16, 82]. Hanika *et al.* [84] studied the hydrogenation of a comprehensive PyGas model containing multiple-component reactants (diolefins, olefins and styrene) as model PyGas and first order kinetics were observed for the hydrogenation of all olefinic double bonds.

Langmuir-Hinshelwood and other distinctively detailed kinetic models have been proposed for styrene and for systems containing a mixture of a few components as a PyGas hydrogenation [4, 18, 82, 85]. However the single compound model cannot accurately represent the hydrogenation of the PyGas mixture. Furthermore, the kinetics and the mechanisms of these compounds are different in mixtures than as pure single compounds reactions. Therefore, kinetics and mechanism of PyGas hydrogenation cannot be considered as the sum of individual components. Thus, further studies are essential on hydrogenation of comprehensive PyGas mixture to give greater insight.

The kinetic studies are mostly presented in a simple concentration, yield and selectivity profile form due to the complex nature of PyGas and the apparent kinetic parameters obtained using an empirical rate model. This type of model is simple, however it is the most reliable kinetic model [53, 63]:

$$r = K \, P_C^b \, P_{H2}^a \qquad (1.11)$$

Where K represents apparent rate constant, P_{H2} partial pressure of hydrogen gas, P_C partial pressure of PyGas component/s; while a and b represent reaction order with respect to hydrogen partial pressure and PyGas component/s partial pressure respectively. The logarithmic form of the equation can be used for determination of the apparent reaction order:

$$\ln(r) = \ln(K \, P_C^b) + a \, \ln(P_{H2}) \qquad (1.12)$$

The apparent reaction order with respect to hydrogen partial pressure can be determined by plotting $\ln(r)$ vs $\ln(P_H)$, whilst keeping the other parameters constant (P_C,T). Similarly, the apparent reaction order with respect to PyGas component/s can be determined by plotting $\ln(r)$ vs $\ln(P_c)$ keeping other parameters constant (P_H, T):

$$\ln(r) = \ln(K \, P_{H2}^a) + b \, \ln(P_c) \qquad (1.13)$$

# 1.5 Catalyst and support

1.5.1 Choosing active agent

The group VIII metals are generally used as active agents for hydrogenation of unsaturated hydrocarbons. Ni, Pt, Pd, Rh, Ru and Ir are most commonly used for hydrogenation reactions. Other transition elements like Cr, Mo, W, Cu and Zn or their oxides or sulfides are also useful in hydrogenation reactions [11, 46, 53]. Complete hydrogenation is not always desired and selective hydrogenation can be achieved by using a suitable catalyst and control of the reaction parameters. The classification of metals according to their hydrogenation activity and selectivity is relatively complex, because catalyst activity and selectivity are dependant on various factors such as catalyst and reaction parameters. However, simple classification has been obtained for the simplest molecules, which is shown in Table 1.6 [11, 53].

Activity and selectivity	Metal
Activity for C_2H_4 hydrogenation	Rh > Pd > Pt > Ni > Fe > W > Cr > Ta
Activity for C_2H_2 hydrogenation	Pd > Pt > Ni, Rh > Fe, Cu, Co, Ir > Ru, Os
Selective hydrogenation of diolefines and acetylenes	Ni, Pd, Co, Fe : High Pt, Os, Rh, Ru : poor
Double bond isomerisation	Ni ≈ Rh≈ Fe > Pd > Ru > Os > Pt ≥ Ir ≈ Cu
Hydrogenation of Aromatics	Pt > Rh > Ru > Ni > Pd > Co > Fe

Table 1.6 Classification of active agents for hydrogenation of unsaturated hydrocarbons [11]

The preferable active agent for PyGas hydrogenation should have good activity, selectivity and also be able to isomerise double bonds to avoid a decrease in octane number. The metals are ranked with respect to selectivity and promotion of double bond migration as below

Pd > Ni > Co > Fe
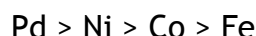
Nickel and palladium metals have good activity, selectivity and a high potential to migrate double bonds [46, 57]. Therefore Ni or Pd catalysts, with or without a promoter, over supported alumina are widely used for the first stage of PyGas hydrogenation [2, 11, 37-45]. Several promoters have been investigated to assess their role in activity and selectivity. The addition of tungsten and molybdenum to nickel catalyst increases activity and as a result, W-Ni and Ni-Mo are also good catalysts for first stage hydrogenation [11, 12, 48, 49, 86]. Qian *et al*. observed an increase in catalyst activity by adding Zn to nickel catalysts [37]. Similarly, a Cr doped palladium catalyst has high activity in the PyGas hydrogenation [12].

1.5.2 Catalyst support

PyGas contains a high quantity of reactive species which can be polymerised to form coke during the reaction. The deposition of coke on catalyst, block the active sites and reduce the accessibility of reactant to these sites. The heavy build up of coke in pores may also fracture the support. Accordingly, the support is required to be inert to polymerisation reactions. However, even with the most inert supports, coke/gum deposition can still occur over the surface of the

catalyst. Consequently, catalyst regeneration and the burning of carbonaceous material deposited on the surface of catalyst, is required periodically. Therefore the catalyst must be mechanically and thermally stable in order to undergo several regenerations at high temperature. Alumina is highly stable, has a reasonable surface area and is relatively inexpensive, so is suitable for this process. Alumina is generally prepared from alumina hydroxide by dehydration. The hydrous alumina converts to anhydrous alumina by calcination above $300^{o}C$ [87].
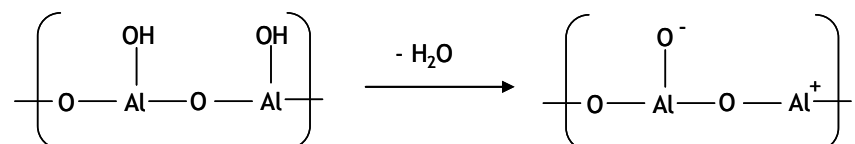
The hydrous oxide $(Al_2O_3 \cdot nH_2O)$ is known as boehmite, with an n value of between 1 to 1.8, which can be converted to crystalline alumina by heat treatment [87]. A wide variety of aluminas are available, depending on the requirements of the catalyst support and reaction process. Alumina can be produced in different phases via heat treatments e.g. drying and calcination. The actual phase change is greatly dependent on the preparation method and other treatment factors such as rate of calcination, environment of calcination. However, an approximate phase changes above $300^{o}C$ is summarised below in Figure 1.6.
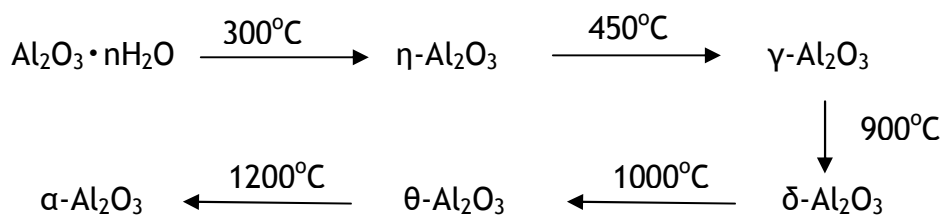
Figure 1.6 Calcination sequence of alumina hydroxide [87]

The aluminas, $\eta\text{-}Al_2O_3$, $\gamma\text{-}Al_2O_3$ and $\delta\text{-}Al_2O_3$ are known as γ-group aluminas and their structures are similar to $Al_2O_3 \cdot nH_2O$, in which n ≈ 0 – 0.6. With a further increase in temperature to above $1000^{o}C$, the alumina converts to anhydrous monoclinic $\theta\text{-}Al_2O_3$ which forms hexagonal $\alpha\text{-}Al_2O_3$ above $1200^{o}C$ [61, 87]. The anhydrous θ and α forms of alumina have low surface areas with high mechanical strength. The conversion of alumina from one phase to another can occur readily during the various treatment stages and therefore most commercial alumina

supports consist of a mixture of phases. The actual form is less important than the surface area, pore distribution and thermal stability for most purposes.

Zirconia and titania have also been tried as catalyst supports for the hydrogenation of PyGas [44, 80, 88, 89]. However due to their high-cost and low surface area compared to alumina, none are seen as a viable replacement for alumina.

1.5.3 Choice of the catalyst

Nickel and palladium supported alumina catalysts have good activity, selectivity and high potential to migrate double bond of the olefins, thus, are suitable catalysts for the hydrogenation of PyGas. The choice between these two catalysts depends on several points e.g. characteristics of the feed stock, product specification, unit operating conditions and the price of Pd vs Ni [90]. Pd/Al_2O_3 is a more selective and active catalyst than Ni/Al_2O_3, however nickel is less expensive than palladium. Nickel catalysts generally contain 10-20 wt.% of nickel metal while palladium catalysts contain 0.2-1 wt.% palladium metal. Thus, nickel catalysts contain 20-100 times more active metal compared to the palladium catalyst and subsequently the nickel catalyst is more tolerant to poisons like mercaptans, disulfides and thiophenes which can be present in the feedstock [12]. Consequently, a nickel is the preferred catalyst when using highly contaminated feed stocks.

1.5.4 Pre-treatment of the catalyst

Palladium and nickel oxides must be reduced to the metallic state before use as a catalyst for hydrogenation reactions. The catalytic activity is highly dependent on the reduction of the catalyst. The reduction of palladium and nickel catalysts depends on reduction temperature, flow of hydrogen, reduction time and metal content. Generally, palladium supported alumina catalysts are reduced at 100-300 ^{o}C under a continuous flow of hydrogen gas [2, 4, 18, 44, 82], whilst nickel supported alumina catalysts are reduced at relatively higher temperature at 400 ^{o}C-500 ^{o}C in a hydrogen gas flow [11, 13, 37, 38, 91]. The reduction rate of both catalysts increases with an increase in reduction temperatures. However, a decrease in the surface area of the catalyst can occur at very higher reduction

temperatures due to sintering, which can cause a decrease in catalyst activity. Therefore, ultra high temperatures are not suitable for the reduction of the catalysts. Cheng *et al.* [2] observed that palladium catalyst activity for PyGas hydrogenation remained the same when the reduction temperature was increased up to 200°C, but a decrease was observed in catalyst activity above 200°C as shown in Figure 1.7:
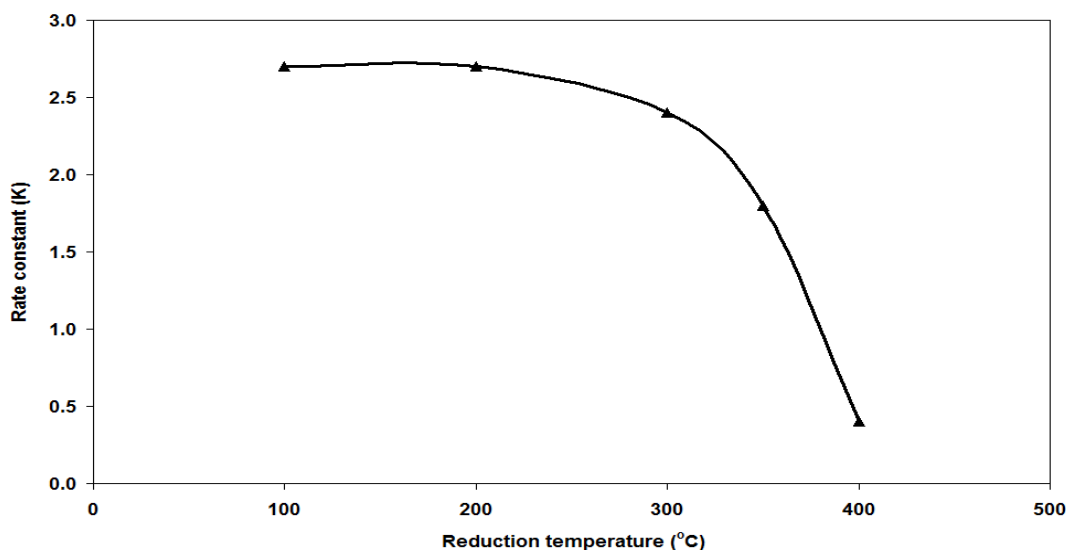

Figure 1.7 Effect of PdO reduction on the PyGas hydrogenation activity [2]

The activity of a Ni/Al$_2$O$_3$ catalyst and chemisorption of hydrogen has been studied after with different reduction temperatures and a maximum activity of the catalyst was observed with a 460°C reduction temperature, as shown in Figure 1.8 [11]:
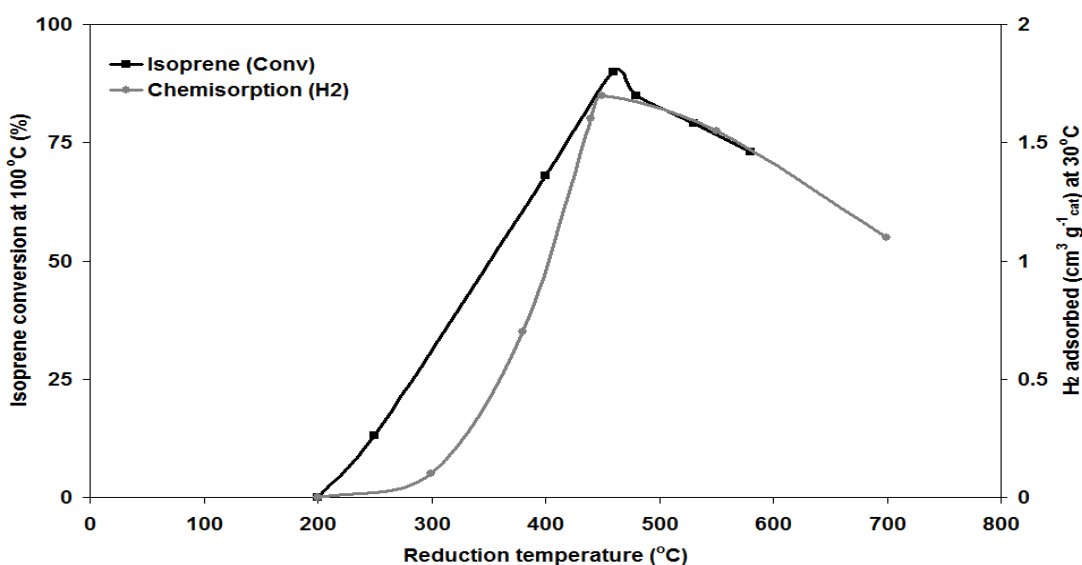
Figure 1.8 Effect of NiO reduction on the catalyst activity

The chemisorption of hydrogen at 30°C by volumetric method. The activity of catalyst is expressed in percentages of isoprene conversion at T = 100°C, P= 40 barg, P$_{H2}$ = 20 barg [11]

The reduction rate is high in the initial stages and becomes slower over time. Bartholomew *et al.* [92] observed that of the nickel oxide in 14% Ni/Al_2O_3, 93% was reduced to metallic nickel under a continuous flow of hydrogen gas over 10 hours at 485^oC, and then only a further 5% was reduced over a further 135 hours.

1.6 Catalyst deactivation

Deactivation of a catalyst is defined as the loss of activity and/or selectivity. Catalysts have a limited lifetime and eventually lose their activity. The lifetime depends on the catalyst and reaction parameters. Some catalysts lose their activity quickly in a few minutes while some remain active for years. A long active catalyst lifetime is desired, as it gives high economic viability in industry. Deactivation cannot be stopped completely; however slow deactivation of the catalysts can increase long term activity. The desired activity of a catalyst can be described by the graph shown in Figure 1.9 [53].
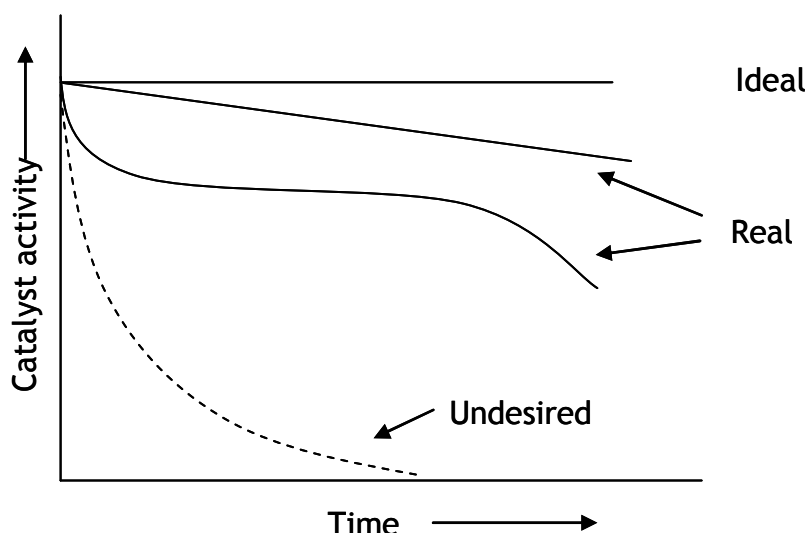
Figure 1.9 Catalyst deactivation behaviour [53]

The main causes of catalyst deactivation are catalyst poisoning, coke or other deposition on the surface of catalyst, sintering, loss of the active component and surface area of the catalyst. Routes for catalyst deactivation can be divided into three main types [87, 93-95];

 1) Chemical deactivation of catalyst e.g. poison adsorption, coking.

 2) Mechanical deactivation of catalyst e.g. blocking of catalyst surface by dust or other material.

3) Thermal deactivation of catalyst e.g. sintering, phase change, active component volatisation.

However these factors cannot be considered independent from each other as temperature has an effect on poison adsorption as well as sintering. Moulijn *et al.* [94] summarised the deactivation routes, which is shown in Figure 1.10.
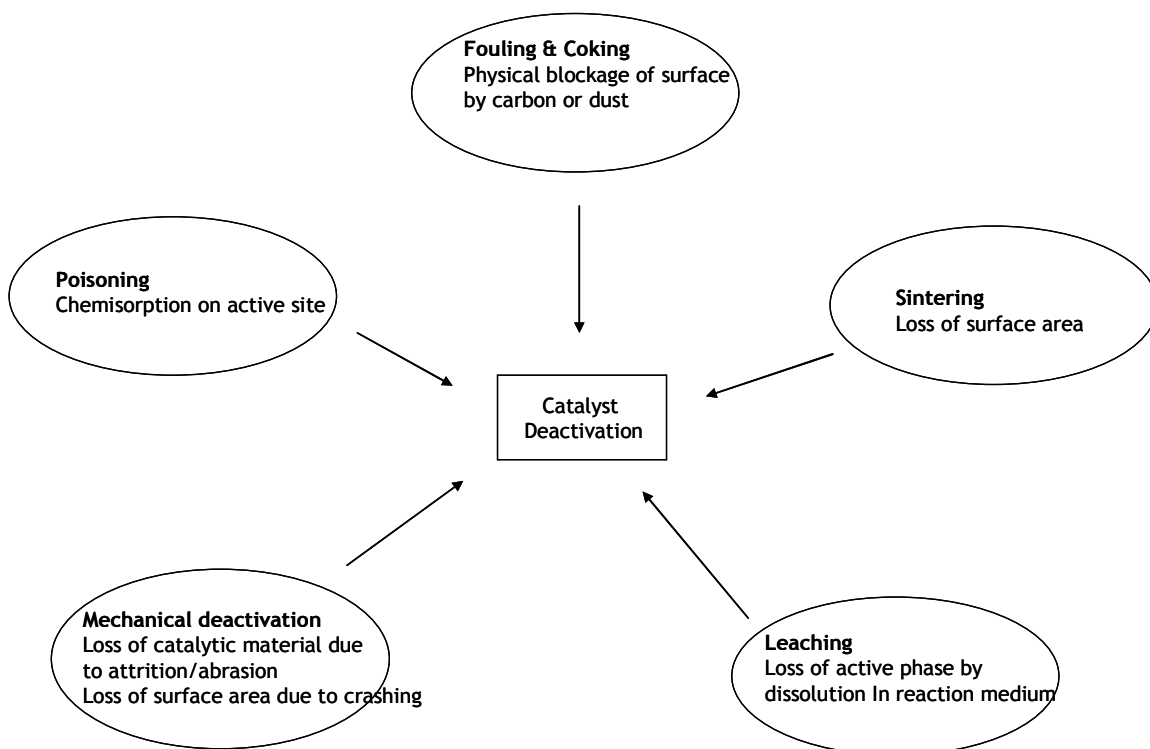

Figure 1.10 Different causes of catalyst deactivation

Generally, catalyst deactivation is initially very fast and then steady state is achieved after a finite amount of time. The reason for this is when fresh catalyst is exposed to the feed, the active sites accommodate poisons especially permanent poisons and deposited coke, and this decreases the activity sharply. The main mode of the catalyst deactivation in PyGas hydrogenation is due to coke/gum deposition and poisons present in the feed [11, 24]. However, catalyst sintering and phase changes can also occur during the catalyst regeneration process.

1.6.1 Poisons

The main poisons present in PyGas are sulfur and nitrogen containing compounds which can decrease the activity and eventually deactivate the catalyst during

PyGas hydrogenation [11, 96]. Trace amounts of arsenic, mercury, lead and phosphorous can also deactivate catalysts when present in PyGas. Therefore, guard beds can be used for the removal of poisons prior to passing feed to the PyGas hydrogenation [14]. However, this is expensive and is not always physically possible. Thus, as an alternative, stable and resistant catalysts with higher regeneration capabilities should be used. The poisons e.g. S, N, P, etc generally have unshared electron pairs or empty valence orbitals and the catalytic metals have d orbitals available for interaction with pairs of electron or empty valence orbitals. Consequently, these poisons adsorb onto the catalyst and decrease activity by blocking active sites for the reactants and also restrict the access of adsorbed species to each other [53, 87, 93, 95]. The degree of poisoning of a compound depends on the pairs of electrons present and empty valence orbitals, as the species which do not have unshared electron pairs or empty valence orbital are nontoxic. Examples are presented in Table 1.7.

Elements	Toxic	Nontoxic
S	H—S—H	$\left[\begin{smallmatrix} O \\ O-S-O \\ O \end{smallmatrix}\right]^{2-}$
	R—S—R	$\left[\begin{smallmatrix} R'' \\ R-S-R' \\ O \end{smallmatrix}\right]^{2-}$
N	H:N̈:H H	$\left[\begin{smallmatrix} H \\ H-N-H \\ H \end{smallmatrix}\right]^{1-}$
P	H:P:H H	$\left[\begin{smallmatrix} O \\ O-P-O \\ O \end{smallmatrix}\right]^{3-}$

Table 1.7 Toxicity of poisons species [87]

Other poisons like Hg^{2+}, Pb^{2+}, etc. have occupied d orbitals with electrons that can bond with the empty orbital of a catalyst metal and cause a decrease in catalyst activity [53, 87].

The most common poisons in PyGas are sulfur containing compounds e.g. thiophene, methylthiophene and mercaptanes [13, 18]. These compounds strongly adsorb on Ni and Pd supported alumina catalysts and deactivate the catalyst. However, some studies have found that small amounts of sulfur containing compounds are beneficial in the selective hydrogenation of PyGas to a high octane mixture [11, 40]. The sulfur containing compounds strongly adsorb

onto the catalyst surface and increase the selectivity of catalyst toward internal olefin formation. Therefore sulfide catalysts have also been used in the first stage of hydrogenation to obtain a higher selectivity towards high octane mixture. For this purpose, the catalyst can be pre-sulfided or a small amount of sulfur containing components can be added to the feed [11, 40].

1.6.2 Coke deposition

The main reason for deactivation of catalysts during PyGas hydrogenation is the deposition of carbonaceous residue (coke) on the surface of catalyst [11, 12]. The nature of the coke depends on the process conditions and length of reaction. The carbonaceous residues deposited vary from hydrocarbons and poly-aromatics to graphitic coke. The deposition of coke decreases accessibility for the reactant to the catalyst surface and can block pores by coke build up. The heavy build up of coke in pores may fracture the support material which can cause plugging of reactor voids [87, 95].

Carbonaceous residue formation is mainly due to the polymerisation of coke precursors present in PyGas e.g. styrene, di-olefins, mono-olefins, cyclo-olefins and aromatic species [7]. The deposited residue converts to polyaromatic hydrocarbons which then further converts to highly condensed polyaromatics and graphitic type coke. The coke formation in PyGas is summarised in Figure 1.11.

Coke and gum precursors
(styrene, olefins and aromatic)

↓

Polymerised hydrocarbons

↓

Polyaromatic hydrocarbons

↓

Carbonaceous residues (Coke)
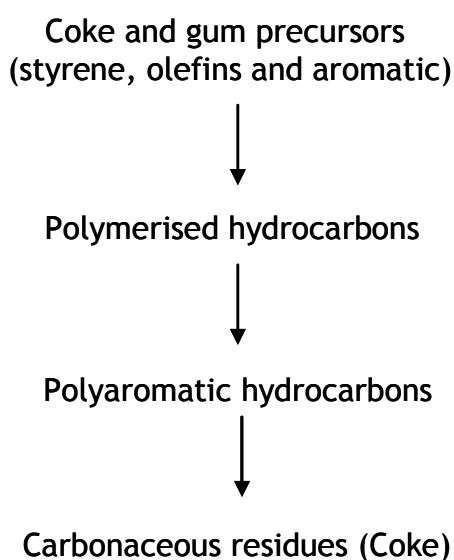
Figure 1.11 Carbonaceous residues (Coke) formation [53, 95]

The nature of the carbonaceous residues changes with reaction time. The change in the nature of the coke is due to polymerisation, multi-side addition and loss of hydrogen content. The deposits convert to more condensed and hydrogen deficient coke with the passage of time, and then finally form graphitic type coke.

The deposition of coke is highly dependent on the reaction conditions, especially on reaction temperature and hydrogen partial pressure. Increases in the reaction temperature of PyGas hydrogenation not only increases the amount of coke deposition but also results in a more condensed hydrogen deficient coke on the surface. Carbon laydown can be decreased by increasing hydrogen partial pressure [2].

1.6.3 Regeneration of used catalyst

Catalyst deactivation is an inevitable process. When deactivation reaches a level where conversion, selectivity or other process parameters are below the required specification, then the catalyst must be replaced or regenerated. The regeneration and re-use of the catalyst is always the preferable option. However, regeneration of the catalyst depends on the nature of deactivation. Some poisoned catalysts are difficult to regenerate. Similarly, catalyst sintering and thermal deactivation is usually irreversible. Coke depositions are the main cause of deactivation in catalysts for PyGas hydrogenation. These catalysts can be regenerated by gasification with O_2, H_2 or H_2O [53, 87, 93]. Coke removal involves a number of reactions which can be represented by;

$$C + O_2 \rightleftharpoons CO_2$$

$$C + 2H_2 \rightleftharpoons CH_4$$

$$C + H_2O \rightleftharpoons CO + H_2$$
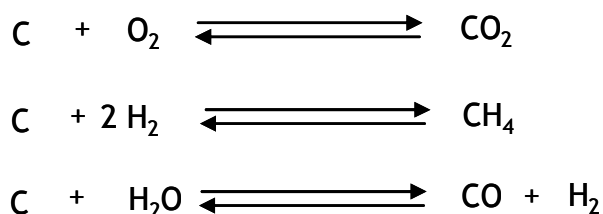
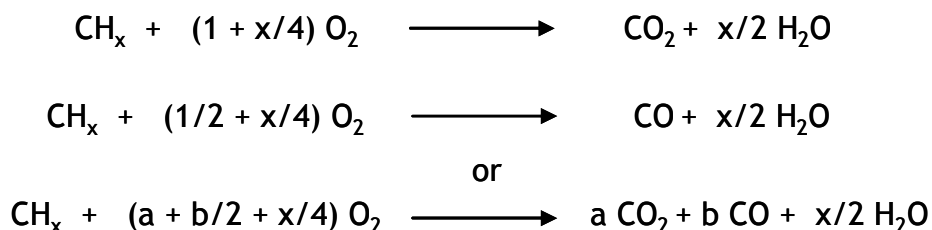The rate of removal of coke by O_2, H_2 or H_2O generally follows the order below [93].
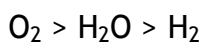
$$O_2 > H_2O > H_2$$

Sulfur is the main poison present in PyGas: This can be also be removed by gasification with O_2, H_2 or H_2O, as shown below.

$$Ni\text{-}S + H_2O \longrightarrow NiO + H_2S$$

$$H_2S + 2\,H_2O \longrightarrow SO_2 + 3H_2$$

$$S + O_2 \longrightarrow SO_2$$

$$S + H_2 \longrightarrow H_2S$$
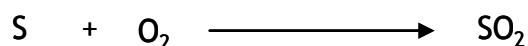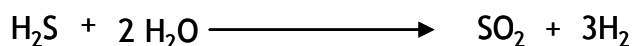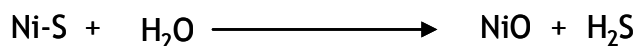
Several treatments have been studied in order to remove sulfur from nickel catalysts with steam (H_2O), hydrogen and oxygen [95]. Nielson *et al.* [97] studied the removal of sulfur with steam and observed that up to 80% surface sulfur can be removed at 700°C, with further removal of sulfur observed by increasing the regeneration temperature. However, higher temperatures can cause sintering and thermal degradation of the catalyst. The regeneration of catalysts to remove sulfur by using hydrogen is generally not satisfactory and the rate of removal of sulfur even at higher temperatures is very low with hydrogen [93, 98]. The regeneration of metal catalysts is more easily accomplished in air (O_2) [12, 93]. The regeneration of metal catalysts with steam or air (O_2) can form sulfates, which are subsequently reduced to sulfides upon reduction with hydrogen. At low oxygen partial pressure, the sulfur converts to SO_2 faster than NiO formation. At higher oxygen partial pressures, the rate of NiO formation is faster than that of SO_2 formation and sulfur is rapidly buried in an NiO layer and $NiSO_4$ is formed inside the nickel oxide layer [93, 98]. Therefore, low oxygen partial pressure and high flow is preferable for the regeneration of supported metal catalysts.

The main issue in catalyst regeneration is over-heating and hot spots. The high temperatures can further deactivate the catalyst by causing sintering and thermal degradation. Therefore a high temperature is not preferable for catalyst regeneration. The preferable temperature for the regeneration of Ni/A_2O_3 and Pd/A_2O_3 catalysts is less than 500°C. The combustion process can be typically controlled by using a low concentration of air (O_2) to avoid temperature overshooting and hot spots. Various ratios of carbon to hydrogen are present in

the carbonaceous residue (CH_x) deposited on the surface of catalyst, hence regeneration with oxygen can be represented by the following reactions.

$$CH_x + (1 + x/4) O_2 \longrightarrow CO_2 + x/2 H_2O$$

$$CH_x + (1/2 + x/4) O_2 \longrightarrow CO + x/2 H_2O$$

or

$$CH_x + (a + b/2 + x/4) O_2 \longrightarrow a CO_2 + b CO + x/2 H_2O$$

Temperature programmed oxidation is a simple and important technique for the investigation into the quantity and nature of coke deposited [99, 100]. The amount of oxygen consumed and the amount of CO_2/CO produced indicates the amount of coke deposited on the surface of the catalyst. The oxygen consumption is commonly mirrored by the production of CO_2, as shown in Figure 1.12.
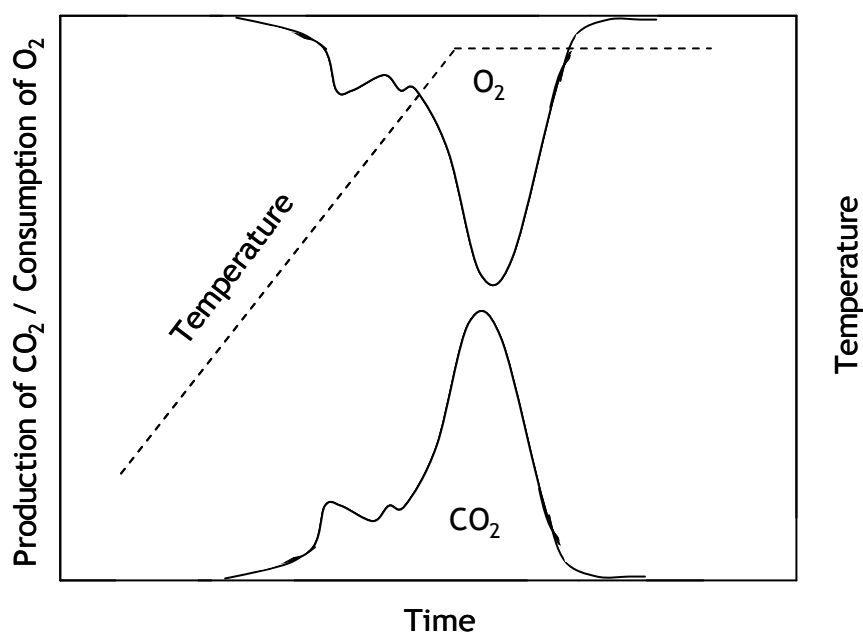
Figure 1.12 Temperature programme oxidation of metal supported alumina catalyst [99, 100]

The combustion of hydrogen rich coke, which is mostly present on catalyst metal, occurs first. This is followed by the combustion of the hydrogen deficient coke present on the surface of the catalyst [101, 102]. The ratio of CO_2/H_2O and CO/H_2O can give insight into the carbon to hydrogen ratio present in the coke. The decreasing hydrogen to carbon ratio represents more condensed polyaromatic type of coke [99].

A regenerated catalyst always exhibits a lower activity compared to the fresh catalyst, due to a small degree of permanent deactivation. However, the catalyst activity can be increased by adjusting the reaction parameters e.g. raising reaction temperature, increasing hydrogen partial pressure [43]. After several regenerations the catalyst may not have sufficient activity to meet the required reaction specification and must be replaced. The deactivation and regeneration process generally follows the pattern shown in Figure 1.13 [53].
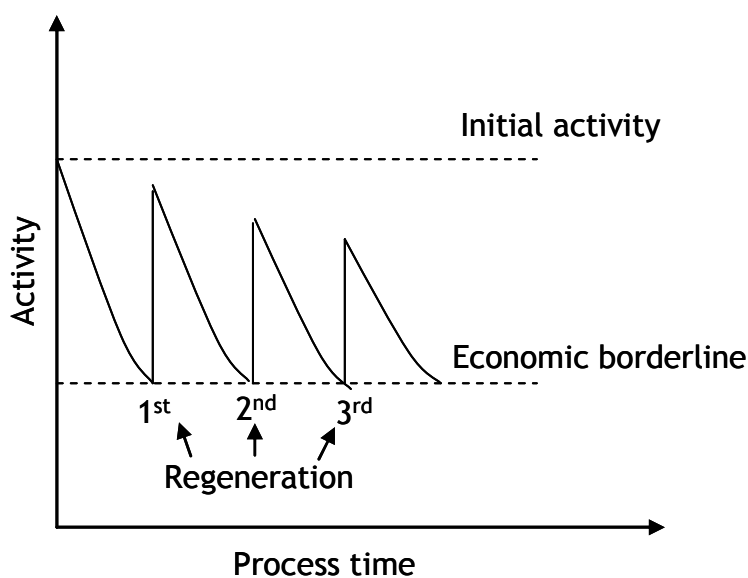
Figure 1.13 Catalyst regeneration and loss of activity during a process

1.7 Project background

Limited work has been performed on the hydrogenation of PyGas and an incomplete picture of the processes has been obtained. Most of the literature available deals only with hydrogenation of a single component or a few components mixture, as a model PyGas, over a limited range of reaction parameters. A single compound cannot realistically represent the hydrogenation of a PyGas mixture, as the kinetics and mechanisms of the complex mixture that is PyGas will behave in a different manner compared to pure single compounds. Consequently, the kinetics and mechanisms of PyGas hydrogenation cannot be considered the sum of individual components.

Furthermore, the hydrogenations of aromatic compounds present in PyGas have not been investigated to a great extent. The aromatic compounds present in PyGas are mainly used in gasoline blending mixtures and/or as an aromatics

source. However, with the introduction of strict fuel regulations, the reduction of aromatics in gasoline has become essential. Therefore, the hydrogenation of aromatic compounds present in PyGas is required to meet fuel regulations or an alternative utilisation of the surplus aromatics need to be found.

Different strategies were proposed for PyGas consumption to obtain; (i) a high octane number gasoline blend, (ii) an aromatic source mixture and (iii) hydrogenation of surplus aromatics present in PyGas. Low temperatures and low hydrogen partial pressures are preferable for the selective hydrogenation of PyGas to a high octane gasoline mixture. However, slightly higher temperatures and higher hydrogen partial pressures are required for the hydrogenation of surplus olefins and aromatics reduction. Therefore, the hydrogenation of PyGas was performed in the gas phase at temperatures between 140°C and 200°C, and at hydrogen partial pressure between 1 and 20 barg to investigate its utilisation for a high octane gasoline blend as well as for aromatic extraction mixtures and the hydrogenation of surplus aromatics.

Coke deposition is one of the main causes of catalyst deactivation during PyGas hydrogenation due to the high amounts of coke precursors present in PyGas. The rate of catalyst deactivation can be reduced with a decrease in coke formation by using appropriate reaction conditions. Regeneration of a used catalyst is also an attractive option for a cost-effective process. Accordingly, extensive research is required for a better understanding of PyGas hydrogenation over a wide range of reaction conditions. Other process issues such as catalyst deactivation and catalyst regeneration also need investigation.

The composition of PyGas is very complex and changes from one plant to another. Therefore, it was decided that the investigation should be carried out with a synthetic PyGas. The synthetic PyGas chosen was made up of the following components: styrene, toluene, 1-octene, cyclopentene, heptane, decane and 1,3-pentadiene/1-pentene. This is a comprehensive model for the broader groups of hydrocarbons (aromatic, diolefins, olefins, cycloolefins, styrene, etc.) present in PyGas. The possible reactions in our model PyGas are shown in Figure 1.14.
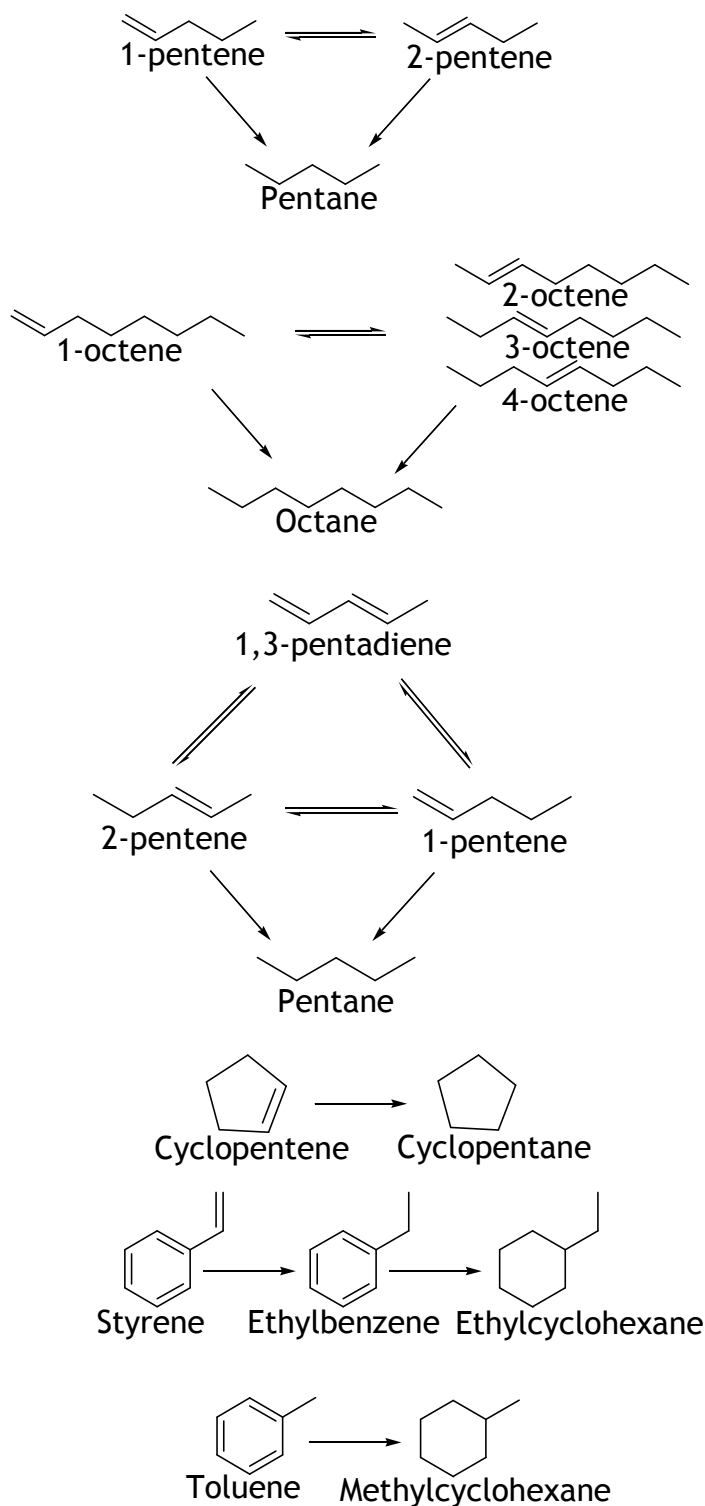
Figure 1.14 Possible reactions in our model PyGas

1.8 Project aims

The aims of the project were:

1.   To study the hydrogenation of a model PyGas over Ni/Al_2O_3 and Pd/Al_2O_3 over a wide range of reaction parameters e.g. hydrogen partial pressure, reaction temperature, total reaction pressure and feed flow rate of PyGas ($WHSV_{PyGas}$).

2. To investigate the useful avenues for PyGas utilisation e.g. high gasoline pool mixture, an aromatics source, etc.

3. To study the reaction kinetics during PyGas hydrogenation.

4. To investigate the nature and amount of coke deposition, and regeneration of the used catalysts by *in-situ* TPO.

2. Experimental

2.1 Catalyst characterisation

2.1.1 Surface area analysis

The surface area of the pre and post-reaction catalysts was determined using a Micromeritics Gemini III 2375 Surface area analyser. Approximately 0.05 g of catalyst was weighed into a glass tube and purged in a flow of N_2 gas overnight at 110^oC before the measurement was carried out.

The BET equation can be expressed as;

$$\frac{P}{V(P_o - P)} = \frac{1}{V_m C} + \frac{(C-1)P}{V_m C P_o}$$

Where

P = pressure of adsorbate gas

P_o = saturated pressure of adsorbate gas

V = volume of adsorbed gas

V_m = volume of monolayer adsorbed gas

C = BET constant ($C = e^{(q_1 - q_L)/RT}$)

q_1 = heat of adsorption on the first layer

q_L = heat of liquefaction on second and higher layers

R = the gas constant

The graph plot $[P / V (P_o - P)]$ vs $[P/P_o]$ gives a straight line with a slope of $[(C - 1)/V_m C]$ and an intercept of $[1/V_m C]$.
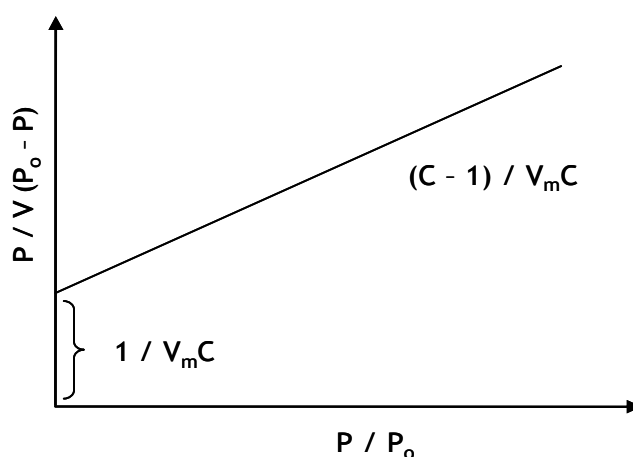
Figure 2.1 BET plot $[P / V (P_o - P)]$ vs $[P / P_o]$

The V_m can be calculated by using the following equation;

$$V_m = 1 / (I + J) \text{ where I and J are intercept and slope respectively.}$$

The surface area of the catalyst can be determined by using the following equation;

$$S_{Total} = V_m \, N \, \sigma \, / \, M_v$$

Where   N = Avogadro number

                  M_v = molar volume of adsorbed gas

                  σ = adsorption cross-section of the adsorbed gas molecule (N_2 gas)

The surface area per unit weight of the catalyst can be calculated from equation;

$$S = S_{Total} / m \qquad \text{(where m is the mass of catalyst)}$$

2.1.2 X-Ray diffraction (XRD)

XRD diffraction patterns of pre and post-reaction catalysts were measured using a Siemens D500 X-ray Diffractometer (40 kV, 40 mA, monochromatised) using a Cu K_{alpha} source (1.5418 Å). The scanning range was 5-85° 2θ with a scanning rate of 1 second step^{-1} and a step size of 0.02°. Crushed catalyst was placed in the sample holder and the sample was levelled with the aid of a glass slide.

Hot-stage analysis was carried out using an Anton-Paar XRK reaction cell. The set up consisted of a water cooled, vacuum tight, stainless steel chamber with a beryllium window. Samples were heated at 15°C min^{-1} and scans were taken at room temperature, 100°C and every 100°C thereafter up to 600°C. The sample was held for 15 minutes at each temperature before the scan was taken. The gas environment was a 5% H_2/N_2 gas mixture.

The Scherrer equation can be used to calculate crystal size from the XRD data.

$$d = K \, \lambda \, / \, \beta \, Cos\theta$$

      Where   d = Average crystal size

                     K = Scherrer constant

                     λ = wavelength of X-ray source (1.5418 Å)

                     β = full width at half maximum (degrees)

                     θ = diffraction angle (degrees)

2.1.3 Thermo-gravimetric analysis

Thermo-gravimetric analysis was performed on catalysts using a combined TGA/DSC SDT Q600 thermal analyser coupled to an ESS mass spectrometer for evolved gas analysis. The samples were heated from room temperature (30°C) to 800°C using a heating ramp of 10°C min^{-1}. This temperature profile was employed using a 2% O_2/Ar or 5% H_2/N_2 (all 100 ml min^{-1}) depending on the sample. Relevant mass fragments were followed by online mass spectrometry. The sample loading was typically 10-15 mg.

2.2 Reaction

Hydrogenation of the synthetic pyrolysis gasoline (PyGas) was investigated over Ni/Al_2O_3 and Pd/Al_2O_3 catalysts in a fixed bed high-pressure continuous flow reactor in gas phase.

2.2.1 Pyrolysis gasoline (PyGas) composition

Two types of synthetic PyGas were used in this study, and the compositions are shown in Table 2.1. The chemicals were mixed to the desired compositions in the synthetic PyGas preparation.

Components	PyGas 1 Wt. % composition	PyGas 2 Wt. % composition
1-Pentene	10.0	-
Cyclopentene	10.0	10.0
1-octene	10.0	10.0
Toluene	55.0	62.5
Styrene	10.0	10.0
n-Heptane	2.5	2.5
n-Decane	2.5	2.5
1,3-Pentadiene	-	2.5

Table 2.1 Weight percent (%) composition of PyGas

2.2.2 Reactor

A diagram of the reactor is shown in Figure 2.2. It consisted of a 1 cm (3/8 inch) internal diameter glass-lined metal reactor tube positioned within a furnace. The catalyst bed within the reactor was carefully positioned in the middle of reactor tube. The thermocouples were present in the furnace and also inside the reactor tube to measure the temperature of the furnace and the catalyst bed. The thermocouples and heater were linked via a West 4400 temperature controller, used to set the temperature programme. The flow rates of the gases were controlled using mass flow controllers that allowed gas flows of between 0 and 700 ml min^{-1}. The HPLC pump fed a desired flow of reactants to the vaporiser. The reactants were vaporised in the vaporiser, mixed with gas and flowed over the catalyst bed through the reactor tube. The reaction products were then condensed in a knockout pot at the base of the reactor. The liquid products were collected from the knockout pot at regular intervals and were analysed using a Thermo Finnigan Focus G.C. Most of the products were condensed in the knockout pot, but very small amounts of the reaction products remained in the gaseous state and therefore the effluent gas was also analysed at regular intervals by online Agilent G.C. The total pressure of the reactor was controlled with a Tescom variable pressure valve. A mass spectrometer was also attached to the reactor for online temperature programme oxidation (TPO) of the post-reaction catalysts.
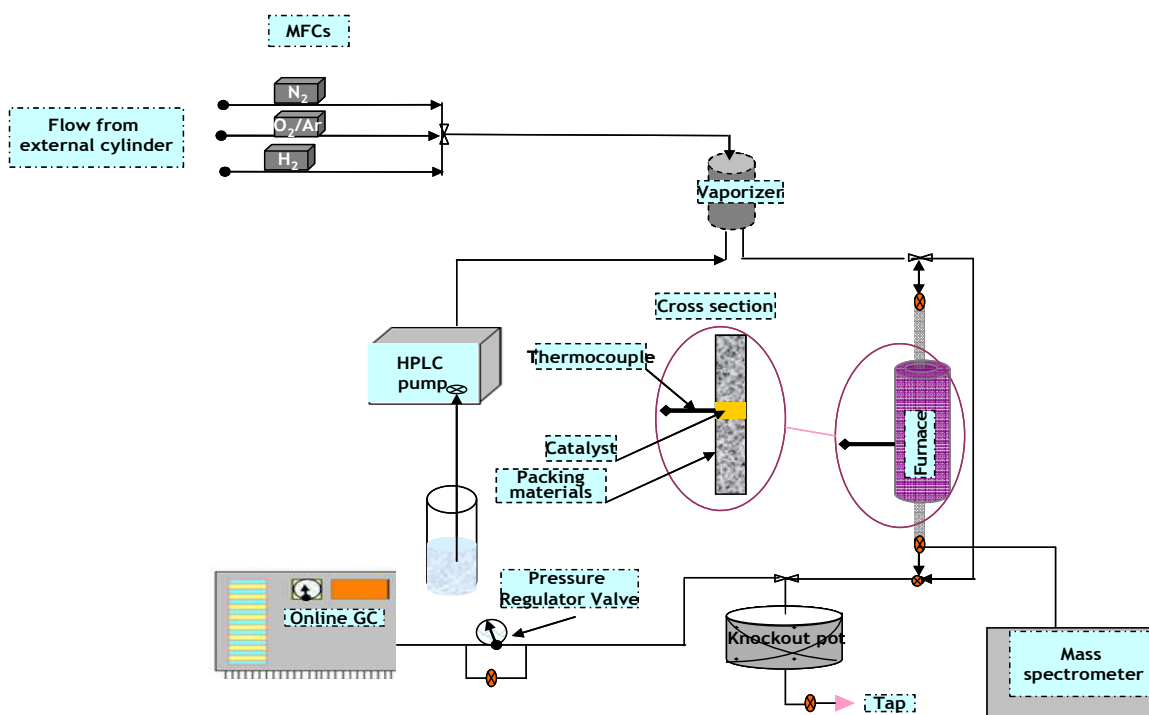
Figure 2.2 Fixed bed high-pressure continuous flow reactor

2.2.3 Mass flow controller (MFC)

The MFC was calibrated for each gas. The MFC was set at a particular flow rate and the gas flow was measured using a digital flow meter. A graph was plotted of actual flow vs MFC set point, and is shown in Figure 2.3.
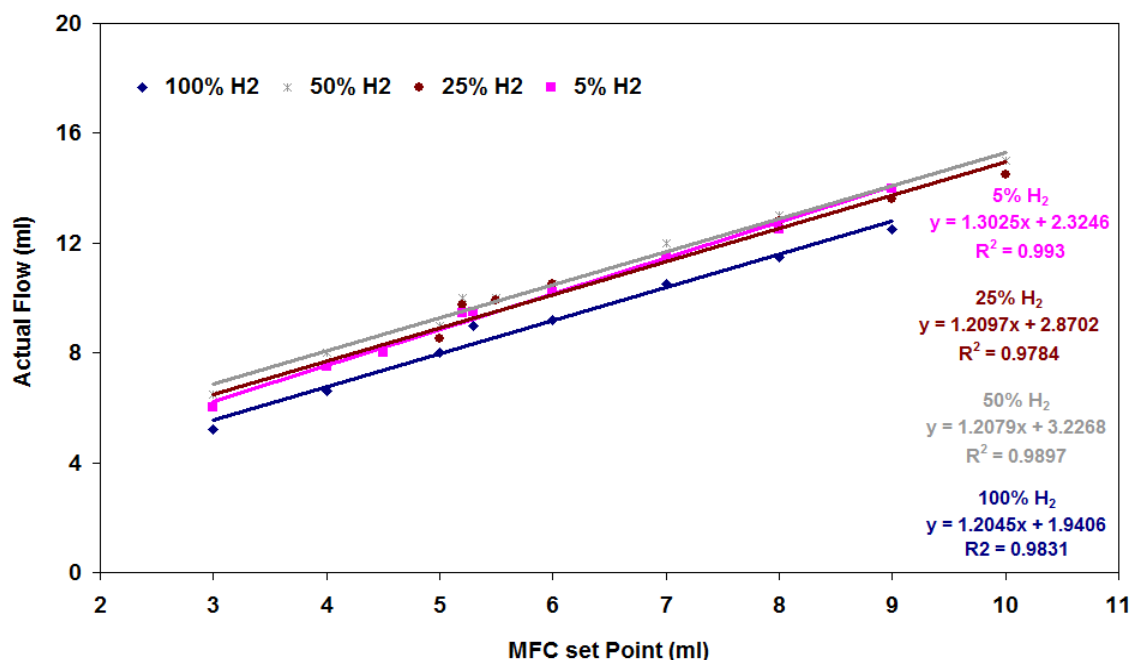
Figure 2.3 MFC calibration graph (actual flow ml vs MFC set points)

2.2.4 Reaction procedure

0.5 or 0.25 g of catalyst (particle size between 250 and 425 microns), depending on the reaction, was added to the reactor tube and positioned in the middle of reactor tube. Both sides of the catalyst bed were packed with a packing material (boiling chips) to keep the catalyst position fixed in the centre of the reactor tube.   The catalysts were reduced *in-situ* with a flow of hydrogen gas. The Ni/Al$_2$O$_3$ catalyst was reduced for 16 hours at a temperature of 450°C, ramped at 10°C min^{-1} from room temperature, under a hydrogen flow of 40 ml min^{-1}. Similarly the Pd/Al$_2$O$_3$ catalyst was reduced for 1 hour at a temperature of 250°C, ramped at 10°C min^{-1} from room temperature, under a hydrogen flow of 40 ml min^{-1}. Following this, the reactor temperature was decreased to the required reaction temperature (140-200°C). The temperature of the vaporiser and the line between vaporiser and reactor tube trace was heated to 140°C. The reactor was then pressurised to the desired pressure (10-20 barg). Once the reactor had obtained the desired conditions, the reaction was started with a

particular flow of PyGas feed depending on the reaction from 0.042 to 0.084 ml min^{-1} (WHSV$_{PyGas}$ 4-8 h^{-1}) and set flow of H$_2$ or H$_2$/N$_2$ mixtures gas (10 ml min^{-1}). The PyGas was vaporised in the vaporiser, where it was mixed with hydrogen and then passed through the catalyst bed. The temperature of the downstream line from the reactor tube to the knockout pot was kept at 200°C to avoid condensation of products material in the line. The products were passed to a knockout pot. The hydrogenated PyGas was condensed in the knockout pot, which was chilled to 0°C. The liquid samples were collected from the knockout pot at every 2 hours intervals during day time and analysed using a Thermo Finnigan Focus G.C. The hydrogenated PyGas mainly condensed in the knockout pot, however very small amounts of the reaction products remained in the gaseous state and therefore the effluent gas was also analysed at regular intervals by online Agilent G.C. All reactions were run for 76 hours. After finishing each reaction, nitrogen gas (40 ml min^{-1}) was passed through the catalyst over night so as to remove any species present in the reactor. The reactor was then cooled down to room temperature in the flow of nitrogen gas and then an *in-situ* TPO was performed on the post reaction catalyst.

2.2.5 *In-Situ* TPO of post reaction catalyst

The gas was switched to a flow of 2% O$_2$/Ar (40 ml min^{-1}) from nitrogen, when the reactor had cooled down after each reaction. The 2% O$_2$/Ar gas mixture was passed through the reactor for a period of time to remove all nitrogen present in the system. The process was monitored by an online Quadrupole Mass Spectrometer (QMS) and when the system became stable then the TPO was started. The temperature was raised to 450°C at a ramp of 5°C min^{-1} and then the reactor temperature was held constant at 450°C until the complete removal of deposited coke on the catalyst had occurred. The TPO process was monitored by an online mass spectrometer (QMS) in which the ion current of main species of mass fragments with m/z 28 (CO), 44 (CO$_2$), 32 (O$_2$), 18 (H$_2$O) were monitored. Other species with m/z 68 (cyclopentene), 70 (1-pentene), 72 (pentane), 78 (benzene), 92 (toluene), 98 (methylcyclohexane), 104 (styrene), 106 (ethylcyclo-hexane), 112 (1-octene), 114 (octane), 15 (CH$_3$), 29 (C$_2$H$_5$) and 2 (H$_2$) were also followed for detailed investigation of deposited coke.

2.3 Gas chromatograph

The liquid samples were analysed by gas chromatography on a Thermo Finnigan Focus GC. The effluent gas was analysed online using an Agilent GC.

2.3.1 Thermo Finnigan Focus G.C

The liquid samples were analysed by Thermo Finnigan Focus G.C with an FID detector. Two types of column were used during this study.

Chrompack DB-1 column

The Chrompack DB-1 column, 50 m in length with 0.32 mm internal diameter, was used for the analysis of the liquid sample taken from reactor at regular interval. The following conditions were employed.

Injector temperature – 300 ^{o}C; Carrier gas – 2 ml min^{-1} helium

The column heating profile is shown in Figure 2.4 and summarised in Table 2.2.
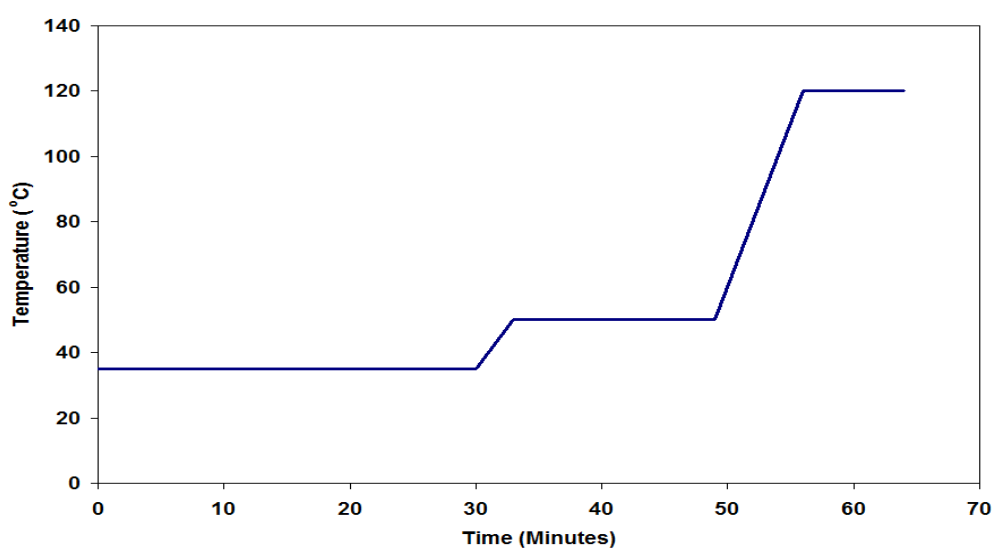
Figure 2.4 Thermo Finnegan Focus GC temperature ramp profile for chrompack DB-1 column

	Rate (^{o}C min^{-1})	Temp (^{o}C)	Hold Time (min)
	-	35	30
Ramp 1	5	50	16
Ramp 2	10	120	8

Table 2.2 Thermo Finnegan Focus GC temperature ramp profile for chrompack DB-1 column

Petrocol™ DH Column

After the Chrompack DB-1 column was no longer useable, a petrocol™ DH Column 150 m in length with 0.25 mm internal diameter was used for the remainder of the project. This column required more time for the analysis of the sample, however separation of the components was superior to that achieved with the previous column. The conditions used are given below;

Injector Temperature – 200 $^{\circ}$C; Carrier gas – 1.5 ml min^{-1} helium

The column heating profile is shown in Figure 2.5 and summarised in Table 2.3.
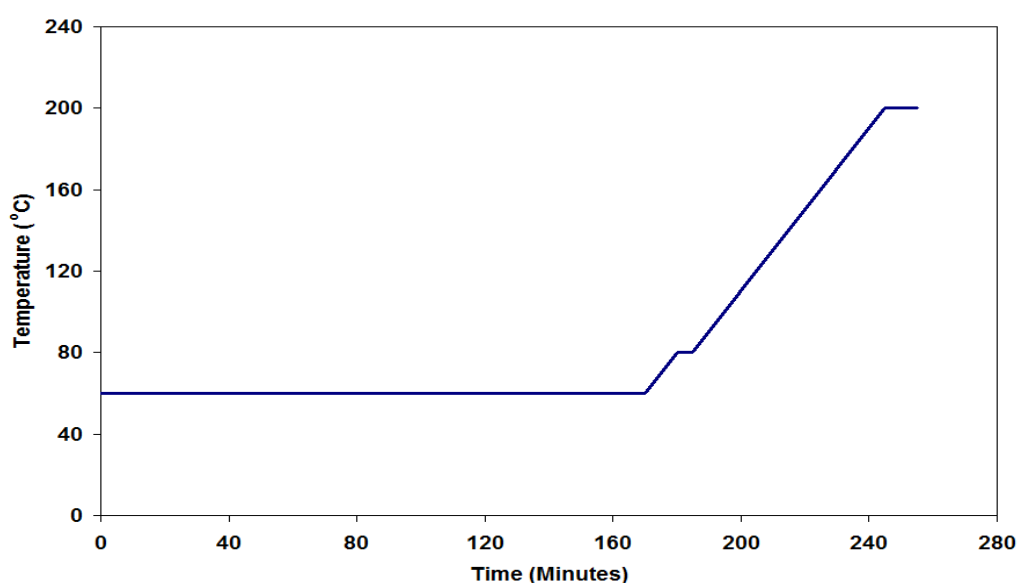
Figure 2.5 Thermo Finnegan Focus GC temperature ramp profile for PetrocolTM DH column

	Rate ($^{\circ}$C min^{-1})	Temp ($^{\circ}$C)	Hold Time (min)
	-	60	170
Ramp 1	2	80	5
Ramp 2	2	200	10

Table 2.3 Thermo Finnegan Focus GC temperature ramp profile for Petrocol^{TM} DH column

2.3.2 Agilent GC

The main liquid sample was trapped in the knockout pot, however a very small amount of volatile hydrocarbons were detected in the effluent gas, which was analysed by online Agilent G.C with an FID detector. The gas samples were injected onto the GC at regular intervals. A CP-Na$_2$SO$_4$ /Al$_2$O$_3$ column, 50 m in

length with 0.25 um internal diameter was used for the online gas samples of effluent gas. The following conditions were employed.

Injector Temperature – 200 $^{\circ}$C; Carrier gas – 3 ml min^{-1} helium

The column heating profile is shown in Figure 2.6 and summarised in Table 2.4.
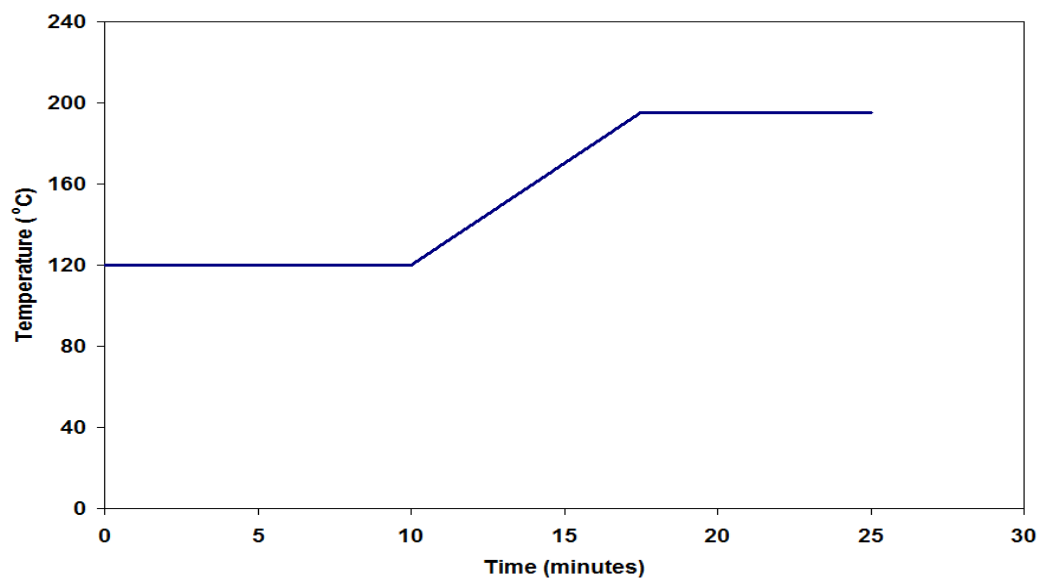
Figure 2.6 Agilent GC temperature ramp profile for CP-Na$_2$SO$_4$ /Al$_2$O$_3$ column

	Rate ($^{\circ}$C min^{-1})	Temp ($^{\circ}$C)	Hold Time (min)
	-	120	10
Ramp 1	10	195	10

Table 2.4 Agilent GC temperature ramp profile for CP-Na$_2$SO$_4$ /Al$_2$O$_3$ column

2.3.3 Calibrations

Calibration standards for all reactants and possible products were prepared in varying concentrations using n-hexane as the solvent. From the peak area responses, linear calibration plots were obtained.

Chrompack DB-1 column

The Chrompack DB-1 column was used for the analysis of liquid samples. The column was capable of separating all the reactants and possible products, with the exception of trans-3-octene, cis-3-octene and cis-4-octene, which gave a

combined single peak. Standards were run and linear calibration plots were obtained, which are shown in Figure 2.7.
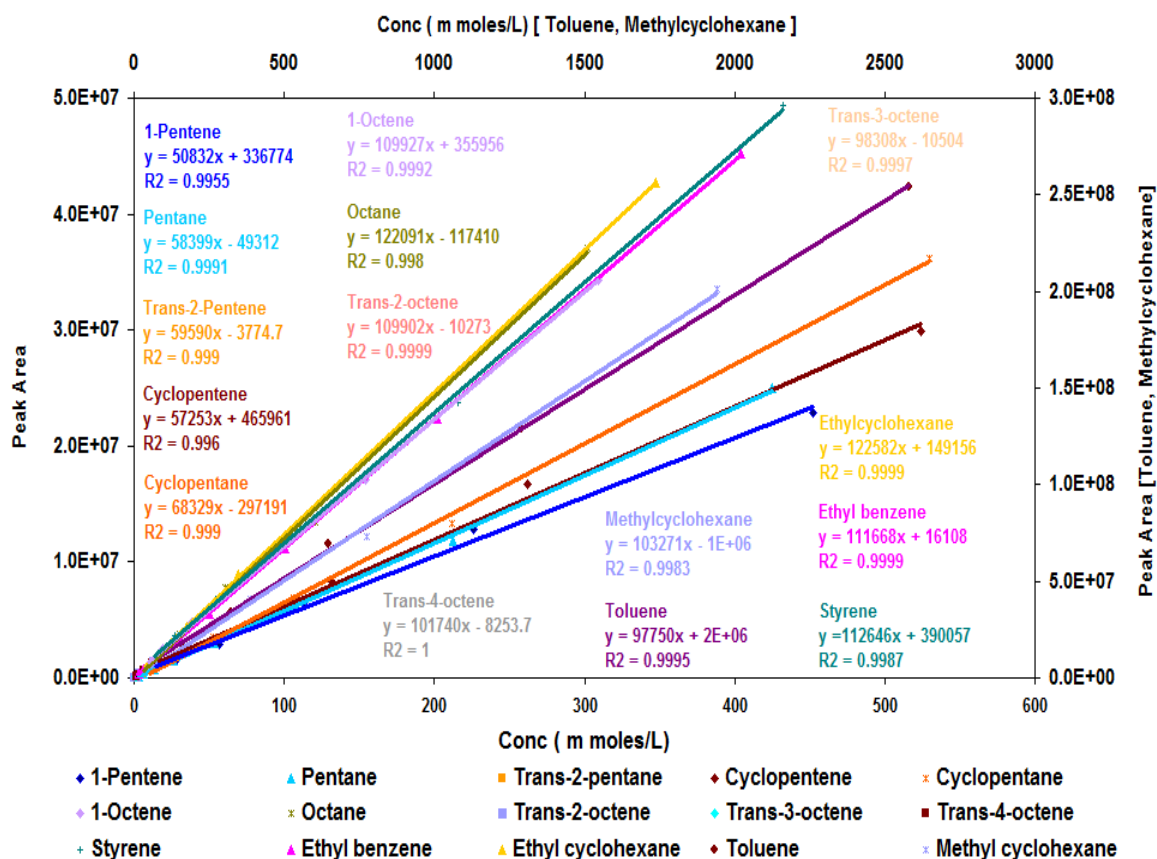
Figure 2.7 Standards calibrations for Chrompack DB-1 column

Petrocol™ DH Column

The Petrocol^{TM} DH was a 150 metre long capillary column. It required a very long time for analysis, however it was able to separate all possible components in the liquid sample. Reasonable linear plots were obtained from standards run on this column, which are shown in Figure 2.8.
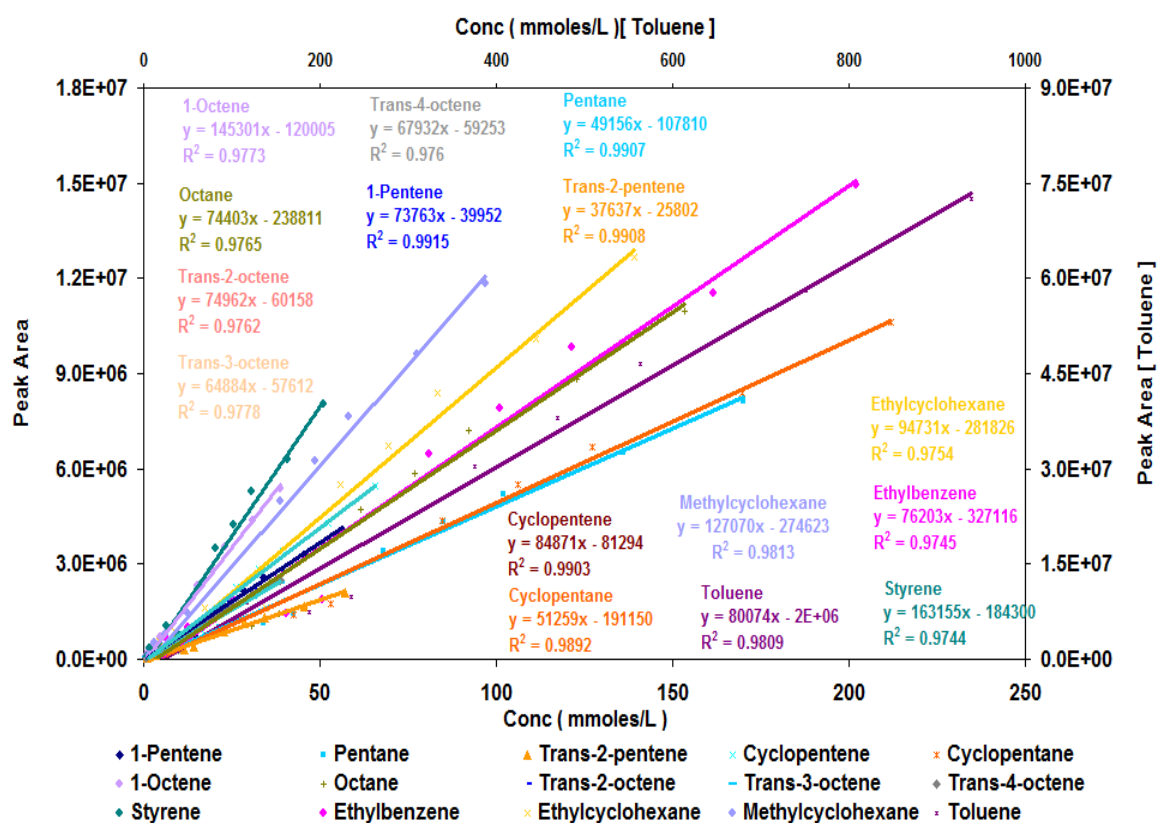
Figure 2.8 Standards calibrations for Petrocol^TM DH column

CP-Na$_2$SO$_4$ /Al$_2$O$_3$ column

A small amount of hydrogenated PyGas components were detected in the effluent gas from the knockout pot. Although the quantity was very small, it was still analysed by online GC for a better understanding of the process and the reactor engineering set up test. The main components present in the effluent gas were C$_5$s compounds such as pentane, pentenes, trans-2-pentene, cis-2-pentene, cyclopentane and cyclopentene. The CP-Na$_2$SO$_4$/Al$_2$O$_3$ column, 25m in length was capable of separating all the C$_5$s compounds *i.e.* 1-pentene, pentane, trans-2-pentene, cis-2-pentene, cyclopentene and cyclopentane. A minute amount of other species such as toluene and methylcyclohexane were also detected in the effluent stream. Standards were also run for this column and graphs were obtained and are shown in Figure 2.9.

Conc (m moles) [Pentane, Cyclopentane]

1-Pentene
y = 4E+09x + 2007.4
R2 = 0.9896

Cyclopentene
y = 4E+09x + 2596.9
R2 = 0.9881

Pentane
y = 6E+09x + 817.26
R2 = 0.9998

Cyclopentane
y = 6E+09x + 2202.8
R2 = 0.9998

Trans-2-pentene
y = 5E+09x + 439.55
R2 = 0.9999

C8 (octane and octene)
y = 1E+10x + 6989.3
R2 = 0.9993

Toluene
y = 1E+10x + 3205
R2 = 0.999

Methylcyclohexane
y = 1E+10x - 674.82
R2 = 0.9991

Ethylcyclohexane
y = 1E+10x - 1281.6
R2 = 0.9991

♦ 1-Pentene   ▲ Trans-2-pentene   ✕ Cyclopentene
♦ C8(octane,octene)   + Methylcyclohexane   Ethylcyclohexane
✳ Toulene   ■ Pentane   ✕ Cyclopentane

Figure 2.9 Standards calibrations for CP-Na$_2$SO$_4$ /Al$_2$O$_3$ column

2.4 Materials

2.4.1 Catalysts

Commercial Ni/Al$_2$O$_3$ (HTC 400) and Pd/Al$_2$O$_3$ catalysts provided by Johnson Matthey, were used in this project. The characterisation data of catalysts provided by catalyst manufacturer are shown in Table 2.5.

Catalyst	Metal loading (% wt)	Metal dispersion (%)	Surface area (m^2 g^{-1})	Pore volume (cm^3 g^{-1})
Ni/Al$_2$O$_3$	16.0	18.0	106	0.39
Pd/Al$_2$O$_3$	1.0	32.5	97.6	0.49

Table 2.5 Properties of catalysts

2.4.2 Gases

The gases were supplied by BOC and used without any further purification. The purities of the gases are shown in Table 2.6.

Gases	Supplier	Purity
Helium	BOC	99.99%
Air	BOC	99.99%
Nitrogen	BOC	99.99%
Hydrogen	BOC	99.99%
50% Hydrogen (H_2:N_2 = 50:50)	BOC	99.99%
25% Hydrogen (H_2:N_2 = 25:75)	BOC	99.99%
5% Hydrogen (H_2:N_2 = 5:95)	BOC	99.99%

Table 2.6 Gases used in the project

2.4.3 Chemicals

The following chemicals without any further purification were used in the reactions and for GC calibration standards. The supplier and purities of the chemicals are shown in Table 2.7.

Chemicals	Supplier	Purity
1-Pentene	Alfa Aesar	97%
Pentane	Alfa Aesar	97%
Trans-2-pentene	Alfa Aesar	99%
Cis-2-pentene	Alfa Aesar	99%
1,3-pentadiene	Sigma Aldrich	90%
Cyclopentene	Alfa Aesar	97%
Cyclopentane	Fluka	99%
n-Hexane	Sigma Aldrich	99%
n-Heptane	Fisher Scientific	99%
1-Octene	Alfa Aesar	97%
Octane	Alfa Aesar	97%
Trans-2-octene	Alfa Aesar	97%
Cis-2-octene	Alfa Aesar	97%
Trans-3-octene	Alfa Aesar	97%
Cis-3-octene	GFS chemicals	97%
Trans-4-octene	Alfa Aesar	97%
Cis-4-octene	Alfa Aesar	97%
n-Decane	Alfa Aesar	99%
Toluene	Fisher Scientific	99%
Styrene	Alfa Aesar	99%
Methylcyclohexane	Sigma Aldrich	99%
Ethylcyclohexane	Sigma Aldrich	99%
Ethyl benzene	Sigma Aldrich	99%

Table 2.7 Chemicals used in the project

2.5 Calculations

2.5.1 Percent (%) conversion

The % conversion of each species was calculated as;

% Conversion = [(moles in –moles out) / (moles in)] × 100

2.5.2 Percent (%) yield

The % yield of each species was calculated as;

% Yield = [(moles of product) / (moles of reactant)] × 100

2.5.3 Percent (%) selectivity

The % selectivity of each species was calculated as;

% Selectivity = [(moles product) / (moles produced of all products)] × 100

All the conversion, yield and selectivity data that are presented in chapter 3, were averages of the five daily samples taken at two hours intervals. Error bars are shown for each average point.

2.5.4 Percent (%) carbon Balance

The % carbon balance was calculated as;

% Carbon Balance = [(moles of carbon out)/(moles of carbon in)] × 100

2.5.5 Oxygen consumption during *in-situ* TPO

The flow of 2% O_2/Ar gas was 40 ml min^{-1} during the *in-situ* TPO. Therefore total consumption of oxygen during TPO was calculated as;

Amount of oxygen consumed (ml) = [time period of oxygen consumed in TPO (min) × 40 ml min^{-1} × 2/100]

The oxygen consumption in m moles was determined by using gas equation;

$$PV = n \, RT$$

Where   P = atmospheric pressure (1 atm)

V = volume of oxygen consumed (ml)

R = Gas constant (0.082 L atm K^{-1} mol^{-1})

T = 298 K (laboratory temperature)

2.6 PyGas hydrogenation reactions

The PyGas hydrogenation reactions were performed over Ni/Al_2O_3 and Pd/Al_2O_3 and are summarised in Tables 2.8-11.

Catalysts	Reaction temperature			
	140°C	160°C	180°C	200°C
Packing material (boiling chips)	√	-	-	-
Catalyst support (Al_2O_3)	√	-	-	-
Ni/Al_2O_3	√	√	√	√
Pd/Al_2O_3	√	√	√	√

Table 2.8 Reactions performed at different reaction temperatures, with other reaction conditions constant [WHSV$_{PyGas}$ = 4 h^{-1}, P$_T$ = 20 barg, P$_{H2}$ = 20 barg]

Catalysts	Hydrogen partial pressure			
	1 barg (5% H_2 gas)	5 barg (25% H_2 gas)	10 barg (50% H_2 gas)	20 barg (100% H_2 gas)
Ni/Al_2O_3	√	√	√	√
Pd/Al_2O_3	√	√	√	√

Table 2.9 Reactions performed with different hydrogen partial pressures, with other reaction conditions kept constant [T= 140°C, WHSV$_{PyGas}$ = 4 h^{-1}, P$_T$ = 20 barg]

Catalysts	Total reaction pressure	
	10 barg	20 barg
Ni/Al_2O_3	√	√
Pd/Al_2O_3	√	√

Table 2.10 Reactions performed with different total reaction pressures, with other reaction conditions kept constant [T= 140°C, WHSV$_{PyGas}$ = 4 h^{-1}, Gas mixture = 50% H_2]

Catalysts	P_{H2} = 5 barg [P_T = 20 barg] (25% H_2 gas)			P_{H2} = 10 barg [P_T = 20 barg] (50% H_2 gas)	
	WHSV= 4 h^{-1} Catalyst wt= 0.5 g	WHSV= 8 h^{-1} Catalyst wt= 0.5 g	WHSV= 8 h^{-1} Catalyst wt= 0.25 g	WHSV= 4 h^{-1} Catalyst wt= 0.5 g	WHSV= 8 h^{-1} Catalyst wt= 0.5 g
Ni/Al$_2$O$_3$	√	√	√	√	√
Pd/Al$_2$O$_3$	√	√	√	√	√

Table 2.11 Reactions performed with different WHSV of PyGas, with other reaction conditions kept constant [T= 140°C, P_T = 20 barg]

3. Results

3.1 Catalyst characterisation

The catalysts were characterised by thermogravimetric analysis (TGA), X-ray diffraction (XRD), and Brunauer, Emmett and Teller (BET) surface area measurement prior to activity testing.

3.1.1 Temperature programme reduction (TPR)

3.1.1.1 TPR of Ni/Al$_2$O$_3$ catalyst

The Ni/Al$_2$O$_3$ catalyst was examined under a 5% H$_2$/N$_2$ atmosphere. Figure 3.1 shows a weight loss up to 800°C, the first major weight loss was observed at around 100°C which was about 3.1% and the second key weight loss of about 3.7% occurred between 300°C and 500°C.
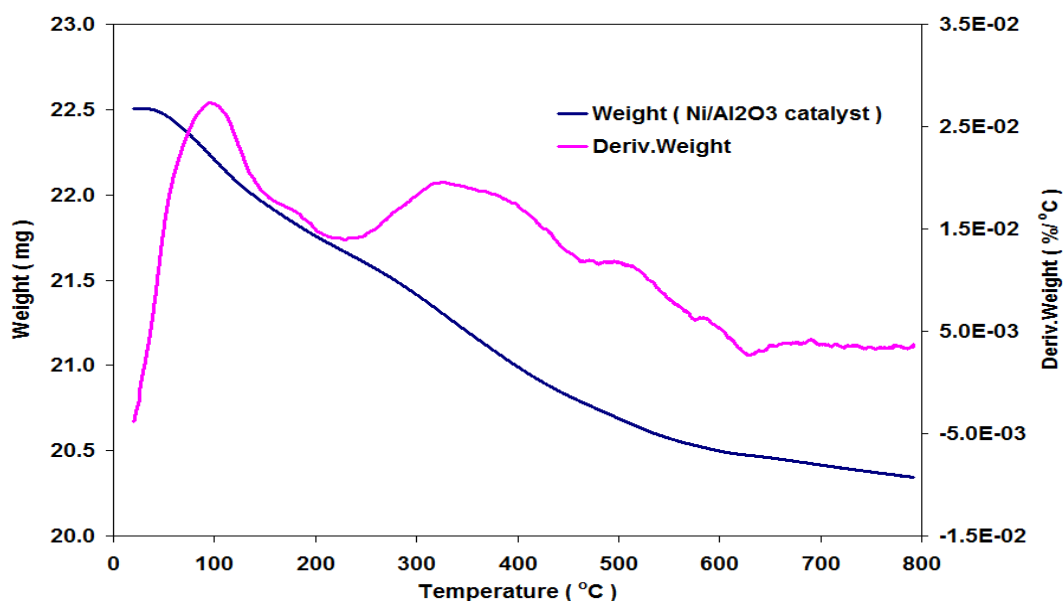
Figure 3.1 TGA profile of Ni/Al$_2$O$_3$ catalyst under 5% H$_2$/N$_2$

The first weight loss mainly corresponded to the loss of physisorbed H$_2$O. The second weight loss corresponded to reduction of nickel oxide, with the uptake of H$_2$ and the evolution of H$_2$O.

3.1.1.2 TPR of Pd/Al$_2$O$_3$ catalyst

The TGA of Pd/Al$_2$O$_3$ indicated that the main weight loss of around 2.2% occurred from room temperature to 200°C. The mass spectrometer data showed an uptake

of H_2 and evolution of H_2O at this temperature. This suggested that the catalyst reduced with the uptake of H_2.
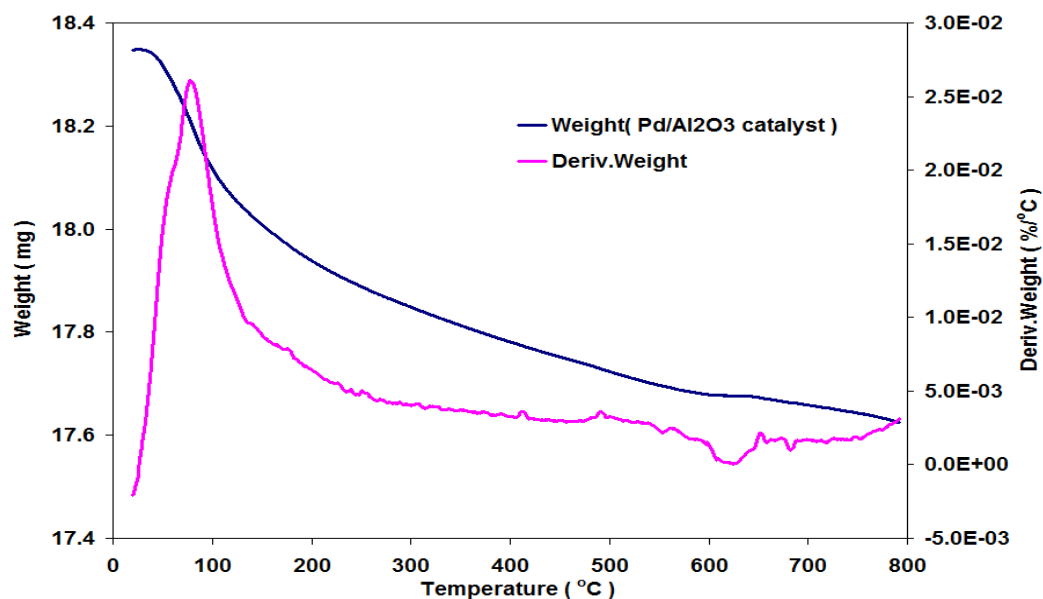
Figure 3.2 TGA profile of Pd/Al$_2$O$_3$ catalyst under 5% H$_2$/N$_2$

3.1.2 X-ray diffraction (XRD)

Powder XRD was used to examine the fresh and reduced catalyst to determine any change in the catalyst morphology. The peaks were identified through the Powder Diffraction Database [103].

3.1.2.1 Ni/Al$_2$O$_3$ catalyst

High temperature *in-situ* XRD analysis of the Ni/Al$_2$O$_3$ was carried under a 5% H$_2$/N$_2$ atmosphere as described in section 2.1.2 and shown in Figure 3.3. There was a noticeable change observed in the Ni peaks at the 52 and 76 (2θ) positions when the temperature was increased. The XRD pattern of Ni/Al$_2$O$_3$ catalyst studies showed that the intensity of the Ni peak increased upon reduction. The alumina peak also became sharper which suggests an increase in crystallinity of the catalyst.
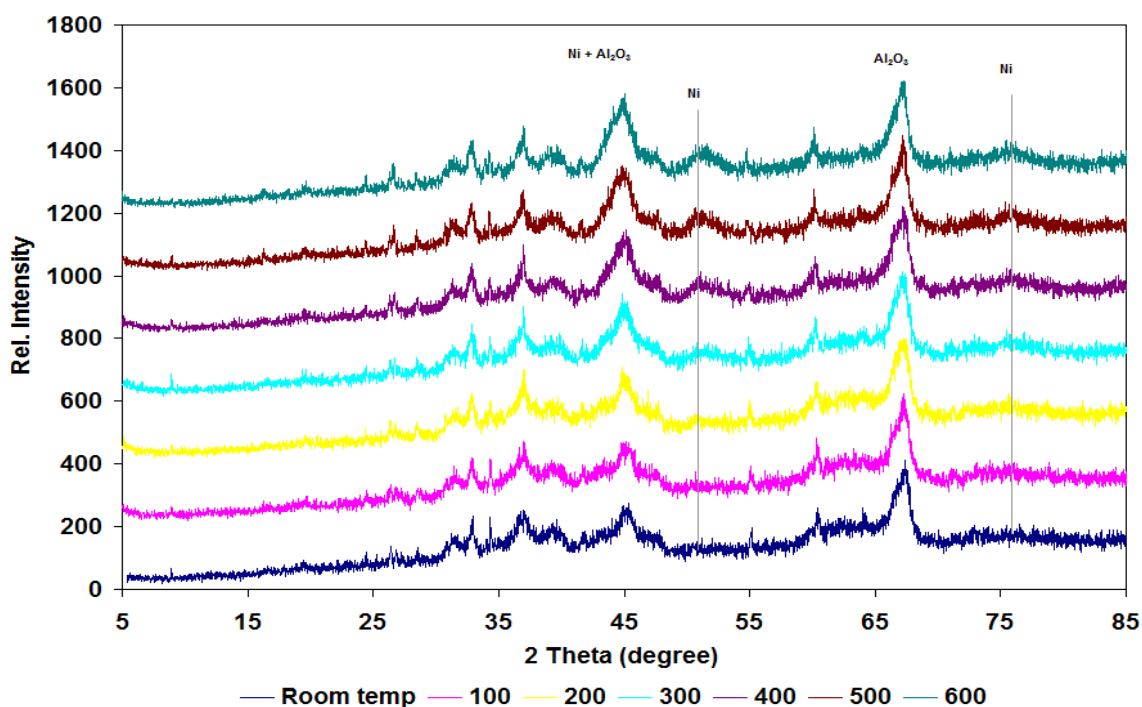
Figure 3.3 *In-situ* XRD spectrum of Ni/Al$_2$O$_3$ catalysts under hydrogen atmosphere

3.1.2.2 Pd/Al$_2$O$_3$ catalyst

Powder XRD analysis was carried out on the Pd/Al$_2$O$_3$ catalyst. The peaks of the support and metal were found to be overlapped with each other in the XRD pattern of the catalyst. The metal content in the Pd/Al$_2$O$_3$ catalyst was only 1% so it is difficult to identify any differences in the XRD patterns of the reduced and unreduced catalyst. However most of the peaks, including alumina support became sharper with reduction.

3.1.3 BET analysis

Surface area analysis was performed for the fresh and reduced catalysts and the data are presented in Table 3.1.

Catalyst	Surface Area (m^{2}g^{-1})	Pore Volume (cm^{3}g^{-1})	Average Pore diameter (Å)
Ni/Al$_2$O$_3$	93	0.35	152
Ni/Al$_2$O$_3$ (Reduced)	106	0.39	150
Pd/Al$_2$O$_3$	99	0.51	208
Pd/Al$_2$O$_3$ (Reduced)	104	0.50	197

Table 3.1 BET analysis of Ni/Al$_2$O$_3$ and Pd/Al$_2$O$_3$ catalysts

The BET results indicate that the surface area of the catalyst increased with reduction.

3.2 Reactions

In this project the hydrogenation of PyGas was investigated over alumina supported nickel and palladium catalysts. The effects of the reaction parameters *i.e.* reaction temperature, hydrogen partial pressure, total reaction pressure and feed flow rate of PyGas (WHSV$_{PyGas}$) on the PyGas hydrogenation were examined. The post reaction catalysts were regenerated, and the amount and nature of coke deposition was investigated by *in-situ* TPO. Moreover, the regenerated catalysts were also characterised to investigate any change that may have occurred in the properties of the catalyst during reaction or *in-situ* TPO.

3.2.1 Blank reactions

Boiling chips were used as an inert packing material in the hydrogenation of PyGas over Ni/Al$_2$O$_3$ and Pd/Al$_2$O$_3$ catalysts as mentioned in section 2.2.4. Therefore, the hydrogenation of PyGas was performed over boiling chips and catalyst support (Al$_2$O$_3$) to examine the behaviour of the inert packing material and the catalyst support under the reaction conditions.

3.2.1.1 Reaction over inert packing material (Boiling chips)

The reaction was performed over packing material (boiling chips) to investigate the inert behaviour of the packing material. The operating conditions used were T = 140°C, WHSV$_{PyGas}$ = 4 h^{-1} and P$_{H2}$ = 20 barg. Very low level hydrogenation of PyGas was observed during the test.

A detectable level of 1-pentene hydrogenation was observed. The yield of pentane was about 1% with small amounts of trans-2-pentene and cis-2-pentene also being produced. Similarly, a very small level of 1-octene hydrogenation was noted in the reaction. The yield of octane formation was found to be less than 0.5% with very small amounts of trans-2-octene and cis-2-octene formed and no 3-octene and 4-octenes formation observed. A low level yield of cyclopentane (< 0.5%) was observed during the reaction. The ratio of trans-olefins was found to be twice that of the respective cis isomer as shown in Table 3.2.

Trans/Cis-2-pentene ratio	Trans/Cis-2-octene ratio
66:34	63:37

Table 3.2 Ratio of formation of trans/cis internal olefins in PyGas hydrogenation [Reaction conditions: T = 140°C, WHSV$_{PyGas}$ = 4 h^{-1}, P$_{H2}$ = 20 barg]

No hydrogenation of toluene to methylcyclohexane was noted. Meanwhile a very small amount of styrene hydrogenation to ethyl benzene (~ 1% yield) was seen, with no ethylcyclohexane formation being observed.

3.2.1.1.1 Post reaction analysis

Post reaction catalyst TPO

In-situ TPO was performed over the post reaction boiling chips to investigate the coke deposited. A reasonable amount of coke was observed over boiling chips, as shown in Figure 3.4.
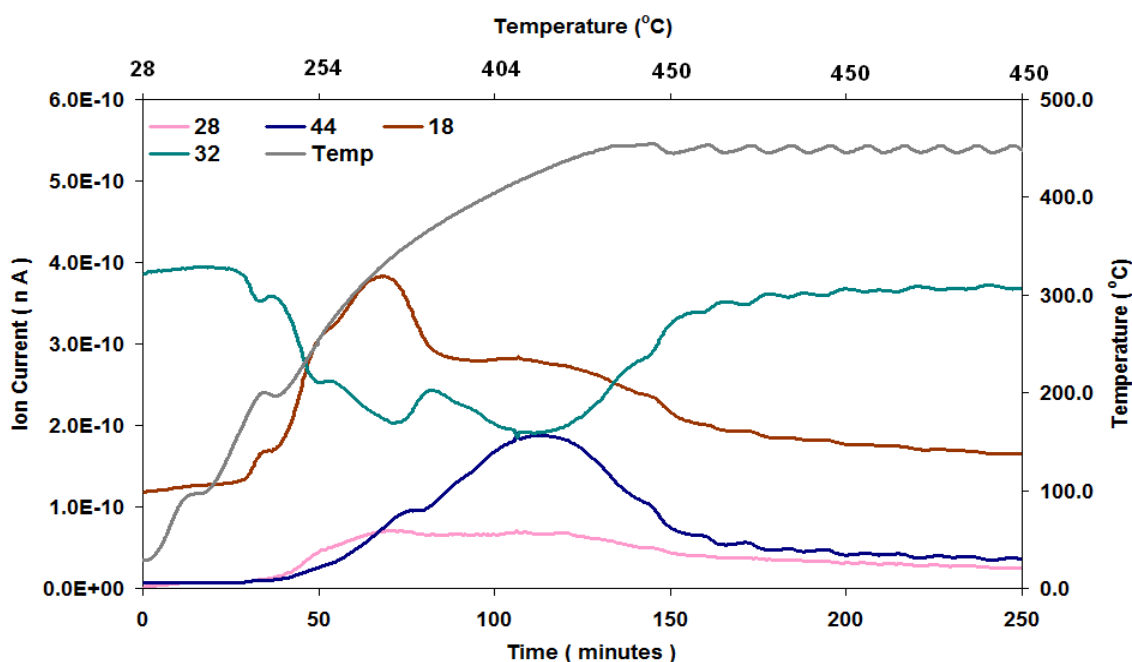
Figure 3.4 Post reaction *in-situ* TPO of boiling chips [Reaction conditions: T = 140°C, WHSV$_{PyGas}$ = 4 h^{-1}, P$_{H2}$ = 20 barg]

Total oxygen consumption in TPO = 1.69 m moles

The evolution of other possible deposited species e.g. reactants and products, was also monitored during TPO analysis. Reasonable amounts of styrene and benzene evolution occurred above 200°C. Whilst, very small levels of 1-pentene, cyclopentene, pentane, toluene, methylcyclohexane, ethylbenzene, 1-octene, and octane evolution were observed as shown in Figure 3.5.
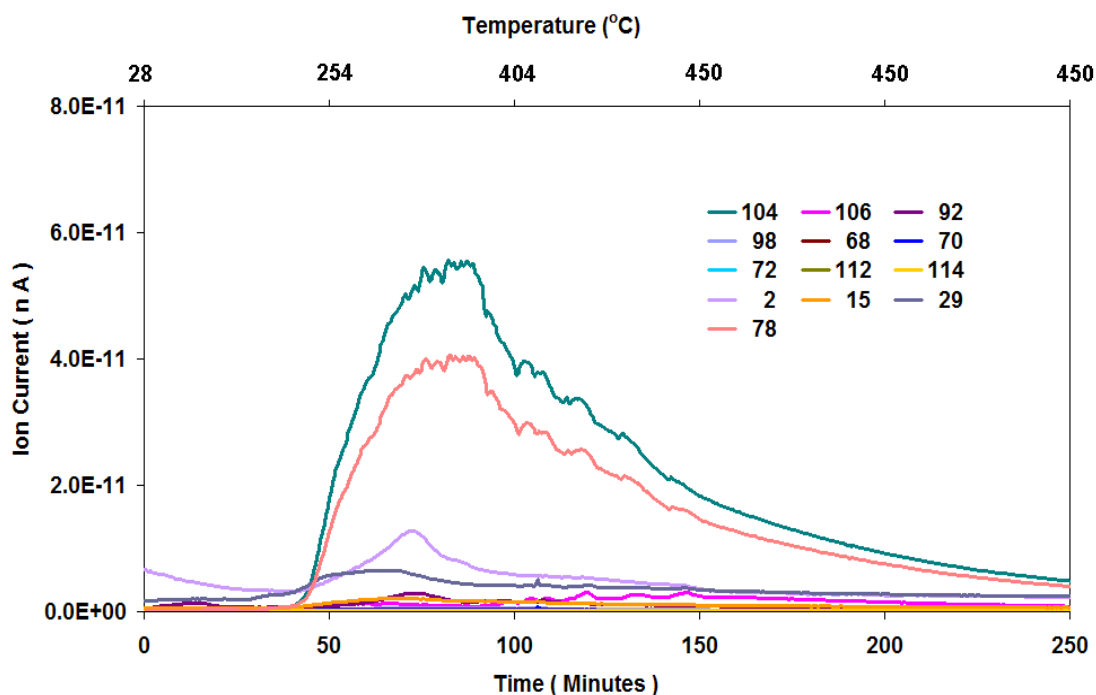
Figure 3.5 Evolution of other possible species during *in-situ* TPO of boiling chips [Reaction conditions: T = 140°C, WHSV$_{PyGas}$ = 4 h^{-1}, P$_{H2}$ = 20 barg]

3.2.1.2 Reaction over catalyst Support (Al$_2$O$_3$)

The reaction was performed over the catalyst support (Al$_2$O$_3$) using operating conditions T = 140°C, WHSV$_{PyGas}$ = 4 h^{-1} and P$_{H2}$ = 20 barg. A very slight hydrogenation of 1-pentene and 1-octene was observed. The yield of pentane and octane was noted at around 1% and small amounts of internal olefins (2-pentens, 2-octenes and 3-octenes) were also produced. No considerable hydrogenation of cyclopentene was noted as the cyclopentane yield was found to be less than 0.5%. The ratio of trans-olefins was found to be twice that of the respective cis isomer, as shown in Table 3.3. The formation of trans-4-octene and cis4-octene was not observed.

Trans/Cis-2-pentene ratio	Trans/Cis-2-octene ratio	Trans/Cis-3-octene ratio
64:36	63:37	65:35

Table 3.3 Ratio of trans/cis internal olefins formation in PyGas hydrogenation [Reaction conditions: T = 140°C, WHSV$_{PyGas}$ = 4 h^{-1}, P$_{H2}$ = 20 barg]

Virtually no formation of methylcyclohexane was observed in PyGas hydrogenation reaction. A small amount of ethylbenzene was formed from hydrogenation of styrene over Al$_2$O$_3$, however no formation of ethylcyclohexane was noted. The yield of ethylbenzene was found to be around 2%.

3.2.1.2.1.1 Post reaction analysis

Post reaction catalyst TPO

The *in-situ* TPO showed a reasonable amount of coke deposited on the catalyst support (Al_2O_3) as shown in Figure 3.6.
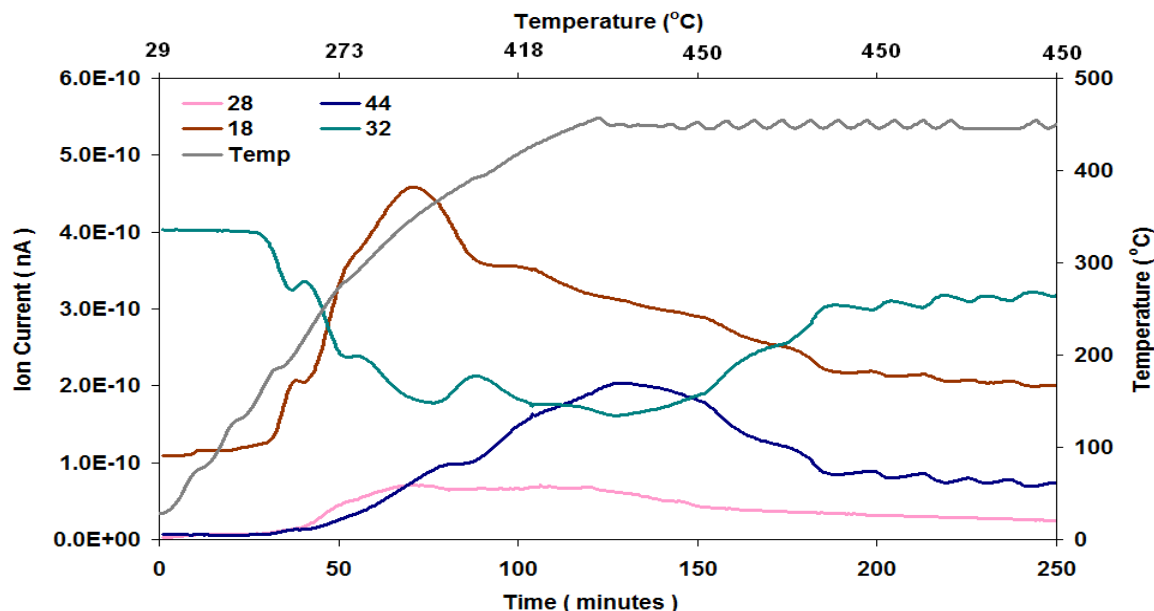
Figure 3.6 Post reaction *in-situ* TPO of Al_2O_3 [Reaction conditions: T= 140 °C, WHSV$_{PyGas}$ = 4 h^{-1}, P$_{H2}$ = 20 barg]

Total oxygen consumption in TPO = 2.20 m moles

Moreover, the levels of styrene and benzene evolved were found to be comparable to that observed over the boiling chips. Similarly, no significant evolution of other species *i.e.* 1-pentene, cyclopentene, pentane, toluene, methylcyclohexane, ethylbenzene, 1-octene, and octane was noted.

3.2.2 PyGas hydrogenation over Ni/Al_2O_3 catalyst

The following parameters were investigated during the PyGas hydrogenation over a Ni/Al_2O_3 catalyst.

a) Effect of reaction temperature

b) Effect of hydrogen partial pressure

c) Effect of total reaction pressure

d) Effect of PyGas feed flow rate (WHSV$_{PyGas}$)

3.2.2.1 Effect of reaction temperature on PyGas hydrogenation

Hydrogenation of PyGas was performed over Ni/Al$_2$O$_3$ catalyst in a fixed bed reactor under the following operating conditions T = 140-200°C, WHSV$_{PyGas}$ = 4 h^{-1} and P$_{H2}$ = 20 barg to study the effect of reaction temperature.

Hydrogenation of PyGas is an exothermic reaction therefore the temperature of the nickel catalyst bed was monitored by a thermocouple positioned within the catalyst bed, as shown in Figure 3.7. The temperature of the catalyst bed rose by about 7°C within the first 20 minutes of the reaction and then became stable at the reaction temperature (±1.5°C) for the rest of the reaction. The temperature profile of catalyst bed was found to be similar in all reactions.
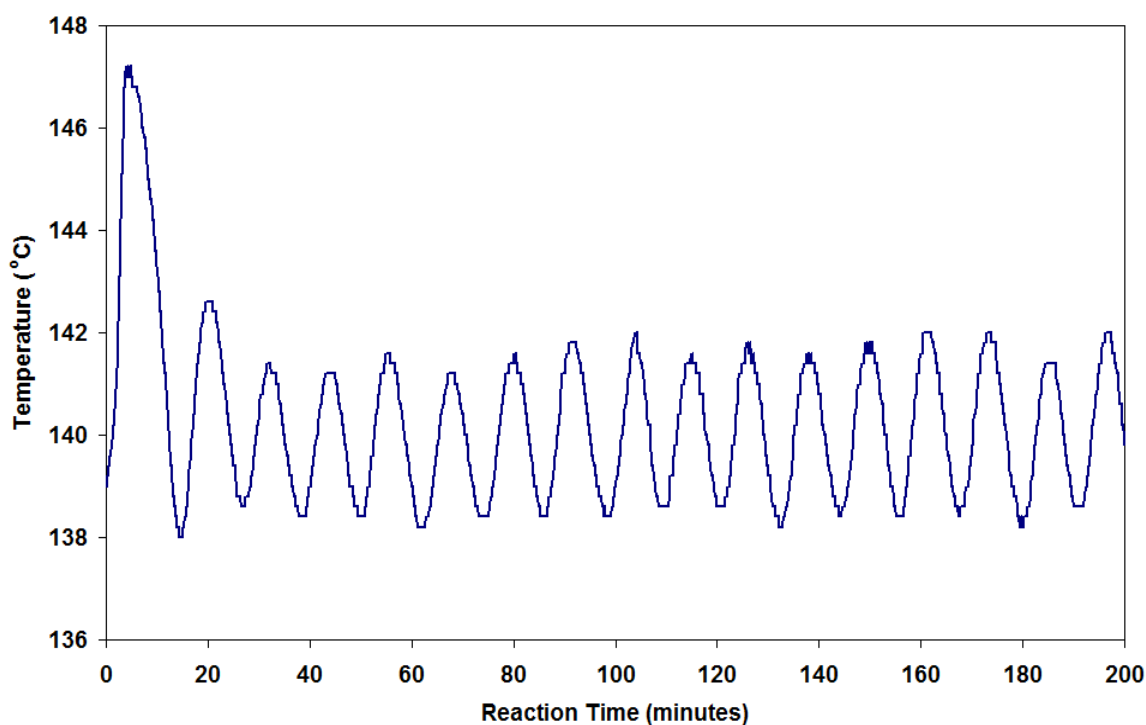
Figure 3.7 Temperature profile of the nickel catalyst bed during PyGas hydrogenation

3.2.2.1.1 PyGas hydrogenation over Ni/Al$_2$O$_3$ at 140°C

The reaction was performed at T = 140°C, WHSV$_{PyGas}$ = 4 h^{-1} and P$_{H2}$ = 20 barg. The concentration profile in Figure 3.8 shows that the catalyst was very active in the initial 11 hours of the reaction and then slightly deactivated to give steady state operation.
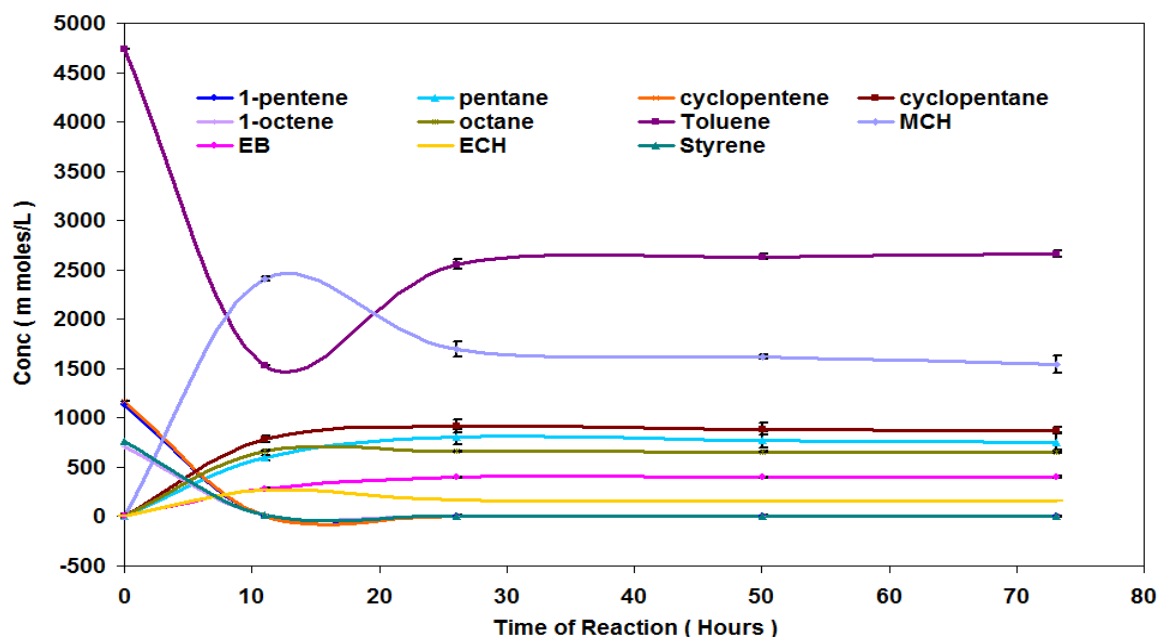
Figure 3.8 Reaction profile of PyGas hydrogenation [Reaction conditions: T=140°C, WHSV$_{PyGas}$ = 4 h^{-1}, P$_{H2}$ = 20 barg]

The conversion of 1-pentene as seen in Figure 3.9 was observed at levels of above 97%. The initial yield of pentane was around 10 % in the first 11 hours of reaction, which increased to 65-70% after steady state was established. Pentane was the main product during 1-pentene hydrogenation. However, small amounts of trans-2-pentene and cis-2-pentene were also produced.
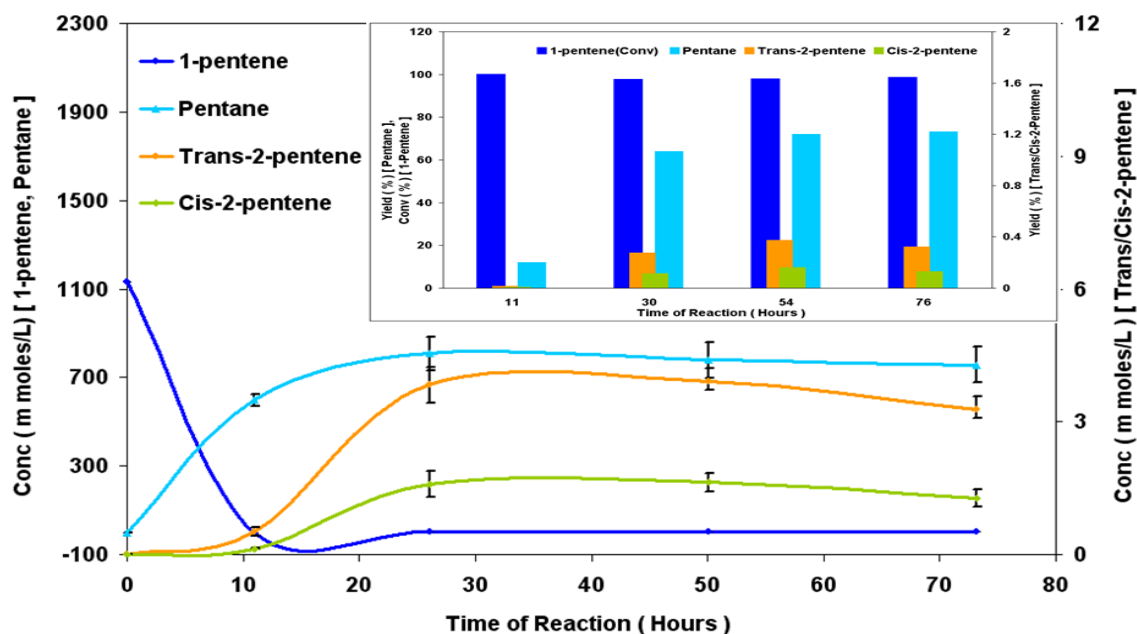
Figure 3.9 Hydrogenation of 1-pentene [Reaction conditions: T = 140°C, WHSV$_{PyGas}$ = 4 h^{-1}, P$_{H2}$ = 20 barg]

High selectivity towards pentane, of around 99% was observed whilst selectivity towards trans-2-pentene and cis-2-pentene formation was less than 1% as shown

in Figure 3.10. The complete saturation of 1-pentene was expected due to favourable reaction conditions for hydrogenation. The formation of trans-2-pentene was twice that of cis-2-pentene, due to the greater thermodynamic stability of trans-2-pentene.
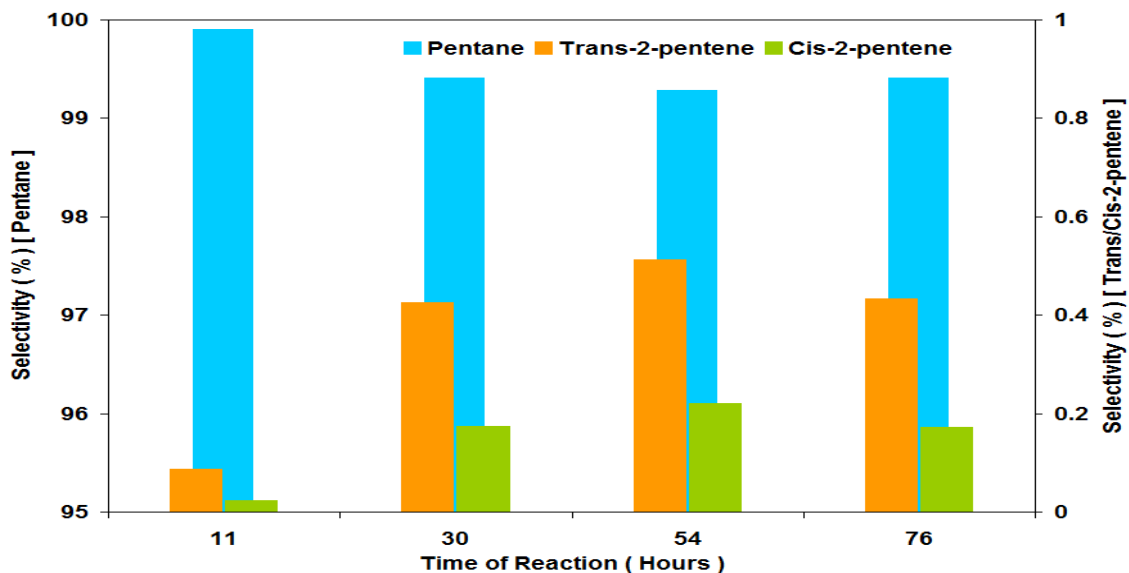
Figure 3.10 Selectivity of pentane, trans-2-pentene and cis-2-pentene during 1-pentene hydrogenation [Reaction conditions: T = 140°C, WHSV$_{PyGas}$ = 4 h^{-1}, P$_{H2}$ = 20 barg]

The reaction profile of 1-octene hydrogenation is shown in Figure 3.11. Conversion of 1-octene was observed at around 99%. Octane was the primary product although small quantities of trans-2-octene and cis-2-octene were also observed.
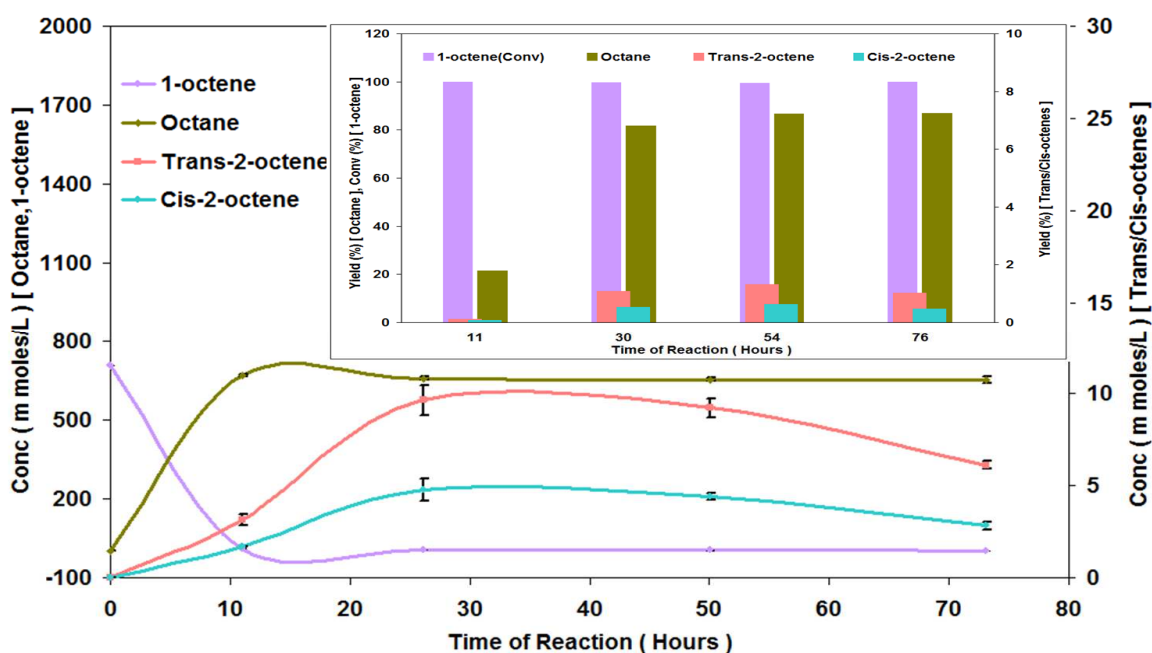
Figure 3.11 Hydrogenation of 1-octene [Reaction conditions: T = 140°C, WHSV$_{PyGas}$ = 4 h^{-1}, P$_{H2}$ = 20 barg]
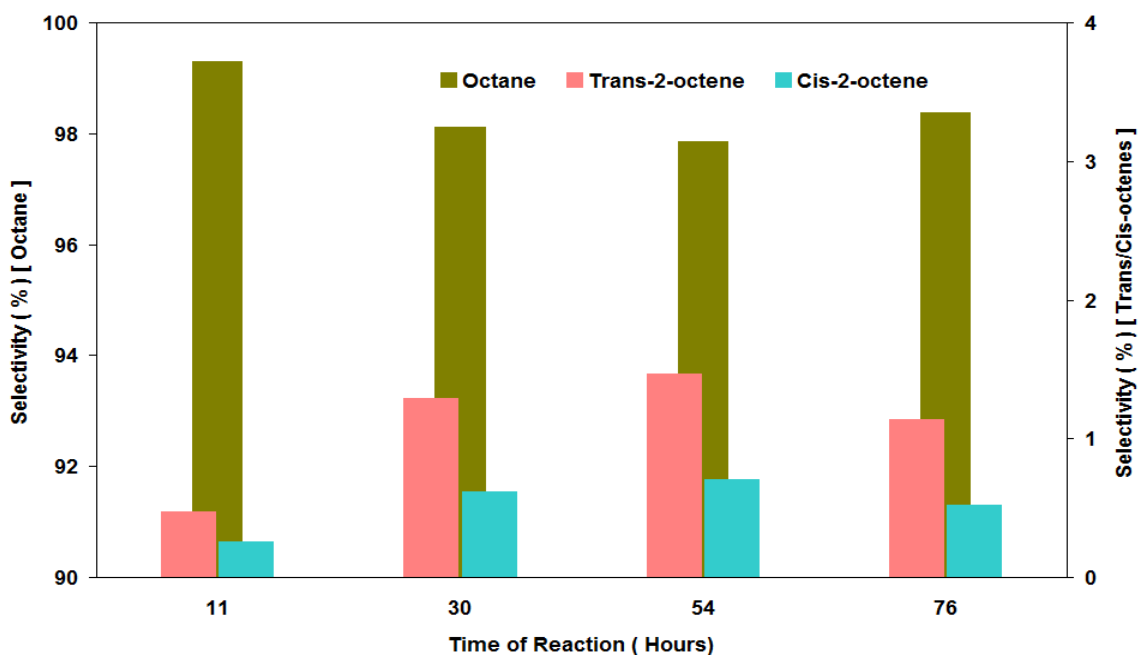
Figure 3.12 Selectivity of octane, trans-2-octene and cis-2-octene during 1-octene hydrogenation [Reaction conditions: T = 140°C, WHSV$_{PyGas}$ = 4 h^{-1}, P$_{H2}$ = 20 barg]

Figure 3.12 shows that the selectivity towards octane formation was greater than 98%. Small amounts of trans-2-octene and cis-2-octene were also produced, while no 3-octene and 4-octene were observed during the reaction. It is interesting to note that the trans isomers were produced at twice the level of the respective cis isomer, which is similar to the trans/cis ratio of 2-pentene as shown in Table 3.4.

Trans/Cis-2-pentene ratio	Trans/Cis-2-octene ratio
70:30	67:33

Table 3.4 Ratio of trans/cis internal olefins formation in PyGas hydrogenation [Reaction conditions: T = 140°C, WHSV$_{PyGas}$ = 4 h^{-1}, P$_{H2}$ = 20 barg]

Cyclopentene in PyGas was used as a model component for cycloolefins hydrogenation. The conversion of cyclopentene was observed at above 90% throughout the reaction. The yield of cyclopentane remained between 70 and 79% once steady state conditions were achieved as shown in Figure 3.13.
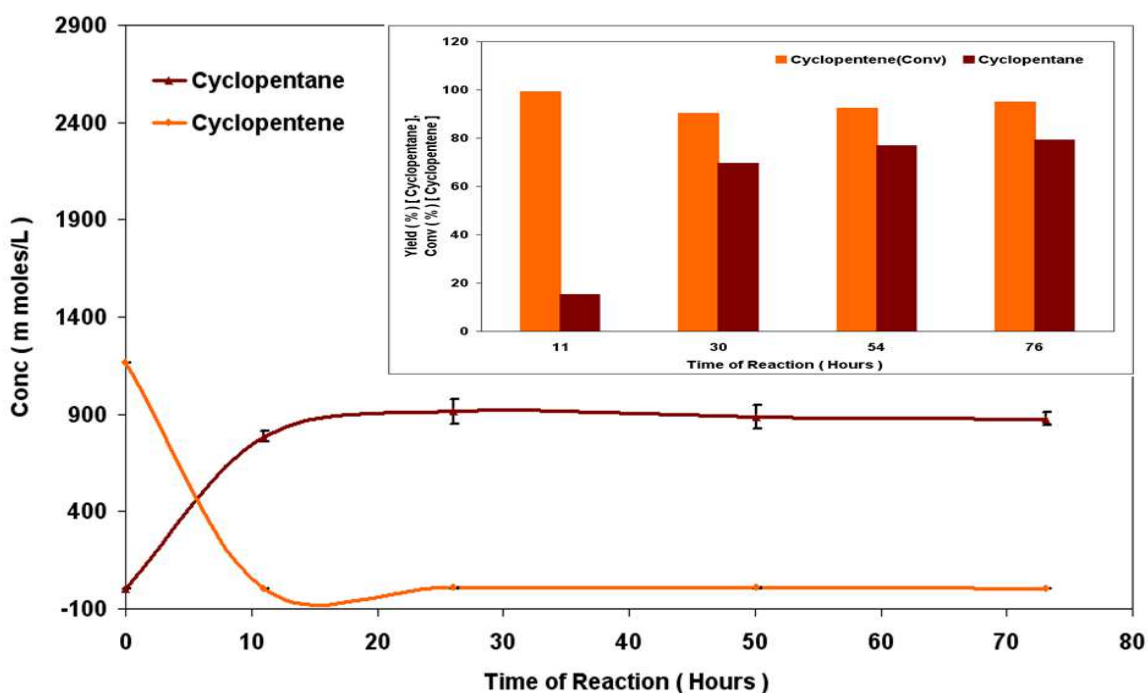
Figure 3.13 Hydrogenation of cyclopentene [Reaction conditions: T = 140°C, WHSV$_{PyGas}$ = 4 h^{-1}, P$_{H2}$ = 20 barg]

Toluene and styrene were used as model components of the aromatic fraction present in PyGas. Toluene is one of the most stable aromatic compounds and hydrogenation of toluene can be used to represent hydrogenation of the comprehensive aromatic contents of PyGas. Styrene is a good model to represent the reactive species of PyGas because it forms large amounts of gum and coke during PyGas hydrogenation. The hydrogenation of styrene is more interesting and informative due to the presence of both alkenyl bonds (alkene) and the aromatic ring.

Figure 3.14 shows that considerable hydrogenation of toluene to methylcyclohexane was observed. Conversion of toluene was around at 93% in the initial 11 hours of reaction, later decreasing to 55% after 30 hours when the reaction obtained steady state conditions. A gentle decrease was observed with further TOS, with a 47% conversion noted after 76 hours of reaction.
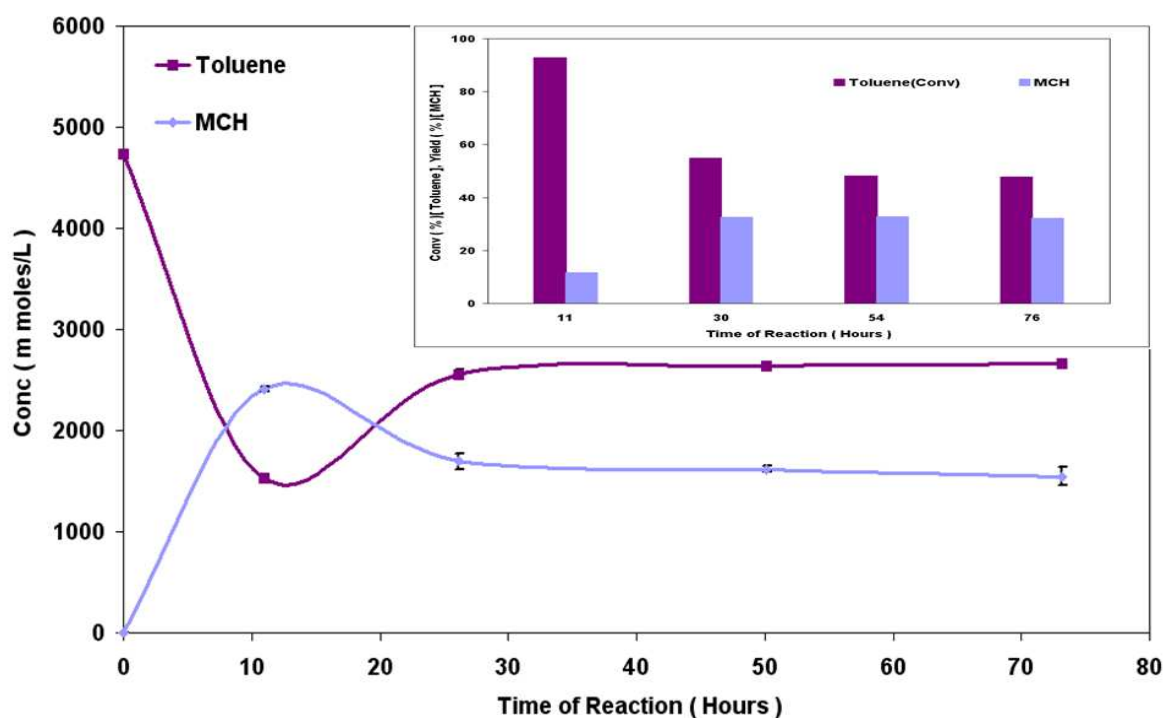
Figure 3.14 Hydrogenation of toluene [Reaction conditions: T = 140°C, WHSV$_{PyGas}$ = 4 h^{-1}, P$_{H2}$ = 20 barg]

Figure 3.15 shows the hydrogenation of styrene. Conversion of styrene remained above 99% throughout the reaction. Styrene was hydrogenated to ethyl benzene, which was then further hydrogenated to ethylcyclohexane. Selectivity towards ethylcyclohexane and ethylbenzene formation was similar during the initial 11 hours of reaction; however the catalyst became twice as selective towards ethylbenzene when steady state was established, as shown in Figure 3.16.
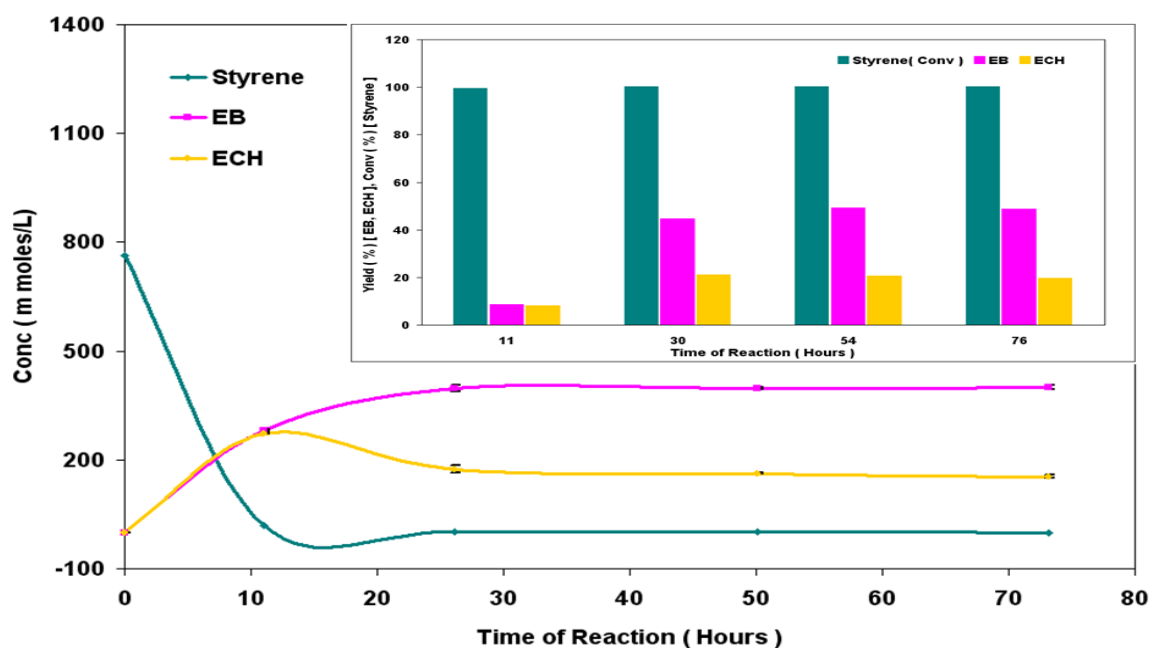
Figure 3.15 Hydrogenation of styrene [Reaction conditions: T = 140°C, WHSV$_{PyGas}$ = 4 h^{-1}, P$_{H2}$ = 20 barg]
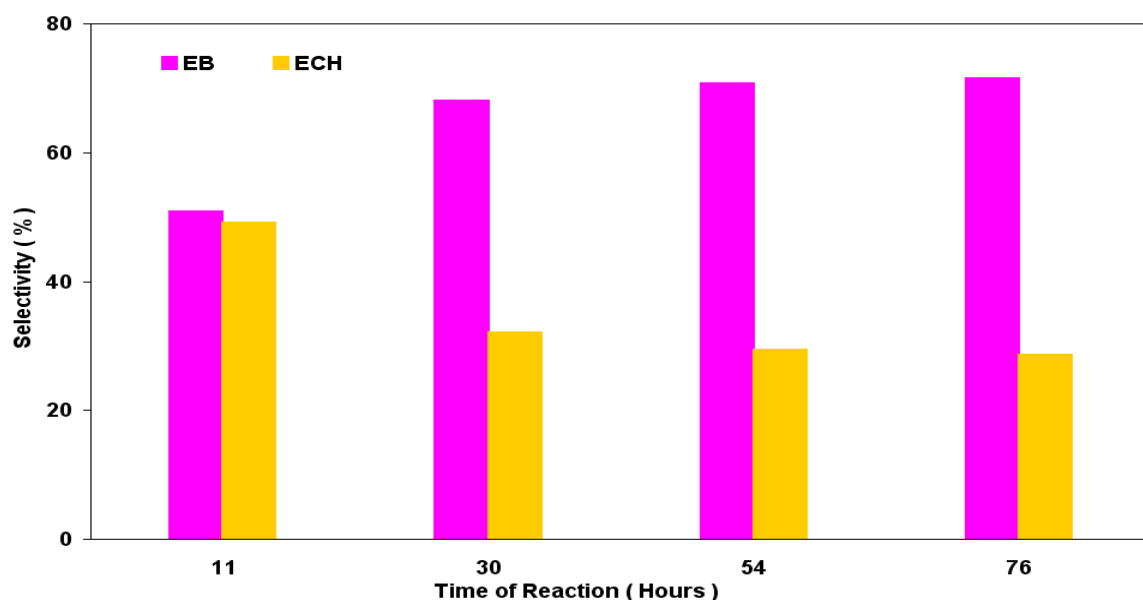
Figure 3.16 Selectivity of ethylbenzene and ethylcyclohexane during styrene hydrogenation [Reaction conditions: T = 140°C, WHSV$_{PyGas}$ = 4 h^{-1}, P$_{H2}$ = 20 barg]

Effluent gas analysis

The main liquid sample was trapped in the knock out pot, however very small amounts of hydrocarbons were detected in the effluent gas stream, which was analysed for a better understanding of the reaction and the reactor engineering set up test. Pentane and cyclopentane were the main components observed in the effluent gas stream with very small amounts of toluene and methylcyclo-hexane, as shown in Figure 3.17.
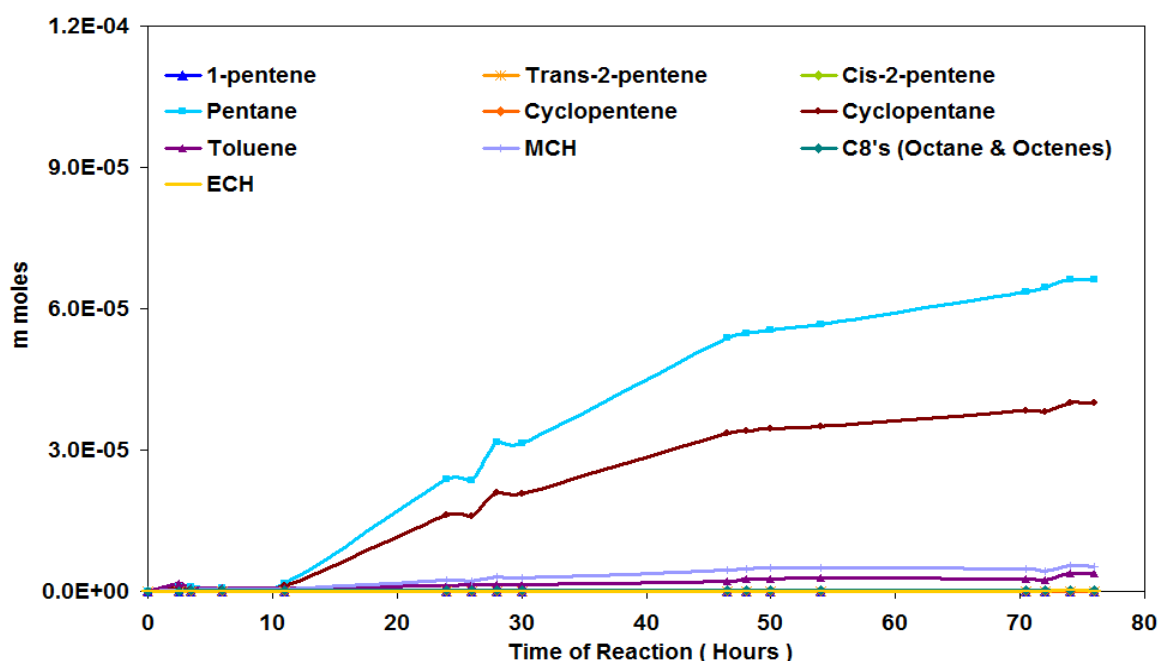
Figure 3.17 Effluent gas analysis [Reaction conditions: T = 140°C, WHSV$_{PyGas}$ = 4 h^{-1}, P$_{H2}$ = 20 barg]

The effluent gas was analysed during subsequent reactions, and similar amounts of hydrocarbons were detected in the gas stream. The presence of hydrocarbons in the effluent gas is considered to be physical phenomena, dependent on the vapour pressure of the components. The high levels of pentane and cyclopentane observed are due to higher vapour pressure of these hydrocarbons than the other components. The hydrocarbons loss from the effluent gas stream was minimal. This demonstrates that the reactor engineering set up was satisfactory.

3.2.2.1.1.1 Post reaction analysis

Post reaction catalyst TPO

A post reaction *in-situ* TPO gave an important insight into the quantity and nature of deposited species on the surface of the catalyst. The catalyst was regenerated in a flow of 2% O_2/Ar gas, as mentioned in section 2.2.5. Figure 3.18 shows the *in-situ* TPO of the post reaction Ni/Al_2O_3 catalyst.
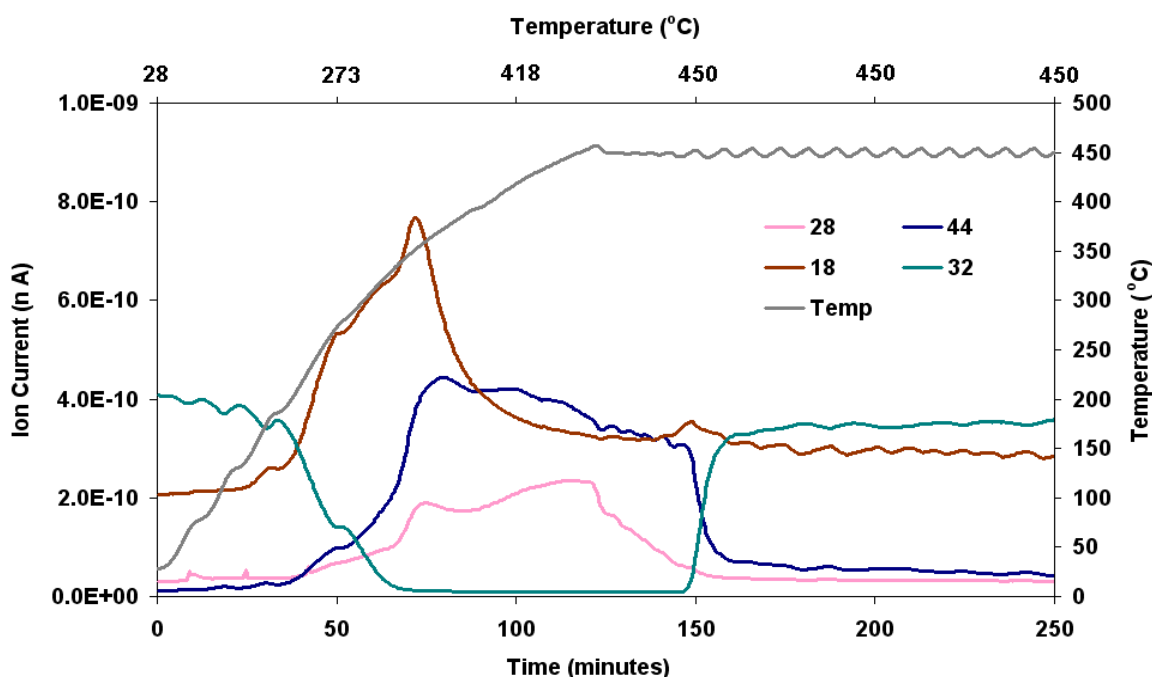
Figure 3.18 Post reaction *in-situ* TPO of Ni/Al_2O_3 catalyst [Reaction conditions: T = 140°C, WHSV$_{PyGas}$ = 4 h^{-1}, P$_{H2}$ = 20 barg]

Total oxygen consumption in TPO = 3.30 m moles

CO_2, CO and H_2O were the principal species detected in the TPO. The other possible deposited species *i.e.* styrene, benzene, 1-pentene, cyclopentene, pentane, toluene, methylcyclohexane, ethylbenzene, 1-octene, octane and H_2 were also monitored for detailed analysis. Figure 3.19 shows that the main

evolution of both styrene and benzene occurred at around 350°C, with small levels of both species also desorbed at below 200°C. A considerable amount of H_2 was desorbed from the catalyst. Whilst, small levels of toluene, 1-pentene and cyclopentene evolution were also noted during TPO.
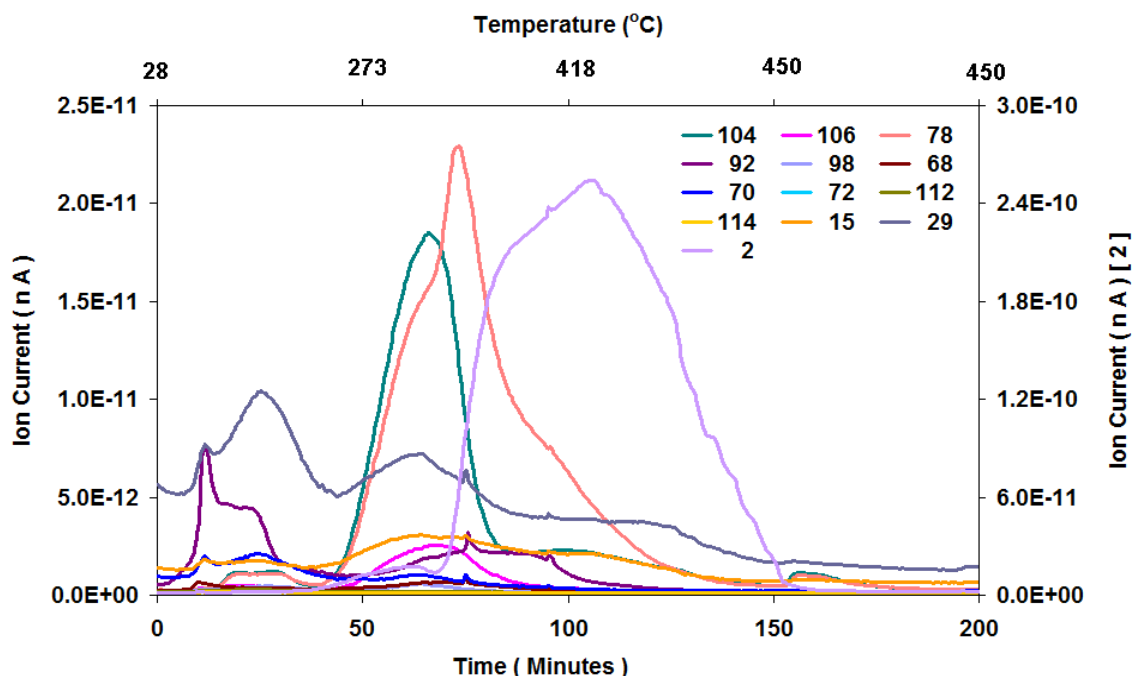
Figure 3.19 Evolution of possible species during *in-situ* TPO of Ni/Al$_2$O$_3$ catalyst [Reaction conditions: T = 140°C, WHSV$_{PyGas}$ = 4 h^{-1}, P$_{H2}$ = 20 barg]

TGA-MS analysis

To confirm that all the deposited coke was removed during *in-Situ* TPO, TGA analysis was performed to a higher temperature (800°C) with a temperature ramp of 10°C/min under 2% O_2/Ar atmosphere, on the regenerated catalyst. A small continuous weight loss (~ 3.5 %) was noted. However a very small quantity of CO_2 was observed at 350°C and about 0.1% weight loss of catalyst was recorded corresponding to CO_2 evolution, as shown in Figure 3.20. This shows that no significant amount of carbonaceous residue was found on the surface of the catalyst after regeneration by *in-situ* TPO.
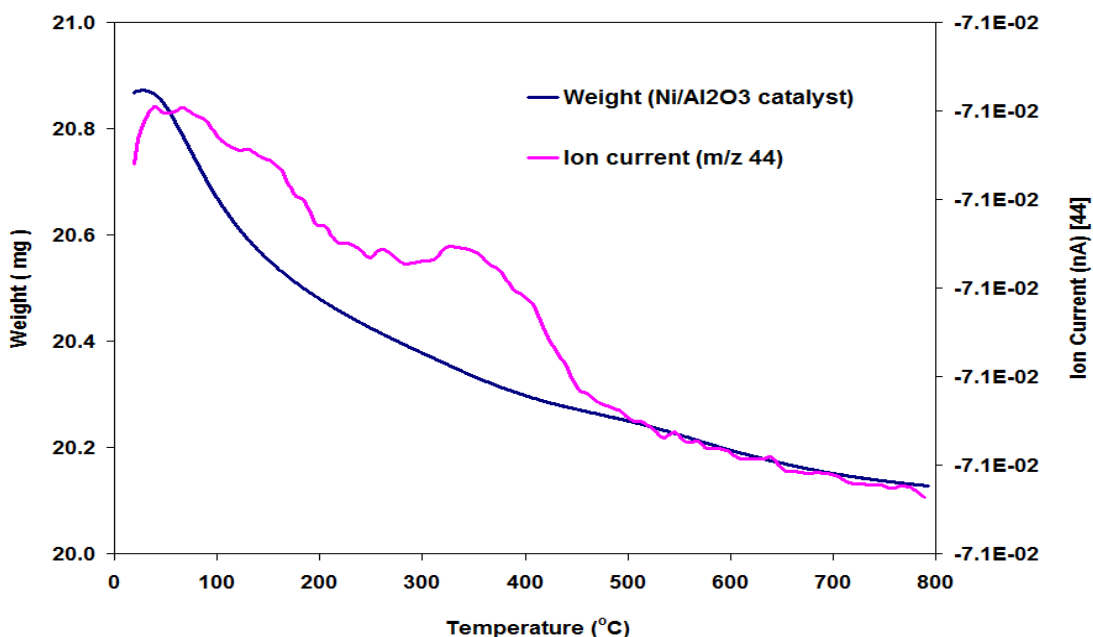
Figure 3.20 TGA- MS analysis of Ni/Al$_2$O$_3$ (Regenerated) catalyst [Reaction conditions: T = 140°C, WHSV$_{PyGas}$ = 4 h^{-1}, P$_{H2}$ = 20 barg]

TGA-MS analysis was performed on the regenerated catalysts of subsequent reactions, up to 800°C with a temperature ramp of 10°C/min under 2% O$_2$/Ar gas and no significant amount of coke was found on the regenerated catalysts. This shows that the coke deposited on the catalysts was effectively removed by *in-situ* TPO.

X-ray diffraction (XRD)

The XRD spectrum of regenerated Ni/Al$_2$O$_3$ catalyst is shown in Figure 3.21. The spectrum was found to be similar to the fresh catalyst, which suggests that no phase change occurred during the hydrogenation and regeneration process. The NiO peak was prominent in the XRD pattern of the regenerated Ni/Al$_2$O$_3$ catalyst due to Ni metal oxidation during regeneration.
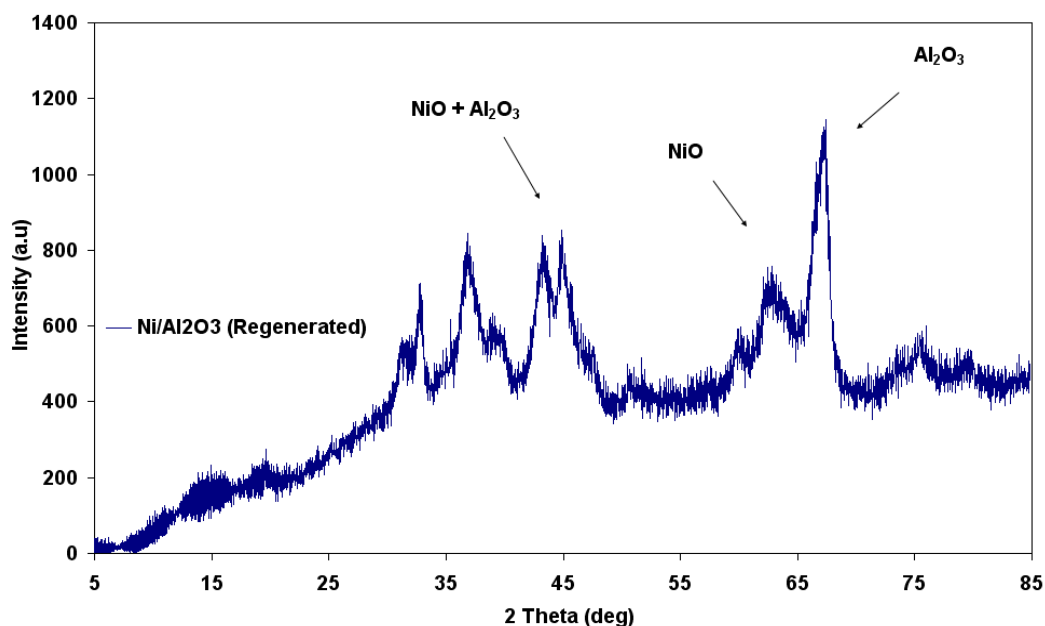
Figure 3.21 XRD Spectrum of Ni/Al$_2$O$_3$ (Regenerated) catalyst [Reaction conditions: T = 140°C, WHSV$_{PyGas}$ = 4 h^{-1}, P$_{H2}$ = 20 barg]

XRD analysis was also performed on the regenerated catalysts of subsequent reactions and the spectra found to be similar to that of the fresh catalyst.

BET analysis

The surface area of the regenerated catalyst was found to be similar to that of the fresh Ni/Al$_2$O$_3$ catalyst, as shown in Table 3.5.

Catalyst	Surface Area (m^{2}g^{-1})	Pore Volume (cm^{3}g^{-1})	Average Pore diameter (Å)
Ni/Al$_2$O$_3$	93	0.35	152
Ni/Al$_2$O$_3$ (Reduced)	106	0.39	150
Ni/Al$_2$O$_3$ (Regenerated)	100	0.38	154

Table 3.5 BET analysis of Ni/Al$_2$O$_3$ (Regenerated) catalyst [Reaction conditions: T = 140°C, WHSV$_{PyGas}$ = 4 h^{-1}, P$_{H2}$ = 20 barg]

The BET results indicate that no significant support sintering was observed in the catalyst during either the reaction or the regeneration process.

3.2.2.1.2 PyGas hydrogenation over Ni/Al$_2$O$_3$ at 160°C

The reaction temperature of PyGas over Ni/Al$_2$O$_3$ was increased to 160°C with all other conditions kept constant [P$_{H2}$ = 20 barg and WHSV$_{PyGas}$ = 4 h^{-1}]. The reaction concentration profile is shown in Figure 3.22.
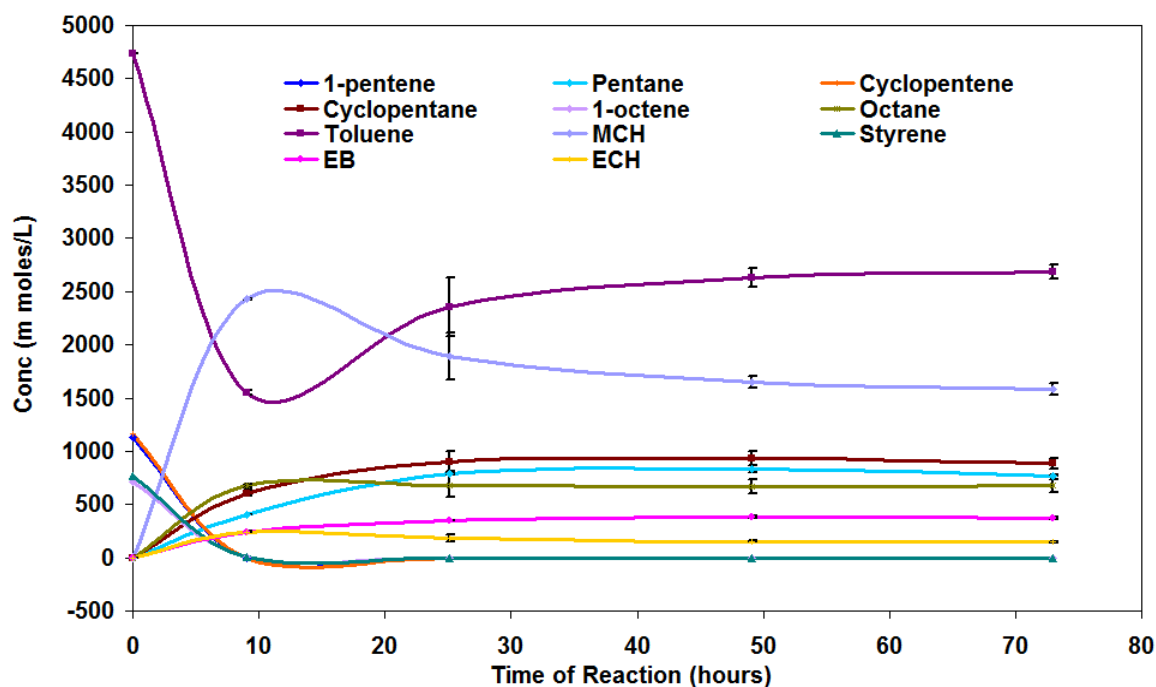
Figure 3.22 Reaction profile of PyGas hydrogenation [Reaction conditions: T = 160°C, WHSV$_{PyGas}$ = 4 h^{-1}, P$_{H2}$ = 20 barg]

Figure 3.23 shows that no considerable change was observed in the hydrogenation of the olefinic fraction of PyGas with an increase in reaction temperature. The conversion of olefins (1-pentene, 1-octene and cyclopentene) was observed to be above 99%. The olefins hydrogenated to their respective saturated components and no formation of internal olefins was observed, bar a very small amount detected in the first 10 hours of reaction.
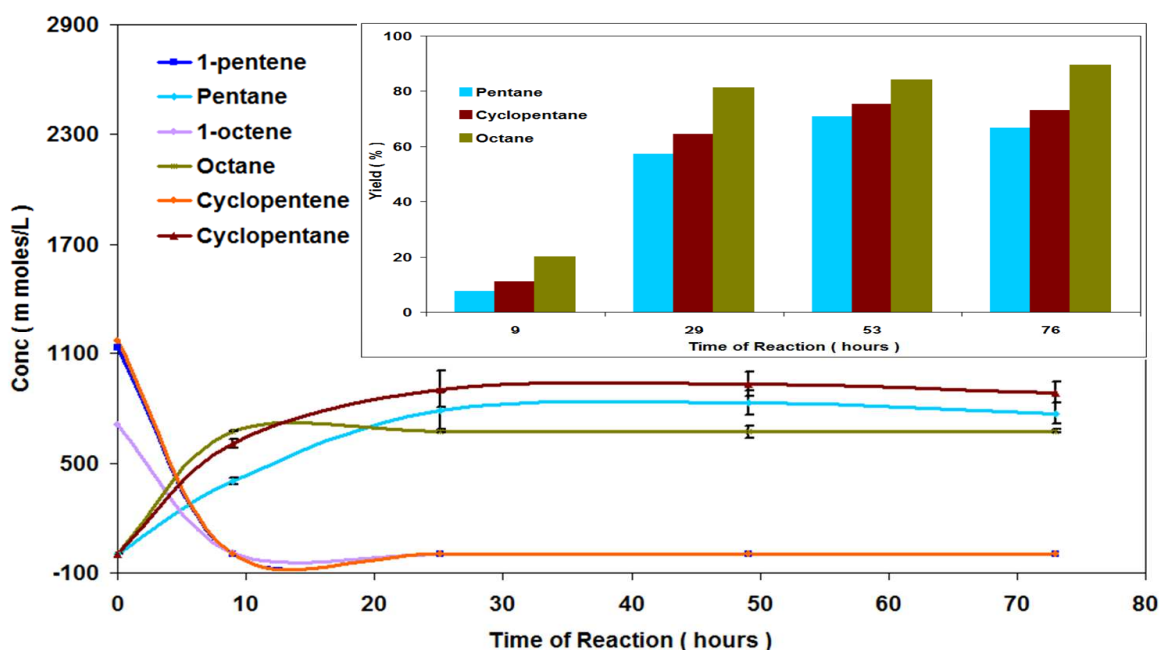
Figure 3.23 Hydrogenation of olefins (1-pentene, 1-octene and cyclopentene) present in PyGas [Reaction conditions: T = 160°C, WHSV$_{PyGas}$ = 4 h^{-1}, P$_{H2}$ = 20 barg]

Figure 3.24 shows that no significant increase was observed in the hydrogenation of toluene to methylcyclohexane with an increase in reaction temperature.
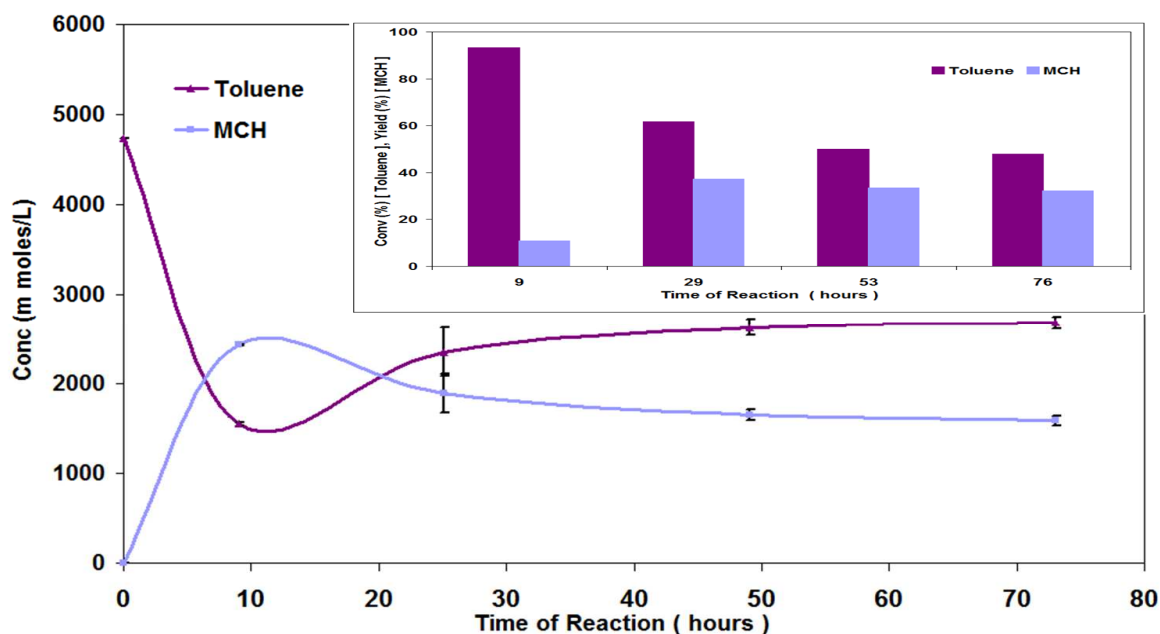
Figure 3.24 Hydrogenation of toluene [Reaction conditions: T = 160°C, WHSV$_{PyGas}$ = 4 h^{-1}, P$_{H2}$ = 20 barg]

The hydrogenation of styrene is shown in Figure 3.25. The styrene hydrogenated to ethylbenzene, which further hydrogenated to ethylcyclohexane. An increase was observed in the further hydrogenation of ethylbenzene to ethylcyclohexane with the increase in reaction temperature; however the total yield of styrene hydrogenation decreased with increase in the reaction temperature due to its higher contribution to coke formation.
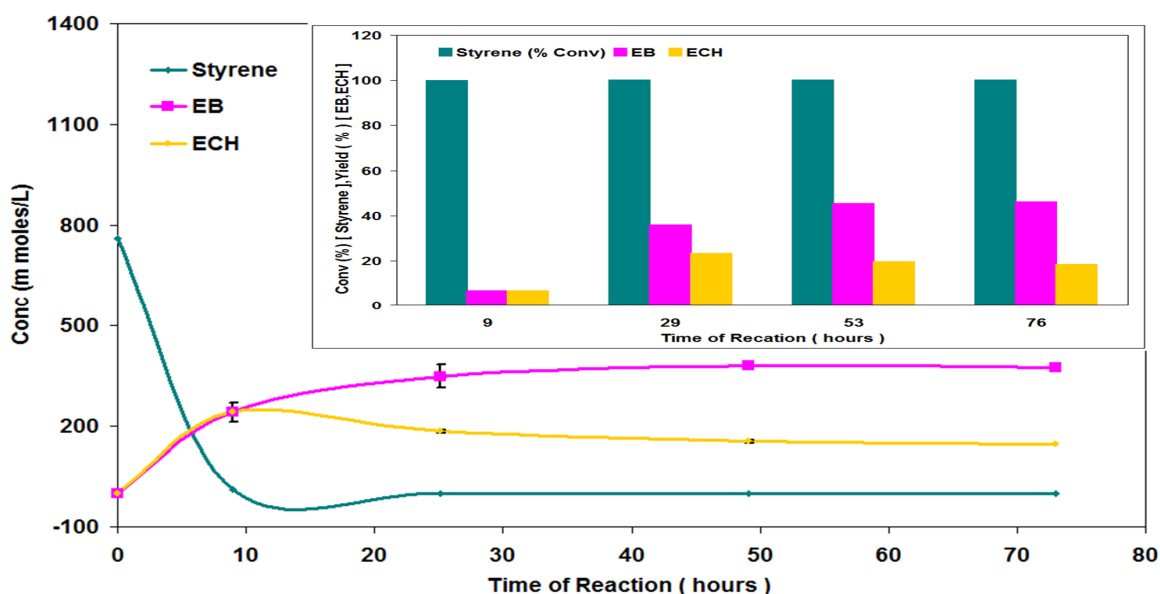
Figure 3.25 Hydrogenation of styrene [Reaction conditions: T = 160°C, WHSV$_{PyGas}$ = 4 h^{-1}, P$_{H2}$ = 20 barg]

Figure 3.26 indicates a decrease in the selectivity towards ethylcyclohexane and an increase in ethylbenzene selectivity with time on stream. This result suggests that the capability of the catalyst to further hydrogenate ethylbenzene to ethylcyclohexane decreased with time on stream due to catalyst deactivation.
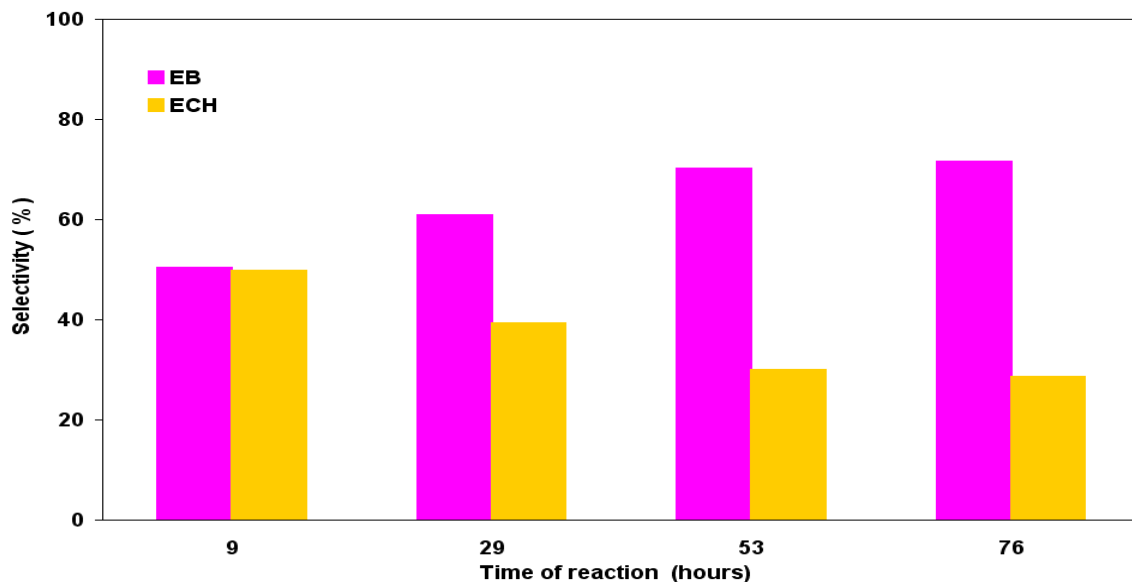
Figure 3.26 Selectivity of ethylbenzene and ethylcyclohexane during styrene hydrogenation [Reaction conditions: T = 160°C, WHSV$_{PyGas}$ = 4 h^{-1}, P$_{H2}$ = 20 barg]

3.2.2.1.2.1 Post reaction analysis

Post reaction catalyst TPO

Figure 3.27 shows that slightly higher amounts of CO_2 and CO desorption and O_2 consumption were observed when compared to the TPO of the catalyst used in previous reaction at 140°C. This indicates that a higher amount of carbonaceous material was deposited on the surface of the catalyst. Moreover, the evolution of other species *i.e.* styrene, benzene, 1-pentene, cyclopentene, pentane, toluene, methylcyclohexane, ethylbenzene, 1-octene, octane and H_2 from the catalyst during TPO was similar to that observed from the catalyst used at 140°C.
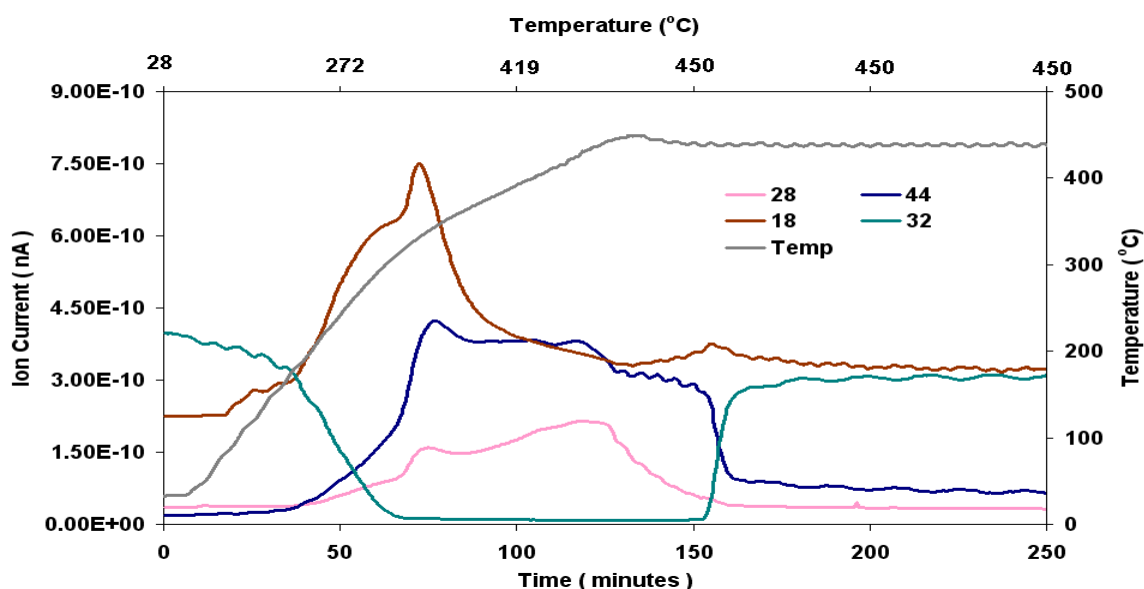
Figure 3.27 Post reaction *in-situ* TPO of Ni/Al$_2$O$_3$ catalyst [Reaction conditions: T = 160°C, WHSV$_{PyGas}$ = 4 h^{-1}, P$_{H2}$ = 20 barg]

Total oxygen consumption in TPO = 3.50 m moles

BET analysis

The surface area, pore volume and pore diameter of the regenerated catalyst were analysed and the results shown in Table 3.6.

Catalyst	Surface Area (m^{2}g^{-1})	Pore Volume (cm^{3}g^{-1})	Average Pore diameter (Å)
Ni/Al$_2$O$_3$	93	0.35	152
Ni/Al$_2$O$_3$ (Reduced)	106	0.39	150
Ni/Al$_2$O$_3$ (Regenerated)	93	0.36	156

Table 3.6 BET analysis of Ni/Al$_2$O$_3$ (Regenerated) catalyst [Reaction conditions: T = 160°C, WHSV$_{PyGas}$ = 4 h^{-1}, P$_{H2}$ = 20 barg]

The surface area of the regenerated catalyst was found to be similar to the fresh catalyst.

3.2.2.1.3 PyGas hydrogenation over Ni/Al$_2$O$_3$ at 180°C

The concentration profile of PyGas hydrogenation over Ni/Al$_2$O$_3$ catalyst under reaction conditions T = 180°C, WHSV$_{PyGas}$ = 4 h^{-1} and P$_{H2}$ = 20 barg is shown in Figure 3.28.
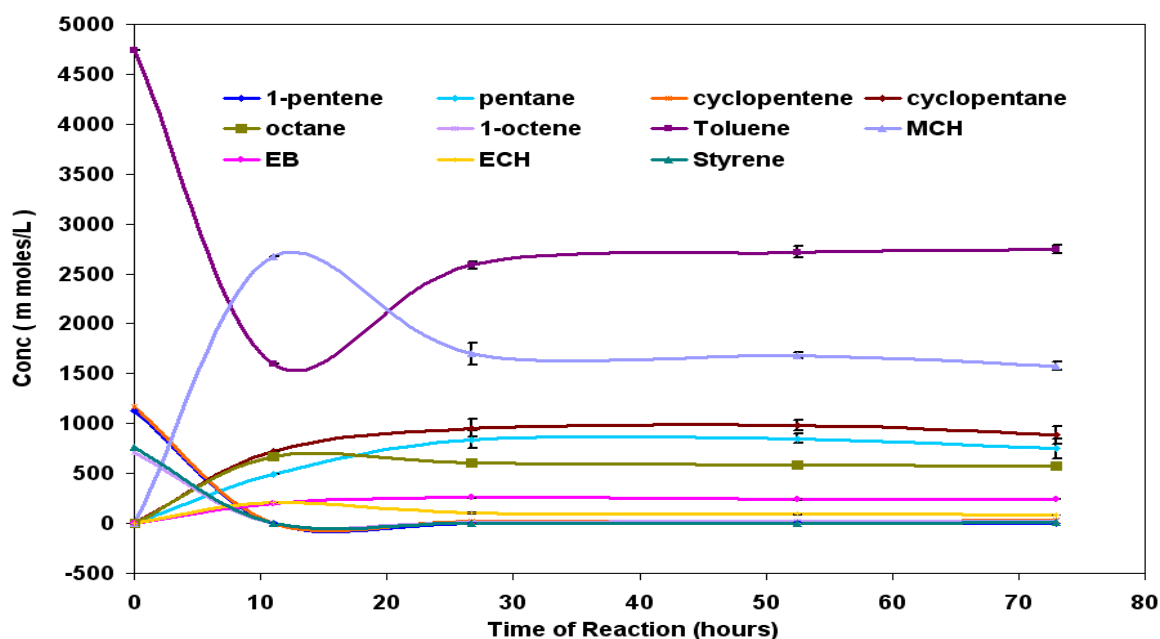
Figure 3.28 Reaction profile of PyGas Hydrogenation [Reaction conditions: T = 180°C, WHSV$_{PyGas}$ = 4 h^{-1}, P$_{H2}$ = 20 barg]

Figures 3.29-30 show that conversion of the 1-pentene was observed at about 99% throughout the reaction. Pentane was the principal product during 1-pentene hydrogenation. The yield of internal pentenes increased with time on stream, however the maximum yield for internal pentenes was only 1%. Selectivity towards trans and cis-2-pentenes formation increased whilst a small decrease was noted in the formation of pentane with time on stream. The trans-2-pentene was formed at twice the levels of the cis-2-pentene, as shown in Table 3.7.
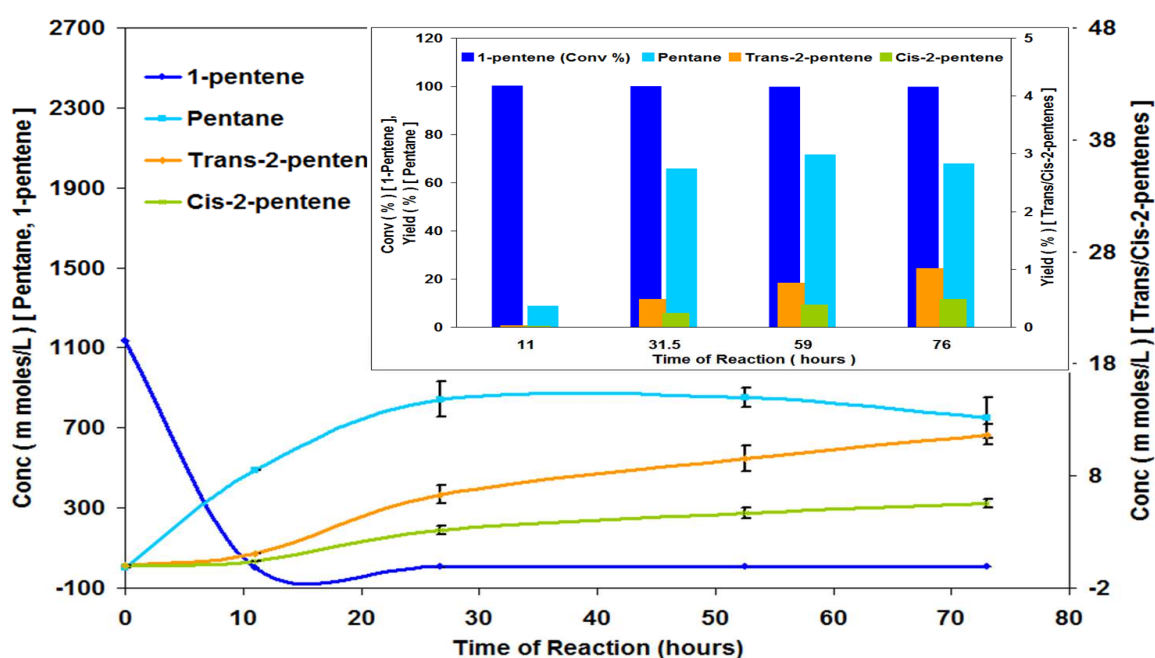
Figure 3.29 Hydrogenation of 1-pentene [Reaction conditions: T = 180°C, WHSV$_{PyGas}$ = 4 h^{-1}, P$_{H2}$ = 20 barg]
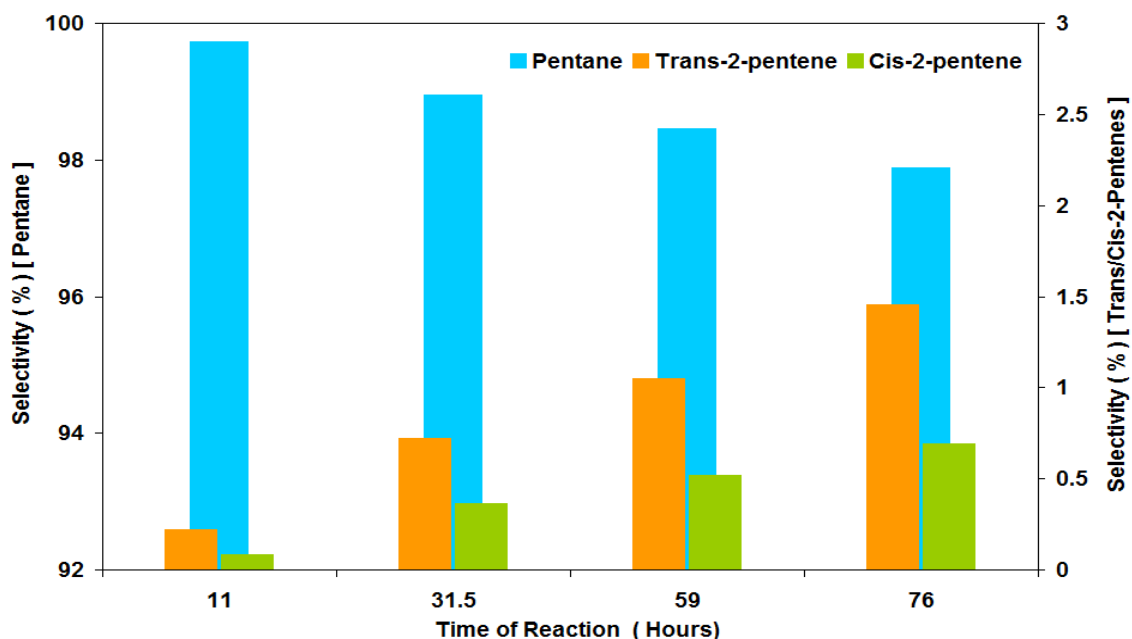
Figure 3.30 Selectivity of pentane, trans-2-pentene and cis-2-pentene during 1-pentene hydrogenation [Reaction conditions: T = 180°C, WHSV$_{PyGas}$ = 4 h^{-1}, P$_{H2}$ = 20 barg]

The reaction profile (Figure 3.31) shows that primarily, 1-octene hydrogenated to octane. However, small amounts of trans-2-octene and cis-2-octene were also produced while no 3-octene or 4-octene were observed. An increase was noted in the formation of tran-2-octene and cis-2-octene with reaction time.
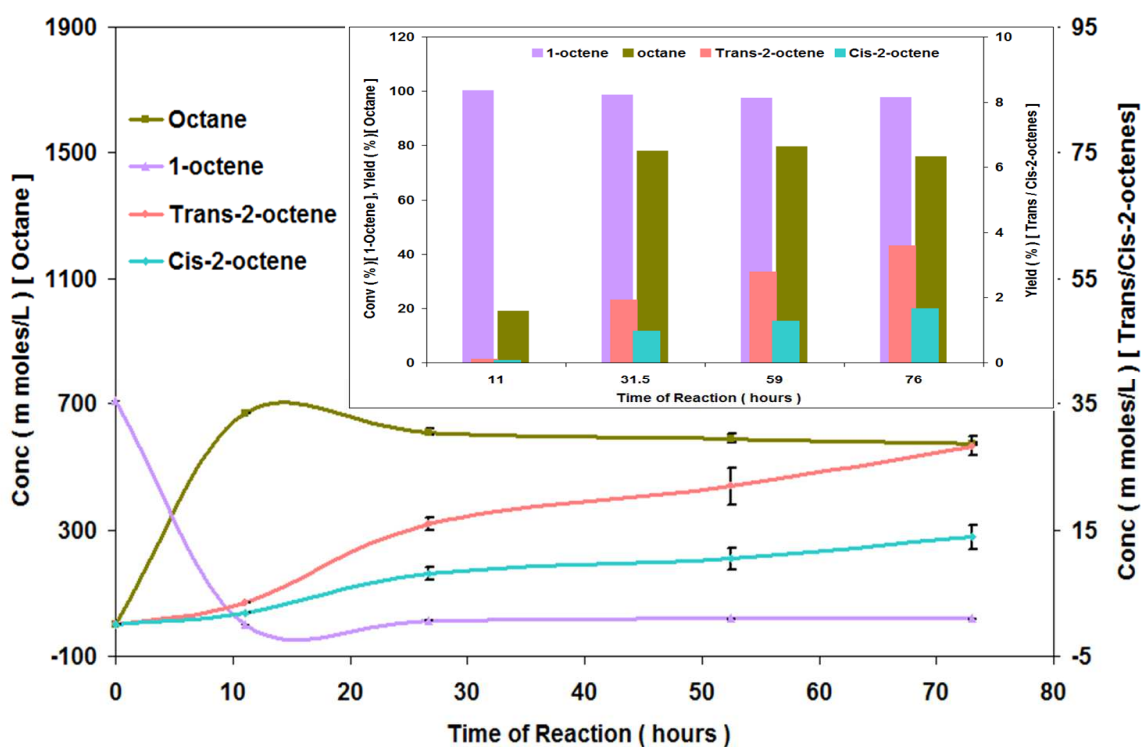
Figure 3.31 Hydrogenation of 1-octene [Reaction conditions: T = 180°C, WHSV$_{PyGas}$ = 4 h^{-1}, P$_{H2}$ = 20 barg]
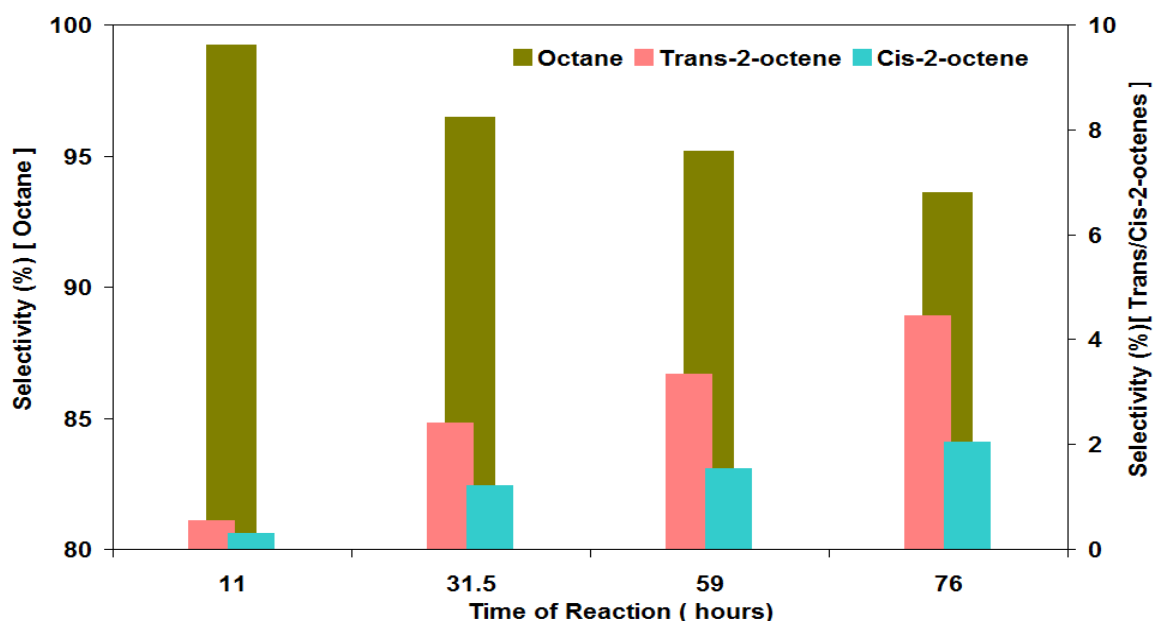
Figure 3.32 Selectivity of octane, trans-2-octene and cis-2-octene during 1-octene hydrogenation [Reaction conditions: T = 180°C, WHSV$_{PyGas}$ = 4 h^{-1}, P$_{H2}$ = 20 barg]

Figure 3.32 shows that selectivity towards trans and cis-2-octene increased with time on stream, however the ratio of trans-2-octene to cis-2-octene remained similar to the trans/cis ratio of pentene as shown in Table 3.7. It was also found that the trans to cis ratio remained constant throughout the reaction.

Trans/Cis-2-pentene ratio	Trans/Cis-2-octene ratio
67:33	66:34

Table 3.7 Ratio of trans/cis internal olefins formation in PyGas Hydrogenation [Reaction conditions: T = 180°C, WHSV$_{PyGas}$ = 4 h^{-1}, P$_{H2}$ = 20 barg]

The conversion of cyclopentene was observed to be more than 97% throughout the reaction, as shown in Figure 3.33.
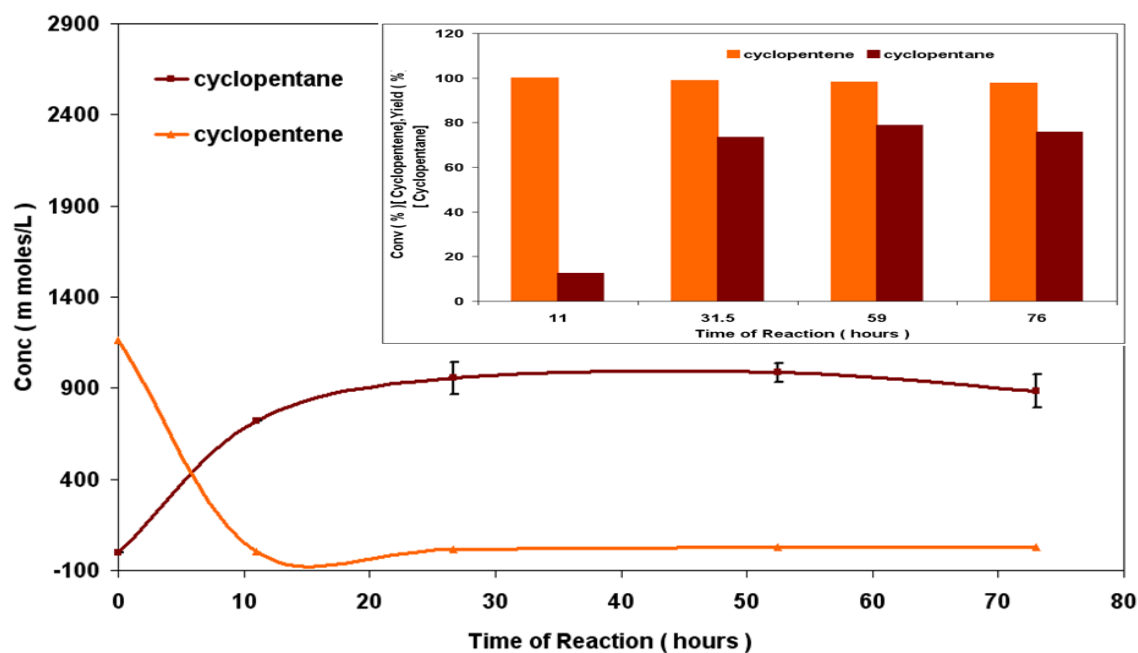
Figure 3.33 Hydrogenation of cyclopentene [Reaction conditions: T = 180°C, WHSV$_{PyGas}$ = 4 h^{-1}, P$_{H2}$ = 20 barg]

Figure 3.34 shows that the conversion of toluene was very high (~93 %) in the first 11 hours of the reaction, then subsequently decreased to 51% once steady state conditions were obtained. However no significant change was observed in the yield of methylcyclohexane with an increase in reaction temperature from 160°C to 180°C.
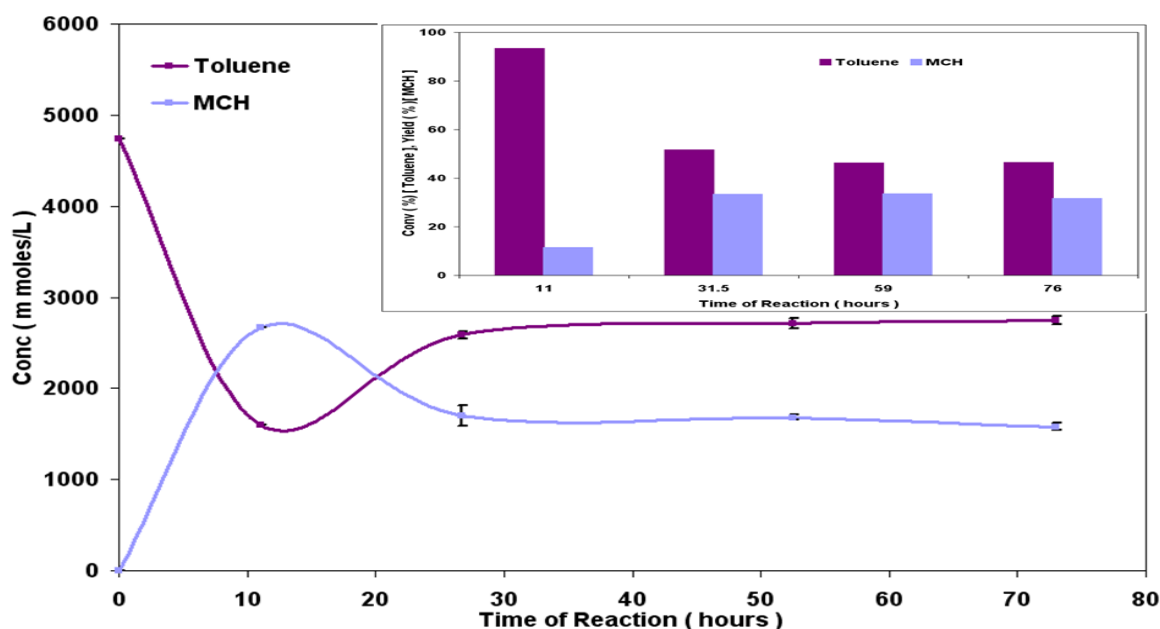
Figure 3.34 Hydrogenation of toluene [Reaction conditions: T = 180°C, WHSV$_{PyGas}$ = 4 h^{-1}, P$_{H2}$ = 20 barg]

A noticeable decrease took place in the yield of both ethylbenzene and ethylcyclohexane with the increase in reaction temperature, although the

conversion of the styrene was greater than 99 %. This shows that contribution of styrene to coke deposition was considerably increased with the increase in reaction temperature from 160°C to 180°C.
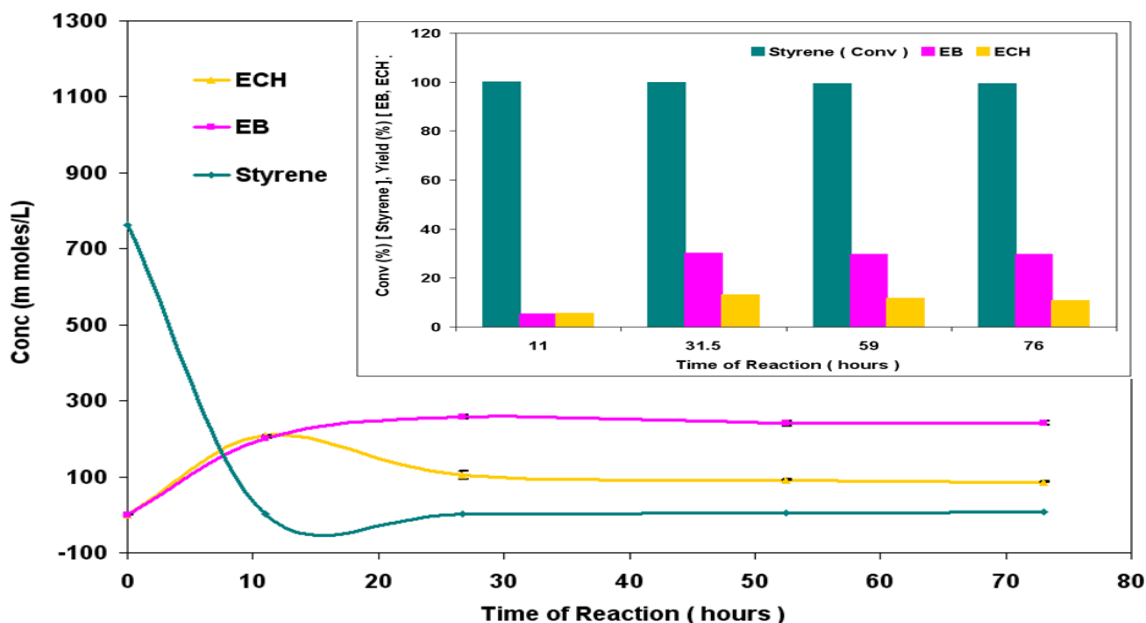
Figure 3.35 Hydrogenation of styrene [Reaction conditions: T = 180°C, WHSV$_{PyGas}$ = 4 h^{-1}, P$_{H2}$ = 20 barg]

No significant change was noted in the selectivity of styrene towards ethylbenzene and ethylcyclohexane with an increase in reaction temperature. In accordance with the previous reaction, the selectivity of ethylbenzene and ethylcyclohexane was initially the same for 11 hours. However, the catalyst was observed to become more selective to ethylbenzene than ethylcyclohexane with time on stream, as shown in Figure 3.36.
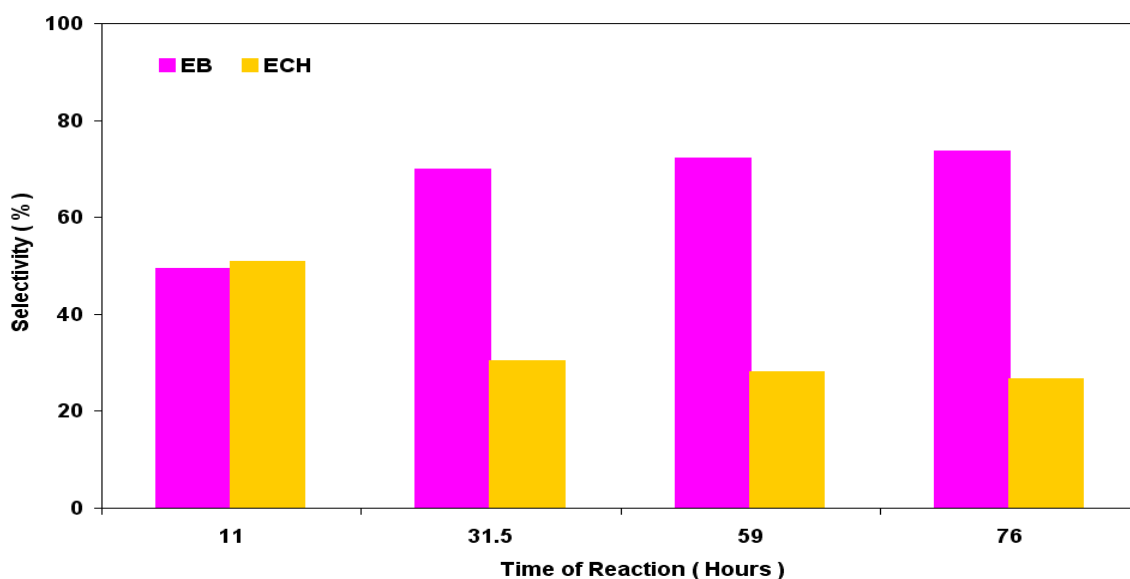
Figure 3.36 Selectivity of ethylbenzene and ethylcyclohexane during styrene hydrogenation [Reaction conditions: T = 180°C, WHSV$_{PyGas}$ = 4 h^{-1}, P$_{H2}$ = 20 barg]

3.2.2.1.3.1 Post reaction analysis

Post reaction catalyst TPO

The *in-situ* TPO shows a large amount of coke deposition on the surface of the catalyst. The evolution of CO_2 and CO became broad and showed a small leading edge of CO_2 and CO at about 350^oC in the TPO, suggesting that the coke was a mixture of different carbonaceous species.
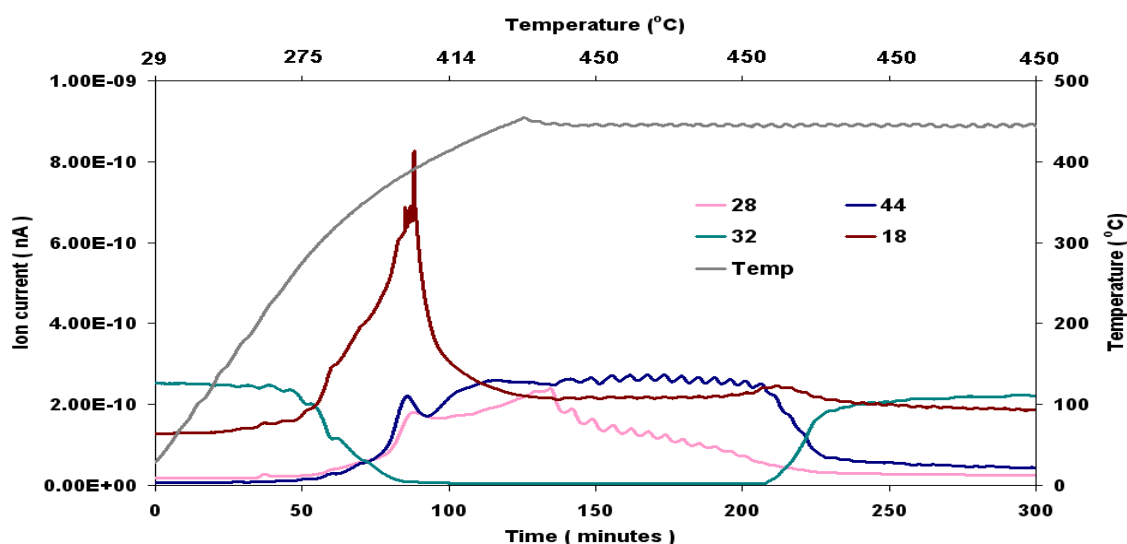
Figure 3.37 Post reaction *in-situ* TPO of Ni/Al$_2$O$_3$ catalyst [Reaction conditions: T = 180°C, WHSV$_{PyGas}$ = 4 h^{-1}, P$_{H2}$ = 20 barg]

Total oxygen consumption in TPO = 5.00 m moles

The small, sharp nature of the H_2O evolution, at 380^oC, indicates a higher C/H ratio in the coke deposited when compared to previous reactions. It is believed that the first small evolution of CO_2 and CO at 350^oC correspond to smaller C/H ratio carbonaceous material while the higher temperature evolutions of CO_2 and CO with the low level of H_2O correspond to higher C/H coke.

BET analysis

The BET results indicate that any surface area lost due to deposition of coke was recovered during regeneration of the catalyst.

Catalyst	Surface Area (m^2g^{-1})	Pore Volume (cm^3g^{-1})	Average Pore diameter (Å)
Ni/Al$_2$O$_3$	93	0.35	152
Ni/Al$_2$O$_3$ (Reduced)	106	0.39	150
Ni/Al$_2$O$_3$ (Regenerated)	90	0.36	163

Table 3.8 BET analysis of Ni/Al$_2$O$_3$ (Regenerated) catalyst [Reaction conditions: T = 180°C, WHSV$_{PyGas}$ = 4 h^{-1}, P$_{H2}$ = 20 barg]

3.2.2.1.4 PyGas hydrogenation over Ni/Al$_2$O$_3$ at 200°C

The reaction temperature was further increased to 200°C and all other reaction conditions were kept constant [P$_{H2}$ = 20 barg and WHSV$_{PyGas}$ = 4 h^{-1}]. The reaction profile is shown in Figure 3.38.
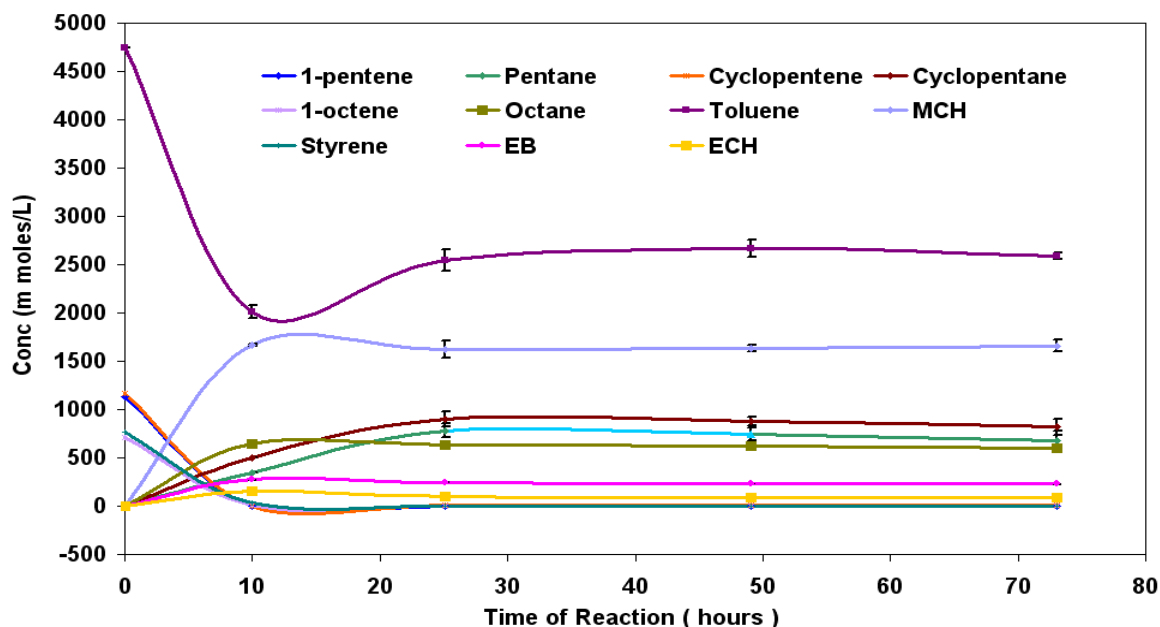
Figure 3.38 Reaction profile of PyGas hydrogenation [Reaction conditions: T = 200°C, WHSV$_{PyGas}$ = 4 h^{-1}, P$_{H2}$ = 20 barg]

Figure 3.39 shows that a slight decrease was found in the yield of pentane with an increase in reaction temperature. However conversion of the 1-pentene was observed to be above 99%.
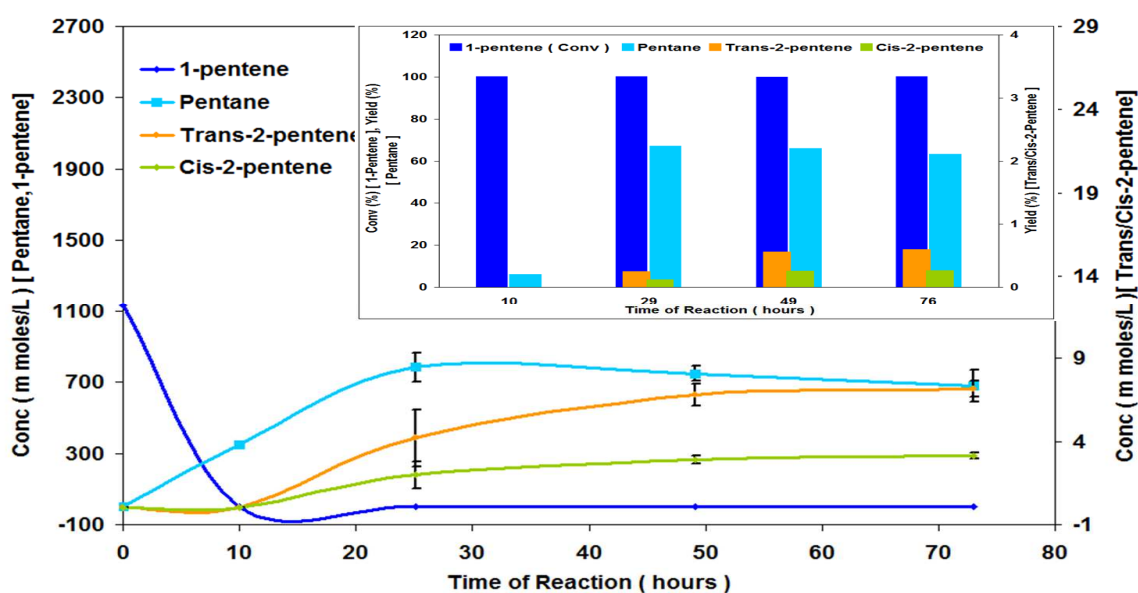
Figure 3.39 Hydrogenation of 1-pentene [Reaction conditions: T = 200°C, WHSV$_{PyGas}$ = 4 h^{-1}, P$_{H2}$ = 20 barg]

Figures 3.39-40 show that pentane was the principal product during the hydrogenation of 1-pentene. However, small amounts of tran-2-pentene and cis-2-pentenes were also observed. An increase was observed in the formation of tran-2-pentene and cis-2-pentene with time on stream. The selectivity of pentane slightly decreased with time on stream whilst an increase was found in the selectivity towards tran-2-pentene and cis-2-pentene. The ratio of trans-2-pentene to cis-2-pentene is shown in Table 3.9 and remained constant throughout the reaction.
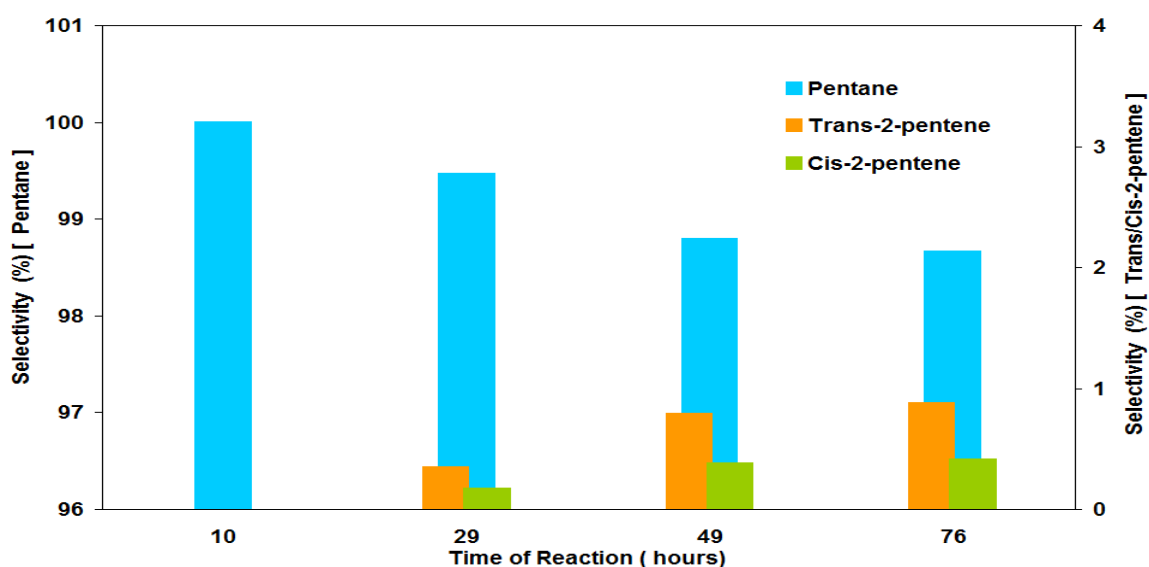
Figure 3.40 Selectivity of pentane, trans-2-pentene and cis-2-pentene during 1-pentene hydrogenation [Reaction conditions: T = 200°C, WHSV$_{PyGas}$ = 4 h^{-1}, P$_{H2}$ = 20 barg]

Figure 3.41-42 shows that octane was the principal product of the 1-octene hydrogenation. However, small amounts of trans-2-octene and cis-2-octene were observed while no 3-octene and 4-octene was noted in the reaction. An increase was observed in the formation of tran-2-octene and cis-2-octene with time on stream.
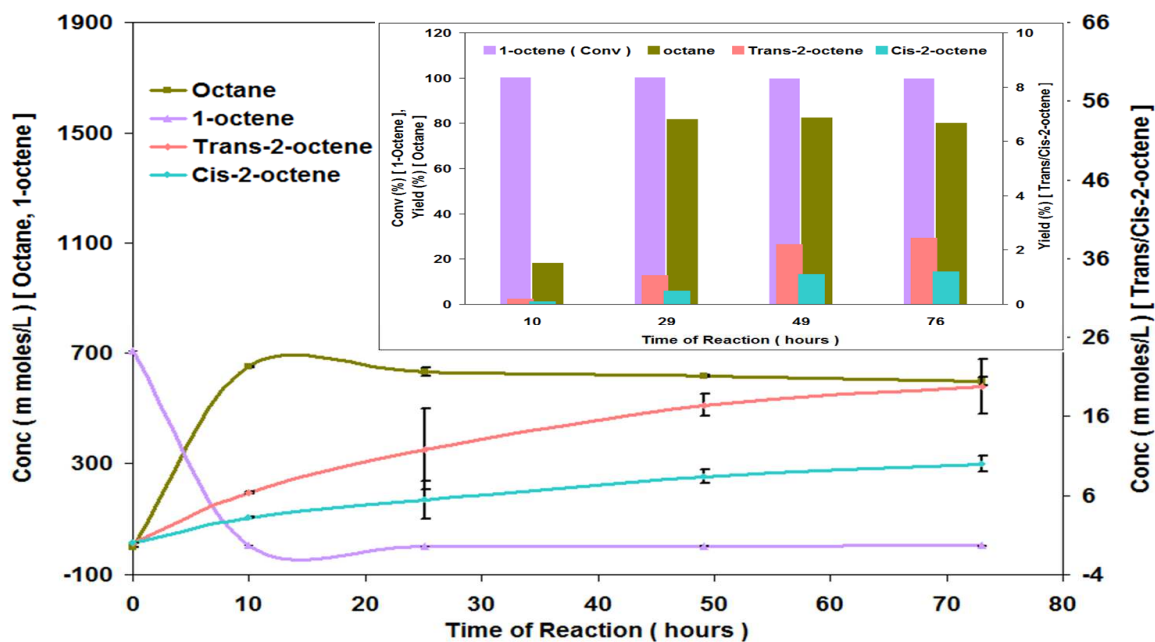
Figure 3.41 Hydrogenation of 1-octene [Reaction conditions: T = 200°C, WHSV$_{PyGas}$ = 4 h^{-1}, P$_{H2}$ = 20 barg]
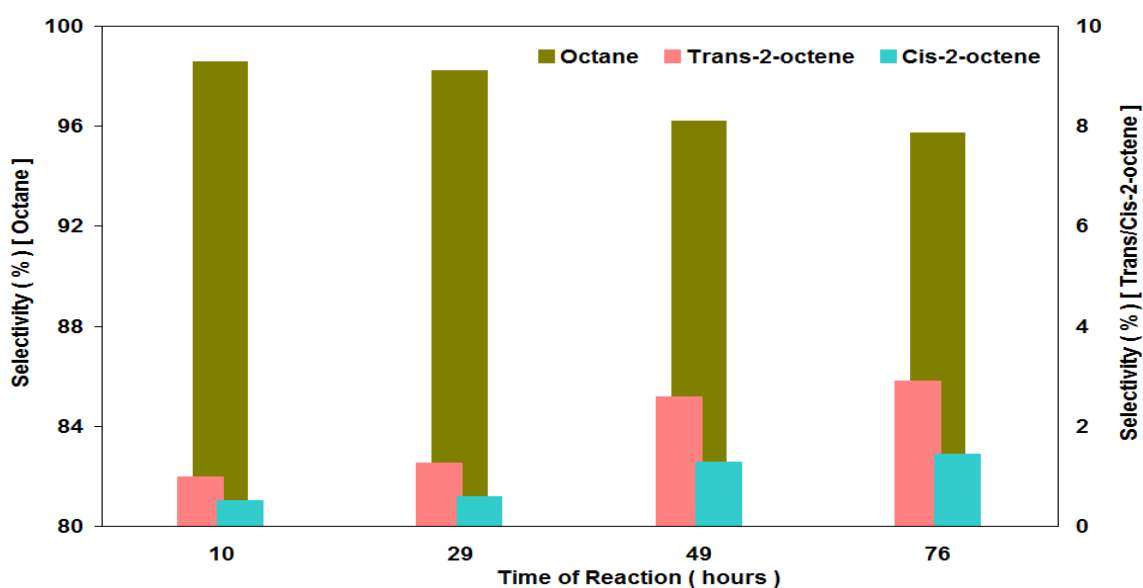
Figure 3.42 Selectivity of octane, trans-2-octene and cis-2-octene during 1-octene hydrogenation [Reaction conditions: T = 200°C, WHSV$_{PyGas}$ = 4 h^{-1}, P$_{H2}$ = 20 barg]

The trans-2-octene was produced at double the amount of the cis-2-octene, as shown in Table 3.9, whilst no 3-octene or 4-octene was observed.

Trans/Cis-2-pentene ratio	Trans/Cis-2-octene ratio
69:31	67:33

Table 3.9 Ratio of trans/cis internal olefins formation in PyGas Hydrogenation [Reaction conditions: T = 200°C, WHSV$_{PyGas}$ = 4 h^{-1}, P$_{H2}$ = 20 barg]

Figure 3.43 shows that no significant change was observed in the hydrogenation of cyclopentene to cyclopentane with the increase in reaction temperature. Conversion of cyclopentene was more than 99% throughout the reaction.
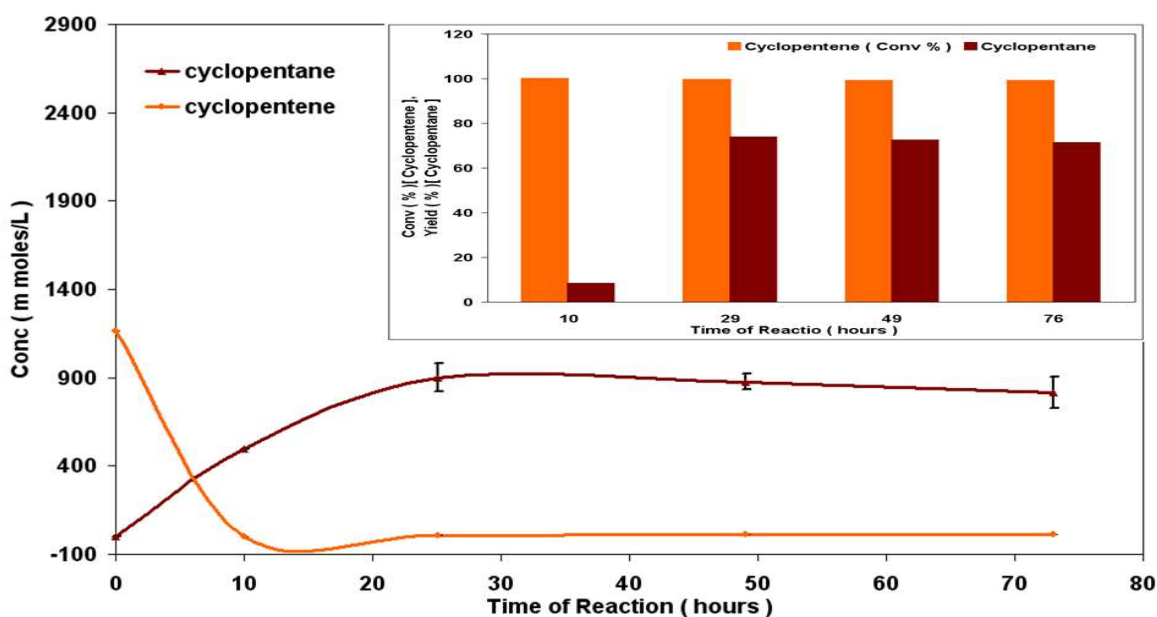
Figure 3.43 Hydrogenation of cyclopentene [Ni/Al$_2$O$_3$, WHSV$_{PyGas}$ = 4 h^{-1}, T = 200°C, P$_{H2}$ = 20 barg]

The conversion of the toluene was around 91% for the first 10 hours of the reaction and decreased to 51% after 29 hours, as shown in Figure 3.44. Conversion and yield remained constant throughout the reaction when steady state conditions were achieved.
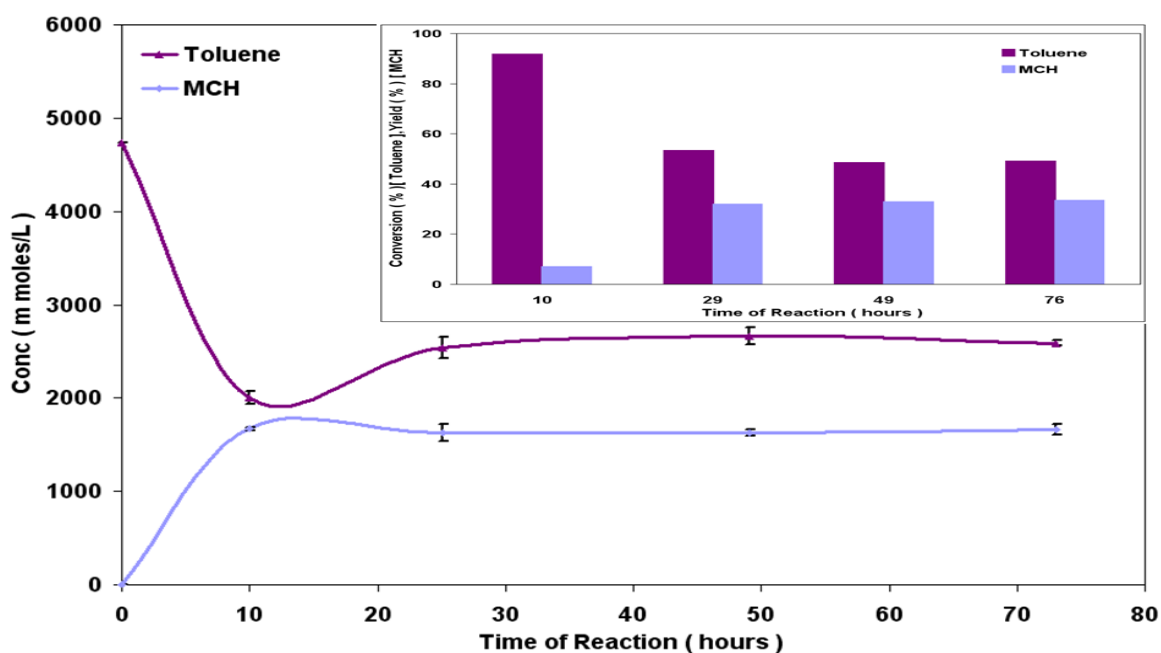
Figure 3.44 Hydrogenation of toluene [Reaction conditions: T = 200°C, WHSV$_{PyGas}$ = 4 h^{-1}, P$_{H2}$ = 20 barg]

From Figure 3.45 it can be seen that a further decrease was observed in the yields of both ethylbenzene and ethylcyclohexane with the increase in reaction temperature from 180°C to 200°C. Conversion of styrene was observed to be above 99%, throughout the reaction.
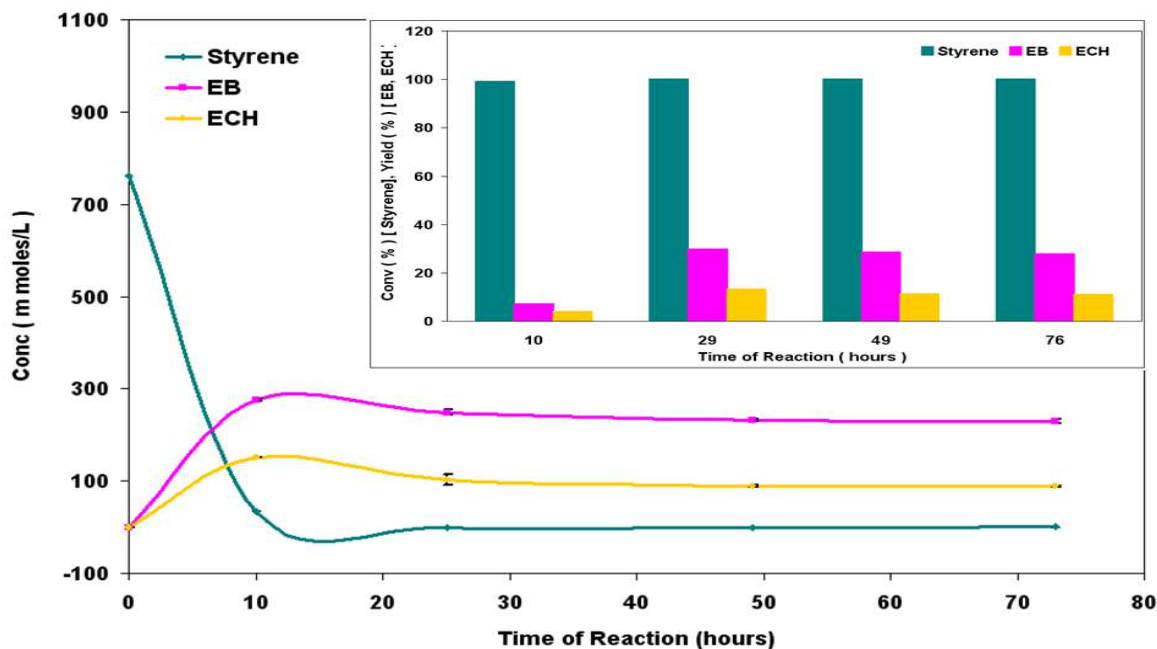
Figure 3.45 Hydrogenation of styrene [Reaction conditions: T = 200°C, WHSV$_{PyGas}$ = 4 h^{-1}, P$_{H2}$ = 20 barg]

The selectivity towards ethylbenzene slightly increased while selectivity towards ethylcyclohexane decreased with time on stream as shown in Figure 3.46.
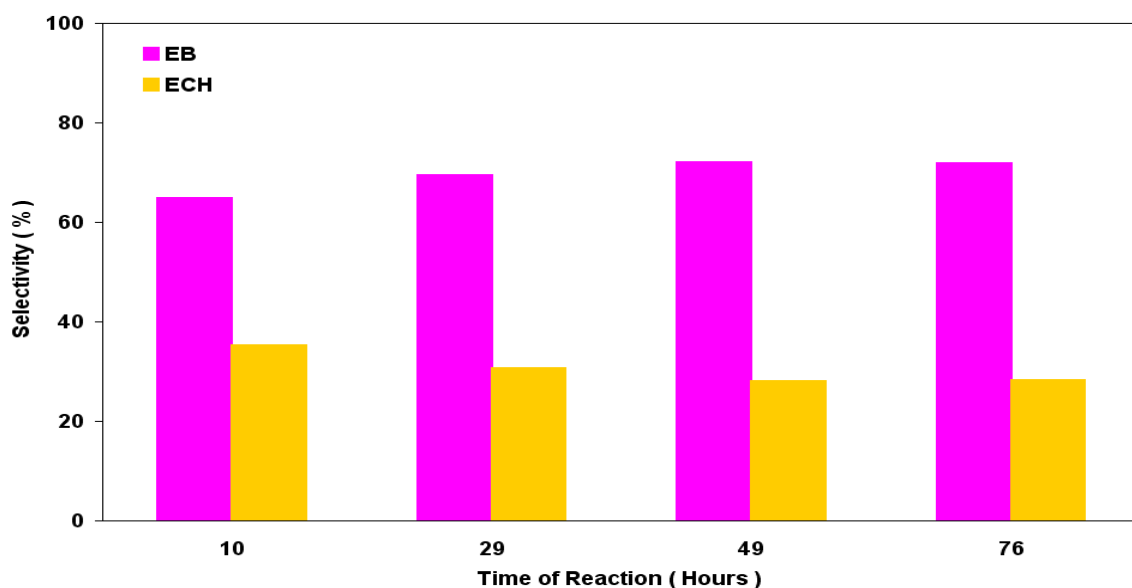
Figure 3.46 Selectivity of ethylbenzene and ethylcyclohexane during styrene hydrogenation [Reaction conditions: T = 200°C, WHSV$_{PyGas}$ = 4 h^{-1}, P$_{H2}$ = 20 barg]

3.2.2.1.4.1 Post reaction analysis

Post reaction catalyst TPO

In-situ TPO of post reaction catalyst shown in Figure 3.47, indicates an increase in coke deposition and a change in the nature of the coke occurring with an increase in reaction temperature. The evolution of H_2O was sharper and smaller when compared to previous TPOs indicating that the C/H ratio in coke had increased with an increase in reaction temperature. The results suggest that the deposited carbonaceous materials on the surface of the catalyst were converted into more condensed polyaromatics with the increase in reaction temperature.
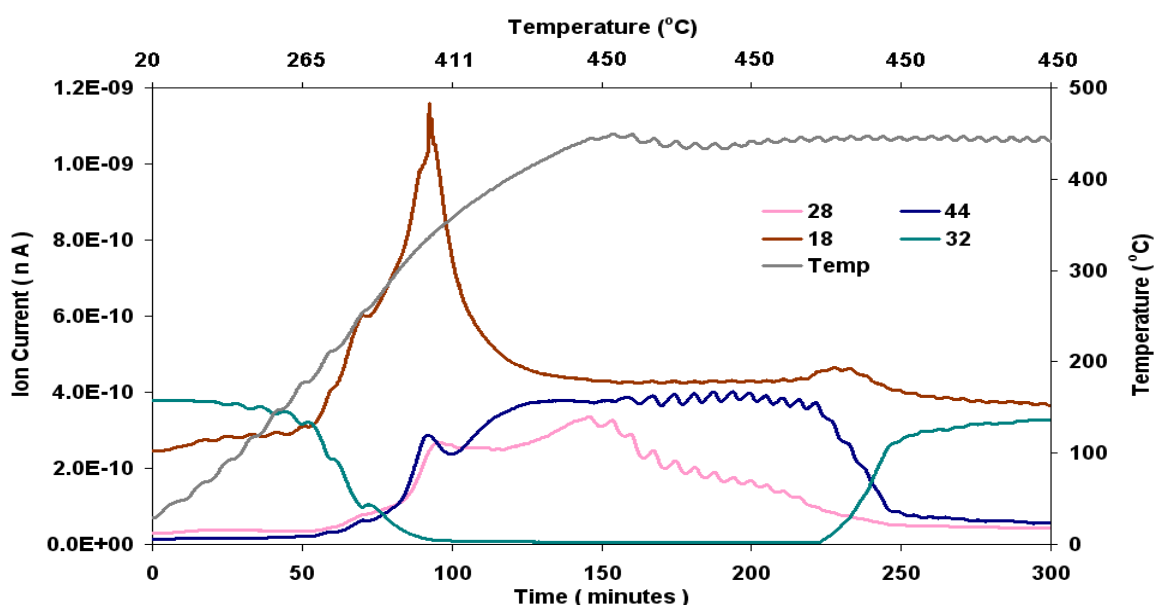
Figure 3.47 Post reaction *in-situ* TPO of Ni/Al$_2$O$_3$ catalyst [Reaction conditions: T = 200°C, WHSV$_{PyGas}$ = 4 h^{-1}, P$_{H2}$ = 20 barg]

Total oxygen consumption in TPO = 5.40 m moles

A noticeable change was observed in the styrene, benzene and hydrogen evolution, which became broader and shifted to higher temperatures as shown in Figure 3.48. Whilst no considerable difference was observed in the evolution of other species *i.e.* 1-pentene, cyclopentene, 1-octene, octane, pentane, toluene, methylcyclohexane, ethylbenzene and ethylcyclohexane.
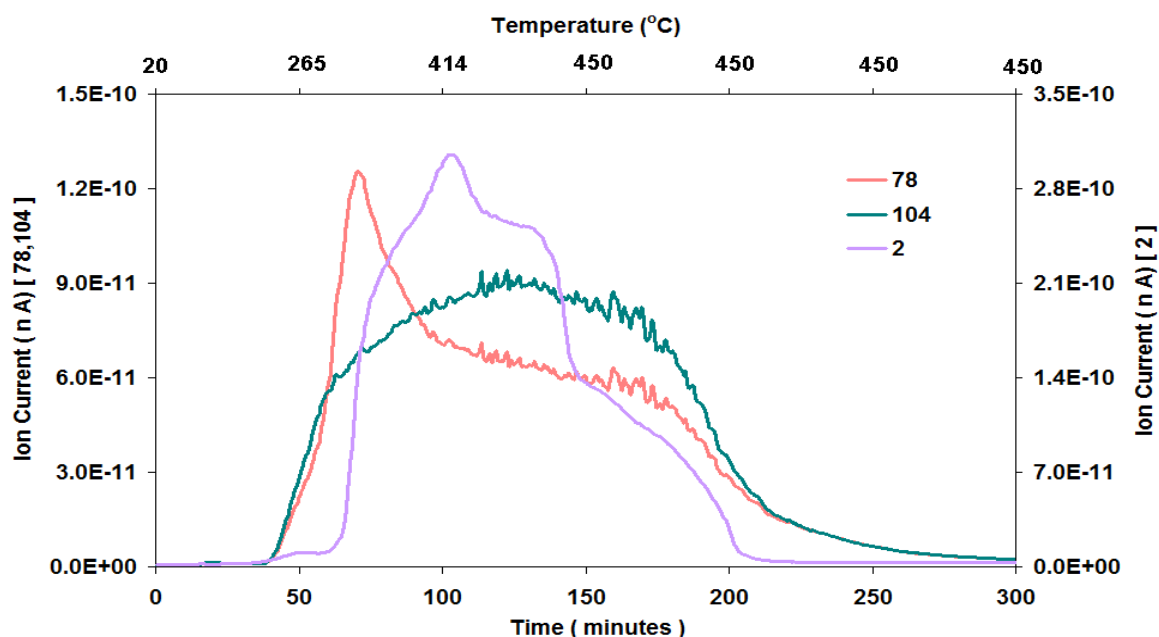
Figure 3.48 Evolution of aromatic species (styrene and benzene) and H$_2$ [Reaction conditions: T = 200°C, WHSV$_{PyGas}$ = 4 h^{-1}, P$_{H2}$ = 20 barg]

TGA-MS Analysis

TGA-MS analysis was performed on the regenerated catalyst. The weight loss of catalyst was about 3.2%. The mass data showed three small evolutions of CO$_2$ as shown in Figure 3.49. It is thought that the first two evolutions at temperatures between 80°C and 400°C corresponded to desorption of the physisorbed species and less condensed carbonaceous materials (with low C/H ratio). Whereas the third evolution observed at 725°C was believed to be highly condensed polyaromatic (graphitic type) coke with a higher C/H ratio. This suggests that hard type coke formation took place at higher reaction temperature. However the weight loss of catalyst corresponding to CO$_2$ desorption at 340°C and 725°C was about 0.3% and 0.2% respectively. This shows that no significant amounts of coke were found on the surface of the catalyst after regeneration by *in-situ* TPO, although a high amount of coke deposition took place at high reaction temperature (200°C).
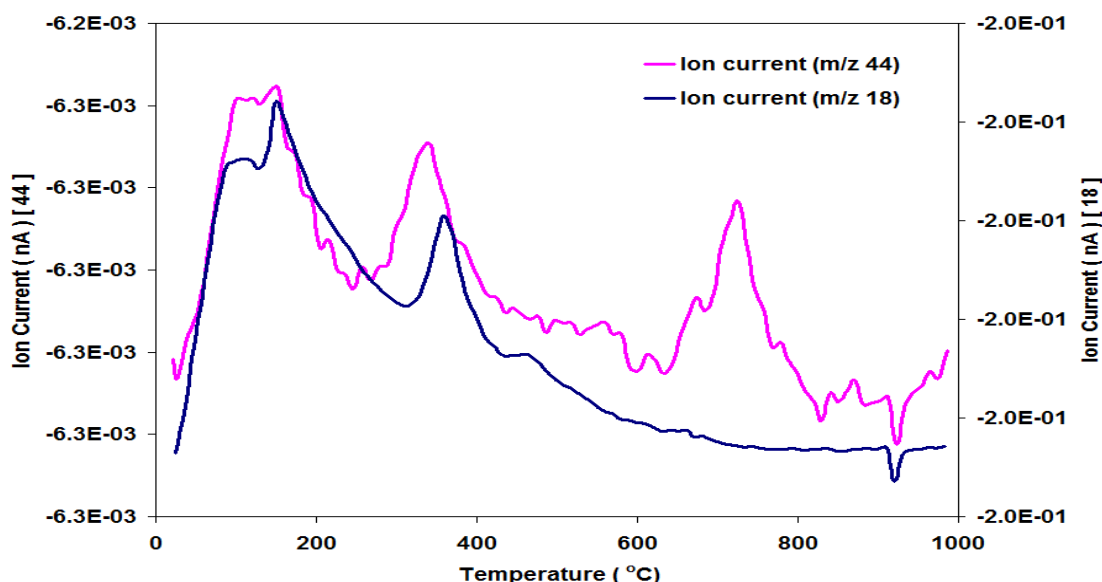
Figure 3.49 TGA-MS of Ni/Al$_2$O$_3$ (Regenerated) catalyst [Reaction conditions: T = 200°C, WHSV$_{PyGas}$ = 4 h^{-1}, P$_{H2}$ = 20 barg]

BET analysis

The surface area, pore volume and average pore diameter of both the fresh and the regenerated catalyst changed insignificantly during the reaction and regeneration process as shown in Table 3.10. Consequently, the results indicated that no support sintering was observed in the catalyst.

Catalyst	Surface Area (m^{2}g^{-1})	Pore Volume (cm^{3}g^{-1})	Average Pore diameter (Å)
Ni/Al$_2$O$_3$	93	0.35	152
Ni/Al$_2$O$_3$ (Reduced)	106	0.39	150
Ni/Al$_2$O$_3$ (Regenerated)	92	0.36	160

Table 3.10 BET analysis of Ni/Al$_2$O$_3$ (Regenerated) catalyst [Reaction conditions: T = 200°C, WHSV$_{PyGas}$ = 4 h^{-1}, P$_{H2}$ = 20 barg]

3.2.2.2 Effect of hydrogen partial pressure on PyGas hydrogenation

Different percentages of hydrogen and nitrogen gas mixtures (100% H$_2$, 50% H$_2$, 25% H$_2$ and 5% H$_2$) were used to investigate the effect of hydrogen partial pressure during the hydrogenation of PyGas. The hydrogenation of PyGas using 100% H$_2$ has been already discussed in section 3.2.2.1.1. The reactions carried out with other hydrogen gas mixtures (50% H$_2$, 25% H$_2$ and 5% H$_2$) are revealed in this section. Different gas mixtures were used whilst the other reaction parameters were kept constant [T = 140°C, WHSV$_{PyGas}$ = 4 h^{-1}, P$_T$ = 20 barg].

3.2.2.2.1 PyGas hydrogenation over Ni/Al$_2$O$_3$ using 50% hydrogen gas mixture

The 50% hydrogen mixed with nitrogen was used to investigate the hydrogenation of PyGas over Ni/Al$_2$O$_3$ catalyst in a fixed bed reactor under the following operating conditions T = 140°C, WHSV$_{PyGas}$ = 4 h^{-1}, P$_T$ = 20 barg and P$_{H2}$ = 10 barg. The reaction profile of PyGas hydrogenation is shown in Figure 3.50.
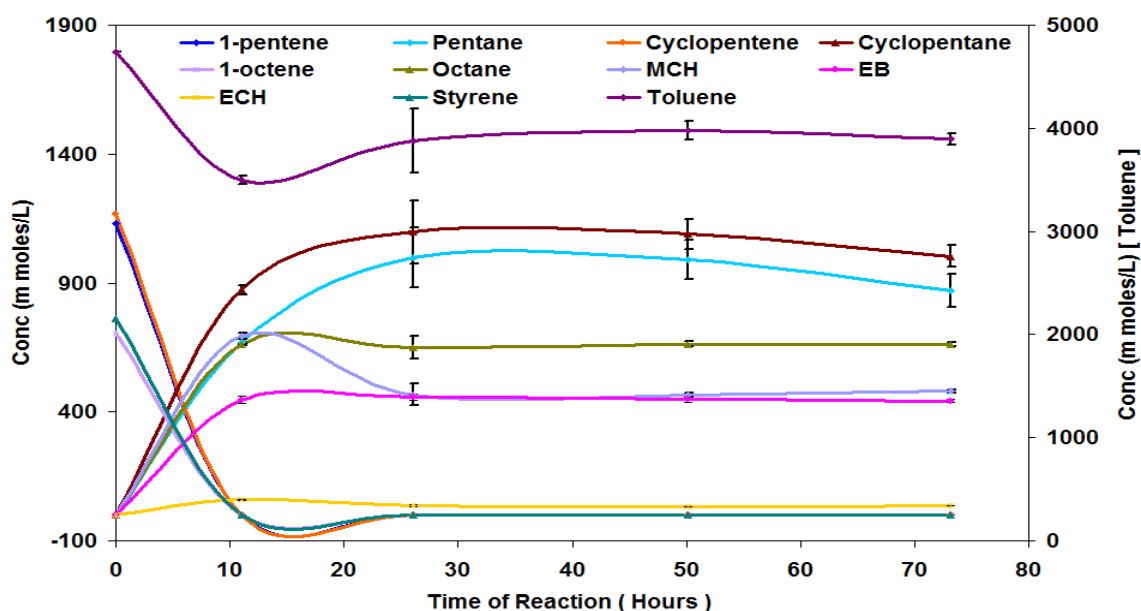
Figure 3.50 Reaction profile of PyGas hydrogenation [Reaction conditions: T = 140°C, WHSV$_{PyGas}$ = 4 h^{-1}, P$_T$ = 20 barg, P$_{H2}$ = 10 barg]

Figure 3.51 shows that conversion of the olefins (1-pentene, 1-octene and cyclopentene) was observed to be above 99%. The olefins were hydrogenated to their respective saturated components with no formation of internal olefins.
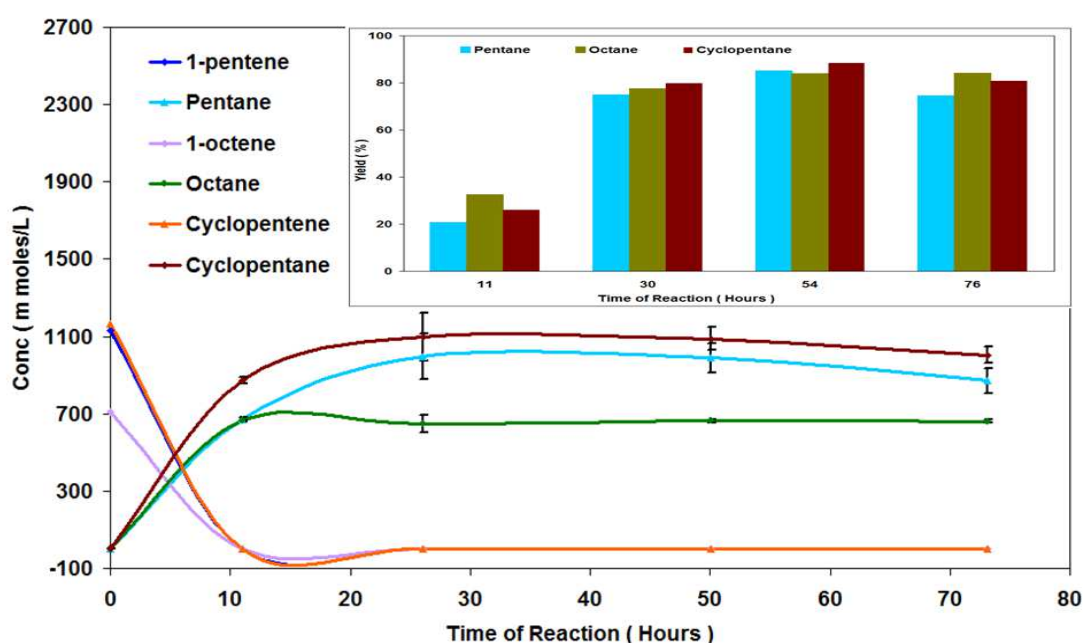
Figure 3.51 Hydrogenation olefins (1-pentene, 1-octene and cyclopentene) present in PyGas [Reaction conditions: T = 140°C, WHSV$_{PyGas}$ = 4 h^{-1}, P$_T$ = 20 barg, P$_{H2}$ = 10 barg]

Figure 3.52 shows that significant decrease was observed in the hydrogenation of toluene to methylcyclohexane with a decrease in hydrogen partial pressure from 20 barg to 10 barg, with a total reactor pressure of 20 barg. The yield of methylcyclohexane was about 5% in the first 11 hours of reaction, which increased to 9% after 30 hours and then remained constant for the rest of the reaction.
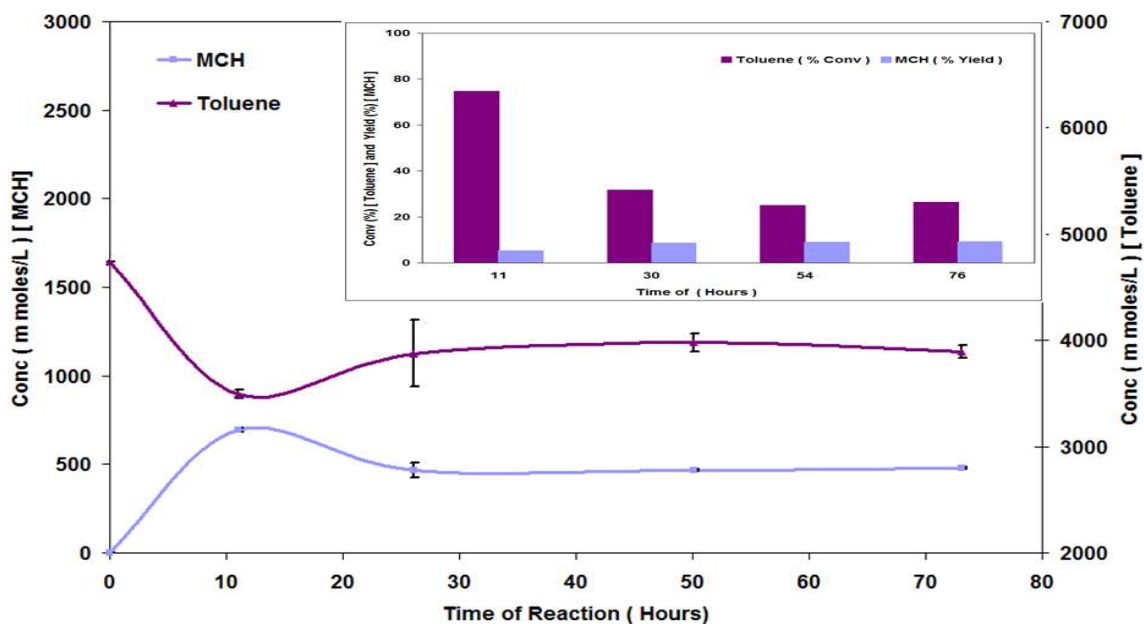
Figure 3.52 Hydrogenation of toluene [Reaction conditions: T = 140°C, WHSV$_{PyGas}$ = 4 h^{-1}, P$_T$ = 20 barg, P$_{H2}$ = 10 barg]

Conversion of styrene remained at above 99% as shown in Figure 3.53. Styrene was hydrogenated to ethyl benzene, which was then further hydrogenated to ethylcyclohexane. The selectivity towards ethylbenzene increased with a decrease in hydrogen partial pressure, as shown in Figure 3.54. However the total yield of styrene hydrogenation decreased with a drop in hydrogen partial pressure due to its higher contribution to gum and coke formation.
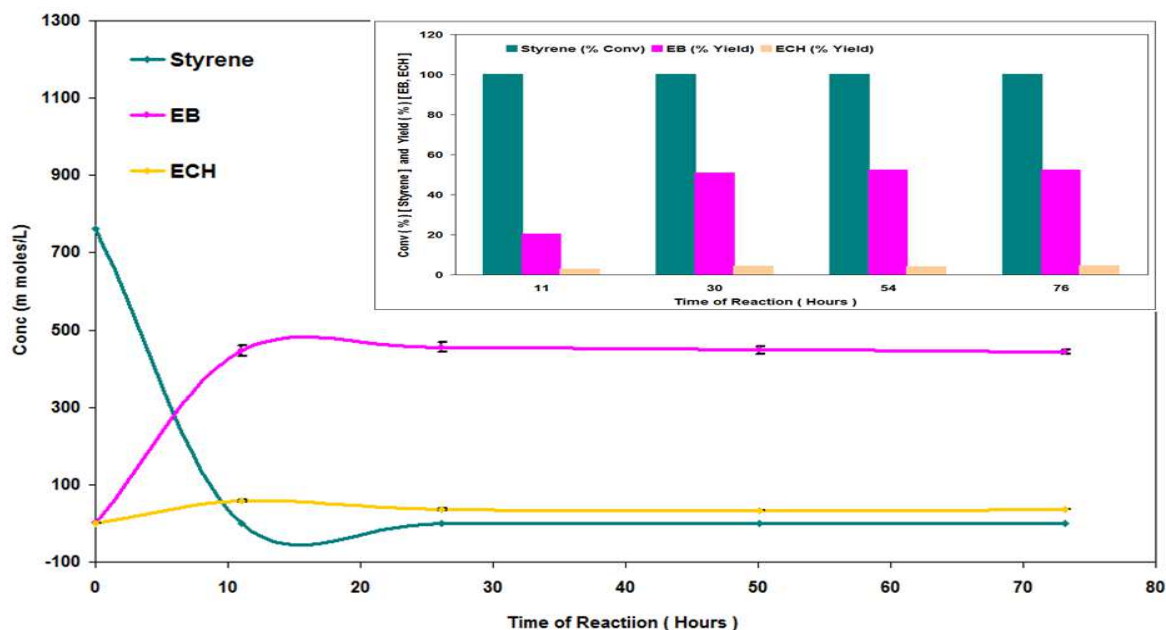
Figure 3.53 Hydrogenation of styrene [Reaction conditions: T = 140°C, WHSV$_{PyGas}$ = 4 h^{-1}, P$_T$ = 20 barg, P$_{H2}$ = 10 barg]
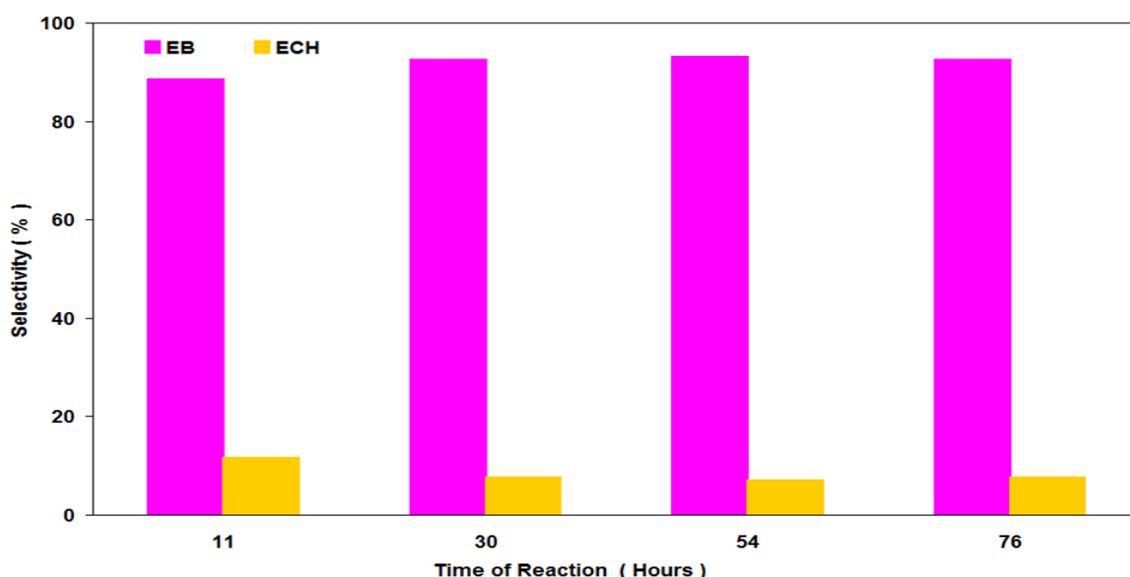
Figure 3.54 Selectivity of ethylbenzene and ethylcyclohexane during styrene hydrogenation [Reaction conditions: T = 140°C, WHSV$_{PyGas}$ = 4 h^{-1}, P$_T$ = 20 barg, P$_{H2}$ = 10 barg]

3.2.2.2.1.1 Post reaction analysis

Post reaction catalyst TPO

In-situ TPO of the post reaction catalyst was carried out and is shown in Figure 3.55. The results indicate a small increase was observed in coke deposition with a change of gas from 100% hydrogen to a 50% hydrogen gas mixture during the reaction. However, no significant difference was observed in the evolution of other species *i.e.* styrene, benzene, 1-pentene, cyclopentene, 1-octene, octane,

pentane, toluene, methylcyclohexane, ethylbenzene, ethylcyclohexane and H_2 during post reaction catalyst TPOs of both reactions.
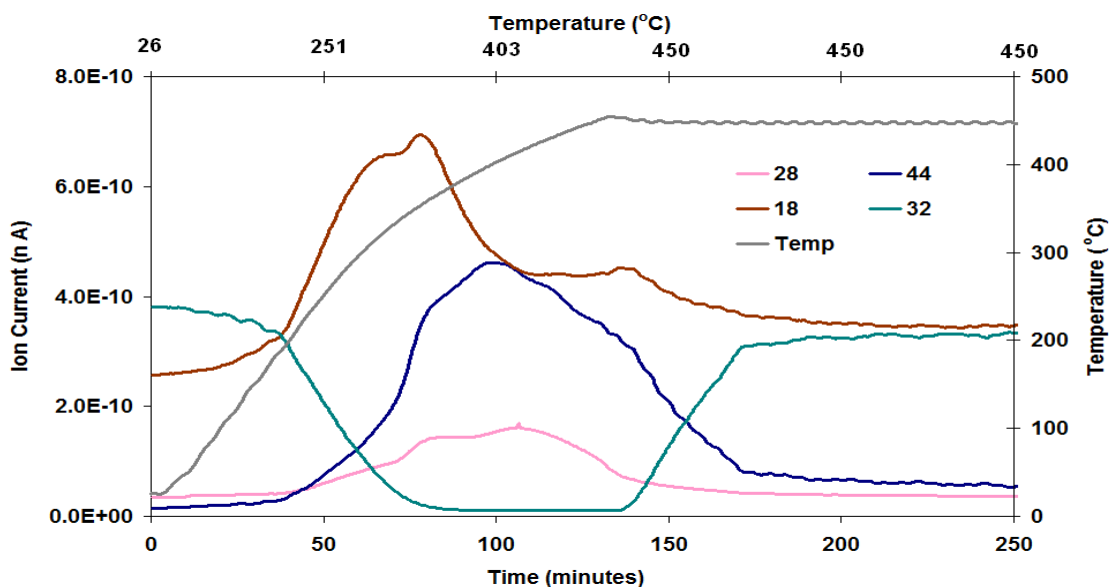
Figure 3.55 Post reaction *in-situ* TPO of Ni/Al$_2$O$_3$ catalyst [Reaction conditions: T = 140°C, WHSV$_{PyGas}$ = 4 h^{-1}, P$_T$ = 20 barg, P$_{H2}$ = 10 barg]

Total oxygen consumption in TPO = 3.37 m moles

BET analysis

The surface area, pore volume and pore diameter of the regenerated Ni/Al$_2$O$_3$ catalyst were analysed and the results presented in Table 3.11.

Catalyst	Surface Area (m^2g^{-1})	Pore Volume (cm^3g^{-1})	Average Pore diameter (Å)
Ni/Al$_2$O$_3$	93	0.35	152
Ni/Al$_2$O$_3$ (Reduced)	106	0.39	150
Ni/Al$_2$O$_3$ (Regenerated)	95	0.37	158

Table 3.11 BET analysis of Ni/Al$_2$O$_3$ (Regenerated) catalyst [Reaction conditions: T = 140°C, WHSV$_{PyGas}$ = 4 h^{-1}, P$_T$ = 20 barg, P$_{H2}$ = 10 barg]

3.2.2.2.2 PyGas Hydrogenation over Ni/Al$_2$O$_3$ using 25% hydrogen gas mixture

The hydrogenation of PyGas was carried out using a 25% hydrogen gas mixture and all other reaction conditions were kept constant [T = 140°C, WHSV$_{PyGas}$ = 4 h^{-1}, P$_T$ = 20 barg]. The reaction profile is shown in Figure 3.56.
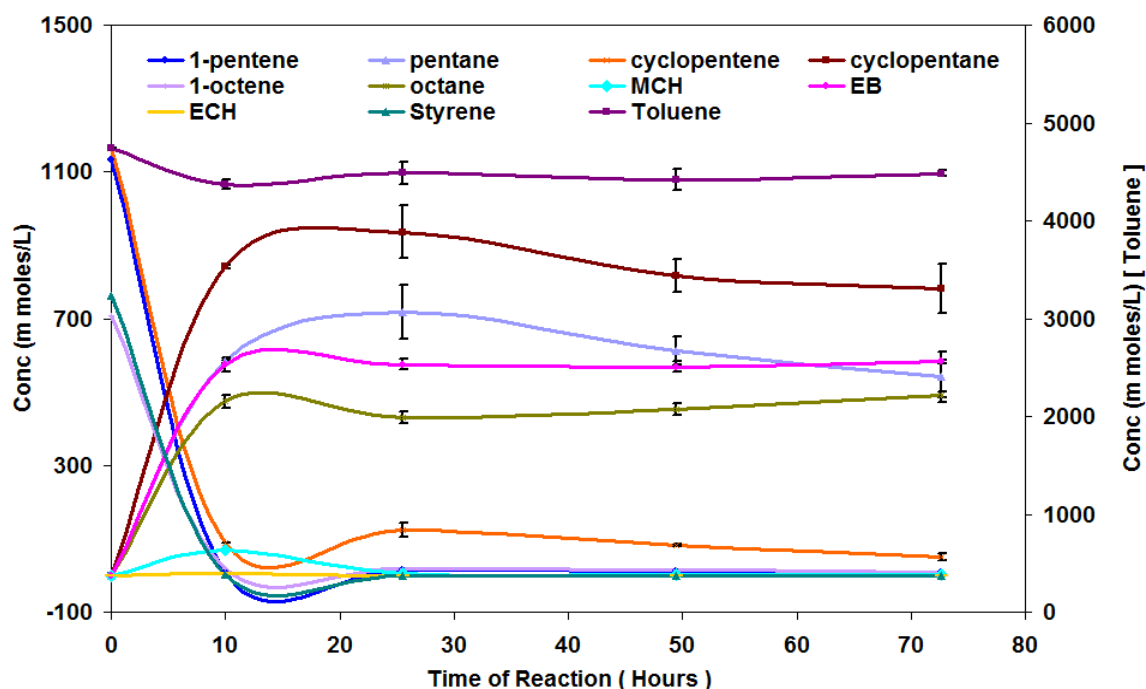
Figure 3.56 Reaction profile of PyGas hydrogenation [Reaction conditions: T = 140°C, WHSV$_{PyGas}$ = 4 h^{-1}, P$_T$ = 20 barg, P$_{H2}$ = 5 barg]

The conversion of 1-pentene remained at more than 90% throughout the reaction. The formation of trans-2-pentene and cis-2-pentene increased with a decrease in the hydrogen partial pressure. However, the total yield of reaction decreased, as shown in Figures 3.57-58.
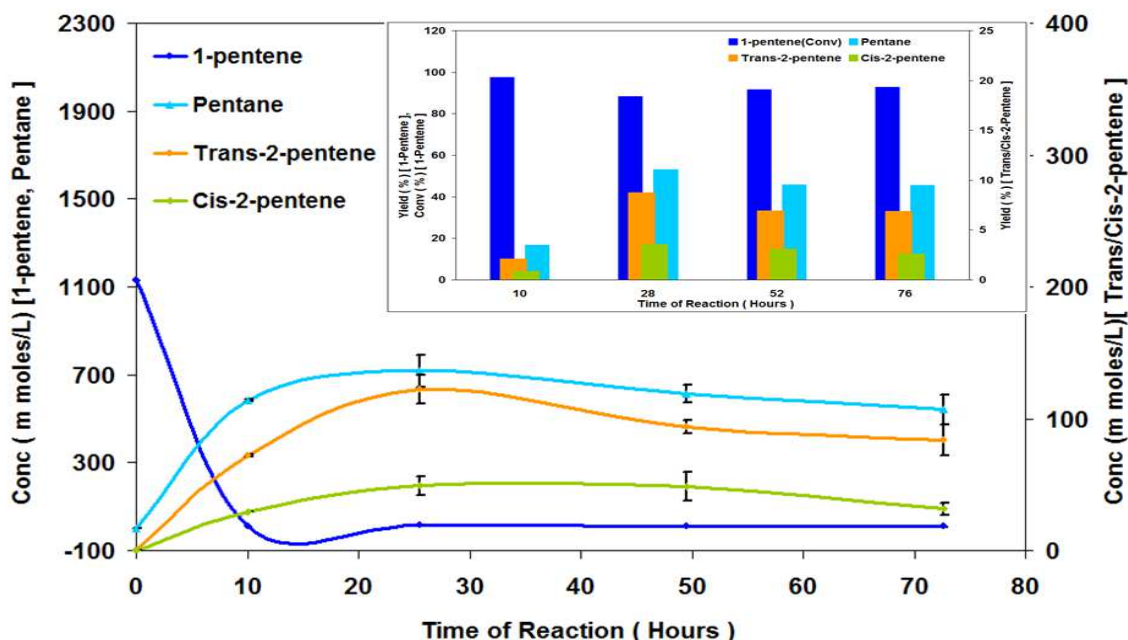
Figure 3.57 Hydrogenation of 1-pentene [Reaction conditions: T = 140°C, WHSV$_{PyGas}$ = 4 h^{-1}, P$_T$ = 20 barg, P$_{H2}$ = 5 barg]
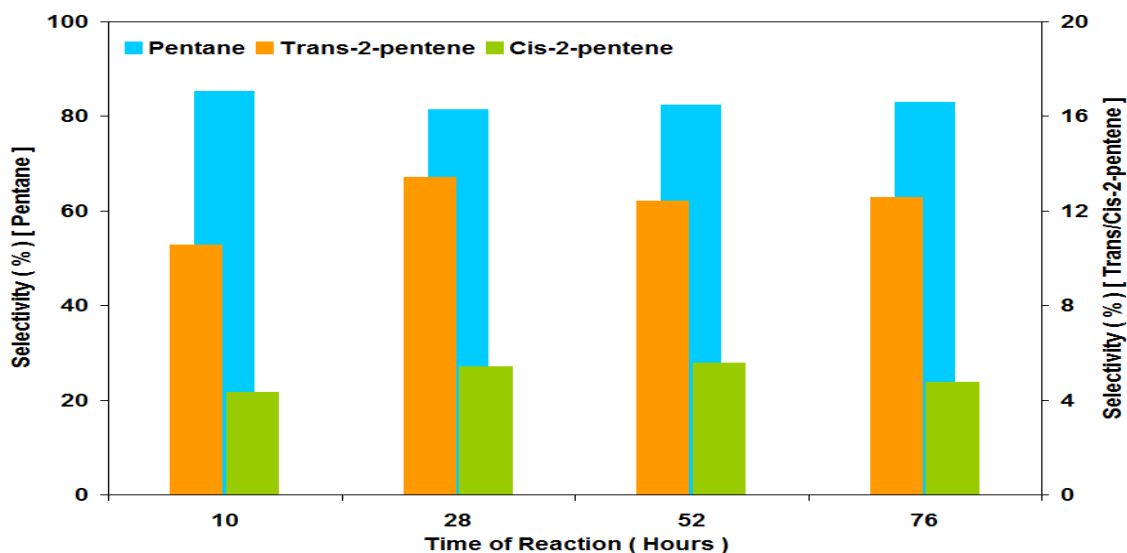
Figure 3.58 Selectivity of pentane, trans-2-pentene and cis-2-pentene during 1-pentene hydrogenation [Reaction conditions: T = 140°C, WHSV$_{PyGas}$ = 4 h^{-1}, P$_T$ = 20 barg, P$_{H2}$ = 5 barg]

Figure 3.59 shows that octane was the primary product in 1-octene hydrogenation, however reasonable amounts of internal octenes were also produced. The internal octenes formation followed the order below.

$$2\text{-octene} > 3\text{-octene} > 4\text{-octene}$$

Trans-3-octene, cis-3-octene and cis-4-octene are presented collectively in the results because the GC column used was only capable of analysing these products as a single peak, as mentioned in section 2.3.3.
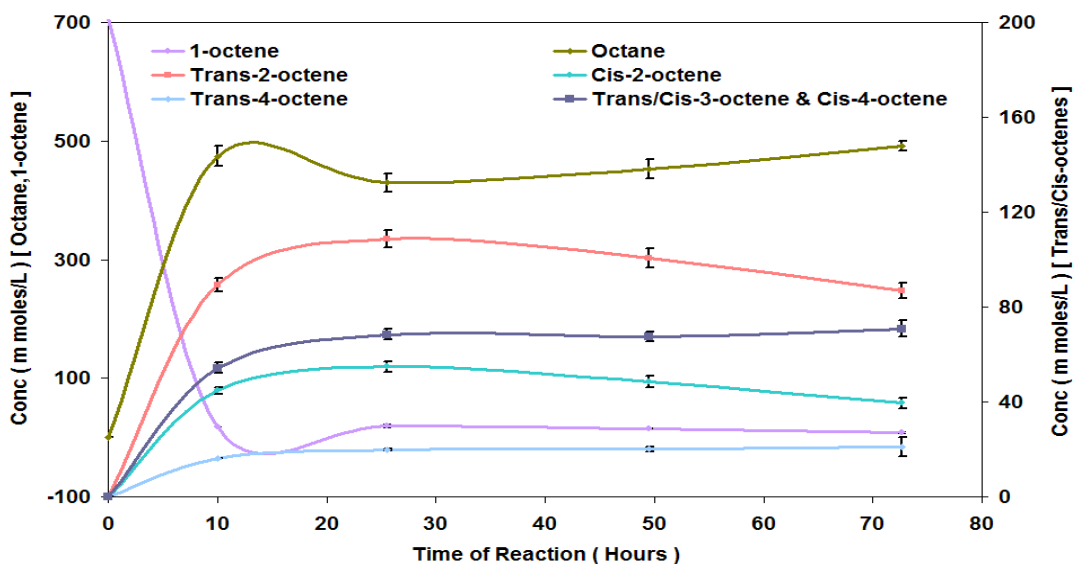
Figure 3.59 Reaction profile of 1-octene hydrogenation [Reaction conditions: T = 140°C, WHSV$_{PyGas}$ = 4 h^{-1}, P$_T$ = 20 barg, P$_{H2}$ = 5 barg]

The conversion of 1-octene remained at more than 97% throughout the reaction, as is shown in Figure 3.60. An increase was observed in the yield of the internal

octenes in the initial 28 hours of the reaction while after obtaining steady state, yield of the internal octenes remained virtually constant. The selectivity of 1-octene towards octane and the internal octenes is shown in Figure 3.61.
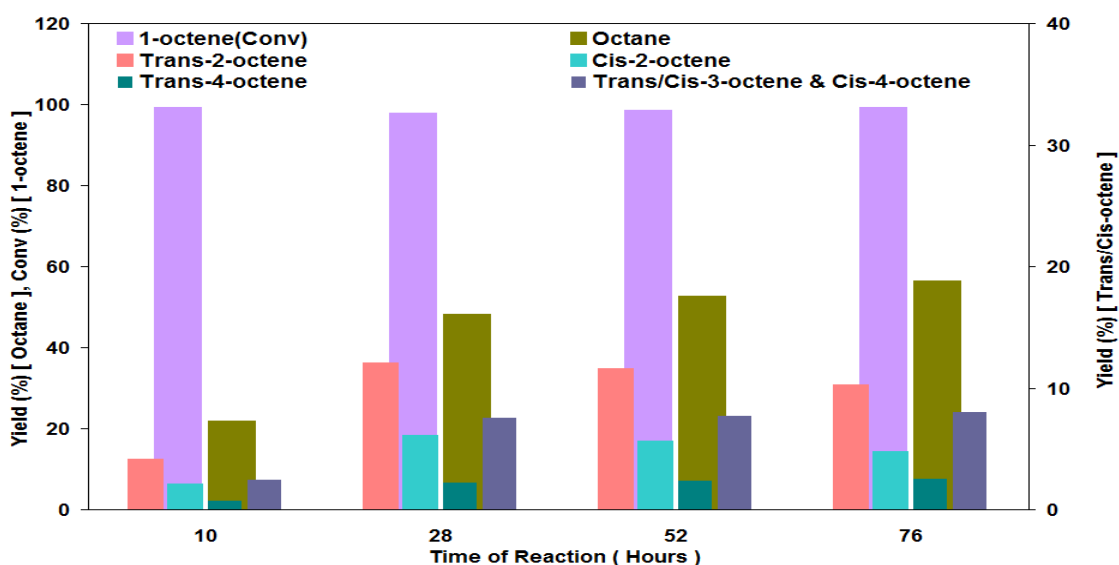
Figure 3.60 Percent yield of 1-octene Hydrogenation [Reaction conditions: T = 140°C, WHSV$_{PyGas}$ = 4 h^{-1}, P$_T$ = 20 barg, P$_{H2}$ = 5 barg]
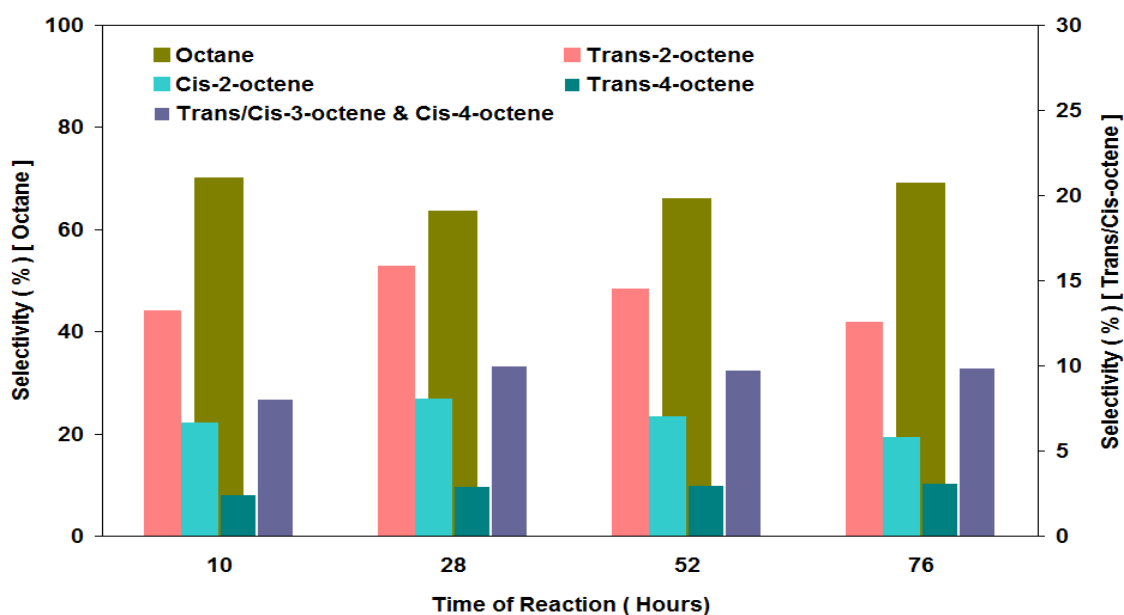
Figure 3.61 Selectivity of octane and internal octenes during 1-octene hydrogenation [Reaction conditions: T = 140°C, WHSV$_{PyGas}$ = 4 h^{-1}, P$_T$ = 20 barg, P$_{H2}$ = 5 barg]

The trans/cis ratio of olefins formed during reaction is shown in Table 3.12.

Trans/Cis-2-pentene ratio	Trans/Cis-2-octene ratio
70:30	67:33

Table 3.12 Ratio of trans/cis internal olefins formation in PyGas Hydrogenation [Reaction conditions: T = 140°C, WHSV$_{PyGas}$ = 4 h^{-1}, P$_T$ = 20 barg, P$_{H2}$ = 5 barg]

The conversion of cyclopentene was found to be more than 90% throughout the reaction. A further decrease was noted in the yield of cyclopentane with the decrease in hydrogen partial pressure from 10 barg to 5 barg, as shown in Figure 3.62.
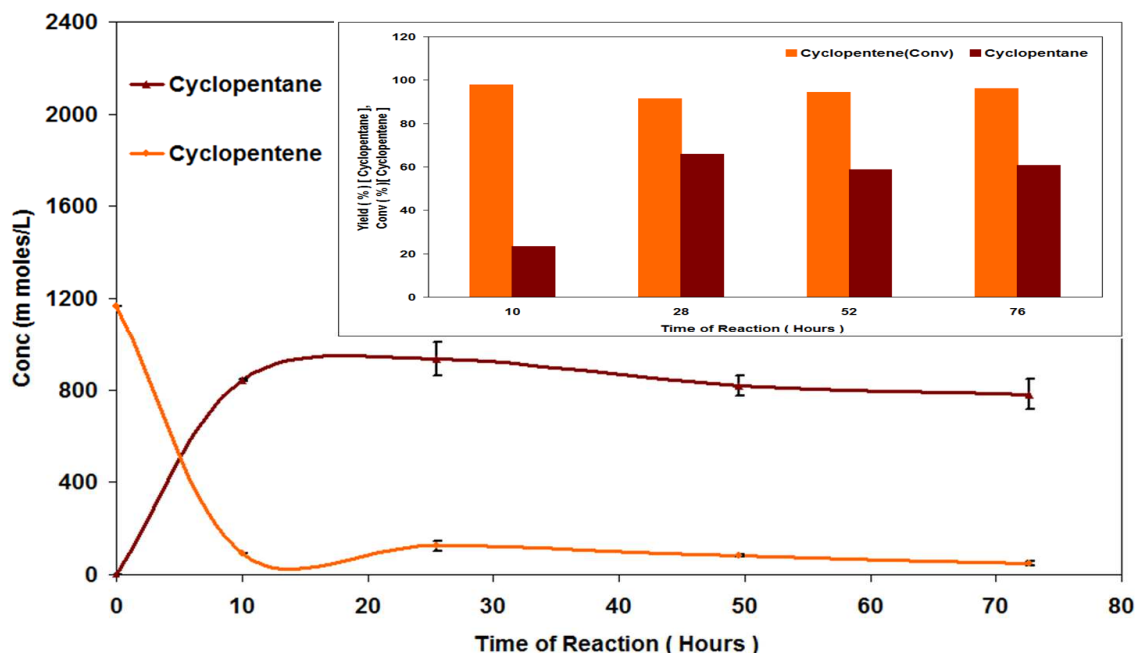
Figure 3.62 Hydrogenation of cyclopentene [Reaction conditions: T = 140°C, WHSV$_{PyGas}$ = 4 h^{-1}, P$_T$ = 20 barg, P$_{H2}$ = 5 barg]

No significant hydrogenation of toluene to methylcyclohexane was seen in the reaction, although a reasonable amount of toluene conversion was observed as shown in Figure 3.63.
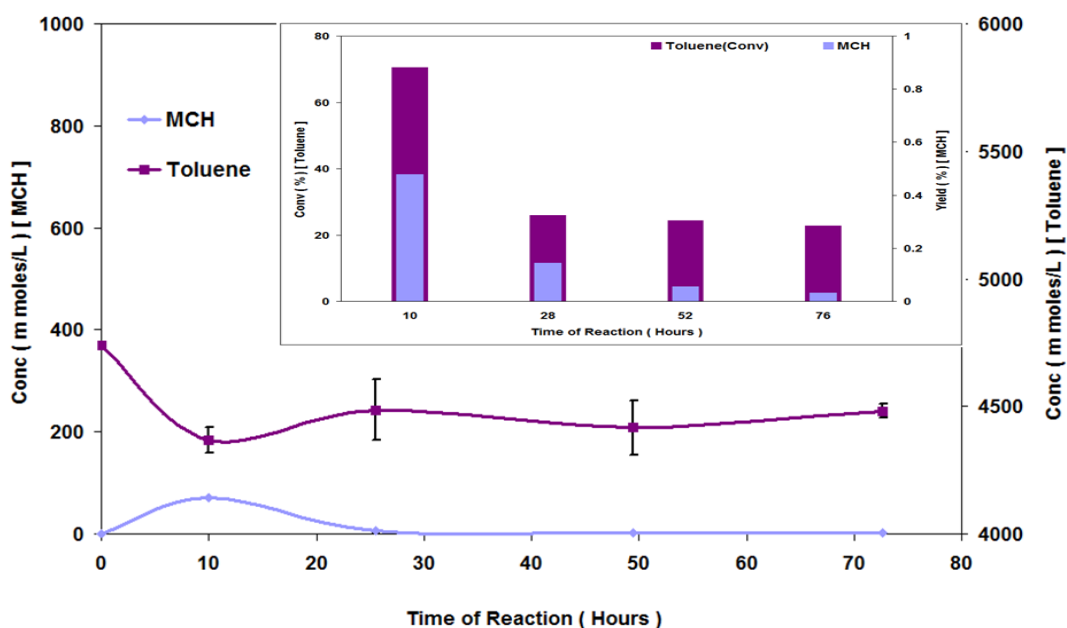
Figure 3.63 Hydrogenation of toluene [Reaction conditions: T = 140°C, WHSV$_{PyGas}$ = 4 h^{-1}, P$_T$ = 20 barg, P$_{H2}$ = 5 barg]

Figure 3.64 shows that the conversion of styrene remained above 99%. The styrene was hydrogenated to ethylbenzene and no further hydrogenation of ethylbenzene to ethylcyclohexane was observed, although a small amount of ethylcyclohexane was seen in the initial 10 hours of the reaction.
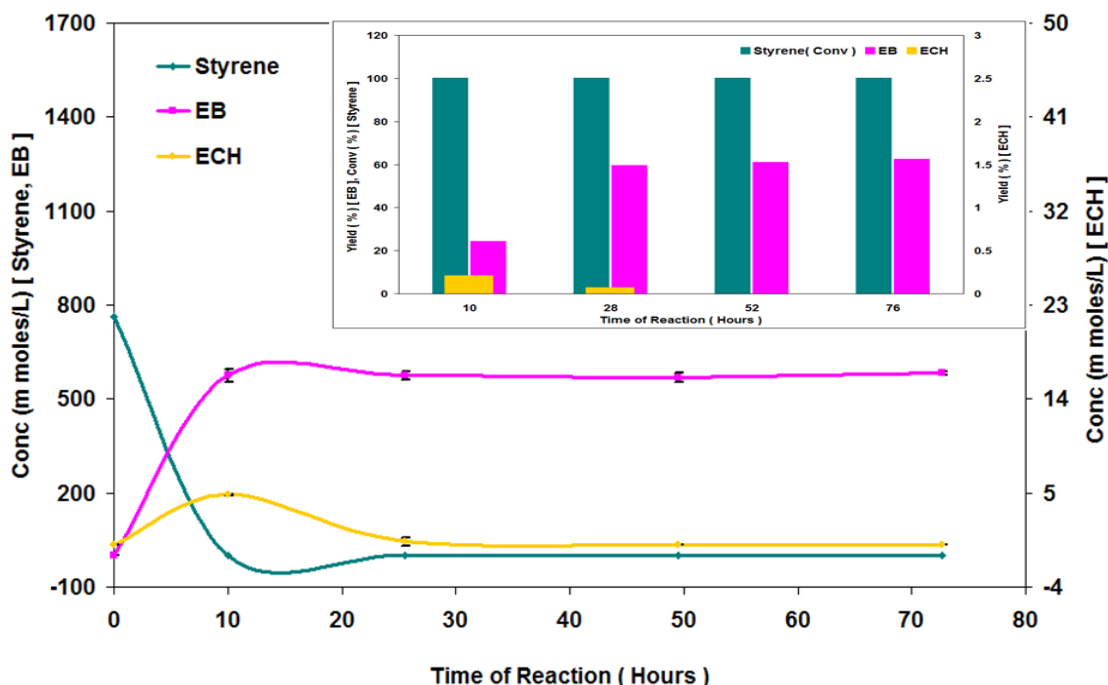
Figure 3.64 Hydrogenation of styrene [Reaction conditions: T = 140°C, WHSV$_{PyGas}$ = 4 h^{-1}, P$_T$ = 20 barg, P$_{H2}$ = 5 barg]

3.2.2.2.2.1 Post reaction analysis

Post reaction catalyst TPO

A post reaction *in-situ* TPO of the catalyst was performed in a flow of 2% O_2/Ar gas. The levels of evolved CO_2, CO, H_2O and O_2 were measured to study the carbon laydown on the surface of the catalyst. A significant amount of coke deposition was observed on the surface of the catalyst, as shown in Figure 3.65. Moreover, the evolution of other species *i.e.* styrene, benzene, 1-pentene, cyclopentene, 1-octene, pentane, octane, toluene, methylcyclohexane, ethylbenzene, ethylcyclohexane and H_2 was also observed and found to be in accordance with TPOs of the catalysts, used in the previous reactions carried out with 100% and 50% hydrogen gas mixtures.
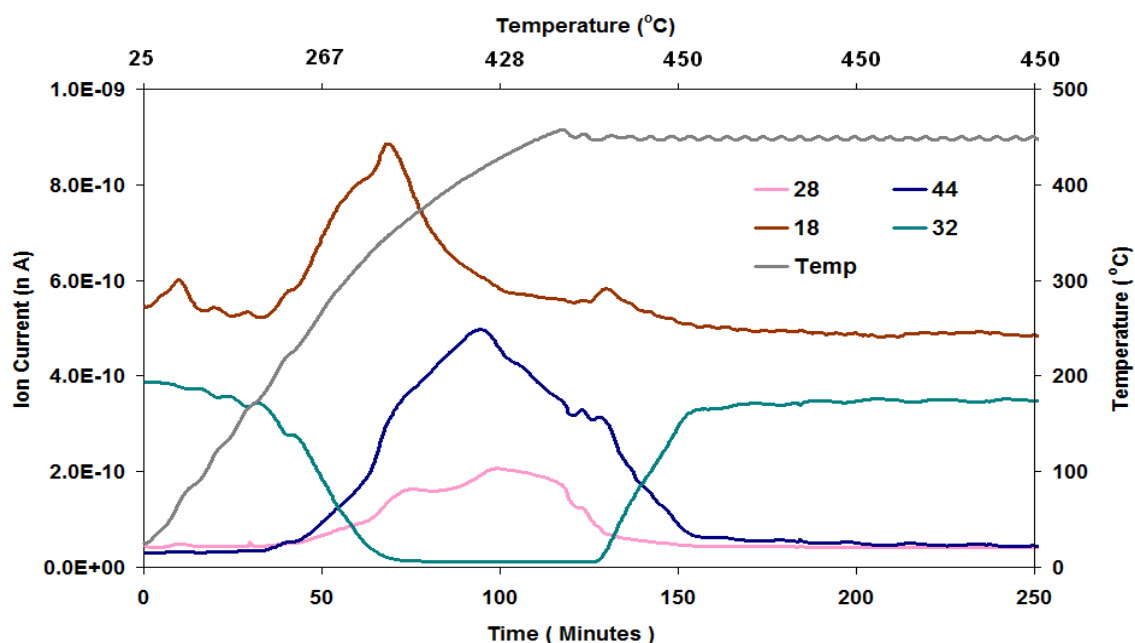
Figure 3.65 Post reaction *in-situ* TPO of Ni/Al$_2$O$_3$ catalyst [Reaction conditions: T = 140°C, WHSV$_{PyGas}$ = 4 h^{-1}, P$_T$ = 20 barg, P$_{H2}$ = 5 barg]

Total oxygen consumption in TPO = 2.97 m moles

BET analysis

The surface area, pore volume and pore diameter of the regenerated Ni/Al$_2$O$_3$ catalyst were analysed and the results are presented in Table 3.13.

Catalyst	Surface Area (m^{2}g^{-1})	Pore Volume (cm^{3}g^{-1})	Average Pore diameter (Å)
Ni/Al$_2$O$_3$	93	0.35	152
Ni/Al$_2$O$_3$ (Reduced)	106	0.39	150
Ni/Al$_2$O$_3$ (Regenerated)	92	0.36	157

Table 3.13 BET analysis of Ni/Al$_2$O$_3$ (Regenerated) catalyst [Reaction conditions: T = 140°C, WHSV$_{PyGas}$ = 4 h^{-1}, P$_T$ = 20 barg, P$_{H2}$ = 5 barg]

3.2.2.2.3 PyGas hydrogenation over Ni/Al$_2$O$_3$ using 5% hydrogen gas mixture

The hydrogenation of PyGas was performed over Ni/Al$_2$O$_3$ catalyst using a 5% hydrogen gas mixture diluted with nitrogen with all other reaction parameter kept constant [T = 140°C, WHSV$_{PyGas}$ = 4 h^{-1} and P$_T$ = 20 barg]. The reaction profile is shown in Figure 3.66.
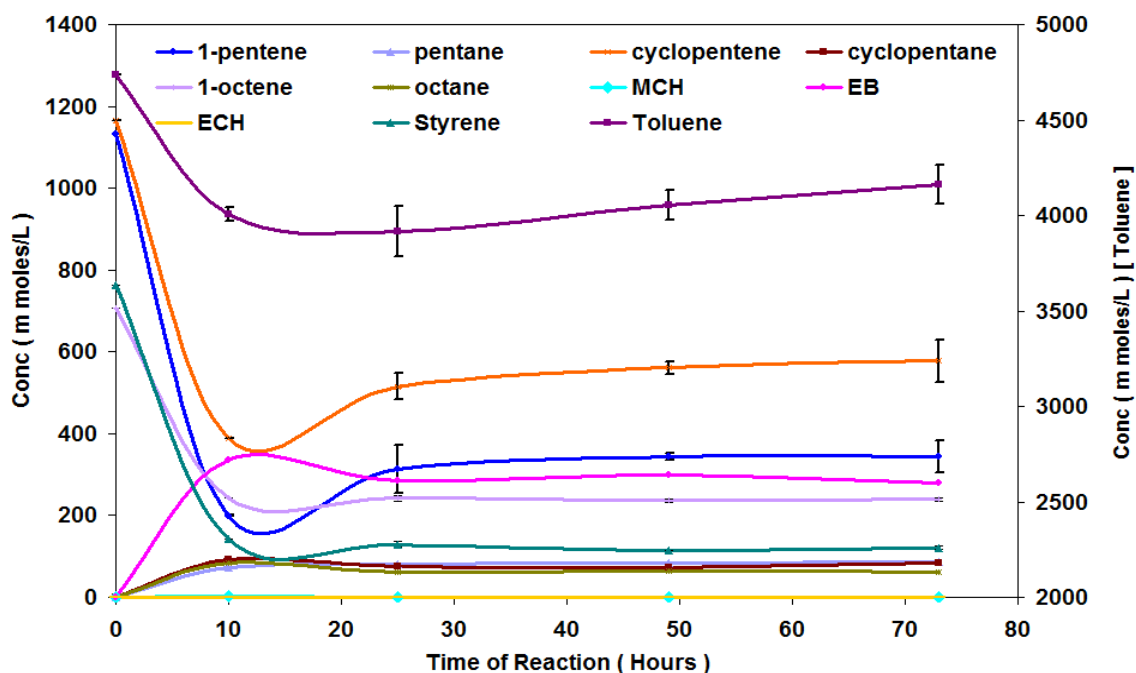
Figure 3.66 Reaction profile of PyGas Hydrogenation [Reaction conditions: T = 140°C, WHSV$_{PyGas}$ = 4 h^{-1}, P$_T$ = 20 barg, P$_{H2}$ = 1 barg]

The conversion of the 1-pentene decreased with time on stream as shown in Figure 3.67. A considerable increase was observed in the formation of internal olefins and the selectivity towards internal pentenes was greatly increased with a decrease in hydrogen partial pressure to 1 barg, as shown in Figures 3.67-68.
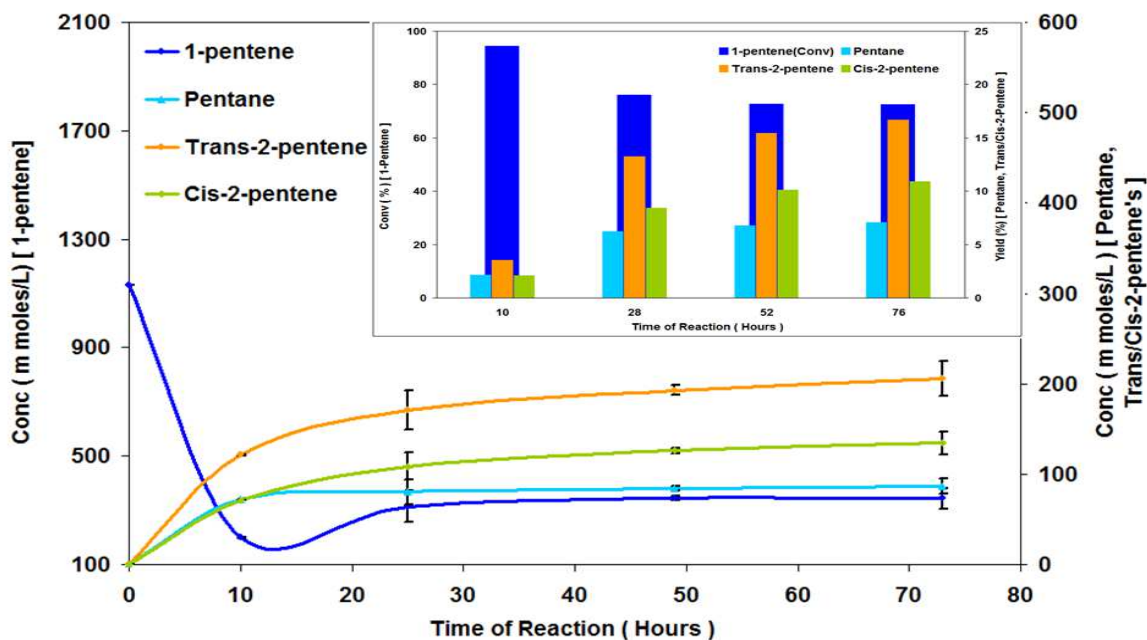

Figure 3.67 Hydrogenation of 1-pentene [Reaction conditions: T = 140°C, WHSV$_{PyGas}$ = 4 h^{-1}, P$_T$ = 20 barg, P$_{H2}$ = 1 barg]
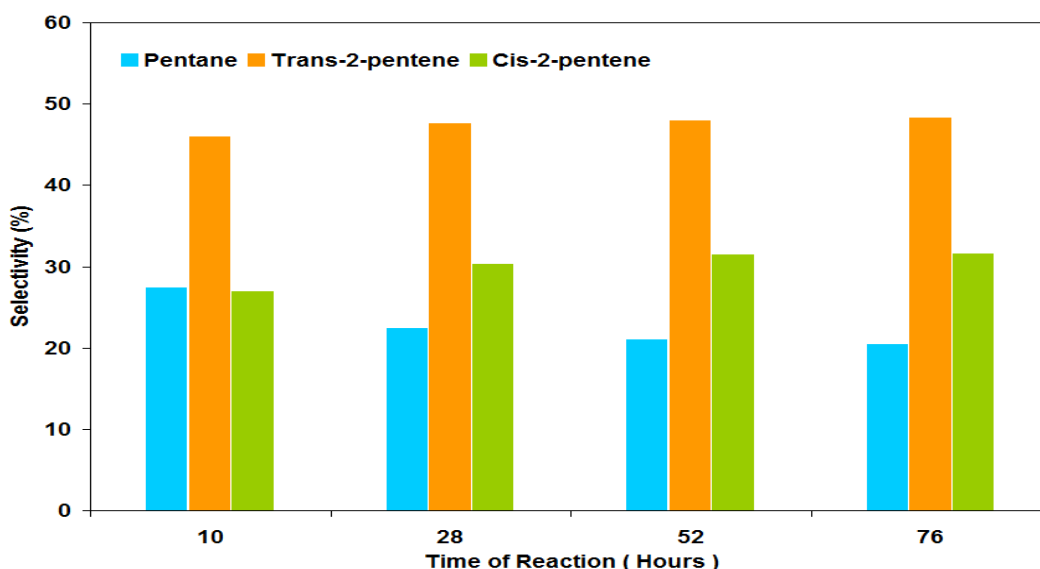
Figure 3.68 Selectivity of pentane, trans-2-pentene and cis-2-pentene during 1-pentene hydrogenation [Reaction conditions: T = 140°C, WHSV$_{PyGas}$ = 4 h^{-1}, P$_T$ = 20 barg, P$_{H2}$ = 1 barg]

Trans-2-octene, cis-2-octene and octane were the principal products during 1-octene hydrogenation. However, a reasonable amount of trans-3-octene was also formed. Moreover, small amounts of cis-3-octene, trans-4-octene and cis-4-octene were also observed.
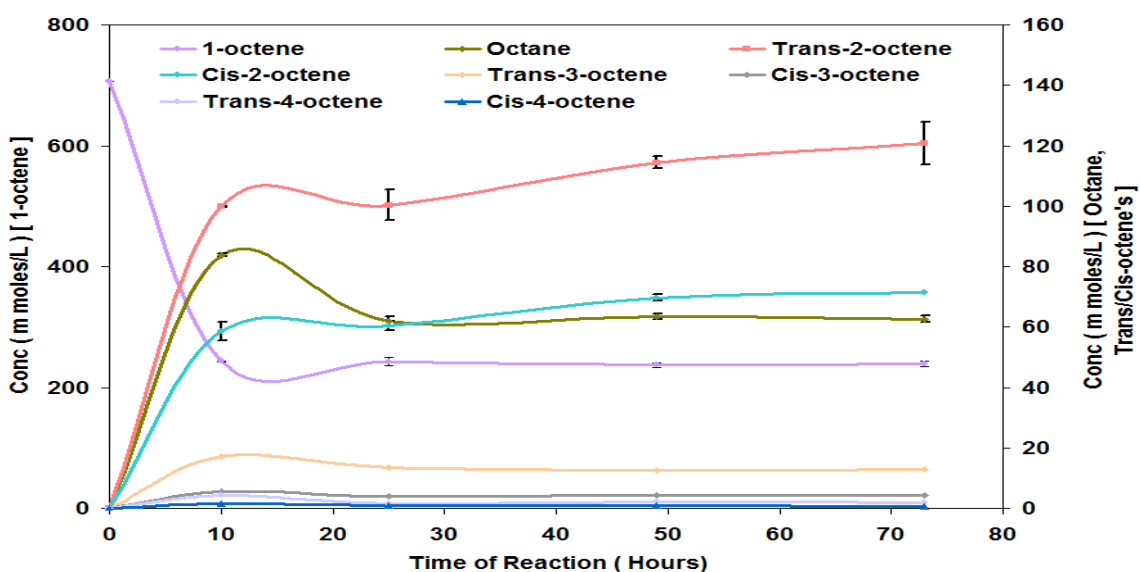

Figure 3.69 Reaction profile of 1-octene hydrogenation [Reaction conditions: T = 140°C, WHSV$_{PyGas}$ = 4 h^{-1}, P$_T$ = 20 barg, P$_{H2}$ = 1 barg]

Figures 3.70-71 show that the yield and selectivity towards internal octenes was significantly increased with the decrease in hydrogen partial pressure. The formation of the product was observed in the following order.

Trans-2-octene > Cis-2-octene ≈ Octane > Trans-3-octene > Cis-3-octene > Trans-4-octene > Cis-4-octene

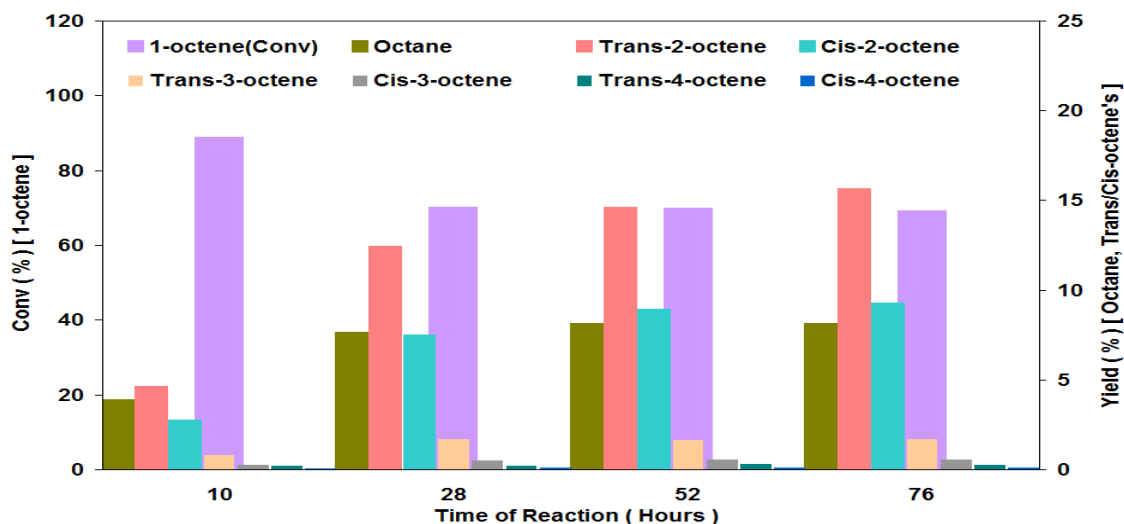**Figure 3.70 Percent yield of 1-octene hydrogenation [Reaction conditions: T = 140°C, WHSV$_{PyGas}$ = 4 h^{-1}, P$_T$ = 20 barg, P$_{H2}$ = 1 barg]**

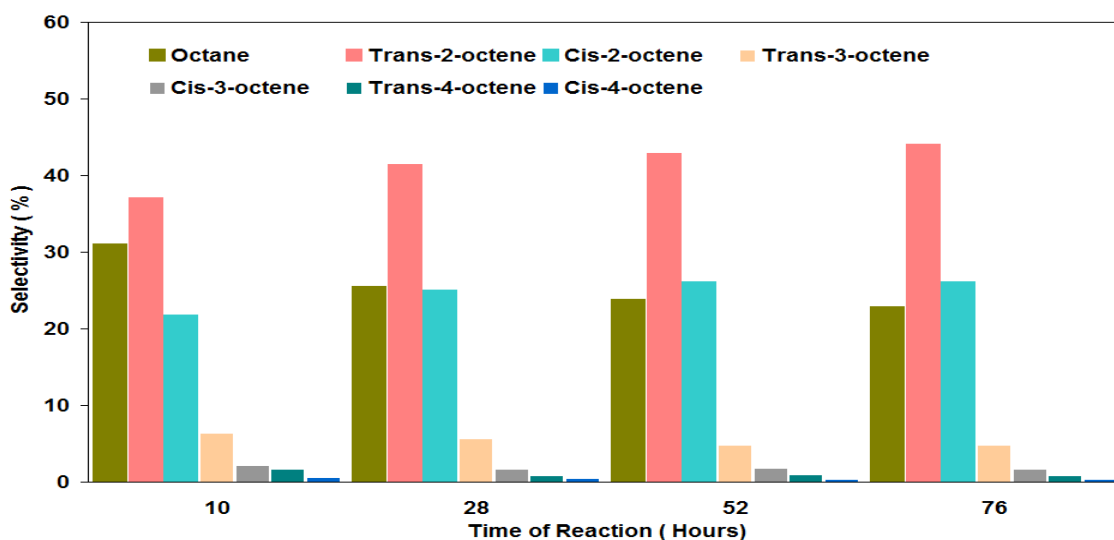**Figure 3.71 Selectivity of octane and internal octenes during 1-octene hydrogenation [Reaction conditions: T = 140°C, WHSV$_{PyGas}$ = 4 h^{-1}, P$_T$ = 20 barg, P$_{H2}$ = 1 barg]**

The ratio of trans/cis in 2-octene was observed to be the same as the trans/cis ratio in 2-pentene. However, a further increase in the trans/cis ratio was seen from 2-octene to 3-octene and 4-octene, as shown in Table 3.14.

Trans/Cis-2-pentene ratio	Trans/Cis-2-octene ratio	Trans/Cis-3-octene ratio	Trans/Cis-4-octene ratio
63:37	63:37	75:25	75:25

Table 3.14 Ratio of trans/cis internal olefins formation in PyGas hydrogenation [Reaction conditions: T = 140°C, WHSV$_{PyGas}$ = 4 h^{-1}, P$_T$ = 20 barg, P$_{H2}$ = 1 barg]

The hydrogenation of cyclopentene to cyclopentane was significantly decreased and the maximum yield of cyclopentane was only about 6% as shown in Figure 3.72.
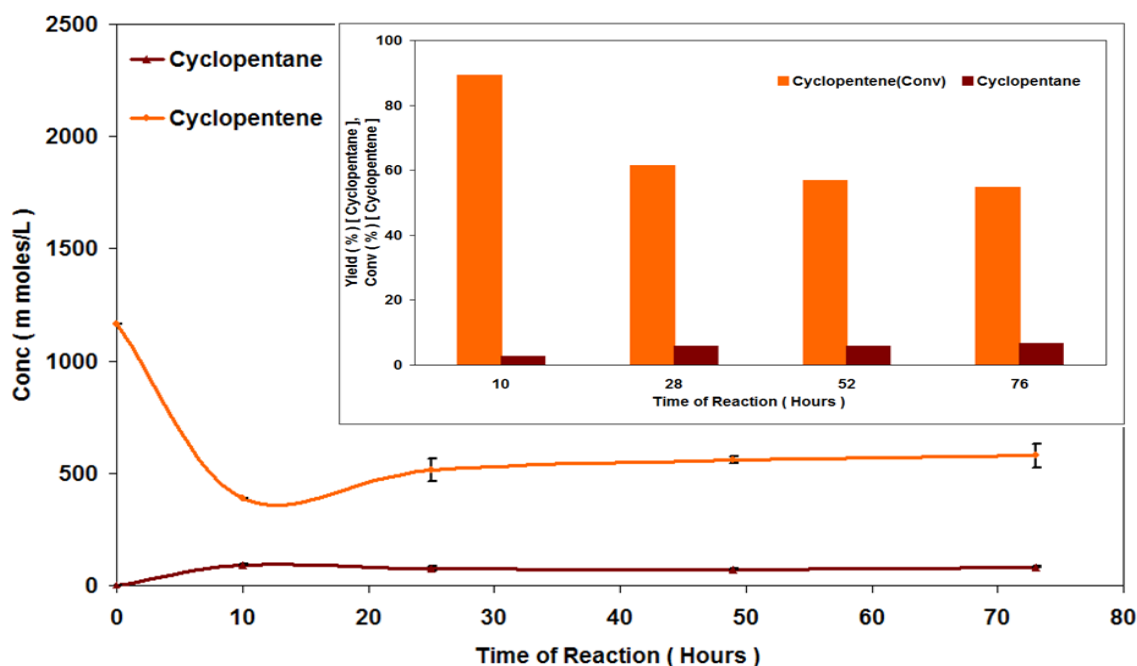
Figure 3.72 Hydrogenation of cyclopentene [Reaction conditions: T = 140°C, WHSV$_{PyGas}$ = 4 h^{-1}, P$_T$ = 20 barg, P$_{H2}$ = 1 barg]

Figure 3.73 shows that virtually no hydrogenation of toluene to methylcyclo-hexane was observed during the reaction.
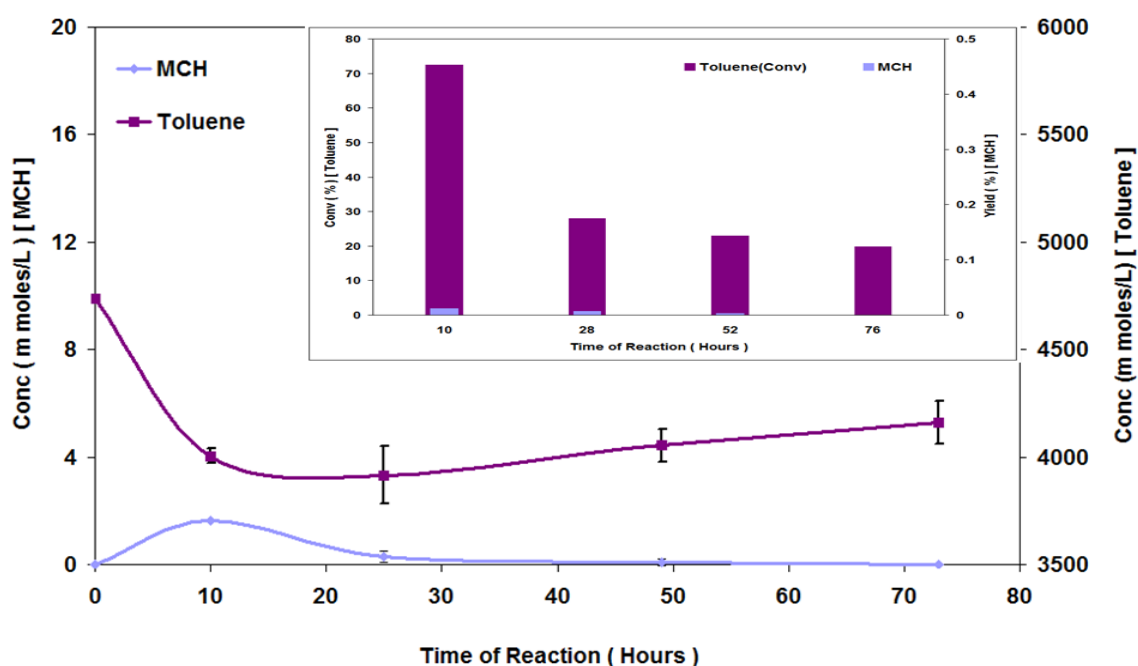

Figure 3.73 Hydrogenation of toluene [Reaction conditions: T = 140°C, WHSV$_{PyGas}$ = 4 h^{-1}, P$_T$ = 20 barg, P$_{H2}$ = 1 barg]

The conversion of styrene was 93% in the initial 10 hours of the reaction and then decreased to 85% after 28 hours when the reaction obtained steady state conditions. The styrene was hydrogenated to ethylbenzene and no ethylcyclohexane was observed in the reaction, as shown in Figure 3.74.
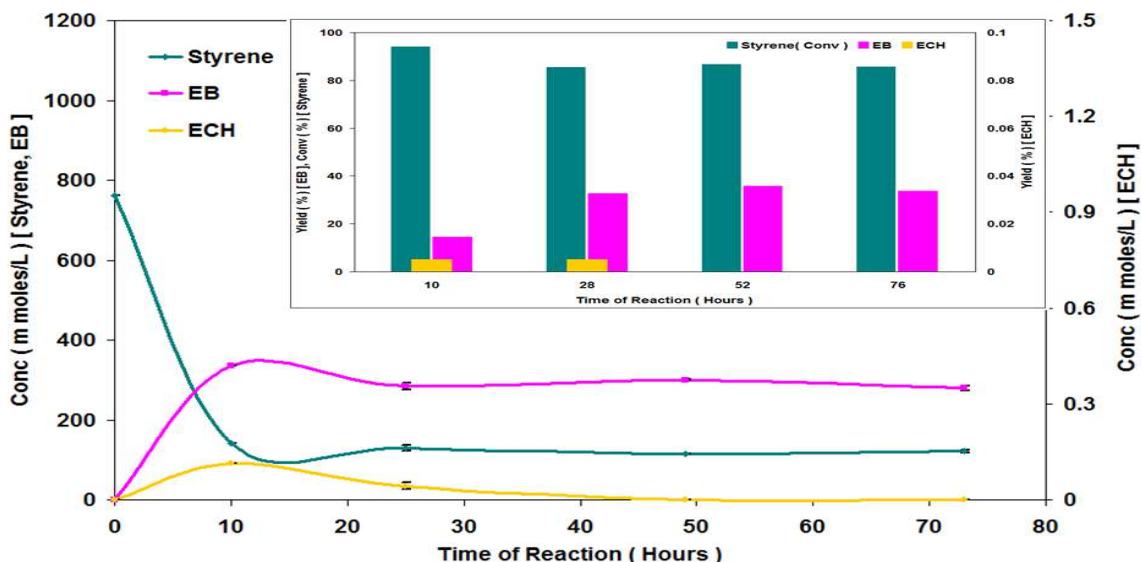
Figure 3.74 Hydrogenation of styrene [Reaction conditions: T = 140°C, WHSV$_{PyGas}$ = 4 h^{-1}, P$_T$ = 20 barg, P$_{H2}$ = 1 barg]

3.2.2.2.3.1 Post reaction analysis

Post reaction catalyst TPO

The post reaction *In-situ* TPO of the catalyst was performed as shown in Figure 3.75. A higher amount of coke deposition was observed over the surface of the catalyst when compared to previous reactions performed with 100%, 50% and 25% hydrogen gas mixtures. This shows that the amount of coke deposition increased with a decrease in the hydrogen partial pressure. Whilst, similar quantities of styrene, benzene, 1-pentene, cyclopentene, 1-octene, pentane, octane, toluene, methylcyclohexane, ethylbenzene, ethylcyclohexane and H$_2$ were evolved as seen with the TPOs of the catalysts, used in the previous reactions carried out with 100%, 50% and 25% hydrogen gas mixtures.
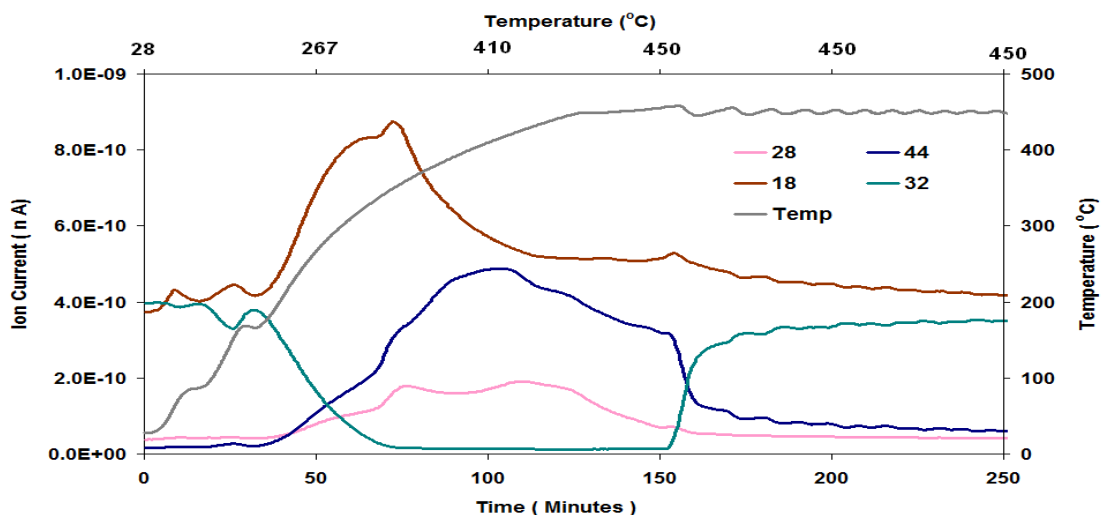

Figure 3.75 Post reaction *in-situ* TPO of Ni/Al$_2$O$_3$ catalyst [Reaction conditions: T = 140°C, WHSV$_{PyGas}$ = 4 h^{-1}, P$_T$ = 20 barg, P$_{H2}$ = 1 barg]

Total oxygen consumption in TPO = 3.41 m moles

BET analysis

The surface area, pore volume and pore diameter of the regenerated Ni/Al$_2$O$_3$ catalyst were analysed and the results are tabulated in Table 3.15 below.

Catalyst	Surface Area (m^{2}g^{-1})	Pore Volume (cm^{3}g^{-1})	Average Pore diameter (Å)
Ni/Al$_2$O$_3$	93	0.35	152
Ni/Al$_2$O$_3$ (Reduced)	106	0.39	150
Ni/Al$_2$O$_3$ (Regenerated)	88	0.34	157

Table 3.15 BET analysis of Ni/Al$_2$O$_3$ (Regenerated) catalyst [Reaction conditions: T = 140°C, WHSV$_{PyGas}$ = 4 h^{-1}, P$_T$ = 20 barg, P$_{H2}$ = 1 barg]

3.2.2.3 Effect of total reaction pressure on PyGas hydrogenation

The reactions were performed at 10 barg and 20 barg total reaction pressure to study the effect of the total reaction pressure on the hydrogenation of PyGas and all other reaction parameters were kept constant [T = 140°C and WHSV$_{PyGas}$ = 4 h^{-1}]. The study was performed with 50% hydrogen gas mixture diluted with nitrogen. The reaction of PyGas hydrogenation at 20 barg was discussed in section 3.2.2.2.1 and the reaction at 10 barg is presented in this section. The reaction profile of PyGas hydrogenation is shown in Figure 3.76.
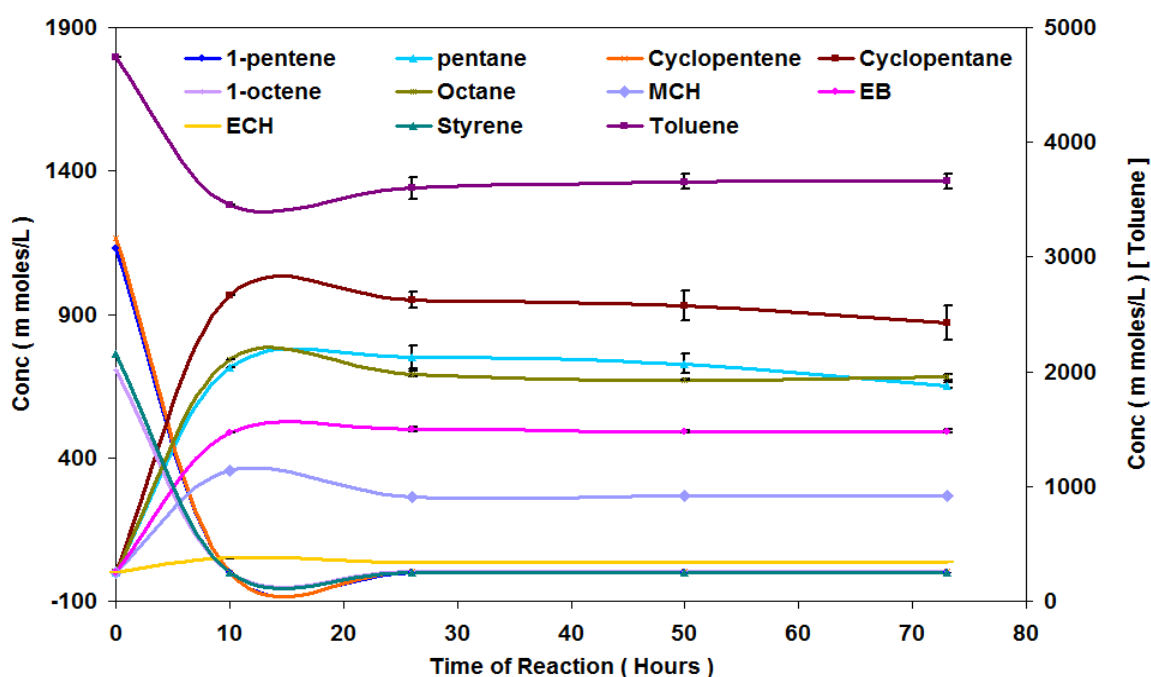

Figure 3.76 Reaction profile of PyGas Hydrogenation [Reaction conditions: T = 140°C, WHSV$_{PyGas}$ = 4 h^{-1}, P$_T$ = 10 barg]

Pentane was the main product of the reaction during the hydrogenation of 1-pentene. However, small amounts of trans-2-pentene and cis-2-pentene were also observed and are shown in Figures 3.77-78. The total yield of the 1-pentene hydrogenation was decreased with a decrease in pressure of reaction from 20 barg to 10 barg.
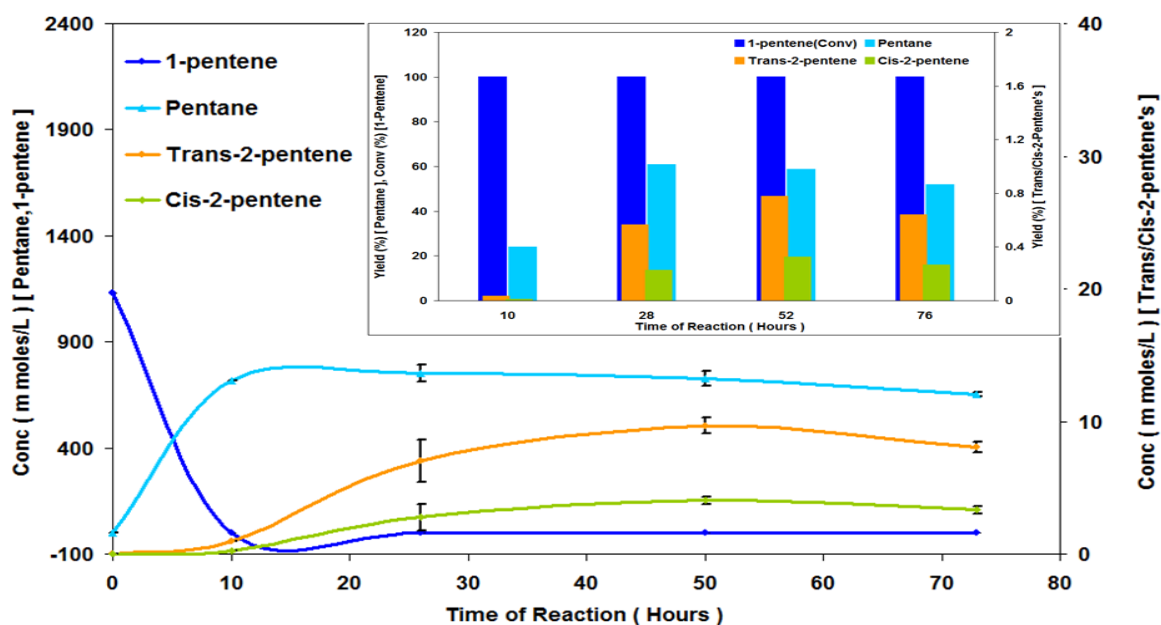

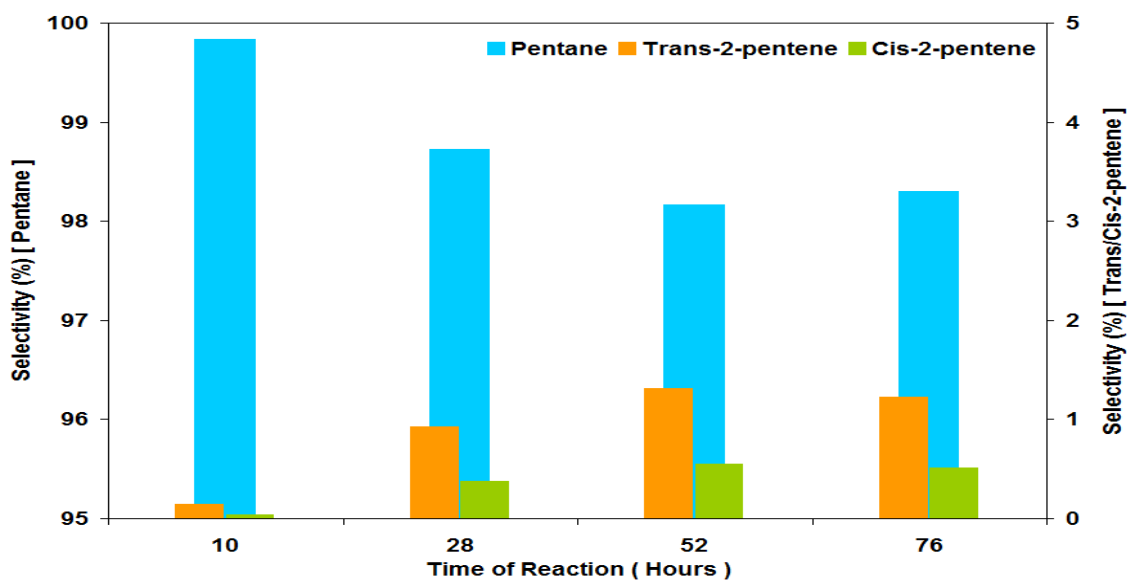**Figure 3.77 Hydrogenation of 1-pentene [Reaction conditions: T = 140°C, WHSV$_{PyGas}$ = 4 h^{-1}, P$_T$ = 10 barg]**

Figure 3.78 Selectivity of pentane, trans-2-pentene and cis-2-pentene during 1-pentene hydrogenation [Reaction conditions: T = 140°C, WHSV$_{PyGas}$ = 4 h^{-1}, P$_T$ = 10 barg]

The 1-octene was hydrogenated to octane whilst small amounts of internal octenes were also observed in the reaction, as shown in Figure 3.79. A slight increase was found in the yield of internal octane with time on stream.
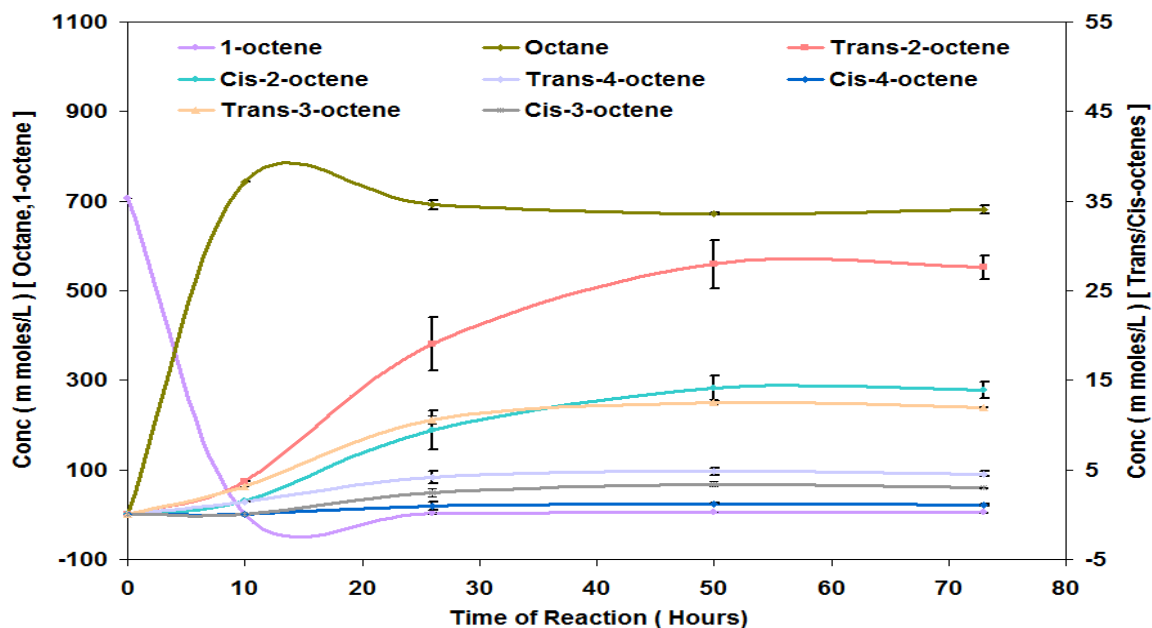
Figure 3.79 Reaction profile of 1-octene hydrogenation [Reaction conditions: T = 140°C, WHSV$_{PyGas}$ = 4 h^{-1}, P$_T$ = 10 barg]

Figures 3.80-81 show that octane was the principal product in the hydrogenation of 1-octene. However, small amounts of internal octenes were also observed. The formation of the products was found to be in the order below,

Octane >> Trans-2-octene > Cis-2-octene ≈ Trans-3-octene > Trans-4-octene > Cis-3-octene > Cis-4-octene

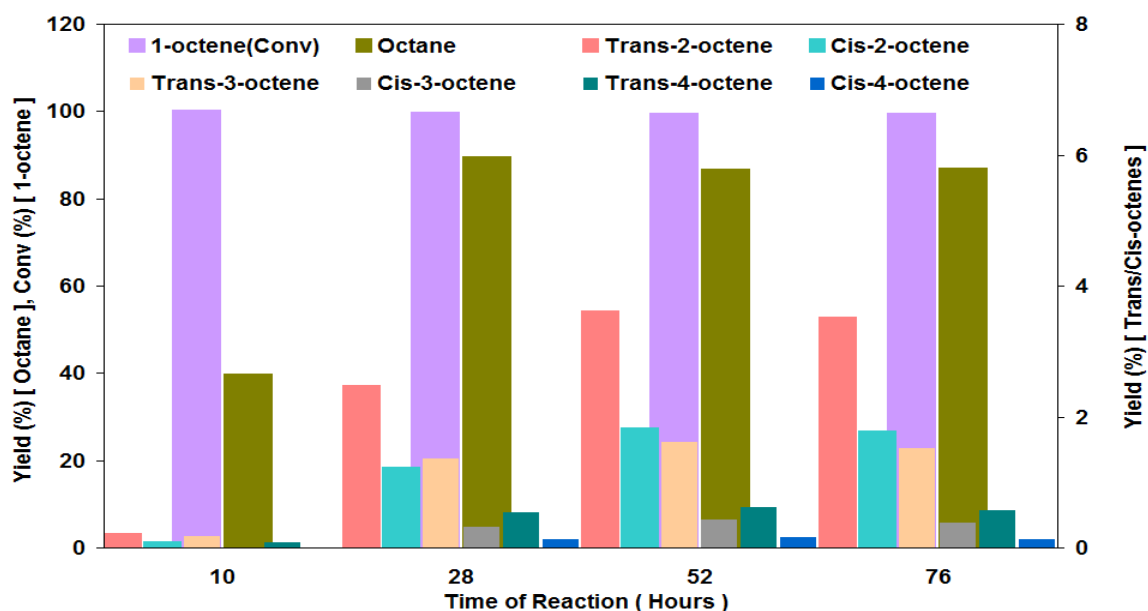**Figure 3.80 Percent yield of 1-octene hydrogenation [Reaction conditions: T = 140°C, WHSV$_{PyGas}$ = 4 h^{-1}, P$_T$ = 10 barg]**

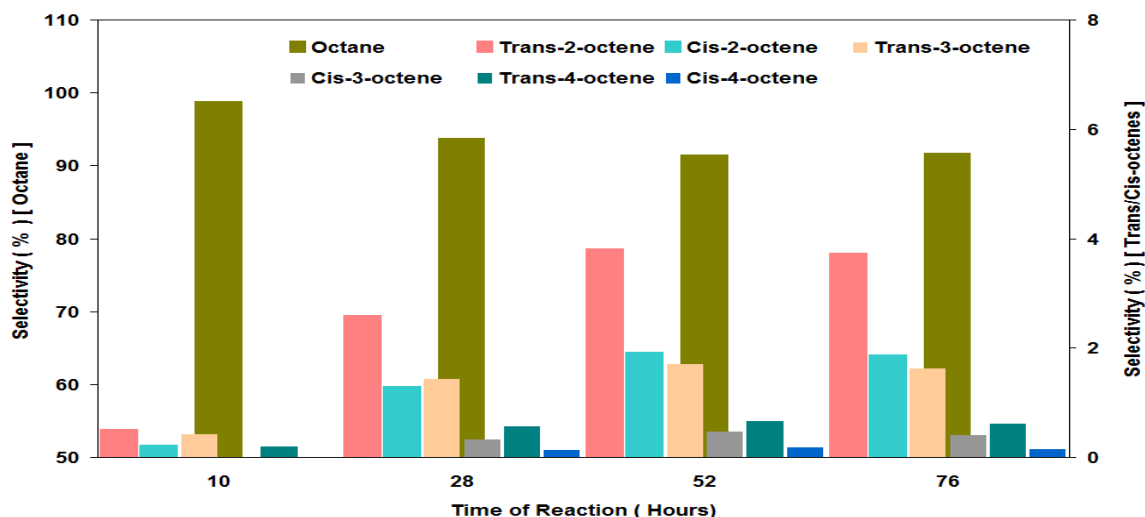**Figure 3.81 Selectivity of octane and internal octenes during 1-octene hydrogenation [Reaction conditions: T = 140°C, WHSV$_{PyGas}$ = 4 h^{-1}, P$_T$ = 10 barg]**

The ratio of trans/cis in 2-octene observed was virtually the same as the trans/cis ratio in 2-pentene. However, a further increase in the trans/cis ratio was seen from 2-octene to 3-octene and 4-octene as shown in Table 3.16.

Trans/Cis-2-pentene ratio	Trans/Cis-2-octene ratio	Trans/Cis-3-octene ratio	Trans/Cis-4-octene ratio
70:30	67:33	80:20	80:20

Table 3.16 Ratio of trans/cis internal olefins formation in PyGas hydrogenation [Reaction conditions: T = 140°C, WHSV$_{PyGas}$ = 4 h^{-1}, P$_T$ = 10 barg]

Conversion of cyclopentene was observed at above 99%. But, a reasonable decrease was observed in the yield of cyclopentane with the decrease in reaction pressure from 20 barg to 10 barg, as shown in Figure 3.82.
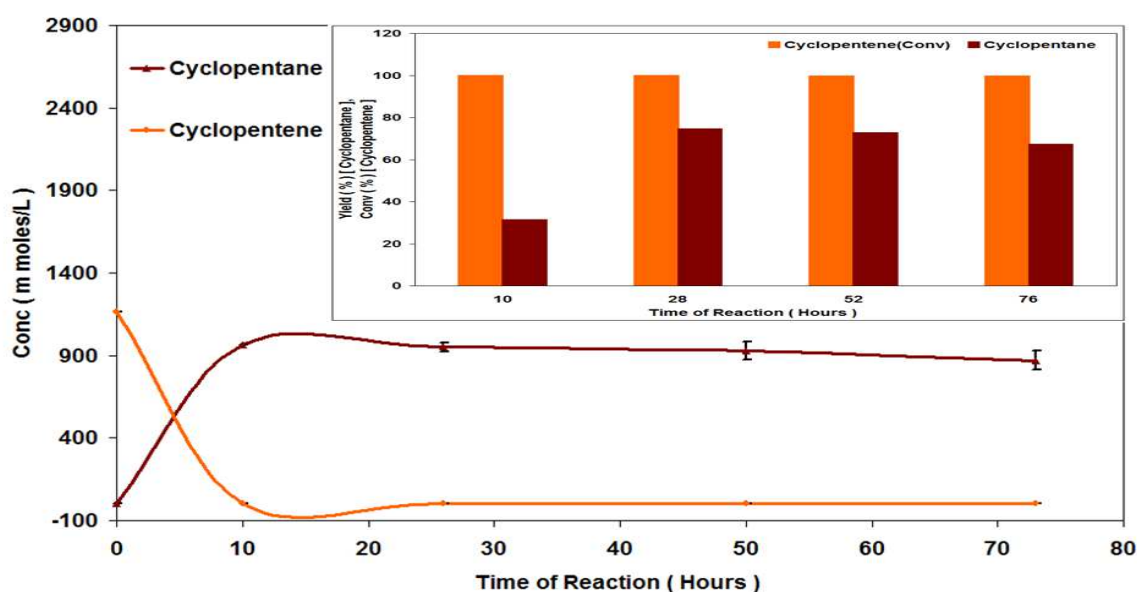

Figure 3.82 Hydrogenation of cyclopentene [Reaction conditions: T = 140°C, WHSV$_{PyGas}$ = 4 h^{-1}, P$_T$ = 10 barg]

No significant change was observed in the conversion of toluene with a decrease in total reactor pressure from 20 to 10 barg. However, a reasonable decrease was observed in the yield of methylcyclohexane, as shown in Figure 3.83. The results suggest that a higher amount of toluene deposition had occurred over the catalyst.
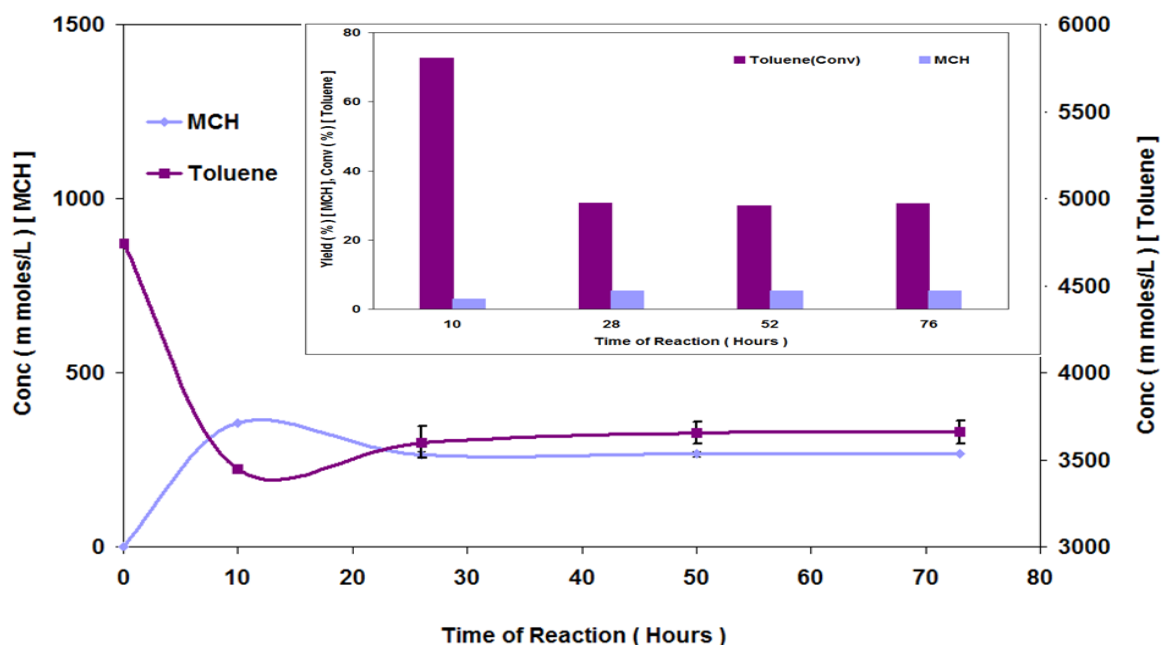

Figure 3.83 Hydrogenation of toluene [Reaction conditions: T = 140°C, WHSV$_{PyGas}$ = 4 h^{-1}, P$_T$ = 10 barg]

The conversion of styrene remained at above 99% throughout the reaction. No significant change was observed in the yield of the products with decrease in total reaction pressure as shown in Figures 3.84-85.
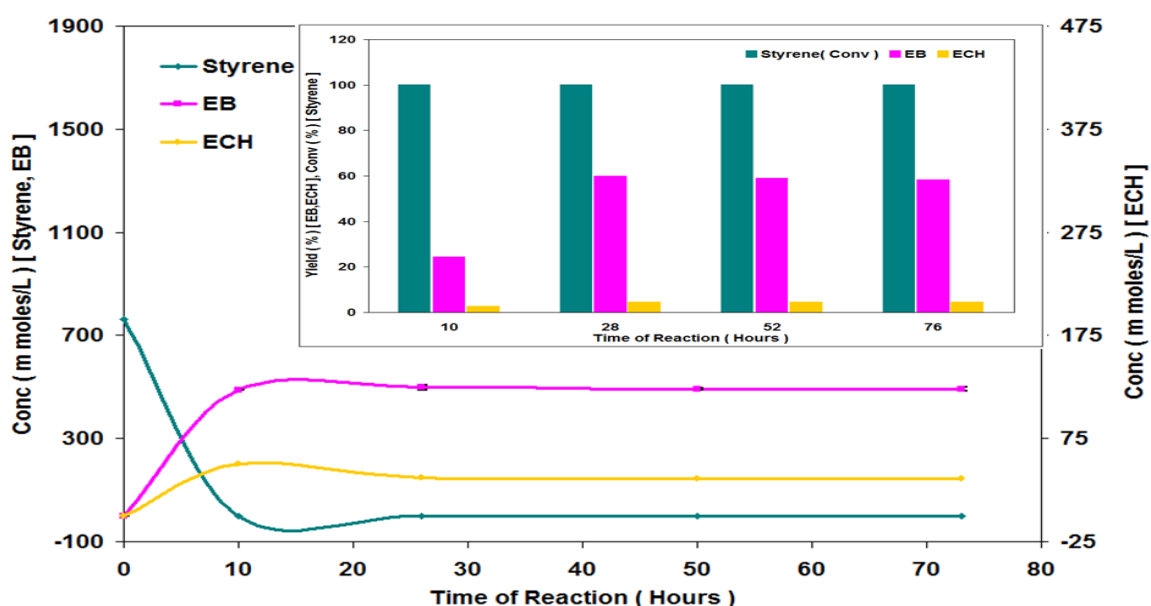

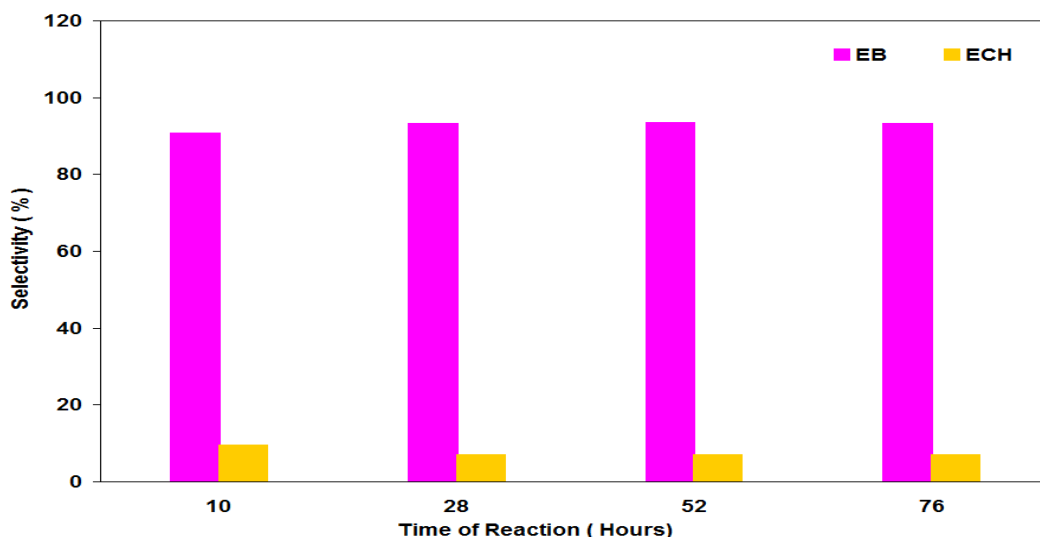**Figure 3.84 Hydrogenation of styrene [Reaction conditions: T = 140°C, WHSV$_{PyGas}$ = 4 h^{-1}, P$_T$ = 10 barg]**

Figure 3.85 Selectivity of ethylbenzene and ethylcyclohexane during hydrogenation of styrene [Reaction conditions: T = 140°C, $WHSV_{PyGas}$ = 4 h^{-1}, P_T = 10 barg]

3.2.2.3.1.1 Post reaction analysis

Post reaction catalyst TPO

The *in-situ* TPO of the post reaction catalyst was carried out and shown in Figure 3.86. The results indicate that a higher amount of coke deposition was observed with the decrease in total reactor pressure, whilst no significant change was observed in the evolution of styrene, benzene, 1-pentene, pentane, 1-octene, cyclopentene, octane, methylcyclohexane, ethylcyclohexane, ethylbenzene, toluene and H_2 in both the TPOs.
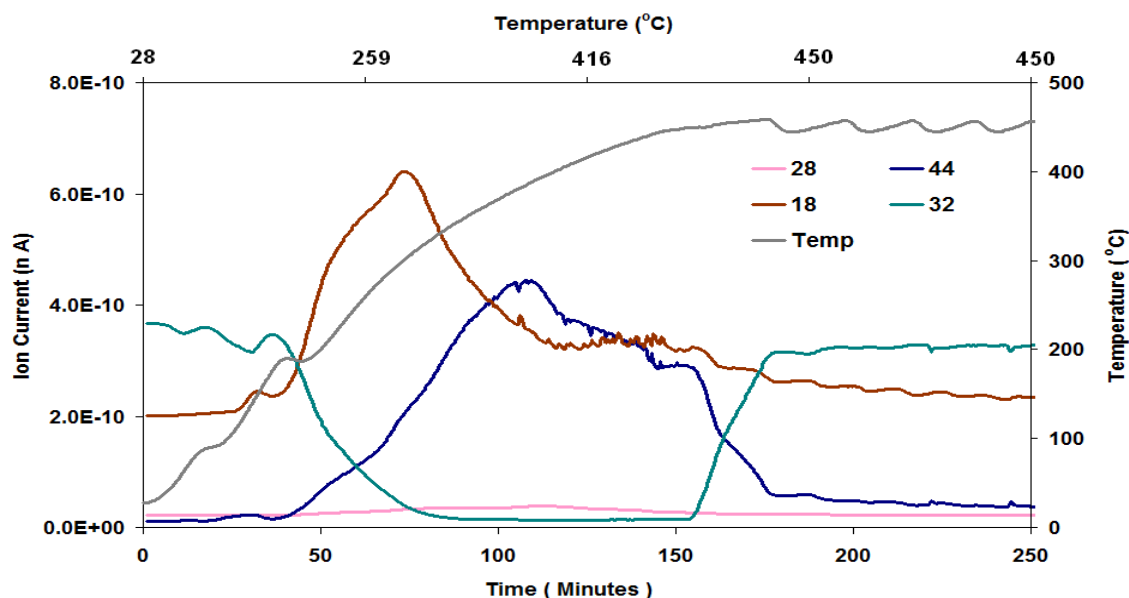

Figure 3.86 Post reaction *in-situ* TPO of Ni/Al$_2$O$_3$ catalyst [Reaction conditions: T = 140°C, $WHSV_{PyGas}$ = 4 h^{-1}, P_T = 10 barg]

Total oxygen consumption in TPO = 3.53 m moles

BET analysis

The surface area, pore volume and pore diameter of the regenerated catalyst were analysed and the results can be seen in Table 3.17 below.

Catalyst	Surface Area (m^2g^{-1})	Pore Volume (cm^3g^{-1})	Average Pore diameter (Å)
Ni/Al_2O_3	93	0.35	152
Ni/Al_2O_3 (Reduced)	106	0.39	150
Ni/Al_2O_3 (Regenerated)	89	0.34	153

Table 3.17 BET analysis of Ni/Al_2O_3 (Regenerated) catalyst [Reaction conditions: T = 140°C, $WHSV_{PyGas}$ = 4 h^{-1}, P_T = 10 barg]

The surface area of regenerated catalyst was observed to be slightly less than that of the fresh catalyst.

3.2.2.4 Effect of PyGas feed flow rate ($WHSV_{PyGas}$) on PyGas hydrogenation

The reactions were performed with different WHSV of PyGas (4-8 h^{-1}) to study the effects of feed flow rate of PyGas ($WHSV_{PyGas}$) on the hydrogenation of PyGas. Different strategies were used to investigate the effect of PyGas feed flow rate ($WHSV_{PyGas}$) on hydrogenation of PyGas. Firstly, the weight of the catalyst was kept constant and feed flow rate of PyGas was changed, whilst in the second case, the PyGas feed was kept the same while the catalyst weight was altered. In addition, the reactions were performed in two types of hydrogen gas mixtures (50% and 25%) for more comprehensive results. The hydrogenation of PyGas carried out at $WHSV_{PyGas}$ 4 h^{-1} using 50% and 25% hydrogen gas mixtures are already discussed in section 3.2.2.2.1 and 3.2.2.2.2 respectively, while the reactions at $WHSV_{PyGas}$ at 8 h^{-1} are revealed in this section.

3.2.2.4.1 PyGas Hydrogenation over Ni/Al_2O_3 at $WHSV_{PyGas}$ = 8 h^{-1} using 50% hydrogen gas [catalyst weight = 0.5 g]

The hydrogenation of PyGas over Ni/Al_2O_3 at $WHSV_{PyGas}$ of 8 h^{-1} by doubling the feed flow rate of PyGas, was carried out using a 50% hydrogen gas and other reaction conditions were kept constant [catalyst weight = 0.5g, T = 140°C and P_T = 20 barg]. The reaction profile is shown in Figure 3.87.
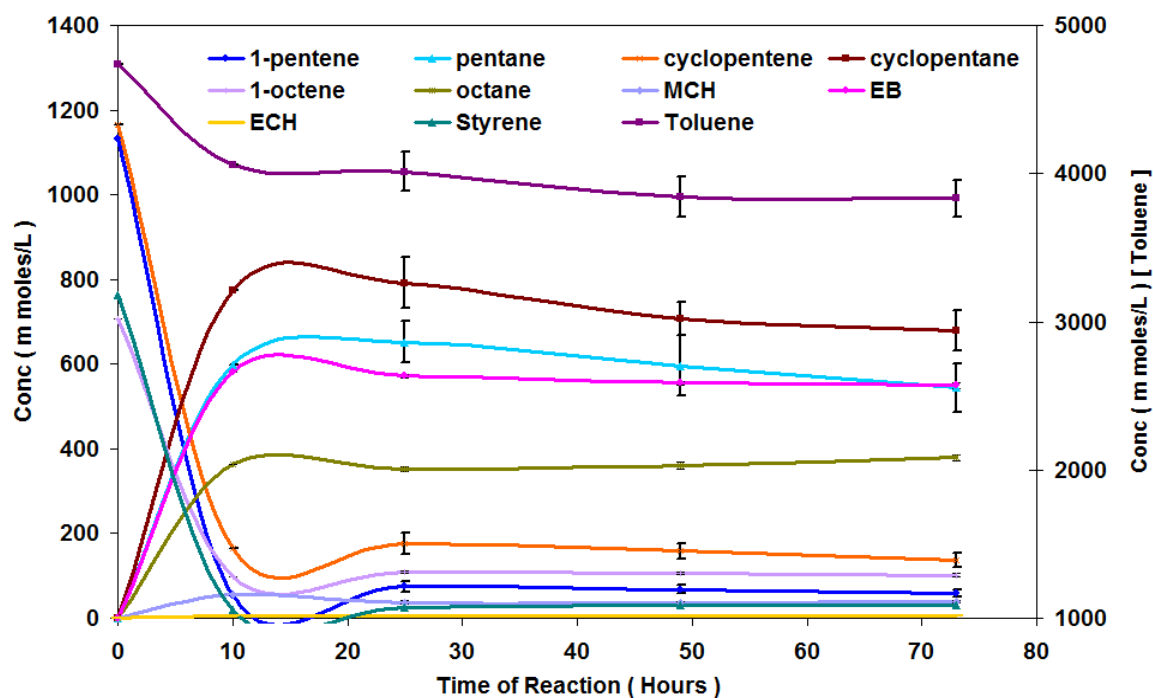
Figure 3.87 Reaction profile of PyGas Hydrogenation [Reaction conditions: T = 140°C, WHSV$_{PyGas}$ = 8 h^{-1}, P$_T$ = 20 barg, P$_{H2}$ = 10 barg]

The conversion of 1-pentene was 97% in the first 10 hours of reaction, which decreased to 94% after 28 hours and remained constant through until the end of the reaction. The catalyst selectivity towards internal pentenes was increased with an increase in WHSV of PyGas. However a decrease was observed in the total yield of the reaction, as shown in Figures 3.88-89.
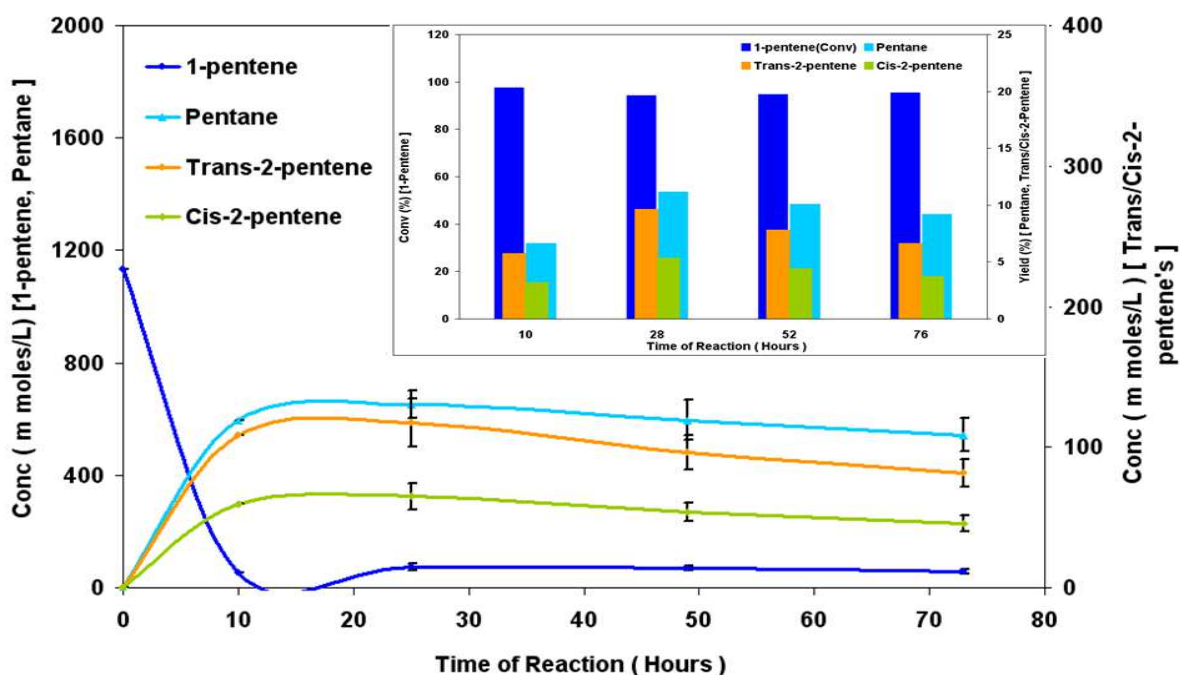

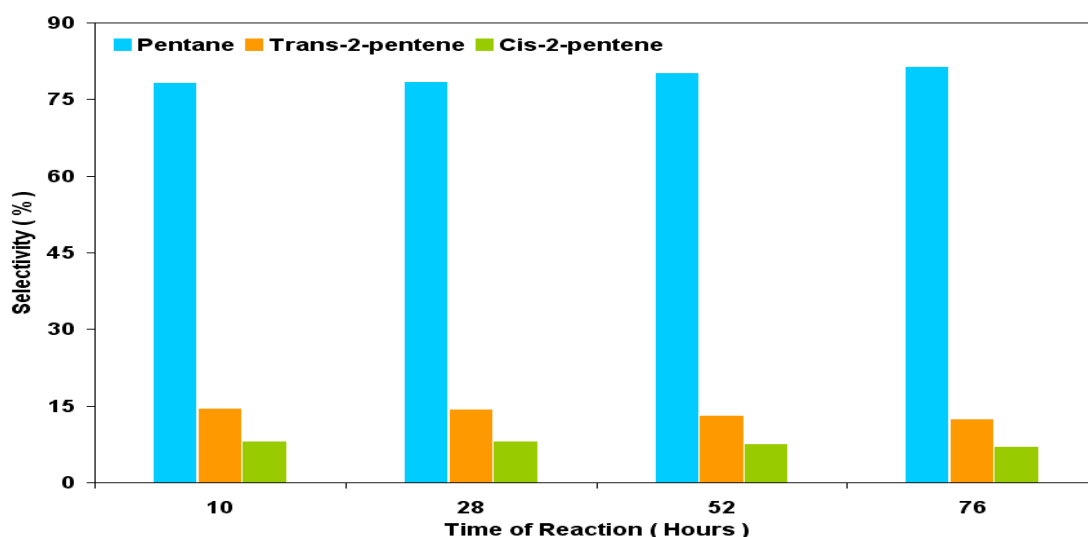**Figure 3.88 Hydrogenation of 1-pentene [Reaction conditions: T = 140°C, WHSV$_{PyGas}$ = 8 h^{-1}, P$_T$ = 20 barg, P$_{H2}$ = 10 barg]**

Figure 3.89 Selectivity of pentane, trans-2-pentene and cis-2-pentene during 1-pentene hydrogenation [Reaction conditions: T = 140°C, WHSV$_{PyGas}$ = 8 h^{-1}, P$_T$ = 20 barg, P$_{H2}$ = 10 barg]

Figure 3.90 represents the concentration profile of the 1-octene hydrogenation. Octane was the primary product however significant amounts of internal octenes were also produced during 1-octene hydrogenation.
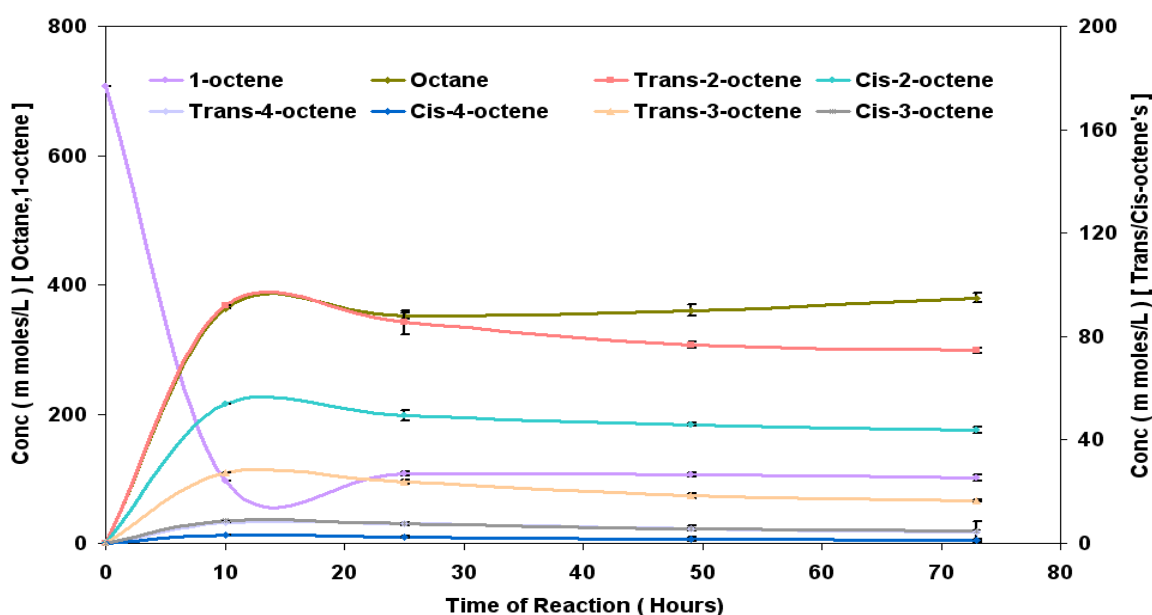
Figure 3.90 Reaction profile of 1-octene hydrogenation [Reaction conditions: T = 140°C, WHSV$_{PyGas}$ = 8 h^{-1}, P$_T$ = 20 barg, P$_{H2}$ = 10 barg]

The conversion of 1-octene was 91% in the first 10 hours of reaction, which decreased to 86% after 28 hours and remained constant for the rest of the reaction. The yield and selectivity of products are shown in Figures 3.91-92. The products formation during 1-octene hydrogenation followed the following order,

Octane >> Trans-2-octene > Cis-2-octene > Trans-3-octene > Cis-3-octene ≈ Trans-4-octene > Cis-4-octene
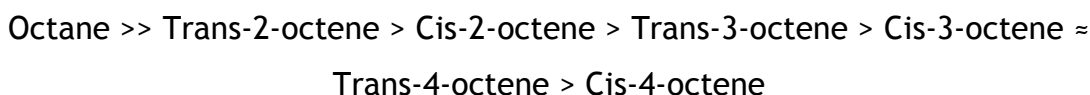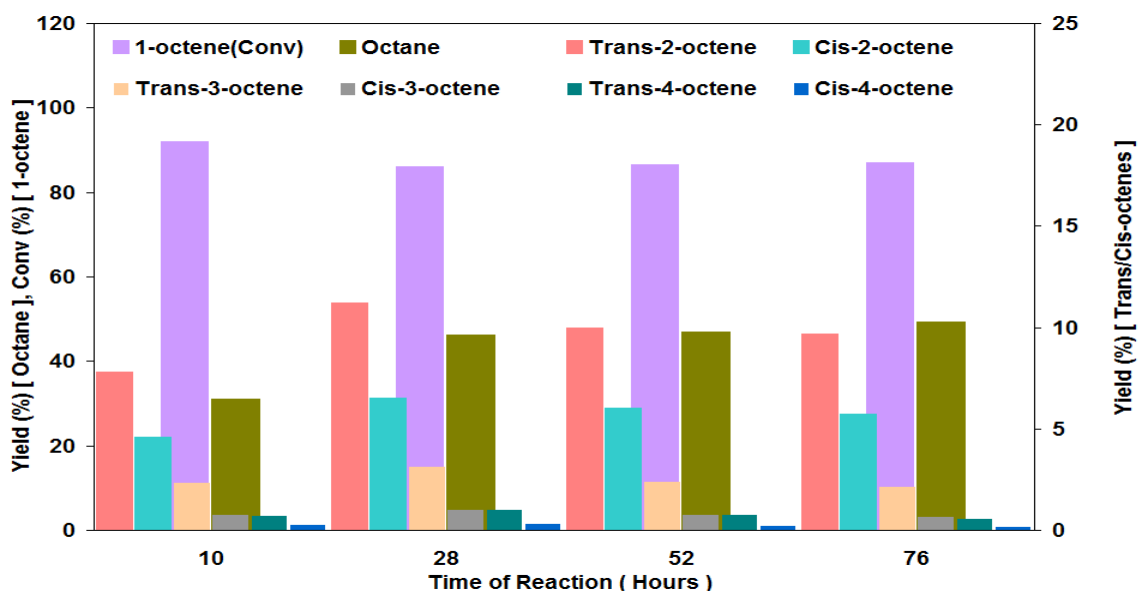
Figure 3.91 Percent yield of 1-octene hydrogenation [Reaction conditions: T = 140°C, WHSV$_{PyGas}$ = 8 h^{-1}, P$_T$ = 20 barg, P$_{H2}$ = 10 barg]
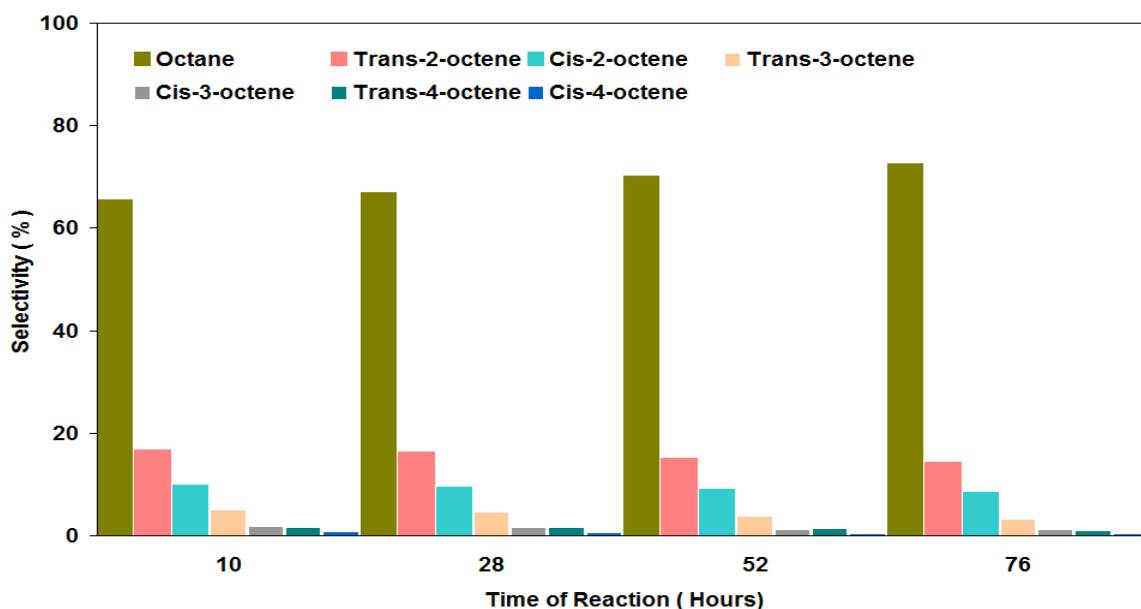
Figure 3.92 Selectivity of octane and internal octenes during 1-octene hydrogenation [Reaction conditions: T = 140°C, WHSV$_{PyGas}$ = 8 h^{-1}, P$_T$ = 20 barg, P$_{H2}$ = 10 barg]

The formation of the trans isomer was found to be greater than for its respective cis isomer due to the trans isomers thermodynamic stability. The ratio of trans/cis isomers is shown in Table 3.18.

Trans/Cis-2-pentene ratio	Trans/Cis-2-octene ratio	Trans/Cis-3-octene ratio	Trans/Cis-4-octene ratio
64:36	63:37	76:23	76:23

Table 3.18 Ratio of trans/cis internal olefins formation in PyGas hydrogenation [Reaction conditions: T = 140°C, WHSV$_{PyGas}$ = 8 h^{-1}, P$_T$ = 20 barg, P$_{H2}$ = 10 barg]

The conversion of cyclopentene was observed to be above 86% during the reaction, although a significant decrease was observed in the yield of cyclopentane with the increase in WHSV of PyGas as shown in Figure 3.93.
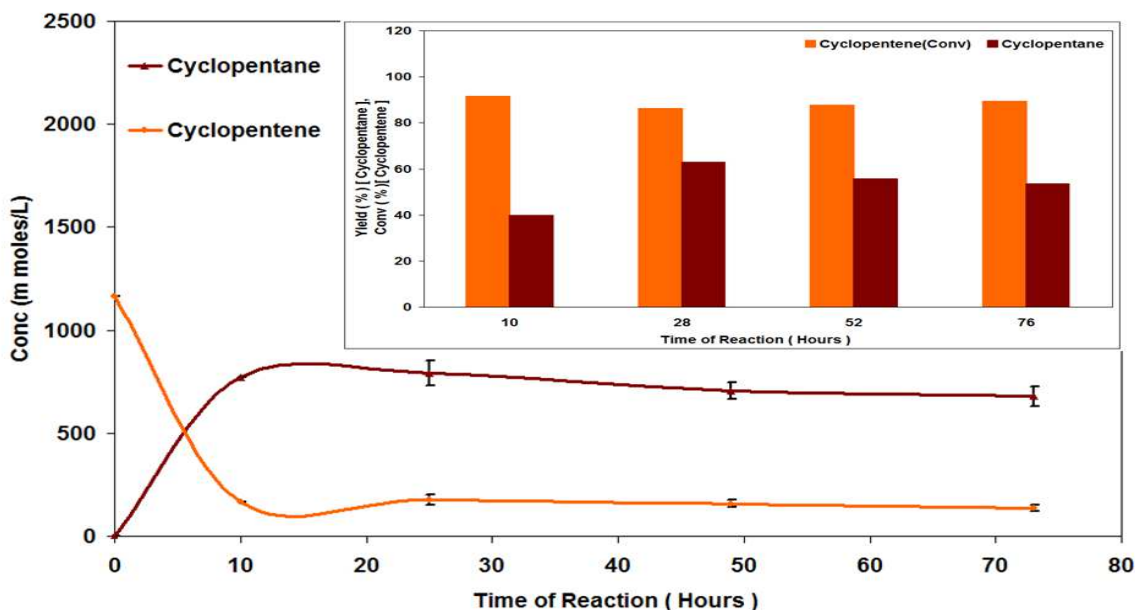
Figure 3.93 Hydrogenation of cyclopentene [Reaction conditions: T = 140°C, WHSV$_{PyGas}$ = 8 h$^-$^{1}, P$_T$ = 20 barg, P$_{H2}$ = 10 barg]

Figure 3.94 shows that negligible amounts of methylcyclohexane formation were seen in the reaction, whilst reasonable conversion of toluene was still observed.
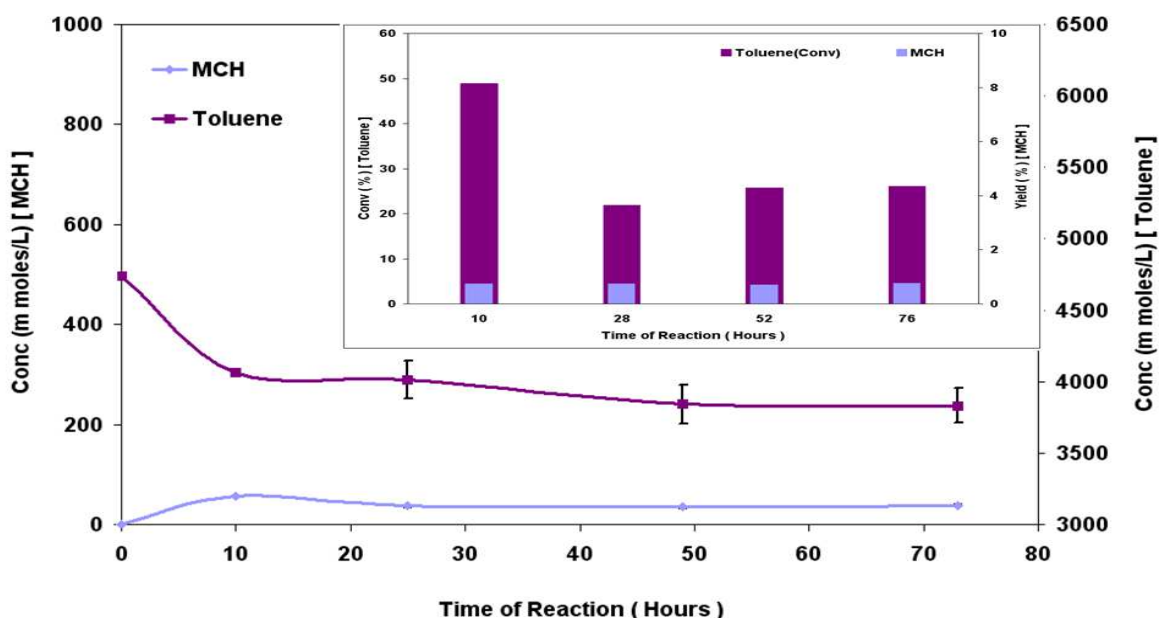
Figure 3.94 Hydrogenation of toluene [Reaction conditions: T = 140°C, WHSV$_{PyGas}$ = 8 h^{-1}, P$_T$ = 20 barg, P$_{H2}$ = 10 barg]

The conversion of styrene remained above 96% throughout the reaction. Ethylbenzene was the primary product of the reaction and virtually no ethylcyclohexane was observed, as shown in Figure 3.95.
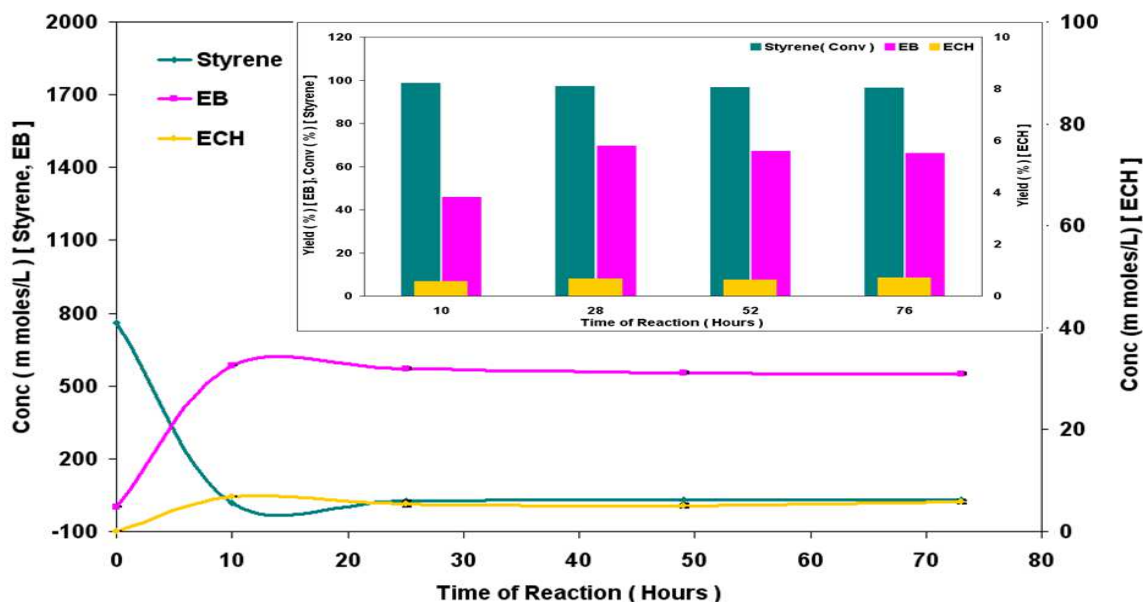
Figure 3.95 Hydrogenation of styrene [Reaction conditions: T = 140°C, WHSV$_{PyGas}$ = 8 h^{-1}, P$_T$ = 20 barg, P$_{H2}$ = 10 barg]

3.2.2.4.1.1 Post reaction analysis

Post reaction catalyst TPO

A post reaction *in-situ* TPO was performed over the catalyst and is shown in Figure 3.96. The results indicate that the amount of coke observed was slightly smaller when compared to the reaction performed at WHSV$_{PyGas}$ 4 h^{-1}. Whilst, the evolution of styrene, benzene, 1-pentene, cyclopentene, 1-octene, pentane, octane, toluene, methylcyclohexane, ethylbenzene, ethylcyclohexane and H$_2$ during TPO was found to be similar to that observed from the catalyst used in the reaction at WHSV$_{PyGas}$ 4 h^{-1}.
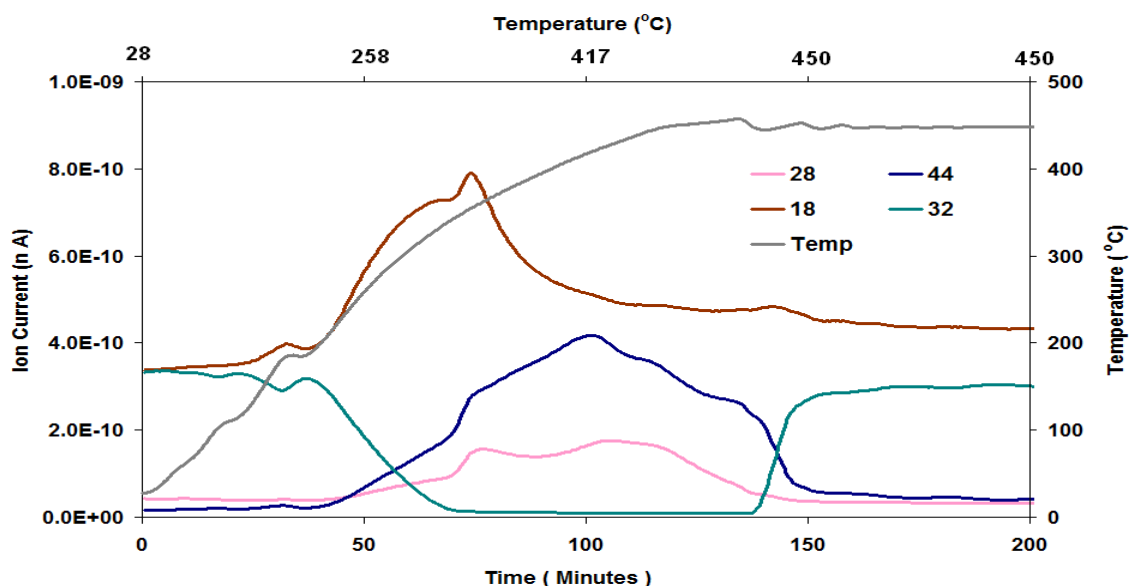
Figure 3.96 Post reaction *in-situ* TPO of Ni/Al$_2$O$_3$ catalyst [Reaction conditions: T = 140°C, WHSV$_{PyGas}$ = 8 h^{-1}, P$_T$ = 20 barg, P$_{H2}$ = 10 barg]

Total oxygen consumption in TPO = 3.06 m moles

BET analysis

The surface area, pore volume and pore diameter of the regenerated catalyst were analysed and the results are shown in Table 3.19 below.

Catalyst	Surface Area (m^2g^{-1})	Pore Volume (cm^3g^{-1})	Average Pore diameter (Å)
Ni/Al$_2$O$_3$	93	0.35	152
Ni/Al$_2$O$_3$ (Reduced)	106	0.39	150
Ni/Al$_2$O$_3$ (Regenerated)	94	0.39	166

Table 3.19 BET analysis of Ni/Al$_2$O$_3$ (Regenerated) catalyst [Reaction conditions: T = 140°C, WHSV$_{PyGas}$ = 8 h^{-1}, P$_T$ = 20 barg, P$_{H2}$ = 10 barg]

3.2.2.4.2 PyGas hydrogenation over Ni/Al$_2$O$_3$ at WHSV$_{PyGas}$ = 8 h^{-1} using 25% hydrogen gas mixture [Catalyst weight = 0.5 g]

The hydrogenation of PyGas over Ni/Al$_2$O$_3$ using a 25% hydrogen gas mixture under reaction conditions [T = 140°C, WHSV$_{PyGas}$ = 4 h^{-1}, P$_T$ = 20 barg and catalyst weight = 0.5 g] is already presented in section 3.2.2.2.2. While, the reaction carried out with the same 25% hydrogen gas mixture at WHSV$_{PyGas}$ 8 h^{-1} by increasing the feed flow rate of PyGas with other reaction conditions kept constant, is discussed in this section. The reaction concentration profile is shown in Figure 3.97.
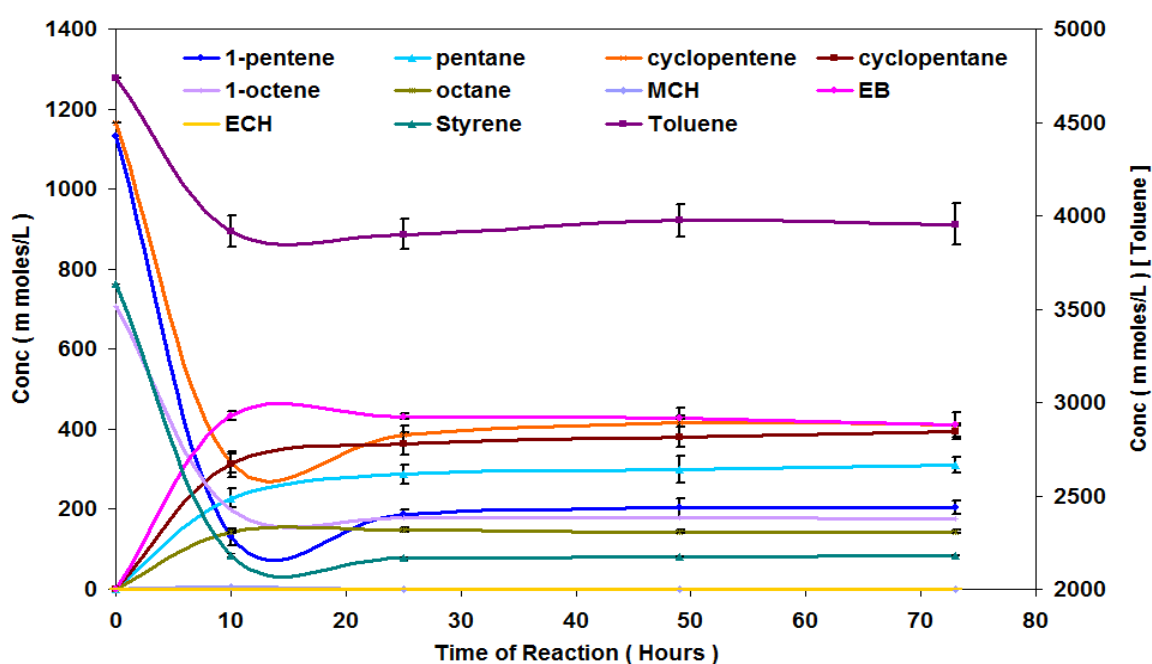
Figure 3.97 Reaction profile of PyGas hydrogenation [Reaction conditions: T = 140°C, WHSV$_{PyGas}$ = 8 h^{-1}, P$_T$ = 20 barg, P$_{H2}$ = 5 barg]

Figure 3.98 shows that the conversion of 1-pentene was 92% in the initial 10 hours of the reaction, which decreased to 84% after 28 hours when reaction had obtained steady state conditions and remained virtually constant for the rest of reaction. The formation of internal pentenes was significantly increased in this reaction. The selectivity of the catalyst towards trans-2-pentene and cis-2-pentene was considerably increased with the change in WHSV of PyGas from 4 h^{-1} to 8 h^{-1}, as shown in Figure 3.99.
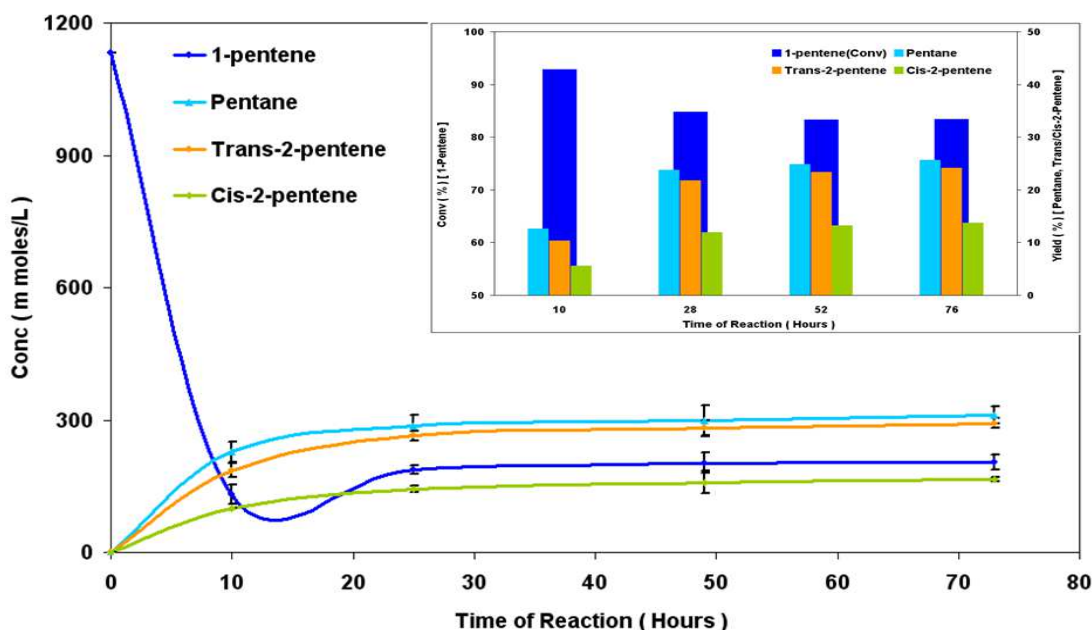
Figure 3.98 Hydrogenation of 1-pentene [Reaction conditions: T = 140°C, WHSV$_{PyGas}$ = 8 h^{-1}, P$_T$ = 20 barg, P$_{H2}$ = 5 barg]
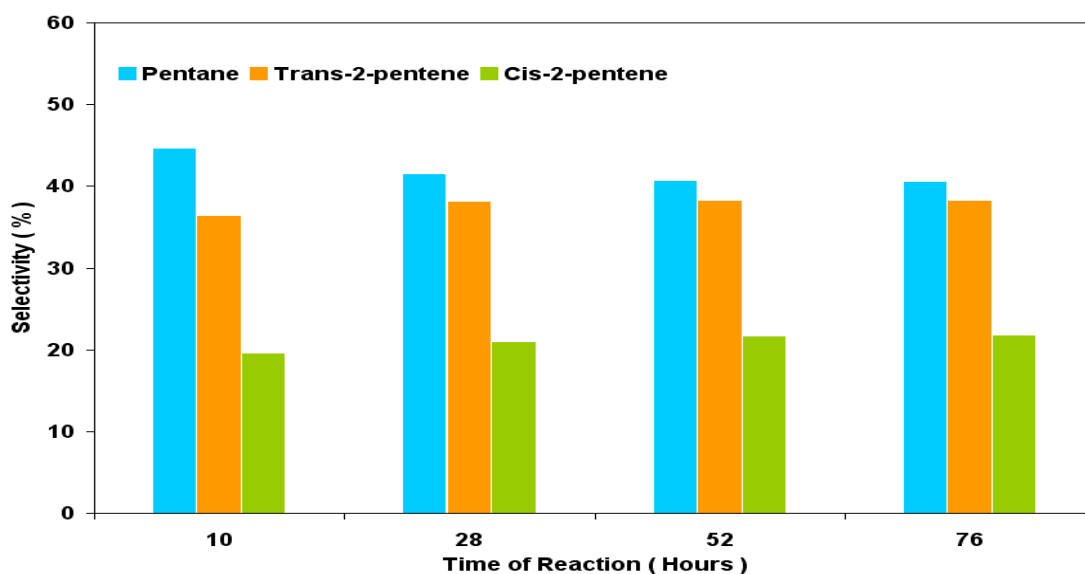
Figure 3.99 Selectivity of Pentane, trans-2-pentene and cis-2-pentene during 1-pentene hydrogenation [Reaction conditions: T = 140°C, WHSV$_{PyGas}$ = 8 h^{-1}, P$_T$ = 20 barg, P$_{H2}$ = 5 barg]

The reaction concentration profile of 1-octene hydrogenation is shown in Figure 3.100. Octane, trans-2-octene, cis-2-octene and trans-3-octene were the main products, with small amounts of cis-3-octene, trans-4-octene and cis-4-octene also being produced during 1-octene hydrogenation.
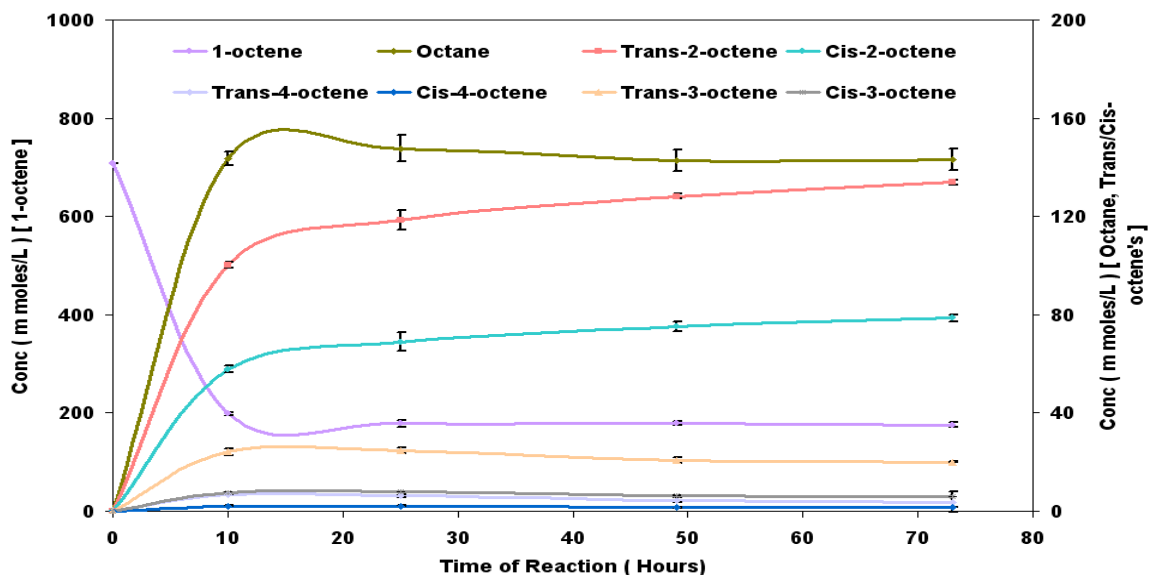
Figure 3.100 Reaction profile of 1-octene hydrogenation [Reaction conditions: T = 140°C, WHSV$_{PyGas}$ = 8 h^{-1}, P$_T$ = 20 barg, P$_{H2}$ = 5 barg]

A significant decrease was observed in the conversion of 1-octene. The conversion of 1-octene was about 82% in the initial 10 hours of the reaction, which decreased to 76% after 28 hours when the reaction had obtained steady state. An increase was observed in the formation and selectivity towards the internal octenes with an increase in the WHSV of PyGas, as shown in Figures 3.101-102.
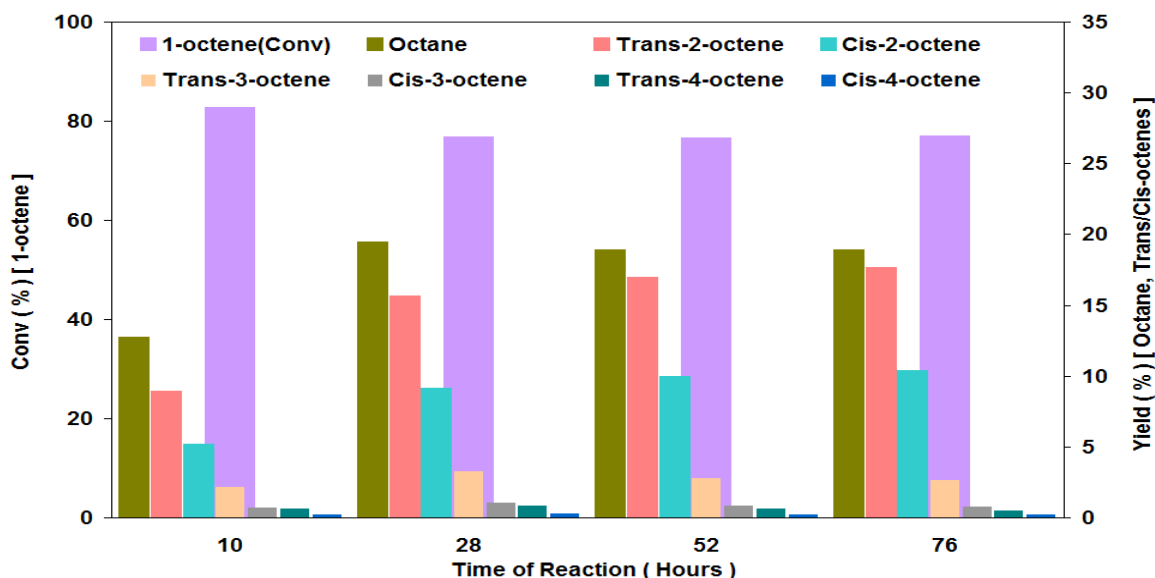
Figure 3.101 Percent yield of 1-octene hydrogenation [Reaction conditions: T = 140°C, WHSV$_{PyGas}$ = 8 h^{-1}, P$_T$ = 20 barg, P$_{H2}$ = 5 barg]
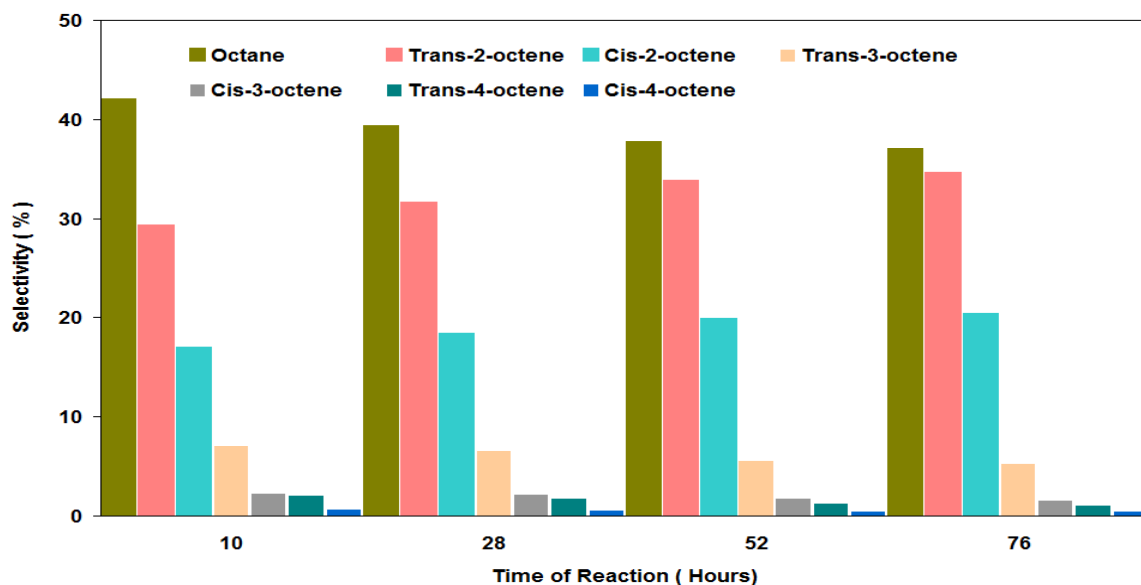
Figure 3.102 Selectivity of octane and internal octenes during 1-octene hydrogenation [Reaction conditions: T = 140°C, WHSV$_{PyGas}$ = 8 h^{-1}, P$_T$ = 20 barg, P$_{H2}$ = 5 barg]

The ratio of trans/cis in 2-octene was observed to be the same as the trans/cis ratio in 2-pentene. However further increases in the trans/cis ratio were seen from 2-octene to 3-octene and 4-octene as shown in Table 3.20.

Trans/Cis-2-pentene ratio	Trans/Cis-2-octene ratio	Trans/Cis-3-octene ratio	Trans/Cis-4-octene ratio
64:36	63:37	75:25	75:25

Table 3.20 Ratio of trans/cis internal olefins formation in PyGas Hydrogenation [Reaction conditions: T = 140°C, WHSV$_{PyGas}$ = 8 h^{-1}, P$_T$ = 20 barg, P$_{H2}$ = 5 barg]

Conversion of cyclopentene was at 83% in the first 10 hours of the reaction, which decreased to 67% after 28 hours when the reaction had obtained steady state, as shown in Figure 3.103. A significant decrease was observed in the yield of cyclopentane with an increase in WHSV$_{PyGas}$ from 4 h^{-1} to 8 h^{-1}.
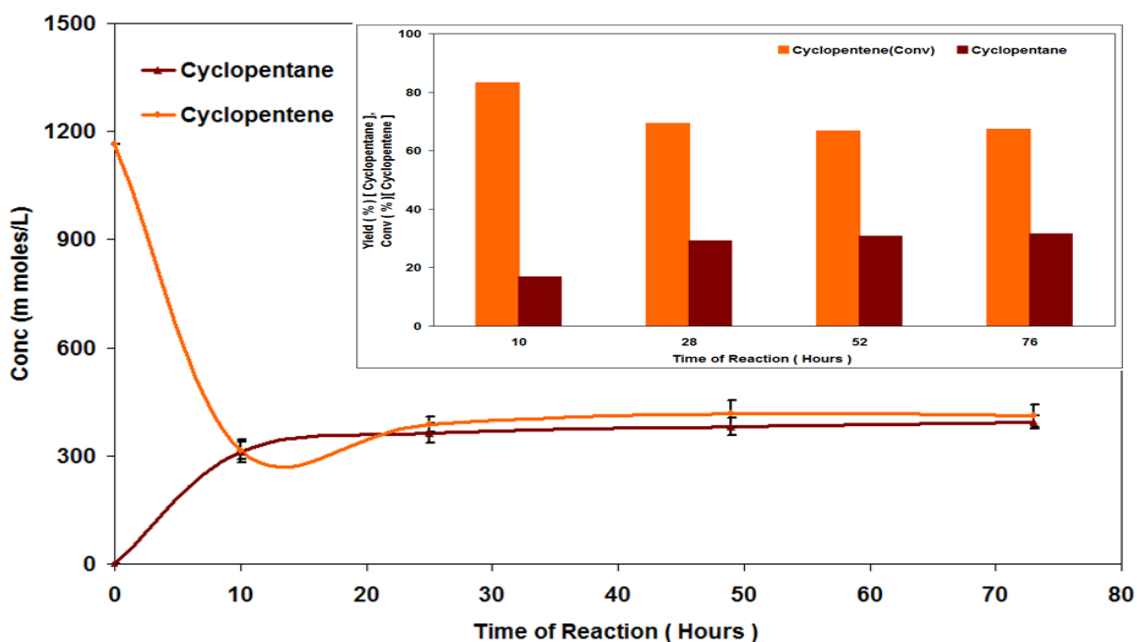
Figure 3.103 Hydrogenation of cyclopentene [Reaction conditions: T = 140°C, WHSV$_{PyGas}$ = 8 h^{-1}, P$_T$ = 20 barg, P$_{H2}$ = 5 barg]

Figure 3.104 indicates that around 48% conversion of toluene was observed in the first 10 hour of the reaction, which then decreased to 23% after 28 hours when the reaction obtained steady state. However, virtually no formation of methylcyclohexane was seen during the reaction.
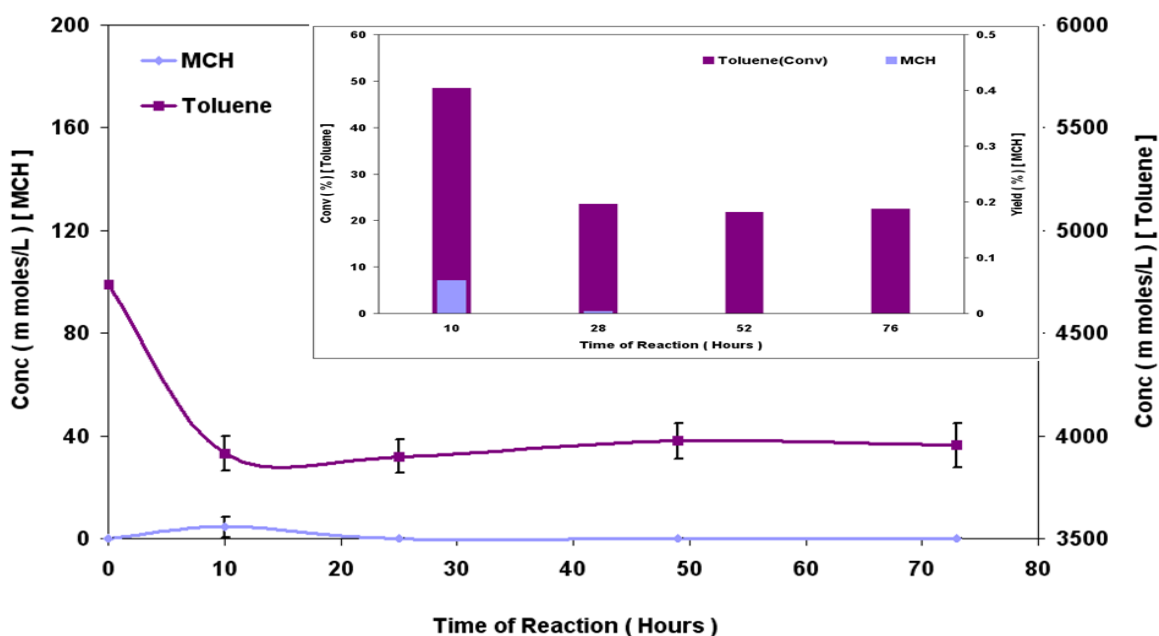
Figure 3.104 Hydrogenation of toluene [Reaction conditions: T = 140°C, WHSV$_{PyGas}$ = 8 h^{-1}, P$_T$ = 20 barg, P$_{H2}$ = 5 barg]

Figure 3.105 shows that ethylbenzene was the single product observed during styrene hydrogenation. However the yield of ethylbenzene was decreased with increase in the WHSV of PyGas from 4 h^{-1} to 8 h^{-1}.
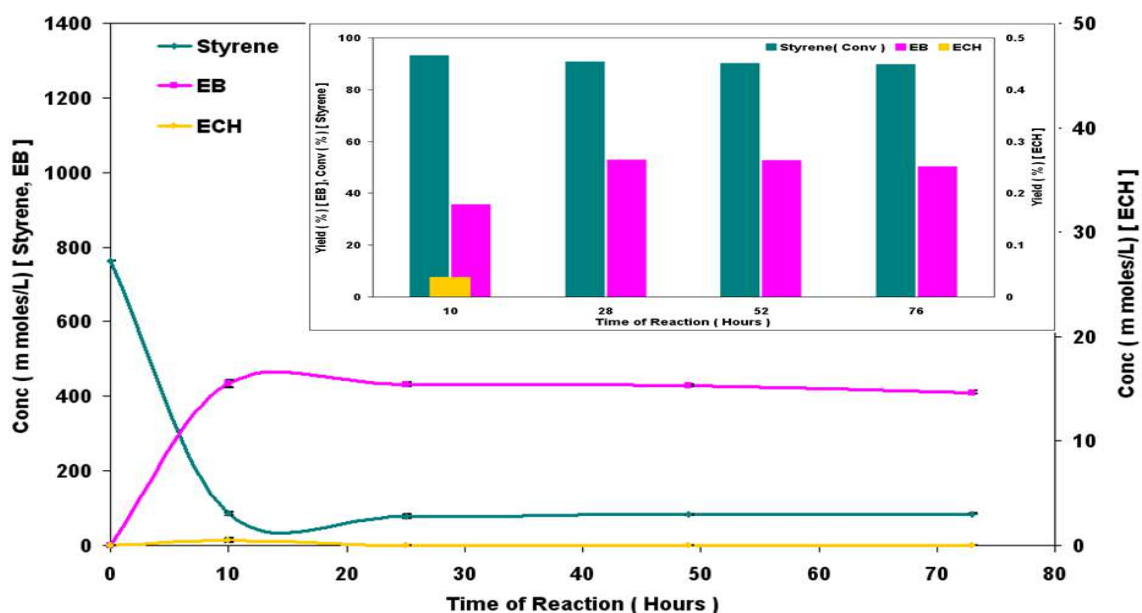
Figure 3.105 Hydrogenation of styrene [Reaction conditions: T = 140°C, WHSV$_{PyGas}$ = 8 h^{-1}, P$_T$ = 20 barg, P$_{H2}$ = 5 barg]

3.2.2.4.2.1 Post reaction analysis

Post reaction catalyst TPO

A post reaction *in-situ* TPO of the catalyst was carried out and is shown in Figure 3.106. The results indicate that a small decrease was observed in the amount of coke deposition with the change in WHSV$_{PyGas}$ from 4 h^{-1} to 8 h^{-1}.
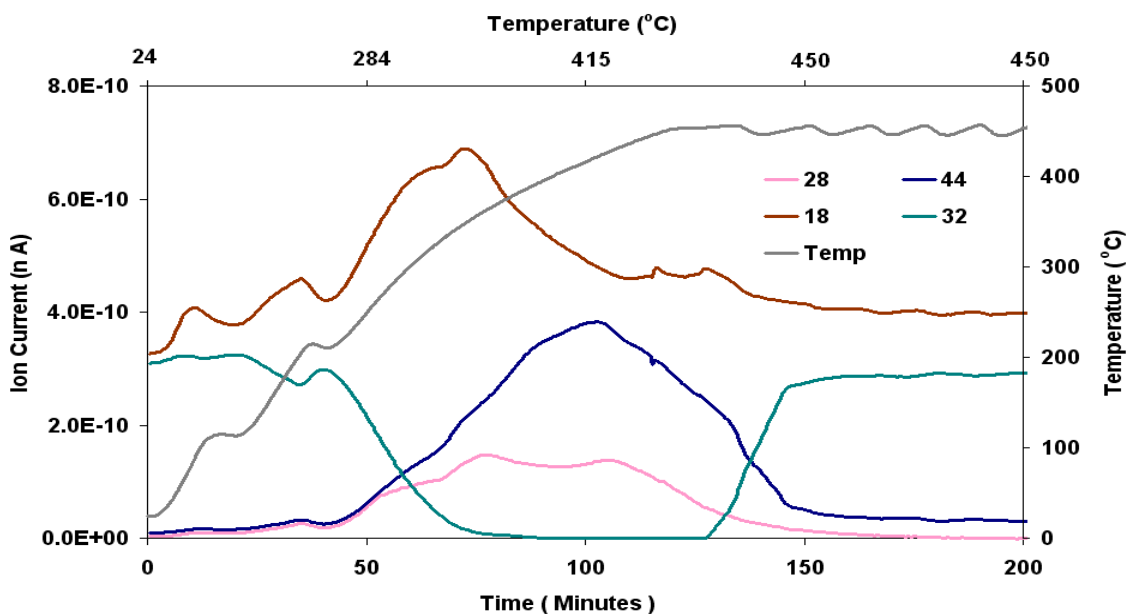
Figure 3.106 Post reaction *in-situ* TPO of Ni/Al$_2$O$_3$ catalyst [Reaction conditions: T = 140°C, WHSV$_{PyGas}$ = 8 h^{-1}, P$_T$ = 20 barg, P$_{H2}$ = 5 barg]

Total oxygen consumption in TPO = 2.66 m moles

A difference was also noted in the evolution of aromatic species (benzene and styrene). Figure 3.107 shows that desorption of styrene and benzene increased below 250°C and the evolution of styrene and benzene decreased at 300-400°C, with an increase in WHSV of PyGas from 4 h^{-1} to 8 h^{-1}. Moreover, the amount of H$_2$ evolved was also slightly decreased. Whilst the evolution of 1-pentene, cyclopentene, 1-octene, pentane, octane, toluene, methylcyclohexane, ethylbenzene and ethylcyclohexane was found to be similar to that observed in the TPO of the catalyst, used in the reaction at WHSV$_{PyGas}$ 4 h^{-1}.
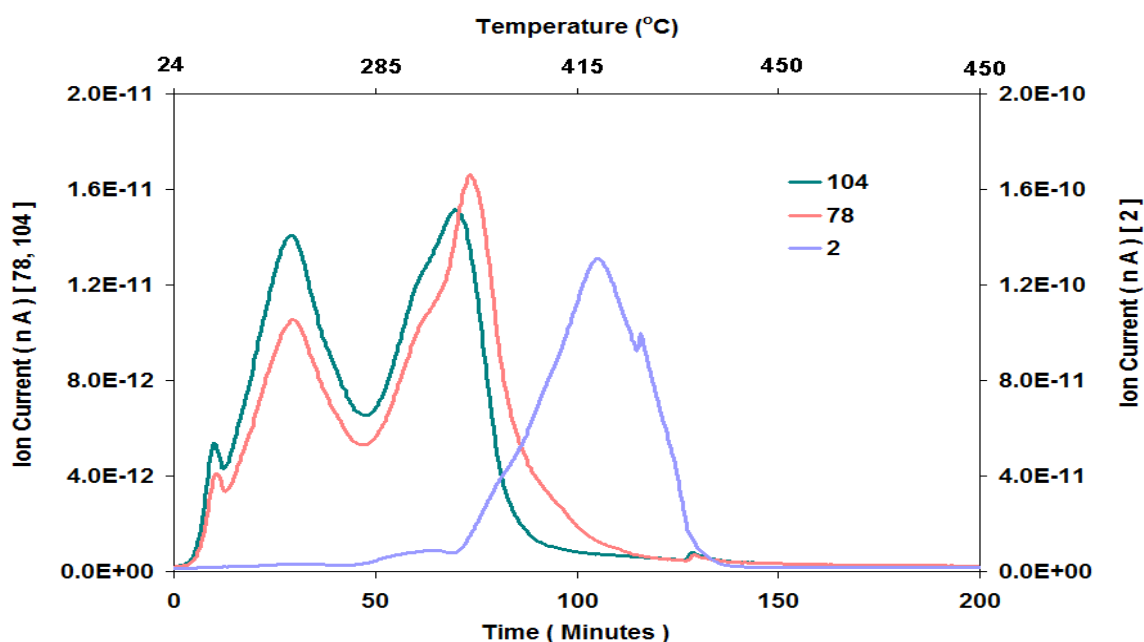
Figure 3.107 Evolution of aromatic species (styrene and benzene) and H$_2$ [Reaction conditions: T = 140°C, WHSV$_{PyGas}$ = 8 h^{-1}, P$_T$ = 20 barg, P$_{H2}$ = 5 barg]

BET analysis

The surface area of the regenerated catalyst was found to be similar to the fresh catalyst as shown in Table 3.21.

Catalyst	Surface Area (m^{2}g^{-1})	Pore Volume (cm^{3}g^{-1})	Average Pore diameter (Å)
Ni/Al$_2$O$_3$	93	0.35	152
Ni/Al$_2$O$_3$ (Reduced)	106	0.39	150
Ni/Al$_2$O$_3$ (Regenerated)	93	0.34	148

Table 3.21 BET analysis of Ni/Al$_2$O$_3$ (Regenerated) catalyst [Reaction conditions: T = 140°C, WHSV$_{PyGas}$ = 8 h^{-1}, P$_T$ = 20 barg, P$_{H2}$ = 5 barg]

3.2.2.4.3 PyGas hydrogenation over Ni/Al$_2$O$_3$ at WHSV$_{PyGas}$ = 8 h^{-1} using 25% hydrogen gas mixture [Catalyst weight = 0.25 g]

The effect of PyGas feed rate (WHSV$_{PyGas}$ 4-8 h^{-1}) on the hydrogenation of PyGas was also studied by keeping feed flow rate of PyGas constant and varying catalyst amount from 0.5 to 0.25 g. This study was performed using a 25% hydrogen gas mixture. The reaction was performed with a WHSV$_{PyGas}$ of 8 h^{-1} using 0.25 g of catalyst while feed flow rate of PyGas and other reaction conditions were kept constant [T = 140°C and P$_T$ = 20 barg]. The reaction profile is shown in Figure 3.108.
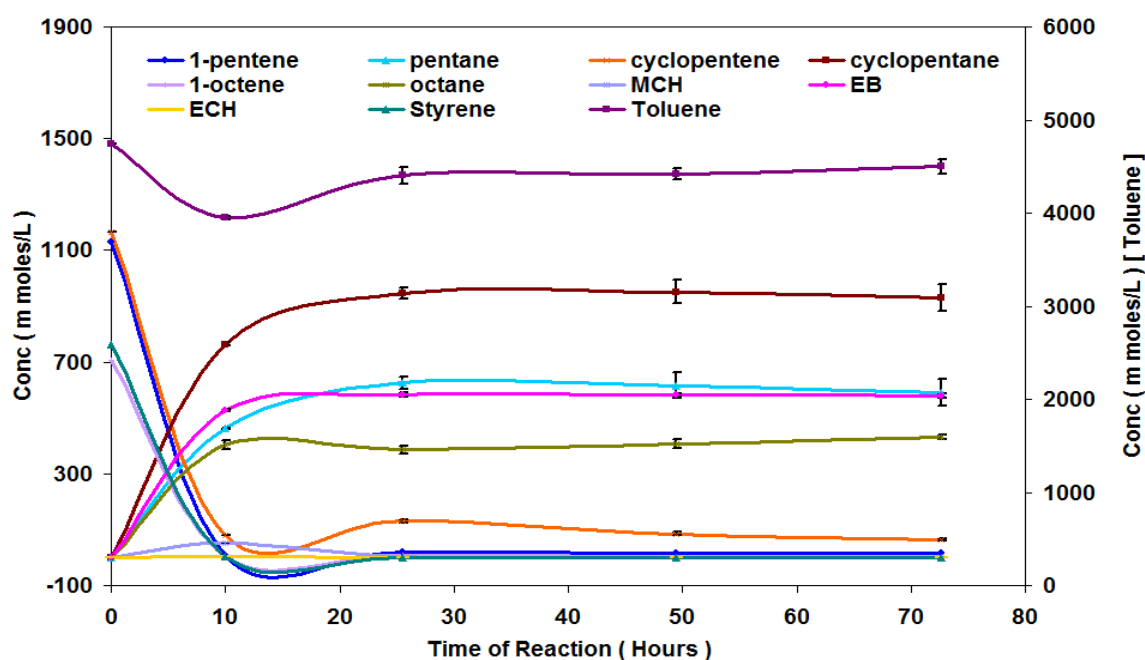
Figure 3.108 Reaction profile of PyGas hydrogenation [Reaction conditions: T = 140°C, WHSV$_{PyGas}$ = 8 h^{-1}, P$_T$ = 20 barg, P$_{H2}$ = 5 barg]

The conversion of 1-pentene was about 97% during the first 10 hours of the reaction, which decreased to 87% after 28 hours when the reaction obtained steady state condition and remained constant during the rest of the reaction. A considerable amount of internal pentenes formation was observed as shown in Figures 3.109-110.
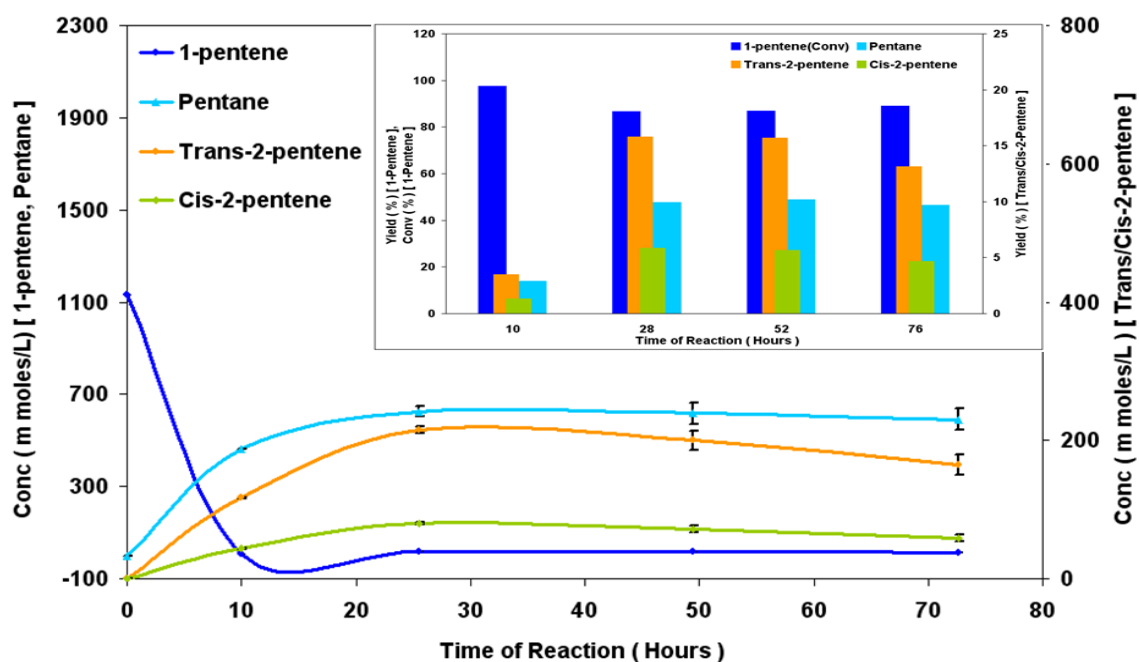
Figure 3.109 Hydrogenation of 1-pentene [Reaction conditions: T = 140°C, WHSV$_{PyGas}$ = 8 h^{-1}, P$_T$ = 20 barg, P$_{H2}$ = 5 barg]
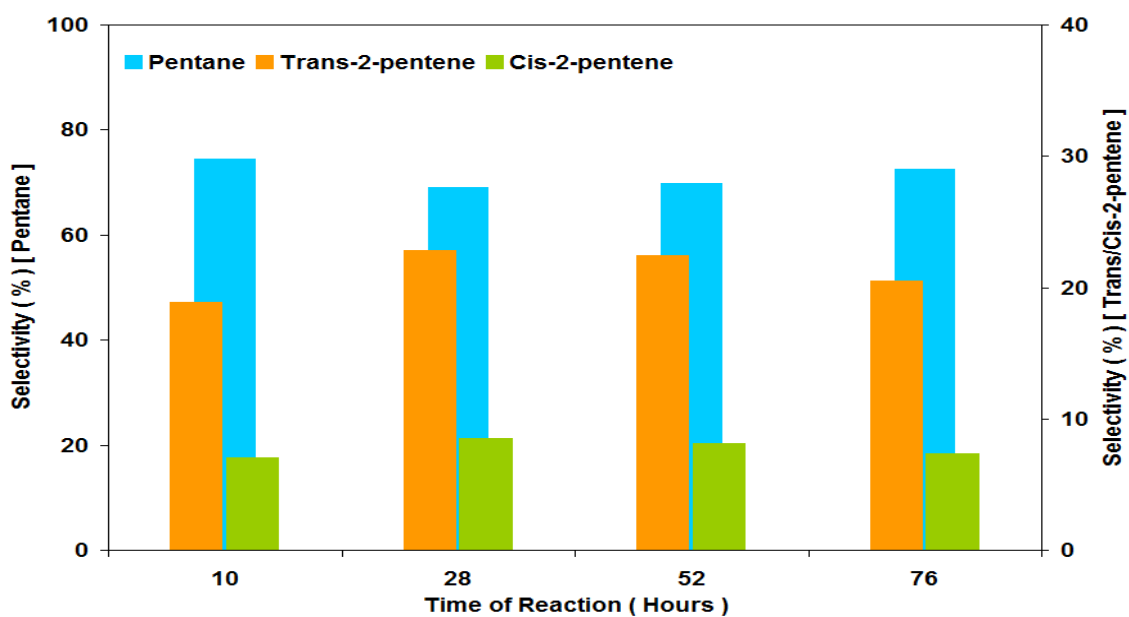
Figure 3.110 Selectivity of pentane, trans-2-pentene and cis-2-pentene during 1-pentene hydrogenation [Reaction conditions: T = 140°C, WHSV$_{PyGas}$ = 8 h^{-1}, P$_T$ = 20 barg, P$_{H2}$ = 5 barg]

Figure 3.111 shows that octane was the principal product, however, reasonable amounts of internal octenes were also produced. The products formation can be presented as the following

Octane >> 2-octene > 3-octene > 4-octene
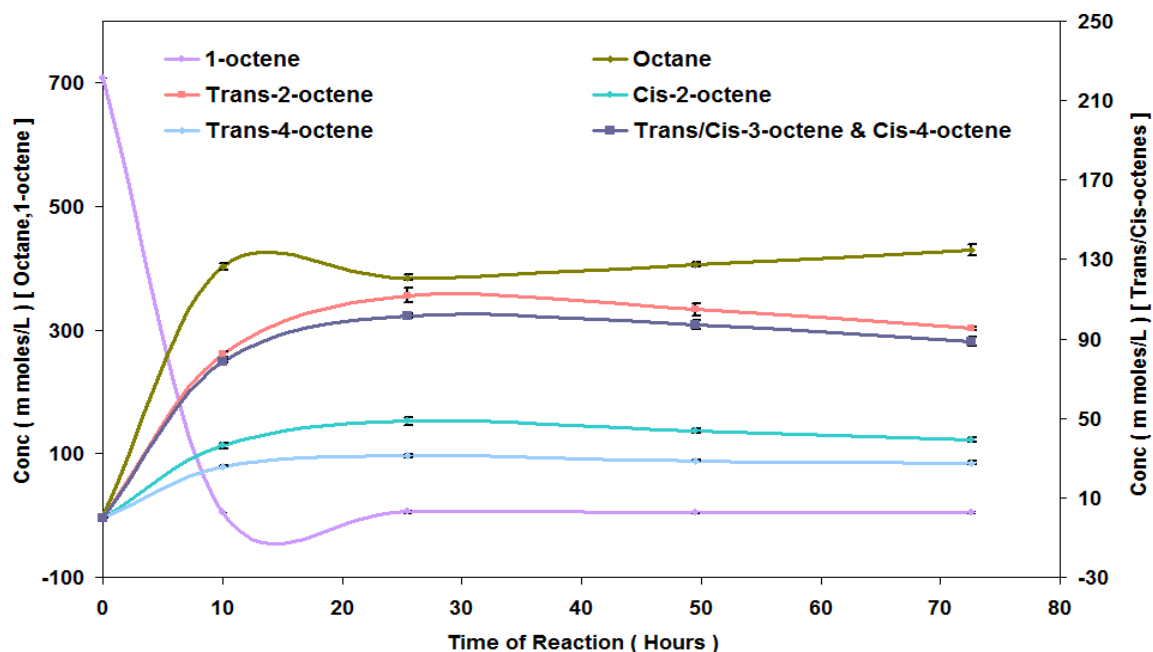
Figure 3.111 Reaction profile of 1-octene hydrogenation [Reaction conditions: T = 140°C, WHSV$_{PyGas}$ = 8 h^{-1}, P$_T$ = 20 barg, P$_{H2}$ = 5 barg]

Conversion of 1-octene remained above 99% throughout the reaction. A slight increase was observed in the yield of the internal octenes in comparison to the reaction performed at WHSV$_{PyGas}$ 4 h^{-1}, mentioned in section 3.2.2.2.2. However, a decrease was observed in the total yield of the reaction, as shown in Figures 3.112-113.
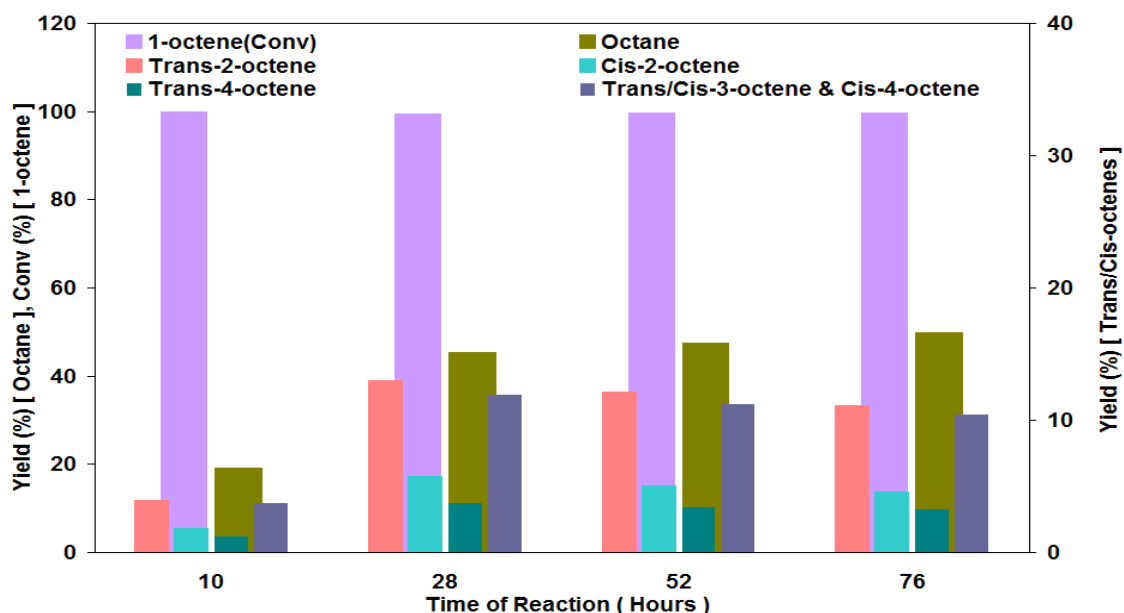
Figure 3.112 Percent yield of 1-octene hydrogenation [Reaction conditions: T = 140°C, WHSV$_{PyGas}$ = 8 h^{-1}, P$_T$ = 20 barg, P$_{H2}$ = 5 barg]
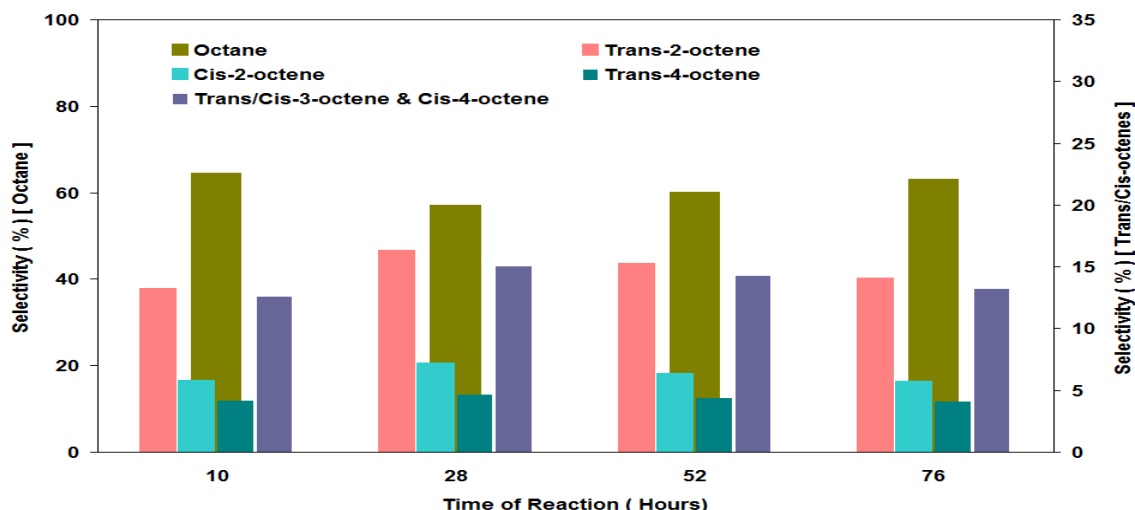
Figure 3.113 Selectivity of octane and internal octenes during 1-octene hydrogenation [Reaction conditions: T = 140°C, WHSV$_{PyGas}$ = 8 h^{-1}, P$_T$ = 20 barg, P$_{H2}$ = 5 barg]

The trans/cis ratio of olefins formed during reaction is shown in Table 3.22.

Trans/Cis-2-pentene ratio	Trans/Cis-2-octene ratio
73:27	70:29

Table 3.22 Ratio of trans/cis internal olefins formation in PyGas Hydrogenation [Reaction conditions: T = 140°C, WHSV$_{PyGas}$ = 8 h^{-1}, P$_T$ = 20 barg, P$_{H2}$ = 5 barg]

Figure 3.114 shows that cyclopentene conversion was observed at above 97% in initial 10 hours of the reaction, which decreased to 93% after 28 hours when the reaction obtained steady state, with no significant change was observed for the remainder of reaction. The yield of cyclopentane was 21% during the first 10 hours and then increased to 69% after 28 hours of the reaction and remained virtually remained constant for the rest of reaction.
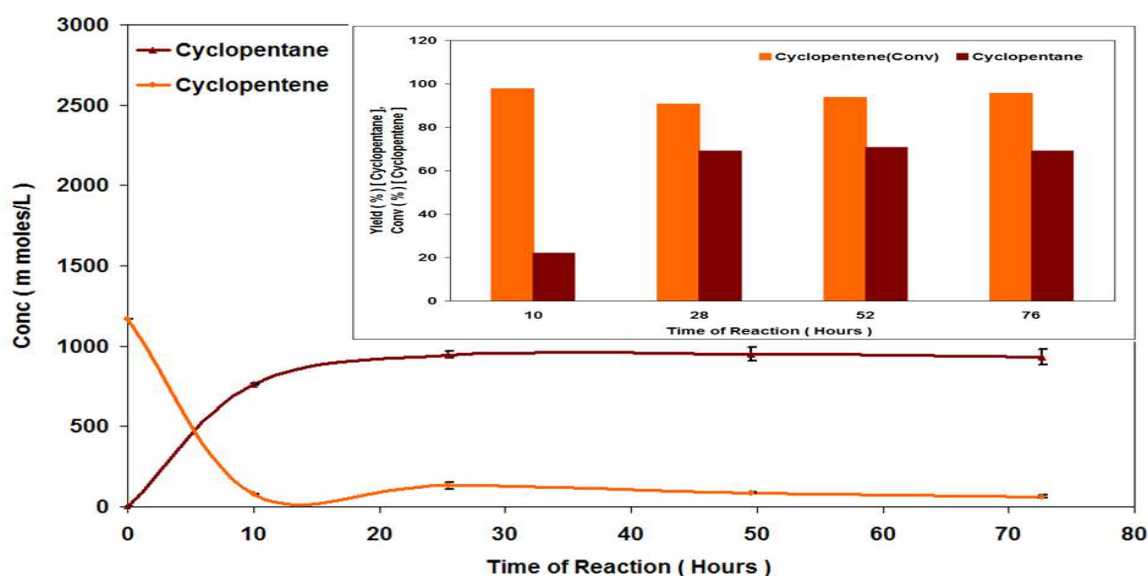
Figure 3.114 Hydrogenation of cyclopentene [Reaction conditions: T = 140°C, WHSV$_{PyGas}$ = 8 h^{-1}, P$_T$ = 20 barg, P$_{H2}$ = 5 barg]

Conversion of toluene was about 72% in the first 10 hours of the reaction, which decreased to 23% when reaction obtained steady state and remained constant throughout the rest of the reaction. However, virtually no formation of methylcyclohexane was observed. The maximum yield of methylcyclohexane observed was less than 0.5%.
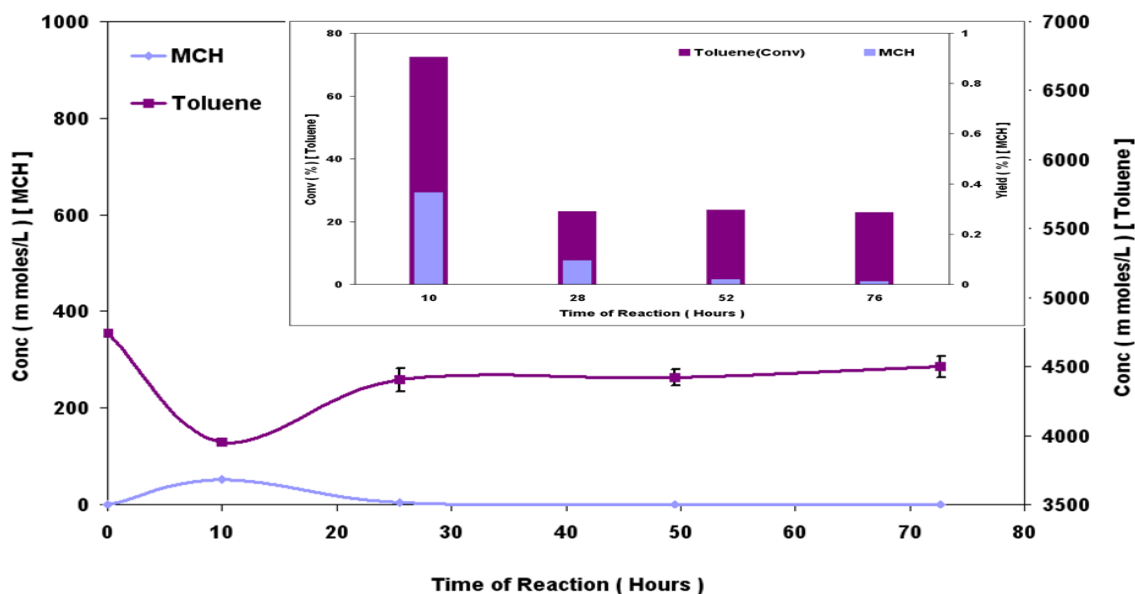
Figure 3.115 Hydrogenation of toluene [Reaction conditions: T = 140°C, WHSV$_{PyGas}$ = 8 h^{-1}, P$_T$ = 20 barg, P$_{H2}$ = 5 barg]

Figure 3.116 shows that the conversion of styrene was above 99% throughout the reaction. Ethylbenzene was the main product observed in the reaction whilst negligible amount of ethylcyclohexane (yield~0.2%) was seen only in initial stages of the reaction.
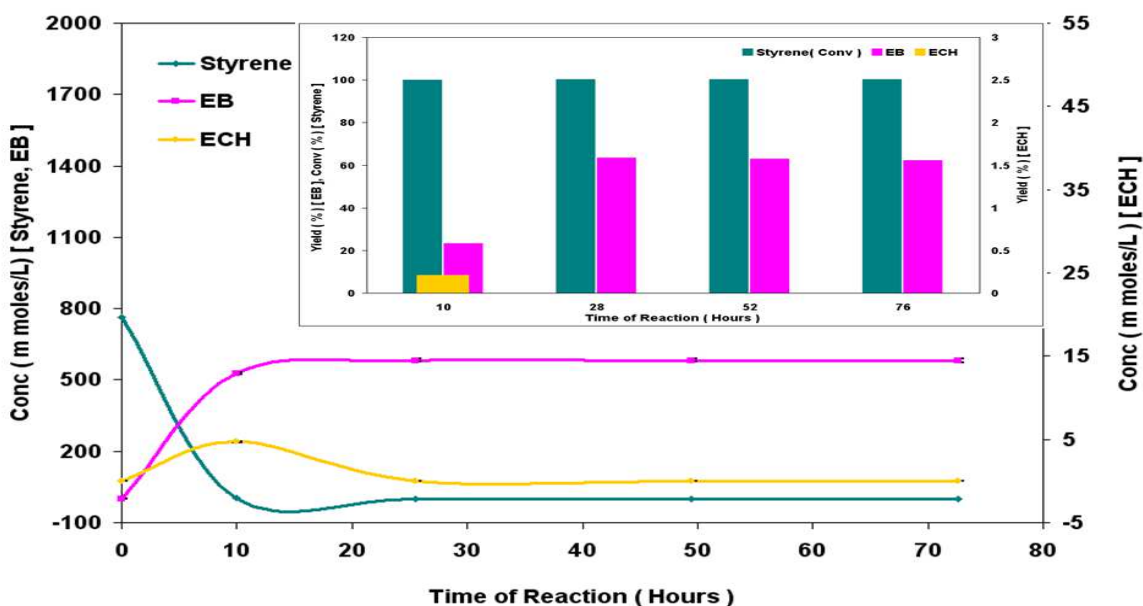
Figure 3.116 Hydrogenation of styrene [Reaction conditions: T = 140°C, WHSV$_{PyGas}$ = 8 h^{-1}, P$_T$ = 20 barg, P$_{H2}$ = 5 barg]

3.2.2.4.3.1 Post reaction analysis

Post reaction catalyst TPO

Post reaction *in-situ* TPO of the catalyst was performed, as shown in Figure 3.117. The results indicate that the amount of coke observed was smaller when compared to the reaction performed at $WHSV_{PyGas}$ 4 h^{-1} over 0.5 g of catalyst described in section 3.2.2.2.2. The amount of coke deposition is less due to the smaller amount of catalyst in this reaction, 0.25 g rather than 0.5 g.
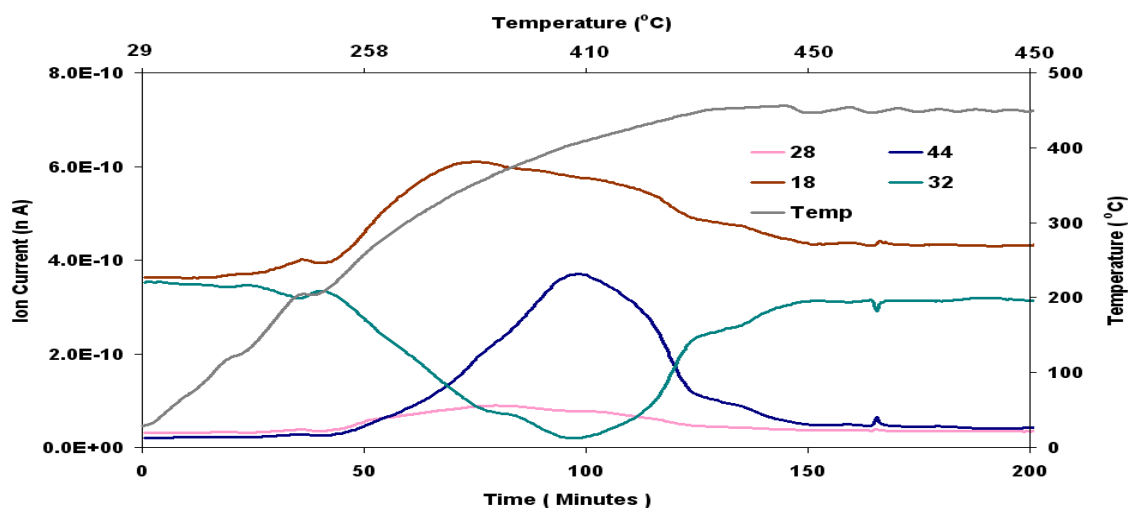
Figure 3.117 Post reaction *in-situ* TPO of Ni/Al$_2$O$_3$ catalyst [Reaction conditions: T = 140°C, $WHSV_{PyGas}$ = 8 h^{-1}, P$_T$ = 20 barg, P$_{H2}$ = 5 barg]

Total oxygen consumption in TPO = 1.88 m moles

Meanwhile, reasonably small amounts of styrene and benzene desorption and virtually no evolution of H$_2$ was observed in the TPO as shown in Figure 3.118. Moreover, no considerable evolution of other species *i.e.* 1-pentene, 1-octene, cyclopentene, pentane, octane, toluene, methylcyclohexane, ethylbenzene and ethylcyclohexane was noted.
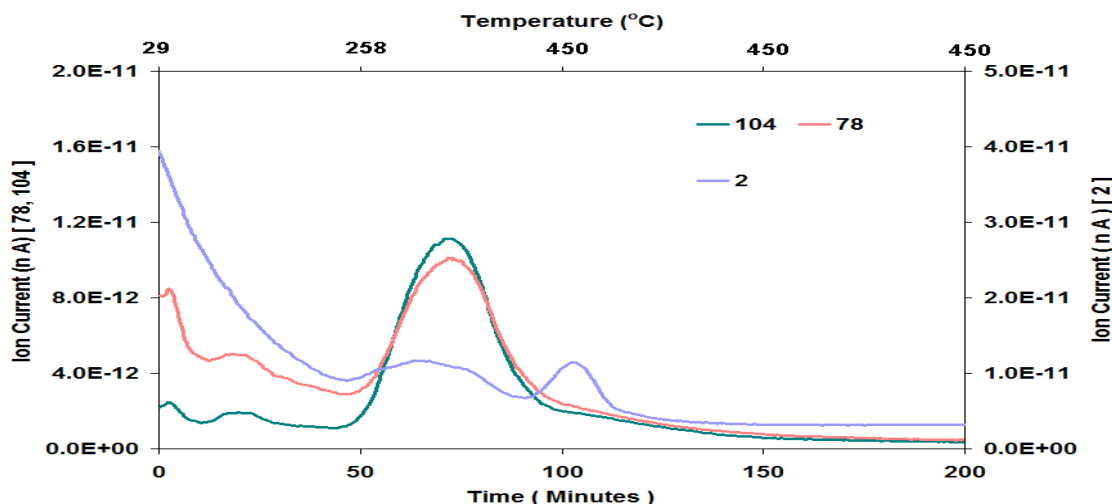
Figure 3.118 Evolution of aromatic species (styrene and benzene) and H$_2$ [Reaction conditions: T = 140°C, $WHSV_{PyGas}$ = 8 h^{-1}, P$_T$ = 20 barg, P$_{H2}$ = 5 barg]

BET analysis

The surface area, pore volume and pore diameter of the regenerated catalyst were analysed and the results are shown in Table 3.23.

Catalyst	Surface Area (m^2g^{-1})	Pore Volume (cm^3g^{-1})	Average Pore diameter ($\mathring{A}$)
Ni/Al_2O_3	93	0.35	152
Ni/Al_2O_3 (Reduced)	106	0.39	150
Ni/Al_2O_3 (Regenerated)	80	0.33	169

Table 3.23 BET analysis of Ni/Al_2O_3 (Regenerated) catalyst [Reaction conditions: T = 140°C, $WHSV_{PyGas}$ = 8 h^{-1}, P_T = 20 barg, P_{H2} = 5 barg]

The BET results indicate that the surface area lost due to the deposition of coke during the reaction was not completely recovered during regeneration and a decrease in the surface area of the catalyst was observed.

3.2.2.5 Reaction with PyGas containing 1,3-pentadiene (PyGas-II)

PyGas generally contains more than 100 species and composition of the PyGas depends on its source and origin. The synthetic PyGas used in this study was a comprehensive model of PyGas. However, diolefines were also included in the synthetic PyGas to study more wide ranging synthetic PyGas for the better understanding of the process. The composition of PyGas used in this reaction given in Table 3.24.

Components	Composition (wt %)
1,3-pentandiene	2.5
1-octene	10
cyclopentene	10
Styrene	10
Toluene	62.5
n-heptane	2.5
n-decane	2.5

Table 3.24 Composition of pyrolysis gasoline (PyGas-II)

The hydrogenation of PyGas was performed over the Ni/Al$_2$O$_3$ using a 25% hydrogen gas mixture under reaction conditions T = 140°C, WHSV$_{PyGas}$ = 4 h^{-1} and P$_T$ = 20 barg. The reaction profile is given in Figure 3.119.
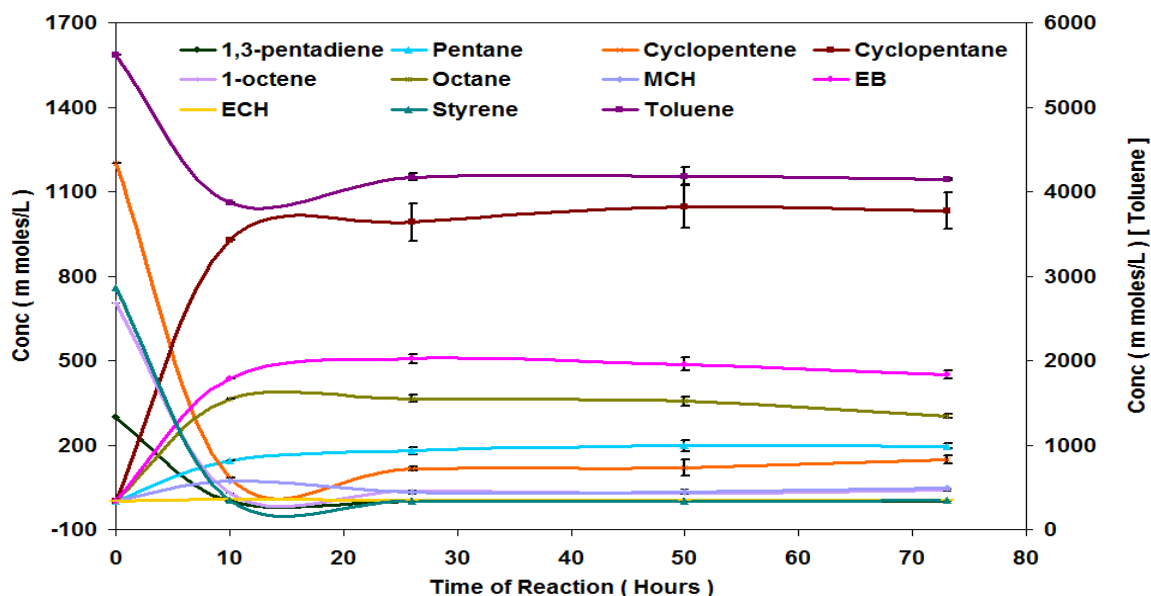
Figure 3.119 Reaction profile of PyGas Hydrogenation [Reaction conditions: T = 140°C, WHSV$_{PyGas}$ = 4 h^{-1}, P$_T$ = 20 barg, P$_{H2}$ = 5 barg]

Figure 3.120-121 show that the conversion of 1,3-pentadiene was virtually 100% throughout the reaction. Pentane was the principal product of the reaction, however, considerable amounts of trans-2-pentene and cis-2-pentene were also produced during the reaction. Virtually no 1-pentene was seen in the reaction stream. An increase was observed in the yield of internal pentenes with time on stream.
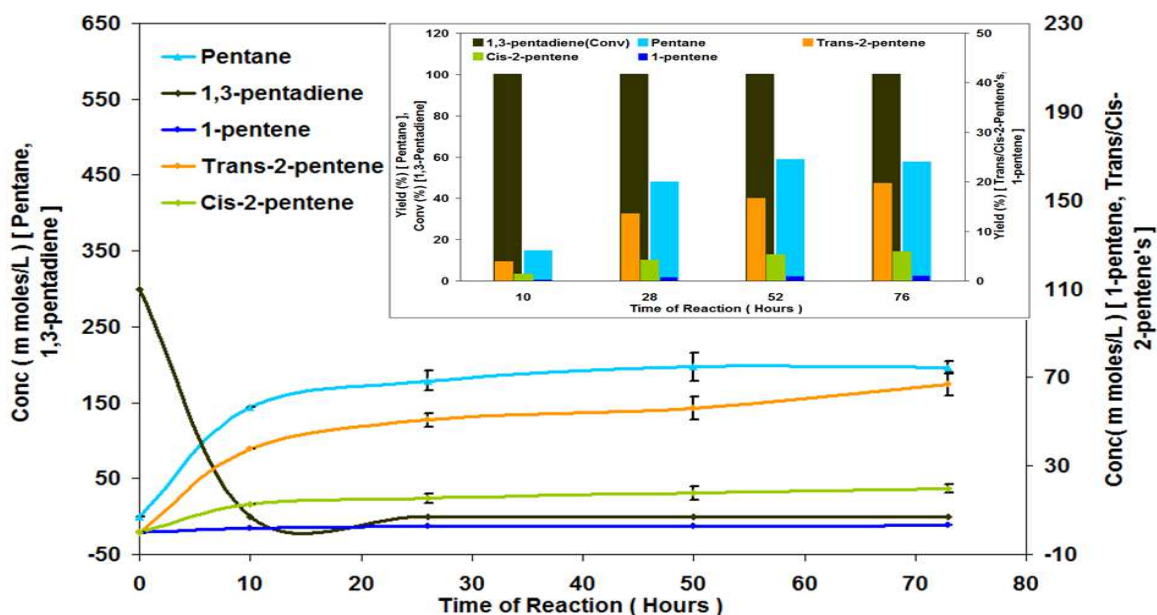
Figure 3.120 Hydrogenation of 1,3-pentadiene [Reaction conditions: T = 140°C, WHSV$_{PyGas}$ = 4 h^{-1}, P$_T$ = 20 barg, P$_{H2}$ = 5 barg]
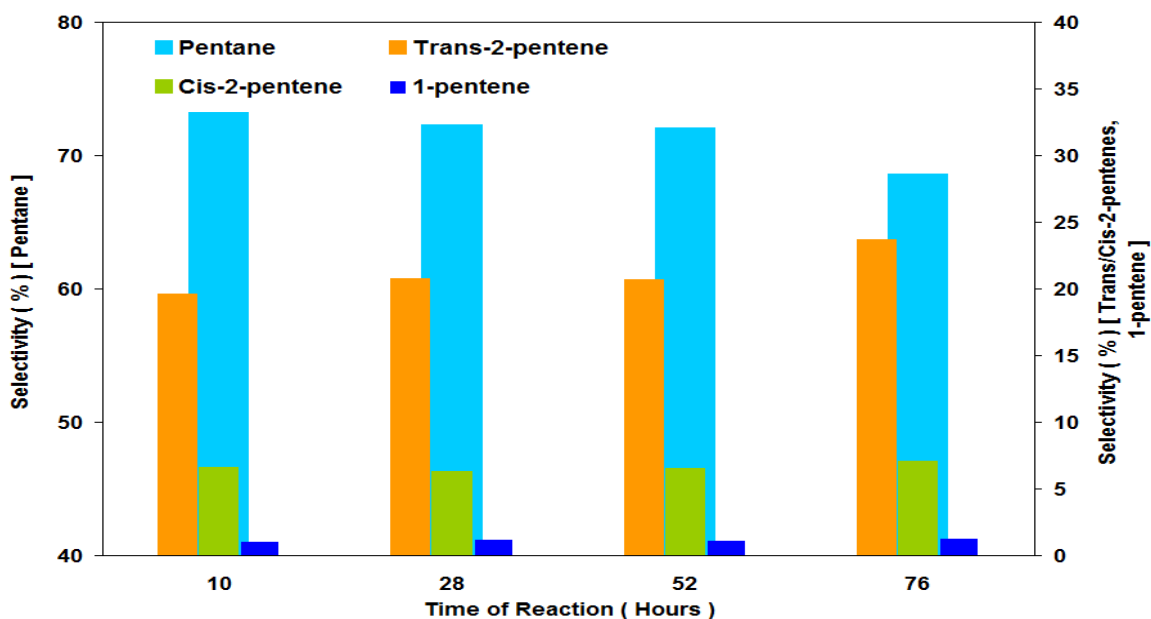
Figure 3.121 Selectivity of pentane, trans-2-pentene and cis-2-pentene, 1-pentene during 1,3-pentadiene hydrogenation [Reaction conditions: T = 140°C, WHSV$_{PyGas}$ = 4 h^{-1}, P$_T$ = 20 barg, P$_{H2}$ = 5 barg]

Octane was the main product formed during 1-octene hydrogenation, while reasonable amounts of internal octenes were also formed in the reaction, as shown in Figure 3.122.
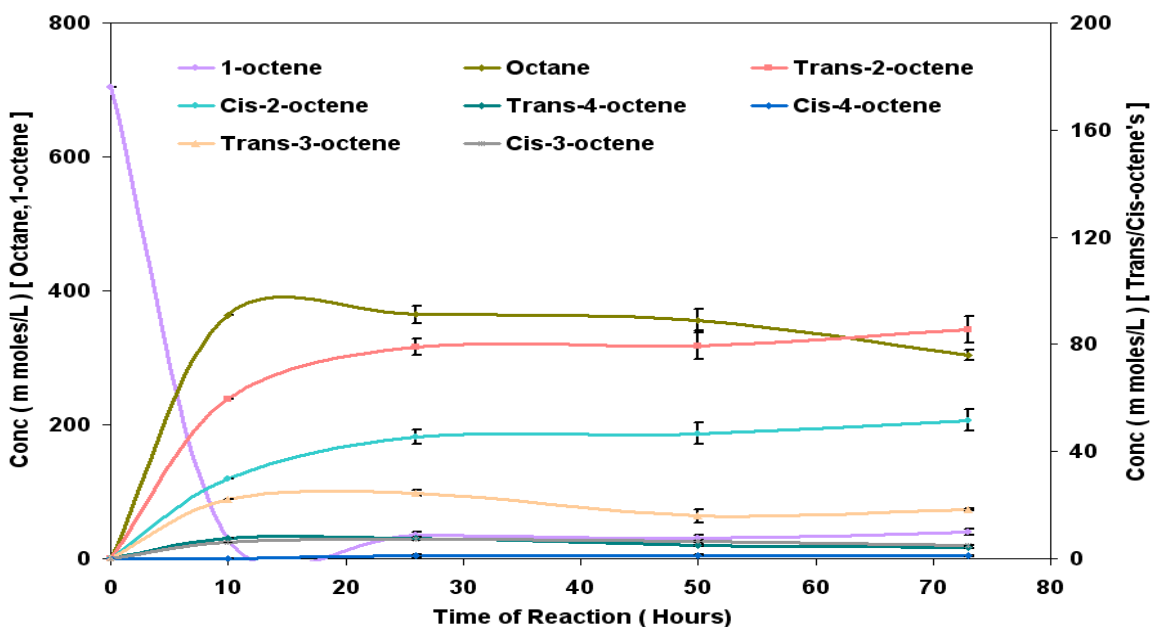
Figure 3.122 Reaction profile of 1-octene hydrogenation [Reaction conditions: T = 140°C, WHSV$_{PyGas}$ = 4 h^{-1}, P$_T$ = 20 barg, P$_{H2}$ = 5 barg]

Conversion of 1-octene was above 96% throughout the reaction. The yields and selectivities of products are given in Figures 3.123-124.
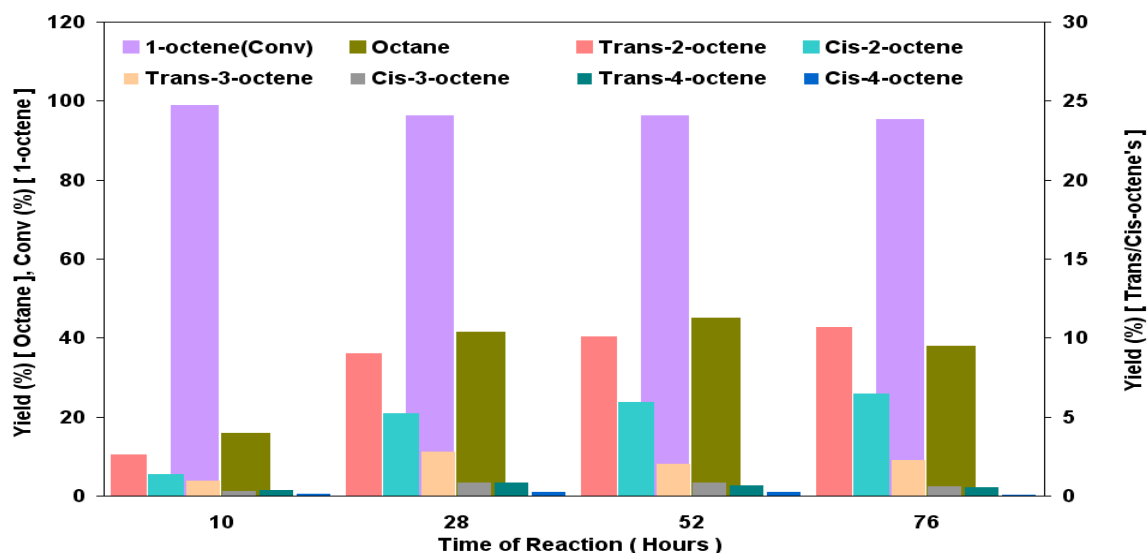
Figure 3.123 Percent yield of 1-octene Hydrogenation [Reaction conditions: T = 140°C, WHSV$_{PyGas}$ = 4 h^{-1}, P$_T$ = 20 barg, P$_{H2}$ = 5 barg]
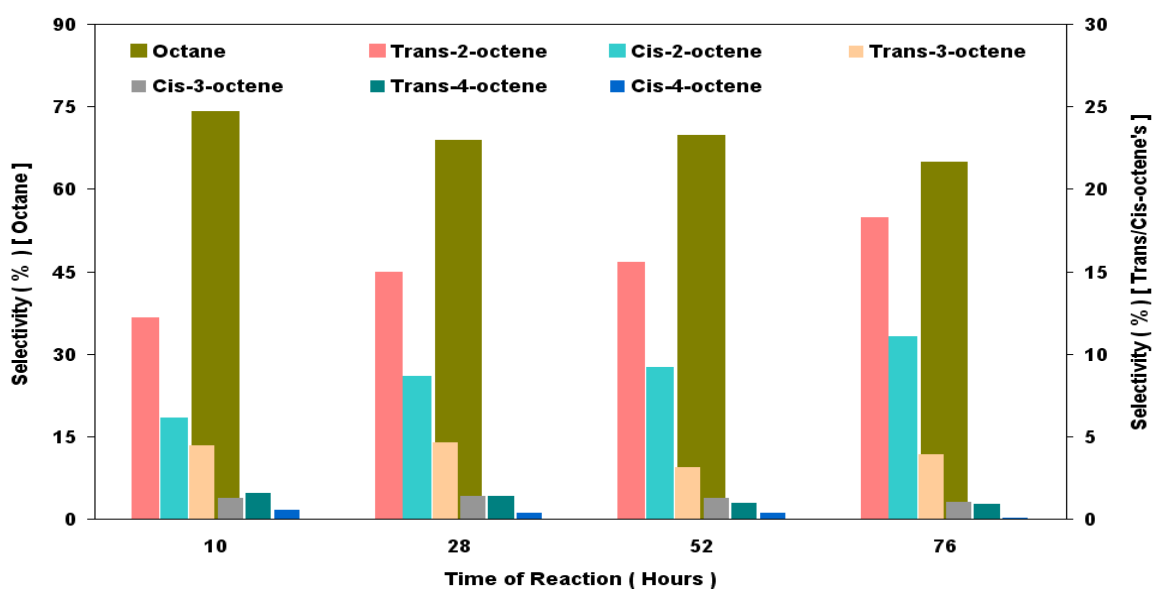
Figure 3.124 Selectivity of octane and internal octenes during 1-octene hydrogenation [Reaction conditions: T = 140°C, WHSV$_{PyGas}$ = 4 h^{-1}, P$_T$ = 20 barg, P$_{H2}$ = 5 barg]

The products distribution during 1-octene can be presented as the following;

Octane >> Trans-2-octene > Cis-2-octene > Trans-3-octene > Cis-3-octene ≈

Trans-4-octene > Cis-4-octene

The formation of the trans isomer was found to be greater than the respective cis isomer. The ratios of trans/cis isomers are shown in Table 3.25.

Trans/Cis-2-pentene ratio	Trans/Cis-2-octene ratio	Trans/Cis-3-octene ratio	Trans/Cis-4-octene ratio
75:25	63:37	75:25	75:25

Table 3.25 Ratio of trans/cis internal olefins formation in PyGas Hydrogenation [Reaction conditions: T = 140°C, WHSV$_{PyGas}$ = 4 h^{-1}, P$_T$ = 20 barg, P$_{H2}$ = 5 barg]

Figure 3.125 shows that the conversion of cyclopentane was 97% during the initial stages of the reaction and slowly decreased with time on stream. The minimum conversion was noted to be 89% after 76 hours of the reaction. Meanwhile, the yield of cyclopentane was only 23% during the first 10 hours of the reaction which increased to 66% after 28 hours when the reaction obtained steady state. Further, gradual increase was observed in the yield of cyclopentane with time on stream.
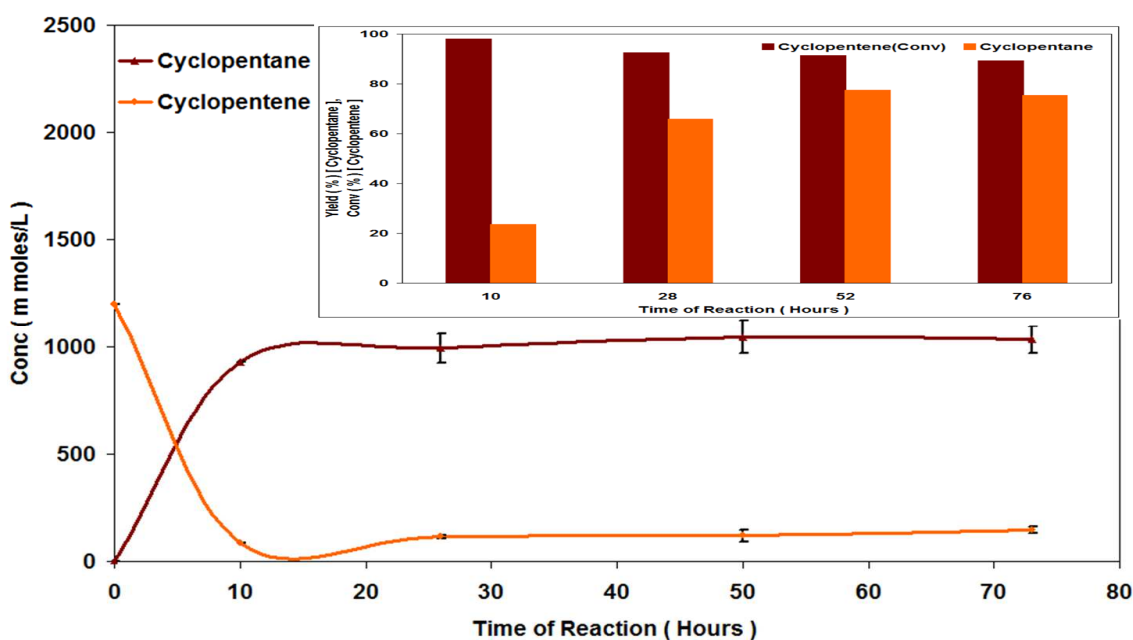
Figure 3.125 Hydrogenation of cyclopentene [Reaction conditions: T = 140°C, WHSV$_{PyGas}$ = 4 h^{-1}, P$_T$ = 20 barg, P$_{H2}$ = 5 barg]

Considerable conversion of toluene was observed during the reaction. However, a negligible amount of methylcyclohexane was seen, as shown in Figure 3.126.
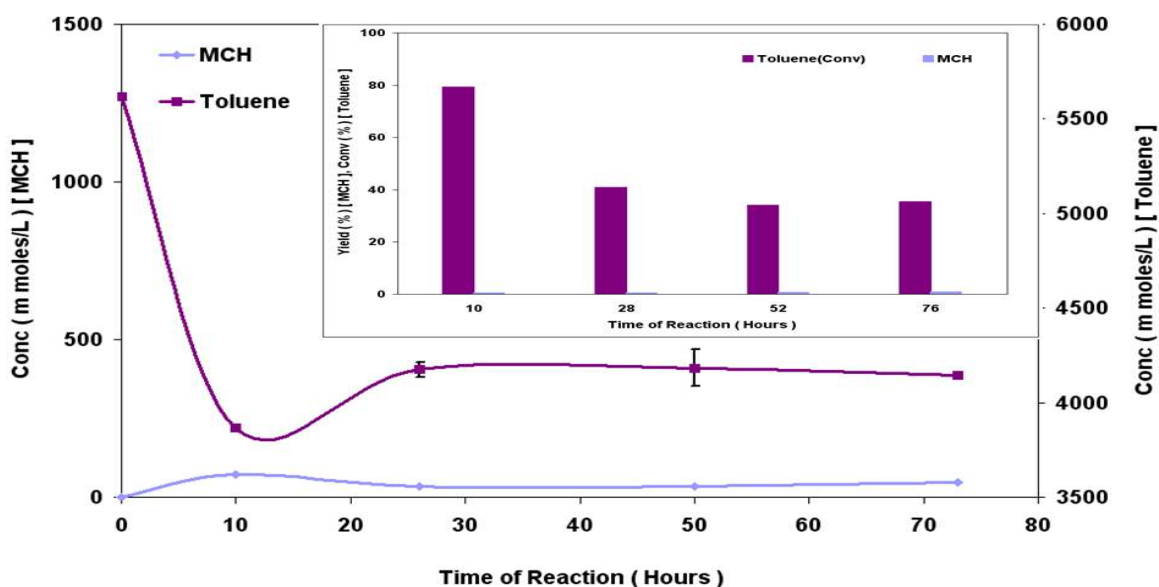
Figure 3.126 Hydrogenation of toluene [Reaction conditions: T = 140°C, WHSV$_{PyGas}$ = 4 h^{-1}, P$_T$ = 20 barg, P$_{H2}$ = 5 barg]

Figure 3.127 shows that the conversion of styrene was above 99% throughout the reaction. Ethylbenzene was the principal product during the reaction whilst a smaller amount, less than 0.5%, of ethylcyclohexane was also formed.
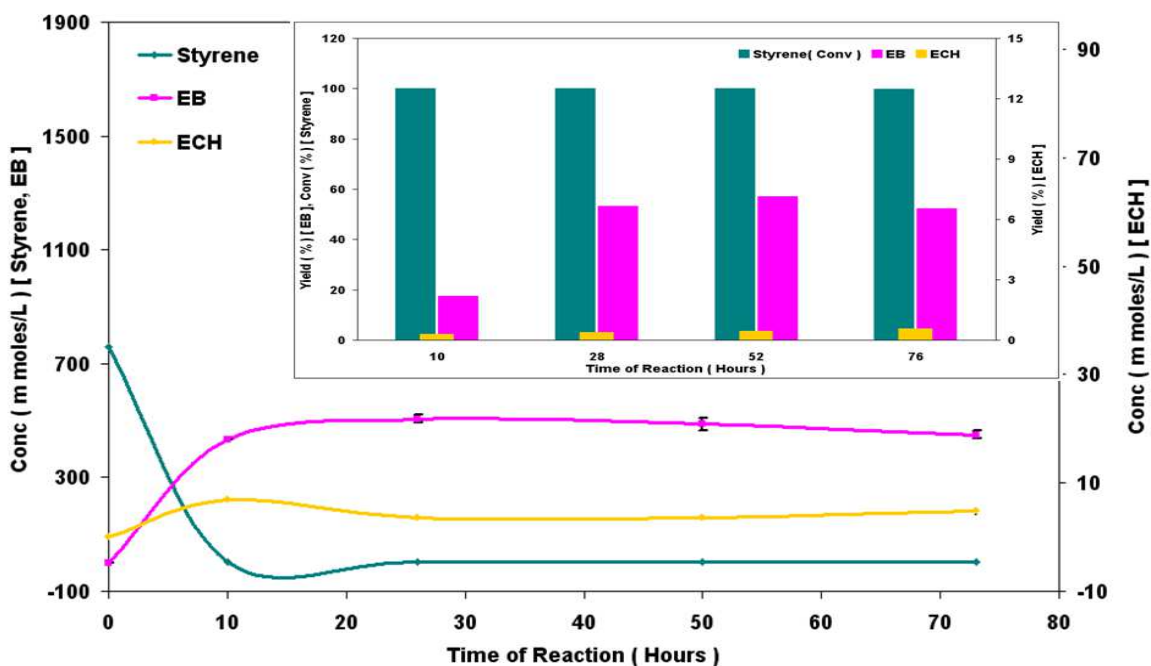
Figure 3.127 Hydrogenation of styrene [Reaction conditions: T = 140°C, WHSV$_{PyGas}$ = 4 h^{-1}, P$_T$ = 20 barg, P$_{H2}$ = 5 barg]

3.2.2.5.1 Post reaction analysis

Post reaction catalyst TPO

A post reaction *in-situ* TPO was carried out over post reaction catalyst. Figure 3.128 shows the oxygen consumption and evolution of CO_2, CO and H_2O. The results indicate that a small decrease occurred in the amount of coke deposition when using PyGas-II instead of PyGas-I in the reaction under similar conditions. The olefins are considered one of the main precursors of coke formation during PyGas hydrogenation. Thus, it is believed that the decrease in coke deposition was due to the smaller amount of olefins present in PyGas-II compared to PyGas-I. However, the evolution of other species *i.e.* styrene, benzene, 1-pentene, cyclopentene, 1-octene, pentane, octane, toluene, methylcyclohexane, ethylcyclohexane and ethylbenzene was found to be similar to that observed in the TPO of the catalyst, used in the reaction carried out with PyGas-I.
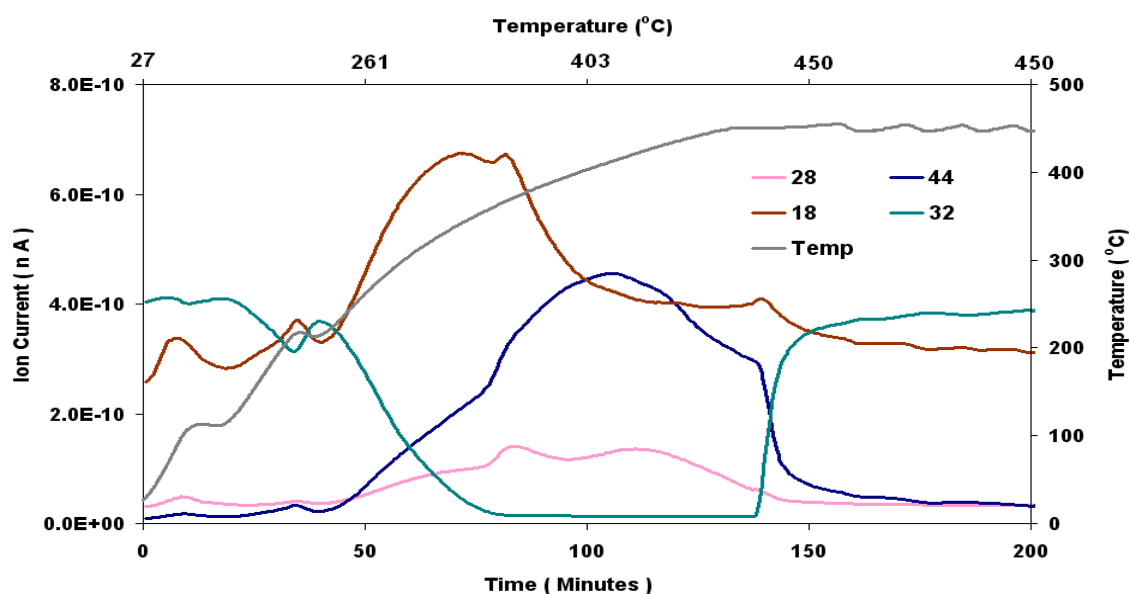
Figure 3.128 Post reaction *in-situ* TPO of Ni/Al$_2$O$_3$ catalyst [Reaction conditions: T = 140°C, WHSV$_{PyGas}$ = 4 h^{-1}, P$_T$ = 20 barg, P$_{H2}$ = 5 barg]

Total oxygen consumption in TPO = 2.84 m moles

BET analysis

The surface area, pore volume and pore diameter of the regenerated catalyst were analysed and the results displayed in Table 3.26.

Catalyst	Surface Area (m^{2}g^{-1})	Pore Volume (cm^{3}g^{-1})	Average Pore diameter (Å)
Ni/Al$_2$O$_3$	93	0.35	152
Ni/Al$_2$O$_3$ (Reduced)	106	0.39	150
Ni/Al$_2$O$_3$ (Regenerated)	94	0.37	158

Table 3.26 BET analysis of Ni/Al$_2$O$_3$ (Regenerated) catalyst [Reaction conditions: T = 140°C, WHSV$_{PyGas}$ = 4 h^{-1}, P$_T$ = 20 barg, P$_{H2}$ = 5 barg]

The BET results indicate the surface area lost due to deposition of coke was recovered during regeneration.

3.2.3 PyGas hydrogenation over Pd/Al$_2$O$_3$ catalyst

The following parameters were investigated during the PyGas hydrogenation over Pd/Al$_2$O$_3$ catalyst.

a) Effect of reaction temperature

b) Effect of hydrogen partial pressure

c) Effect of total reaction pressure

d) Effect of PyGas feed flow rate (WHSV$_{PyGas}$)

3.2.3.1 Effect of reaction temperature on PyGas hydrogenation

To study the effect of reaction temperature, the hydrogenation of PyGas was performed over Pd/Al$_2$O$_3$ catalyst in a fixed bed reactor under the following operating conditions T = 140-200°C, WHSV$_{PyGas}$ = 4 h^{-1} and P$_{H2}$ = 20 barg.

Hydrogenation of PyGas is an exothermic reaction therefore the temperature of the palladium catalyst bed was monitored by a thermocouple positioned within the catalyst bed, as shown in Figure 3.129. The temperature of the catalyst bed rose by about 7°C within the first 5 minutes of the reaction and then became stable at the reaction temperature (±1.5^{o}C) for the rest of the reaction. The temperature profile of catalyst bed was found to be similar in all reactions.
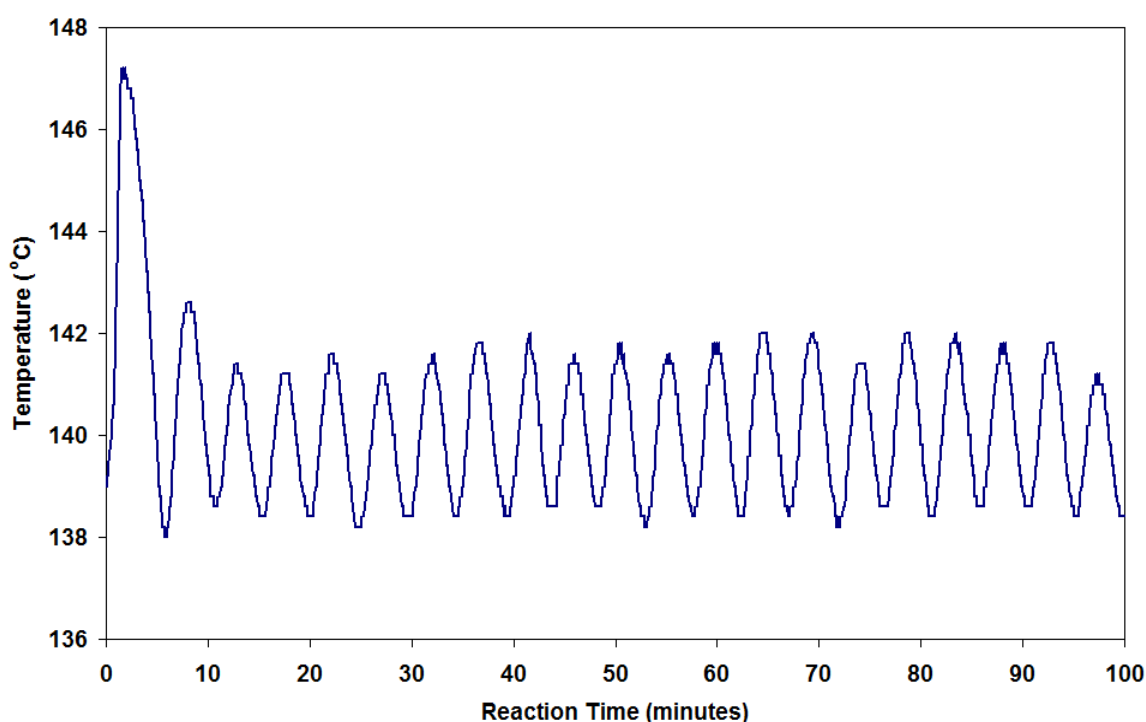
Figure 3.129 Temperature profile of the palladium catalyst bed during PyGas hydrogenation

3.2.3.1.1 PyGas hydrogenation over Pd/Al$_2$O$_3$ at 140 ^{o}C

The PyGas hydrogenation was performed over Pd/Al$_2$O$_3$ catalyst using reaction conditions T = 140°C, WHSV$_{PyGas}$ = 4 h^{-1} and P$_{H2}$ = 20 barg. The reaction profile is shown in Figure 3.130.
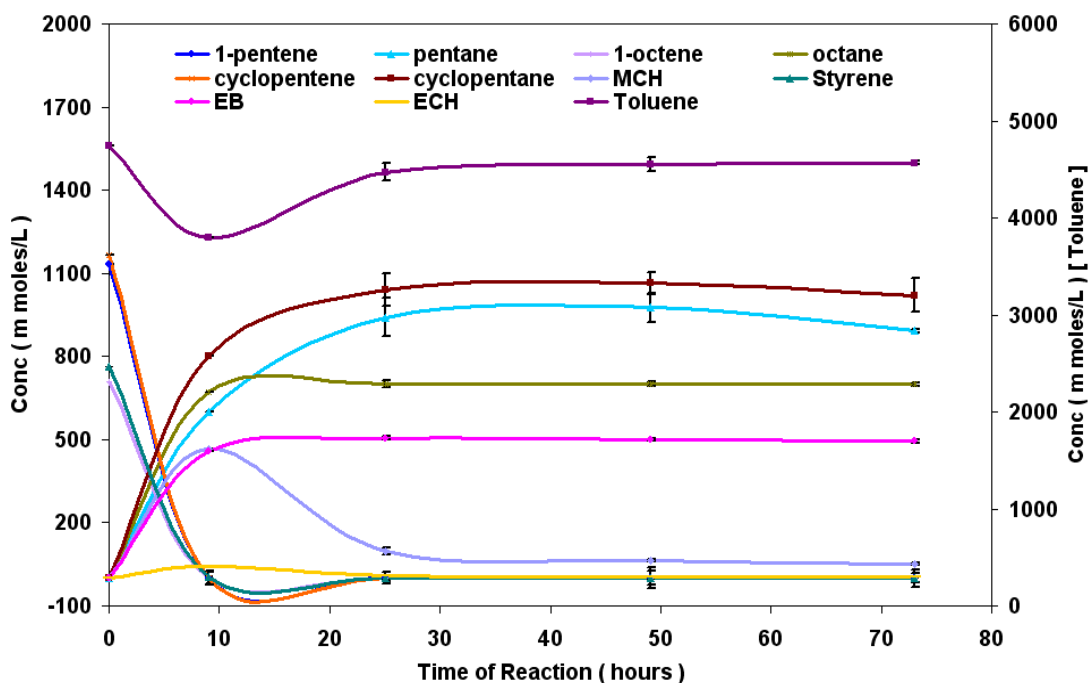
Figure 3.130 Reaction profile of PyGas hydrogenation [Reaction conditions: T = 140°C, WHSV$_{PyGas}$ = 4 h^{-1}, P$_{H2}$ = 20 barg]

Figure 3.131 shows that olefins (1-pentene, cyclopentene and 1-octene) present in the PyGas hydrogenated to their respective saturated compounds and no internal olefins formation was observed. Conversion of the olefins was above 99% throughout TOS of the reaction. The yields of pentane, cyclopentane and octane were noted at 17%, 23% and 31% respectively over the first 9 hours of the reaction. An increase was observed in formation of the paraffins and the yields of pentane, cyclopentane and octane increased to 80%, 85% and 89% respectively after 29 hour of TOS. These remained virtually constant for the rest of reaction.
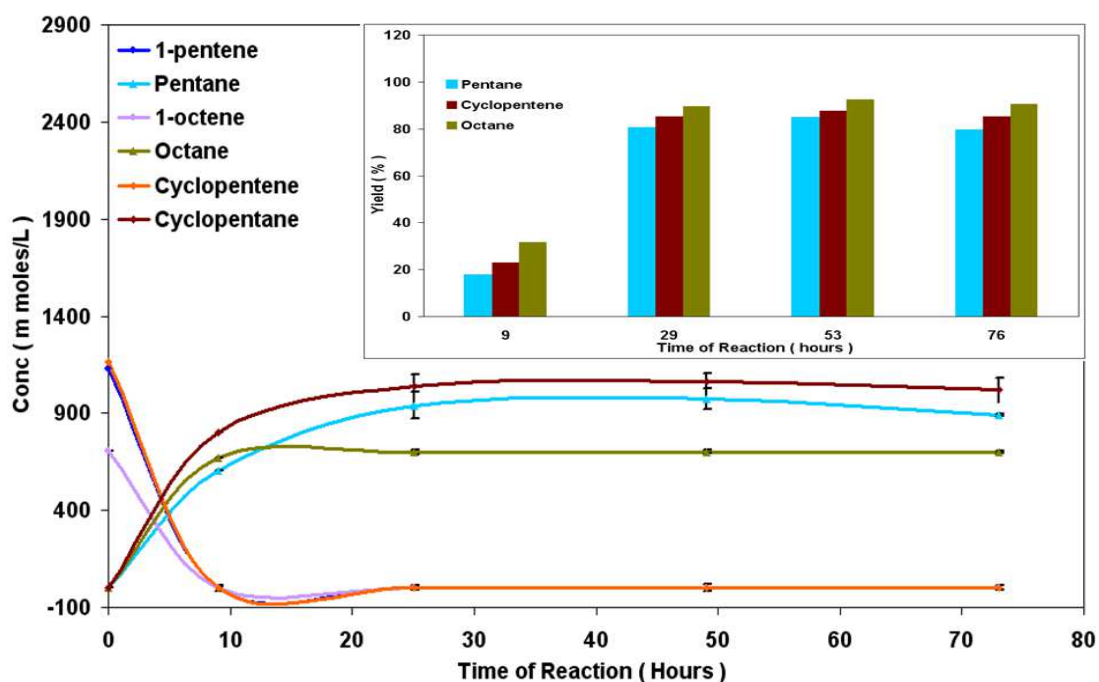
Figure 3.131 Hydrogenation of olefins (1-pentene, 1-octene and cyclopentene) present in PyGas [Reaction conditions: T = 140°C, WHSV$_{PyGas}$ = 4 h^{-1}, P$_{H2}$ = 20 barg]

Figure 3.132 shows that conversion of the toluene was about 73% in the first 9 hours of reaction, this decreased to 14% after 29 hours when reaction obtained steady state condition. After that a gentle decrease was observed and conversion decreased to 11% after 76 hours of reaction. In contrast to Ni/Al$_2$O$_3$ catalyst, the yield of methylcyclohexane formation over Pd/Al$_2$O$_3$ catalyst was significantly less. The yield of methylcyclohexane was 3% at 9 hours of reaction and a gradual decrease was observed in the yield to 1% at 76 hours of reaction.
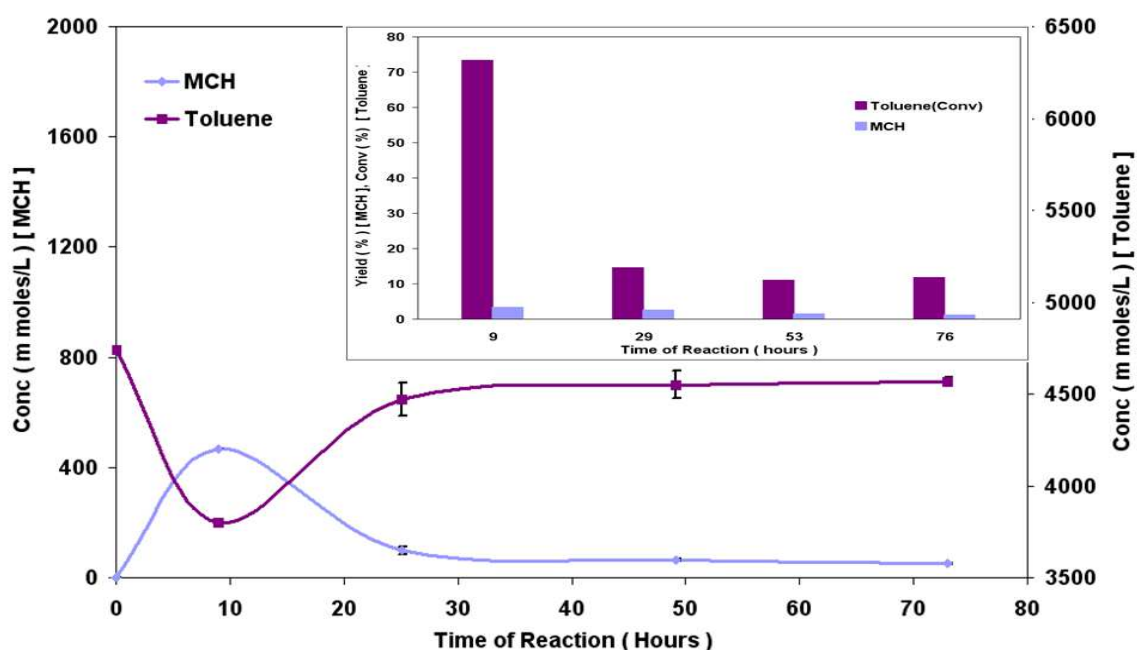
Figure 3.132 Hydrogenation of toluene [Reaction conditions: T = 140°C, WHSV$_{PyGas}$ = 4 h^{-1}, P$_{H2}$ = 20 barg]

Figure 3.133 shows that conversion of the styrene remained above 99%. Ethylbenzene was the main product of the reaction and a very small amount of ethylbenzene further hydrogenated to ethylcyclohexane. The yield of ethylbenzene was 20% at 9 hours of the reaction which increased to 60% at 29 hours and no significant change was observed with further time on stream. The yield of ethylcyclohexane was 2% in initial 9 hours of reaction. This was followed by a steady decrease in formation of ethylcyclohexane with time on stream. The results show that hydrogenation of aromatic over the Pd/Al_2O_3 catalyst was significantly smaller compared to the Ni/Al_2O_3 catalyst under these reaction conditions.
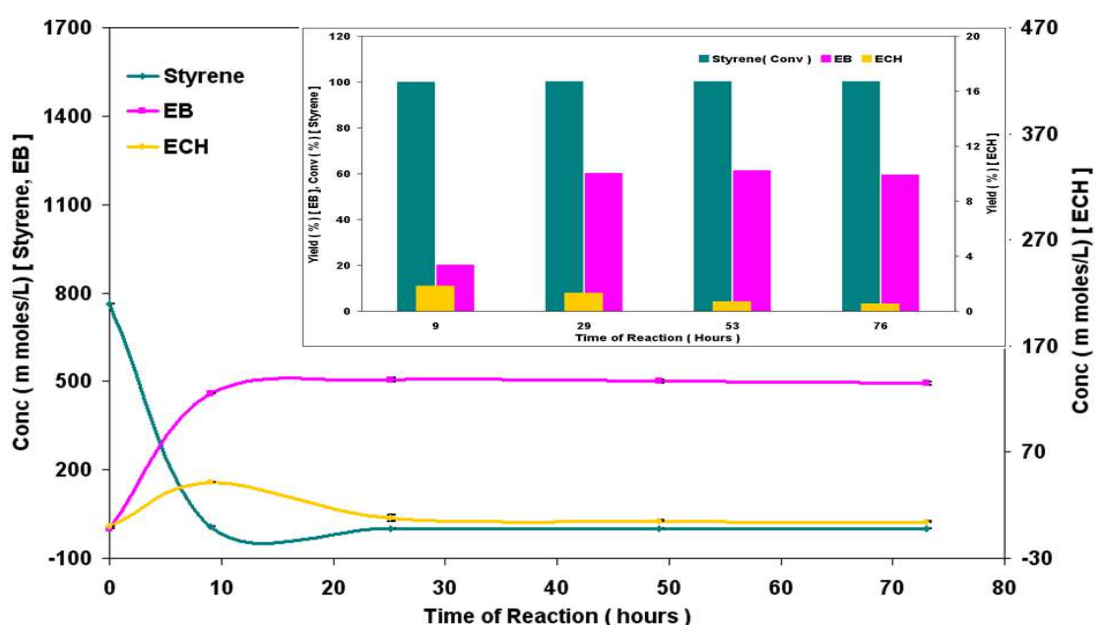
Figure 3.133 Hydrogenation of styrene [Reaction conditions: T = 140°C, WHSV$_{PyGas}$ = 4 h^{-1}, P$_{H2}$ = 20 barg]

Effluent gas analysis

Similar to Ni/Al_2O_3 system, the main liquid sample was trapped in the knockout pot, however very small amounts of hydrocarbons were detected in the effluent gas. Pentane and cyclopentane were the main components observed in effluent gas with very small amounts of toluene and methylcyclohexane, as shown in Figure 3.134.
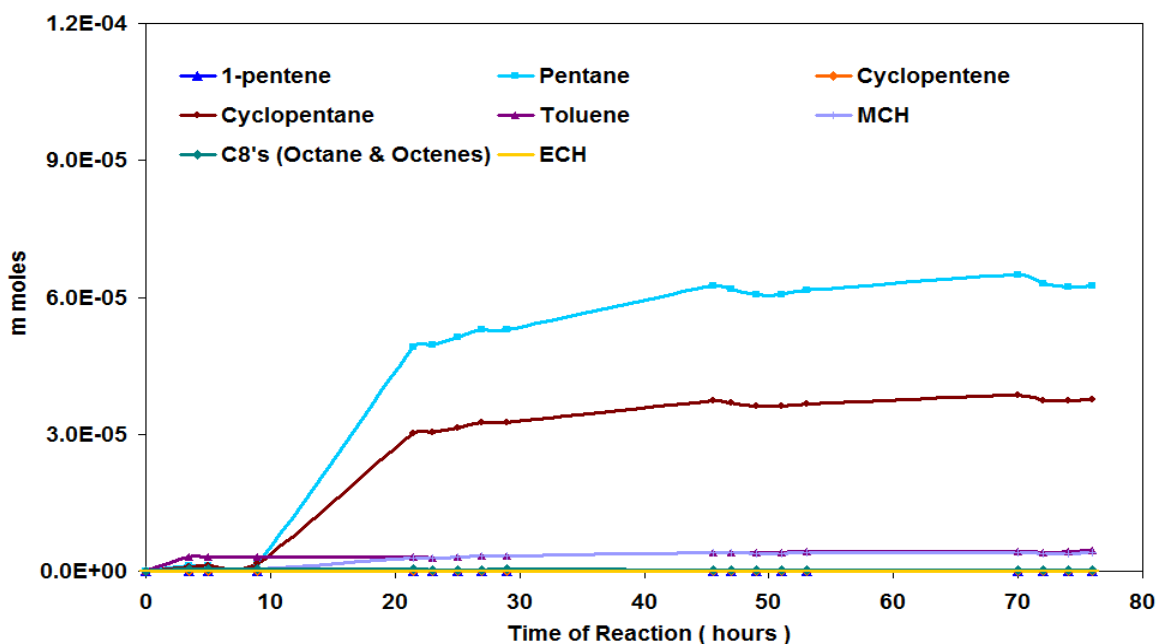
Figure 3.134 Effluent gas analysis [Reaction conditions: T = 140°C, WHSV$_{PyGas}$ = 4 h^{-1}, P$_{H2}$ = 20 barg]

The effluent gas was analysed during subsequent reactions over Pd/Al$_2$O$_3$ catalyst, and comparable amounts of hydrocarbons were observed in the effluent gas. Moreover, no significant change was observed in the quantity of hydrocarbons in the effluent gas when compared to the reactions over Ni/Al$_2$O$_3$ catalyst. This shows that the presence of hydrocarbons in the effluent gas is only physical phenomena, dependent on the vapour pressure of the components.

3.2.3.1.1.1 Post reaction analysis

Post reaction catalyst TPO

The catalyst was regenerated in a flow of 2% O$_2$/Ar gas and the process monitored by online Mass Spectrometer as mentioned in section 2.2.5. Figure 3.135 shows the *in-situ* TPO of post reaction Pd/Al$_2$O$_3$. The amount of coke deposition over the Pd/Al$_2$O$_3$ was comparable with the Ni/Al$_2$O$_3$ under the identical reaction conditions. However a higher amount of the H$_2$O evolution was observed in the TPO over palladium catalyst. This indicates that soft type coke deposition (with a lower C/H ratio) took place over the Pd/Al$_2$O$_3$ when compared to coke deposited over the Ni/Al$_2$O$_3$ under the same reaction conditions.

Temprature (°C)
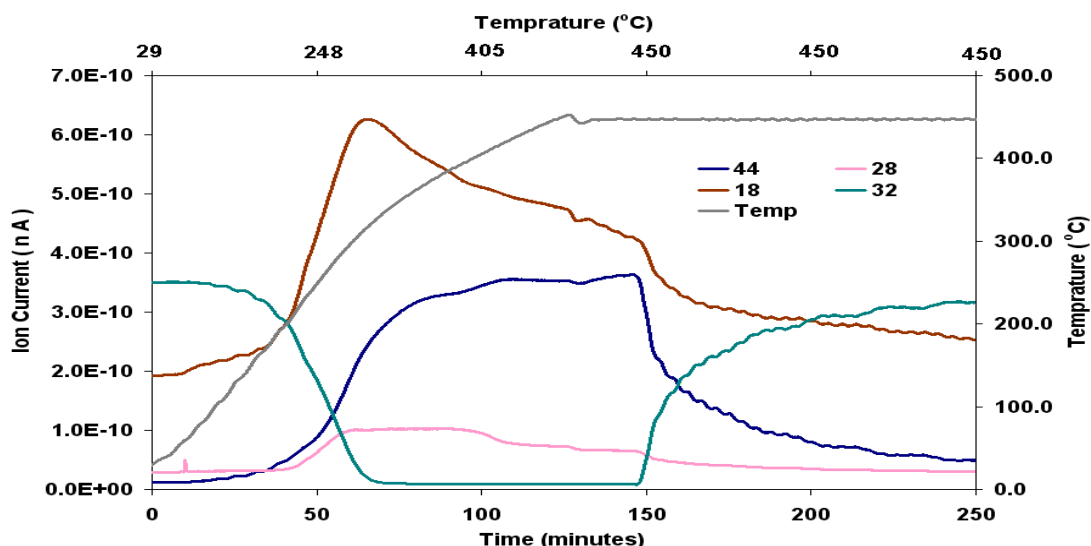
Figure 3.135 Post reaction *in-situ* TPO of Pd/Al$_2$O$_3$ catalyst [Reaction conditions: T = 140°C, WHSV$_{PyGas}$ = 4 h^{-1}, P$_{H2}$ = 20 barg]

Total oxygen consumption in TPO = 3.62 m moles

TGA-MS analysis

The catalyst was regenerated by *in-situ* TPO. However, TGA-MS analysis was performed up to 800°C, with a temperature ramp of 10°C/min under 2% O$_2$/Ar atmospheres on the regenerated catalyst to investigate if any coke was still present on the catalyst surface. A continuous weight loss (~3.0%) was noted. However a small evolution of CO$_2$ was observed in temperature between 360 and 400°C and about 0.6% weight loss was found corresponding to CO$_2$ evolution, as shown in Figure 3.136. This showed that no significant amount of carbonaceous residue was found on the surface of the catalyst after regeneration by *in-situ* TPO.
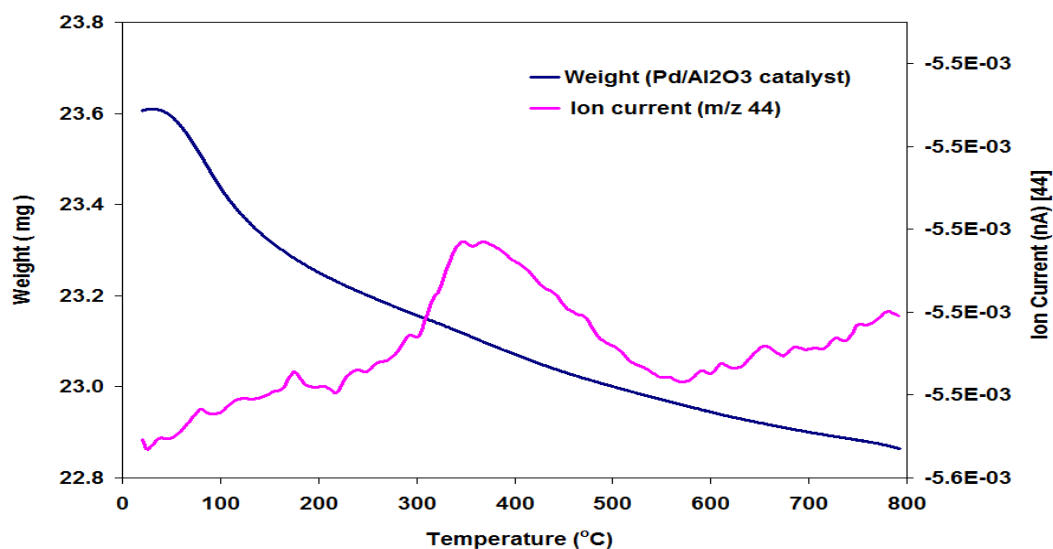
Figure 3.136 TGA-MS analysis of Pd/Al$_2$O$_3$ (Regenerated) catalyst [Reaction conditions: T = 140°C, WHSV$_{PyGas}$ = 4 h^{-1}, P$_{H2}$ = 20 barg]

TGA-MS analysis was performed on the regenerated Pd/Al_2O_3 catalysts of subsequent reactions up to 800°C, with a temperature ramp of 10°C/min, under 2% O_2/Ar gas and no significant amounts of coke was found on the regenerated catalysts.

X-ray diffraction (XRD)

The XRD analysis was carried out over the regenerated Pd/Al_2O_3 catalyst. No significant change was observed in XRD analysis, which suggests that no phase change occurred in the catalyst support during hydrogenation and regeneration. XRD analysis was also performed on the regenerated catalysts of subsequent reactions and the spectra found to be similar to that of the fresh catalyst.

BET analysis

The surface area, pore volume and pore diameter of the regenerated Pd/Al_2O_3 catalyst was analysed and compared with fresh the Pd/Al_2O_3 catalyst as shown in Table 3.27.

Catalyst	Surface Area (m^2g^{-1})	Pore Volume (cm^3g^{-1})	Average Pore diameter (Å)
Pd/Al_2O_3	99	0.51	208
Pd/Al_2O_3 (Reduced)	104	0.50	197
Pd/Al_2O_3 (Regenerated)	93	0.45	172

Table 3.27 BET analysis of Pd/Al_2O_3 (Regenerated) catalyst [Reaction conditions: T = 140°C, $WHSV_{PyGas}$ = 4 h^{-1}, P_{H2} = 20 barg]

The surface area of the regenerated catalyst was found to be similar to the fresh catalyst.

3.2.3.1.2 PyGas hydrogenation over Pd/Al_2O_3 at 160°C

The reaction temperature of PyGas over Pd/Al_2O_3 was increased to 160°C with all other conditions kept constant [$WHSV_{PyGas}$ = 4 h^{-1} and P_{H2} = 20 barg]. The reaction concentration profile is shown in Figure 3.137.
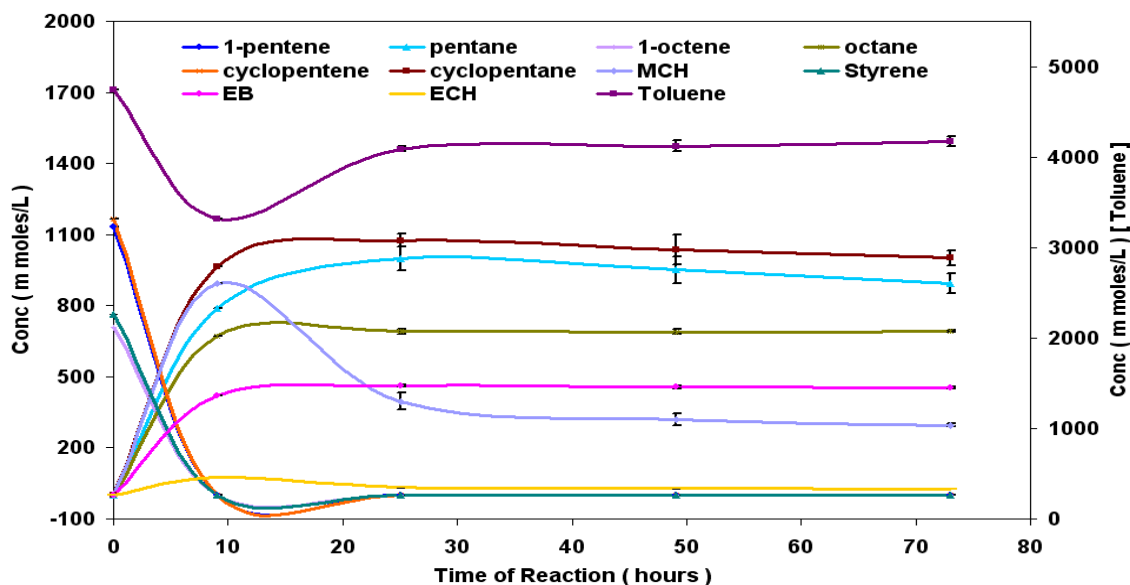
Figure 3.137 Reaction profile of PyGas hydrogenation [Reaction conditions: T = 160°C, WHSV$_{PyGas}$ = 4 h^{-1}, P$_{H2}$ = 20 barg]

Figure 3.138 shows that no significant change was observed in the hydrogenation of olefins with an increase in reaction temperature. The conversion of olefins (1-pentene, 1-octene and cyclopentene) was found to be above 99%. The olefins hydrogenated to their respective saturated components with no formation of internal olefins. The yield of paraffins was small for the first 9 hours of reaction however this increased when reaction achieved steady state condition. The yields of pentane, cyclopentane and octane were 86%, 89% and 92% respectively after 29 hours of the reaction and a very slow decrease was observed in these yields with time on stream.
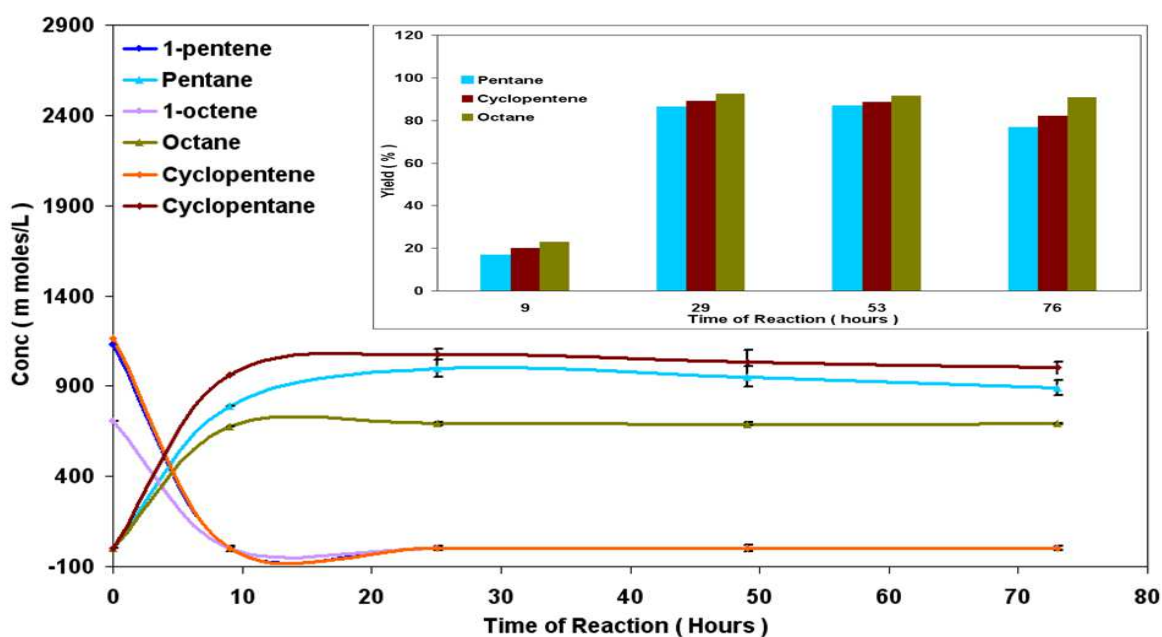
Figure 3.138 Hydrogenation of olefins (1-pentene, 1-octene and cyclopentene) present in PyGas [Reaction conditions: T = 160°C, WHSV$_{PyGas}$ = 4 h^{-1}, P$_{H2}$ = 20 barg]

Figure 3.139 shows that an increase took place in the hydrogenation of toluene to methylcyclohexane with an increase in reaction temperature. The conversion of toluene was 83% in the initial 9 hours of the reaction, this decreased to 19% after 29 hours of the reaction and remained constant throughout the remainder of the reaction. The yield of methylcyclohexane was 5% at 10 hours of reaction, this increased to 9% when the reaction obtained steady state after 29 hours. There then followed a slow decrease with time on stream.
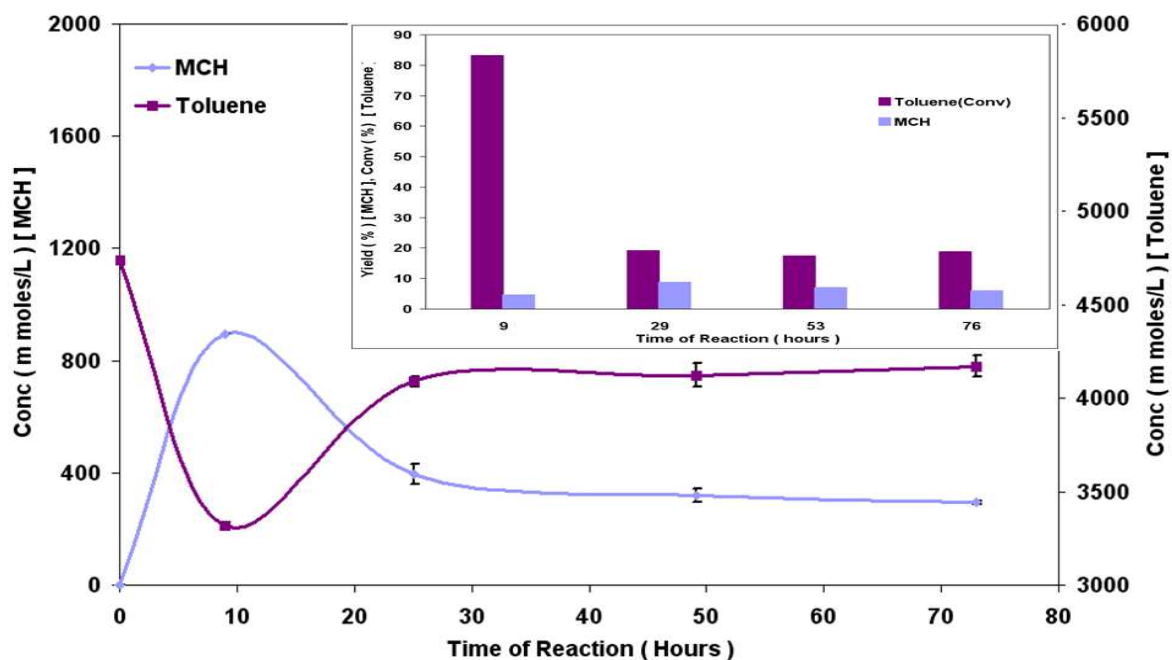
Figure 3.139 Hydrogenation of toluene [Reaction conditions: T = 160°C, WHSV$_{PyGas}$ = 4 h^{-1}, P$_{H2}$ = 20 barg]

Figure 3.140 shows that an increase was also observed in the further hydrogenation of ethylbenzene to ethylcyclohexane with an increase in reaction temperature. The yield of ethylbenzene was 13% in initial 9 hours of reaction which increased to 58% after 29 hours, with no significant change observed to the end of the reaction. The yield of ethylcyclohexane was 2% at 9 hours of the reaction which increased to 5% after 29 hours followed by a slow decreased with time on stream.
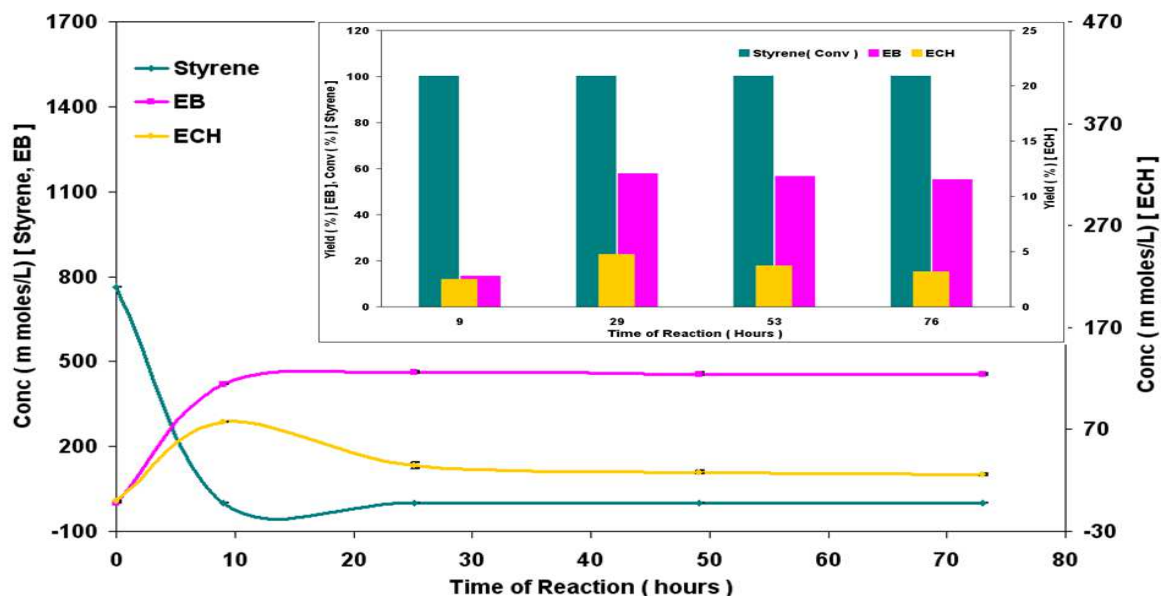
Figure 3.140 Hydrogenation of styrene [Reaction conditions: T = 160°C, WHSV$_{PyGas}$ = 4 h^{-1}, P$_{H2}$ = 20 barg]

Figure 3.141 indicates a slight decrease in selectivity of ethylcyclohexane and a small increase in ethylbenzene selectivity with time on stream. This suggests that the capability of the catalyst to further hydrogenate ethylbenzene to ethylcyclohexane decreased with time on stream.
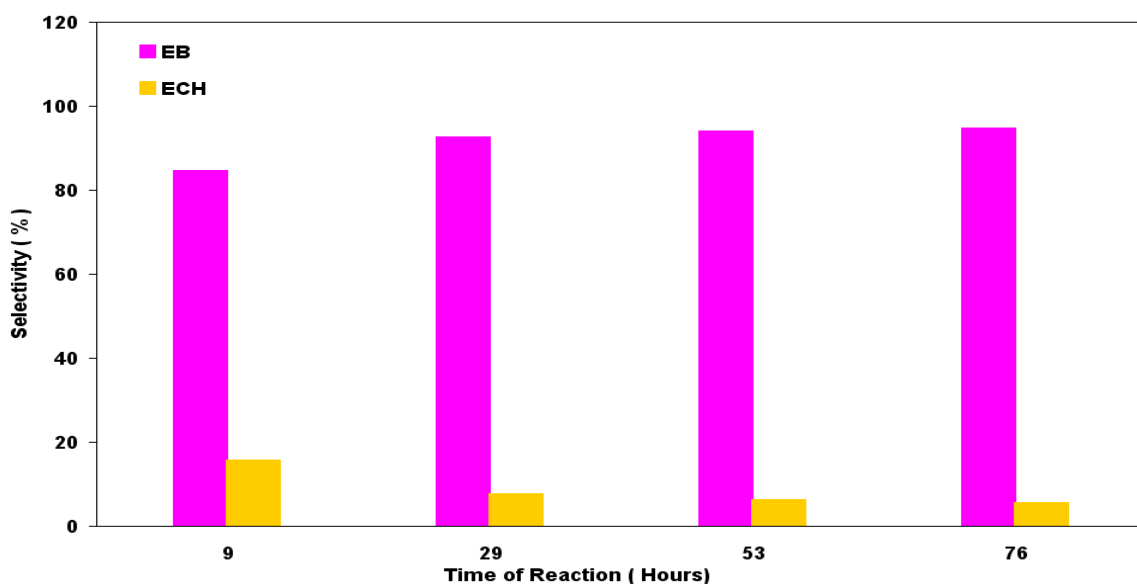
Figure 3.141 Selectivity of ethylbenzene and ethylcyclohexane during hydrogenation of styrene [Reaction conditions: T = 160°C, WHSV$_{PyGas}$ = 4 h^{-1}, P$_{H2}$ = 20 barg]

3.2.3.1.2.1 Post Reaction Analysis

Post reaction catalyst TPO

Figure 3.142 shows that similar amounts of CO_2, CO, H_2O desorption and O_2 consumption were observed in the TPO when compared to that observed from

the catalyst used in the previous reaction at 140°C. This indicates that there was no noticeable change in the amount and nature of carbonaceous material deposited on the surface of the catalyst with an increase in reaction temperature from 140°C to 160°C.
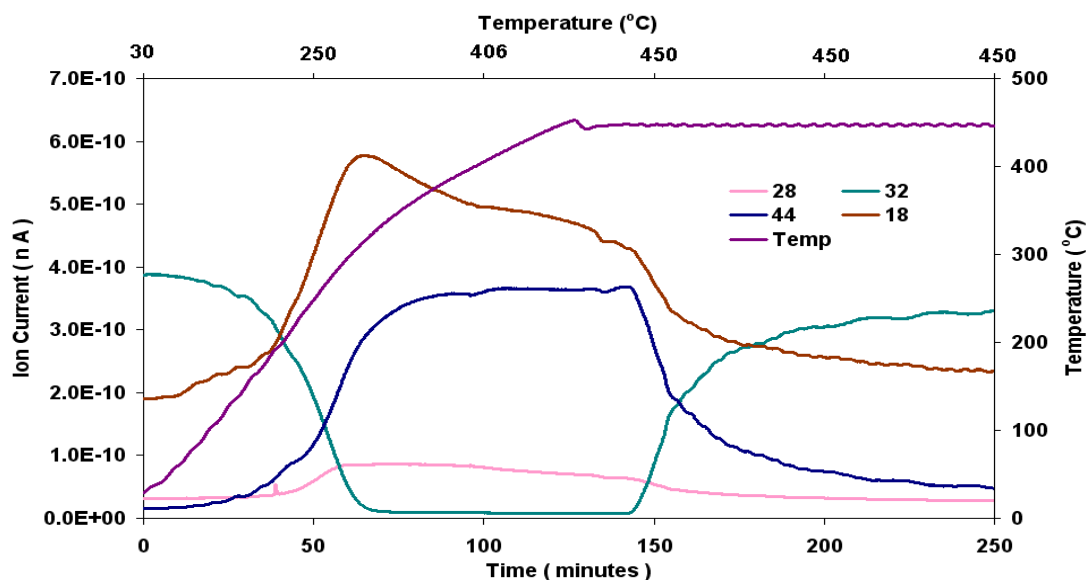
Figure 3.142 Post reaction *in-situ* TPO of Pd /Al$_2$O$_3$ catalyst [Reaction conditions: T = 160°C, WHSV$_{PyGas}$ = 4 h^{-1}, P$_{H2}$ = 20 barg]

Total oxygen consumption in TPO = 3.68 m moles

BET analysis

The surface area, pore volume and pore diameter of the regenerated Pd/Al$_2$O$_3$ catalyst were analysed. No significant change was observed in the surface area of regenerated catalyst when compared to fresh the catalyst as shown in Table 3.28.

Catalyst	Surface Area (m^{2}g^{-1})	Pore Volume (cm^{3}g^{-1})	Average Pore diameter (Å)
Pd/Al$_2$O$_3$	99	0.51	208
Pd/Al$_2$O$_3$ (Reduced)	104	0.50	197
Pd/Al$_2$O$_3$ (Regenerated)	95	0.49	208

Table 3.28 BET analysis of Pd/Al$_2$O$_3$ (Regenerated) catalyst [Reaction conditions: T = 160°C, WHSV$_{PyGas}$ = 4 h^{-1}, P$_{H2}$ = 20 barg]

3.2.3.1.3 PyGas hydrogenation over Pd/Al$_2$O$_3$ at 180°C

The concentration profile of PyGas hydrogenation over Pd/Al$_2$O$_3$ under reaction conditions T = 180°C, WHSV$_{PyGas}$ = 4 h^{-1} and P$_{H2}$ = 20 barg is shown in Figure 3.143.
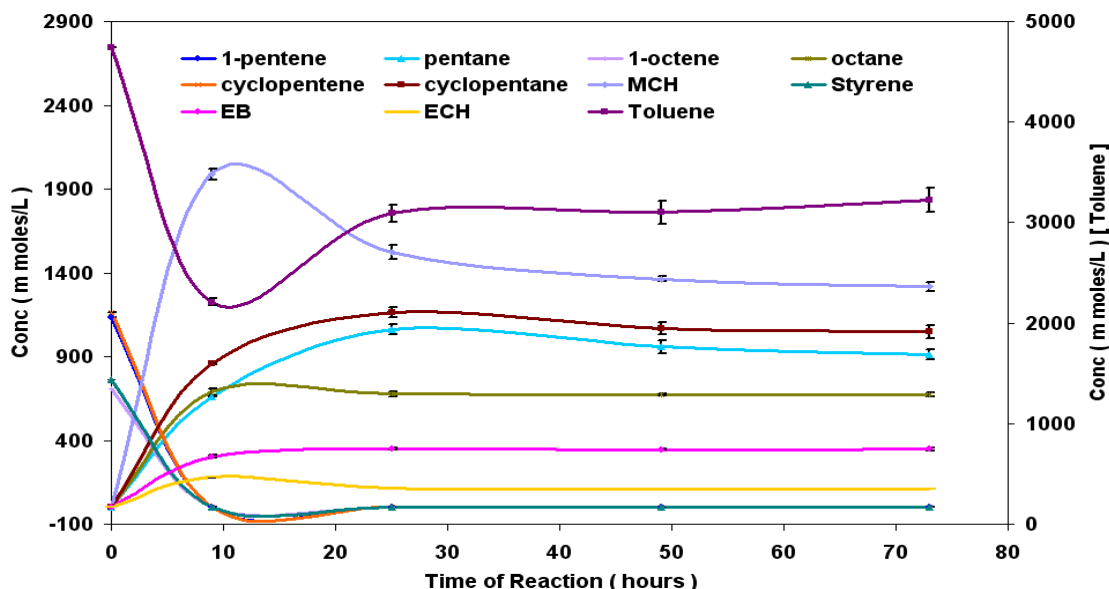
Figure 3.143 Reaction profile of PyGas hydrogenation [Reaction conditions: T = 180°C, WHSV$_{PyGas}$ = 4 h^{-1}, P$_{H2}$ = 20 barg]

Figure 3.144 shows that olefins hydrogenated to saturated compounds with no formation of internal olefins. No significant change was observed in the yield of saturated paraffins with an increase in temperature from 160°C to 180°C. Compared to the reaction with the Ni/Al$_2$O$_3$ catalyst, the yield of paraffins was considerably higher over the Pd/Al$_2$O$_3$ catalyst under the same reaction conditions.
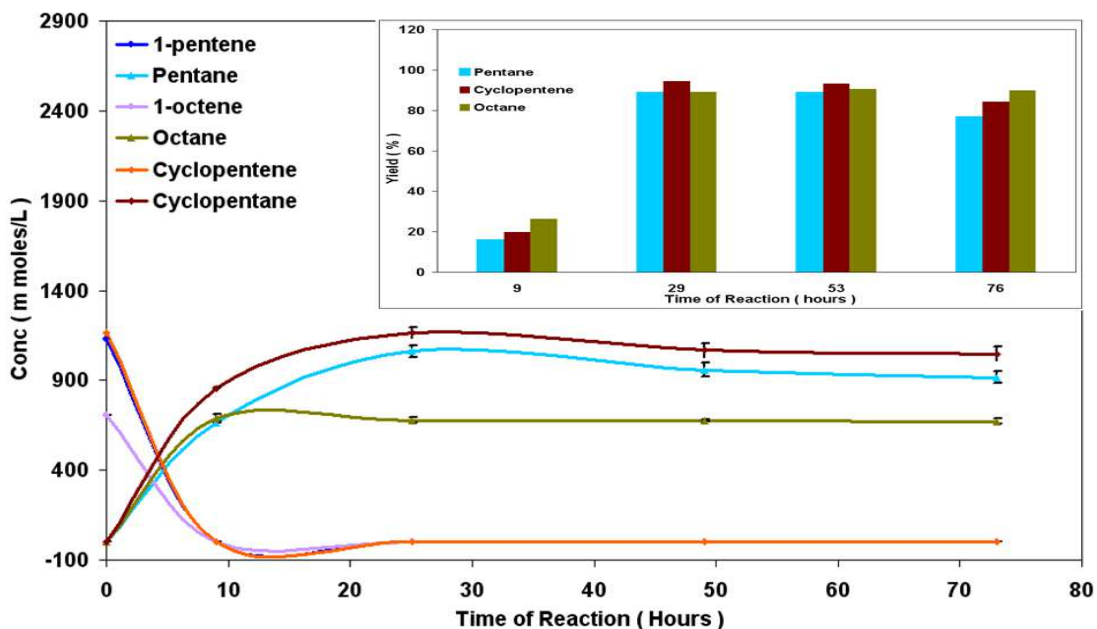
Figure 3.144 Hydrogenation of olefins (1-pentene, 1-octene and cyclopentene) present in PyGas [Reaction conditions: T = 180°C, WHSV$_{PyGas}$ = 4 h^{-1}, P$_{H2}$ = 20 barg]

Figure 3.145 shows that a considerable increase was observed in the hydrogenation of toluene with the increase in reaction temperature from 160°C

to 180°C. Conversion of toluene was very high (~ 87%) in the initial 9 hours of the reaction, which decreased to 40% after 29 hours once steady state was achieved. A gradual decrease was observed in conversion of the toluene in the rest of the reaction. The yield of methylcyclohexane was 11% in the initial 9 hours of the reaction which increased to 30% after 29 hours of the reaction. This was followed by a steady decrease with time on stream. Comparable rate of toluene hydrogenation was observed over both the Pd/Al$_2$O$_3$ and Ni/Al$_2$O$_3$ catalysts at 180°C.
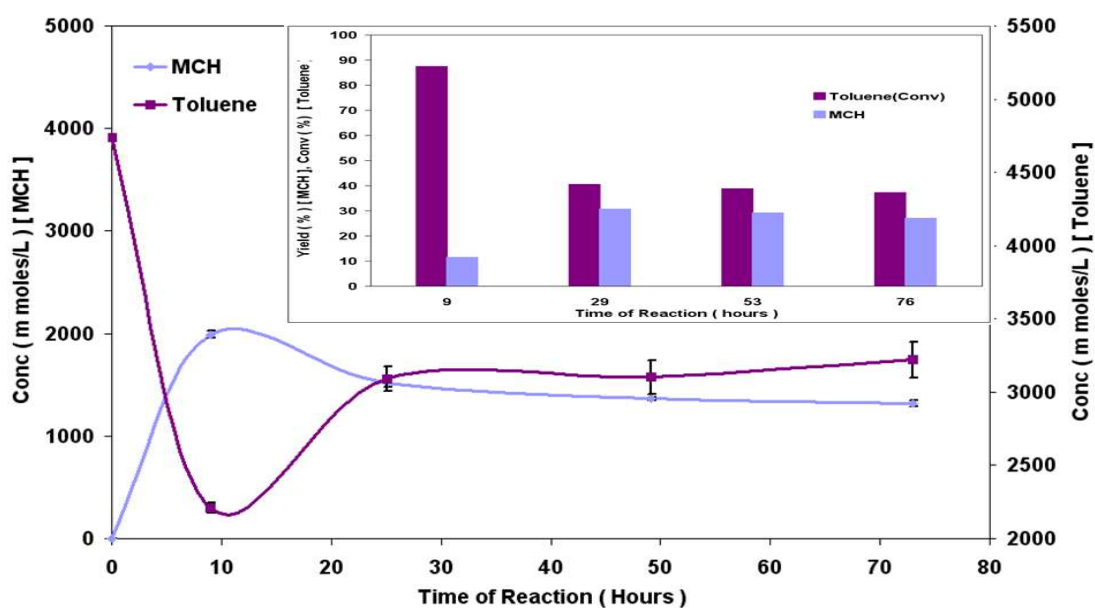
Figure 3.145 Hydrogenation of toluene [Reaction conditions: T = 180°C, WHSV$_{PyGas}$ = 4 h^{-1}, P$_{H2}$ = 20 barg]

Similarly, a reasonable increase also occurred in formation of the ethylcyclohexane during styrene hydrogenation with an increase in the reaction temperature as shown in Figures 3.146-147. The results suggest that high temperature is favourable for further hydrogenation of ethylbenzene to ethylcyclohexane. The yield of ethylcyclohexane was found to be similar while the yield of ethylbenzene was found to be considerably higher than that for the reaction performed over Ni/Al$_2$O$_3$ catalyst at 180°C. This suggests that a smaller amount of styrene polymerised to form coke over the Pd/Al$_2$O$_3$ catalyst compared to the Ni/Al$_2$O$_3$ catalyst under these reaction conditions.
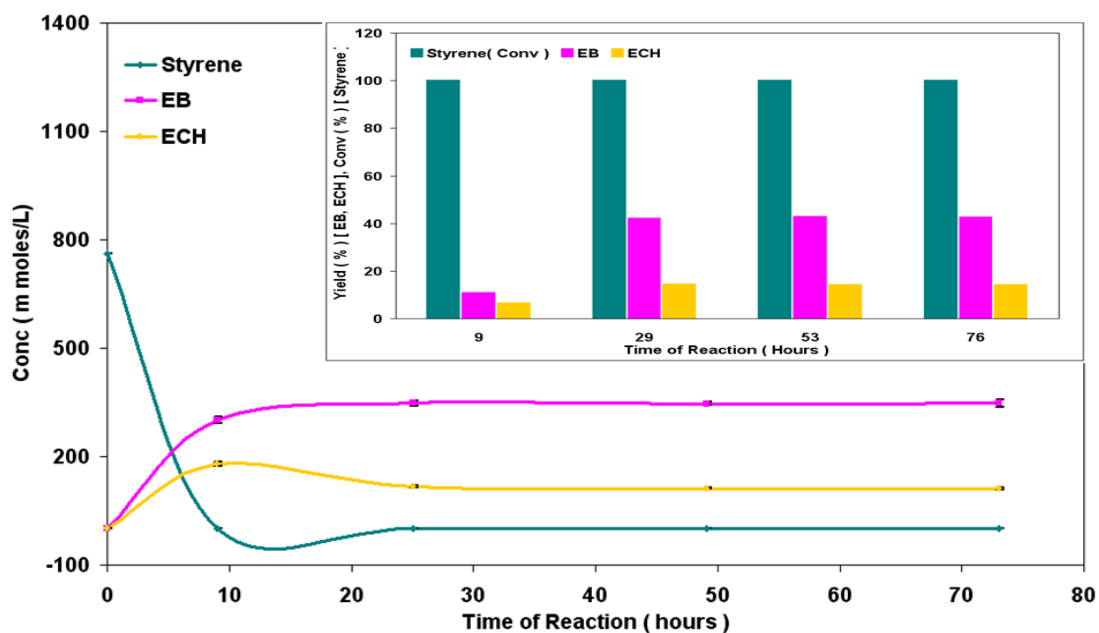
Figure 3.146 Hydrogenation of styrene [Reaction conditions: T = 180°C, WHSV$_{PyGas}$ = 4 h^{-1}, P$_{H2}$ = 20 barg]
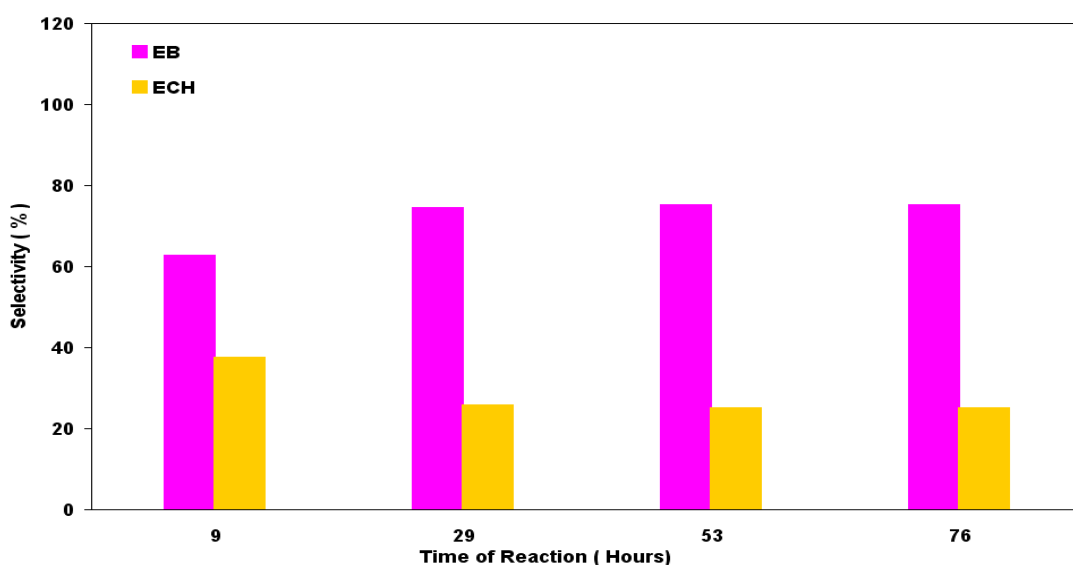
Figure 3.147 Selectivity of ethylbenzene and ethylcyclohexane during styrene hydrogenation [Reaction conditions: T = 180°C, WHSV$_{PyGas}$ = 4 h^{-1}, P$_{H2}$ = 20 barg]

3.2.3.1.3.1 Post reaction analysis

Post reaction catalyst TPO

The *in-situ* TPO was carried out over post reaction Pd/Al$_2$O$_3$ catalyst, and shown in Figure 3.148. An increase was noted in the evolution of CO$_2$, CO and consumption of O$_2$ during TPO with an increase in reaction temperature. This suggests that an increase occurred in coke deposition with an increase in reaction temperature from 160°C to 180°C. Moreover, a decrease was observed

in the amount of H_2O evolved. This illustrates that the C/H ratio in the deposited coke increased with an increase in reaction temperature from 160°C to 180°C.
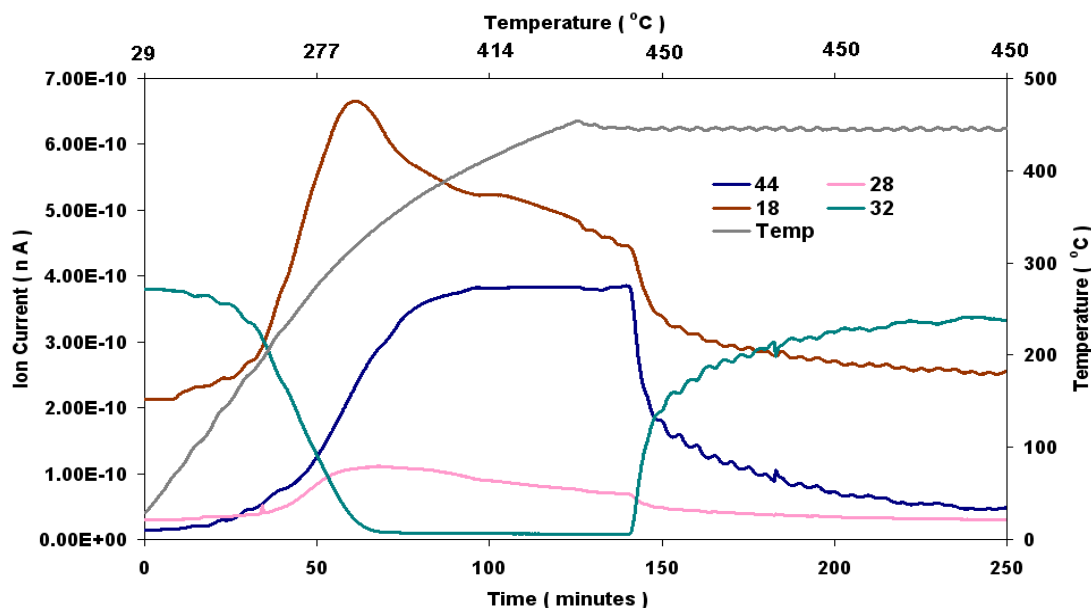
Figure 3.148 Post reaction *in-situ* TPO of Pd/Al₂O₃ catalyst [Reaction conditions: T = 180°C, WHSV_PyGas = 4 h⁻¹, P_H2 = 20 barg]

Total oxygen consumption in TPO = 3.86 m moles

BET analysis

The results indicate the surface area lost due to deposition of coke was recovered during regeneration, as shown in Table 3.29.

Catalyst	Surface Area (m²g⁻¹)	Pore Volume (cm³g⁻¹)	Average Pore diameter (Å)
Pd/Al₂O₃	99	0.51	208
Pd/Al₂O₃ (Reduced)	104	0.50	197
Pd/Al₂O₃ (Regenerated)	95	0.46	196

Table 3.29 BET analysis of Pd/Al₂O₃ (Regenerated) catalyst [Reaction conditions: T = 180°C, WHSV_PyGas = 4 h⁻¹, P_H2 = 20 barg]

3.2.3.1.4 PyGas hydrogenation over Pd/Al₂O₃ at 200°C

The reaction temperature was further increased to 200°C and all other reaction conditions kept constant [WHSV_PyGas = 4 h⁻¹ and P_H2 = 20 barg], the reaction profile is shown in Figure 3.149.
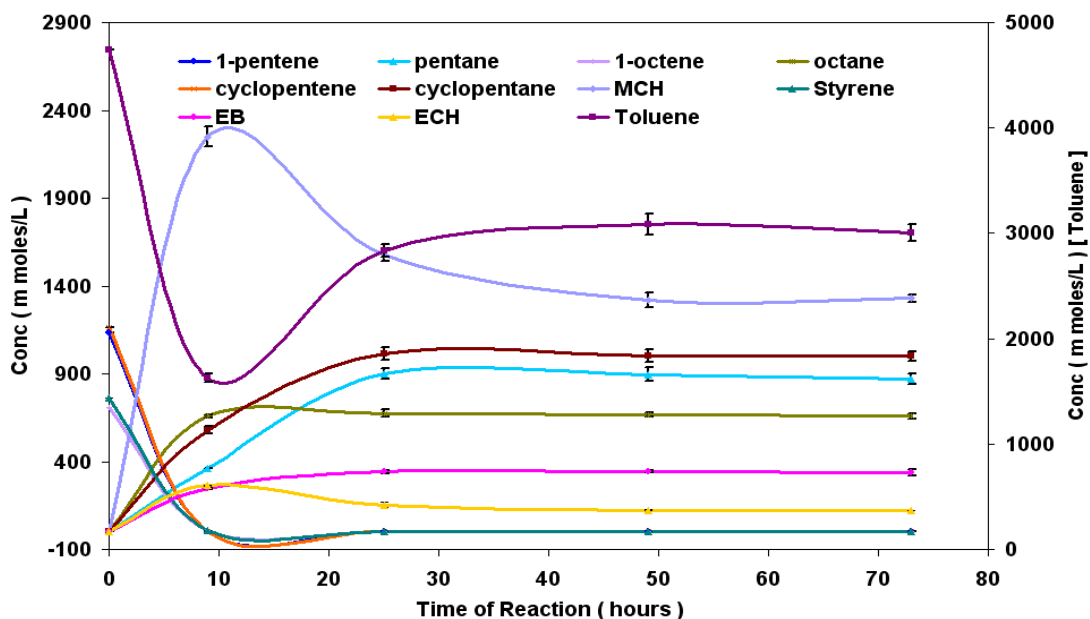
Figure 3.149 Reaction profile of PyGas hydrogenation [Reaction conditions: T = 200°C, WHSV$_{PyGas}$ = 4 h^{-1}, P$_{H2}$ = 20 barg]

Figure 3.150 shows that olefins (1-pentene, cyclopentene and 1-octene) present in the PyGas hydrogenated to their respective saturated compounds and no internal olefin formation was observed. A small decrease in the yield of paraffins was observed with an increase in the reaction temperature although the conversion of olefins was above 99%.

Figure 3.150 Hydrogenation of olefins (1-pentene, 1-octene and cyclopentene) present in PyGas [Reaction conditions: T = 200°C, WHSV$_{PyGas}$ = 4 h^{-1}, P$_{H2}$ = 20 barg]

Figure 3.151 shows that conversion of the toluene was around 93% for first 9 hours of the reaction, which decreased to 49% after 29 hours when reaction

obtained steady state. Then a small decrease was observed in the conversion of toluene with time on stream. The yield of methylcyclohexane was 9% in the initial 9 hours of the reaction which increased to 31% after 29 hours and then a very gradual decrease was observed in the formation of methylcyclohexane with time on stream. The hydrogenation of toluene was found to be similar to the reaction carried out over Ni/Al$_2$O$_3$ catalyst under the same reaction conditions.
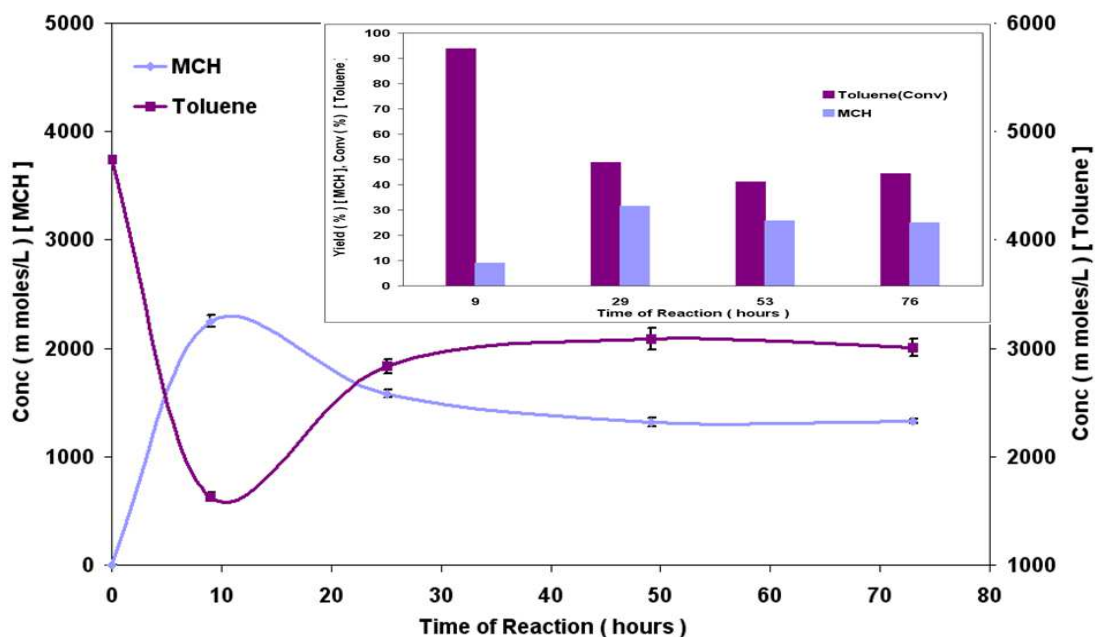
Figure 3.151 Hydrogenation of toluene [Reaction conditions: T = 200°C, WHSV$_{PyGas}$ = 4 h^{-1}, P$_{H2}$ = 20 barg]

From Figures 3.152-153 it can be seen that a further increase took place in the yield of ethylcyclohexane with an increase in reaction temperature from 180°C to 200 °C. Conversion of the styrene was observed to be above 99 % throughout the reaction. The yields of ethylbenzene and ethylcyclohexane were 6% and 7% respectively in the initial 9 hours of reaction. This increased to 40% and 20% respectively after 29 hours of reaction. Subsequently, the yield of ethylbenzene was virtually constant while a steady decrease was observed in the yield of ethylcyclohexane with time on stream. Higher amounts of both the ethylbenzene and the ethylcyclohexane formation were observed over the Pd/Al$_2$O$_3$ catalyst when compared to the Ni/Al$_2$O$_3$ catalyst under these reaction conditions.
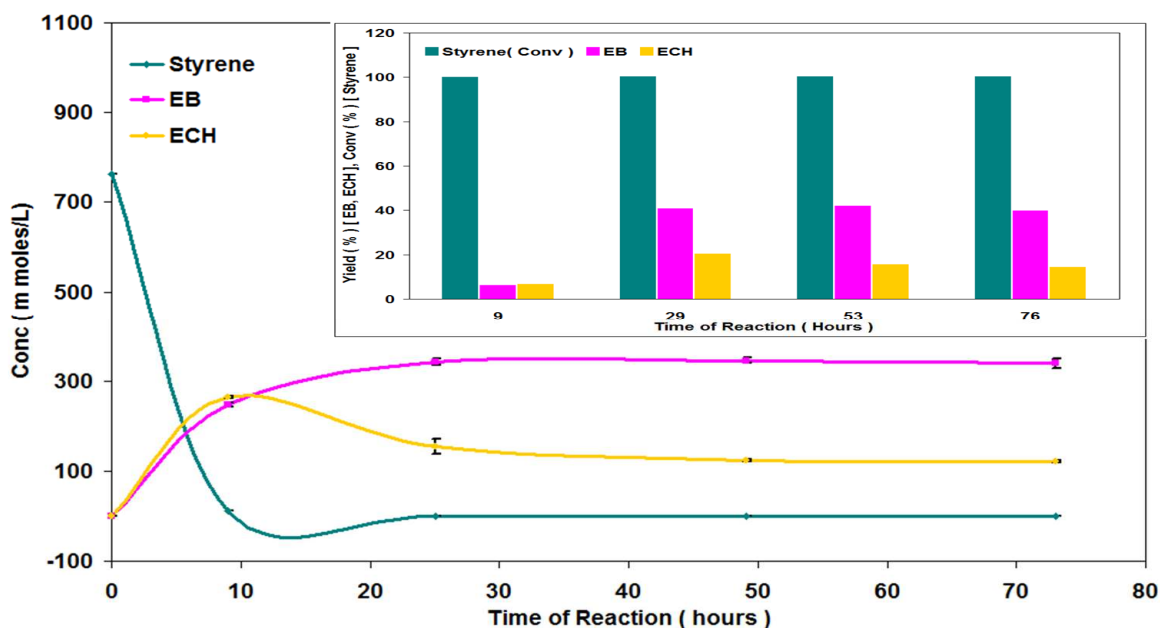
Figure 3.152 Hydrogenation of styrene [Reaction conditions: T = 200°C, WHSV$_{PyGas}$ = 4 h^{-1}, P$_{H2}$ = 20 barg]
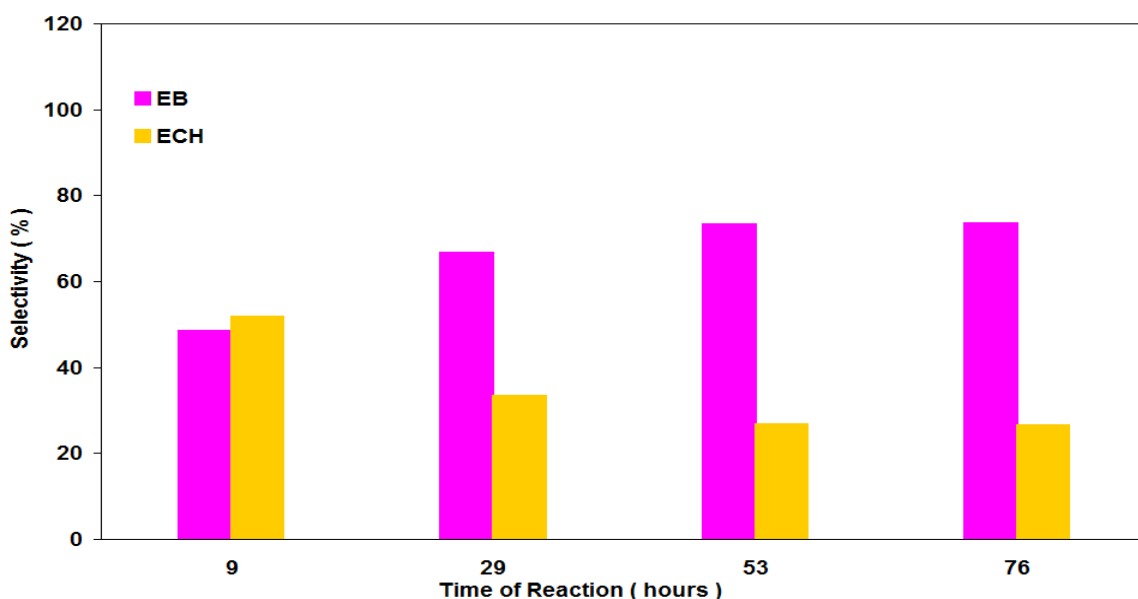
Figure 3.153 Selectivity of ethylbenzene and ethylcyclohexane during hydrogenation of styrene [Reaction conditions: T = 200°C, WHSV$_{PyGas}$ = 4 h^{-1}, P$_{H2}$ = 20 barg]

3.2.3.1.4.1 Post reaction analysis

Post reaction catalyst TPO

Post reaction *in-situ* TPO of the Pd/Al$_2$O$_3$ catalyst was carried out in a continuous flow of 2% O$_2$/Ar, as shown in Figure 3.154. The results indicate an increase in coke deposition and a change in the nature of the coke took place, with an increase in reaction temperature. The evolution of H$_2$O was sharper and smaller when compared to previous TPOs indicating that the C/H ratio in carbonaceous material increased with an increase in reaction temperature.
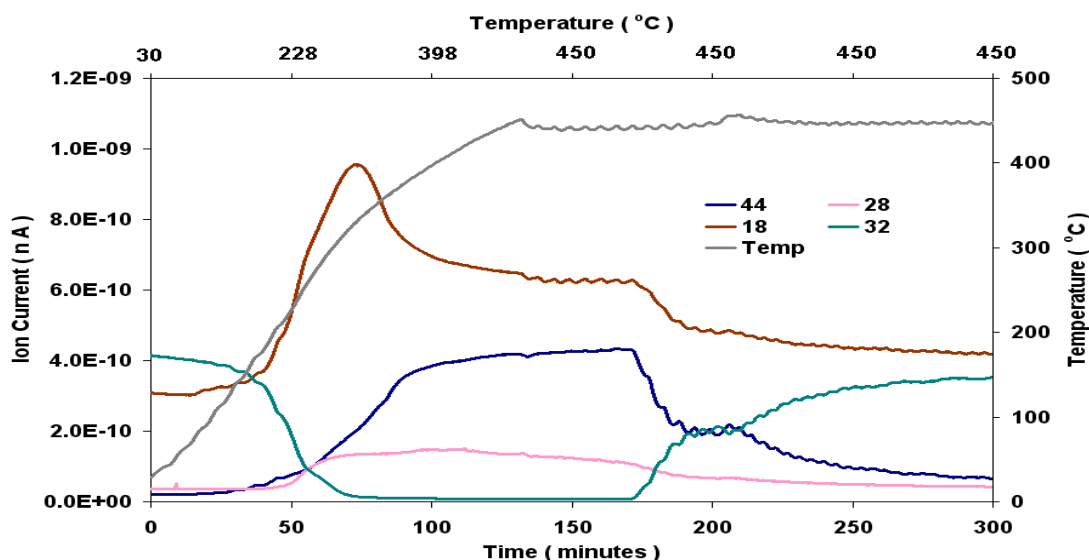
Figure 3.154 Post reaction *in-situ* TPO of Pd/Al$_2$O$_3$ catalyst [Reaction conditions: T = 200°C, WHSV$_{PyGas}$ = 4 h^{-1}, P$_{H2}$ = 20 barg]

Total oxygen consumption in TPO = 4.80 m moles

TGA-MS analysis

The TGA-MS analysis performed on the regenerated catalyst up to 800°C with temperature ramp 10°C under 2% O$_2$/Ar. A small continuous weight loss (~3.7%) was observed. Figure 3.155 shows that the main CO$_2$ evolution was observed at 365°C and about 1% weight loss of catalyst corresponded to this CO$_2$ evolution. This showed that no significant amount of coke was found on the surface of the catalyst after regeneration by *in-situ* TPO, although a high amount of coke deposition took place at high reaction temperature (200°C).
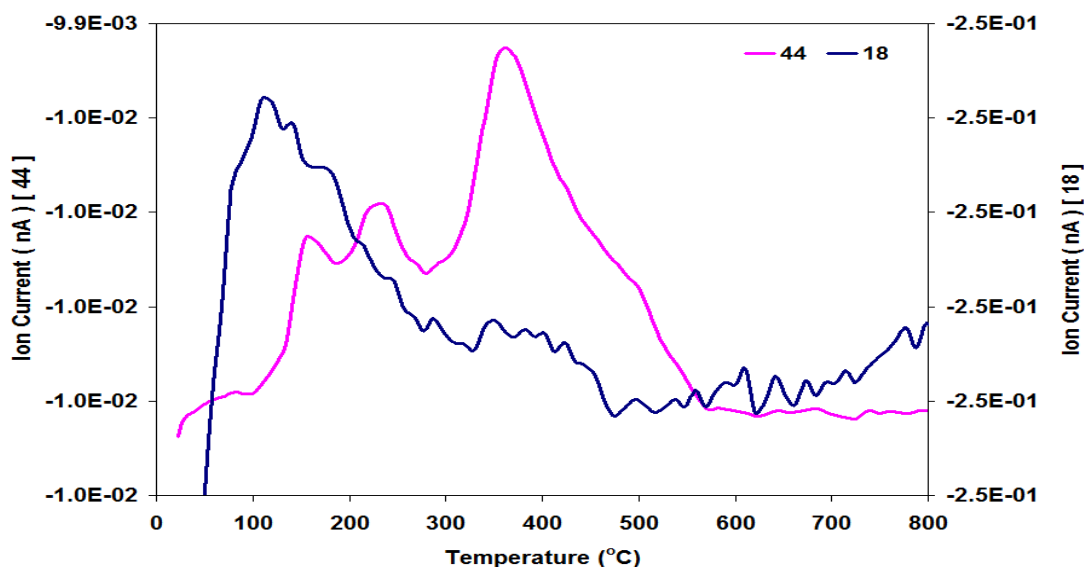
Figure 3.155 TGA- MS of Pd/Al$_2$O$_3$ (Regenerated) catalyst [Reaction conditions: T = 200°C, WHSV$_{PyGas}$ = 4 h^{-1}, P$_{H2}$ = 20 barg]

BET analysis

The surface area, pore volume and average pore diameter of both the fresh and the regenerated catalyst changed insignificantly as shown in Table 3.30. Consequently the results indicated that no sintering was observed in the catalyst.

Catalyst	Surface Area (m^2g^{-1})	Pore Volume (cm^3g^{-1})	Average Pore diameter ($\mathring{A}$)
Pd/Al$_2$O$_3$	99	0.51	208
Pd/Al$_2$O$_3$ (Reduced)	104	0.50	197
Pd/Al$_2$O$_3$ (Regenerated)	101	0.49	197

Table 3.30 BET analysis of Pd/Al$_2$O$_3$ (Regenerated) catalyst [Reaction conditions: T = 200°C, WHSV$_{PyGas}$ = 4 h^{-1}, P$_{H2}$ = 20 barg]

3.2.3.2 Effect of hydrogen partial pressure on PyGas hydrogenation

Similar to Ni/Al$_2$O$_3$ system, different hydrogen gas mixtures (100% H$_2$, 50% H$_2$, 25% H$_2$ and 5% H$_2$) diluted with nitrogen were used to investigate the effect of hydrogen partial pressure during the hydrogenation of PyGas over Pd/Al$_2$O$_3$ catalyst. Only the hydrogen gas mixtures were changed while other reaction parameters were kept constant [T = 140°C, WHSV$_{PyGas}$ = 4 h^{-1}, P$_T$ = 20 barg]. The reaction over 100% H$_2$ is already presented in section 3.2.3.1.1 and other reactions are discussed below.

3.2.3.2.1 PyGas hydrogenation over Pd/Al$_2$O$_3$ using 50% hydrogen gas mixture

The 50% hydrogen diluted with nitrogen was used to investigate the hydrogenation of PyGas over Pd/Al$_2$O$_3$ in a fixed bed reactor under the following operating conditions T = 140°C, WHSV$_{PyGas}$ = 4 h^{-1}, P$_T$ = 20 barg and P$_{H2}$ = 10 barg. The reaction profile of PyGas hydrogenation is shown in Figure 3.156.
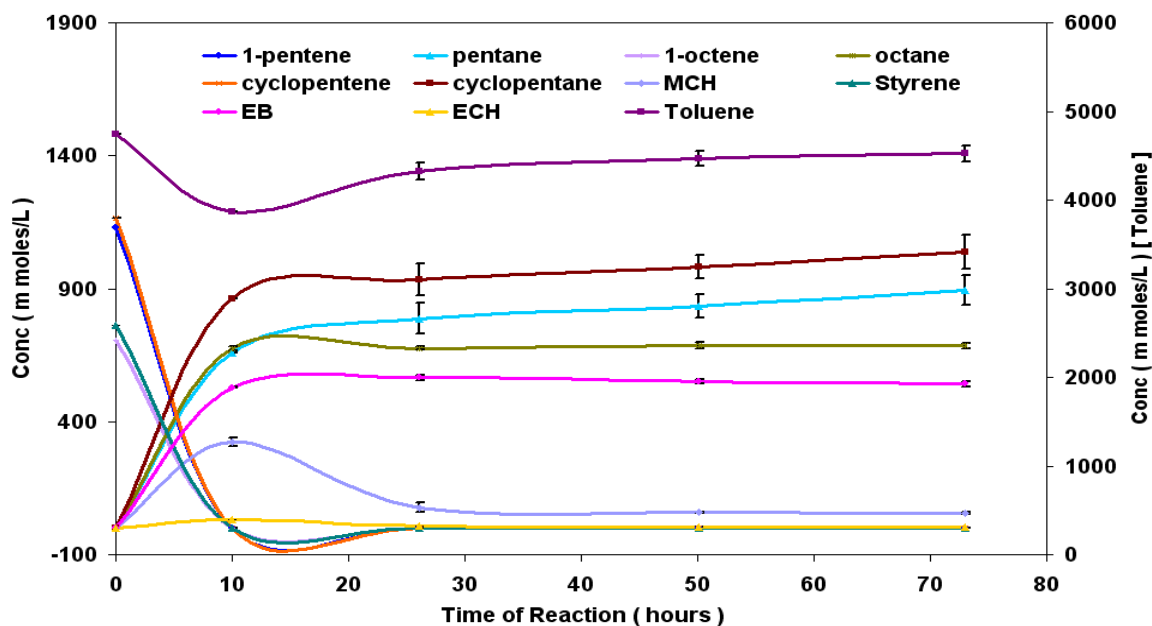
Figure 3.156 Reaction profile of PyGas Hydrogenation [Reaction conditions: T = 140°C, WHSV$_{PyGas}$ = 4 h^{-1}, P$_T$ = 20 barg, P$_{H2}$ = 10 barg]

The olefins (1-pentene, 1-octene and cyclopentene) hydrogenated to their respective saturated components with no formation of internal olefins. A considerable decrease was observed in the yield of paraffins with a decrease in hydrogen partial pressure from 20 barg to 10 barg although conversion of olefins was above 99%. The yields of pentane, cyclopentane and octane were 19%, 24%, and 31% respectively in the first 10 hours of reaction which subsequently increased to 67%, 73% and 78% respectively at 30 hours of the reaction and then remained constant till to the end of reaction, as shown in Figure 3.157.
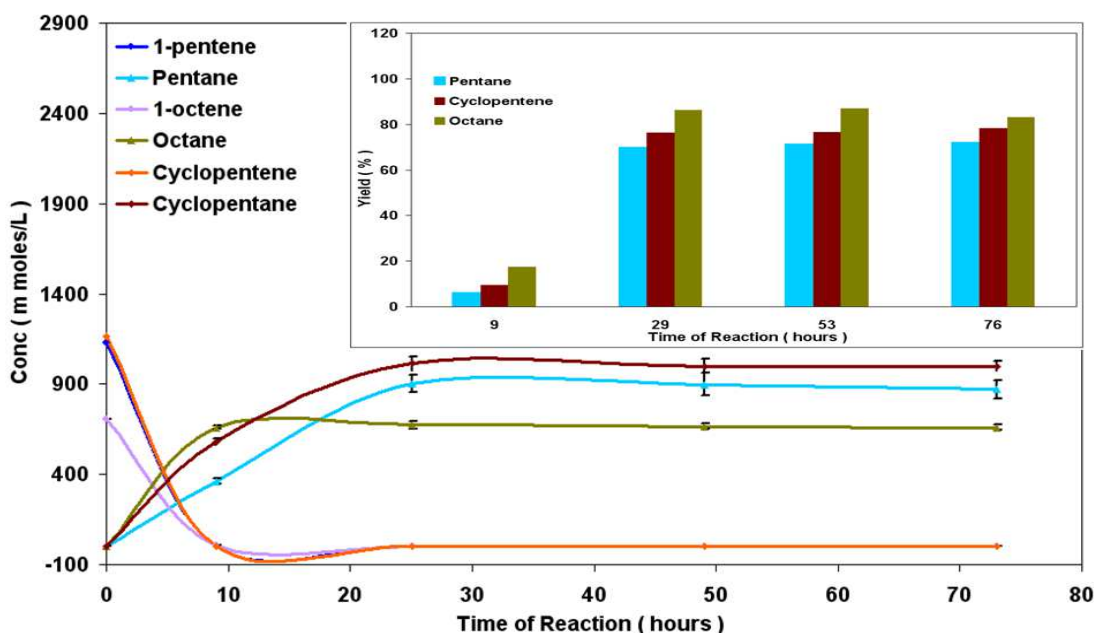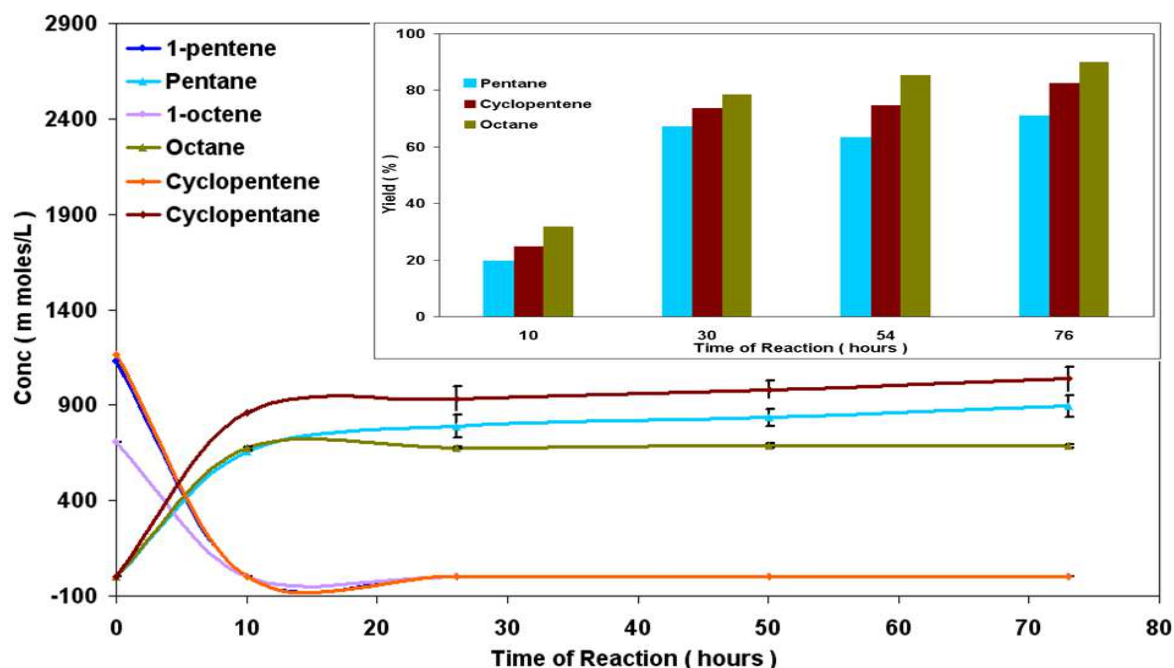

Figure 3.157 Hydrogenation of olefins (1-pentene, 1-octene and cyclopentene) present in PyGas [Reaction conditions: T = 140°C, WHSV$_{PyGas}$ = 4 h^{-1}, P$_T$ = 20 barg, P$_{H2}$ = 10 barg]

Figure 3.158 shows that a decrease was observed in the hydrogenation of toluene to methylcyclohexane with a decrease in hydrogen partial pressure. The yield of methylcyclohexane was about 2% in the first 10 hours of the reaction and then a steady decrease was observed with time on stream.
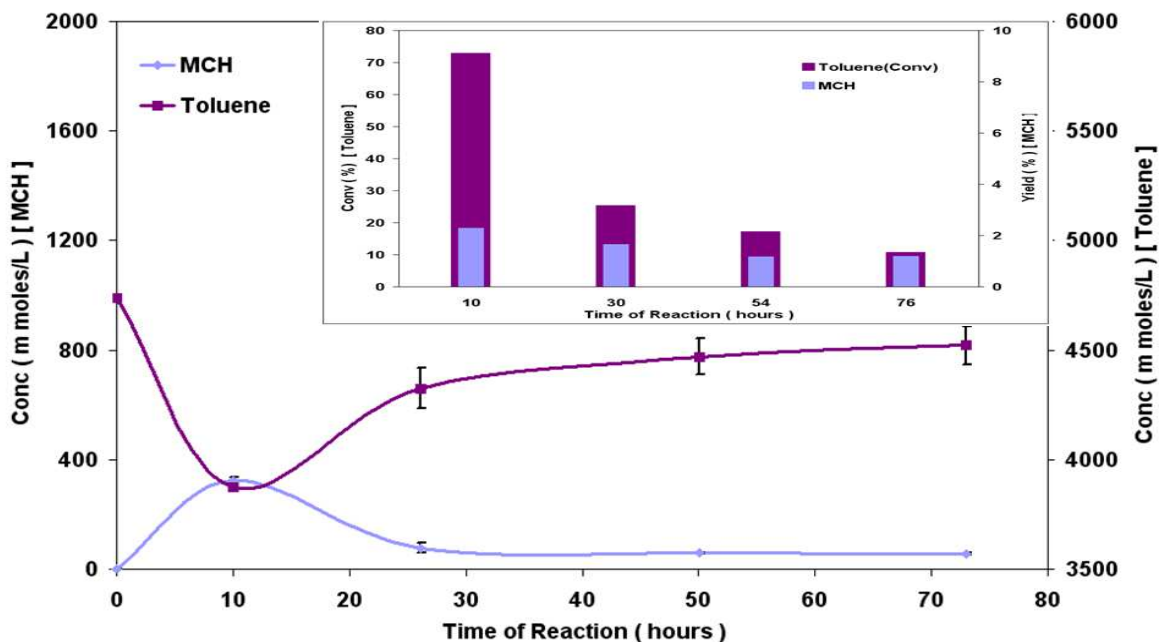
Figure 3.158 Hydrogenation of toluene [Reaction conditions: T = 140°C, WHSV$_{PyGas}$ = 4 h^{-1}, P$_T$ = 20 barg, P$_{H2}$ = 10 barg]

Conversion of styrene remained above 99% as shown in Figure 3.159. Ethyl benzene was the principal product in styrene hydrogenation while a small amount of ethylcyclohexane (~1% yield) was also produced.
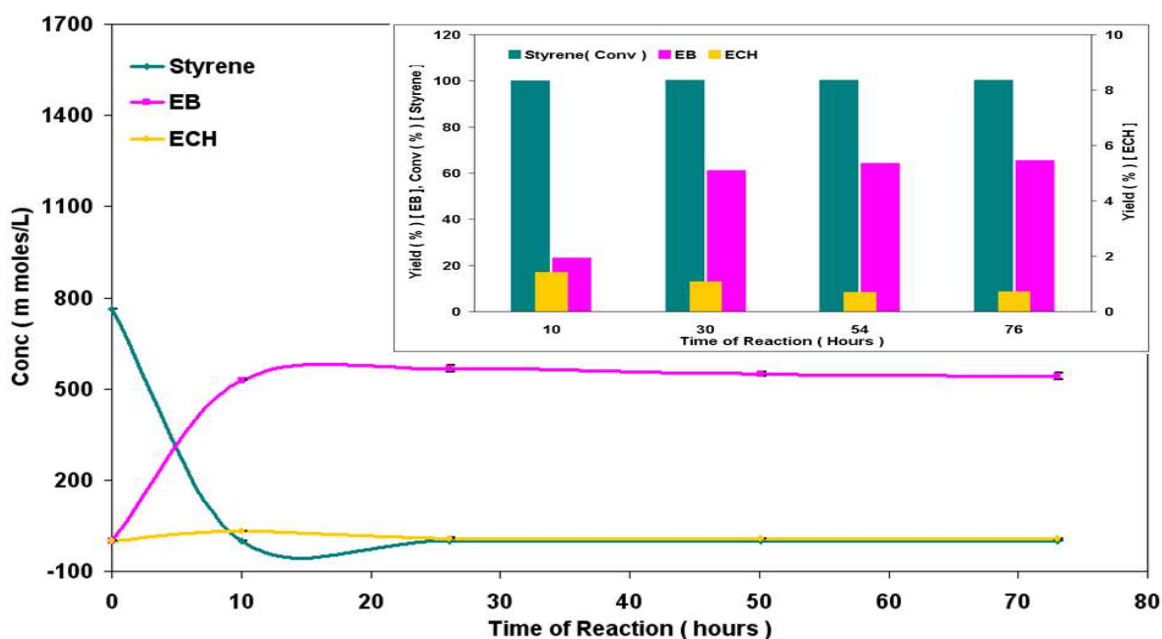
Figure 3.159 Hydrogenation of styrene [Reaction conditions: T = 140°C, WHSV$_{PyGas}$ = 4 h^{-1}, P$_T$ = 20 barg, P$_{H2}$ = 10 barg]

3.2.3.2.1.1 Post reaction analysis

Post reaction catalyst TPO

Post reaction *in-situ* TPO of the catalyst was carried out, as shown in Figure 3.160. The amount of CO_2, CO produced and the amount of O_2 consumed were proportional to the amount of coke deposited on the surface of the catalyst. A considerable amount of coke was observed on the surface of catalyst.
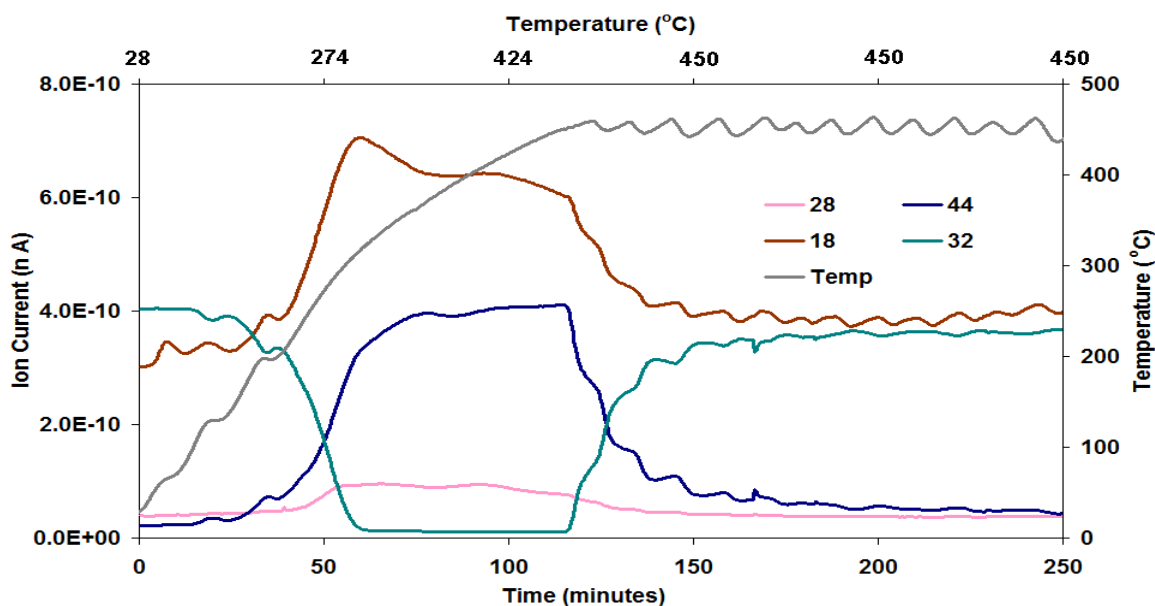
Figure 3.160 Post reaction *in-situ* TPO of Pd/Al_2O_3 catalyst [Reaction conditions: T = 140°C, $WHSV_{PyGas}$ = 4 h^{-1}, P_T = 20 barg, P_{H2} = 10 barg]

Total oxygen consumption in TPO = 3.08 m moles

CO_2, CO and H_2O were the principal species detected in the TPO. The other possible deposited species *i.e.* styrene, benzene, 1-pentene, cyclopentene, pentane, toluene, methylcyclohexane, ethylbenzene, 1-octene, octane and H_2 were also monitored for detailed analysis and shown in Figure 3.161. Reasonable amounts of styrene and benzene desorption was observed at 320°C and 430°C, whilst small quantities of 1-pentene, cyclopentene, 1-octene, pentane, octene, toluene, methylcyclohexane, ethylbenzene and ethylcyclohexane were evolved below 200°C. Moreover a considerable amount of H_2 evolution was also observed above 300°C.
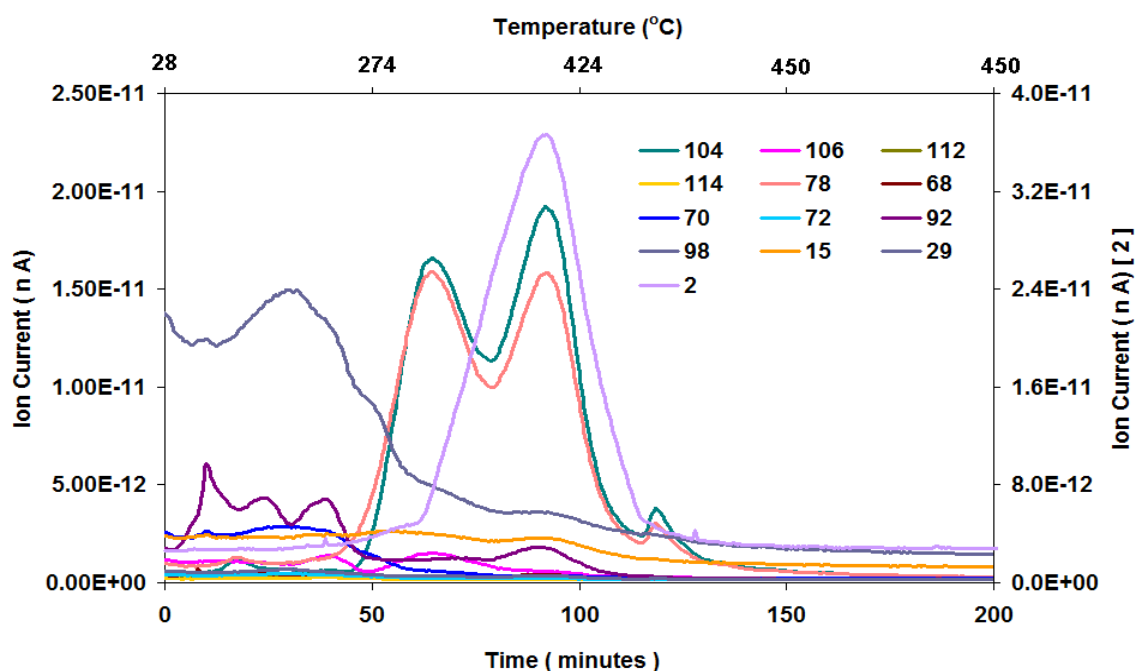
Figure 3.161 Evolution of other species during *in-situ* TPO of Pd/Al$_2$O$_3$ catalyst [Reaction conditions: T = 140°C, WHSV$_{PyGas}$ = 4 h^{-1}, P$_T$ = 20 barg, P$_{H2}$ = 10 barg]

BET analysis

The BET results indicate that surface area loss of the catalyst due to deposition of coke was recovered during regeneration as shown in Table 3.31 below.

Catalyst	Surface Area (m^{2}g^{-1})	Pore Volume (cm^{3}g^{-1})	Average Pore diameter (Å)
Pd/Al$_2$O$_3$	99	0.51	208
Pd/Al$_2$O$_3$ (Reduced)	104	0.50	197
Pd/Al$_2$O$_3$ (Regenerated)	98	0.47	194

Table 3.31 BET analysis of Pd/Al$_2$O$_3$ (Regenerated) catalyst [Reaction conditions: T = 140°C, WHSV$_{PyGas}$ = 4 h^{-1}, P$_T$ = 20 barg, P$_{H2}$ = 10 barg]

3.2.3.2.2 PyGas hydrogenation over Pd/Al$_2$O$_3$ using 25% hydrogen gas mixture

The reaction was performed using 25% hydrogen, with all other reaction conditions were similar to the previous reaction [T = 140°C, WHSV$_{PyGas}$ = 4 h^{-1}, P$_T$ = 20 barg]. The reaction profile is shown in Figure 3.162.
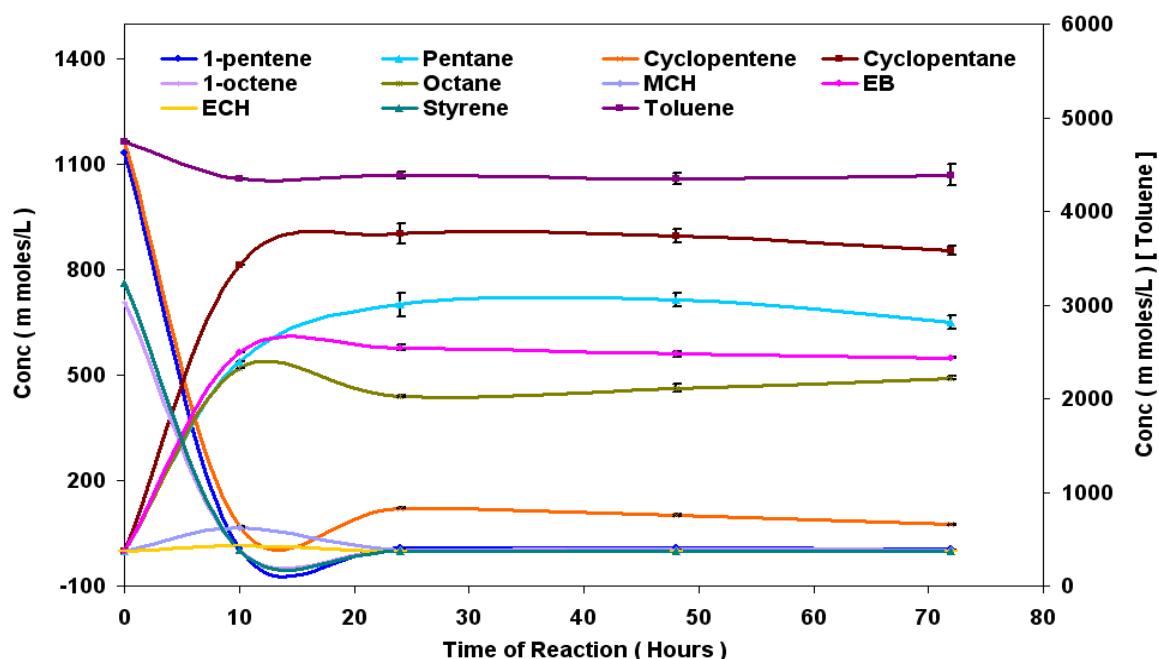
Figure 3.162 Reaction profile of PyGas hydrogenation [Reaction conditions: T = 140°C, WHSV$_{PyGas}$ = 4 h^{-1}, P$_T$ = 20 barg, P$_{H2}$ = 5 barg]

The conversion of 1-pentene was 98% in the first 10 hours of reaction which decreased to 92% after 28 hours and remained virtually constant with TOS. The formation of trans-2-pentene and cis-2-pentene were increased with a decrease in hydrogen partial pressure however the total yield of 1-pentene hydrogenation decreased, as shown in Figures 3.163-164.
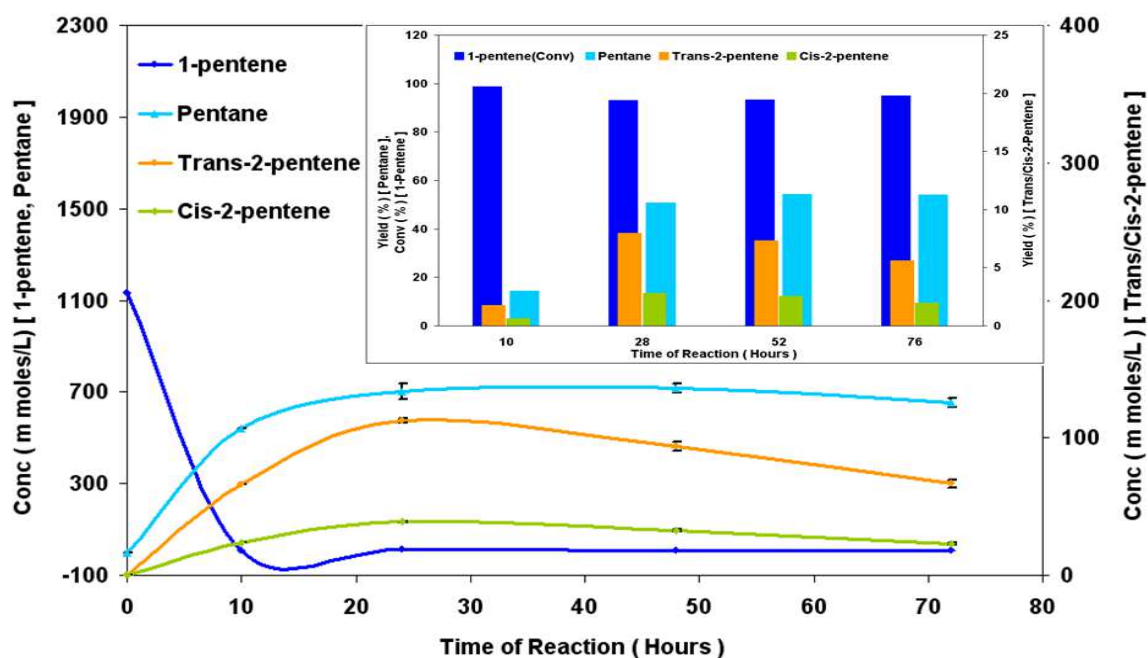
Figure 3.163 Hydrogenation of 1-pentene [Reaction conditions: T = 140°C, WHSV$_{PyGas}$ = 4 h^{-1}, P$_T$ = 20 barg, P$_{H2}$ = 5 barg]
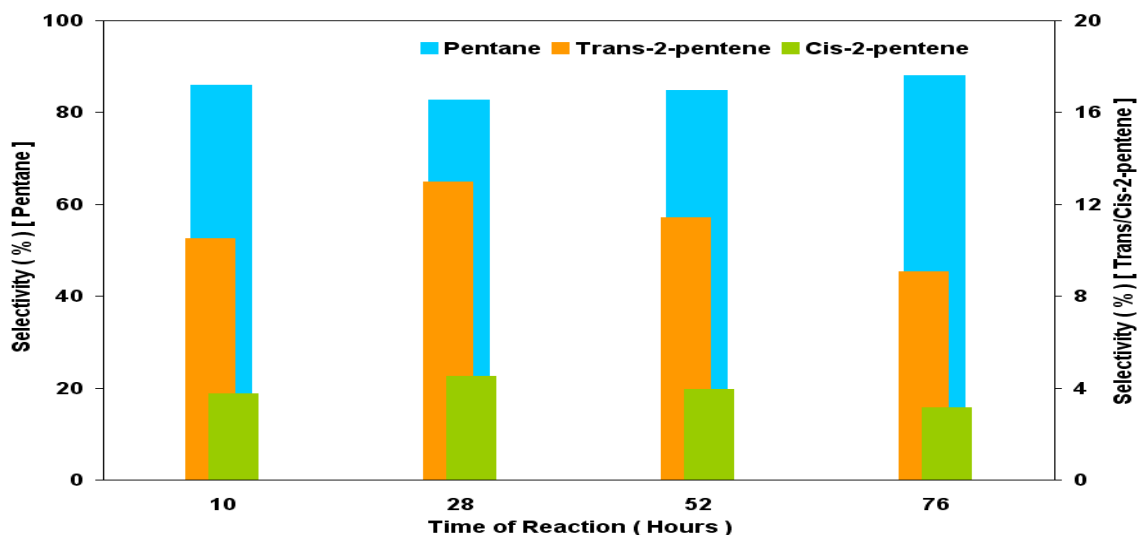
Figure 3.164 Selectivity of pentane, trans-2-pentene and cis-2-pentene during 1-pentene hydrogenation [Reaction conditions: T = 140°C, WHSV$_{PyGas}$ = 4 h^{-1}, P$_T$ = 20 barg, P$_{H2}$ = 5 barg]

Figure 3.165 shows that octane was the principal product in 1-octene hydrogenation however reasonable amounts of internal octenes were also produced. Trans-3-octene, cis-3-octene and cis-4-octene are presented collectively in the results because the GC column used was only capable of analysing these products as a single peak, as mentioned in section 2.3.3.
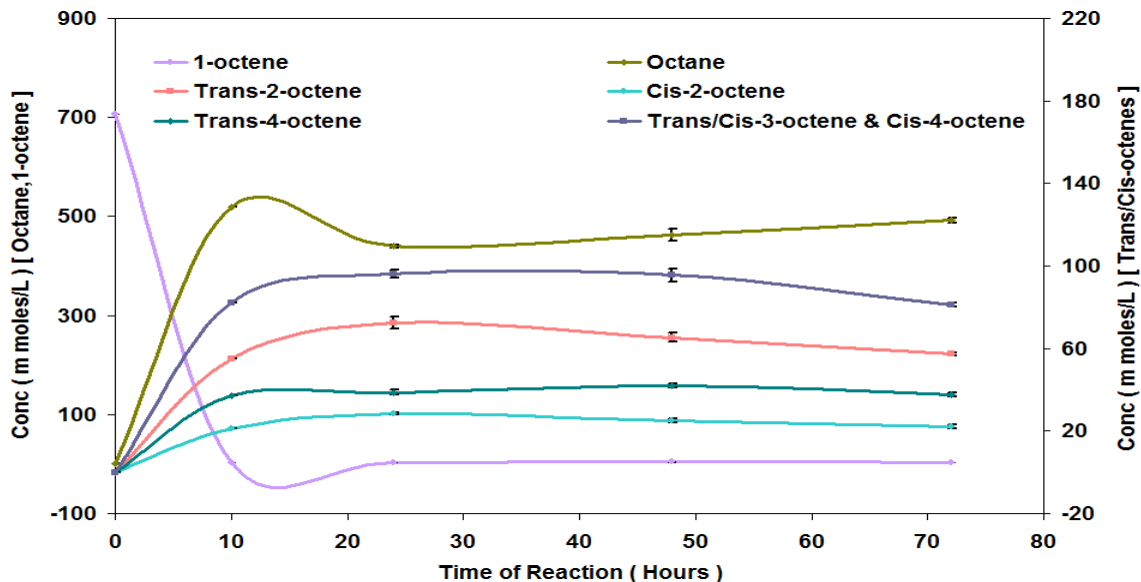
Figure 3.165 Reaction profile of 1-octene hydrogenation [Reaction conditions: T = 140°C, WHSV$_{PyGas}$ = 4 h^{-1}, P$_T$ = 20 barg, P$_{H2}$ = 5 barg]

Conversion of 1-octene remained more than 99% throughout TOS of the reaction as shown in Figure 3.166. A significant increase was observed in the internal octenes with a decrease in hydrogen partial pressure from 10 barg to 5 barg within 20 barg total pressure. Compared to the Ni/Al$_2$O$_3$ catalyst, no noticeable change was observed in the yield of octane and total internal octenes under the

same reaction conditions, however an increase was found in selectivity towards 3-octene and 4-octene formation within internal octene over the Pd/Al$_2$O$_3$. The results suggest that the Pd/Al$_2$O$_3$ has a higher capability to shift the double bond further towards 3-octene and 4-octene, as shown in figure 3.166-167.
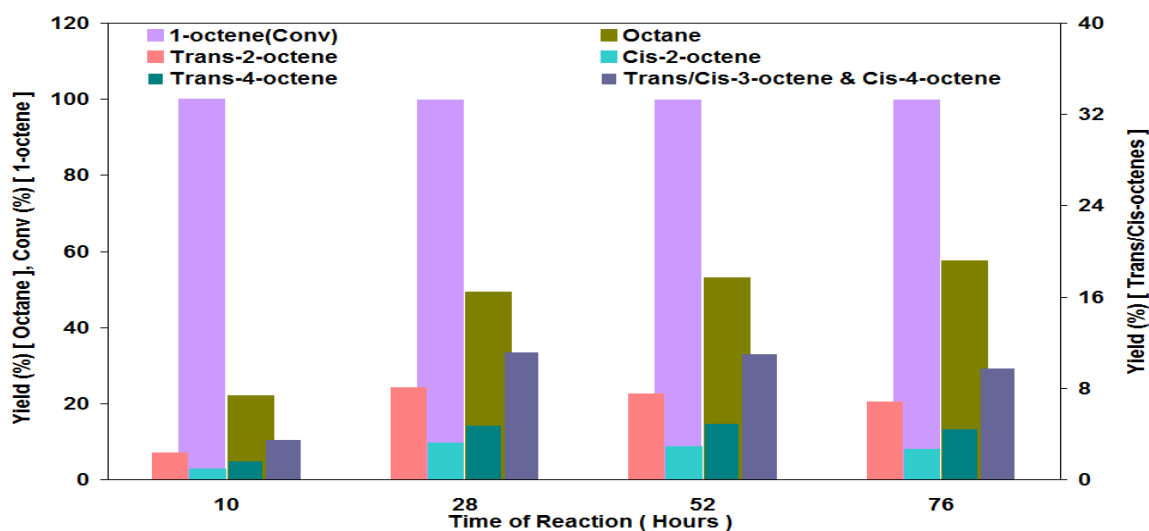
Figure 3.166 Percent yield of 1-octene hydrogenation [Reaction conditions: T = 140°C, WHSV$_{PyGas}$ = 4 h^{-1}, P$_T$ = 20 barg, P$_{H2}$ = 5 barg]
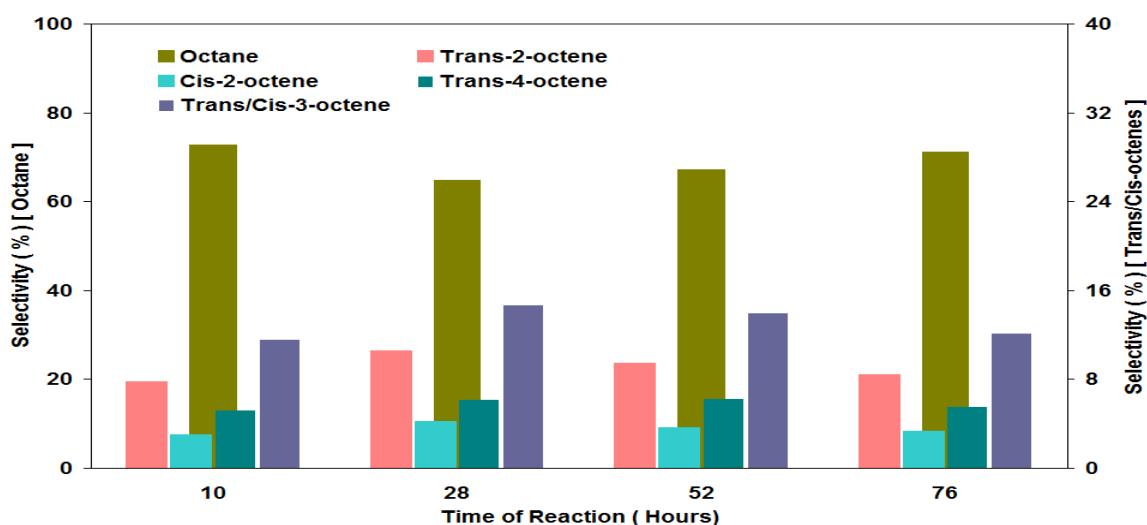
Figure 3.167 Selectivity of octane and internal octenes during 1-octene hydrogenation [Reaction conditions: T = 140°C, WHSV$_{PyGas}$ = 4 h^{-1}, P$_T$ = 20 barg, P$_{H2}$ = 5 barg]

The trans/cis ratio of olefins formed during reaction is shown in Table 3.32. It was observed that the trans to cis ratio was slightly higher when compared to Ni/Al$_2$O$_3$ catalyst under similar reaction conditions.

Trans/Cis-2-pentene ratio	Trans/Cis-2-octene ratio
74:26	72:28

Table 3.32 Ratio of trans/cis internal olefins formation in PyGas Hydrogenation [Reaction conditions: T = 140°C, WHSV$_{PyGas}$ = 4 h^{-1}, P$_T$ = 20 barg, P$_{H2}$ = 5 barg]

Figure 3.168 shows that the conversion of cyclopentene was about 98% in the first 10 hours of reaction which decreased to 91% after 28 hours as the reaction obtained steady state. A decrease was noted in the cyclopentane yield with a decrease in hydrogen partial pressure from 10 barg to 5 barg.
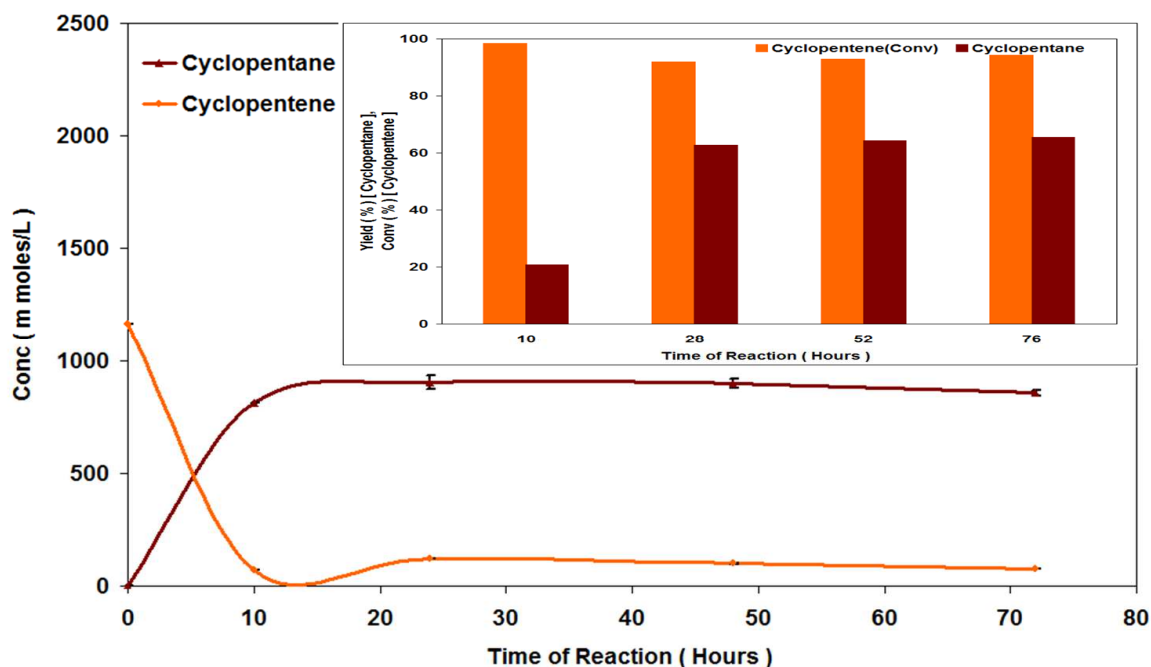
Figure 3.168 Hydrogenation of cyclopentene [Reaction conditions: T = 140°C, WHSV$_{PyGas}$ = 4 h^{-1}, P$_T$ = 20 barg, P$_{H2}$ = 5 barg]

Conversion of toluene was 72% in the first 10 hours of the reaction which decreased to 27% after 28 hours and a gradual decrease was observed with further TOS. Virtually no formation of methylcyclohexane was noted, as shown in Figure 3.169.
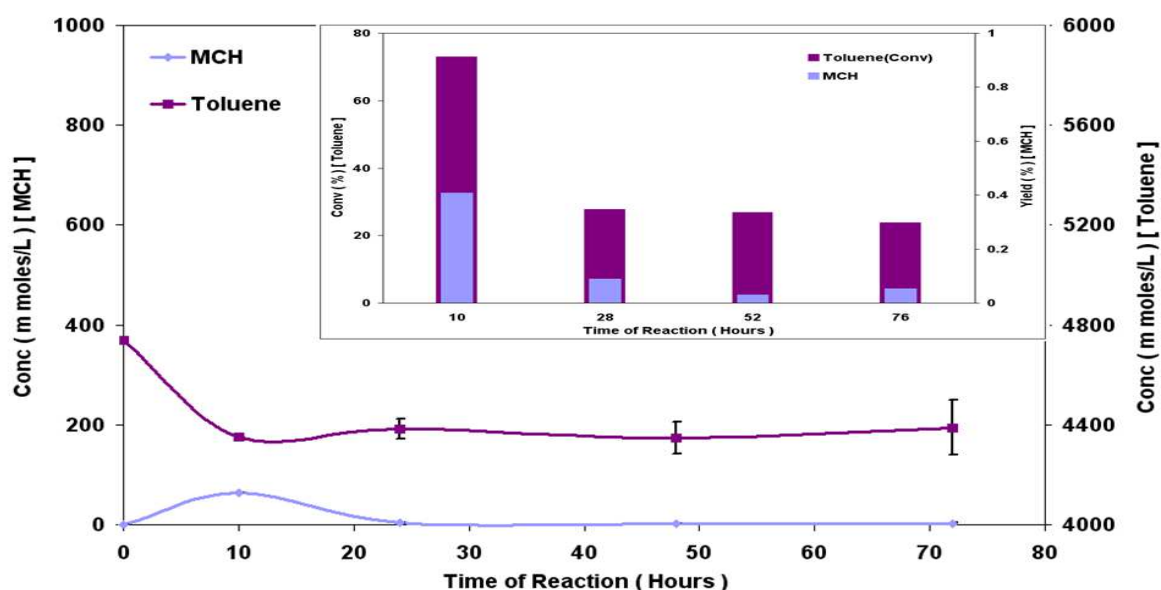
Figure 3.169 Hydrogenation of toluene [Reaction conditions: T = 140°C, WHSV$_{PyGas}$ = 4 h^{-1}, P$_T$ = 20 barg, P$_{H2}$ = 5 barg]

Conversion of styrene hydrogenation remained above 99%. The styrene hydrogenated to ethylbenzene, however very small amount of ethylcyclohexane was seen in the initial 10 hours of reaction.
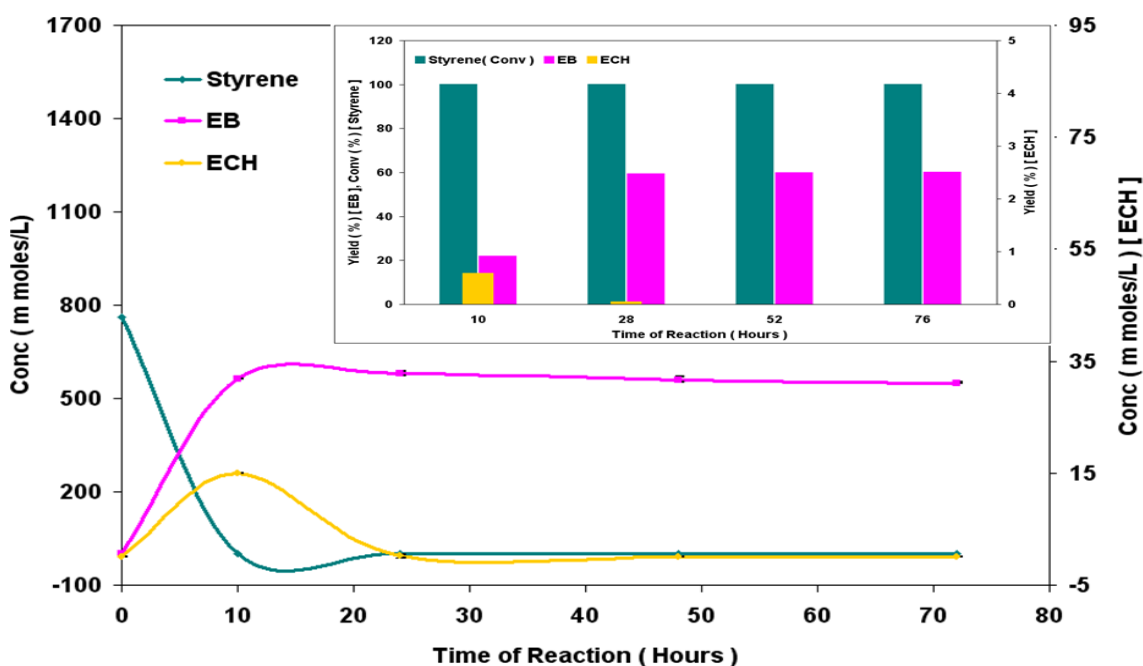
Figure 3.170 Hydrogenation of styrene [Reaction conditions: T = 140°C, WHSV$_{PyGas}$ = 4 h^{-1}, P$_T$ = 20 barg, P$_{H2}$ = 5 barg]

3.2.3.2.2.1 Post reaction analysis

Post reaction catalyst TPO

Post reaction *in-situ* TPO over Pd/Al$_2$O$_3$ catalyst was performed in a continuous flow of 2% O$_2$/Ar. The ion currents for CO$_2$, CO, H$_2$O and O$_2$ were measured to study the carbon laydown on the surface of the catalyst and the results are shown in Figure 3.171. Higher level of CO$_2$ evolution and O$_2$ consumption was noted when compared to that observed in the TPO of the catalyst used in the previous reaction carried out with 50% hydrogen gas. However the evolution of other species *i.e.* styrene, benzene, 1-pentene, cyclopentene, pentane, methylcyclohexane, toluene, ethylbenzene, 1-octene, octane and H$_2$ remained similar in both TPOs.
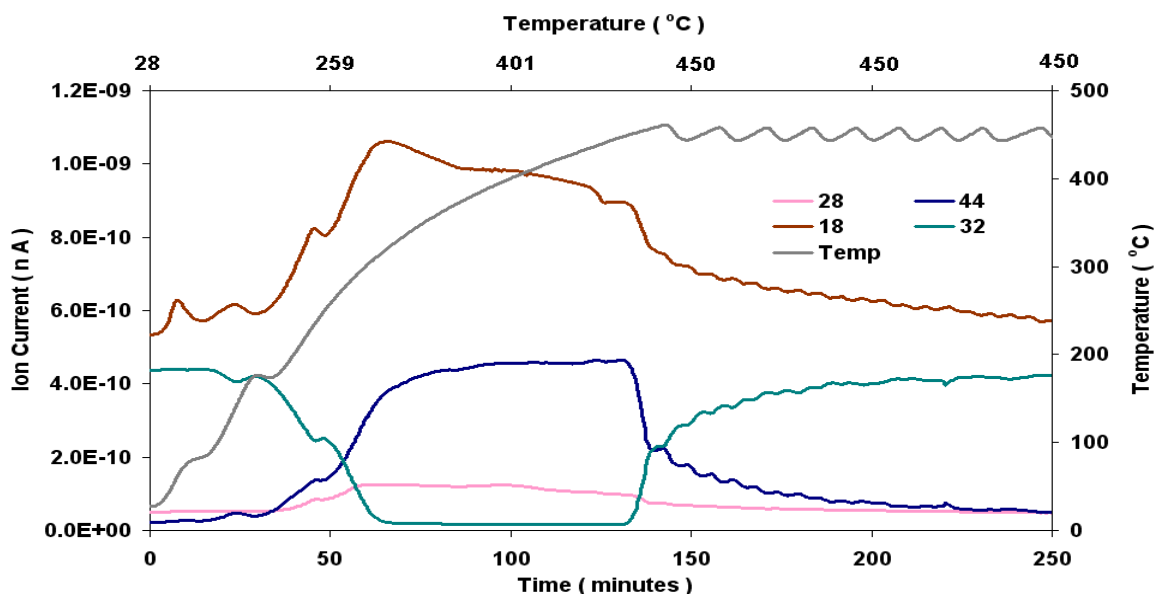
Figure 3.171 Post reaction *in-situ* TPO of Pd/Al$_2$O$_3$ catalyst [Reaction conditions: T = 140°C, WHSV$_{PyGas}$ = 4 h^{-1}, P$_T$ = 20 barg, P$_{H2}$ = 5 barg]

Total oxygen consumption in TPO = 3.51 m moles

BET analysis

The surface area, pore volume and pore diameter of the regenerated catalyst was found to be similar to the fresh catalyst as shown in Table 3.33.

Catalyst	Surface Area (m^{2}g^{-1})	Pore Volume (cm^{3}g^{-1})	Average Pore diameter (Å)
Pd/Al$_2$O$_3$	99	0.51	208
Pd/Al$_2$O$_3$ (Reduced)	104	0.50	197
Pd/Al$_2$O$_3$ (Regenerated)	97	0.47	198

Table 3.33 BET analysis of Pd/Al$_2$O$_3$ (Regenerated) catalyst [Reaction conditions: T = 140°C, WHSV$_{PyGas}$ = 4 h^{-1}, P$_T$ = 20 barg, P$_{H2}$ = 5 barg]

3.2.3.2.3 PyGas hydrogenation over Pd/Al$_2$O$_3$ using 5% hydrogen gas mixture

The hydrogenation of PyGas was performed over Pd/Al$_2$O$_3$ using 5% hydrogen gas mixture diluted with nitrogen, with reaction parameter T = 140°C, WHSV$_{PyGas}$ = 4 h^{-1}, P$_T$ = 20 barg and P$_{H2}$ = 1 barg. The reaction profile is shown in Figure 3.172.
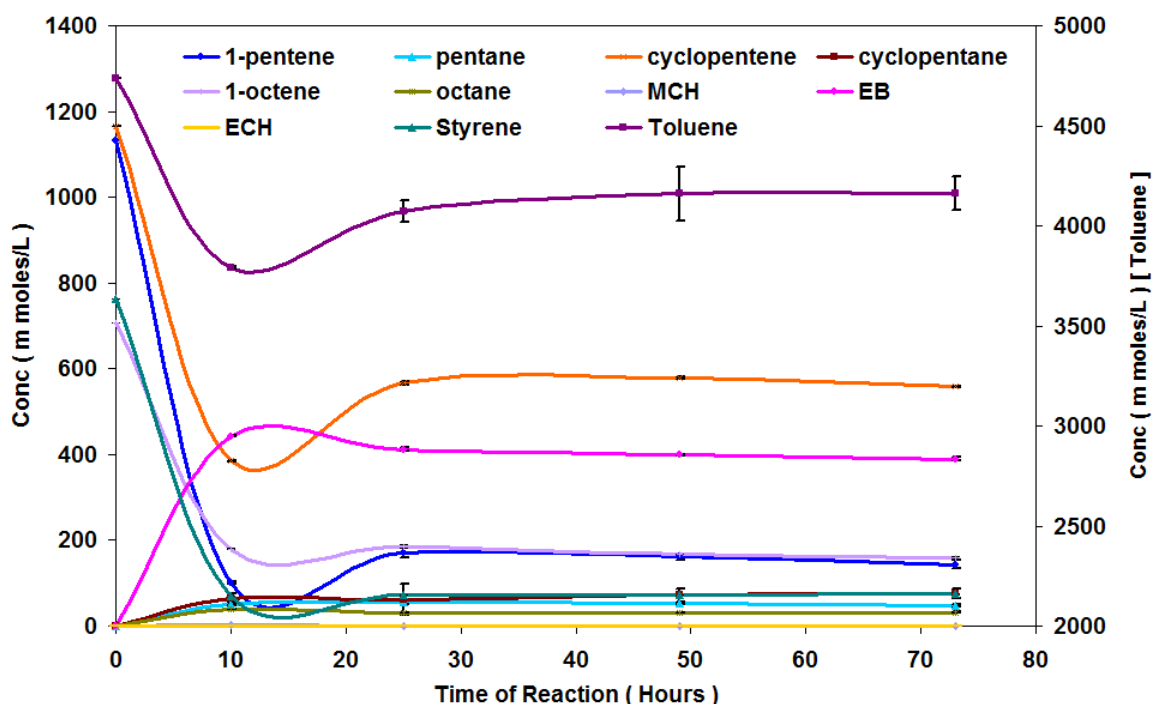
Figure 3.172 Reaction profile of PyGas Hydrogenation [Reaction conditions: T = 140°C, WHSV$_{PyGas}$ = 4 h^{-1}, P$_T$ = 20 barg, P$_{H2}$ = 1 barg]

Conversion of the 1-pentene was 97% in the first 10 hours of reaction which decreased to 86% after 29 hours and remained constant with further TOS, as shown in Figure 3.173. A considerable increase was observed in the formation of internal pentenes as shown in Figures 3.173-174. Compared to the Ni/Al$_2$O$_3$ catalyst, the formation of internal pentene was noticeably higher over the Pd/Al$_2$O$_3$ catalyst.
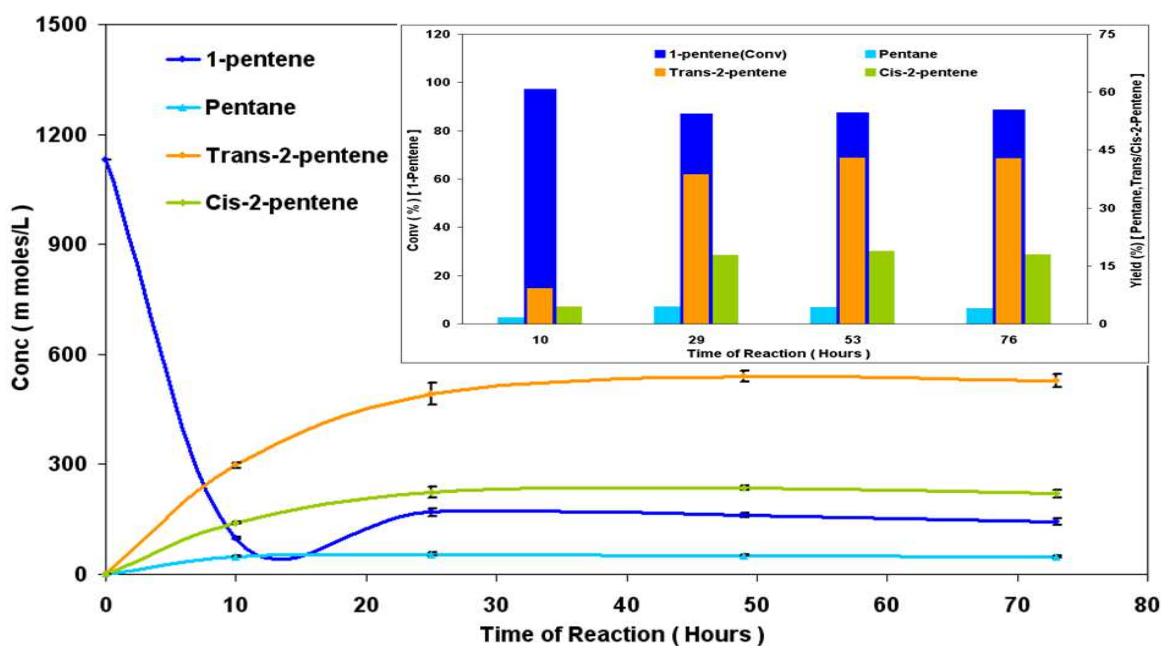
Figure 3.173 Hydrogenation of 1-pentene [Reaction conditions: T = 140°C, WHSV$_{PyGas}$ = 4 h^{-1}, P$_T$ = 20 barg, P$_{H2}$ = 1 barg]
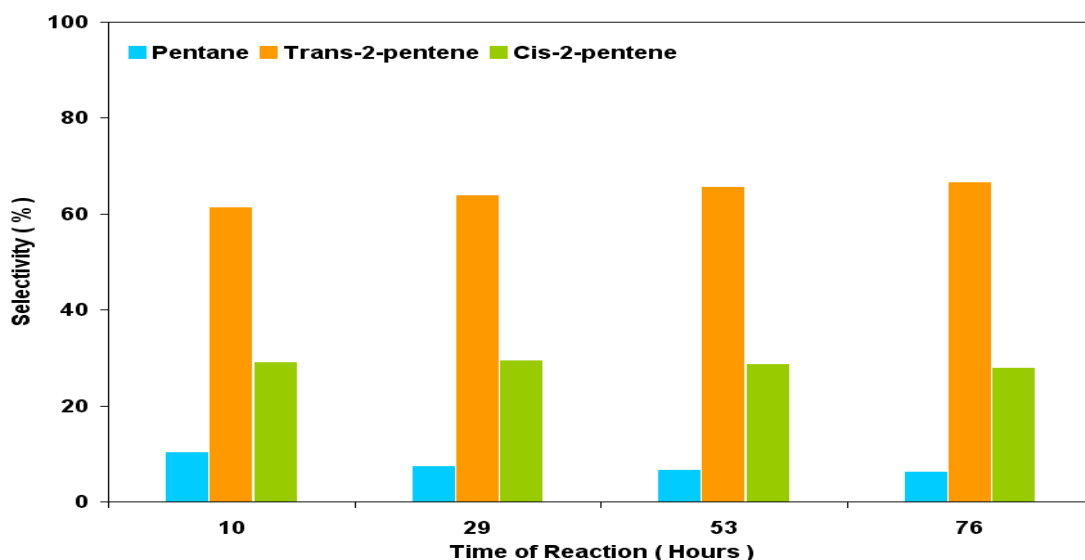
Figure 3.174 Selectivity of pentane, trans-2-pentene and cis-2-pentene during 1-pentene hydrogenation [Reaction conditions: T = 140°C, WHSV$_{PyGas}$ = 4 h^{-1}, P$_T$ = 20 barg, P$_{H2}$ = 1 barg]

Figure 3.175 shows the concentration profile of 1-octene hydrogenation. An Increase was observed in the yield of internal octenes with a decrease in hydrogen partial pressure. Moreover, the formation of internal octenes was also higher when compared to the Ni/Al$_2$O$_3$ catalyst under identical reaction conditions. A higher tendency of double bond migration was observed and the selectivity towards 3-octene and 4-octene was increased.
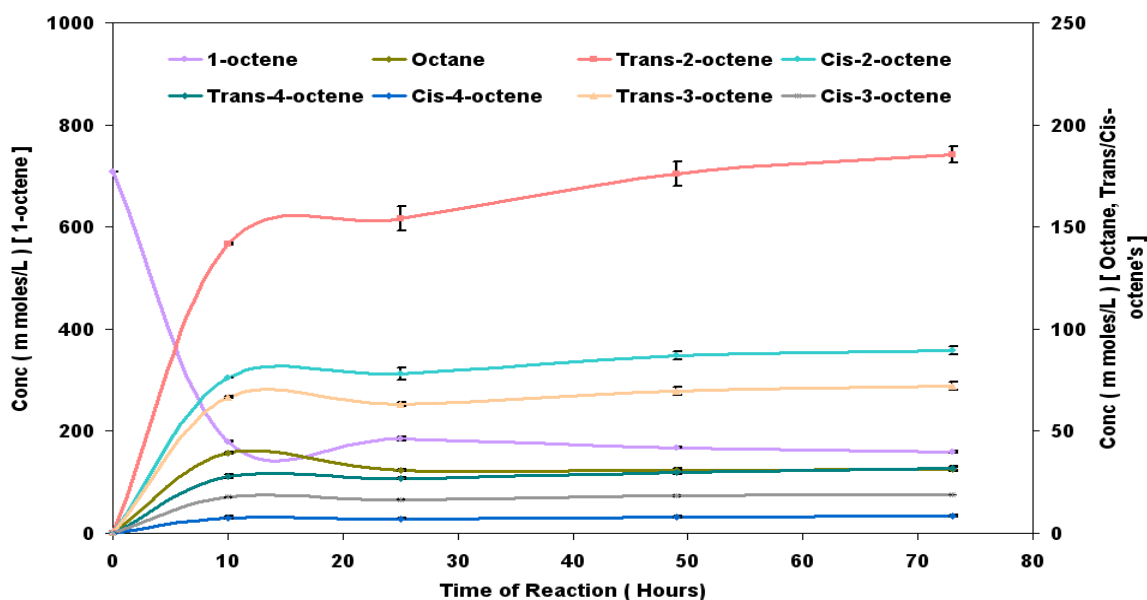
Figure 3.175 Reaction profile of 1-octene hydrogenation [Reaction conditions: T = 140°C, WHSV$_{PyGas}$ = 4 h^{-1}, P$_T$ = 20 barg, P$_{H2}$ = 1 barg]

Figures 3.176-177 show that the yield and selectivity of internal octenes considerably increased. The formation of the products followed the order set out below,

Trans-2-octene > Cis-2-octene > Trans-3-octene > Octane ≈ Trans-4-octene> Cis-3-octene > Cis-4-octene
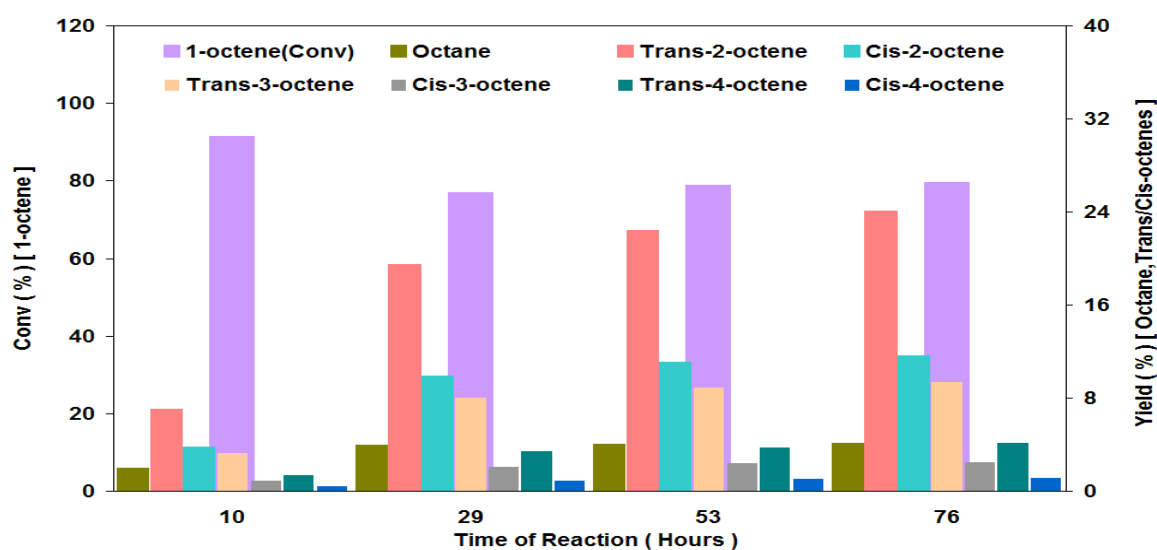
Figure 3.176 Percent yield of 1-octene hydrogenation [Reaction conditions: T = 140°C, $WHSV_{PyGas}$ = 4 h^{-1}, P_T = 20 barg, P_{H2} = 1 barg]
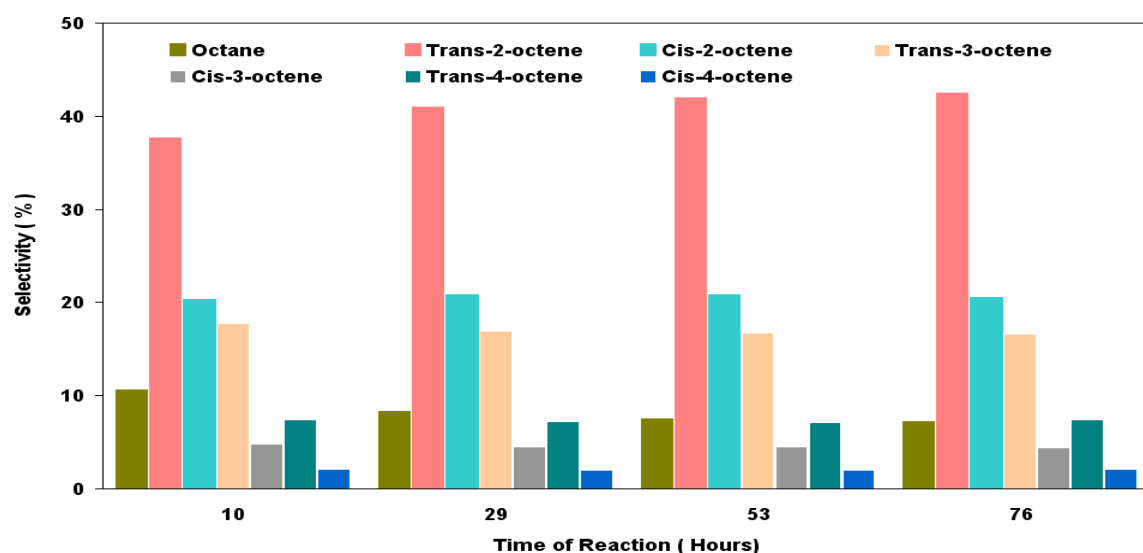
Figure 3.177 Selectivity of octane and internal octenes during 1-octene hydrogenation [Reaction conditions: T = 140°C, $WHSV_{PyGas}$ = 4 h^{-1}, P_T = 20 barg, P_{H2} = 1 barg]

The ratio of trans/cis in 2-octene was found to be the same as the trans/cis ratio in 2-pentene however a further increase in trans/cis ratio was seen from 2-octene to 3-octene and 4-octene as shown in Table 3.34.

Trans/Cis-2-pentene ratio	Trans/Cis-2-octene ratio	Trans/Cis-3-octene ratio	Trans/Cis-4-octene ratio
68:32	67:33	79:21	79:21

Table 3.34 Ratio of trans/cis internal olefins formation in PyGas Hydrogenation [Reaction conditions: T = 140°C, $WHSV_{PyGas}$ = 4 h^{-1}, P_T = 20 barg, P_{H2} = 1 barg]

Conversion of cyclopentene was 88% in the first 10 hours of reaction which decreased to 56% after 29 hours and remained constant for the reminder of the reaction. A significant decrease was observed in the yield of cyclopentane with a decrease in hydrogen partial pressure to 1 barg. The formation of cyclopentane increased slightly with TOS and only 6% maximum yield of cyclopentane was observed, as shown in Figure 3.178. Compared to the Ni/Al$_2$O$_3$ catalyst, the amount of cyclopentane formation was similar under these reaction conditions.
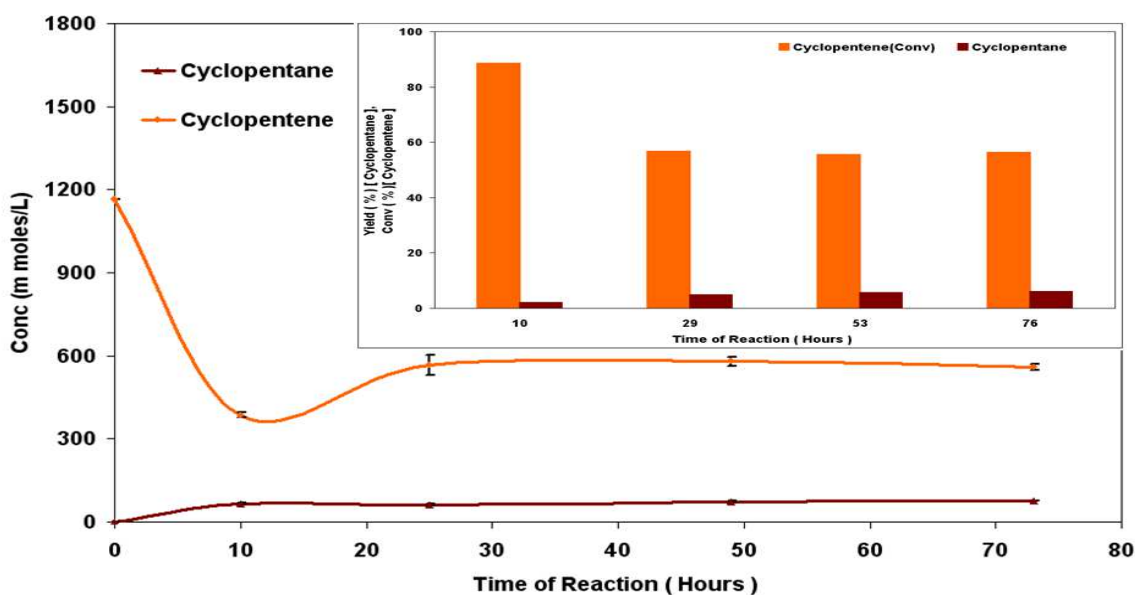
Figure 3.178 Hydrogenation of cyclopentene [Reaction conditions: T = 140°C, WHSV$_{PyGas}$ = 4 h^{-1}, P$_T$ = 20 barg, P$_{H2}$ = 1 barg]

Figure 3.179 shows that virtually no formation of methylcyclohexane was observed during the reaction although a considerable amount of toluene conversion was observed.
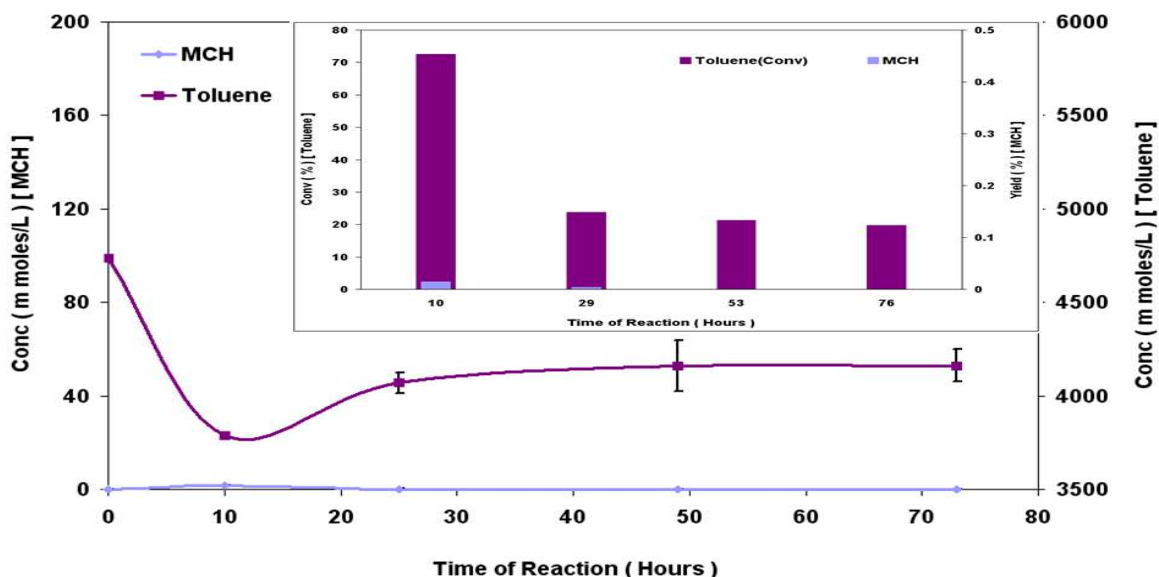
Figure 3.179 Hydrogenation of toluene [Reaction conditions: T = 140°C, WHSV$_{PyGas}$ = 4 h^{-1}, P$_T$ = 20 barg, P$_{H2}$ = 1 barg]

Conversion of styrene was 96% in the initial 10 hours of the reaction and then decreased to 91% after 29 hours when the reaction obtained steady state. The styrene hydrogenated to ethylbenzene and in effect no ethylcyclohexane was observed in the reaction as shown in Figure 3.180.
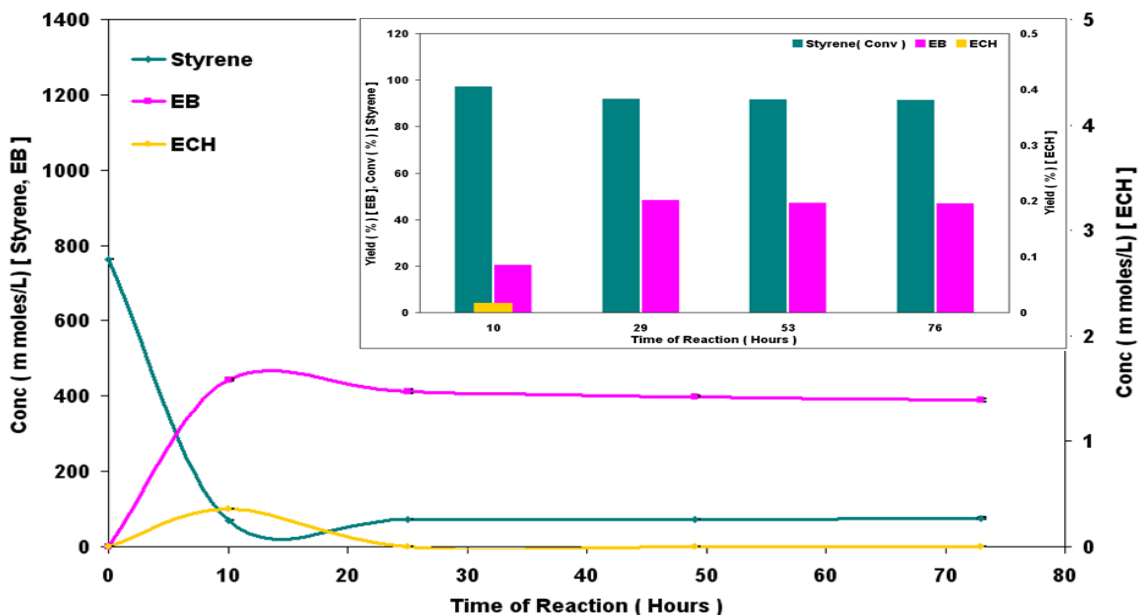
Figure 3.180 Hydrogenation of styrene [Reaction conditions: T = 140°C, WHSV$_{PyGas}$ = 4 h^{-1}, P$_T$ = 20 barg, P$_{H2}$ = 1 barg]

3.2.3.2.3.1 Post reaction analysis

Post reaction catalyst TPO

Post reaction *in-situ* TPO over Pd/Al$_2$O$_3$ catalyst and shown in Figure 3.181. A higher amount of coke deposition was observed on the catalyst when compared to previous reactions carried out with 100%, 50% and 25% hydrogen gas mixtures. However, similar levels of styrene, benzene, 1-pentene, 1-octene, pentane, octane, cyclopentene, toluene, methylcyclohexane, ethylbenzene and ethyl-cyclohexane evolution were seen when compared to TPOs of the catalysts, used in the previous reactions carried out with 50% and 25% hydrogen gas mixtures.
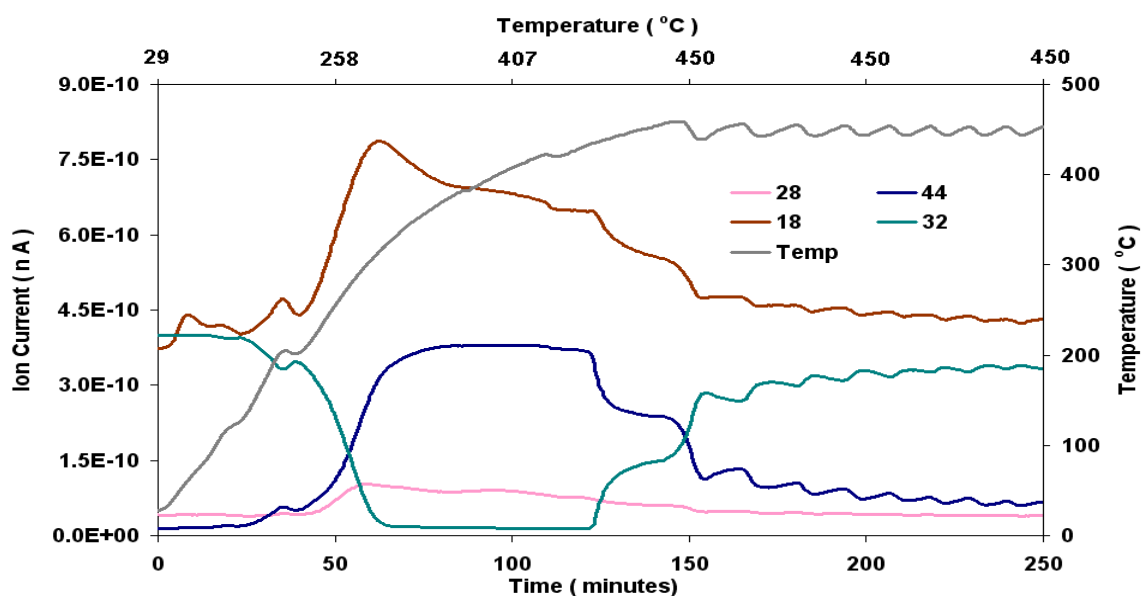
Figure 3.181 Post reaction *in-situ* TPO of Pd/Al$_2$O$_3$ catalyst [Reaction conditions: T = 140°C, WHSV$_{PyGas}$ = 4 h^{-1}, P$_T$ = 20 barg, P$_{H2}$ = 1 barg]

Total oxygen consumption in TPO = 3.94 m moles

BET analysis

The BET results show that no significant difference was found in the surface area, pore volume and average pore diameter of both fresh and the regenerated catalyst, as shown in Table 3.35.

Catalyst	Surface Area (m^{2}g^{-1})	Pore Volume (cm^{3}g^{-1})	Average Pore diameter (Å)
Pd/Al$_2$O$_3$	99	0.51	208
Pd/Al$_2$O$_3$ (Reduced)	104	0.50	197
Pd/Al$_2$O$_3$ (Regenerated)	95	0.46	199

Table 3.35 BET analysis of Pd/Al$_2$O$_3$ (Regenerated) catalyst [Reaction conditions: T = 140°C, WHSV$_{PyGas}$ = 4 h^{-1}, P$_T$ = 20 barg, P$_{H2}$ = 1 barg]

3.2.3.3 Effect of total reaction pressure on PyGas hydrogenation

Similar to the Ni/Al$_2$O$_3$ system, the reactions was performed at 10 barg and 20 barg total reaction pressures using a 50% hydrogen gas mixture to study effect of total reaction pressure on the hydrogenation of PyGas. All other reaction parameters were kept constant [T = 140°C and WHSV$_{PyGas}$ = 4 h^{-1}]. The PyGas hydrogenation over the Pd/Al$_2$O$_3$ catalyst at 20 barg is already presented in section 3.2.3.2.1, while the reaction at 10 barg pressure is discussed in this section. The reaction profile of PyGas hydrogenation is shown in Figure 3.182.
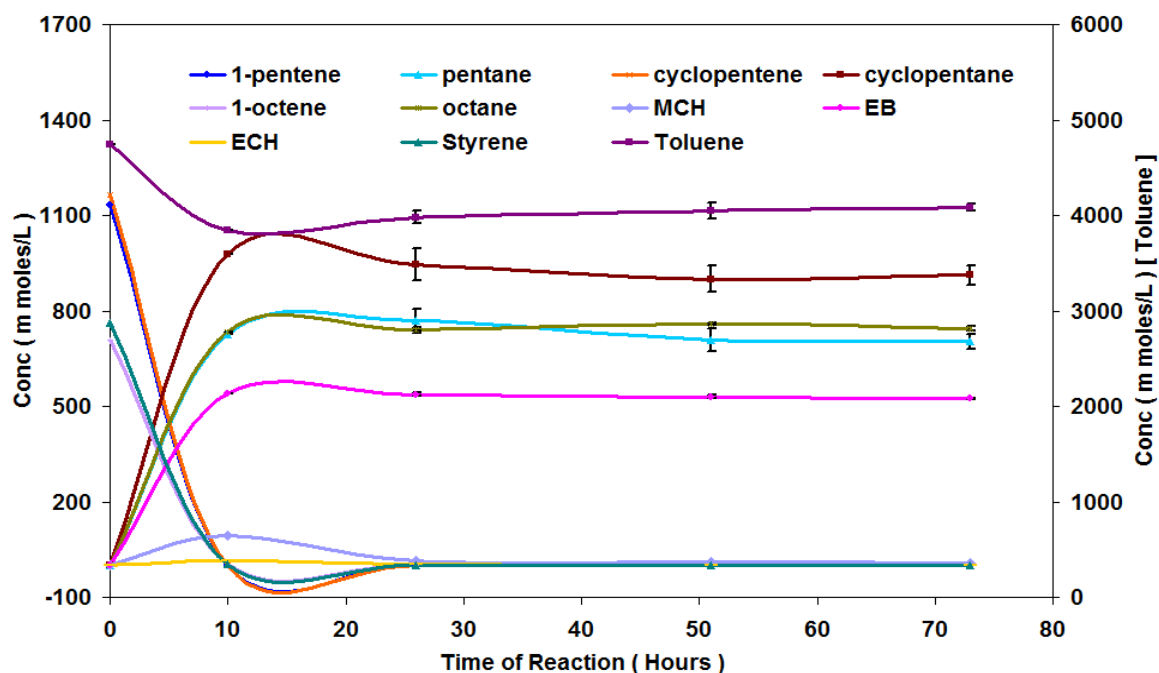
Figure 3.182 Reaction profile of PyGas Hydrogenation [Reaction conditions: T = 140°C, WHSV$_{PyGas}$ = 4 h^{-1}, P$_T$ = 10 barg]

Figure 3.183 shows that the olefins (1-pentene, 1-octene and cyclopentene) hydrogenated to their saturated components with virtually no formation of internal olefins. Only a very small amount (< 0.2%) of internal olefins was seen in the first 10 hours of reaction. Conversion of olefins was above 99% throughout the reaction. A significant decrease was observed in the yield of pentane and cyclopentane with a decrease in reaction pressure from 20 barg to 10 barg.
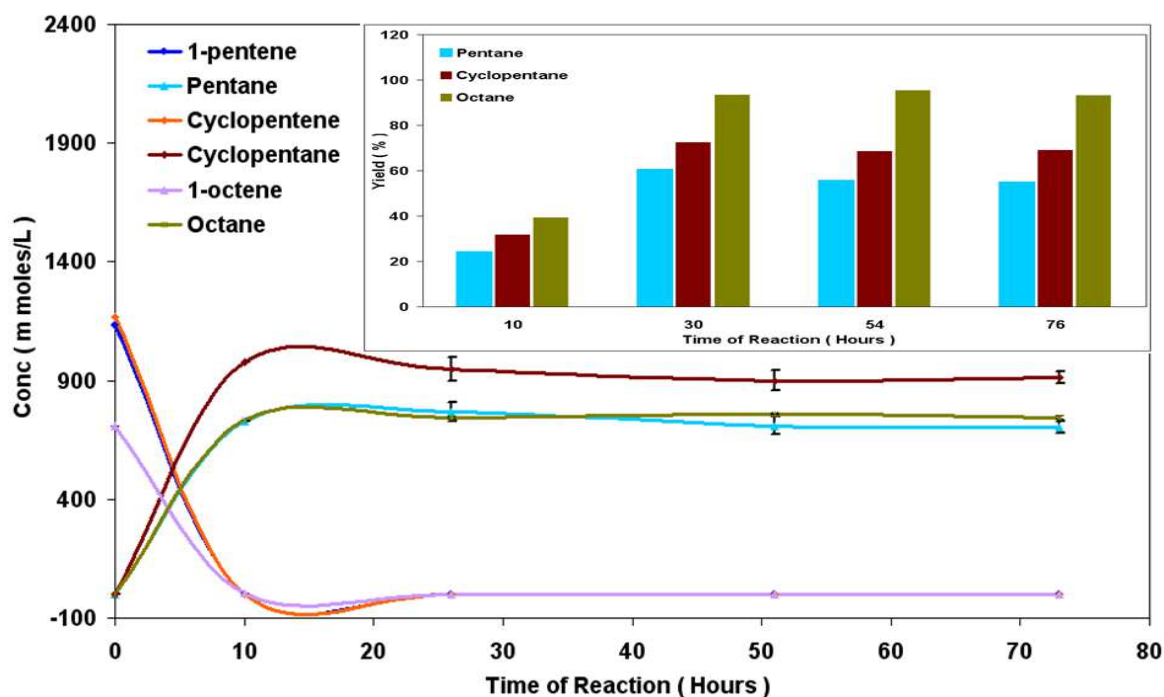
Figure 3.183 Hydrogenation of olefins (1-pentene, 1-octene and cyclopentene) present in PyGas [Reaction conditions: T = 140°C, WHSV$_{PyGas}$ = 4 h^{-1}, P$_T$ = 10 barg]

No methylcyclohexane was observed in the reaction while considerable conversion of toluene was observed, as shown in Figure 3.184.
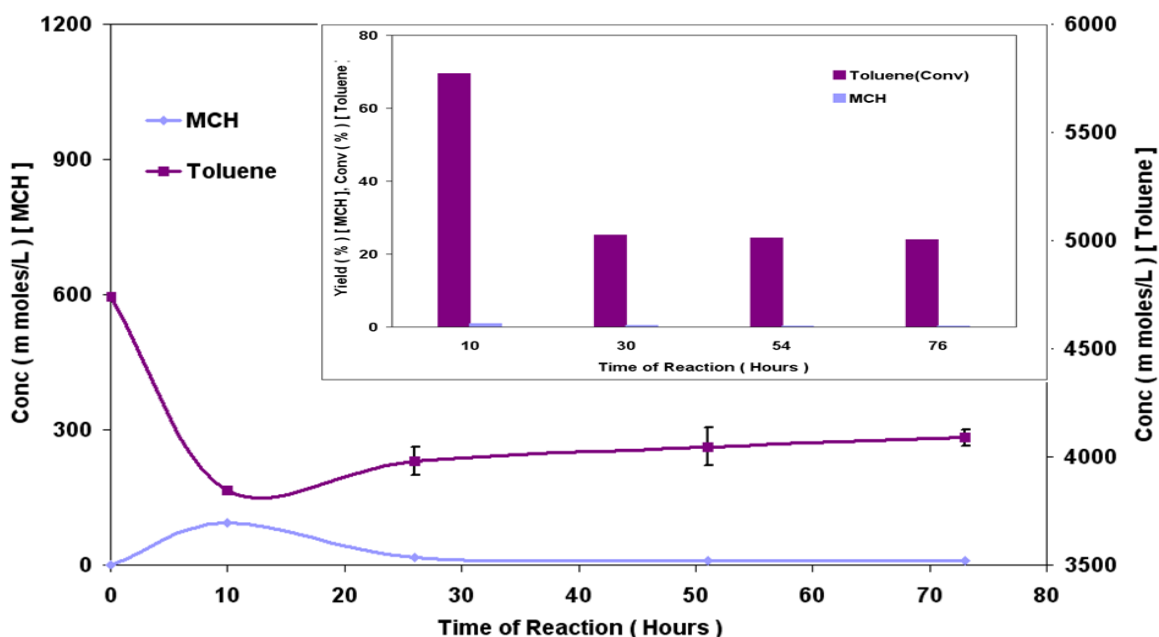
Figure 3.184 Hydrogenation of toluene [Reaction conditions: T = 140°C, WHSV$_{PyGas}$ = 4 h^{-1}, P$_T$ = 10 barg]

Figure 3.185 shows that the conversion of styrene remained above 99% throughout the reaction. Ethylbenzene was the principal product and no significant change was observed in the yield with a decrease in total reaction pressure from 20 barg to 10 barg. Moreover, only a trace amount of ethylcyclohexane was seen in the reaction.
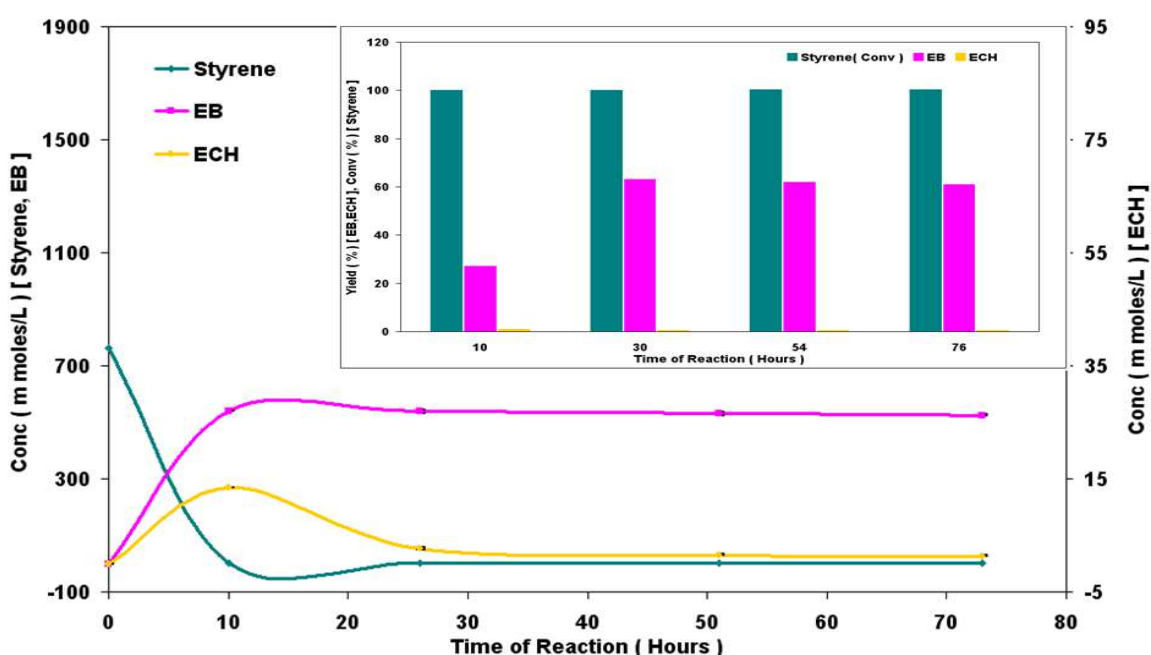
Figure 3.185 Hydrogenation of styrene [Reaction conditions: T = 140°C, WHSV$_{PyGas}$ = 4 h^{-1}, P$_T$ = 10 barg]

3.2.3.3.1 Post reaction analysis

Post reaction catalyst TPO

Post reaction *in-situ* TPO of the catalyst was carried out and shown in Figure 3.186. The results indicate that an increase occurred in the amount of coke deposition with a decrease in total reaction pressure from 20 barg to 10 barg. However, no considerable change was seen in the evolution of styrene, benzene, 1-pentene, cyclopentene, pentane, methylcyclohexane, toluene, ethylbenzene, 1-octene, octane and H_2 in both the TPOs.
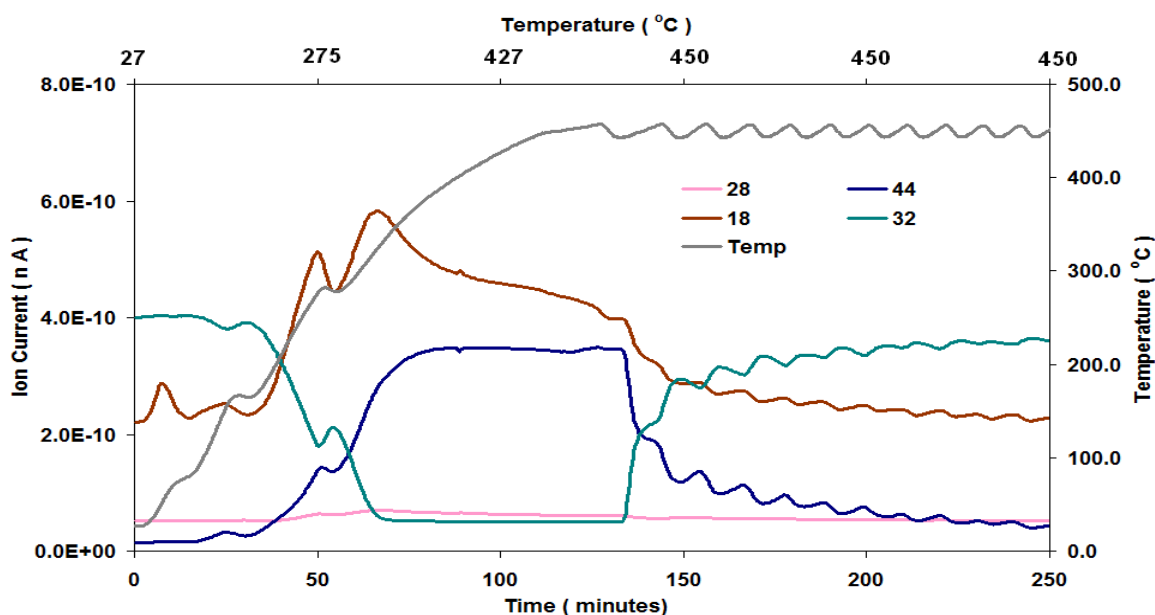
Figure 3.186 Post reaction *in-situ* TPO of Pd/Al_2O_3 catalyst [Reaction conditions: T = 140°C, $WHSV_{PyGas}$ = 4 h^{-1}, P_T = 10 barg]

Total oxygen consumption in TPO = 3.56 m moles

BET analysis

The surface area, pore volume and pore diameter of the regenerated Pd/Al_2O_3 catalyst were to found to be similar to fresh catalyst as shown in Table 3.36.

Catalyst	Surface Area (m^2g^{-1})	Pore Volume (cm^3g^{-1})	Average Pore diameter (Å)
Pd/Al_2O_3	99	0.51	208
Pd/Al_2O_3 (Reduced)	104	0.50	197
Pd/Al_2O_3 (Regenerated)	98	0.47	193

Table 3.36 BET analysis of Pd/Al_2O_3 (Regenerated) catalyst [Reaction conditions: T = 140°C, $WHSV_{PyGas}$ = 4 h^{-1}, P_T = 10 barg]

3.2.3.4 Effect of PyGas feed flow rate (WHSV$_{PyGas}$) on PyGas hydrogenation

The reaction was performed with different WHSV of PyGas (4-8 h^{-1}) to study the effects of feed flow rate of PyGas (WHSV$_{PyGas}$) on the hydrogenation of PyGas. As like the Ni/Al$_2$O$_3$ system, different methods were used to investigate the effect of PyGas feed flow rate (WHSV$_{PyGas}$) on hydrogenation of PyGas over Pd/Al$_2$O$_3$ catalyst. Firstly, the weight of the catalyst was kept constant and feed flow rate of PyGas was changed, whilst in the second case, the PyGas feed was kept the same while the catalyst weight was altered. In addition, the reactions were performed in two types of hydrogen gas mixtures (50% and 25% hydrogen) for more comprehensive results. The hydrogenation of PyGas carried out at WHSV$_{PyGas}$ 4 h^{-1} using 50% and 25% hydrogen gas mixtures are already presented in section 3.2.3.2.1 and 3.2.3.2.2 respectively, while the reactions at WHSV$_{PyGas}$ at 8 h^{-1} are discussed in this section.

3.2.3.4.1 PyGas Hydrogenation over Pd/Al$_2$O$_3$ at WHSV$_{PyGas}$ = 8 h^{-1} using 50% hydrogen gas mixture [catalyst weight = 0.5 g]

The hydrogenation of PyGas over the Pd/Al$_2$O$_3$ catalyst using a 50% hydrogen gas mixture was performed at WHSV$_{PyGas}$ 8 h^{-1} by increasing the feed flow rate of PyGas, whilst keeping other reaction conditions constant [T = 140°C, P$_T$ = 20 barg and catalyst weight = 0.5 g]. The reaction profile of PyGas hydrogenation is shown in Figure 3.187.
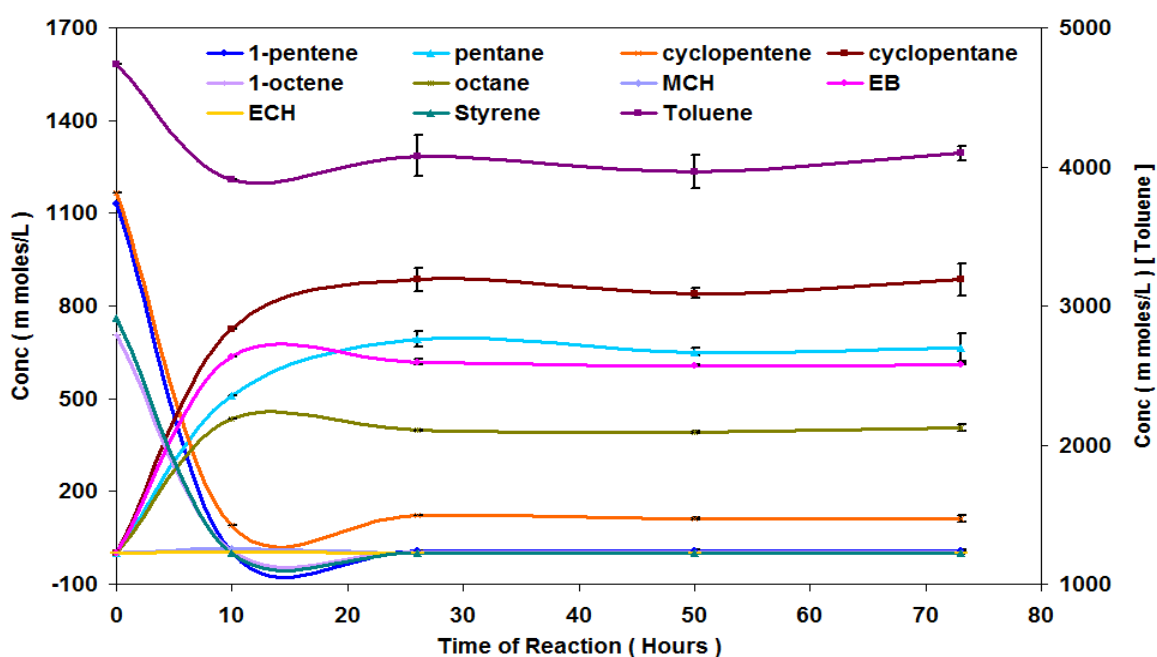
Figure 3.187 Reaction profile of PyGas Hydrogenation [Reaction conditions: T = 140°C, WHSV$_{PyGas}$ = 8 h^{-1}, P$_T$ = 20 barg, P$_{H2}$ = 10 barg]

Conversion of 1-pentene was 99% throughout TOS of the reaction. A considerable amount of internal pentene formation was observed with an increase in WHSV of PyGas, as shown in Figure 3.188-189. Moreover, a noticeably high amount of internal pentene formation was noted over the Pd/Al_2O_3, when compared to the Ni/Al_2O_3 under identical reaction conditions.
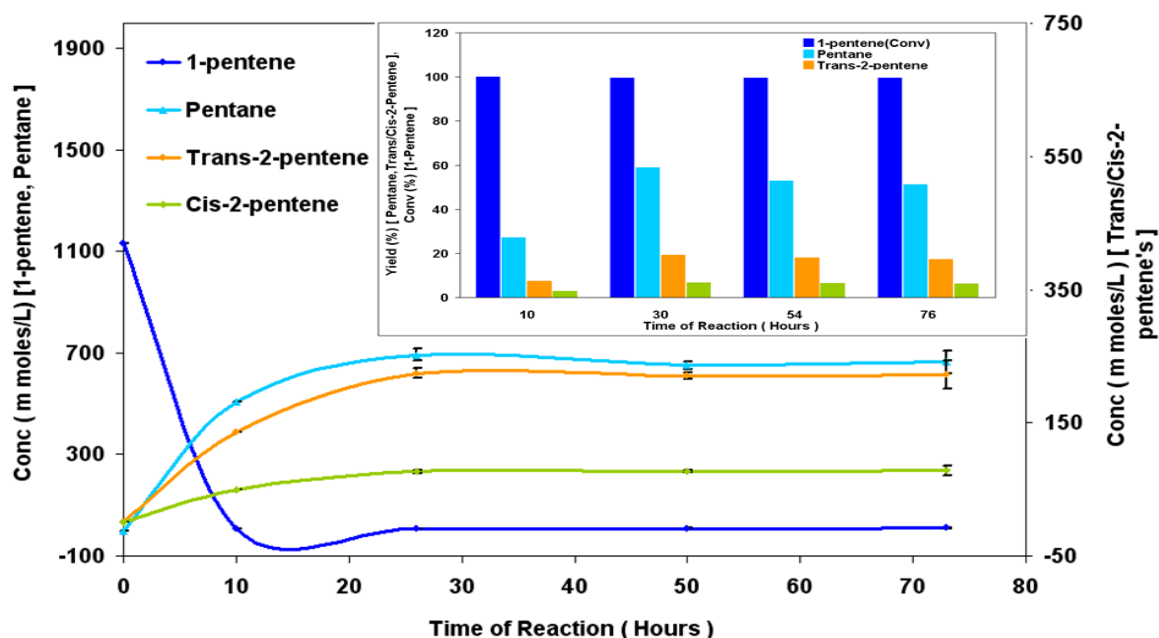
Figure 3.188 Hydrogenation of 1-pentene [Reaction conditions: T = 140°C, WHSV$_{PyGas}$ = 8 h^{-1}, P$_T$ = 20 barg, P$_{H2}$ = 10 barg]
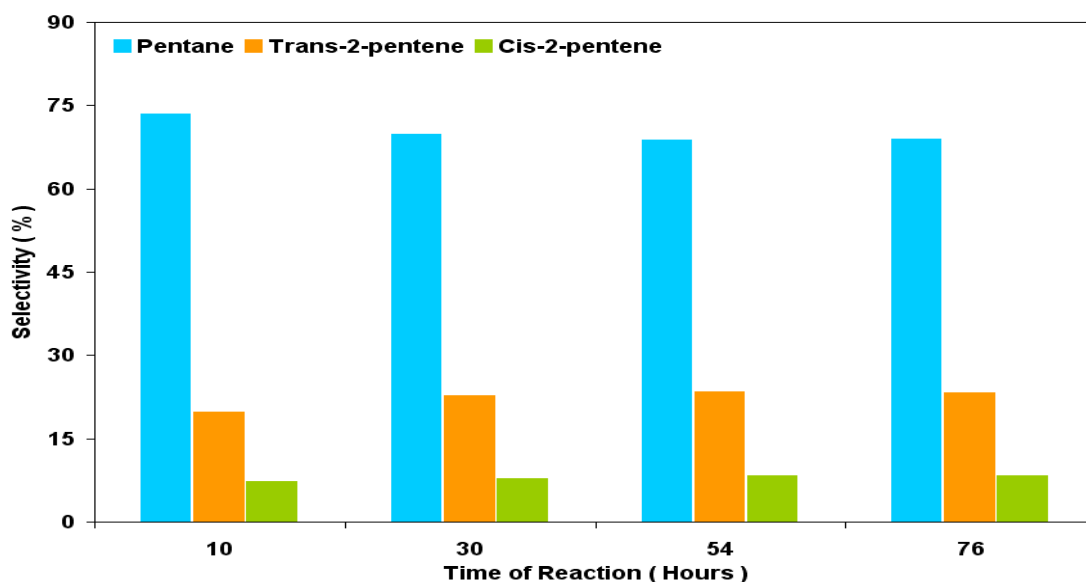
Figure 3.189 Selectivity of pentane, trans-2-pentene and cis-2-pentene during 1-pentene hydrogenation [Reaction conditions: T = 140°C, WHSV$_{PyGas}$ = 8 h^{-1}, P$_T$ = 20 barg, P$_{H2}$ = 10 barg]

Figure 3.190 represents the concentration profile of the 1-octene hydrogenation. Octane was the primary product however significant amounts of internal octenes were also produced during the reaction.
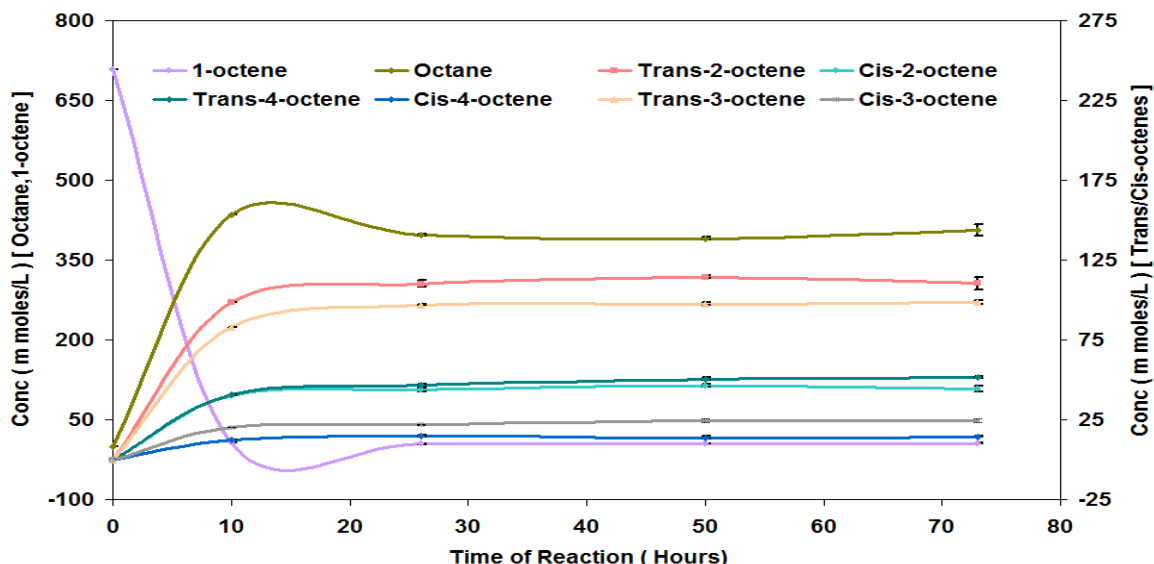
Figure 3.190 Reaction profile of 1-octene Hydrogenation [Reaction conditions: T = 140°C, WHSV$_{PyGas}$ = 8 h^{-1}, P$_T$ = 20 barg, P$_{H2}$ = 10 barg]

Conversion of 1-octene was above 99% throughout the reaction. The yield and selectivity of products are shown in Figures 3.191-192. An increase was observed in the formation of internal octenes with an increase in WHSV of PyGas from 4 h^{-1} to 8 h^{-1}. The formation of internal octenes was also found in higher amounts when compared to Ni/Al$_2$O$_3$ catalyst under these reaction conditions. Moreover, the selectivity towards 3-octene and 4-octene was found to be higher over Pd/Al$_2$O$_3$ catalyst.

The formation of products during 1-octene hydrogenation followed the order outlined below,

Octane >> Trans-2-octene > Trans-3-octene > Trans-4-octene ≈ Cis-2-octene >

Cis-3-octene > Cis-4-octene
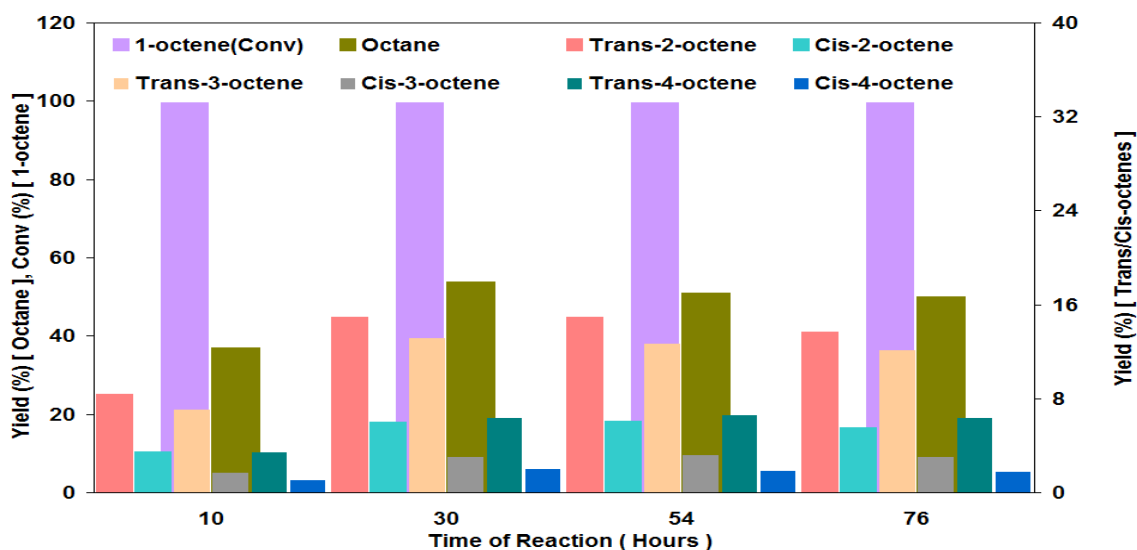
Figure 3.191 Percent yield of 1-octene Hydrogenation [Reaction conditions: T = 140°C, WHSV$_{PyGas}$ = 8 h^{-1}, P$_T$ = 20 barg, P$_{H2}$ = 10 barg]
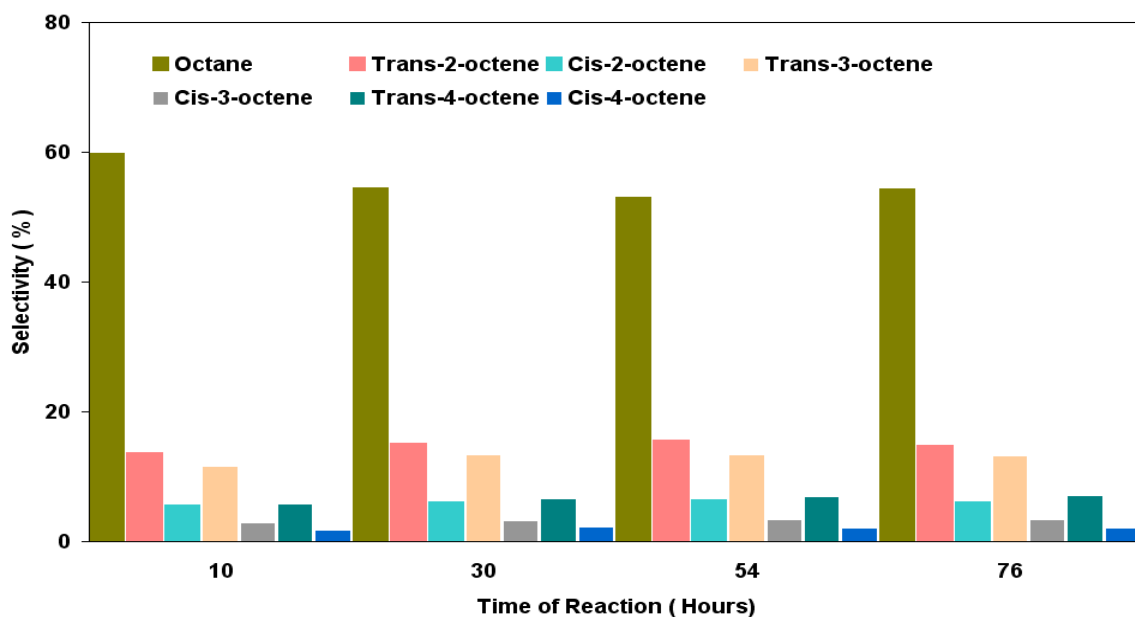
Figure 3.192 Selectivity of octane and internal octenes during 1-octene hydrogenation [Reaction conditions: T = 140°C, WHSV$_{PyGas}$ = 8 h^{-1}, P$_T$ = 20 barg, P$_{H2}$ = 10 barg]

The formation of the trans isomer was found to be higher than that of its respective cis isomer due to the thermodynamic stability of the trans isomer. The ratio of trans/cis isomers are shown in Table 3.37.

Trans/Cis-2-pentene ratio	Trans/Cis-2-octene ratio	Trans/Cis-3-octene ratio	Trans/Cis-4-octene ratio
74:26	71:29	80:20	78:22

Table 3.37 Ratio of trans/cis internal olefins formation in PyGas Hydrogenation [Reaction conditions: T = 140°C, WHSV$_{PyGas}$ = 8 h^{-1}, P$_T$ = 20 barg, P$_{H2}$ = 10 barg]

Conversion of cyclopentene was observed above 90% as shown in Figure 3.193. A considerable decrease was observed in the yield of cyclopentane with an increase in WHSV$_{PyGas}$. However, a higher yield of cyclopentane was observed when compared to the reaction performed over the Ni/Al$_2$O$_3$ catalyst under these reaction conditions.
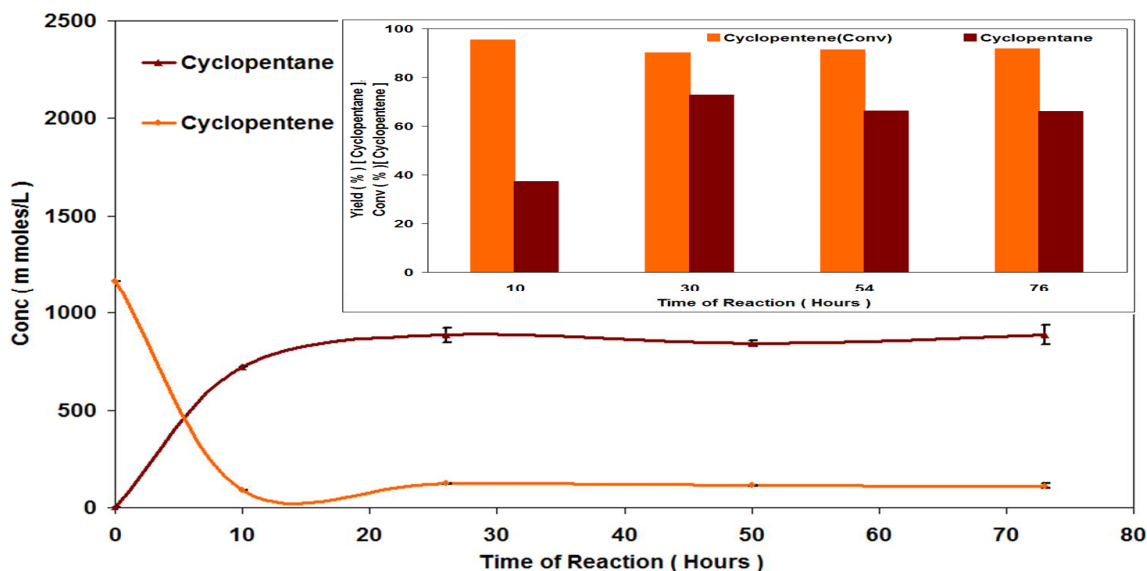
Figure 3.193 Hydrogenation of cyclopentene [Reaction conditions: T = 140°C, WHSV$_{PyGas}$ = 8 h^{-1}, P$_T$ = 20 barg, P$_{H2}$ = 10 barg]

Figure 3.194 shows that virtually no formation of methylcyclohexane occurred in the reaction whilst a reasonable conversion of toluene was observed.
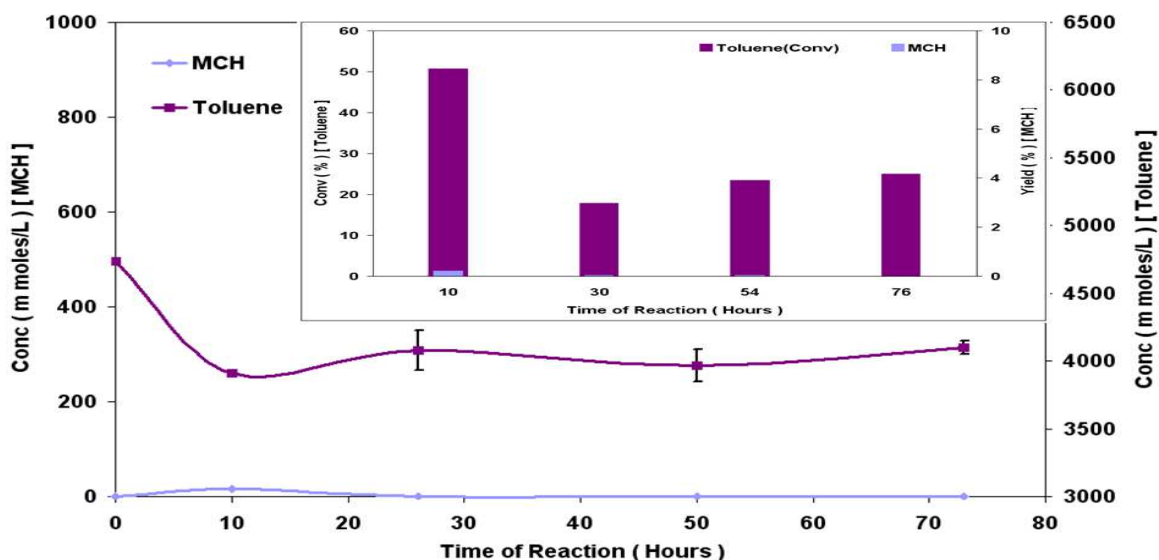
Figure 3.194 Hydrogenation of toluene [Reaction conditions: T = 140°C, WHSV$_{PyGas}$ = 8 h^{-1}, P$_T$ = 20 barg, P$_{H2}$ = 10 barg]

Conversion of styrene remained above 99%. Ethylbenzene was the primary product of reaction and virtually no ethylcyclohexane was observed, as shown in Figure 3.195. No significant change was observed in the yield of ethylbenzene with an increase in WHSV$_{PyGas}$ from 4 h^{-1} to 8 h^{-1}. The yield of ethylbenzene was noted at 49% in the first 10 hours of reaction. This increased to 77% after 30 hours and then a very slow decrease was found with TOS. In addition, the yield of ethylbenzene was slightly higher when compared to the reaction carried out over the Ni/Al$_2$O$_3$ catalyst under these reaction conditions.
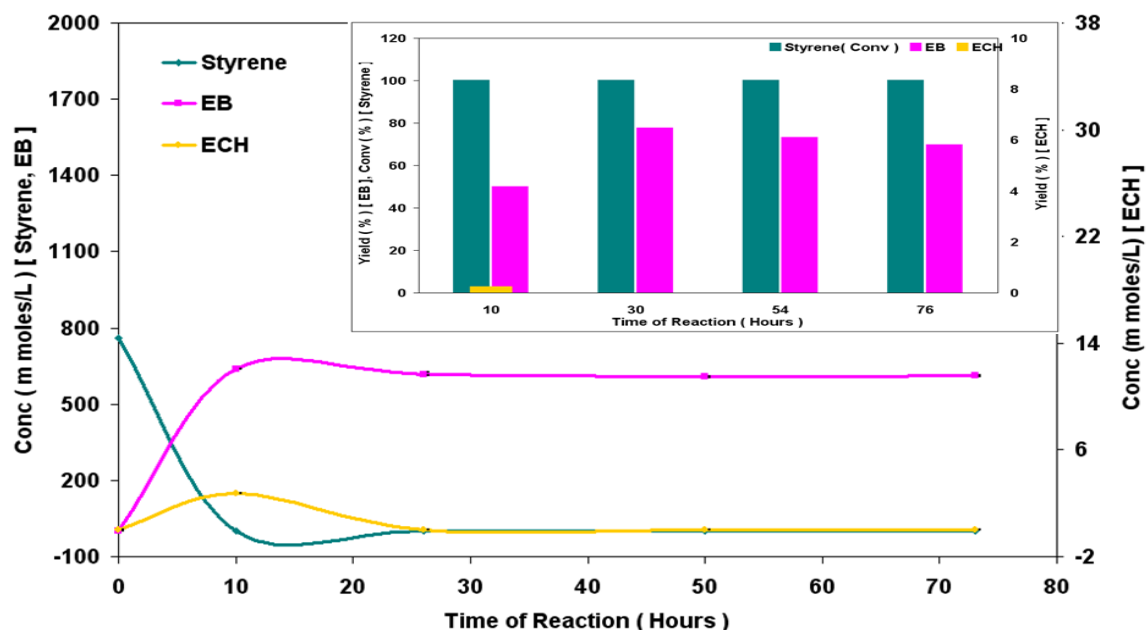
Figure 3.195 Hydrogenation of styrene [Reaction conditions: T = 140°C, WHSV$_{PyGas}$ = 8 h^{-1}, P$_T$ = 20 barg, P$_{H2}$ = 10 barg]

3.2.3.4.1.1 Post reaction analysis

Post reaction catalyst TPO

Post reaction *in-situ* TPO was performed over the Pd/Al$_2$O$_3$ and is shown in Figure 3.196. The results indicate that no significant change was observed in coke deposition with the change of WHSV$_{PyGas}$ from 4 h^{-1} to 8 h^{-1} during PyGas hydrogenation. Moreover, the evolution of styrene, benzene, 1-pentene, pentane, 1-octene, octane, cyclopentene, methylcyclohexane, toluene, ethylbenzene and H$_2$ was also found to be comparable to that observed with the TPO of the catalyst, used in the reaction carried out at WHSV$_{PyGas}$ 4 h^{-1}.
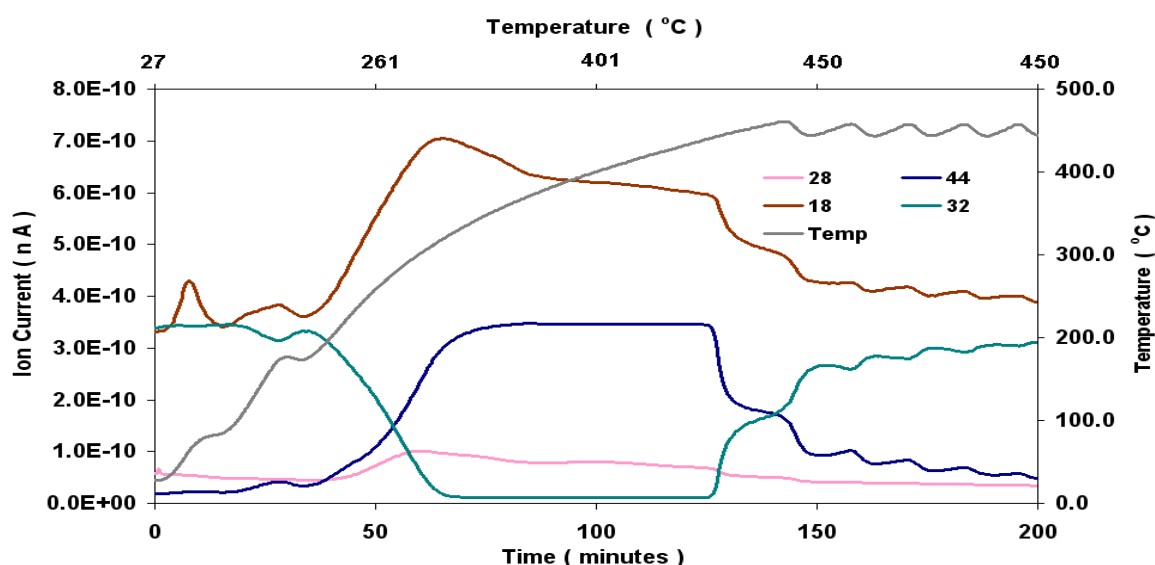
Figure 3.196 Post reaction *in-situ* TPO of Pd/Al$_2$O$_3$ catalyst [Reaction conditions: T = 140°C, WHSV$_{PyGas}$ = 8 h^{-1}, P$_T$ = 20 barg, P$_{H2}$ = 10 barg]

Total oxygen consumption in TPO = 2.91 m moles

BET analysis

The BET results show the surface area lost due to deposition of coke was recovered during regeneration as shown in Table 3.38.

Catalyst	Surface Area (m^2g^{-1})	Pore Volume (cm^3g^{-1})	Average Pore diameter (Å)
Pd/Al_2O_3	99	0.51	208
Pd/Al_2O_3 (Reduced)	104	0.50	197
Pd/Al_2O_3 (Regenerated)	97	0.44	185

Table 3.38 BET analysis of Pd/Al_2O_3 (Regenerated) catalyst [Reaction conditions: T = 140°C, $WHSV_{PyGas}$ = 8 h^{-1}, P_T = 20 barg, P_{H2} = 10 barg]

3.2.3.4.2 PyGas hydrogenation over Pd/Al$_2$O$_3$ at $WHSV_{PyGas}$ = 8 h^{-1} using 25% hydrogen gas mixture [Catalyst weight = 0.5 g]

The hydrogenation of PyGas over Pd/Al_2O_3 catalyst using a 25% hydrogen gas mixture under reaction conditions [T = 140°C, $WHSV_{PyGas}$ = 4 h^{-1}, P_T = 20 barg, and catalyst weight = 0.5 g] is already presented in section 3.2.3.2.2. The reaction performed with 25% hydrogen gas mixture at $WHSV_{PyGas}$ 8 h^{-1} achieved by doubling the feed flow rate of PyGas while all other reaction conditions constant, is discussed in this section. The reaction concentration profile is shown in Figure 3.197.
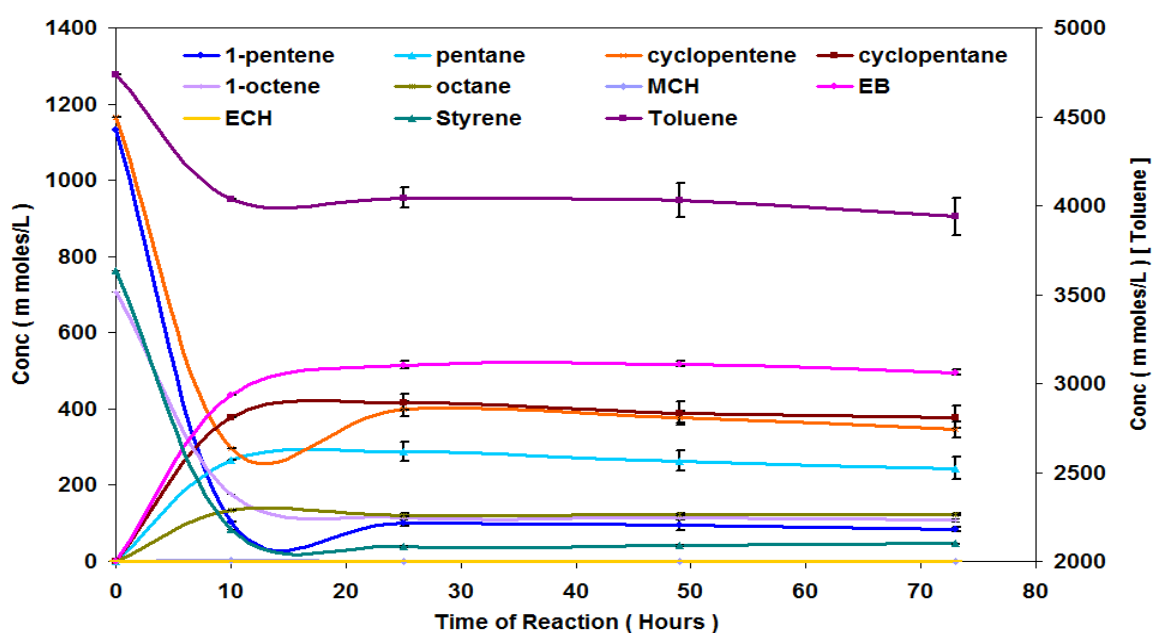
Figure 3.197 Reaction profile of PyGas hydrogenation [Reaction conditions: T = 140°C, $WHSV_{PyGas}$ = 8 h^{-1}, P_T = 20 barg, P_{H2} = 5 barg]

Figure 3.198 shows that conversion of 1-pentene was 94% in the first 10 hours of the reaction, which decreased to 90% after 29 hours and remained virtually constant for the rest of the reaction. The formation of internal pentene was considerably increased. The selectivity of the catalyst towards trans-2-pentene and cis-2-pentene increased with a change of $WHSV_{PyGas}$ from 4 h $^{-1}$ to 8 h $^{-1}$ as shown in Figure 3.199. Moreover, the formation of internal pentene was also found to be higher than for the reaction performed over the Ni/Al_2O_3 catalyst under these reaction conditions.
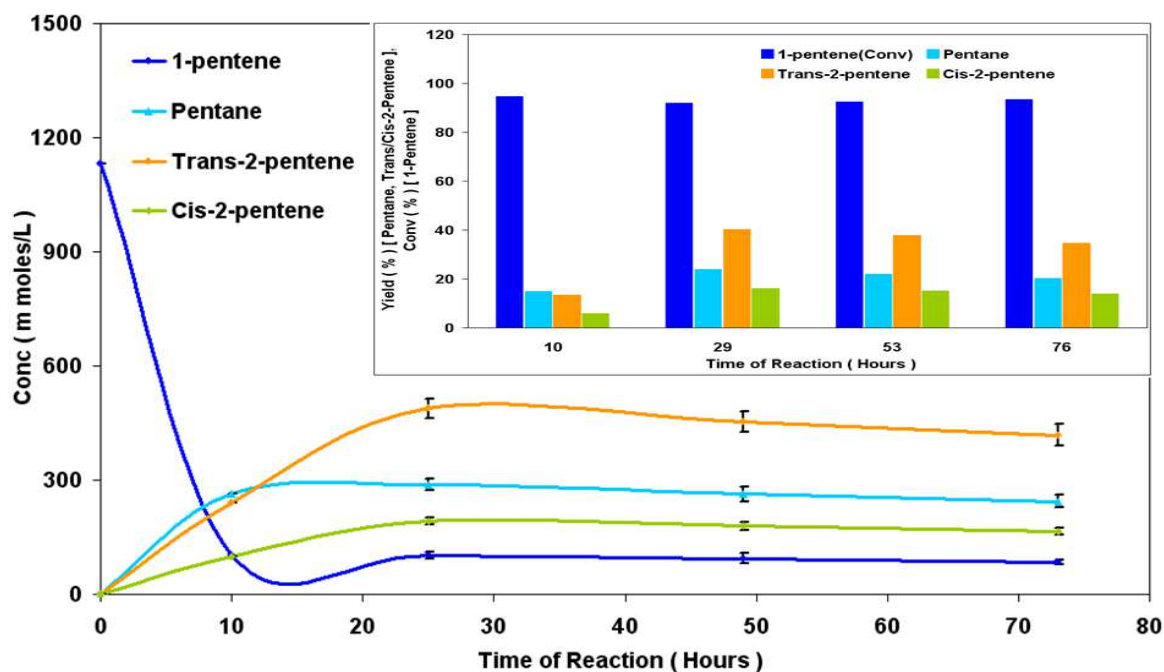
Figure 3.198 Hydrogenation of 1-pentene [Reaction conditions: T = 140°C, $WHSV_{PyGas}$ = 8 h^{-1}, P_T = 20 barg, P_{H2} = 5 barg]
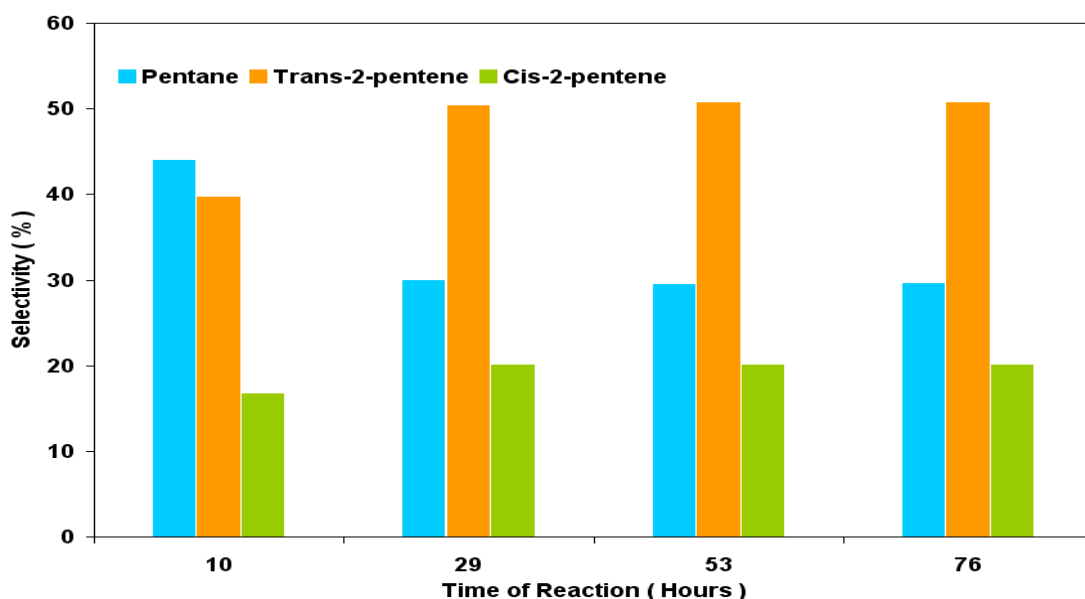
Figure 3.199 Selectivity of Pentane, trans-2-pentene and cis-2-pentene during 1-pentene hydrogenation [Reaction conditions: T = 140°C, $WHSV_{PyGas}$ = 8 h^{-1}, P_T = 20 barg, P_{H2} = 5 barg]

The reaction concentration profile of 1-octene hydrogenation is shown in Figure 3.200. Octane, trans-2-octene, cis-2-octene and trans-3-octene were the main products. However, a noticeable amount of cis-3-octene, trans-4-octene and cis-4-octene were also produced during 1-octene hydrogenation.
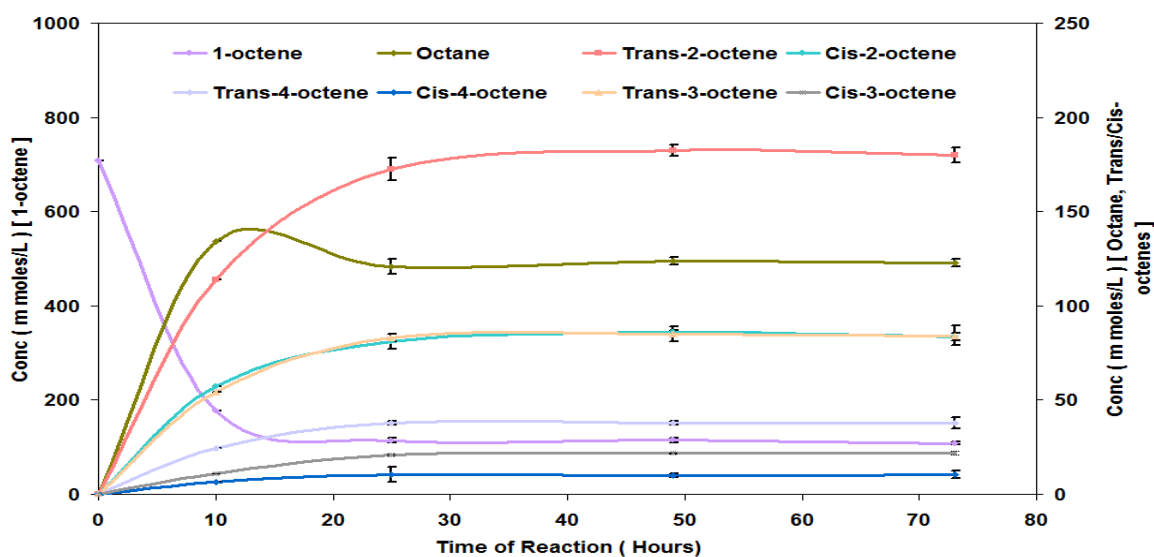
Figure 3.200 Reaction profile of 1-octene Hydrogenation [Reaction conditions: T = 140°C, WHSV$_{PyGas}$ = 8 h^{-1}, P$_T$ = 20 barg, P$_{H2}$ = 5 barg]

The conversion of 1-octene was about 84% throughout TOS of the reaction. A considerable increase was observed in the formation of internal octenes, however a noticeable decrease was observed in the conversion of 1-octene with an increase in WHSV$_{PyGas}$ from 4 h^{-1} to 8 h^{-1}. The yield and selectivity of 1-octene hydrogenation are shown in Figures 3.201-202. The higher selectivity towards 3-octene and 4-octene was observed when compared to the Ni/Al$_2$O$_3$ catalyst under similar reaction conditions.
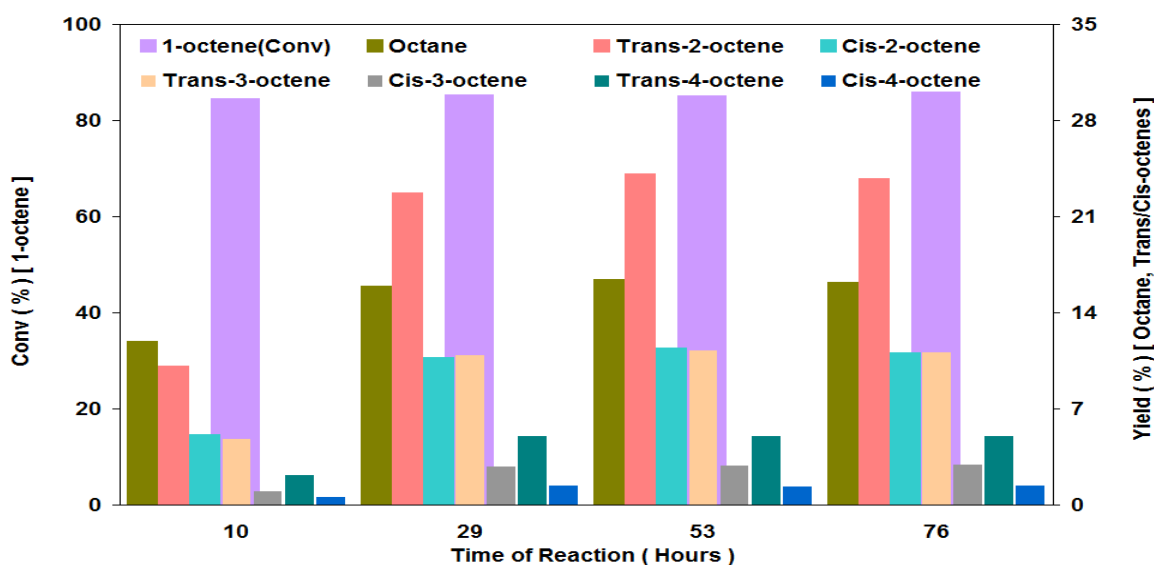
Figure 3.201 Percent yield of 1-octene Hydrogenation [Reaction conditions: T = 140°C, WHSV$_{PyGas}$ = 8 h^{-1}, P$_T$ = 20 barg, P$_{H2}$ = 5 barg]
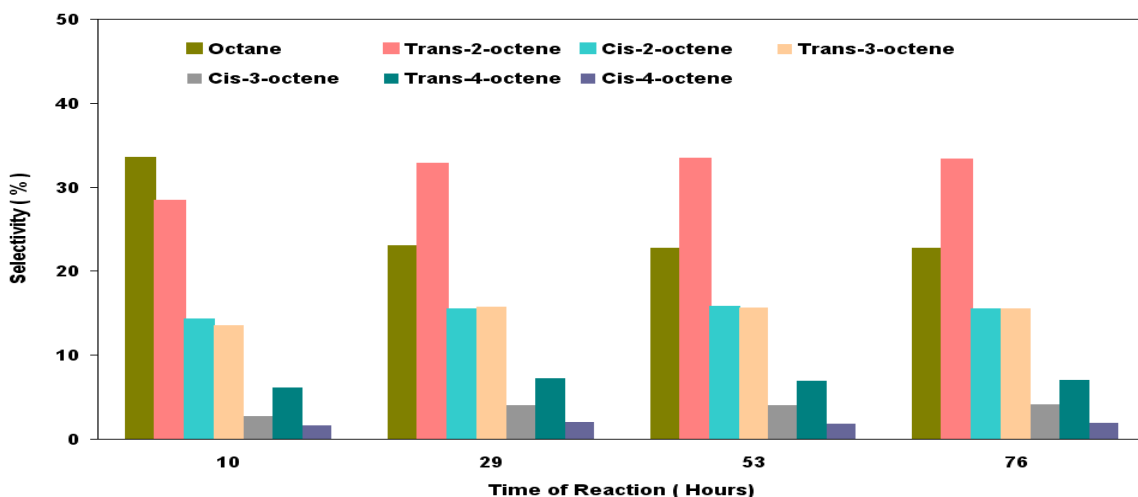
Figure 3.202 Selectivity of octane and internal octenes during 1-octene hydrogenation [Reaction conditions: T = 140°C, WHSV$_{PyGas}$ = 8 h^{-1}, P$_T$ = 20 barg, P$_{H2}$ = 5 barg]

The formation of the trans isomer was found to be higher than that of its respective cis isomer due to the thermodynamic stability of trans isomer. The ratio of trans/cis isomers are shown in Table 3.39.

Trans/Cis-2-pentene ratio	Trans/Cis-2-octene ratio	Trans/Cis-3-octene ratio	Trans/Cis-4-octene ratio
71:29	67:33	79:21	79:21

Table 3.39 Ratio of trans/cis internal olefins formation in PyGas Hydrogenation [Reaction conditions: T = 140°C, WHSV$_{PyGas}$ = 8 h^{-1}, P$_T$ = 20 barg, P$_{H2}$ = 5 barg]

Conversion of cyclopentene was 84% in the first 10 hours of the reaction, which decreased to 70% after 29 hours when reaction obtained steady state. A noticeable decrease was observed in the yield of cyclopentane with an increase in WHSV$_{PyGas}$ from 4 h^{-1} to 8 h^{-1}.
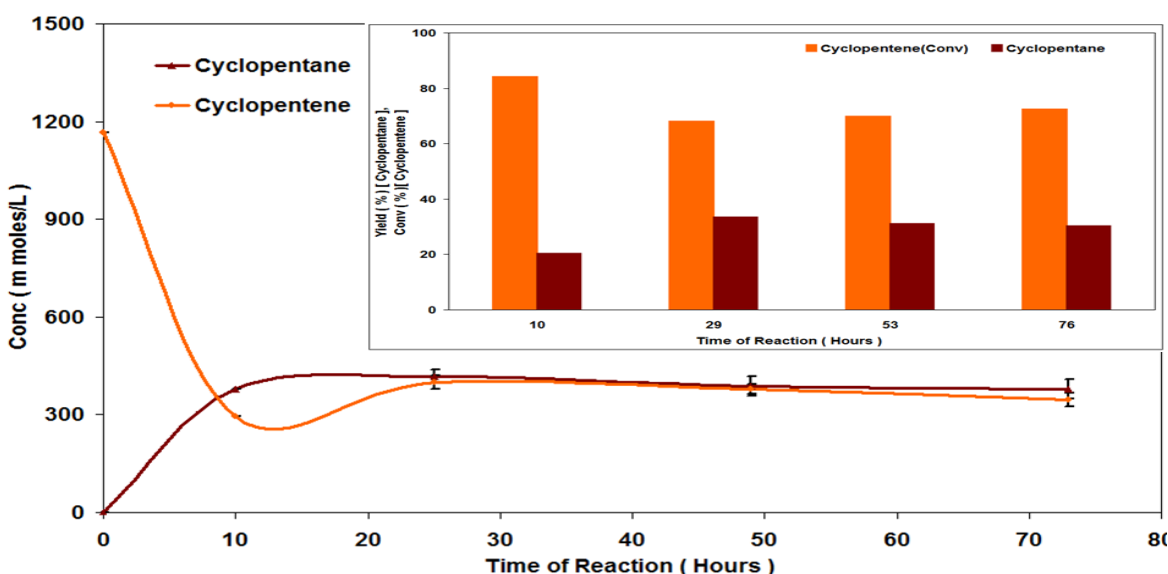
Figure 3.203 Hydrogenation of cyclopentene [Reaction conditions: T = 140°C, WHSV$_{PyGas}$ = 8 h^{-1}, P$_T$ = 20 barg, P$_{H2}$ = 5 barg]

Figure 3.204 shows that around 47% conversion of toluene was observed in the first 10 hours of reaction which decreased to 21% after 29 hours when the reaction obtained steady state. This remained constant throughout the remainder of the reaction. Virtually no formation of methylcyclohexane was seen in the reaction.
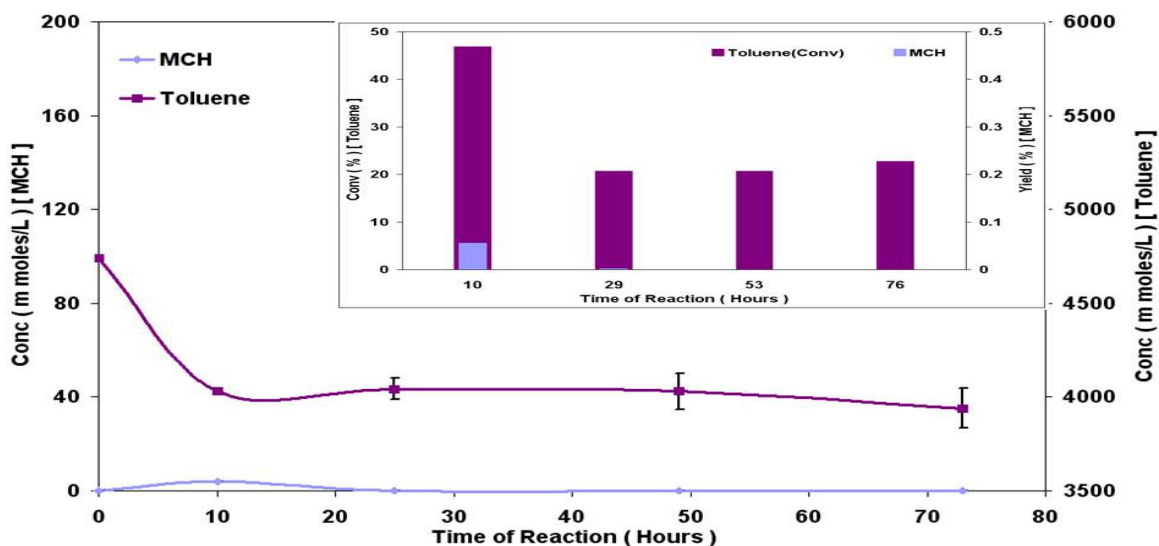
Figure 3.204 Hydrogenation of toluene [Reaction conditions: T = 140°C, WHSV$_{PyGas}$ = 8 h^{-1}, P$_T$ = 20 barg, P$_{H2}$ = 5 barg]

Figure 3.205 shows that conversion of the styrene was above 94% in the reaction. Ethylbenzene was the single product observed during styrene hydrogenation. The yield of ethylbenzene was 36% in the first 10 hours of the reaction which increased to 62% after 29 hours and then remained constant in the rest of reaction. No significant change was observed in the yield of the ethylbenzene with an increase in WHSV$_{PyGas}$ from 4 h^{-1} to 8 h^{-1}.
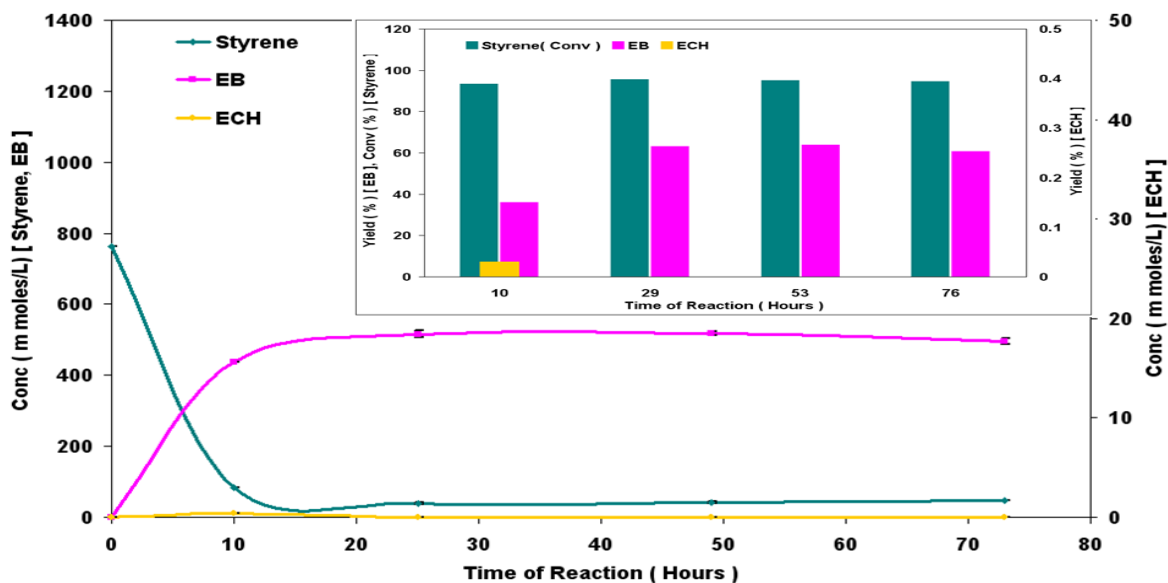
Figure 3.205 Hydrogenation of styrene [Reaction conditions: T = 140°C, WHSV$_{PyGas}$ = 8 h^{-1}, P$_T$ = 20 barg, P$_{H2}$ = 5 barg]

3.2.3.4.2.1 Post reaction analysis

Post reaction catalyst TPO

Post reaction *in-situ* TPO of the Pd/Al_2O_3 catalyst was carried out, which is shown in Figure 3.206. These results indicate that a small decrease was observed in the amount of coke deposition with a change of $WHSV_{PyGas}$ from 4 h^{-1} to 8 h^{-1}.
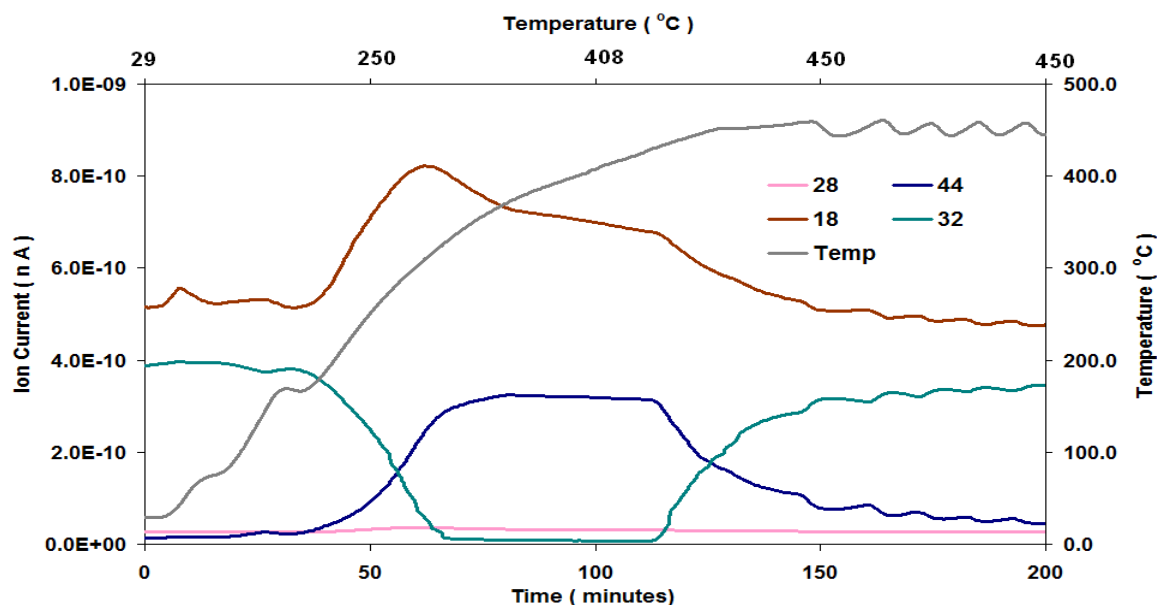
Figure 3.206 Post reaction *in-situ* TPO of Pd/Al_2O_3 catalyst [Reaction conditions: T = 140°C, $WHSV_{PyGas}$ = 8 h^{-1}, P_T = 20 barg, P_{H2} = 5 barg]

Total oxygen consumption in TPO = 2.93 m moles

Moreover, higher level of aromatic species (styrene and benzene) desorption was observed in the temperature range 250-350°C, while small amounts of styrene and benzene evolution occurred at 400°C with an increase in WHSV of PyGas from 4 h^{-1} to 8 h^{-1}, as shown in Figure 3.207. Moreover, the amount of H_2 evolved also slightly decreased. Whilst the levels of 1-pentene, cyclopentene, 1-octene, pentane, octane, toluene, methylcyclohexane, ethylbenzene and ethylcyclo-hexane evolution were found to be similar to that observed in the TPO of the catalyst, used in the reaction at $WHSV_{PyGas}$ 4 h^{-1}.
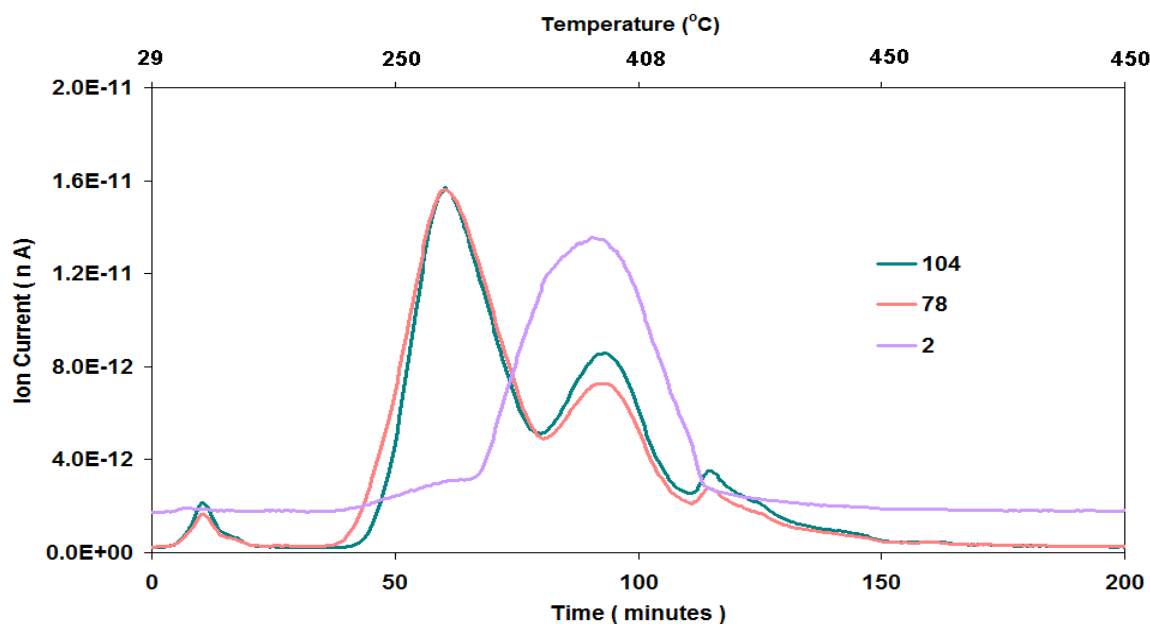
Figure 3.207 Evolution of aromatic species (styrene and benzene) and H_2 [Reaction conditions: T = 140°C, $WHSV_{PyGas}$ = 8 h^{-1}, P_T = 20 barg, P_{H2} = 5 barg]

BET analysis

The surface area of the regenerated catalyst was found to be similar to the fresh catalyst as shown in Table 3.40.

Catalyst	Surface Area (m^2g^{-1})	Pore Volume (cm^3g^{-1})	Average Pore diameter (Å)
Pd/Al$_2$O$_3$	99	0.51	208
Pd/Al$_2$O$_3$ (Reduced)	104	0.50	197
Pd/Al$_2$O$_3$ (Regenerated)	93	0.46	202

Table 3.40 BET analysis of Pd/Al$_2$O$_3$ (Regenerated) catalyst [Reaction conditions: T = 140°C, $WHSV_{PyGas}$ = 8 h^{-1}, P_T = 20 barg, P_{H2} = 5 barg]

3.2.3.4.3 PyGas hydrogenation over Pd/Al$_2$O$_3$ at $WHSV_{PyGas}$ = 8 h^{-1} using 25% hydrogen gas mixture [Catalyst weight = 0.25 g]

Effect of $WHSV_{PyGas}$ during the PyGas hydrogenation was also studied by keeping the feed low rate of PyGas constant and varying the catalyst amount from 0.5 to 0.25 g. This study was performed using a 25% hydrogen gas mixture. The hydrogenation of PyGas at $WHSV_{PyGas}$ = 4 h^{-1} using 0.5 g catalyst is revealed in section 3.2.3.2.2. The reaction presented in this section was performed with a same feed flow rate of PyGas using 0.25 g of catalyst ($WHSV_{PyGas}$ 8 h^{-1}) with other reaction conditions kept constant [T = 140°C and P_T = 20 barg]. The reaction profile is shown in Figure 3.208.
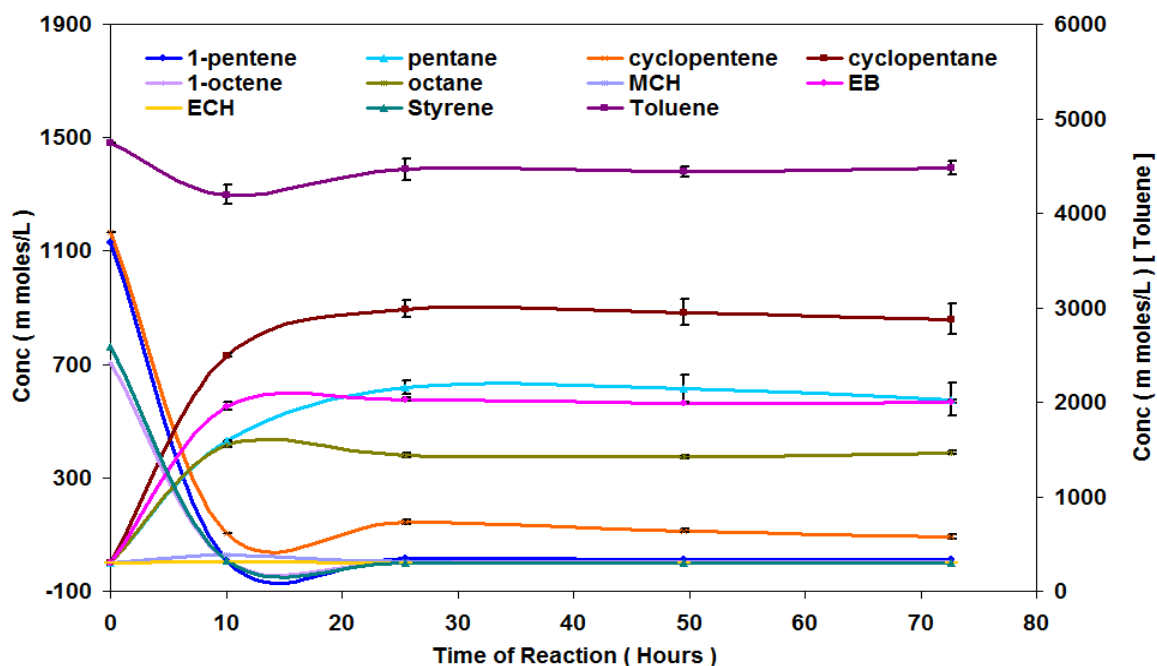
Figure 3.208 Reaction profile of PyGas Hydrogenation [Reaction conditions: T = 140°C, WHSV$_{PyGas}$ = 8 h^{-1}, P$_T$ = 20 barg, P$_{H2}$ = 5 barg]

Figure 3.209-210 show that conversion of 1-pentene was about 97% during the first 10 hours of the reaction which decreased to about 89% after 30 hours when the reaction obtained steady state condition and remained constant during the rest of reaction. Small amount of internal pentenes formation was observed contrast to previous reaction carried out at WHSV$_{PyGas}$ 8 h^{-1} with using 0.5 g of the catalyst.
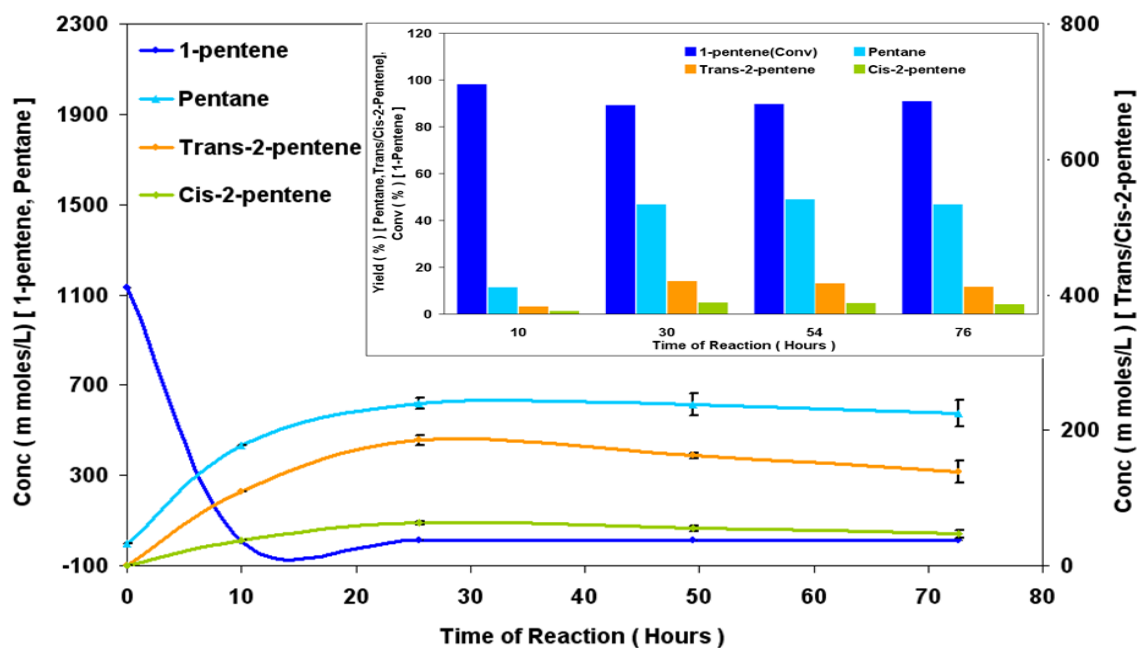
Figure 3.209 Hydrogenation of 1-pentene [Reaction conditions: T = 140°C, WHSV$_{PyGas}$ = 8 h^{-1}, P$_T$ = 20 barg, P$_{H2}$ = 5 barg]
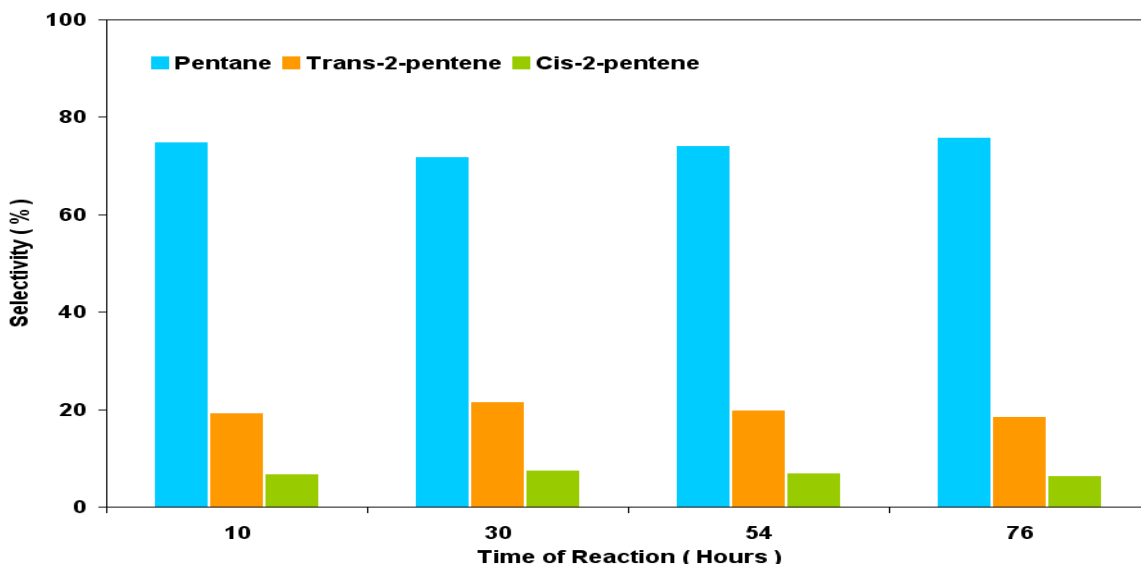
Figure 3.210 Selectivity of pentane, trans-2-pentene and cis-2-pentene during 1-pentene hydrogenation [Reaction conditions: T = 140°C, WHSV$_{PyGas}$ = 8 h^{-1}, P$_T$ = 20 barg, P$_{H2}$ = 5 barg]

Octane was the principal product however a reasonable amount of internal octenes were also produced during 1-octene hydrogenation as shown in Figure 3.211. The products formation can be presented as following order,

Octane >> 2-octene > 3-octene > 4-octene
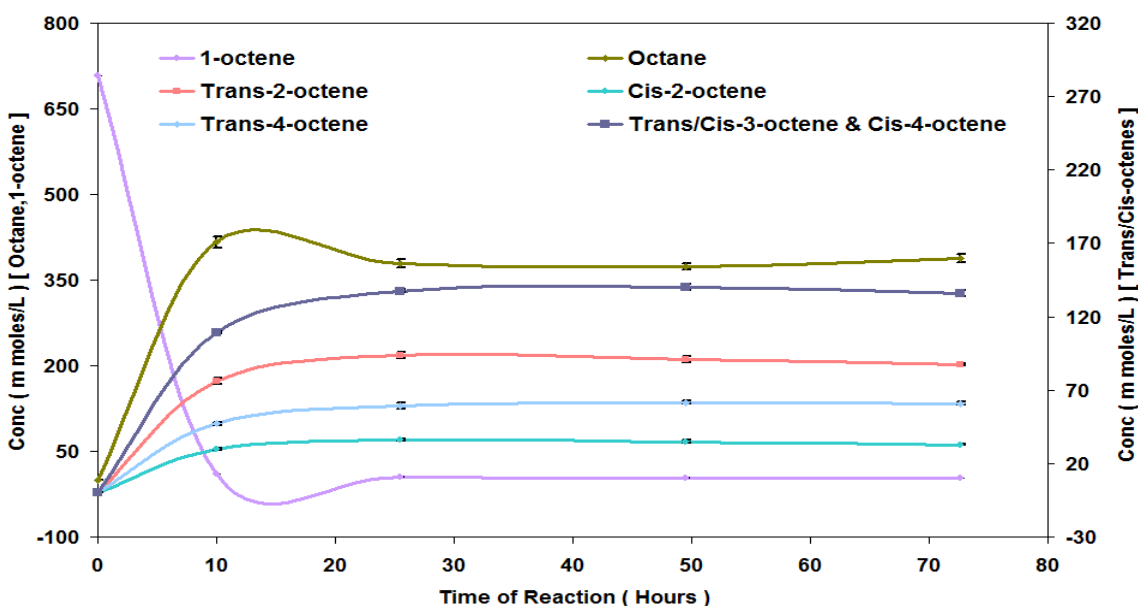
Figure 3.211 Reaction profile of 1-octene hydrogenation [Reaction conditions: T = 140°C, WHSV$_{PyGas}$ = 8 h^{-1}, P$_T$ = 20 barg, P$_{H2}$ = 5 barg]

Figures 3.212-213 show that the conversion of 1-octene remained above 99% throughout the reaction. A small increase was observed in the formation of internal octene when compared to the reaction carried out at WHSV$_{PyGas}$ 4 h^{-1}. However the internal formation was found in small amount contrast to the previous reaction carried out at WHSV$_{PyGas}$ 8 h^{-1} with using 0.5 g of the catalyst.
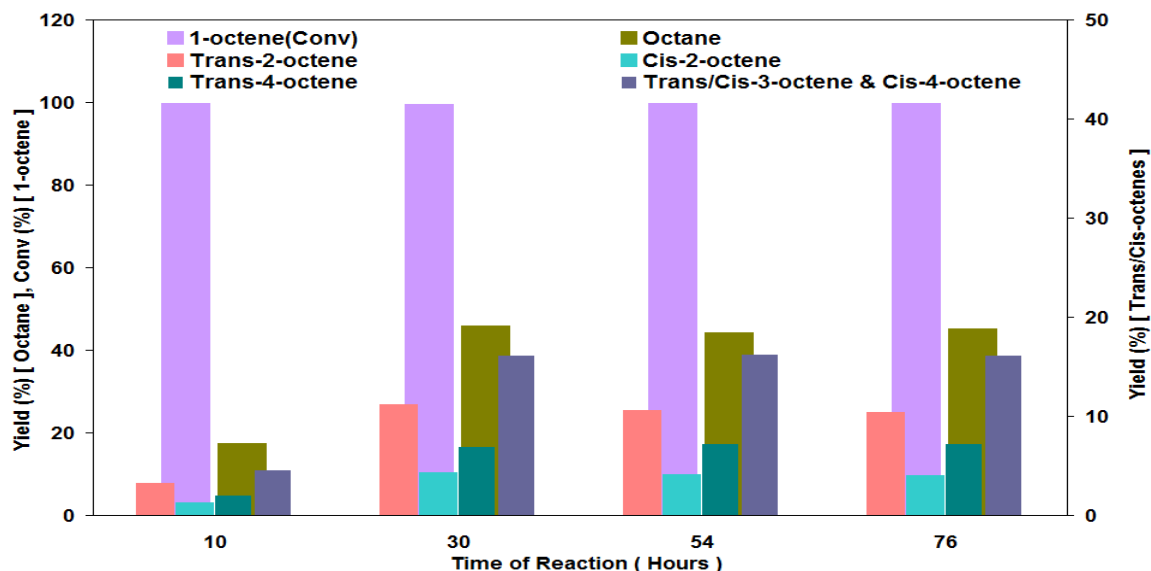
Figure 3.212 Percent yield of 1-octene hydrogenation [Reaction conditions: T = 140°C, WHSV$_{PyGas}$ = 8 h^{-1}, P$_T$ = 20 barg, P$_{H2}$ = 5 barg]
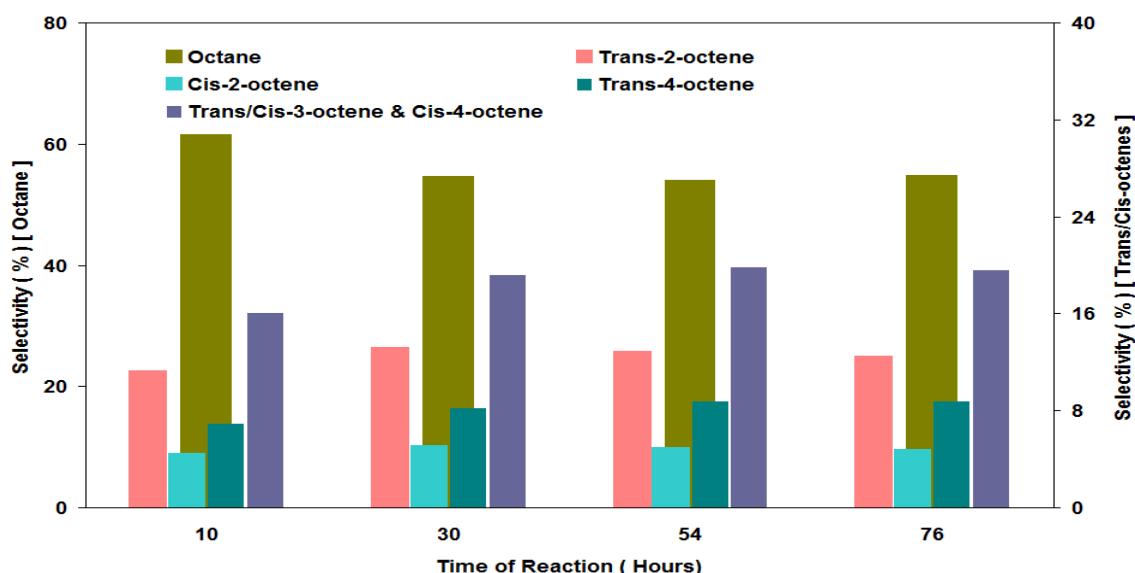
Figure 3.213 Selectivity of octane and internal octenes during 1-octene hydrogenation [Reaction conditions: T = 140°C, WHSV$_{PyGas}$ = 8 h^{-1}, P$_T$ = 20 barg, P$_{H2}$ = 5 barg]

The ratio of trans/cis 2-octene was found to be similar to the trans/cis ratio of 2-pentene as shown in Table 3.41.

Trans/Cis-2-pentene ratio	Trans/Cis-2-octene ratio
75:25	73:27

Table 3.41 Ratio of trans/cis internal olefins formation in PyGas Hydrogenation [Reaction conditions: T = 140°C, WHSV$_{PyGas}$ = 8 h^{-1}, P$_T$ = 20 barg, P$_{H2}$ = 5 barg]

Figure 3.214 shows that the conversion of cyclopentene was above 97% in the first 10 hours of the reaction, which decreased to 90% after 30 hour and no

significant change was observed in the rest of reaction. The yield of cyclopentane was 18% during the first 10 hours, which increased to 65% after 30 hours of the reaction and remained constant for the rest of reaction.
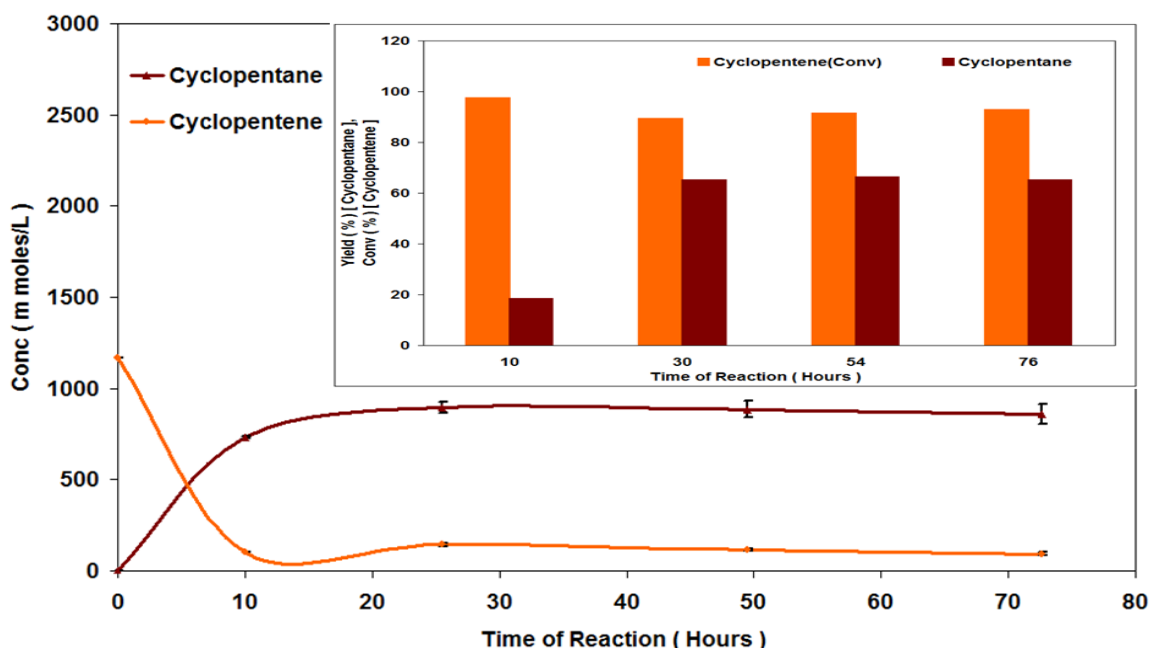
Figure 3.214 Hydrogenation of cyclopentene [Reaction conditions: T = 140°C, WHSV$_{PyGas}$ = 8 h^{-1}, P$_T$ = 20 barg, P$_{H2}$ = 5 barg]

Figure 3.215 shows that the conversion of toluene was about 74% in the initial 10 hours of reaction, which decreased to 21% when reaction obtained steady state and remained constant throughout the rest of reaction. However, virtually no formation of methylcyclohexane was observed.
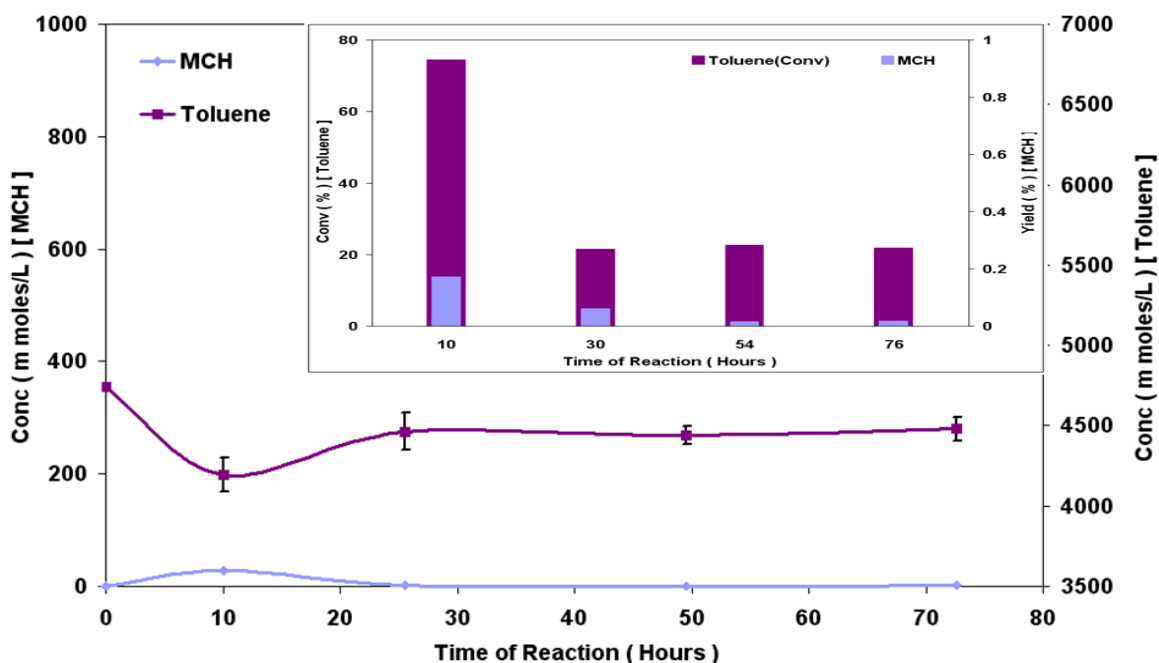
Figure 3.215 Hydrogenation of toluene [Reaction conditions: T = 140°C, WHSV$_{PyGas}$ = 8 h^{-1}, P$_T$ = 20 barg, P$_{H2}$ = 5 barg]

Figure 3.216 shows that conversion of the styrene was above 99% throughout the reaction. Ethylbenzene was the single product observed in the reaction.
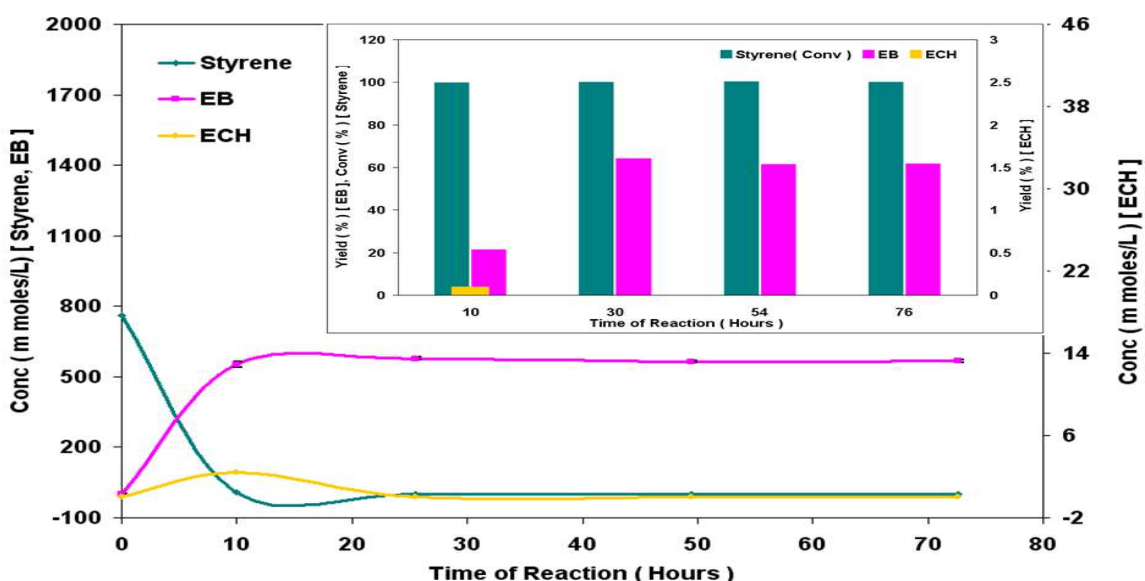
Figure 3.216 Hydrogenation of styrene [Reaction conditions: T = 140°C, WHSV$_{PyGas}$ = 8 h^{-1}, P$_T$ = 20 barg, P$_{H2}$ = 5 barg]

3.2.3.4.3.1 Post reaction analysis

Post reaction catalyst TPO

Post reaction *in-situ* TPO of the catalyst was performed, as shown in Figure 3.217. The results indicate that the amount of coke deposited on the catalyst during this reaction was small when compare to the reaction performed with WHSV$_{PyGas}$ = 4 h^{-1} using 0.5 g of catalyst described in section 3.2.3.2.2. The amount of coke deposition is less due to smaller amount of catalyst used in this reaction, 0.25 g rather than of 0.5 g.
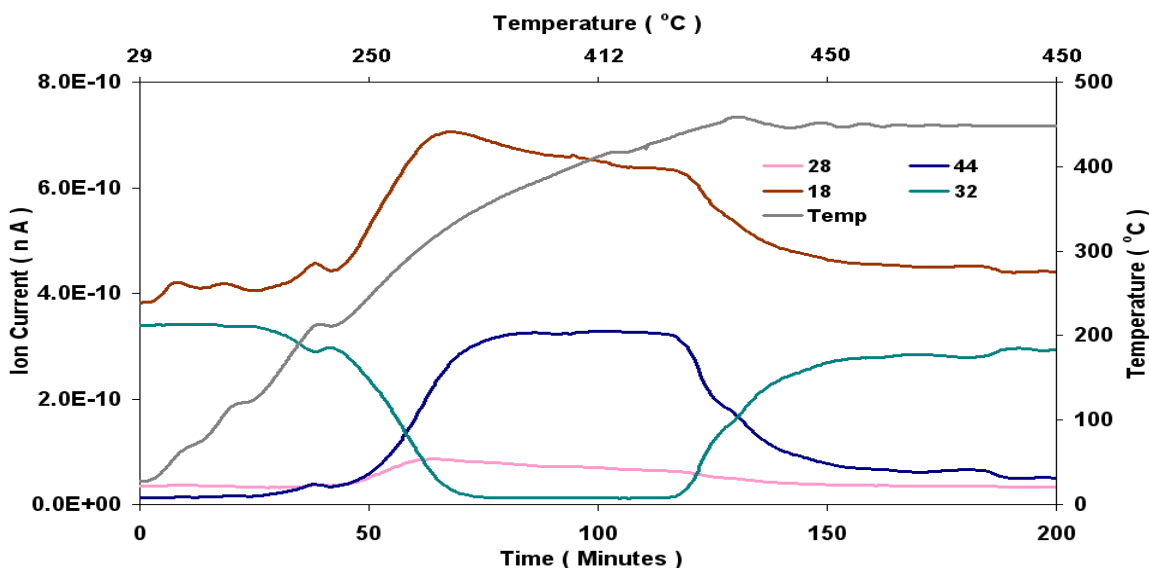
Figure 3.217 Post reaction *in-situ* TPO of Pd/Al$_2$O$_3$ catalyst [Reaction conditions: T = 140°C, WHSV$_{PyGas}$ = 8 h^{-1}, P$_T$ = 20 barg, P$_{H2}$ = 5 barg]

Total oxygen consumption in TPO = 2.60 m moles

Meanwhile, small levels of styrene, benzene and H_2 evolution were observed in the TPO as shown in Figure 3.218. Moreover, no considerable evolution of 1-pentene, cyclopentene, 1-octene, pentane, octane, toluene, methylcyclo-hexane, ethylbenzene and ethylcyclohexane were noted.
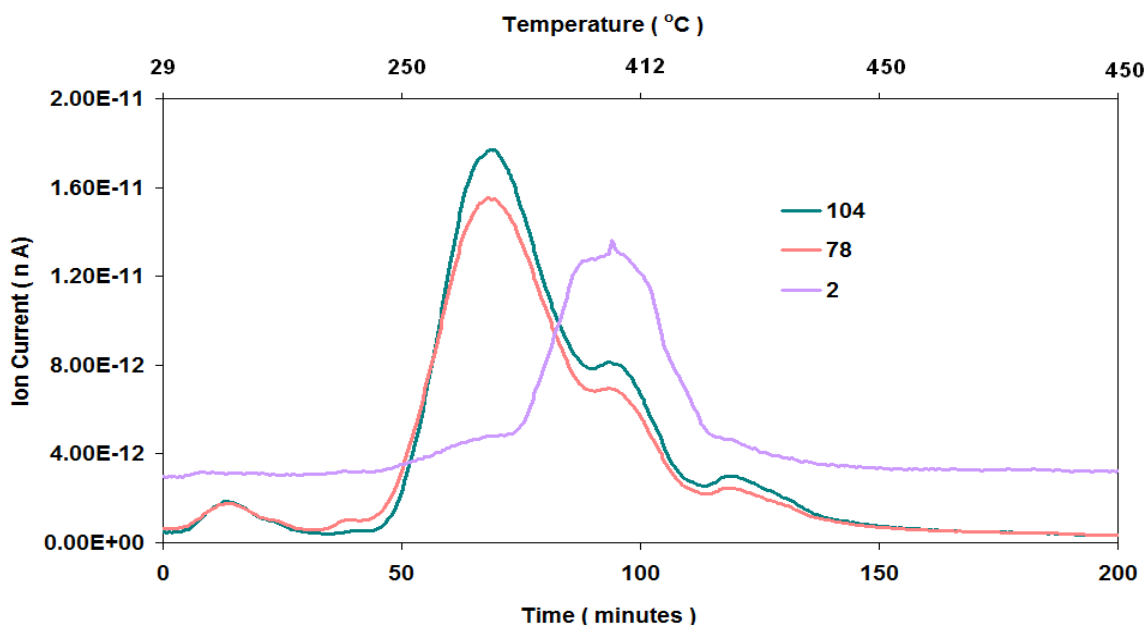
Figure 3.218 Evolution of aromatic species (styrene and benzene) and H_2 [Reaction conditions: T = 140°C, $WHSV_{PyGas}$ = 8 h^{-1}, P_T = 20 barg, P_{H2} = 5 barg]

BET analysis

The surface area, pore volume and pore diameter of the regenerated Pd/Al_2O_3 were analysed and presented in Table 3.42.

Catalyst	Surface Area (m^2g^{-1})	Pore Volume (cm^3g^{-1})	Average Pore diameter (Å)
Pd/Al_2O_3	99	0.51	208
Pd/Al_2O_3 (Reduced)	104	0.50	197
Pd/Al_2O_3 (Regenerated)	85	0.44	209

Table 3.42 BET analysis of Pd/Al_2O_3 (Regenerated) catalyst [Reaction conditions: T = 140°C, $WHSV_{PyGas}$ = 8 h^{-1}, P_T = 20 barg, P_{H2} = 5 barg]

The BET results indicate that the surface area lost due to the deposition of coke during the reaction was not completely recovered during regeneration and a decrease in the surface area of the catalyst was observed.

3.2.3.5 Reaction with PyGas containing 1,3-pentadiene (PyGas-II)

PyGas containing 1,3-pentadiene instead of 1-pentene was used for this reaction to investigate the di-olefin hydrogenation in PyGas over the Pd/Al$_2$O$_3$. The composition of PyGas used in this reaction is given in Table 3.24. The Hydrogenation of PyGas was performed over the Pd/Al$_2$O$_3$ catalyst using 25% hydrogen gas under reaction conditions T = 140°C, WHSV$_{PyGas}$ = 4 h^{-1} and P$_T$ = 20 barg. The reaction profile is given in Figure 3.219.
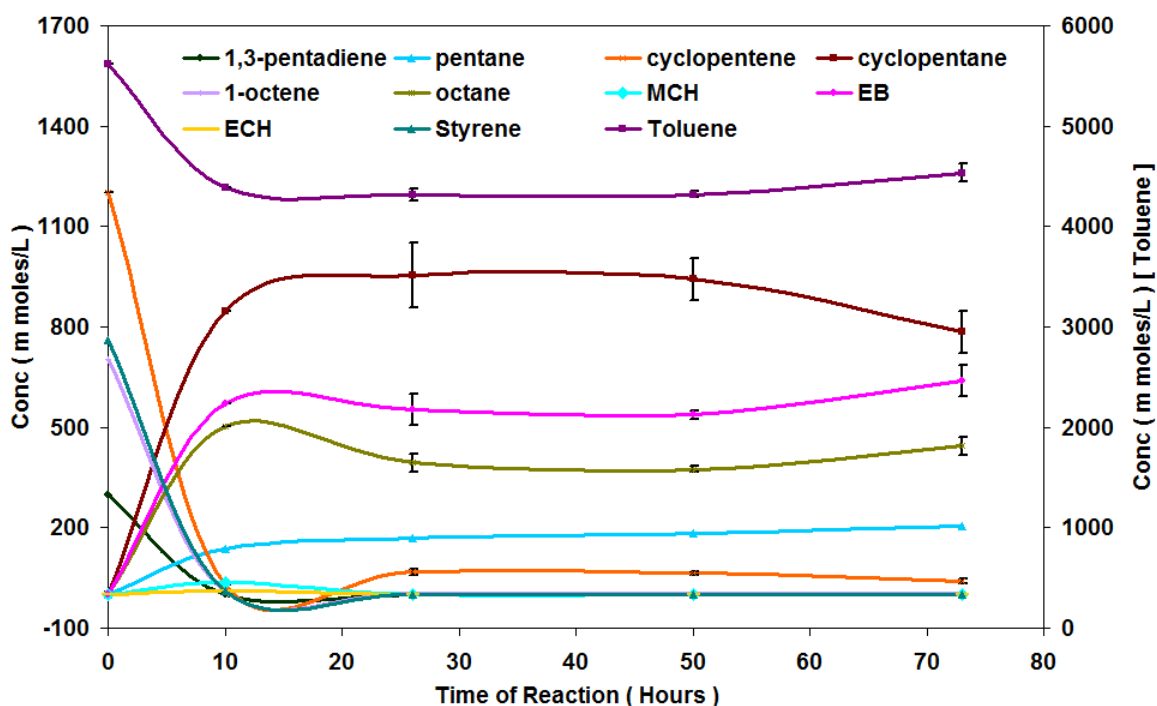
Figure 3.219 Reaction profile of PyGas Hydrogenation [Reaction conditions: T = 140°C, WHSV$_{PyGas}$ = 4 h^{-1}, P$_T$ = 20 barg, P$_{H2}$ = 5 barg]

Figures 3.220-221 present that conversion of 1,3-pentadiene was virtually 100% throughout the reaction. Pentane was the principal product of the reaction however a reasonable amount of trans-2-pentene and cis-2-pentene was also produced during the reaction. Moreover, almost no 1-pentene was seen in the reaction.
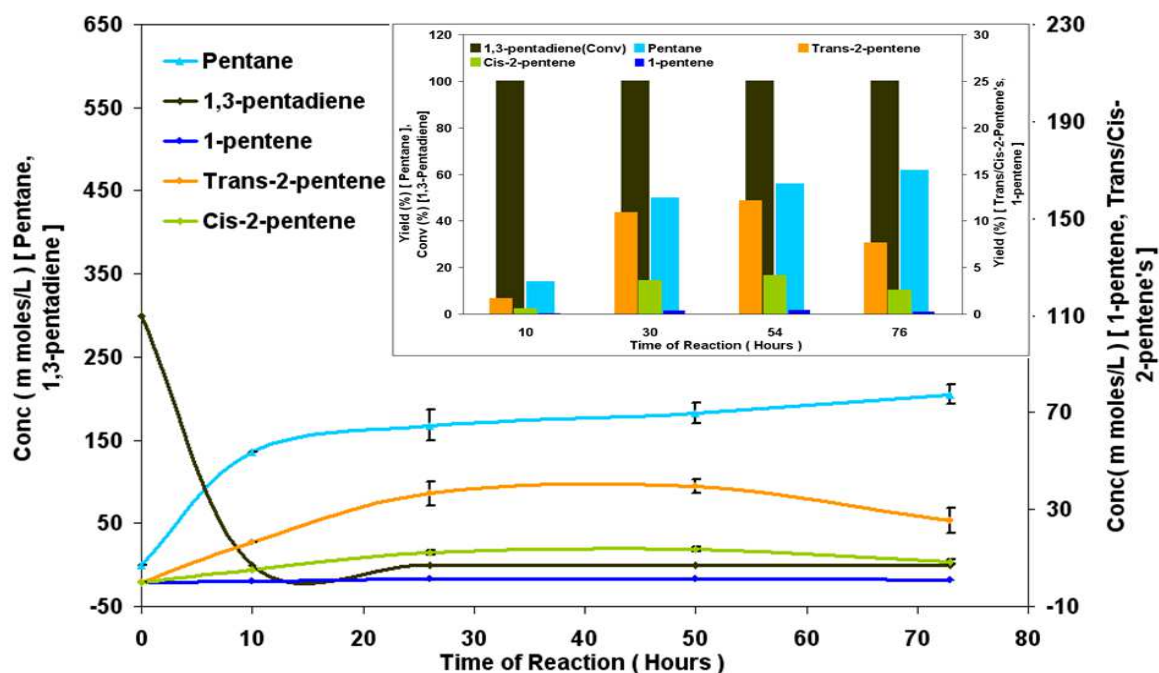
Figure 3.220 Hydrogenation of 1,3-pentadiene [Reaction conditions: T = 140°C, WHSV$_{PyGas}$ = 4 h^{-1}, P$_T$ = 20 barg, P$_{H2}$ = 5 barg]
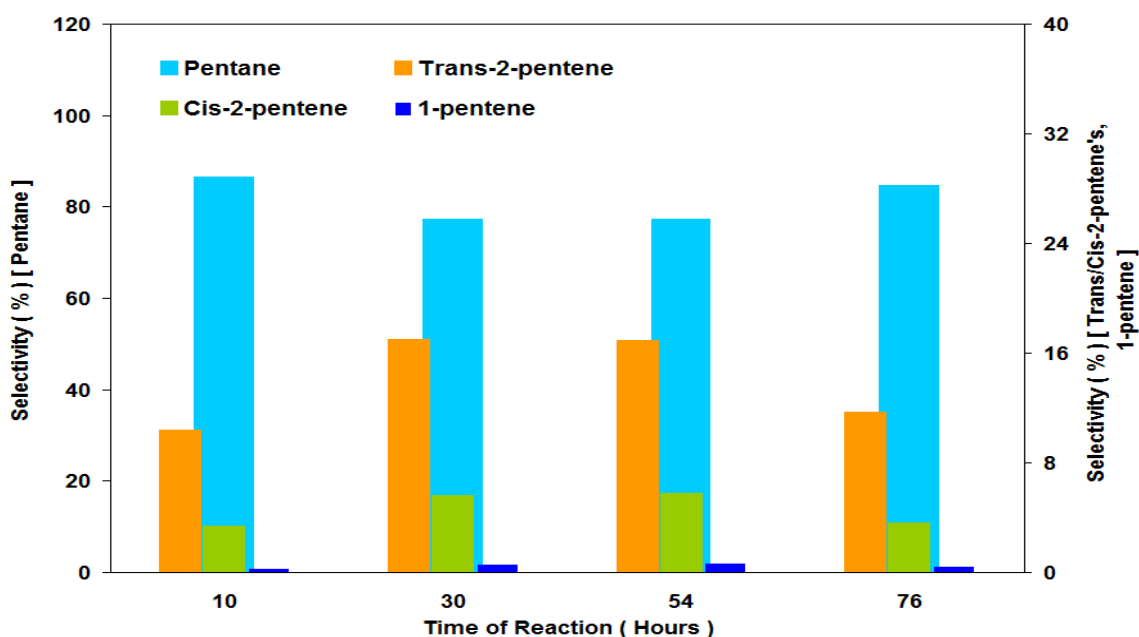
Figure 3.221 Selectivity of pentane, trans-2-pentene and cis-2-pentene, 1-pentene during 1,3-pentadiene hydrogenation [Reaction conditions: T = 140°C, WHSV$_{PyGas}$ = 4 h^{-1}, P$_T$ = 20 barg, P$_{H2}$ = 5 barg]

Figure 3.222 shows the 1-octene hydrogenation exhibited a similar selectivity profile to that of the reaction performed with PyGas-I as discussed in section 3.2.3.2.2. Octane was the main product during 1-octene hydrogenation, however reasonable amounts of internal octenes were also formed.
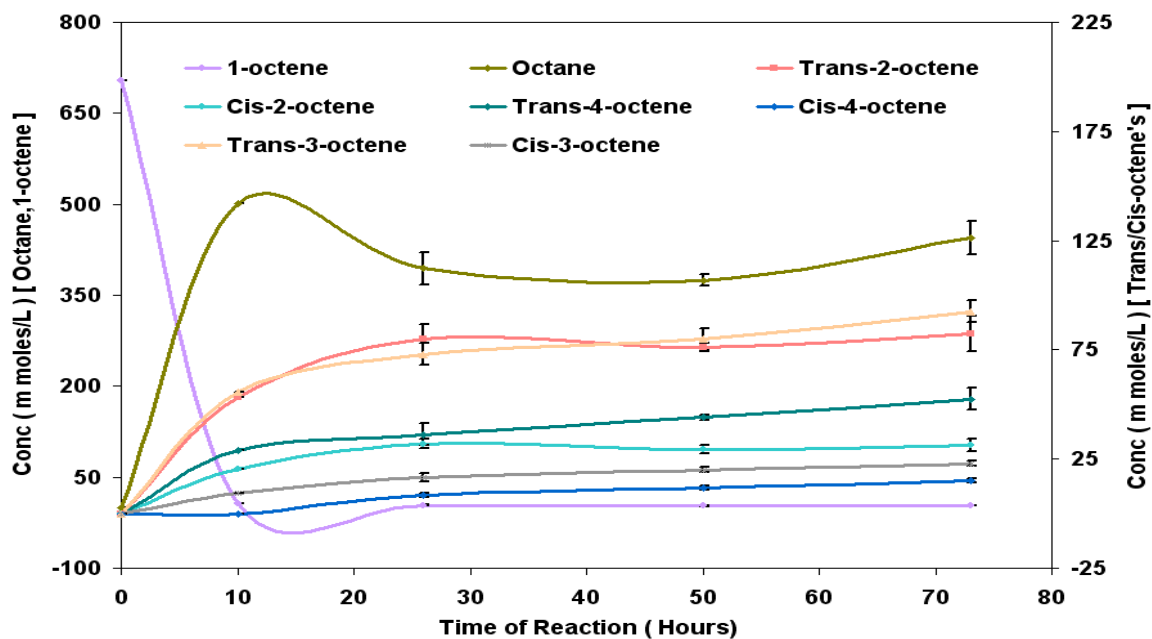
Figure 3.222 Reaction profile of 1-octene Hydrogenation [Reaction conditions: T = 140°C, WHSV_PyGas = 4 h⁻¹, P_T = 20 barg, P_H2 = 5 barg]

Conversion of 1-octene was above 96% throughout the reaction. The yield and selectivity of products are given in Figures 3.223-224.
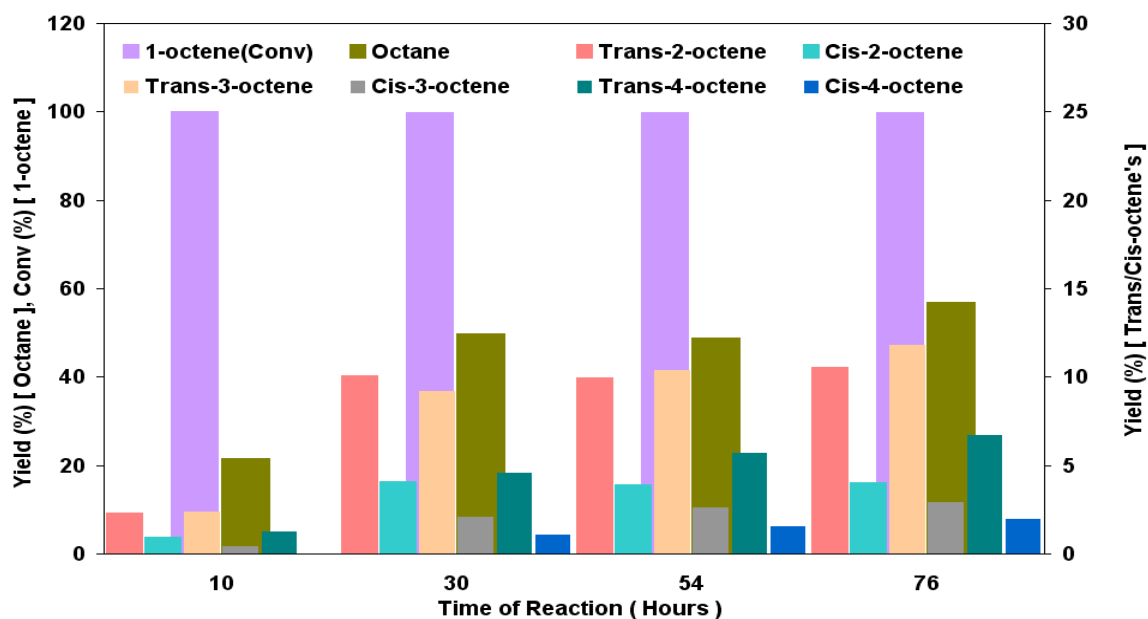
Figure 3.223 Percent yield of 1-octene hydrogenation [Reaction conditions: T = 140°C, WHSV_PyGas = 4 h⁻¹, P_T = 20 barg, P_H2 = 5 barg]
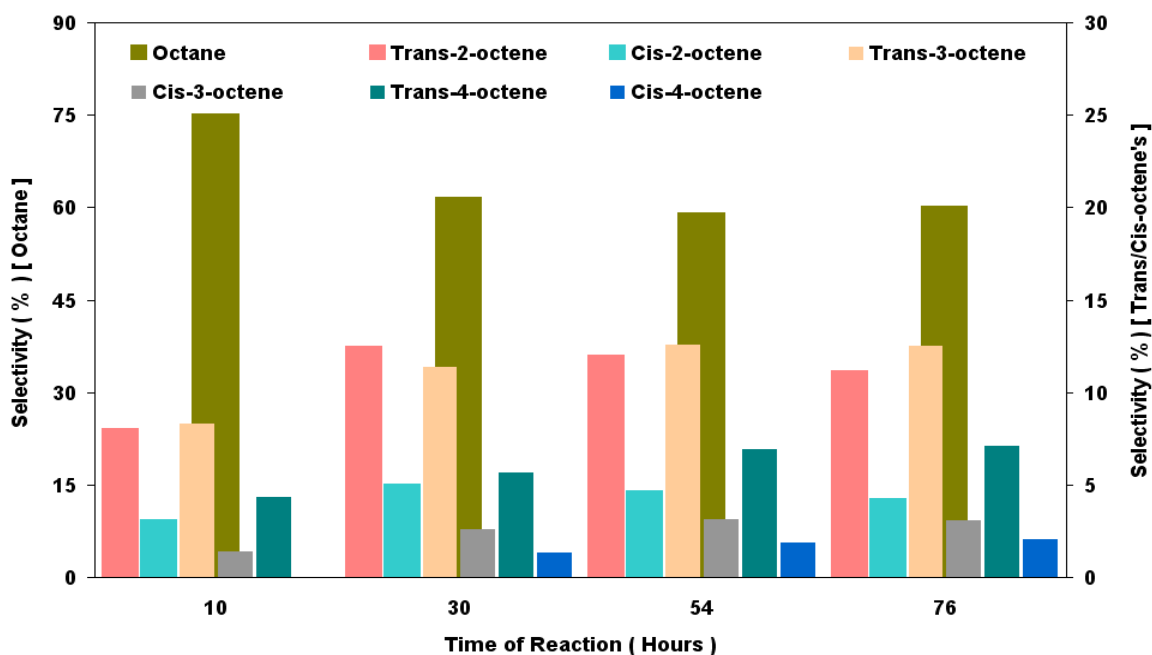
Figure 3.224 Selectivity of octane and internal octenes during 1-octene hydrogenation [Reaction conditions: T = 140°C, WHSV$_{PyGas}$ = 4 h^{-1}, P$_T$ = 20 barg, P$_{H2}$ = 5 barg]

The formation of products during 1-octene can be presented as follows,

Octane >> Trans-2-octene ≈ Trans-3-octene > Trans-4-octene > Cis-2-octene > Cis-3-octene > Cis-4-octene
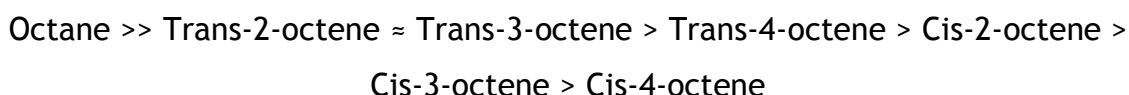
The formation of the trans isomer was found to be higher than its respective cis isomer. The ratios of trans/cis isomers are shown in Table 3.43.

Trans/Cis-2-pentene ratio	Trans/Cis-2-octene ratio	Trans/Cis-3-octene ratio	Trans/Cis-4-octene ratio
75:25	72:28	80:20	80:20

Table 3.43 Ratio of trans/cis internal olefins formation in PyGas hydrogenation [Reaction conditions: T = 140°C, WHSV$_{PyGas}$ = 4 h^{-1}, P$_T$ = 20 barg, P$_{H2}$ = 5 barg]

Figure 3.225 shows that conversion of cyclopentane was 99% in the first 10 hours of the reaction and a slight decrease was observed with time on stream. The minimum conversion was noted about 95%. The yield of cyclopentane was 21% during the first 10 hours of the reaction, which increased to 70% after 30 hours when the reaction obtained steady state.
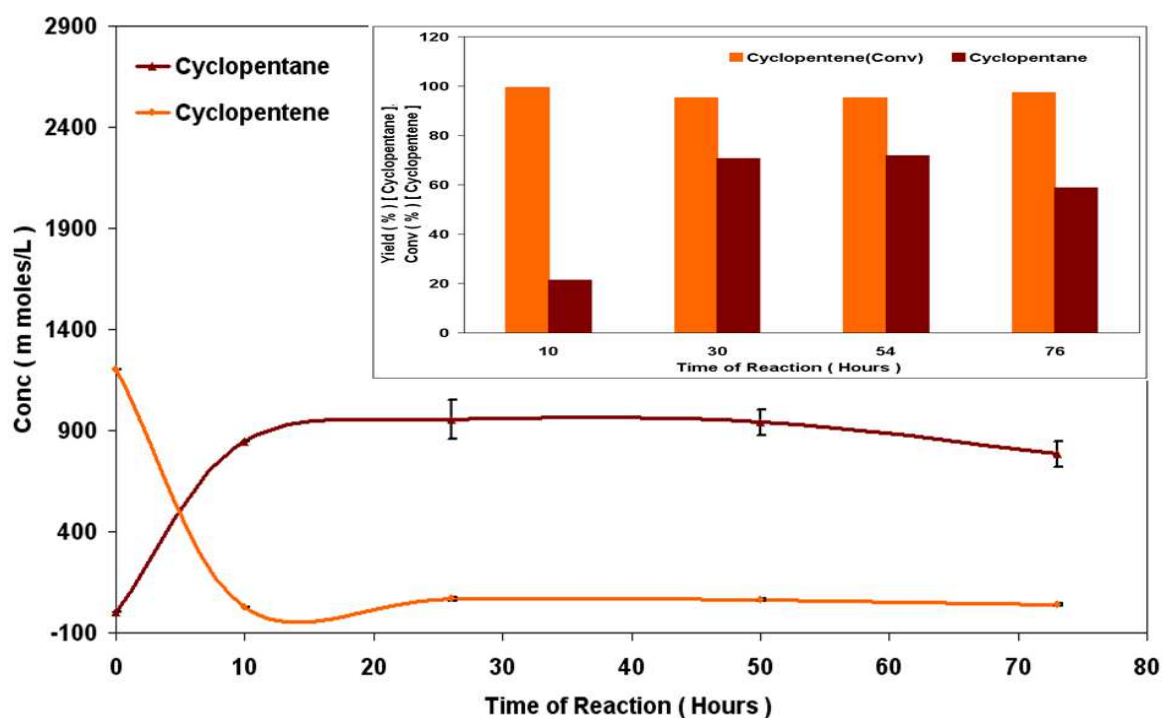
Figure 3.225 Hydrogenation of cyclopentene [Reaction conditions: T = 140°C, WHSV$_{PyGas}$ = 4 h^{-1}, P$_T$ = 20 barg, P$_{H2}$ = 5 barg]

A considerable conversion of toluene was observed during the reaction however no formation of methylcyclohexane was seen as shown in Figure 3.226.
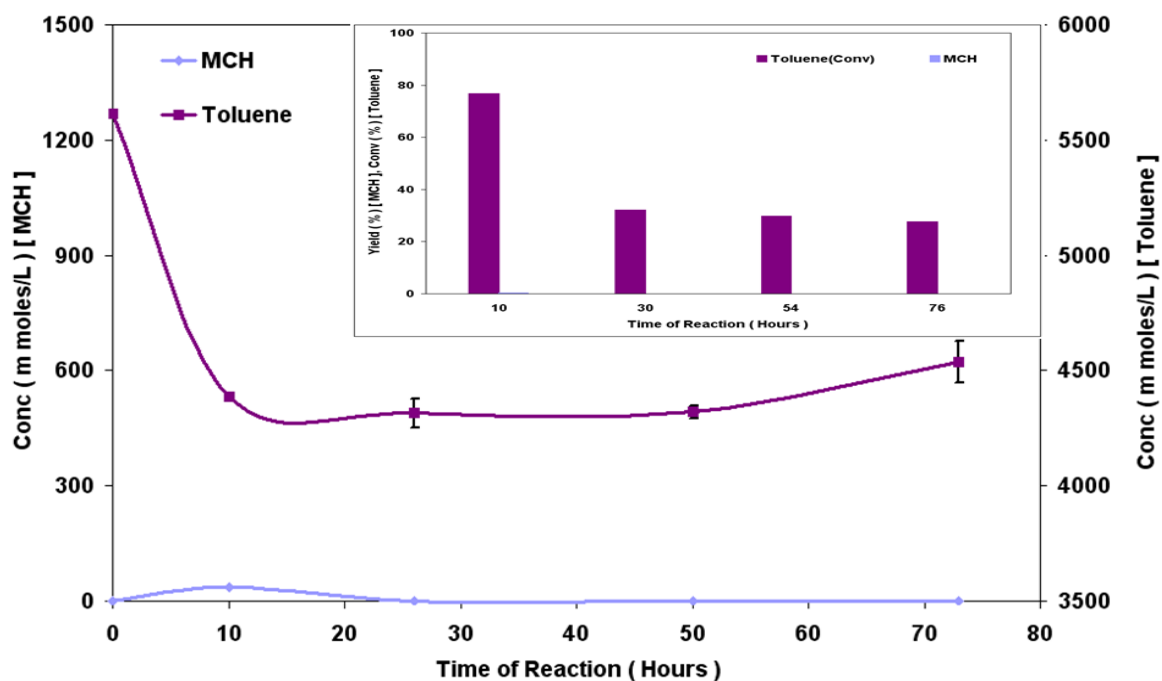
Figure 3.226 Hydrogenation of toluene [Reaction conditions: T = 140°C, WHSV$_{PyGas}$ = 4 h^{-1}, P$_T$ = 20 barg, P$_{H2}$ = 5 barg]

Figure 3.227 shows that conversion of styrene was above 99% throughout the reaction. Ethylbenzene was the principal product during the reaction whilst a

small amount (~0.4%) of ethylcyclohexane was also formed in first 10 hours of reaction. No significant change was observed in the yield of ethylbenzene when compared to the reaction performed with PyGas containing 1-pentene instead of 1,3-pentadiene.
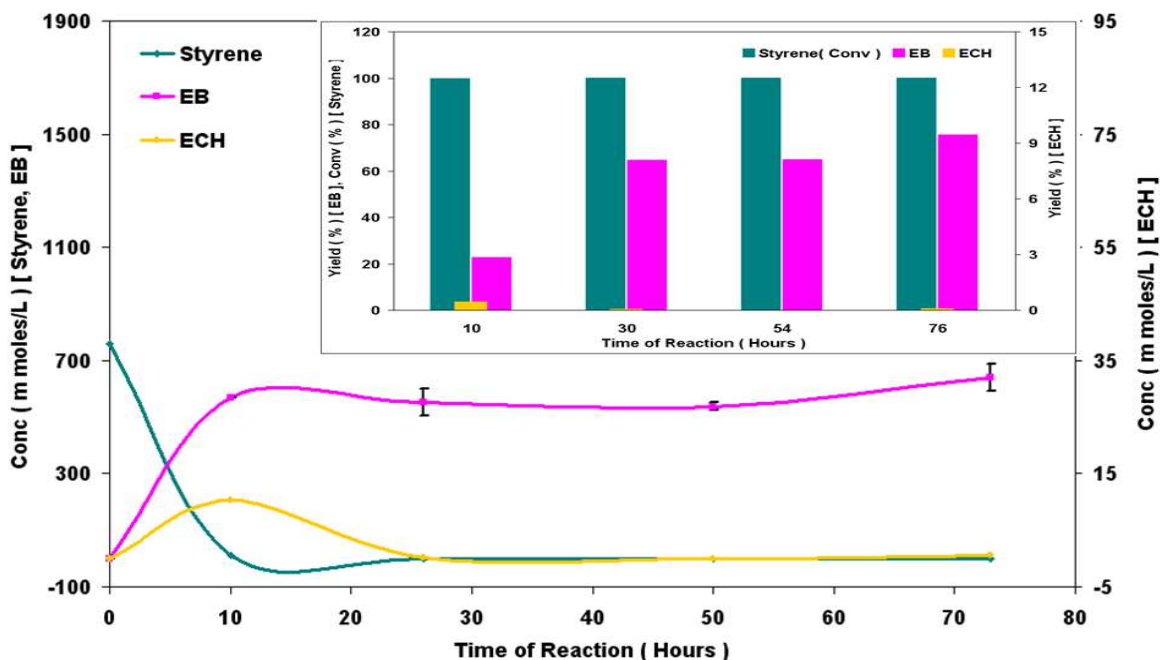
Figure 3.227 Hydrogenation of styrene [Reaction conditions: T = 140°C, WHSV$_{PyGas}$ = 4 h^{-1}, P$_T$ = 20 barg, P$_{H2}$ = 5 barg]

3.2.3.5.1 Post reaction analysis

Post reaction catalyst TPO

A post reaction *in-situ* TPO was carried out and shown in Figure 3.228. The results indicate that a small decrease occurred in the amount of coke deposition when using PyGas-II instead of PyGas-I in the reaction under similar conditions. The olefins are considered one of the main precursors of coke formation during PyGas hydrogenation. Thus, it is believed that the decrease in coke deposition was due to the smaller amount olefins present in PyGas-II compared to PyGas-I.
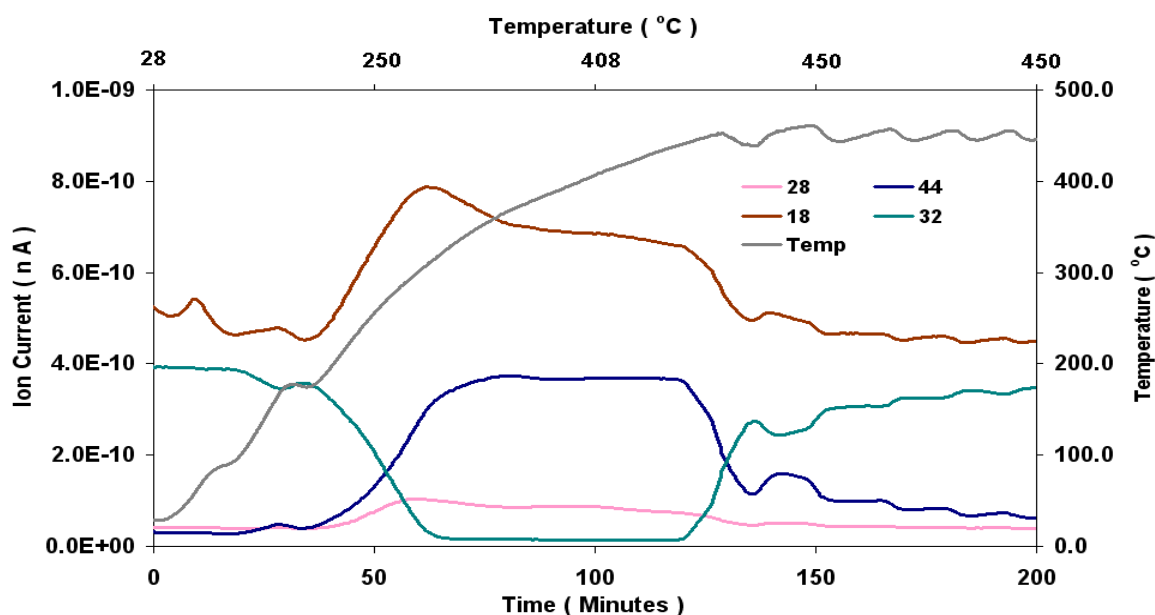
Figure 3.228 Post reaction *in-situ* TPO of Pd/Al$_2$O$_3$ catalyst [Reaction conditions: T = 140°C, WHSV$_{PyGas}$ = 4 h^{-1}, P$_T$ = 20 barg, P$_{H2}$ = 5 barg]

Total oxygen consumption in TPO = 3.02 m moles

BET analysis

The surface area, pore volume and pore diameter of the regenerated catalyst were analysed and the results are presented in Table 3.44.

Catalyst	Surface Area (m^{2}g^{-1})	Pore Volume (cm^{3}g^{-1})	Average Pore diameter (Å)
Pd/Al$_2$O$_3$	99	0.51	208
Pd/Al$_2$O$_3$ (Reduced)	104	0.50	197
Pd/Al$_2$O$_3$ (Regenerated)	105	0.49	191

Table 3.44 BET analysis of Pd/Al$_2$O$_3$ (Regenerated) catalyst [Reaction conditions: T = 140°C, WHSV$_{PyGas}$ = 4 h^{-1}, P$_T$ = 20 barg, P$_{H2}$ = 5 barg]

The BET results indicate the surface area lost due to deposition of coke was recovered during regeneration.

4. Discussion

This chapter consists of three main sections: catalyst characterisation, catalyst activity during PyGas hydrogenation, and catalyst deactivation and regeneration. The catalyst characterisation section includes an explanation of the TPRs of the Ni/Al_2O_3 and Pd/Al_2O_3 catalysts. The PyGas hydrogenation and effect of reaction conditions *i.e.* reaction temperature, hydrogen partial pressure of reaction, total reaction pressure and PyGas feed flow rate ($WHSV_{PyGas}$) on the hydrogenation of PyGas are discussed in the catalyst activity section. Coke deposition is believed to be the main reason for catalyst deactivation during PyGas hydrogenation. The nature and amount of coke deposited, and the regeneration of used catalyst by *in-situ* TPO are discussed in the catalyst deactivation and regeneration section.

4.1 Catalyst characterisation

4.1.1 Reduction of Ni/Al$_2$O$_3$ catalyst

Figure 3.1 shows that the main weight loss, about 3.7%, of the nickel catalyst occurred in a temperature range between $300^{\circ}C$ and $500^{\circ}C$. The mass spectrometry data showed the consumption of H_2 gas and evolution of H_2O suggesting the occurrence of nickel oxide reduction, which is in close agreement with literature [104-107];

$$NiO + H_2 \longrightarrow Ni + H_2O$$
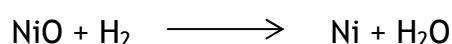
The theoretical weight loss of the catalyst associated with the reduction of NiO to Ni was determined to be 3.4%, confirming that the main weight loss between $300^{\circ}C$ and $500^{\circ}C$ was due to NiO reduction. However, a small weight loss of the catalyst and hydrogen consumption was also observed at a higher temperature in the TPR analysis, probably due to the reduction of $NiAl_2O_4$ which requires a higher reduction temperature than NiO. This is found to be similar to previous studies, which revealed that the reduction of $NiAl_2O_4$ in the alumina supported nickel catalyst at high temperature [104, 108, 109].

The *in-situ* XRD of the alumina supported nickel catalyst is shown in Figure 3.3. The broad peaks of alumina, at $2\theta = 37, 46, 67$, indicate poor crystallinity and the presence of amorphous type alumina. The peaks that occurred at $2\theta = 37$,

43, 63 are assigned to the NiO phase and the peaks observed at 2θ = 52, 76 to Ni metal [103, 110-113]. An increase was seen in the intensity of the peaks at 2θ = 52, 76 with an increase in temperature in the hot-stage XRD analysis indicating that a larger amount of NiO was reduced to Ni metal at a higher temperature under a flow of hydrogen.

4.1.2 Reduction of Pd/Al$_2$O$_3$ catalyst

The TPR profile of the palladium catalyst, shown in Figure 3.2, illustrates that the main weight loss of about 2.2% occurred between room temperature and 200°C. The mass spectrometry data showed an uptake of H$_2$ and an evolution of H$_2$O in this temperature range. This indicates that the PdO was reduced to Pd in this temperature range under a flow of hydrogen, which is in close agreement to that cited in the literature [114-116];

$$PdO + H_2 \longrightarrow Pd + H_2O$$
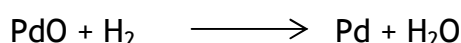
The theoretical weight loss of the catalyst associated with the reduction of PdO to Pd was determined to be about 0.13%. However, a large weight loss was observed for palladium catalyst in the TPR analysis because of considerable amounts of physisorbed species, like H$_2$O, present on the surface of catalyst.

4.2 Catalyst activity

The PyGas hydrogenation over Ni/Al$_2$O$_3$ and Pd/Al$_2$O$_3$ catalysts are discussed respectively in the following sections.

4.2.1 PyGas hydrogenation over Ni/Al$_2$O$_3$ catalyst

The effects of the following reaction parameters during the PyGas hydrogenation over the Ni/Al$_2$O$_3$ catalyst are discussed in this section.

   a) Effect of reaction temperature

   b) Effect of hydrogen partial pressure

   c) Effect of total reaction pressure

   d) Effect of PyGas feed flow rate (WHSV$_{PyGas}$)

The kinetic analysis and reaction orders of hydrogenation/isomerisation of the PyGas components were also investigated and are discussed in section 4.2.1.5.

4.2.1.1 Effect of reaction temperature on PyGas hydrogenation

The effect of reaction temperature on the hydrogenation of PyGas was investigated with reaction conditions [T = 140-200°C, P$_{H2}$ = 20 barg, WHSV$_{PyGas}$ = 4 h^{-1}]. The olefins and cycloolefins were completely hydrogenated to saturated paraffins along with the formation of trace amounts of internal olefins. The reaction conditions were favourable for hydrogenation [46, 117] and therefore complete hydrogenation of the olefinic fraction of PyGas was practical. Moreover, a considerable amount of aromatic hydrogenation was observed in our system during PyGas hydrogenation and the rate of aromatic hydrogenation was found to be constant in the temperature range from 140°C to 200°C. The maximum rate of hydrogenation of monoaromatic and substituted monoaromatic compounds, e.g. benzene and toluene, over a supported nickel catalyst has been quoted at 150°C [118], 185°C [72] and 200°C [119] in the literature. However, many researchers have reported a range of temperatures for maximum rate rather than one specific temperature. For example, the maximum rate of toluene hydrogenation was observed in the temperature range of 170°C to 185°C [66, 67] and from 157°C to 187°C [120], whereas the maximum rate of hydrogenation of benzene has been reported to be between 135°C and 180°C [77].

The yields of ethylbenzene and ethylcyclohexane decreased with an increase in the reaction temperature, although the conversion of styrene remained constant at ~100%. This is due to a higher contribution from styrene to coke and gum formation at higher temperatures, which is in close agreement with a previous study [2]. The effect of reaction temperature on the conversions and yields of the different components of PyGas are summarised in Figures 4.1 and 4.2.
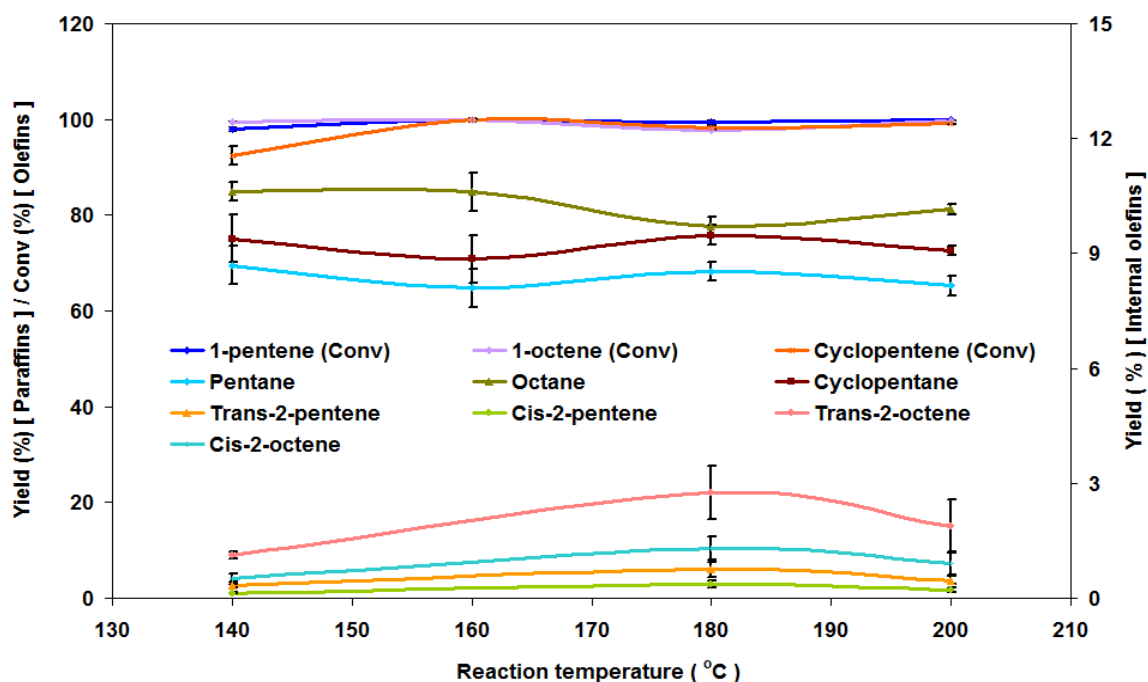
Figure 4.1 Effect of reaction temperature on the hydrogenation of olefinic species of PyGas [T = 140-200°C, P_{H2} = 20 barg, $WHSV_{PyGas}$ = 4 h^{-1}], (Average conversion and average yield at steady state)
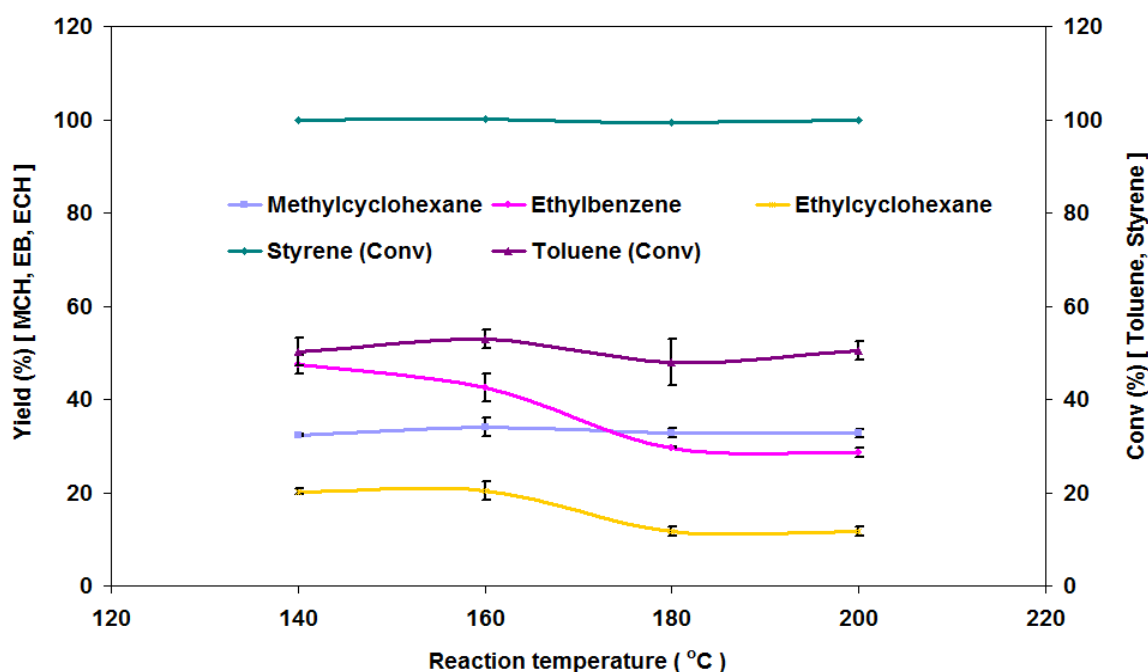
Figure 4.2 Effect of reaction temperature on the hydrogenation of aromatic species of PyGas [T = 140-200°C, P_{H2} = 20 barg, $WHSV_{PyGas}$ = 4 h^{-1}], (Average conversion and average yield at steady state)

The blank reactions performed on both the catalyst support (Al_2O_3) and the packing material (boiling chips) showed that practically no hydrogenation of PyGas took place. Hence, the hydrogenation of the unsaturated hydrocarbons occurred on the metal and no hydrogenation reaction took place over the catalyst support, which is in close agreement with the literature [47]. The

unsaturated hydrocarbons have π bonds, which can easily adsorb onto the metal surface of the catalyst and form π-complexes. These can subsequently make σ-bonds with the metal, which actively take part in the hydrogenation reaction. The olefin hydrogenation reaction is most likely to follow the Horiuti-Polanyi mechanism [46, 57], as explained in Section 1.4.1. The hydrogenation of aromatic hydrocarbons is most likely to follow stepwise hydrogenation, as shown in Figure 4.3 [63, 66-68, 70-74, 121-123].

$$H_{2(g)} + 2\,M \rightleftharpoons 2\,H\!-\!M$$

$$A_{(g)} + M \rightleftharpoons A\!-\!M$$

$$A\!-\!M + H\!-\!M \longrightarrow AH\!-\!M + M$$

$$AH\!-\!M + H\!-\!M \rightleftharpoons AH_2\!-\!M + M$$

$$AH_2\!-\!M + 4\,H\!-\!M \rightleftharpoons AH_6\!-\!M + 4\,M$$

$$AH_6\!-\!M \rightleftharpoons AH_{6\,(g)} + M$$
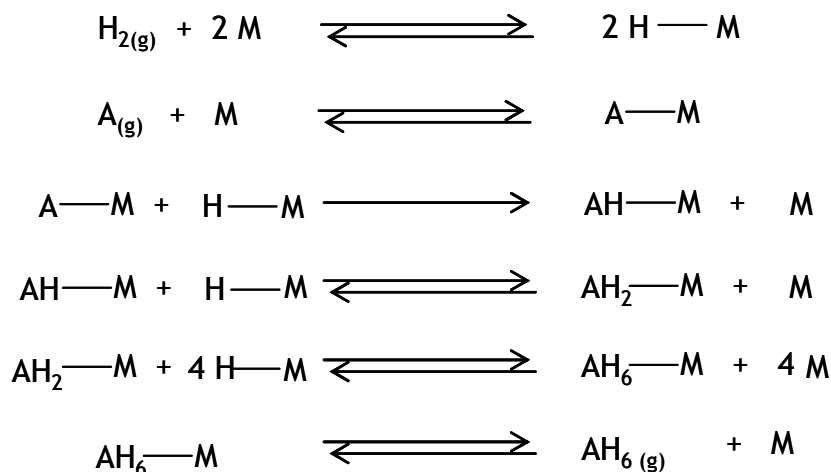
Figure 4.3 Mechanism of catalytic hydrogenation of aromatics over group VIII metals catalyst [Where M is metal site, A represent aromatic compound]

However, only completely hydrogenated products of the aromatic compounds were observed and no intermediate species were detected throughout the entire study, because the heat of hydrogenation of benzene to cyclohexane is 206 kJ mol^{-1}, while the heat of hydrogenation of cyclohexadiene to cyclohexane is 232 kJ mol^{-1}. Therefore the formation of cyclohexadiene is unlikely during the hydrogenation of benzene. The heat of hydrogenation of cyclohexene is 120 kJ mol^{-1}. So, cyclohexene formation during benzene hydrogenation is possible. However, due to its high reactivity, it readily hydrogenates to cyclohexane [46].

4.2.1.2 Effect of hydrogen partial pressure on PyGas hydrogenation

Hydrogen partial pressure has a significant effect on PyGas hydrogenation as well as the product distribution and is an important parameter for achieving optimum yields and selectivities of the products. The hydrogenation of PyGas increased with an increase in hydrogen partial pressure. However, the selectivity of PyGas hydrogenation towards a high octane gasoline mixture decreased at very high hydrogen partial pressures. Therefore, optimised hydrogen partial

pressures are required to obtain desired products and to maintain economical viability.

In this study, a P_{H2} value of 5 barg with P_T = 20 barg was found to be appropriate for the selective hydrogenation of PyGas to a high octane mixture. By further decreasing the hydrogen partial pressure, the process became more selective towards internal olefin formation but the overall hydrogenation of PyGas was significantly decreased and fast catalyst deactivation took place, due to high amounts of coke deposition on the catalyst. Consequently, a very low hydrogen partial pressure was found to not be suitable for the selective hydrogenation of PyGas.

The hydrogenation of aromatics increased with an increase in hydrogen partial pressure. Therefore, a high partial pressure is preferable if the hydrogenation of aromatic components is desired. Table 4.1 shows a summary of the product distribution, yield and conversion of PyGas hydrogenation at different hydrogen partial pressures.

Conversion/Yield	Hydrogen Partial Pressure (barg) [P_T = 20 barg]			
	P_{H2} = 1 barg	P_{H2} = 5 barg	P_{H2} = 10 barg	P_{H2} = 20 barg
Conversion (%)				
1-pentene	73.5	90.6	99.5	97.9
Yield (%)				
Pentane	6.6	47.9	78.1	69.4
Trans-2-pentene	15.0	7.4	-	0.3
Cis-2-pentene	9.7	3.0	-	0.1
Conversion (%)				
1-octene	69.6	98.3	100	99.5
Yield (%)				
Octane	8.0	52.2	81.7	84.8
Trans-2-octene	15.1	11.2	-	1.1
Cis-2-octene	9.0	5.4	-	0.5
Trans-3-octene	1.6		-	-
Cis -3-octene	Trace	7.7	-	-
Cis-4-octene	Trace		-	-
Trans-4-octene	Trace	2.3	-	-
Conversion (%)				
Cyclopentene	57.5	93.8	100	92.3
Yield (%)				
Cyclopentane	5.9	61.5	83.0	75.0
Conversion (%)				
Toluene	23.4	24.1	27.5	50.1
Yield (%)				
Methylcyclohexane	Trace	0.1	8.8	32.3
Conversion (%)				
Styrene	85.6	99.9	99.9	99.9
Yield (%)				
Ethylbenzene	33.8	60.8	51.7	47.3
Ethylcyclohexane	Trace	Trace	4.1	20.2

Table 4.1 Effect of hydrogen partial pressure on PyGas hydrogenation [P_{H2} = 1-20 barg, P_T = 20 barg, T = 140°C, $WHSV_{PyGas}$ = 4 h^{-1}], (Average conversion and average yield at steady state)

The hydrogenation of olefins most likely follows the Horiuti-Polanyi mechanism, as explained in Section 1.4.1. Complete hydrogenation of olefins gives saturated paraffins; however selective hydrogenation and isomerisation of olefins to internal olefins takes place when using suitable reaction conditions. A greater extent of olefin isomerisation takes place when small amounts of adsorbed

hydrogen are present on the surface of the catalyst, while their conversion to saturated paraffins increases when high amounts of hydrogen are available on surface of the catalyst [47].

Therefore the 1-pentene hydrogenated to pentane, at high hydrogen partial pressure, while isomerisation of 1-pentene to 2-pentene increased with a decrease in hydrogen partial pressure during the reaction. Trans-2-pentene was observed in quantities of about twice the amount of cis-2-pentene (trans/cis ratio ~ 66:33) during isomerisation of 1-pentene to 2-pentene. The higher amount of the trans-isomer is due to greater thermodynamic stability of the trans-isomer [46]. Cis-2-pentene isomer can also preferentially adsorbs onto the surface of the catalyst compared to the trans-isomer, which then converts to trans-2-pentene or hydrogenates to pentane [58]. Therefore the high trans/cis ratio was an expected result.

Similarly, the hydrogenation of 1-octene to octane took place when high hydrogen partial pressures were used during the PyGas hydrogenation, whilst 1-octene isomerisation to internal octenes was achieved by using low hydrogen partial pressures. The extent of bond migration during 1-octene hydrogenation is highly dependent upon the reaction conditions. The π-bond of 1-octene first adsorbs onto the catalyst and makes π-complex with catalyst, then consequently makes di σ-bonds with the metal [46, 117]. The product formation in the reaction is dependent on the hydrogen addition and abstraction, as shown in Figure 4.4.
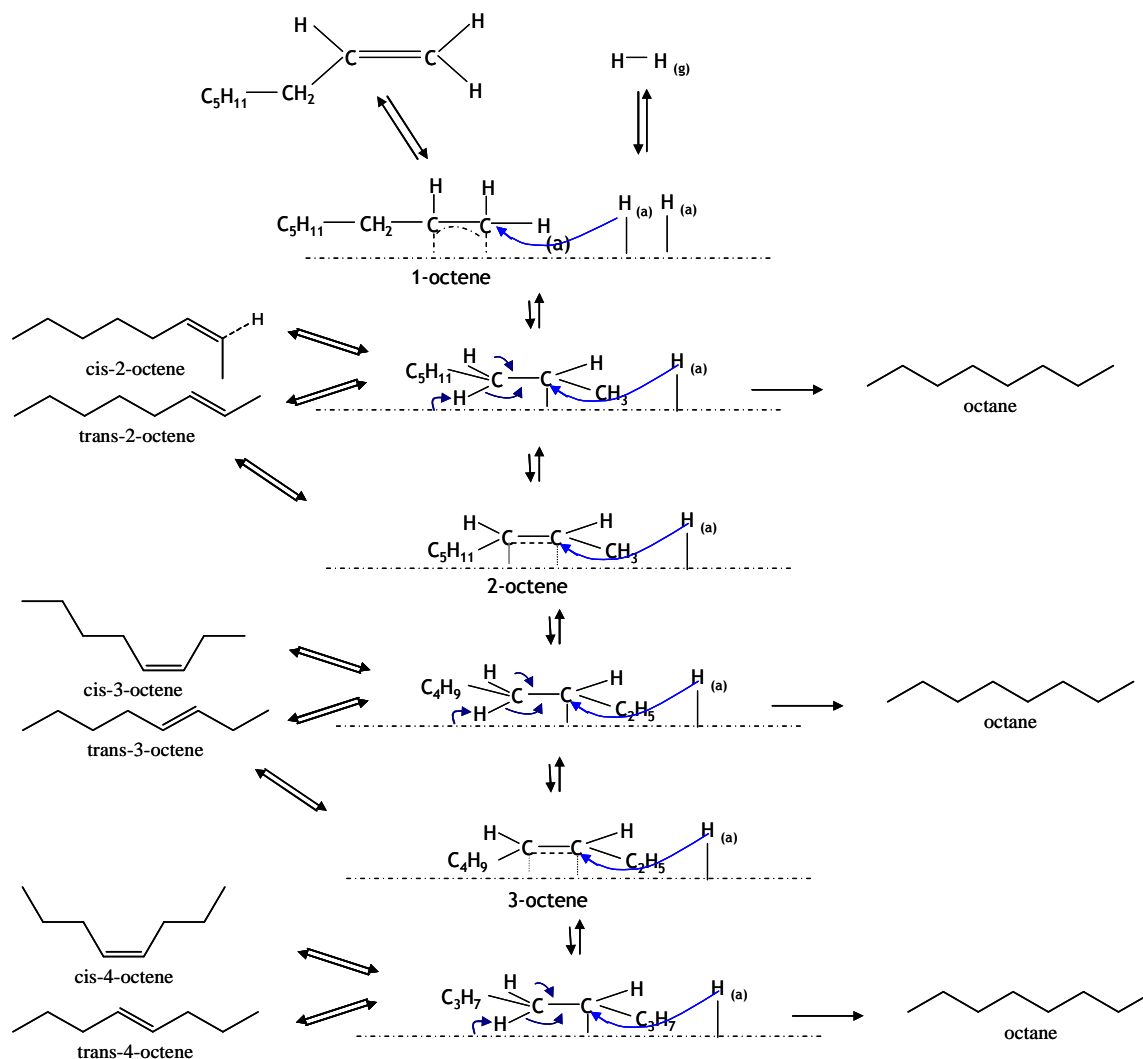
Figure 4.4 hydrogenation/ isomerisation of 1-octene during PyGas hydrogenation

The addition of hydrogen to both σ-bonded carbons produces octane. While the addition of hydrogen to one carbon makes half hydrogenated octene, which then further hydrogenates to octane with the addition of another hydrogen atom or isomerises to form 2-octene by hydrogen-abstraction from the opposite side [46, 117]. The isomerisation of 1-octene is favourable when a small amount of hydrogen is present on the surface on the catalyst. The formation of trans and cis-2-octene isomers during 1-octene isomerisation are mainly dependent on the adsorption mode of the half hydrogenated 1-octene intermediate and the mode of hydrogen addition and abstraction.

A higher amount of trans-2-octene formation was observed in our system due to a greater thermodynamic stability of the trans-isomer. The trans/cis ratio was about 66:33, which was similar to the trans/cis ratio observed for 2-pentene in the PyGas hydrogenation. The 2-octene either remained adsorbed or became

reabsorbed onto the surface of catalyst and was further isomerised to 3-octene and 4-octene, in a similar manner to that of 1-octene isomerisation, or hydrogenated to octane as shown in Figure 4.4. The high amount of trans isomers to the respective cis isomers was also observed in the formation of 3-octene and 4-octene. The trans/cis ratio for 3-octene and 4-octene was about 70:30.

Stepwise bond migration of 1-octene to internal octenes took place and can be presented as;

1-octene ⟶ 2-octene ⟶ 3-octene ⟶ 4-octene
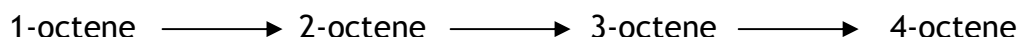
The rates of formation of internal octenes during PyGas were observed in the following order;

2-octene > 3-octene > 4-octene

Low hydrogen partial pressure is favourable for isomerisation of olefin. Therefore, an increase was observed in the formation of internal octenes with a decrease in the hydrogen partial pressure down to 5 barg during PyGas hydrogenation. Moreover, a greater extent of bond migration was also observed with decrease in hydrogen partial pressure and subsequently the selectivity towards 3-octene and 4-octene was increased.

However, the isomerisation and bond migration involves hydrogen addition and abstraction steps. Therefore the presence of adsorbed hydrogen on the catalyst is essential for the isomerisation reaction and bond migration could decrease when a very small amount of hydrogen is present on the surface of catalyst. Consequently, no significant amount of 3-octene or 4-octene formation was observed during PyGas hydrogenation when the hydrogen partial pressure was further decreased to 1 barg from 5 barg.

Trans isomers are more stable and therefore cis-trans isomerisations also take place during the reaction and are likely to follow the Horiuti-Polanyi mechanism, as shown in Figure 4.5.
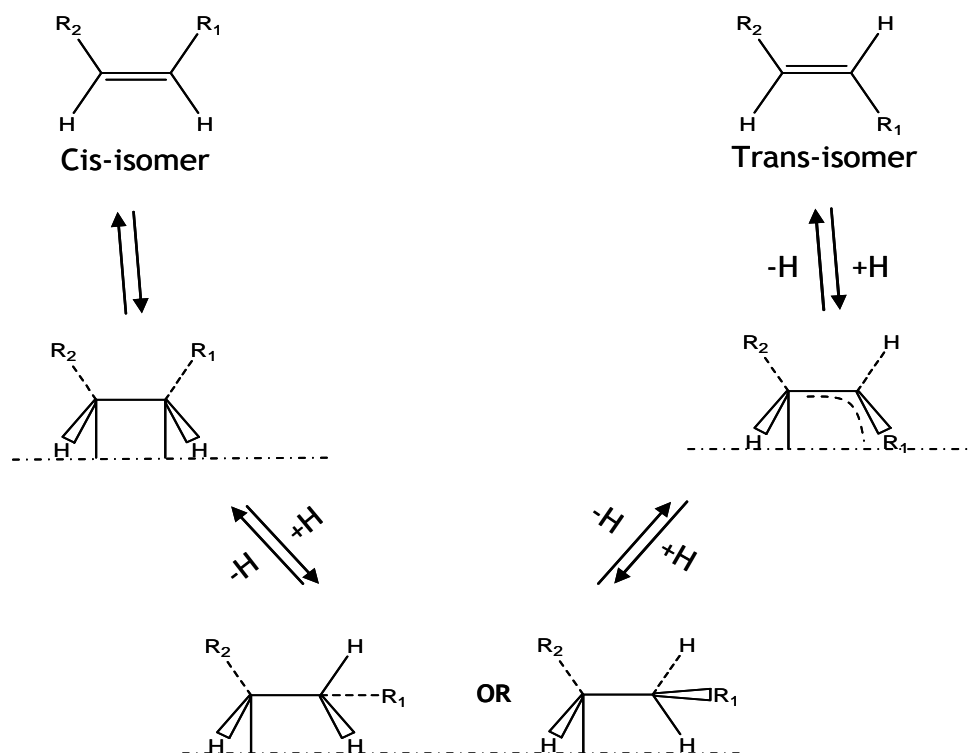
Figure 4.5 Cis-trans isomerisation of olefins

The cis-trans transformation involves adsorption, an intermediate surface reaction and desorption. Therefore, direct cis-trans transformations are not expected without adsorption of the isomer onto the catalyst surface. The cis isomer can preferentially adsorb onto the surface of the catalyst than the respective trans-isomer, due to lower steric hindrance, then converts to trans-isomer, or further bond migration or hydrogenation could take place [58, 124]. Therefore, a greater trans to cis ratio was an expected result during olefin isomerisation.

Hydrogenation of the PyGas containing 1,3-pentadiene instead of 1-pentene (PyGas-II) was also performed to investigate the behaviour of diolefins present in PyGas. The hydrogenation of diolefins with terminal double bonds like, 1,4-pentadiene or 1,3-butadiene is well known. These diolefins selectively hydrogenate to 1-pentene and 1-butene respectively, which can be further isomerised to trans/cis-2-olefins or hydrogenated to respective paraffins, depending on the reaction conditions [46, 59, 125, 126]. However, the selective hydrogenation of 1,3-pentadiene is more complex because different conformations and hydrogen additions are possible, as shown in Figure 4.6.
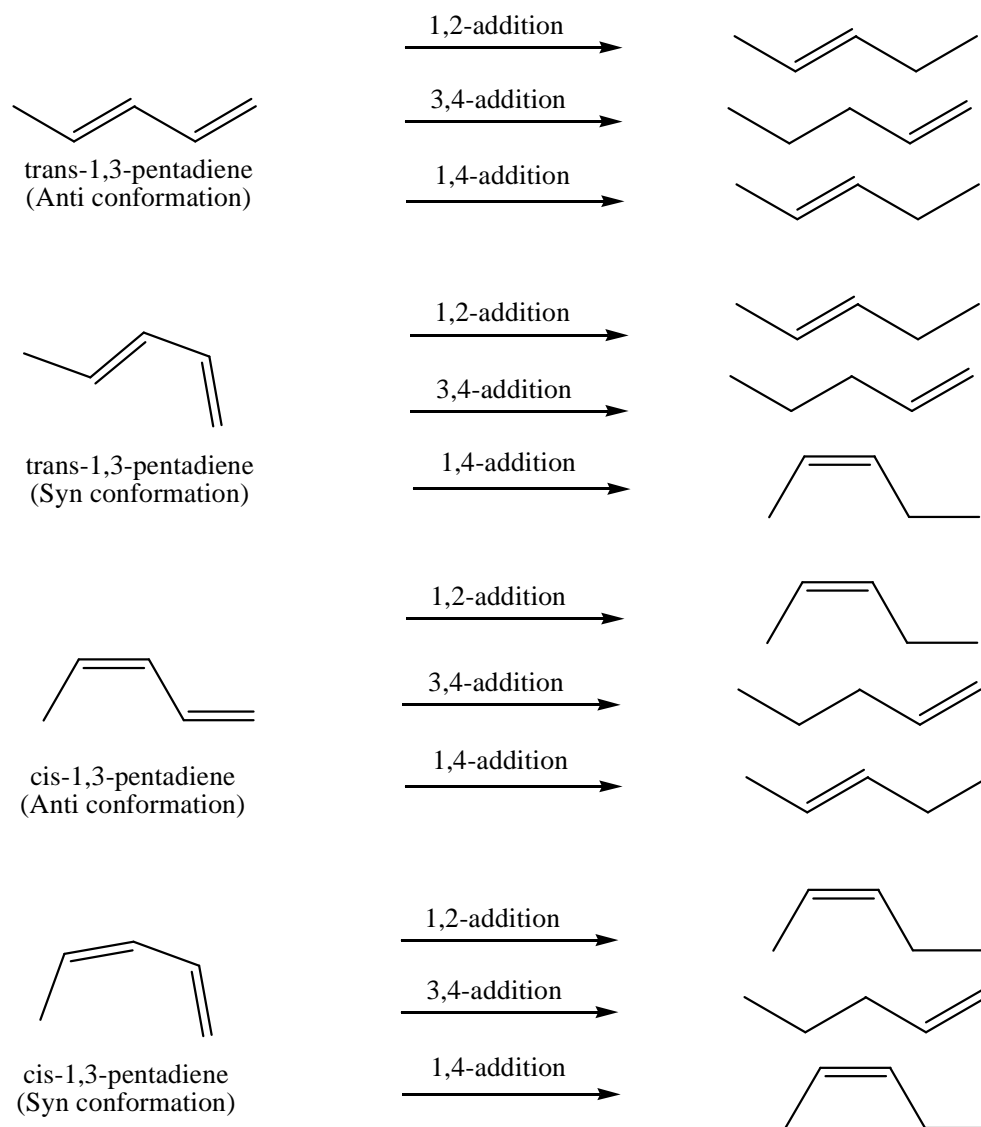
Figure 4.6 Possible pathways of 1,3-pentadiene hydrogenation to pentene

This shows that the product distribution depends on the adsorbed conformation and the mode of hydrogen addition. The hydrogenation of the anti conformers can produce a higher ratio of trans-2-pentene to cis-2-pentene, while the syn conformers produce a higher ratio of cis-2-pentene to trans-2-pentene. The anti conformers are more stable than syn conformers, and consequently there is a higher amount of 1,3-pentadiene present in the form of anti conformers [46]. The mode of hydrogen addition to the adsorbed species has an important role in determining product distribution.

Opera *et al.* [127] observed that trans-2-pentene was a solo intermediate during the selective hydrogenation of 1,3-pentadiene. They suggested that 1,2-hydrogen addition took place most readily and therefore terminal double bond hydrogenation occurred in advance of the internal double bond. No formation of

cis-2-pentene was observed in their study and therefore it was revealed that cis-1,3-pentadiene present in the 1,3-pentadiene mixture, was first isomerised to trans-1,3-pentadiene and then 1,2-hydrogen addition took place. However, other catalytic literature studies [46, 126, 128] observed the formation of 1-pentene, trans-2-pentene and cis-2-pentene intermediates during the hydrogenation of 1,3-pentadiene. This suggests that the 1,3-pentadiene adsorbs in the various conformer orientations and different modes of hydrogen addition take place which produces a wide range of intermediate products. These studies also reported that 3,4-hydrogen addition is preferential because the methyl group increases the reactivity of the adjacent double bond to overcome any negative bias through the increase in steric crowding.

The selectivity of 1-pentene, trans-2-pentene, cis-2-pentene and pentane during the 1,3-pentadiene hydrogenation in our system was observed to be 1%, 21%, 7% and 69% respectively. This suggests that most likely adsorption of the various types of 1,3-pentadiene conformers took place and different modes of hydrogen addition occurred which produced these wide range of pentene isomers. The 1-pentene and 2-pentene then further hydrogenated and produced high amount of pentane. A higher amount of trans-2-pentene formation than cis-2-pentene was formed during the 1,3-pentadiene hydrogenation in our system and the 2-pentene trans : cis ratio was found to be 75:25. The high trans to cis ratio suggests that higher amounts of 1,3-pentadiene were present in the anti conformers and this produces a higher amount of trans isomers than the cis isomer, which is in close agreement with the literature [46].

The hydrogenation of styrene was also highly dependent on the reaction conditions. Ethylbenzene was the sole product during hydrogenation of styrene when the hydrogen partial pressure was increased up to 5 barg and the formation of ethylcyclohexane took place with a further increase in hydrogen partial pressure. This suggests that styrene was first hydrogenated to ethylbenzene, which could then be further hydrogenated to ethylcyclohexane by increasing the hydrogen partial pressure, and similar behaviour has been reported in a previous study [40]. Therefore, the styrene hydrogenation reaction can be presented as;

Styrene   Ethylbenzene Ethylcyclohexane
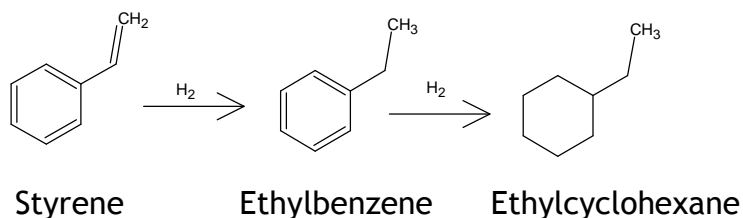
4.2.1.3 Effect of total reaction pressure on PyGas hydrogenation

A decrease was observed in the hydrogenation of PyGas with a decrease in the total reaction pressure from 20 barg to 10 barg, using a 50% hydrogen gas mixture. However, the product distribution remained virtually the same, as the olefins were fully hydrogenated to saturated paraffins with no significant formation of the internal olefins. Whereas reasonable amounts of internal olefins formation were observed by using a 25% hydrogen gas mixture at 20 barg pressure. This suggests that using a diluted hydrogen gas mixture at higher total reaction pressure is more favourable for selective hydrogenation of PyGas than carrying out the reaction at a lower total reaction pressure. Table 4.2 shows a summary of the product distribution, yield and conversion of PyGas hydrogenation at different total reaction pressures. The feed flow rate of PyGas was kept constant for all the reactions.

Conversion/Yield	50% hydrogen gas mixture		25% hydrogen gas
	P_T = 20 barg	P_T = 10 barg	P_T = 20 barg
Conversion (%) 1-pentene	99.5	99.9	90.6
Yield (%) Pentane	78.1	56.9	47.9
Trans-2-pentene	-	0.6	7.4
Cis-2-pentene	-	0.2	3.0
Conversion (%) 1-octene	100	99.4	98.3
Yield (%) Octane	81.7	87.5	52.2
Trans-2-octene	-	3.1	11.2
Cis-2-octene	-	1.5	5.4
Trans-3-octene	-	1.5	
Cis -3-octene	-	0.4	7.7
Cis-4-octene	-	0.1	
Trans-4-octene	-	0.5	2.3
Conversion (%) Cyclopentene	100	99.7	93.8
Yield (%) Cyclopentane	83.0	71.4	61.5
Conversion (%) Toluene	27.5	30.2	24.1
Yield (%) Methylcyclohexane	8.8	5.0	0.1
Conversion (%) Styrene	99.9	99.9	99.9
Yield (%) Ethylbenzene	51.7	58.8	60.8
Ethylcyclohexane	4.1	4.3	Trace

Table 4.2 Effect of total reaction pressure on PyGas hydrogenation [P_T = 10-20 barg, T = 140°C, WHSV$_{PyGas}$ = 4 h^{-1}], (Average conversion and average yield at steady state)

4.2.1.4 Effect of PyGas feed flow rate (WHSV$_{PyGas}$) on PyGas hydrogenation

The hydrogenation of PyGas decreased with an increase in WHSV$_{PyGas}$ from 4 h^{-1} to 8 h^{-1} with the other reaction conditions kept constant [P_T = 20 barg, P_{H2} = 5 barg, T = 140°C]. The concentration of reactants increased on the surface of

catalyst with an increase in PyGas feed from $WHSV_{PyGas}$ 4 h^{-1} to 8 h^{-1}. Subsequently the numbers of reactants were increased per active site. The H_2/PyGas molar ratio in the feed was also decreased from 5 to 2.5 with an increase in WHSV of PyGas from 4 to 8 h^{-1}. Consequently, a decrease occurred in the hydrogenation of PyGas and an increase took place in the isomerisation of olefins to internal olefins with the increase in WHSV of PyGas. Competitive hydrogenation was observed between the reactants. The hydrogenation of 1-pentene and 1-octene decreased during PyGas hydrogenation with an increase in WHSV of PyGas from 4 h^{-1} to 8 h^{-1}. Moreover, small amounts of 3-octene and 4-octene were observed which suggests that a decrease in the extent of bond migration also took place with increase in PyGas feed flow rate. Similarly, cyclopentene hydrogenation was also considerably decreased. However, no substantial decrease was observed in the hydrogenation of styrene to ethylbenzene because the styrene adsorbed more strongly onto the catalyst than the olefins. This shows that the hydrogenation of both olefins and cycloolefins was depressed by the stronger adsorption of styrene during PyGas hydrogenation with an increase in feed flow rate, similar behaviour has been reported in previous studies [40, 82, 83, 117].

The effect of PyGas feed flow rate ($WHSV_{PyGas}$ 4-8 h^{-1}) on the hydrogenation of PyGas was also investigated at a high hydrogen partial pressure (10 barg) using a 50% hydrogen gas mixture. The H_2/PyGas molar ratio in the feed decreased from 10 to 5 with an increase in WHSV of PyGas from 4 h^{-1} to 8 h^{-1}. This time the hydrogenation of PyGas also decreased and an increase took place in the isomerisation of olefins to internal olefins with an increase in the WHSV of PyGas from 4 h^{-1} to 8 h^{-1}. Accordingly, a similar effect was observed with an increase in $WHSV_{PyGas}$ when compared to reactions performed using a 25% hydrogen gas mixture. The hydrogenation of aromatic species was considerably suppressed by increasing the WHSV of PyGas, which illustrates that the competitive adsorption of aromatics and olefins took place on the same active site on the surface of the catalyst, which is in close agreement with literature [41].

The hydrogenation of PyGas with a $WHSV_{PyGas}$ of 8 h^{-1} when using a 50% hydrogenation gas mixture was found to be comparable to the reaction carried out at $WHSV_{PyGas}$ 4 h^{-1} using a 25% hydrogen gas mixture. This shows that the

decrease in PyGas hydrogenation with the increase in $WHSV_{PyGas}$ can be restored by increasing the hydrogen partial pressure.

The hydrogenation of PyGas was also performed at $WHSV_{PyGas}$ 8 h^{-1} using a 25% hydrogen gas mixture and keeping the feed flow rate of PyGas similar to the reaction carried out at $WHSV_{PyGas}$ of 4 h^{-1} and decreasing the amount of catalyst from 0.5 g to 0.25 g. Thus, the H_2/PyGas molar ratio in the feed and other reaction conditions remained the same, while the $WHSV_{PyGas}$ increased from 4 h^{-1} to 8 h^{-1} with the decrease in catalyst weight from 0.5 g to 0.25 g. Therefore in Table 4.3 the 0.25 g catalyst sample with a $WHSV_{PyGas}$ of 8 h^{-1} can be considered as the top half of the catalyst bed of the 0.5 g sample with a $WHSV_{PyGas}$ of 4 h^{-1}. No significant change was observed in the hydrogenation of PyGas when compared to the reaction performed at $WHSV_{PyGas}$ 4 h^{-1}. Whereas a considerable decrease took place in the hydrogenation of PyGas when the reaction was carried out at WHSV 8 h^{-1} by increasing the feed flow rate of PyGas. This suggests that the molar ratio of H_2/PyGas in the feed is also a very important factor in the hydrogenation of PyGas and a decrease in PyGas hydrogenation takes place when the feed ratio of H_2/PyGas decreases in the reaction. The results of PyGas hydrogenation at various $WHSV_{PyGas}$ (4-8 h^{-1}) are summarised in Table 4.3.

Conversion/ Yield	P_{H2} = 5 barg [P_T = 20 barg]			P_{H2} = 10 barg [P_T = 20 barg]	
	WHSV= 4 h^{-1} Catalyst wt= 0.5 g (H$_2$/PyGas mol ratio=5)	WHSV= 8 h^{-1} Catalyst wt= 0.25 g (H$_2$/PyGas mol ratio=5)	WHSV= 8 h^{-1} Catalyst wt= 0.5 g (H$_2$/PyGas mol ratio=2.5)	WHSV= 4 h^{-1} Catalyst wt= 0.5 g (H$_2$/PyGas mol ratio=10)	WHSV= 8 h^{-1} Catalyst wt= 0.5 g (H$_2$/PyGas mol ratio=5)
Conversion (%) 1-pentene	90.6	87.3	83.7	99.5	94.5
Yield (%) Pentane	47.9	47.4	24.6	78.1	48.5
Trans-2-pentene	7.4	14.8	22.9	-	7.9
Cis-2-pentene	3.0	5.3	12.8	-	4.4
Conversion (%) 1-octene	98.3	99.3	76.6	100	86.3
Yield (%) Octane	52.2	47.3	19.0	81.7	47.2
Trans-2-octene	11.2	11.9	16.7	-	10.2
Cis-2-octene	5.4	5.0	9.7	-	6.0
Trans-3-octene	} 7.7	} 11.1	2.8	-	2.5
Cis -3-octene			0.9	-	0.8
Cis-4-octene			0.2	-	0.2
Trans-4-octene	2.3	3.4	0.6	-	0.8
Conversion (%) Cyclopentene	93.8	93.1	67.6	100	87.5
Yield (%) Cyclopentane	61.5	69.5	30.3	83.0	57.2
Conversion (%) Toluene	24.1	23.1	22.4	27.5	24.4
Yield (%) Methyl-cyclohexane	0.1	Trace	Trace	8.8	0.7
Conversion (%) Styrene	99.9	99.9	90.0	99.9	96.5
Yield (%) Ethylbenzene	60.8	62.7	51.7	51.7	67.0
Ethylcyclohexane	Trace	Trace	-	4.1	0.6

Table 4.3 Effect of WHSV$_{PyGas}$ on PyGas hydrogenation [WHSV$_{PyGas}$ = 4-8 h^{-1}, T = 140°C, P_T = 20 barg], (Average conversion and average yield at steady state)

4.2.1.5 Kinetic analysis of PyGas hydrogenation over Ni/Al$_2$O$_3$ catalyst

The rate of olefin hydrogenation to the respective saturated paraffin within PyGas increased with an increase in hydrogen partial pressure up to 10 barg and then the rate of paraffin formation remained constant or a small decrease was observed with further increase in hydrogen partial pressure up to 20 barg. In contrast, the rate of olefin isomerisation to internal olefins decreased with an increase in the hydrogen partial pressure.

No noticeable hydrogenation of the PyGas aromatic species was observed with increasing the hydrogen partial pressure up to 5 barg. However, a clear increase was noticed in the hydrogenation of aromatic species with a further increase in hydrogen pressure from 5 barg up to 20 barg.

Moreover, a very small increase was observed in the rate of styrene hydrogenation to ethylbenzene when the hydrogen partial pressure was increased to 5 barg and a further increase in hydrogen partial pressure facilitated the hydrogenation of ethylbenzene to ethylcyclohexane.

This shows that the hydrogenation of PyGas components generally increased with increasing hydrogen partial pressure. The rates of hydrogenation of PyGas components with respect to hydrogen partial pressure are shown in Figure 4.7-8.
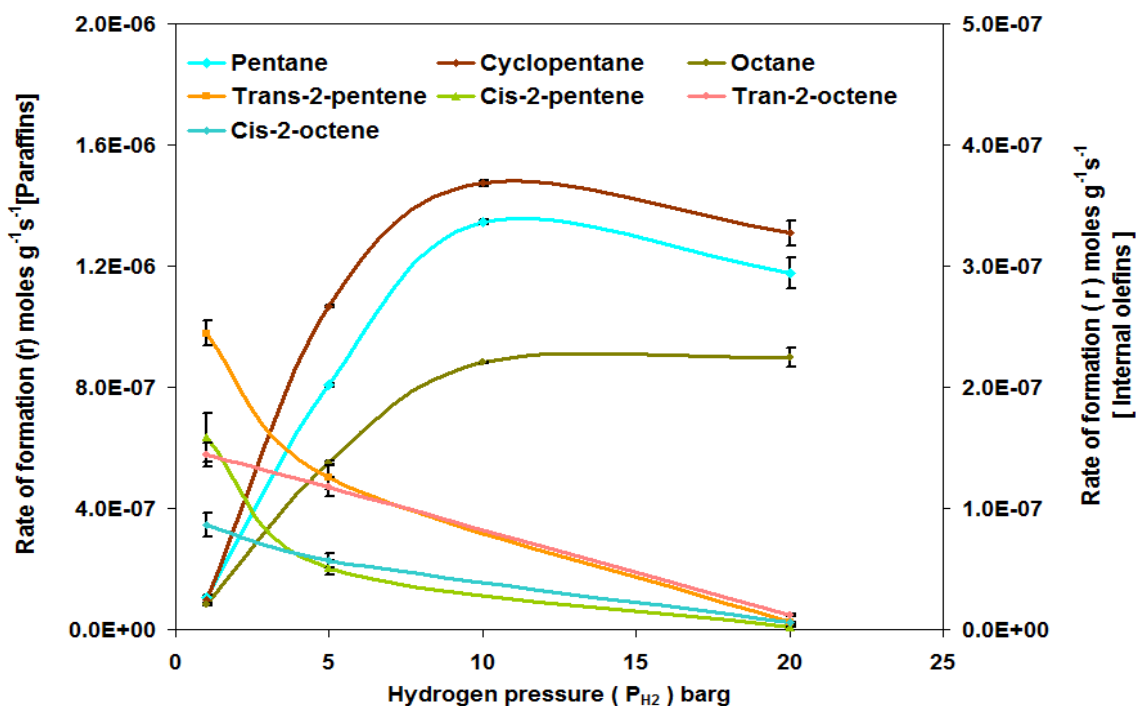
Figure 4.7 Effect of hydrogen partial pressure on hydrogenation of olefinic species of PyGas [P$_{H2}$ = 1-20 barg, P$_T$ = 20 barg, T = 140°C, WHSV$_{PyGas}$ = 4 h^{-1}], (Average rate at steady state)
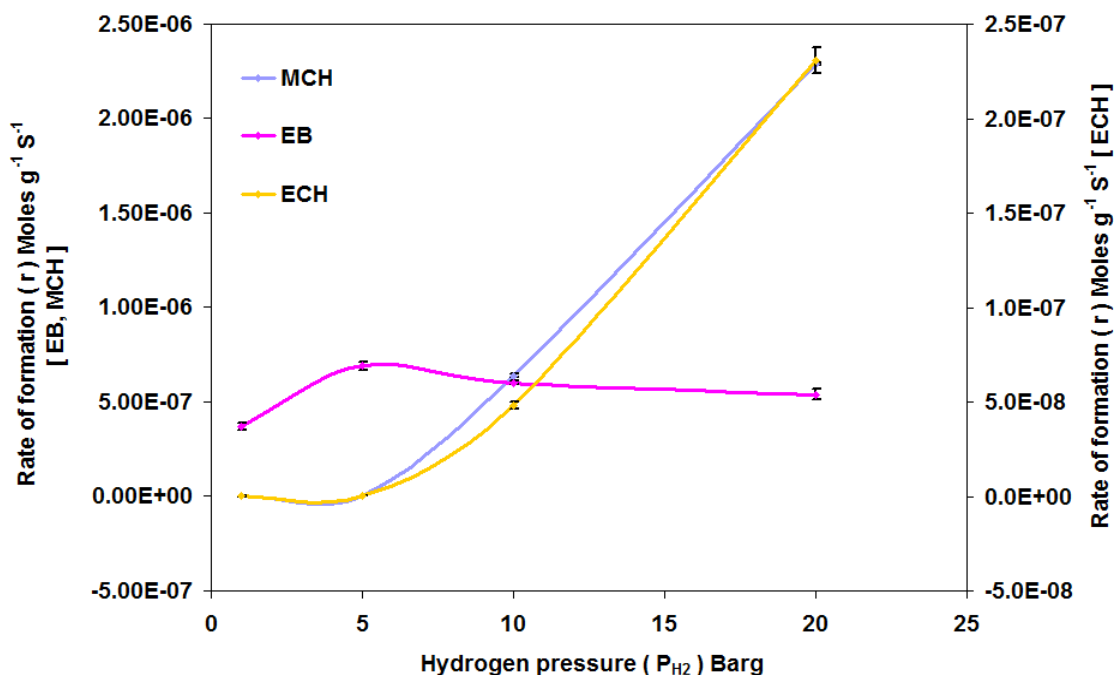
Figure 4.8 Effect of hydrogen partial pressure on hydrogenation of aromatic components of PyGas [P_{H2} = 1-20 barg, P_T = 20 barg, T = 140°C, WHSV$_{PyGas}$ = 4 h^{-1}], (Average rate at steady state)

A simple empirical rate equation was used for the determination of the apparent reaction order of the hydrogenation/isomerisation of PyGas components, and although simple, it is considered a reliable model [46, 53, 63].

$$r_A = k\, P^a_A\, P^b_{H2} \qquad (4.1)$$

r_A: rate of hydrogenation/isomerisation, k: kinetic rate constant, P_A and P_{H2} : partial pressures of PyGas component/s A and hydrogen respectively, a and b: apparent orders with respect to PyGas and hydrogen respectively.

In order to determine the apparent orders of the reactions with respect to hydrogen, the rate of reaction was measured by varying the partial pressure of hydrogen and the partial pressures of the PyGas components were kept constant. Then Eq. (4.1) becomes;

$$r_A = k_1\, P^b_{H2} \qquad (4.2)$$

Where $k_1 = k\, P^a_A$ = constant.

The logarithmic form of reaction becomes;

$$\ln(r_A) = \ln(k_1) + b\, \ln(P_{H2}) \qquad (4.3)$$

The apparent order with respect to hydrogen was determined by plotting $\ln(r_A)$ vs $\ln(P_{H2})$.

First order kinetics (1.1 to 1.3) were observed for the hydrogenation of olefins to their respective paraffins with respect to hydrogen during the hydrogenation of PyGas when the hydrogen pressure was ≤ 10 barg. This changed to zero or slightly negative orders reactions (0.0 to -0.2) when the hydrogen partial pressure was between 10-20 barg. While, negative order kinetics were observed for olefin isomerisation to their internal olefins with increasing hydrogen partial pressure. The results are in close agreement with literature in which first order kinetics were generally observed for the hydrogenation of double bonds of olefins within PyGas with an increase in hydrogen pressure and then become zero order when a sufficient amount of hydrogen is available on the surface of the catalyst [46, 84]. The detailed kinetic orders of the reactions during PyGas hydrogenation are presented in Table 4.4.

Reactions		Orders of reactions wrt H_2	
Reactants	Products	P_{H2} (1-10 barg)	P_{H2} (10-20 barg)
1-pentene	Pentane	1.1	-0.2
1-pentene	Trans-2-pentene	-0.4	-2.2
1-pentene	Cis-2-pentene	-0.7	-2.2
1-octene	Octane	1.1	0.0
1-octene	Trans-2-octene	-0.1	-1.7
1-octene	Cis-2-octene	-0.2	-1.7
Cyclopentene	Cyclopentane	1.3	-0.2

Table 4.4 Kinetics of olefin hydrogenation with respect to hydrogen [P_{H2} = 1-20 barg, P_T = 20 barg, T = 140°C, WHSV$_{PyGas}$ = 4 h^{-1}]

Virtually no hydrogenation of toluene to methylcyclohexane took place during PyGas hydrogenation up to 5 barg hydrogen partial pressure, while third order (3.3) reaction kinetics were observed for toluene hydrogenation to methylcyclohexane in the range of 5 barg to 20 barg hydrogen partial pressure. For the hydrogenation of styrene to ethylbenzene, zero order kinetics were observed with respect to hydrogen in the entire range of hydrogen partial pressures (1-20 barg). Zero order kinetics for styrene hydrogenation suggest that stronger adsorption of the styrene took place on the catalyst than the other components of PyGas, which is in close agreement with the literature [18, 40,

83]. The further hydrogenation of ethylbenzene to ethylcyclohexane followed similar order kinetics to toluene hydrogenation. The hydrogenation of aromatics such as toluene and benzene over supported Ni, Pd and Pt catalyst are found in the literature with a wide range of kinetic orders from 0.5 to 0.7 below 100°C and from 0.7 to 4 above 100°C with respect to hydrogenation [63, 65-67, 74-77]. However, the kinetics of aromatic hydrogenation in PyGas have not been explored in detail. The detailed reaction kinetic order data of the aromatic components in the PyGas in our system are presented in Table 4.5.

Reactions		Orders of reactions wrt H$_2$	
Reactants	Products		
		P$_{H2}$ (1-20 barg)	
Styrene	Ethyl benzene	0.1	
		P$_{H2}$ (1-5 barg)	P$_{H2}$ (5-20 barg)
Toluene	Methylcyclohexane	-	3.3
Ethylbenzene	Ethylcyclohexane	-	3.3

Table 4.5 Kinetics of aromatic hydrogenation with respect to hydrogen [P$_{H2}$ = 1-20 barg, P$_T$ = 20 barg, T = 140°C, WHSV$_{PyGas}$ = 4 h^{-1}]

PyGas contains a large number of unsaturated components, therefore it not always feasible to measure the reaction kinetics of each of the components. Subsequently, the components which followed analogous reactions can be summed to obtain more general and simple reaction kinetics for PyGas hydrogenation [23]. Therefore, the rate of formation of paraffin was taken to be the sum of all the paraffins formed during the PyGas hydrogenation, the rate of internal olefin formation was taken to be the sum of all the internal olefins formed and the rate of aromatic hydrogenation was considered to be the sum of formation of all saturated components of aromatics during the reaction to obtain simple and general reaction kinetics for our system.

Rate of formation of paraffins = r $_{Paraffins}$ = r $_{(pentane + octane + cyclopentane)}$

Rate of formation of internal olefins = r $_{Internal olefins}$ = r $_{(Trans-2-pentene + Cis-2-pentene + Trans-2-octene + Cins-2-octene + Trans-3-octene + Cins-3-octene + Trans-4-octene + Cins-4-octene)}$

Rate of formation of saturated compounds of aromatics = r $_{saturated compounds of aromatics}$ = r $_{(MCH + ECH)}$

By using this approach, the results obtained are presented in Figure 4.9 and the orders of reactions with respect to hydrogen, are presented in Table 4.6.

Figure 4.9 Effect of hydrogen pressure on PyGas hydrogenation, [P_{H2} = 1-20 barg, P_T = 20 barg, T = 140°C, WHSV$_{PyGas}$ = 4 h^{-1}]

Reactions		Orders of reactions wrt H$_2$	
Reactants	Products		
Olefin hydrogenation		P_{H2} (1-10 barg)	P_{H2} (10-20 barg)
Olefins (1-pentene, 1-octene, Cyclopentane)	Paraffins (Pentane, Octane, Cyclopentane)	1.1	-0.1
Olefins (1-pentene, 1-octene)	Internal olefins	-0.1	-2.2
Aromatic hydrogenation		P_{H2} (1-20 barg)	
Styrene	Ethylbenzene	0.1	
		P_{H2} (1-5 barg)	P_{H2} (5-20 barg)
Aromatics (Toluene, Ethylbenzene)	Saturated compounds of aromatic (MCH + ECH)	-	3.3

Table 4.6 Kinetics of PyGas hydrogenation with respect to hydrogen pressure [P_{H2} = 1-20 barg, P_T = 20 barg, T = 140°C, WHSV$_{PyGas}$ = 4 h^{-1}]

The hydrogenation of PyGas was also investigated using different WHSV of PyGas (4-8 h^{-1}) with the other reaction conditions kept constant [P_T = 20 barg (25%

Hydrogen gas mixture), P_{H2} = 5, T = 140°C]. The results are summarised in Figure 4.10. The rate of hydrogenation of olefins to their saturated paraffins remained the same or a small decrease took place with an increase in the WHSV of PyGas from 4 to 8 h^{-1}. However, a considerable increase was observed in the rate of formation of internal olefins. An increase was observed in the rate of styrene hydrogenation to ethylbenzene with an increase in the PyGas feed flow rate. This suggests that the styrene is comparatively more strongly adsorbed onto the catalyst, similar behaviour has been reported in previous studies [40, 82, 83, 117].

The hydrogenation of aromatics to their corresponding saturated compounds was depressed during PyGas hydrogenation when the WHSV of PyGas was increased from 4 h^{-1} to 8 h^{-1}, due to the stronger adsorption of styrene and olefins onto the catalyst than aromatic species, similar observations have been reported in the literature [41, 59].
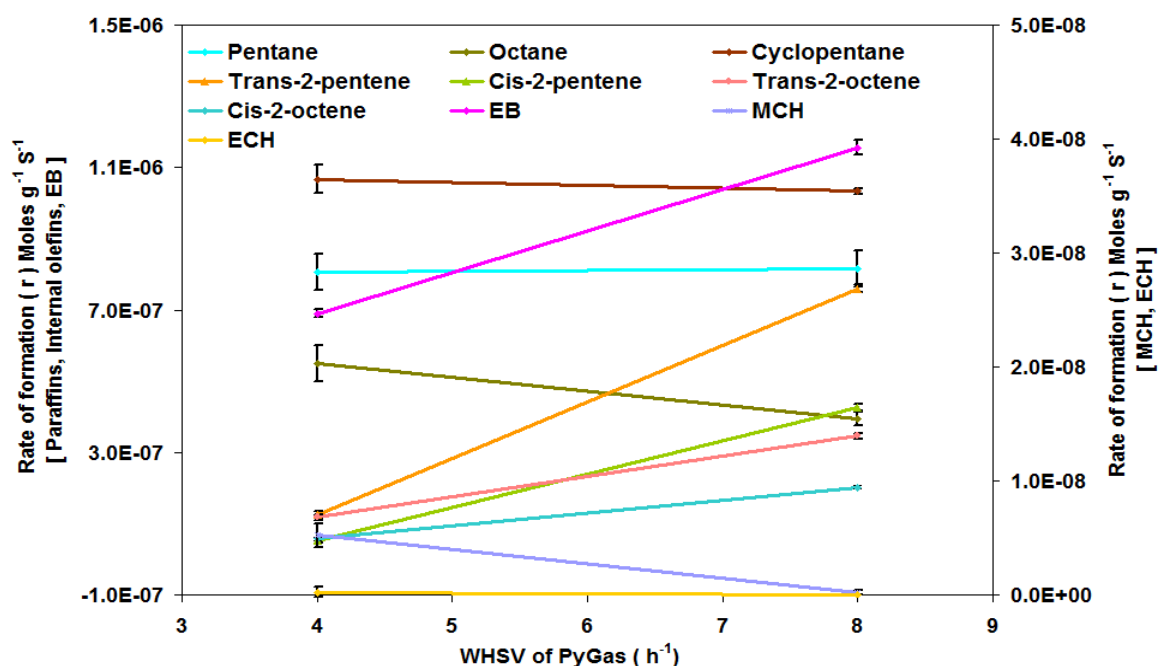
Figure 4.10 Effect of PyGas feed flow rate (WHSV$_{PyGas}$) on hydrogenation of PyGas [WHSV$_{PyGas}$ = 4-8 h^{-1}, T = 140°C, P$_T$ = 20 barg, P$_{H2}$ = 5 barg]

The influence of PyGas feed flow rate (WHSV$_{PyGas}$) was also determined at a high hydrogen partial pressure by using a 50% hydrogen gas mixture, while all other reaction conditions were kept constant [P$_T$ = 20 barg, P$_{H2}$ = 10 barg, T = 140°C]. The effect was found to be similar to reactions performed at lower partial pressure of hydrogen when using a 25% hydrogen gas mixture. An increase was

also observed in the rate of formation of internal olefins with an increase in PyGas feed flow rate (WHSV$_{PyGas}$). However the effect was not as pronounced as when using the 25% hydrogen gas mixture, where the olefins converted to paraffins due to a high amount of hydrogen present on the surface of the catalyst.

Moreover, the hydrogenation of aromatics to the corresponding saturated compounds was also depressed with an increase in feed flow rate of PyGas using a 50% hydrogen gas mixture due to the stronger adsorption of styrene and olefins than aromatic species onto the catalyst, which is in close agreement with literature [41, 59]. The effect of PyGas feed flow rate (WHSV$_{PyGas}$ 4-8 h^{-1}) on the rate of formation of different components during PyGas hydrogenation is summarised in Figure 4.11.
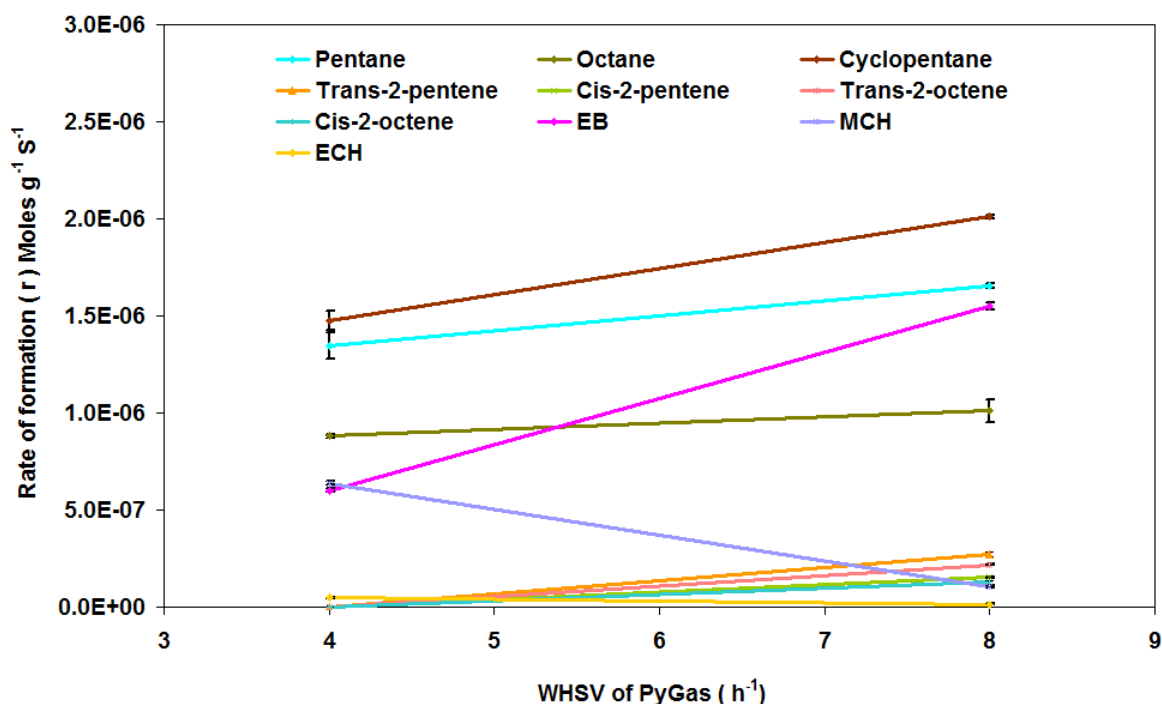
Figure 4.11 Effect of PyGas feed flow rate (WHSV$_{PyGas}$) on hydrogenation of PyGas [WHSV$_{PyGas}$ = 4-8 h^{-1}, T = 140°C, P$_T$ = 20 barg, P$_{H2}$ = 10 barg]

Similarly, the reaction orders for hydrogenation/isomerisation of components with respect to PyGas were calculated by using the empirical rate equation (4.1);

$$r_A = k \, P_A^a \, P_{H2}^b \qquad\qquad (4.1)$$

The partial pressure of the PyGas component/s increases with an increase in the feed flow rate of PyGas ($WHSV_{PyGas}$) when all other parameters of the reaction keep constant [129]. Thus,

$$P_A \propto (WHSV \text{ of } PyGas) \qquad (4.4)$$

$$P_A = C_1 * (WHSV \text{ of } PyGas) \qquad (4.5)$$

By putting equation (4.5) into equation (4.1) the empirical rate formula becomes [129];

$$r_A = k_2 P^b_{H2} * (WHSV \text{ of } PyGas)^a \qquad (4.6)$$

$$r_A = k_3 * (WHSV \text{ of } PyGas)^a \qquad (4.7)$$

Where $k_3 = k_2 P^b_{H2}$ because P^b_{H2} is constant at constant hydrogen partial pressure.

The logarithmic form then becomes;

$$\ln(r_A) = \ln(k_3) + a \ln(WHSV \text{ of } PyGas) \qquad (4.8)$$

The apparent reaction orders of the PyGas component/s with respect to PyGas were determined by plotting $\ln(r_A)$ vs $\ln(WHSV_{PyGas})$ and are shown in Table 4.7. The hydrogenation of olefins to their paraffins followed zero to negative half order (0.0 to -0.5) kinetics with respect to PyGas. However, these increased to positive order kinetics (0.2-0.4) by using a higher hydrogen partial pressure (50% hydrogen gas mixture). Positive order kinetics were observed for olefins isomerisation to internal olefins with both 25% and 50% hydrogen gas mixtures. Moreover, positive order kinetics were also observed for styrene hydrogenation to ethylbenzene with respect to PyGas.

Negative order kinetics were observed for aromatic hydrogenation during PyGas hydrogenation with respect to PyGas. Generally, zero order kinetics have been reported in the literature for the hydrogenation of aromatic compounds with respect to aromatic concentration/partial pressure when the hydrogenation of the individual aromatic compounds is carried out [46, 65, 77, 78]. The negative order reaction of aromatic components to the corresponding saturated compounds during PyGas hydrogenation was due to competitive adsorption of styrene, olefins and aromatics taking place on the same active sites on the catalyst. The adsorption of aromatic compounds were depressed by the stronger adsorption of styrene and olefins, similar behaviour was observed in previous studies [41].

Reactions		Order of Reactions wrt PyGas (WHSV$_{PyGas}$ 4-8 h^{-1})	
Reactants	Products	P_{H2} = 5 barg, P_T = 20 barg (25 % Hydrogen gas)	P_{H2} = 10 barg, P_T = 20 barg (50 % Hydrogen gas)
1-pentene	Pentane	0.0	0.3
1-pentene	Trans-2-pentene	2.6	-
1-pentene	Cis-2-pentene	3.0	-
1-octene	Octane	-0.5	0.2
1-octene	Trans-2-octene	1.6	-
1-octene	Cis-2-octene	1.8	-
Cyclopentene	Cyclopentane	0.0	0.4
Styrene	Ethylbenzene	0.7	1.4
Ethylbenzene	Ethylcyclohexane	-	-
Toluene	Methylcyclohexane	-	-2.5

Table 4.7 Kinetics of PyGas hydrogenation with respect to PyGas (WHSV$_{PyGas}$ 4-8 h^{-1})

To obtain more general and simple kinetics for the hydrogenation of PyGas, the formation of similar components were taken combined as discussed earlier in this section. The results are presented in Figures 4.12-13 and the reaction orders obtained are shown in Table 4.8.
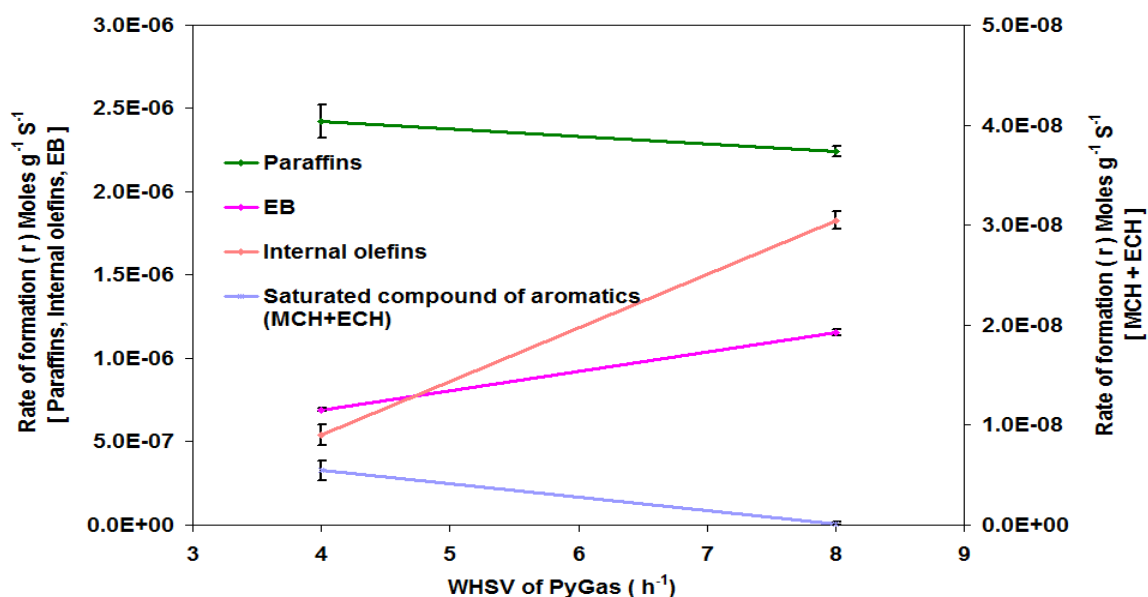
Figure 4.12 Effect of PyGas feed flow rate (WHSV$_{PyGas}$) on hydrogenation of PyGas [WHSV$_{PyGas}$ = 4-8 h^{-1}, T = 140°C, P_T = 20 barg, P_{H2} = 5 barg]
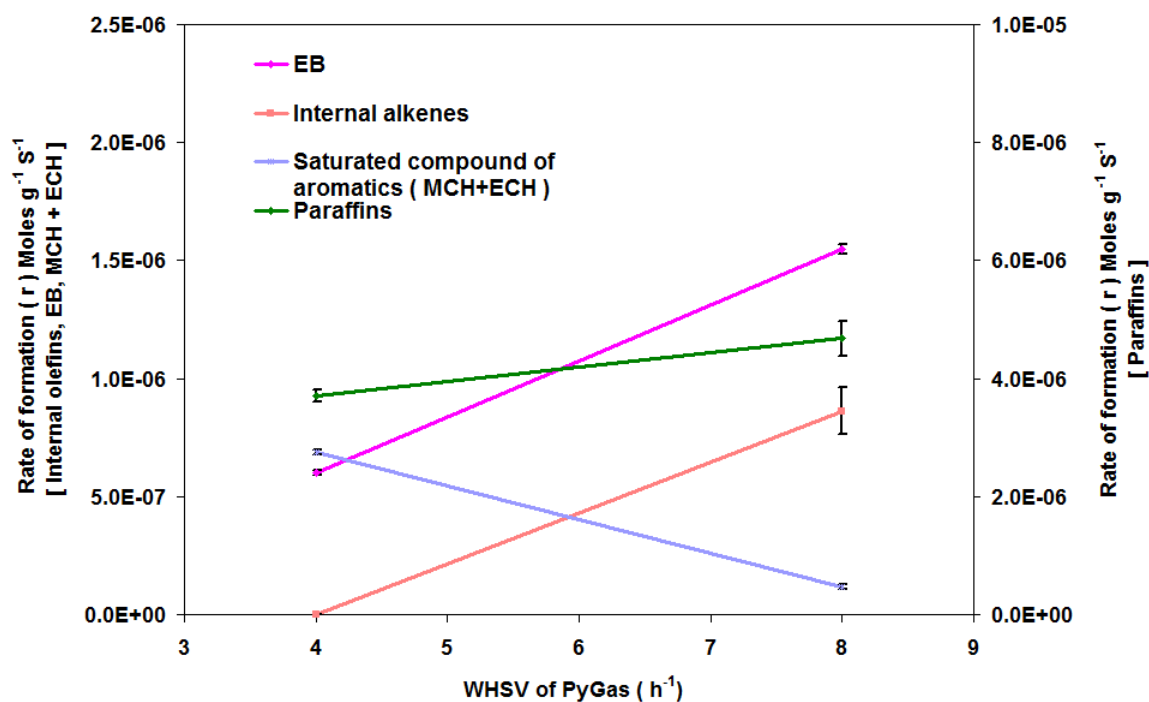
Figure 4.13 Effect of PyGas feed flow rate (WHSV$_{PyGas}$) on hydrogenation of PyGas [WHSV$_{PyGas}$ = 4-8 h^{-1}, T = 140°C, P$_T$ = 20 barg, P$_{H2}$ = 10 barg]

Reactions		Orders of reactions wrt PyGas (WHSV$_{PyGas}$ 4-8 h^{-1})	
Reactants	**Products**	P$_{H2}$ = 5 barg, P$_T$ = 20 barg (25 % Hydrogen gas used)	P$_{H2}$ = 10 barg, P$_T$ = 20 barg (50 % Hydrogen gas used)
Olefins (1-pentene, 1-octene, Cyclopentane)	Paraffins (Pentane, Octane, Cyclopentane)	-0.1	0.3
Olefins (1-pentene, 1-octene)	Internal olefins	1.8	-
Styrene	Ethylbenzene	0.7	1.4
Aromatics (Toluene, Ethylbenzene)	Saturated compounds of aromatic (MCH+ECH)	-	-2.5

Table 4.8 Kinetics of PyGas hydrogenation with respect to PyGas (WHSV$_{PyGas}$ 4-8 h^{-1})

4.2.2 Pyrolysis gasoline hydrogenation over Pd/Al$_2$O$_3$ catalyst

The effects of the following reaction parameters during the PyGas hydrogenation over the Pd/Al$_2$O$_3$ catalyst are discussed in this section.

e) Effect of reaction temperature

f) Effect of hydrogen partial pressure

g) Effect of total reaction pressure

h) Effect of PyGas feed flow rate (WHSV$_{PyGas}$)

The kinetic analysis and reaction orders of hydrogenation/isomerisation of the PyGas components over the palladium catalyst are also investigated and are discussed in section 4.2.2.5.

4.2.2.1 Effect of reaction temperature on PyGas hydrogenation

The hydrogenation of PyGas was performed at various reaction temperatures (140-200°C) with the other reaction conditions kept constant. The hydrogenation of olefins over palladium catalyst was comparable with that over the nickel catalyst. The olefins were hydrogenated to their saturated paraffins and no internal olefins formation was observed due to favourable reaction conditions for hydrogenation.

However, only very small amounts of the aromatics hydrogenation were observed at 140°C, with about 1% yield of both methylcyclohexane and ethylcyclohexane. The literature also shows that palladium is less active for aromatic hydrogenation and was placed below nickel for aromatic hydrogenation [46, 65, 76, 130].

$$Pt > Ni > Pd$$
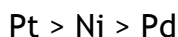
A similar mechanism for aromatic hydrogenation over palladium metals is generally accepted, as discussed in Section 4.2.1.1 and shown in Figure 4.3. However, palladium has a comparatively higher tendency to stabilise the π-complexes of unsaturated hydrocarbons than nickel and platinum [131-133]. Therefore, the hydrocarbons are likely to remain as π-complexes on the palladium catalyst and consequently the tendency to make σ-bonded complexes decrease. The σ-bonded complex is required for the hydrogenation of aromatics

and thus a small amount of aromatic hydrogenation took place over the palladium catalyst. This illustrates that palladium is highly selective to olefins and styrene hydrogenation without hydrogenating the aromatic components of PyGas at lower reaction temperatures. This behaviour is highly desirable for the selective hydrogenation of PyGas [4, 11, 44].

However, an increase in the hydrogenation of aromatics was observed during PyGas hydrogenation over the palladium catalyst with an increase in reaction temperature. The maximum rate of aromatic hydrogenation was observed at $180^{o}C$ and then remained constant or slightly decreased with a further increase in reaction temperature, which is similar to Jen *et al.* [122] study, where the maximum rate of aromatic hydrogenation over a palladium catalyst was noted at $187^{o}C$. However, a higher temperature (~ $220^{o}C$) was also cited in some studies [134]. The rate of aromatic hydrogenation decreases with a further increase in the reaction temperature, which is most likely due to a decrease in surface coverage of the aromatic compounds on the surface of catalyst and/or catalyst deactivation [74, 122].

Ethylbenzene was the main product from styrene hydrogenation during PyGas hydrogenation over the palladium catalyst at $140^{o}C$ and a very small amount of ethylcyclohexane (~ 1% yield) was observed. This suggests that palladium is capable of selectively hydrogenating the alkenyl bond of styrene without hydrogenation of the aromatic ring of styrene at low reaction temperature ($140^{o}C$). However, the formation of ethylcyclohexane increased with an increase in the reaction temperature. This shows that styrene is first hydrogenated to ethylbenzene, which is then further hydrogenated to ethylcyclohexane with increasing reaction temperature. The effect of reaction temperature (140-$200^{o}C$) on the hydrogenation of PyGas is summarised in Figure 4.14.
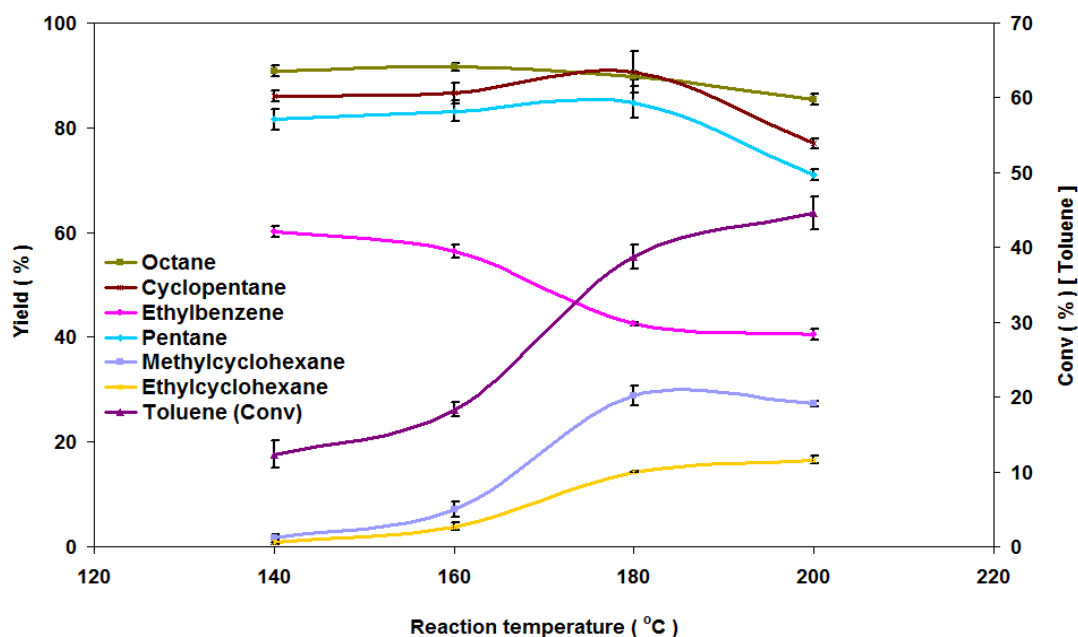
Figure 4.14 Effect of reaction temperature on hydrogenation of PyGas [T = 140-200°C, P_{H2} = 20 barg, $WHSV_{PyGas}$=4 h^{-1}], (Average conversion and average yield at steady state)

4.2.2.2 Effect of Hydrogen pressure on PyGas hydrogenation

A significant effect of hydrogen partial pressure was observed on the hydrogenation of PyGas over the palladium catalyst. The extent of PyGas hydrogenation increased with an increase in hydrogen partial pressure. However, an optimised hydrogen partial pressure is required to obtain the desired selectivity and yield during PyGas hydrogenation, because a high degree of saturation of the olefins and the aromatic components took place and a smaller extent of olefin isomerisation to internal olefins occurred at a very high hydrogen partial pressure. Consequently, the selectivity of PyGas hydrogenation towards a high octane mixture decreased. In contrast, the selectivity of PyGas hydrogenation increased with a decrease in the hydrogen partial pressure but the total yield of PyGas hydrogenation was considerably decreased and rapid catalyst deactivation took place due to high amount of coke deposition. Therefore, a very small hydrogen partial pressure was also found to not be suitable for PyGas hydrogenation. The effect of hydrogen partial pressure (1-20 barg) on the hydrogenation of PyGas over the palladium catalyst is summarised in Table 4.9.

Conversion/ Yield	Hydrogen Partial Pressure (barg) [P_T = 20 barg]			
	P_{H2} = 1 barg	P_{H2} = 5 barg	P_{H2} = 10 barg	P_{H2} = 20 barg
Conversion (%) 1-pentene	87.4	93.6	99.9	99.8
Yield (%)				
Pentane	4.1	52.8	66.9	81.5
Trans-2-pentene	41.3	6.9	-	-
Cis-2-pentene	18.0	2.4	-	-
Conversion (%) 1-octene	78.2	99.8	100	100
Yield (%)				
Octane	4.0	53.0	84.5	90.8
Trans-2-octene	21.9	7.4	-	-
Cis-2-octene	10.8	2.9	-	-
Trans-3-octene	8.7		-	-
Cis -3-octene	2.3	10.6	-	-
Cis-4-octene	1.0		-	-
Trans-4-octene	3.8	4.7	-	-
Conversion (%) Cyclopentene	56.1	92.9	100	100
Yield (%) Cyclopentane	5.4	63.9	76.9	85.9
Conversion (%) Toluene	21.4	26.0	17.6	12.3
Yield (%) Methylcyclohexane	Trace	0.1	1.3	1.6
Conversion (%) Styrene	100	100	100	100
Yield (%)				
Ethylbenzene	47.2	59.7	63.3	60.1
Ethylcyclohexane	-	Trace	0.8	0.8

Table 4.9 Effect of hydrogen partial pressure on PyGas hydrogenation [P_{H2} = 1-20 barg, P_T = 20 barg, T = 140°C, WHSV$_{PyGas}$ = 4 h^{-1}], (Average conversion and average yield at steady state)

The hydrogenation of PyGas over the palladium catalyst was comparable with the PyGas hydrogenation over the nickel catalyst in the range of hydrogen partial pressures between 5 and 20 barg. However, the yield of the PyGas hydrogenation over the palladium catalyst with 1 barg hydrogen partial pressure was considerably higher when compared to the reaction over the nickel catalyst

under similar reaction conditions. This shows that the palladium catalyst was comparatively more active than the nickel catalyst at 1 barg hydrogen partial pressure. The stronger adsorption of hydrogen onto palladium compared with nickel has been reported in the literature [135, 136]. Therefore the higher activity of the palladium at low hydrogen partial pressure (1 barg) is most likely due to the stronger adsorption of hydrogen onto palladium compared with nickel. The higher activity over the palladium catalyst was more pronounced at lower hydrogen partial pressure (1 barg). However similar hydrogenation of the PyGas over the both catalysts was observed with increasing hydrogen partial pressure due to higher availability of hydrogen.

The hydrogenation of olefins over palladium follows the Horiuti-Polanyi mechanism, as explained in Section 1.4.1. The 1-pentene present in the PyGas was hydrogenated to n-pentane at high hydrogen partial pressure. However, formation of trans-2-pentene and cis-2-pentene took place with a decrease in hydrogen partial pressure. This shows that isomerisation of 1-pentene to 2-pentene increases when a small amount of adsorbed hydrogen is present on the surface of the catalyst.

A higher amount of the 2-pentene isomers was observed over the palladium catalyst when compared to the nickel catalyst. Trans-2-pentene was observed in quantities of about twice the amount of cis-2-pentene (trans/cis ratio ~68/32). The higher amount of the trans-isomer is due to the greater thermodynamic stability of the trans-isomer [46].

Similarly, the 1-octene present in the PyGas hydrogenated to octane at high hydrogen partial pressure while isomerisation to internal octenes took place at low hydrogen partial pressure. The mechanism of hydrogenation/isomerisation of 1-octene was likely to be similar to that over nickel, which is explained in Figure 4.4. However, a higher extent of internal olefin formation was observed over the palladium catalyst when compared to the nickel catalyst under identical reaction conditions. Moreover, a high degree of bond migration occurred and therefore greater amounts of 3-octene and 4-octene formation occurred over the palladium. The selective hydrogenation and greater extent of internal olefin formation during PyGas hydrogenation over the palladium catalyst

is most likely due to its higher tendency to stabilise the π-complex of unsaturated hydrocarbons than nickel and platinum [131-133].

A high trans/cis ratio of internal octene isomers was observed due to the greater thermodynamic stability of the trans isomers. The trans/cis ratio in the 2-octene was about 67/33, which slightly increased to 79:21 in the 3-octene and 4-octene.

The results suggest that the palladium catalyst has a higher isomerisation capability for olefins than the nickel catalyst, which is in close agreement with the literature [11, 60]. Consequently, the palladium catalyst is preferable to the nickel catalyst for the highly selective hydrogenation of PyGas, and a similar view has been reported in previous studies [12, 90].

Hydrogenation of PyGas containing 1,3-pentadiene was also performed to investigate the hydrogenation behaviour of diolefins present in PyGas over the palladium catalyst. The hydrogenation of 1,3-pentadiene during PyGas hydrogenation was comparable to the reaction performed over the nickel catalyst under identical reaction conditions. The selectivity towards 1-pentene, trans-2-pentene, cis-2-pentene and pentane during the 1,3-pentadiene hydrogenation over the palladium was found to be 0.5%, 15%, 5% and 79% respectively. This result suggests that most likely the adsorption of various 1,3-pentadiene conformers took place and different modes of hydrogen addition occurred. These produced the wide range of pentene isomers, as shown in Figure 4.6 and were discussed in detail in Section 4.2.1.2. The 1-pentene and 2-pentene then further hydrogenated and produced a high amount of pentane.

Similar to the nickel catalyst, a higher amount of trans-2-pentene formation occurred than cis-2-pentene formation during the hydrogenation of 1,3-pentadiene over the palladium catalyst and the ratio of trans to cis in 2-pentene was found to be 75:25. The high trans to cis ratio suggests that higher amounts of 1,3-pentadiene were present as the anti conformers and produced a higher amount of the trans isomers than the respective cis isomers, which is closely in agreement with the literature [46].

Ethylbenzene was the only product observed in the hydrogenation of styrene over the palladium catalyst and virtually no formation of ethylcyclohexane was

noted over the entire range of hydrogen partial pressures (1-20 barg). These results suggest that the palladium catalyst has a high selectivity for hydrogenation of the alkenyl bond of styrene without hydrogenation of the aromatic ring of the styrene. This behaviour is highly desirable for the selective hydrogenation of PyGas without aromatic saturation e.g. for aromatic extraction [4, 44].

4.2.2.3 Effect of Total reaction pressure on PyGas hydrogenation

As with the nickel catalyst, a decrease was observed in the hydrogenation of PyGas with a decrease in total pressure from 20 barg to 10 barg when using a 50% hydrogen gas mixture. However, the product distribution was unchanged and no internal isomerisation was observed. Whereas a reasonable amount of internal olefin formation was observed using a 25% hydrogen gas mixture at 20 barg total reaction pressure. This is similar behaviour to that observed with the nickel catalyst during PyGas hydrogenation. These results suggest that the use of a diluted hydrogen gas mixture at a higher total reaction pressure is more favourable for the selective hydrogenation of PyGas than performing the reaction at a lower total pressure over both the nickel and the palladium catalysts. Table 4.10 shows a summary of the product distribution, yield (%) and conversion (%) of PyGas hydrogenation at different total pressures. The feed rate of PyGas was kept constant for all the reactions.

Conversion/Yield	50% hydrogen gas mixture		25% hydrogen gas
	P_T = 20 barg	P_T = 10 barg	P_T = 20 barg
Conversion (%) 1-pentene	99.9	99.9	93.6
Yield (%) Pentane	66.9	57.0	52.8
Trans-2-pentene	-	Trace	6.9
Cis-2-pentene	-	Trace	2.4
Conversion (%) 1-octene	100	99.9	99.8
Yield (%) Octane	84.5	93.9	53.0
Trans-2-octene	-	Trace	7.4
Cis-2-octene	-	Trace	2.9
Trans-3-octene	-	Trace	
Cis -3-octene	-	Trace	10.6
Cis-4-octene	-	Trace	
Trans-4-octene	-	Trace	4.7
Conversion (%) Cyclopentene	100	99.9	92.9
Yield (%) Cyclopentane	76.9	70.0	63.9
Conversion (%) Toluene	17.6	24.4	26.0
Yield (%) Methylcyclohexane	1.3	0.2	0.1
Conversion (%) Styrene	100	99.9	100
Yield (%) Ethylbenzene	63.3	61.8	59.7
Ethylcyclohexane	0.8	0.2	Trace

Table 4.10 Effect of total pressure on PyGas hydrogenation [P_T = 10-20 barg, T = 140°C, WHSV$_{PyGas}$ = 4 h^{-1}], (Average conversion and average yield at steady state)

4.2.2.4 Effect of PyGas feed flow rate (WHSV$_{PyGas}$) on PyGas hydrogenation

Similar to the nickel system, the hydrogenation of PyGas over the palladium catalyst decreased with an increase in WHSV of PyGas from 4 h^{-1} to 8 h^{-1} when all the other reaction conditions were kept constant [P_T = 20 barg, P_{H2} = 5 barg, T =

140°C]. The concentration of reactants increased on the surface of palladium with an increase in the feed flow rate of PyGas (WHSV$_{PyGas}$) and therefore the numbers of reactants increased per active site. Moreover, the H$_2$/PyGas molar ratio in the feed also decreased from 5 to 2.5 with an increase in WHSV of PyGas from 4 to 8 h^{-1}. Consequently, a decrease occurred in the hydrogenation of PyGas increased and an increase took place in the isomerisation of olefins to internal olefins with an increase in the feed flow rate of PyGas. Competitive hydrogenation was observed between the PyGas components with an increase in the PyGas feed flow rate. The hydrogenation of olefins and cycloolefins decreased, while no noticeable decrease was observed in the hydrogenation of styrene during PyGas hydrogenation with an increase in the feed flow rate of PyGas because the styrene more strongly adsorbed onto the catalyst than the olefins, similar results have been reported in previous studies [40, 82, 83, 117].

However, a higher amount of internal olefin formation was achieved over the palladium than the nickel at WHSV$_{PyGas}$ of 8 h^{-1} under identical reaction conditions. Moreover, high amounts of 3-octene and 4-octene formation were also observed over the palladium compared to the nickel at WHSV$_{PyGas}$ of 8 h^{-1}. This shows that the palladium has high potential for olefin isomerisation and bond migration, which is in close agreement with literature [11, 60].

The effect of PyGas feed flow rate (WHSV$_{PyGas}$ 4-8 h^{-1}) on the hydrogenation of PyGas over the palladium catalyst was also investigated at higher hydrogen partial pressure (10 barg) using a 50% hydrogen gas mixture. This time the hydrogenation of PyGas also decreased and an increase in the isomerisation of olefins to internal olefins took place with an increase in the WHSV of PyGas from 4 h^{-1} to 8 h^{-1}. A similar effect was observed with an increase in WHSV$_{PyGas}$ when compared to reactions performed with a 25% hydrogen gas mixture. The hydrogenation of aromatic compounds over the palladium was very small when compared with the nickel. Even so the hydrogenation of aromatic species was suppressed by increasing the feed flow rate of PyGas, which illustrates the competitive adsorption of aromatics and olefins on the same active site on the surface of the catalyst, which is in close agreement with literature [41].

The hydrogenation of PyGas at WHSV$_{PyGas}$ 8 h^{-1} using a 50% hydrogen gas mixture was found to be comparable to the reaction carried out at WHSV$_{PyGas}$ 4 h^{-1} with a

25% hydrogen gas mixture. This shows that the decrease in PyGas hydrogenation with an increase in the $WHSV_{PyGas}$ can be restored by increasing the hydrogen partial pressure.

The hydrogenation of PyGas was also performed at $WHSV_{PyGas}$ 8 h^{-1} using a 25% hydrogen gas mixture whilst keeping the feed flow rate of PyGas similar to the reaction carried out at $WHSV_{PyGas}$ of 4 h^{-1} and decreasing the amount of catalyst from 0.5 g to 0.25 g. Thus, the H_2/PyGas molar ratio in the feed and other reaction conditions remained the same, while the $WHSV_{PyGas}$ increased from 4 h^{-1} to 8 h^{-1} with a decrease in catalyst weight from 0.5 g to 0.25 g. Therefore, in Table 4.11 the 0.25 g sample with a $WHSV_{PyGas}$ of 8 h^{-1} can be considered as the top half of the catalyst bed of the 0.5 g sample with a $WHSV_{PyGas}$ of 4 h^{-1}. No significant change was observed in the hydrogenation of PyGas when compared to the reaction performed at $WHSV_{PyGas}$ 4 h^{-1}. Whereas a considerable decrease took place in the hydrogenation of PyGas when the reaction was carried out at WHSV 8 h^{-1} by increasing feed flow rate of the PyGas. This suggests that the molar ratio of H_2/PyGas in the feed is also a very important factor in the hydrogenation of PyGas and a decrease in PyGas hydrogenation takes place when the feed ratio of H_2/PyGas decreases in the reaction. The results of PyGas hydrogenation at various $WHSV_{PyGas}$ (4-8 h^{-1}) are summarised in Table 4.11.

Conversion/ Yield	P_{H2} = 5 barg [P_T = 20 barg]			P_{H2} = 10 barg [P_T = 20 barg]	
	WHSV= 4 h^{-1} Catalyst wt= 0.5 g (H$_2$/PyGas mol ratio=5)	WHSV= 8 h^{-1} Catalyst wt= 0.25 g (H$_2$/PyGas mol ratio=5)	WHSV= 8 h^{-1} Catalyst wt= 0.5 g (H$_2$/PyGas mol ratio=2.5)	WHSV= 4 h^{-1} Catalyst wt= 0.5 g (H$_2$/PyGas mol ratio=10)	WHSV= 8 h^{-1} Catalyst wt= 0.5 g (H$_2$/PyGas mol ratio=5)
Conversion (%) 1-pentene	93.6	89.6	92.3	99.9	99.3
Yield (%) Pentane	52.8	47.1	21.8	66.9	54.1
Trans-2-pentene	6.9	12.6	37.3	-	18.0
Cis-2-pentene	2.4	4.3	14.7	-	6.2
Conversion (%) 1-octene	99.8	99.6	85.3	100	99.4
Yield (%) Octane	53.0	44.9	16.1	84.5	51.4
Trans-2-octene	7.4	10.6	23.5	-	14.4
Cis-2-octene	2.9	4.0	10.9	-	5.8
Trans-3-octene	10.6	16.1	11.0	-	12.6
Cis -3-octene			2.8	-	3.2
Cis-4-octene			1.4	-	1.9
Trans-4-octene	4.7	7.0	4.9	-	6.4
Conversion (%) Cyclopentene	92.9	91.2	70.0	100	96.9
Yield (%) Cyclopentane	63.9	65.5	31.5	76.9	68.2
Conversion (%) Toluene	26.0	21.8	21.3	17.6	22.0
Yield (%) Methyl-cyclohexane	0.1	Trace	-	1.3	Trace
Conversion (%) Styrene	100	99.9	94.8	100	99.9
Yield (%) Ethylbenzene	59.7	62.2	62.3	63.3	73.4
Ethylcyclohexane	Trace	-	-	0.8	0.0

Table 4.11 Effect of WHSV$_{PyGas}$ on PyGas hydrogenation [WHSV$_{PyGas}$ = 4-8 h^{-1}, T = 140°C, P_T = 20 barg], (Average conversion and average yield at steady state)

4.2.2.5 Kinetic analysis of PyGas hydrogenation over Pd/Al$_2$O$_3$ catalyst

The hydrogenation of PyGas over the palladium catalyst increased with an increase in hydrogen partial pressure. The rates of olefins hydrogenation to the respective saturated paraffins increased rapidly with an increase in the hydrogen pressure up to 5 barg and then a slow increase was observed in the rate of paraffins formation with a further increase in the hydrogen partial pressure up to 20 barg. Conversely, the rates of internal olefins formation decreased with an increase in hydrogen partial pressure up to 5 barg and then no internal olefin formation was observed with a further increase in hydrogen partial pressure up to 20 barg. A small increase was observed in the rate of formation of ethylbenzene when the hydrogen partial pressure was increased up to 5 barg and then remained constant with any further increase in hydrogen partial pressure up to 20 barg. A very small amount of aromatic hydrogenation took place over the palladium catalyst, even so a small increase was observed with an increase in the reaction hydrogen partial pressure. The rates of hydrogenation of the PyGas components with respect to hydrogen partial pressure are shown in Figures 4.15-16.
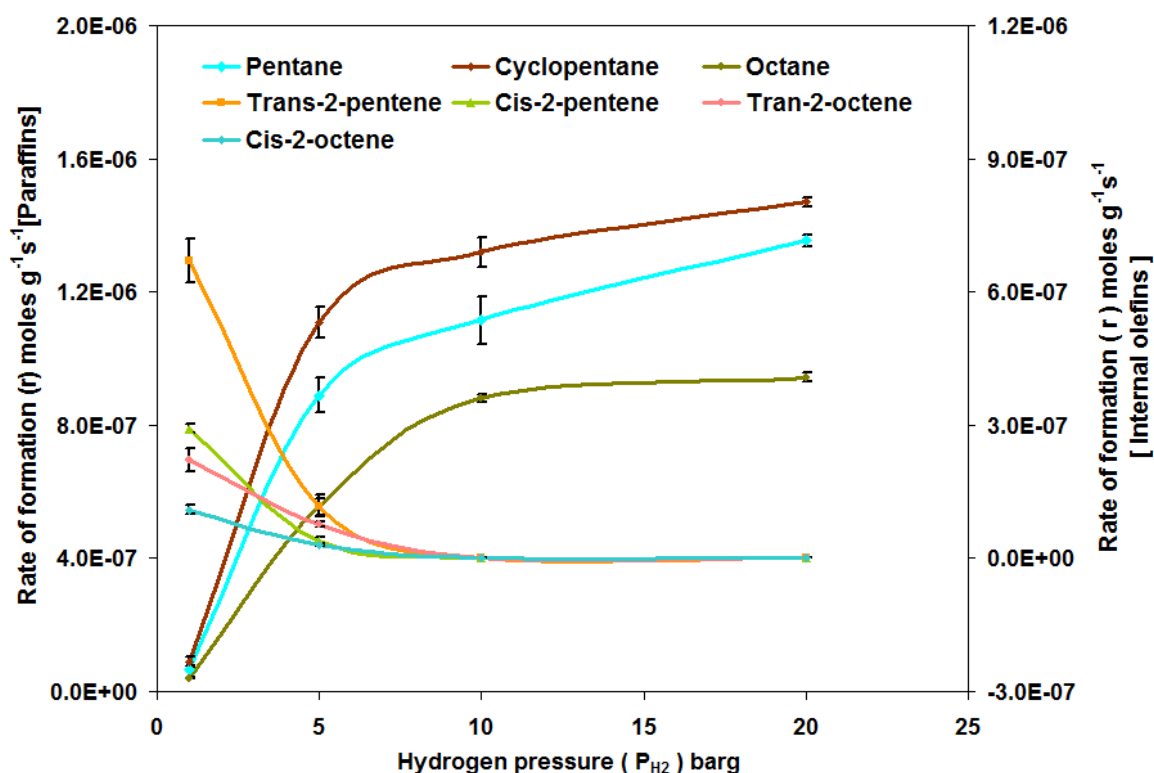
Figure 4.15 Effect of hydrogen partial pressure on hydrogenation of olefinic species of PyGas [P$_{H2}$ = 1-20 barg, P$_T$ = 20 barg, T = 140°C, WHSV$_{PyGas}$ = 4 h^{-1}] (Average rate at steady state)
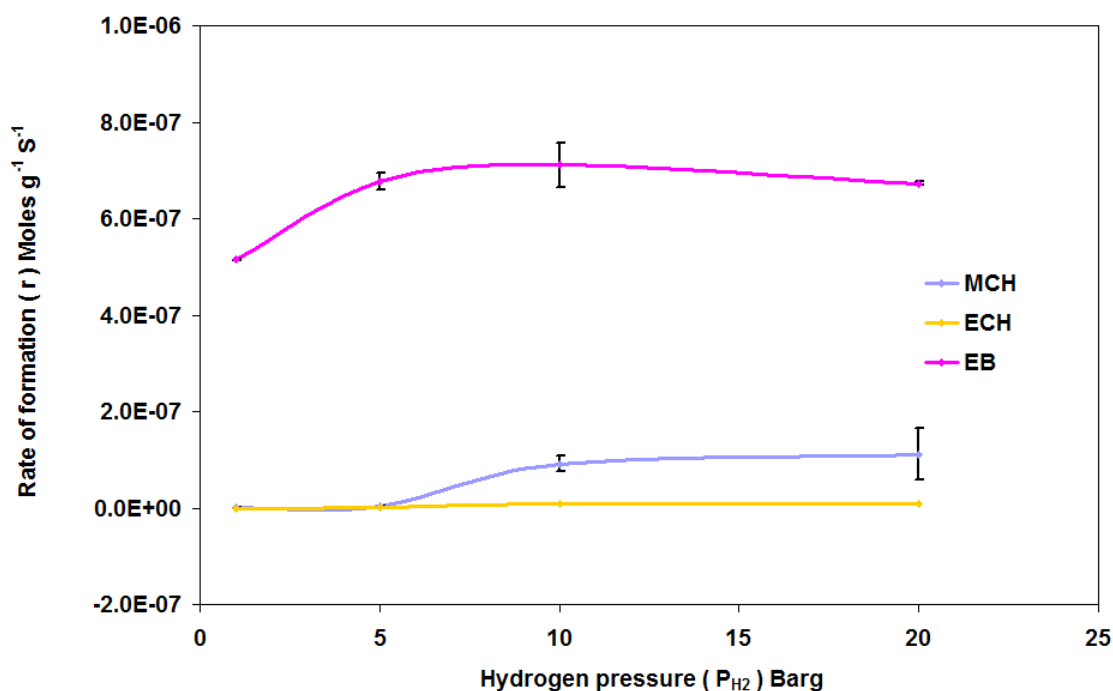
Figure 4.16 Effect of hydrogen partial pressure on hydrogenation of aromatic components of PyGas [P_{H2} = 1-20 barg, P_T = 20 barg, T = 140°C, WHSV$_{PyGas}$ = 4 h^{-1}], (Average rate at steady state)

Similar to the nickel catalyst, the logarithmic form of the empirical rate equation (equation 4.3) was used to determine the apparent orders of hydrogenation/isomerisation of PyGas components reactions over the palladium catalyst. Positive order (1.6) kinetics were observed for the hydrogenation of olefins to saturated paraffins when the hydrogen partial pressure was increased up to 5 barg and then the reaction orders decreased (0.2-0.3) with hydrogen partial pressures in the range of 5 barg to 20 barg. Moreover, the isomerisation of olefins to internal olefins decreased with an increase in hydrogen partial pressure. About negative half to negative first order (-0.7 to -1.2) reaction kinetics were observed for the formation of internal olefins up to 5 barg hydrogen partial pressure and no internal olefin formation was observed with a further increase in hydrogen pressure up to 20 barg. The results obtained were in close agreement with the literature, in which first order kinetics were observed for the hydrogenation of olefinic components during PyGas hydrogenation with an increase in the hydrogen partial pressure and then decrease to zero order kinetics when the surface of the catalyst becomes saturated with hydrogen [46, 84]. The detailed kinetic order data for our system are presented in Table 4.12.

Reactions		Orders of reactions wrt H_2	
Reactants	Products	P_{H2} (1-5 barg)	P_{H2} (5-20 barg)
1-pentene	Pentane	1.6	0.3
1-pentene	Trans-2-pentene	-1.1	-
1-pentene	Cis-2-pentene	-1.2	-
1-octene	Octane	1.6	0.3
1-octene	Trans-2-octene	-0.7	-
1-octene	Cis-2-octene	-0.8	-
Cyclopentene	Cyclopentane	1.6	0.2

Table 4.12 Kinetic of olefin hydrogenation with respect to hydrogen [P_{H2} = 1-20 barg, P_T = 20 barg, T = 140°C, WHSV$_{PyGas}$ = 4 h^{-1}]

A very small amount of aromatic hydrogenation to the corresponding saturated compounds was observed over the palladium catalyst during PyGas hydrogenation at above 5 barg hydrogen partial pressure. However, positive order kinetics were observed with respect to hydrogen. The kinetic order of toluene hydrogenation to methylcyclohexane was observed at about 2.4. Whereas zero order kinetics were noted for the hydrogenation of styrene to ethylbenzene. The zero order kinetics of styrene hydrogenation illustrate the stronger adsorption of the styrene than the other components of PyGas to the catalyst, and similar behaviour has been reported in previous studies [18, 40, 83]. Third order kinetics (2.9) were observed for the further hydrogenation of ethylbenzene to ethylcyclohexane, which is similar to the reaction orders of the toluene hydrogenation to methylcyclohexane. This shows that the hydrogenation of aromatic rings during PyGas hydrogenation over the palladium catalyst followed third order kinetics in the range of 5 barg to 20 barg hydrogen partial pressure. The detailed reaction order data of the aromatic components in PyGas over the palladium catalyst are presented in Table 4.13.

Reactions		Orders of reactions wrt H$_2$	
Reactants	Products		
		P$_{H2}$ (1-20 barg)	
Styrene	Ethyl benzene	0.1	
		P$_{H2}$ (1-5 barg)	P$_{H2}$ (5-20 barg)
Toluene	Methylcyclohexane	-	2.4
Ethylbenzene	Ethylcyclohexane	-	2.9

Table 4.13 Kinetic of aromatic hydrogenation with respect to hydrogen [P$_{H2}$ = 1-20 barg, P$_T$ = 20 barg, T = 140°C, WHSV$_{PyGas}$ = 4 h^{-1}]

To obtain more general and simple reaction kinetics for the hydrogenation of PyGas, the formation of similar components of PyGas were taken combined, as discussed earlier in section 4.2.1.5. The results are presented in Figure 4.17 and the reaction orders are shown in Table 4.14.
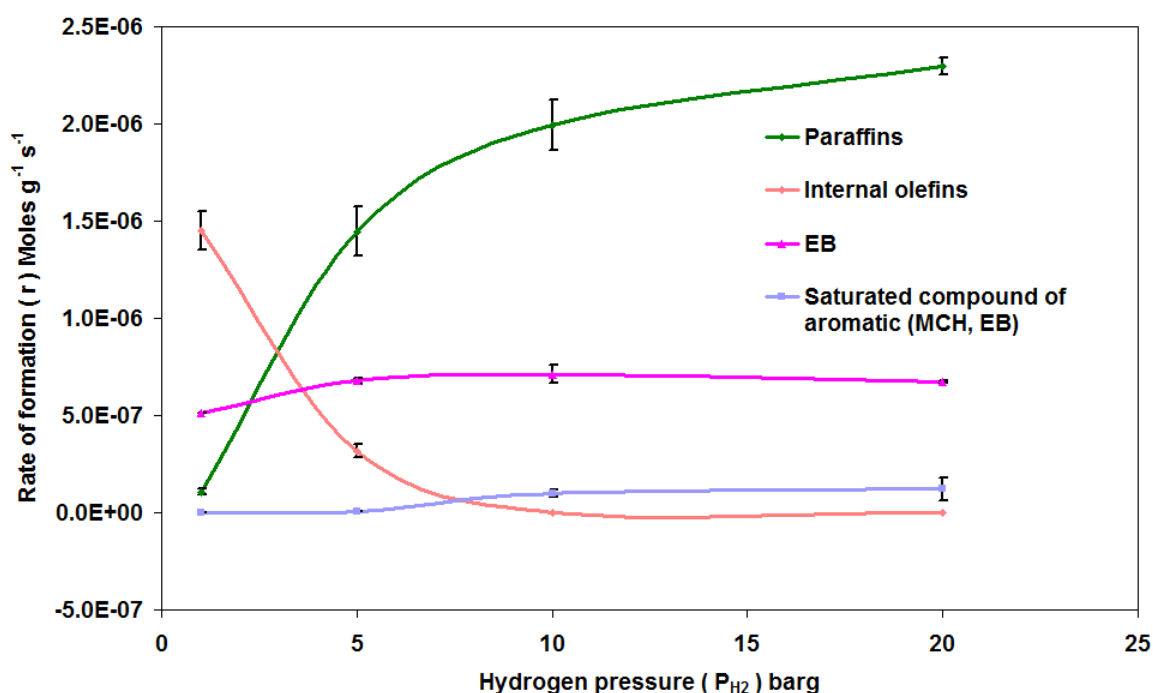
Figure 4.17 Effect of hydrogen pressure on PyGas hydrogenation [P$_{H2}$ = 1-20 barg, P$_T$ = 20 barg, T = 140°C, WHSV$_{PyGas}$ = 4 h^{-1}]

Reactions		Orders of reactions wrt H_2	
Reactants	Products		
Olefin hydrogenation		P_{H2} (1-10 barg) P_{H2} (10-20 barg)	
Olefins (1-pentene, 1-octene, Cyclopentane)	Paraffins (Pentane, Octane, Cyclopentane)	1.6	0.3
Olefins (1-pentene, 1-octene)	Internal olefins	-0.9	-
Aromatic hydrogenation		P_{H2} (1-20 barg)	
Styrene	Ethylbenzene	0.1	
		P_{H2} (1-5 barg) P_{H2} (5-20 barg)	
Aromatics (Toluene, Ethylbenzene)	Saturated compounds of aromatic (MCH + ECH)	-	2.4

Table 4.14 Kinetic of PyGas hydrogenation with respect to hydrogen pressure PyGas [P_{H2} = 1-20 barg, P_T = 20 barg, T = 140°C, WHSV$_{PyGas}$ = 4 h^{-1}]

The hydrogenation of PyGas was also investigated using different WHSV of PyGas (4-8 h^{-1}) with the other reaction conditions kept constant [P_T = 20 barg (25% hydrogen gas mix), P_{H2} = 5, T = 140°C]. The rates of formation of internal olefins increased and rates of paraffins formation slightly decreased or remained constant during PyGas hydrogenation with an increase in the WHSV of PyGas from 4 to 8 h^{-1}. An increase was observed in the rate of formation of ethylbenzene, which is due to a high rate of styrene adsorption onto the catalyst [40, 82, 83, 117]. Aromatic hydrogenation over the palladium catalyst was very low compared to the nickel catalyst. However, the aromatic hydrogenation was still depressed by stronger adsorption of olefins and styrene. The results are presented in Figure 4.18.
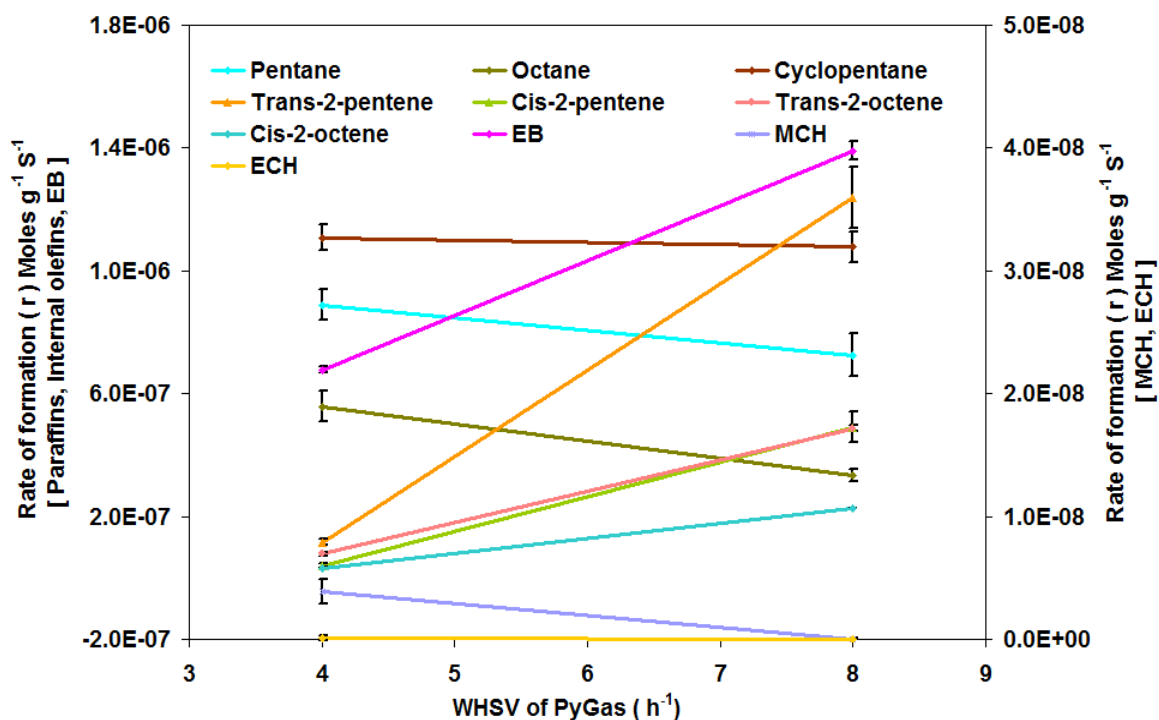
Figure 4.18 Effect of PyGas feed flow rate (WHSV$_{PyGas}$) on hydrogenation of PyGas [WHSV$_{PyGas}$ = 4-8 h^{-1}, T = 140°C, P$_T$ = 20 barg, P$_{H2}$ = 5 barg]

The hydrogenation of PyGas was also investigated using a 50% hydrogen gas mixture instead of a 25% hydrogen gas mixture with different WHSV$_{PyGas}$ (4-8 h^{-1}). The hydrogenation of PyGas decreased with an increase in the WHSV of PyGas from 4 to 8 h^{-1}. However, a smaller increase was observed in the isomerisation of olefins to internal olefins when compared to the reactions using a 25% hydrogen gas mixture. This shows that the olefins were hydrogenated to the respective saturated paraffins and a small amount of isomerisation to internal olefins took place when higher amounts of adsorbed hydrogen were present on the surface of the catalyst.

The aromatic hydrogenation was depressed during PyGas hydrogenation with an increase in WHSV of PyGas from 4 to 8 h^{-1} due to the stronger adsorption of styrene and olefinic species onto the surface of catalyst, which is in close agreement with literature [41, 59]. The effect of PyGas feed flow rate (WHSV$_{PyGas}$ 4-8 h^{-1}) on the rate of formation of different components during PyGas hydrogenation is summarised in Figure 4.19.
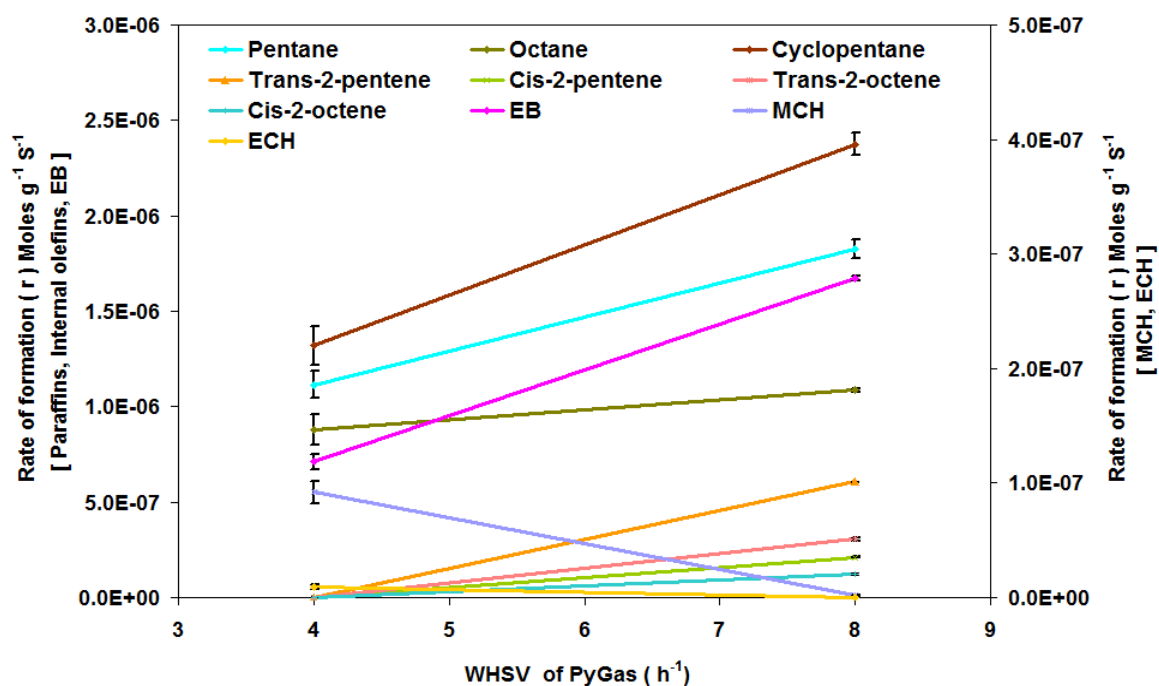
Figure 4.19 Effect of PyGas feed flow rate (WHSV$_{PyGas}$) on hydrogenation of PyGas [WHSV$_{PyGas}$ = 4-8 h^{-1}, T = 140°C, P$_T$ = 20 barg, P$_{H2}$ = 10 barg]

The apparent reaction orders of the PyGas component/s with respect to PyGas were determined by plotting $ln(r_A)$ vs $ln(WHSV_{PyGas})$ using equation (4.8) and are shown in Table 4.15. The hydrogenation of olefins to the saturated paraffins followed 0.0 to -0.7 order kinetics with respect to PyGas during the hydrogenation of PyGas using a 25% hydrogen gas mixture. This increased to positive order kinetics (0.3 to 0.8) using a higher hydrogen partial pressure (50% hydrogen gas mixture). Positive order kinetics were observed for olefins isomerisation to internal olefins with an increase in the WHSV of PyGas from 4 h^{-1} to 8 h^{-1} with both the 25% and 50% hydrogen gas mixtures. Moreover, positive order kinetics were also observed for styrene hydrogenation to ethylbenzene with respect to PyGas.

Negative order kinetics with respect to PyGas were noted for aromatic hydrogenation over the palladium catalyst during hydrogenation of PyGas. The hydrogenation of aromatics over palladium catalyst generally followed zero order reaction kinetics with respect to the aromatic concentration/partial pressure when hydrogenation of the individual aromatic compounds are carried out [46, 63, 74, 130]. This suggests that the negative order reaction of aromatic components to their corresponding saturated compounds during PyGas hydrogenation is due to the competitive adsorption of styrene, olefins and

aromatics on the same active sites over the palladium catalyst and the adsorption of aromatic compounds was depressed by the stronger adsorption of styrene and olefins.

Reactions		Orders of Reactions wrt PyGas (WHSV$_{PyGas}$ 4-8 h^{-1})	
Reactants	Products	P_{H2} = 5 barg, P_T = 20 barg (25% hydrogen gas)	P_{H2} = 10 barg, P_T = 20 barg (50% hydrogen gas)
1-pentene	Pentane	-0.3	0.7
1-pentene	Trans-2-pentene	3.4	-
1-pentene	Cis-2-pentene	3.6	-
1-octene	Octane	-0.7	0.3
1-octene	Trans-2-octene	2.6	-
1-octene	Cis-2-octene	2.9	-
Cyclopentene	Cyclopentane	0.0	0.8
Styrene	Ethylbenzene	1.0	1.2
Ethylbenzene	Ethylcyclohexane	-	-
Toluene	Methylcyclohexane	-	-

Table 4.15 Kinetic of PyGas hydrogenation with respect to PyGas (WHSV$_{PyGas}$ 4-8 h^{-1})

To obtain more general and simple kinetics for PyGas hydrogenation, the formations of similar components of PyGas were taken combined, as discussed earlier in section 4.2.1.5. The results are presented in Figure 4.20-21 and the apparent reaction orders obtained are shown in Table 4.16.
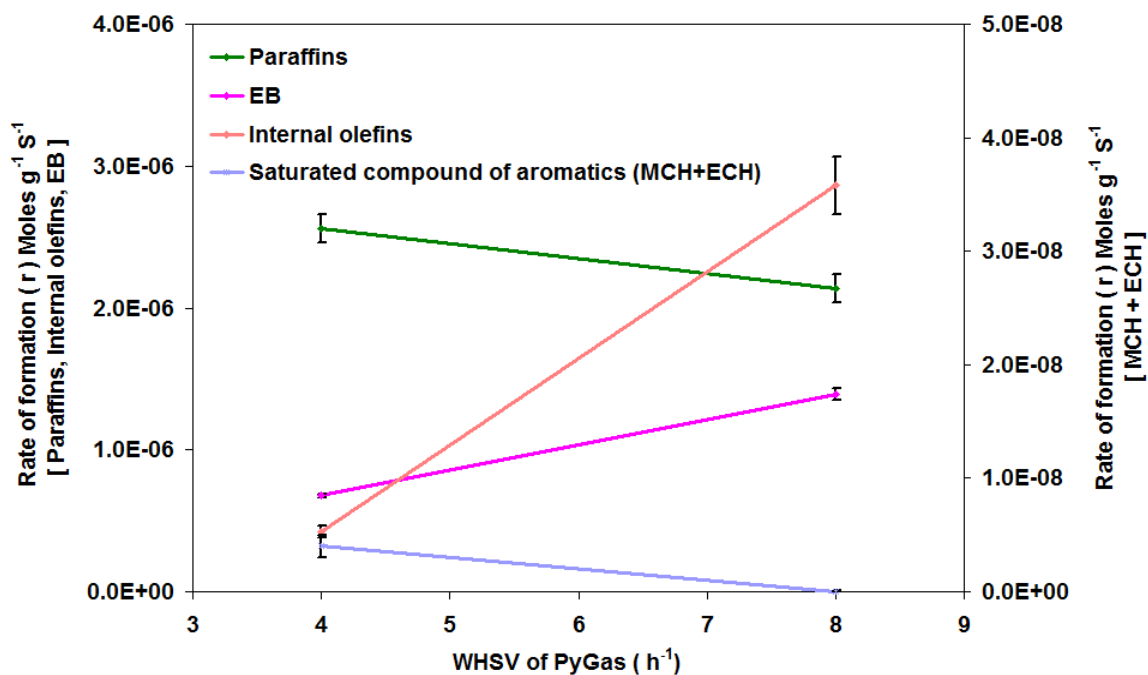
Figure 4.20 Effect of PyGas feed flow rate (WHSV$_{PyGas}$) on hydrogenation of PyGas, [WHSV$_{PyGas}$ = 4-8 h^{-1}, T = 140°C, P$_T$ = 20 barg, P$_{H2}$ = 5 barg]
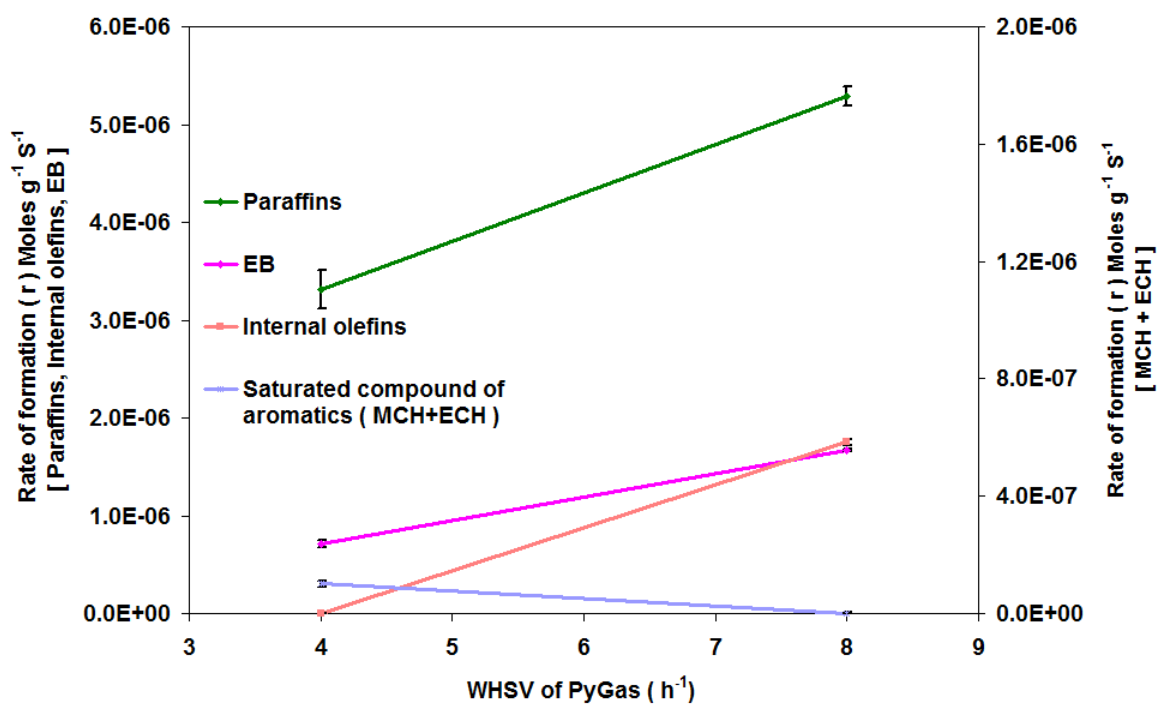
Figure 4.21 Effect of PyGas feed flow rate (WHSV$_{PyGas}$) on hydrogenation of PyGas [WHSV$_{PyGas}$ = 4-8 h^{-1}, T = 140°C, P$_T$ = 20 barg, P$_{H2}$ = 10 barg]

Reactions		Orders of reactions wrt PyGas (WHSV$_{PyGas}$ 4-8 h^{-1})	
Reactants	**Products**	P$_{H2}$ = 5 barg, P$_T$ = 20 barg (25 % Hydrogen gas used)	P$_{H2}$ = 10 barg, P$_T$ = 20 barg (50 % Hydrogen gas used)
Olefins (1-pentene, 1-octene, Cyclopentane)	Paraffins (Pentane, Octane, Cyclopentane)	-0.2	0.7
Olefins (1-pentene, 1-octene)	Internal olefins	2.8	-
Styrene	Ethylbenzene	1.0	1.2
Aromatics (Toluene, Ethylbenzene)	Saturated compounds of aromatic (MCH+ECH)	-	-

Table 4.16 Kinetic of PyGas hydrogenation with respect to PyGas (WHSV$_{PyGas}$ 4-8 h^{-1})

4.3 Deactivation and regeneration of catalyst

Coke deposition is believed to be the main reason for catalyst deactivation during PyGas hydrogenation [11, 12]. The deposition of gum and carbonaceous residues on catalyst, block the active sites and reduce the accessibility of reactant to these sites. Consequently, the activity of the catalyst decreases. The heavy build up of coke in pores may also fracture the support material which can cause the plugging of reactor voids [87, 95]. Therefore, when deactivation reaches a level where conversion, selectivity or other process parameters are below the required specification, then the catalyst must be replaced or regenerated. The regeneration and reuse of the catalyst is always the preferable option. In this study, a substantial amount of coke deposition took place on the catalyst during PyGas hydrogenation, although no noticeable decrease was found in the activity of both the Ni/Al$_2$O$_3$ and Pd/Al$_2$O$_3$ catalysts during 76 hours of reaction. However, it is believed that the catalysts would be deactivated due to further coke deposition when the reactions are run for longer periods. Accordingly, the amount and nature of coke deposition on the post reaction catalysts was investigated and the catalysts were regenerated by *in-situ* TPO.

4.3.1 Coke deposition during PyGas hydrogenation and subsequent regeneration of Ni/Al$_2$O$_3$

Coke deposition took place during PyGas hydrogenation over the Ni/Al$_2$O$_3$ which blocked the catalyst pores and consequently reduced the surface area of the post reaction catalyst, as shown in the Table 4.17.

Catalyst	Surface Area (m^{2}g^{-1})	Pore Volume (cm^{3}g^{-1})	Average Pore diameter (Å)
Ni/Al$_2$O$_3$	93	0.35	152
Ni/Al$_2$O$_3$ (Reduced)	106	0.39	150
Ni/Al$_2$O$_3$ (Post reaction)	78	0.31	159
Ni/Al$_2$O$_3$ (Regenerated)	100	0.38	154

Table 4.17 BET analysis of Ni/Al$_2$O$_3$ (fresh, reduced, post reaction and regenerated catalyst), [Reaction conditions: T = 140°C, WHSV$_{PyGas}$ = 4 h^{-1}, P$_{H2}$ = 20 barg]

The amounts and nature of coke deposition on the post reaction nickel catalysts were investigated and the catalysts were regenerated by *in-situ* TPO. The detailed results are shown in Section 3.2.2. Figure 4.22 is an example of the *in-situ* TPO of Ni/Al$_2$O$_3$.
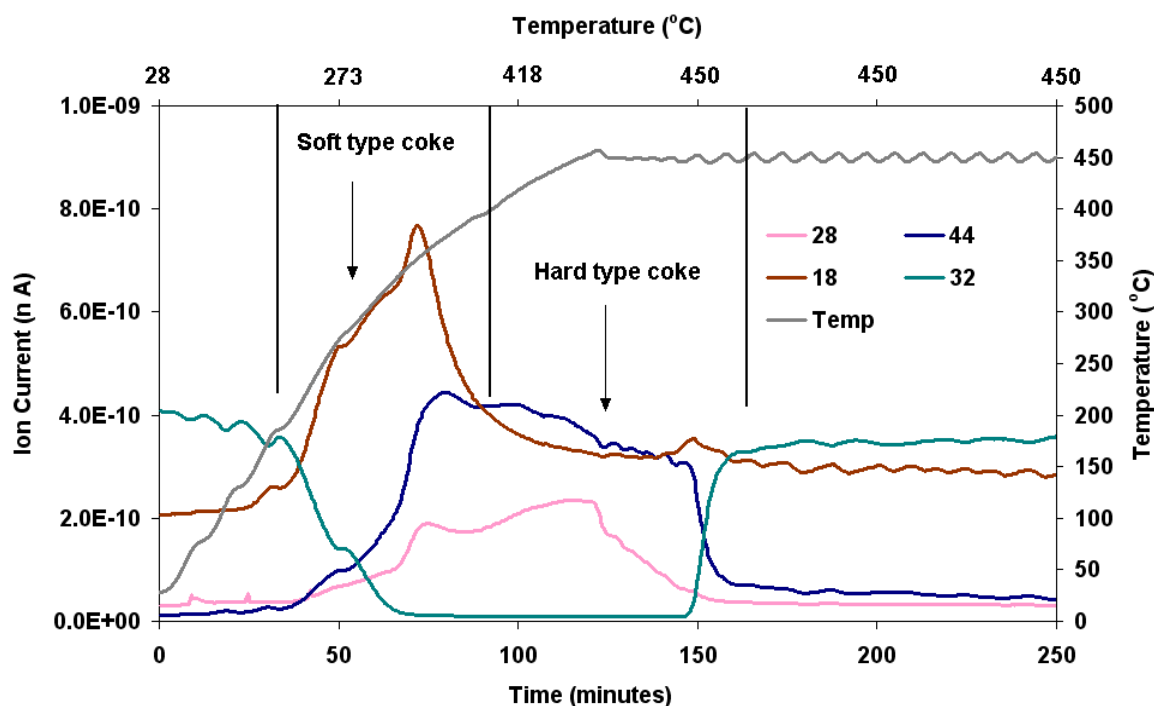
Figure 4.22 Post reaction *in-situ* TPO of Ni/Al$_2$O$_3$ catalyst [Reaction conditions: T = 140°C, WHSV$_{PyGas}$ = 4 h^{-1}, P$_{H2}$ = 20 barg]

The coke deposited on the catalyst was oxidised to CO_2/CO and H_2O in the presence of oxygen during the *in-situ* TPO. However, the combustion of coke is not simple and a number of reactions could take place during the *in-situ* TPO, which mainly depend on the nature of coke, temperature during the TPO and amount of oxygen available. The main possible reactions are summarised below.

$$C + O_2 \longrightarrow CO_2$$

$$C + \tfrac{1}{2}\,O_2 \longrightarrow CO$$

$$2CH + 2\tfrac{1}{2}\,O_2 \longrightarrow 2CO_2 + H_2O$$

$$2CH + 1\tfrac{1}{2}\,O_2 \longrightarrow 2CO + H_2O$$

$$CH_2 + 1\tfrac{1}{2}\,O_2 \longrightarrow CO_2 + H_2O$$

$$CH_2 + O_2 \longrightarrow CO + H_2O$$

$$\dots\dots\dots\dots\dots\dots\dots\dots\dots\dots\dots\dots\dots\dots\dots$$
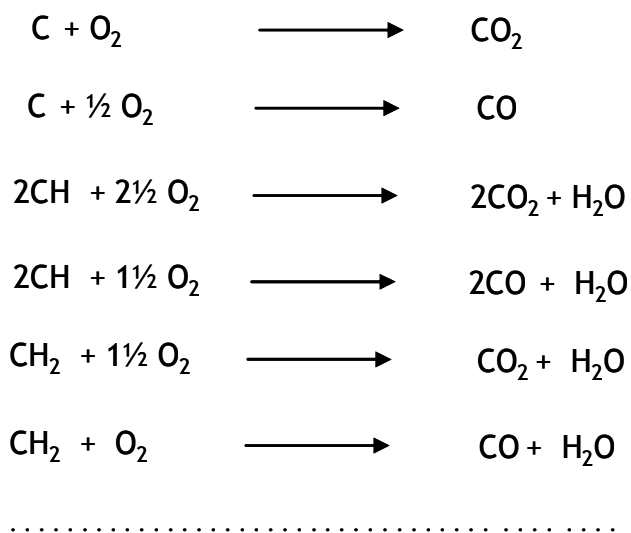
These can be generalised as;

$$CH_x + (1 + x/4)\,O_2 \longrightarrow CO_2 + x/2\,H_2O$$

$$CH_x + (1/2 + x/4)\,O_2 \longrightarrow CO + x/2\,H_2O$$

or

$$CH_x + (a + b/2 + x/4)\,O_2 \longrightarrow a\,CO_2 + b\,CO + x/2\,H_2O$$
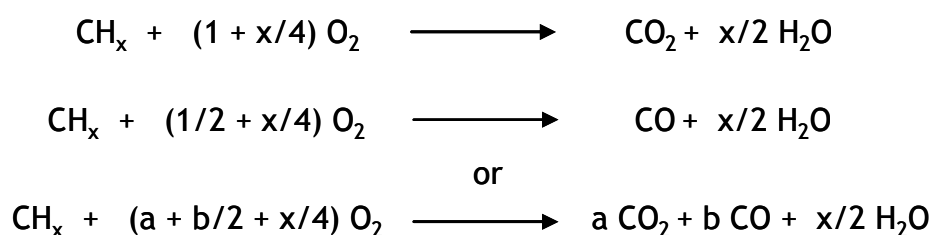
Hence the amounts of CO_2, CO and H_2O evolution during the *in-situ* TPO mainly illustrate the quantity and nature of coke deposited. The amount of CO_2 and CO produced and amount of O_2 consumed is proportional to the amount of coke deposited on the catalyst. The evolution of H_2O observed below 200^oC can be ascribed to physisorbed H_2O on the catalyst and the H_2O produced during coke combustion was evolved above 200^oC. The ratio of H_2O to CO_2/CO illustrated the H/C ratio present in the coke. A higher ratio of H_2O to CO_2/CO was observed in the initial stages before a decrease occurred in the ratio of H_2O to CO_2/CO above 400^oC. This suggests that the combustion of soft coke occurred first in the initial stages of the TPO and subsequently the removal of hard coke took place at higher temperatures.

The formation of CO_2, CO, H_2O and the consumption of O_2 primarily reveals the amount and nature of coke and therefore most previous studies monitored only these species during *in-situ* TPO. However, the evolutions of other species like un-oxidised hydrocarbons e.g. reactants and products, and hydrogen could also take place. Therefore the evolution of the following m/z fragments were also recorded during the *in-situ* TPO: 68 (cyclopentene), 70 (1-pentene), 72 (pentane), 78 (benzene), 92 (toluene), 98 (methylcyclohexane), 104 (styrene), 106 (ethyl benzene), 112 (1-octene/ethylcyclohexane), 114 (octane) and 2 (H_2) for a detailed analysis of the deposited coke. The analysis showed that reasonable amounts of styrene, benzene and H_2 with small amounts of 1-pentene, cyclopentene, 1-octene toluene and ethylcyclohexane evolved during the TPO, as shown in Figure 4.23.

No considerable amount of saturated hydrocarbons *i.e.* reaction products, were found on the catalyst during the TPO analysis. This suggests that hydrogenated products formed in the reaction are weakly adsorbed on the catalyst and therefore desorbed very easily. Consequently no significant amounts of hydrogenated hydrocarbons remained on the surface of catalyst. Whereas, small levels of cyclopentene, 1-pentene, 1-octene and toluene desorption at temperatures below $200^{\circ}C$ suggest that a small amount of the reactant species remained on the surface of catalyst.

Benzene was neither fed within the reactants nor detected in the products, however a considerable amount of benzene evolution took place which is most likely a fragment of the styrene and other aromatics/polyaromatic species that were present on the surface of the catalyst. Stepwise evolution of styrene and benzene at different temperatures during the TPO illustrates that various polymers of aromatic species were present on the surface of the catalyst. The evolution of benzene and styrene below $250^{\circ}C$ was mainly from adsorbed aromatic compounds and their oligomers while desorption at higher temperature was from polymerised aromatic species (polystyrene/polyaromatics). Previous studies also revealed that the evolution of styrene (m/z = 104) and benzene (m/z = 78) at temperatures below $250^{\circ}C$ are due to adsorbed compounds and oligomers present on the catalyst while evolution at higher temperatures (300-$450^{\circ}C$) are mainly from polymerised aromatic species (polystyrene/poly-aromatics) [137-142] . Therefore these results suggest that the polymerisation of

coke precursors took place and mainly produced polyaromatic species and a very small amount of oligomers present on the surface of the catalyst.

Moreover, the evolution of hydrogen was observed at temperatures above 340°C. This result shows the hard type coke also had a reasonable hydrogen content however it is desorbed in the form of hydrogen rather than H_2O.
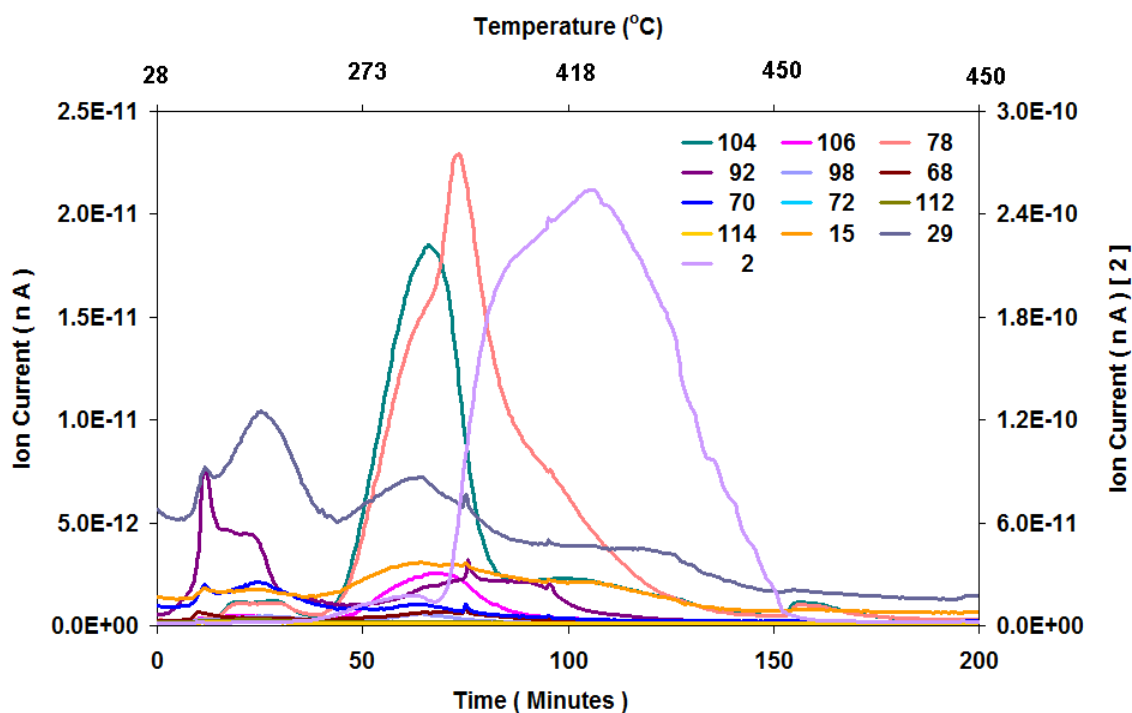
Figure 4.23 Evolution of other species during *in-situ* TPO of Ni/Al$_2$O$_3$ catalyst [Reaction conditions: T = 140°C, WHSV$_{PyGas}$ = 4 h^{-1}, P$_{H2}$ = 20 barg]

The results show that the combustion of soft coke with high hydrogen content took place first at lower temperatures and produced CO_2/CO and H_2O. Subsequently, hard coke combustion occurred at higher temperatures and produced H_2 instead H_2O.

The evolution of H_2 at higher temperatures was most likely due to selective oxidation of carbon to CO_2 and CO because of the comparatively high content of carbon in the hard coke. However, other possible routes could also be considered, like gasification and water gas shift reactions because water was produced in the reaction which could further react with coke or CO and produce H_2, as shown below;

$$2C \; + \; 3\,H_2O \longrightarrow CO_2 + CO + \; 3H_2 \qquad \text{(Gasification reaction)}$$

$$CO \; + \; H_2O \longrightarrow CO_2 + H_2 \qquad \text{(Water-Gas shift reaction)}$$
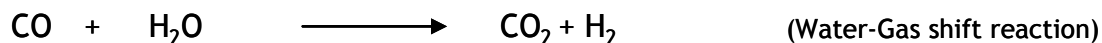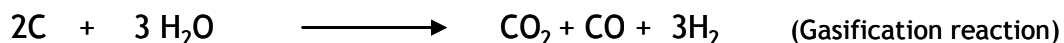
However whichever route was followed, the reaction could be reduced to the below form by ignoring intermediate steps during the TPO;

$$CH_x \; + \; (a + b/2)\,O_2 \longrightarrow a\,CO_2 + b\,CO + \; x/2\,H_2$$
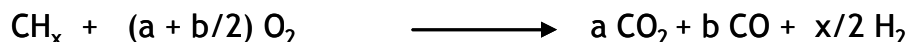
The investigation of the hydrogen species during the TPO is an attractive advancement and demonstrates a supplementary insight into the nature of coke and regeneration process. Therefore, monitoring of H_2 evolution is very important during the TPO. Ignoring the evolution of hydrogen during the TPO and determining the C/H ratio solely from CO_2/CO and H_2O evolution could underestimate the hydrogen content and misinterpret the C/H ratio of coke.

Carbonaceous residue formation was mainly due to the polymerisation of coke precursors present in PyGas [7, 11, 17]. Styrene was found to be the main precursor of coke formation, as discussed in sections 4.3.1.1 and 4.3.1.2. The deposited species convert to polyaromatic hydrocarbons which further convert to highly condensed polyaromatic residues and hard type coke with the passage of time [53, 95]. The coke formation during hydrogenation of PyGas is summarised in Figure 4.24.

Coke and gum precursors
(styrene, olefins and aromatic)

↓

Polymerised hydrocarbons

↓

Polyaromatic hydrocarbons

↓

Carbonaceous residues (Coke)
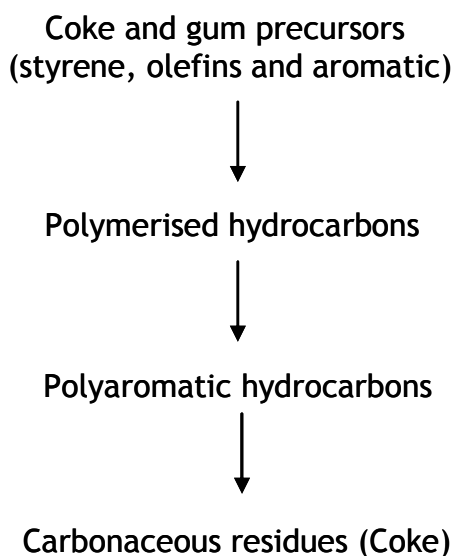
Figure 4.24 Carbonaceous residues (Coke) formation [53, 95]

The BET analysis of the regenerated catalyst was performed. The surface area and pore volume of both fresh and regenerated catalysts were found to be similar, which suggests that the surface area lost due to coke deposition was successfully recovered during the regeneration of the catalyst by *in-situ* TPO. This illustrates that no significant support sintering occurred in the catalyst, either during the reaction or in the regeneration process. Both the fresh and regenerated catalyst samples showed similar XRD patterns, which suggests that no phase change had occurred during the reaction or the regeneration process. These results illustrate that coke deposition is the main cause of catalyst deactivation during PyGas hydrogenation, which is in close agreement with previous studies [11-13].

4.3.1.1 Effect of reaction temperature on coke deposition

The deposition of coke is highly dependent upon the reaction conditions and especially on the reaction temperature. The increase in reaction temperature during PyGas hydrogenation not only increased the amount of coke deposition but also produced a more condensed hydrogen deficient type coke. The TPO results of catalysts used in the reactions preformed at $140^{\circ}C$ and $200^{\circ}C$ are compared below in Figure 4.25 and detailed results are described in section 3.2.2.1.
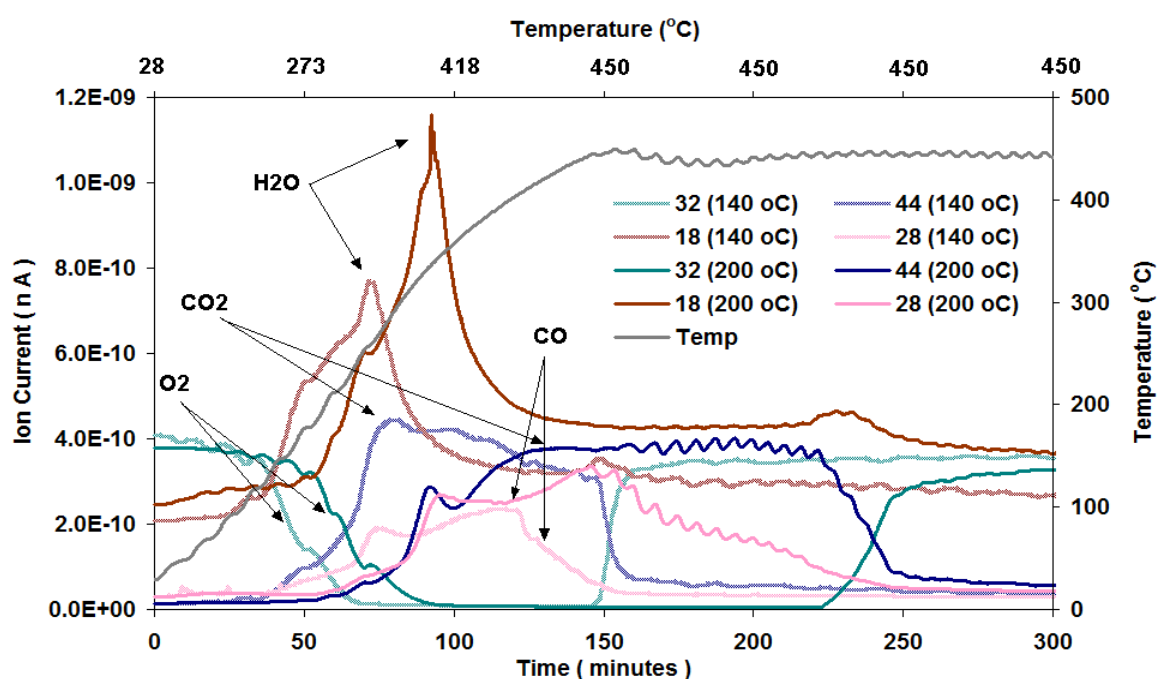
Figure 4.25 Comparison of *in-situ* TPO of Ni/Al_2O_3 at reaction temperature $140^{\circ}C$ and $200^{\circ}C$ [$WHSV_{PyGas}$ = 4 h^{-1}, P_{H2} = 20 barg]

These results show that a higher amount of coke deposition was observed with an increase in the reaction temperature. The evolution of CO_2, CO and H_2O also start at comparatively higher temperatures suggesting hard type coke formation at the higher reaction temperature. A considerable increase was also observed in the evolution of aromatic species (styrene and benzene) and hydrogen in the TPO with the increase in reaction temperature, as shown in Figure 4.26. However, the evolution of other species *i.e.* cyclopentene, 1-pentene, pentane, toluene, methylcyclohexane, ethylbenzene, 1-octene, ethylcyclohexane and octane were found to be similar in both TPOs.
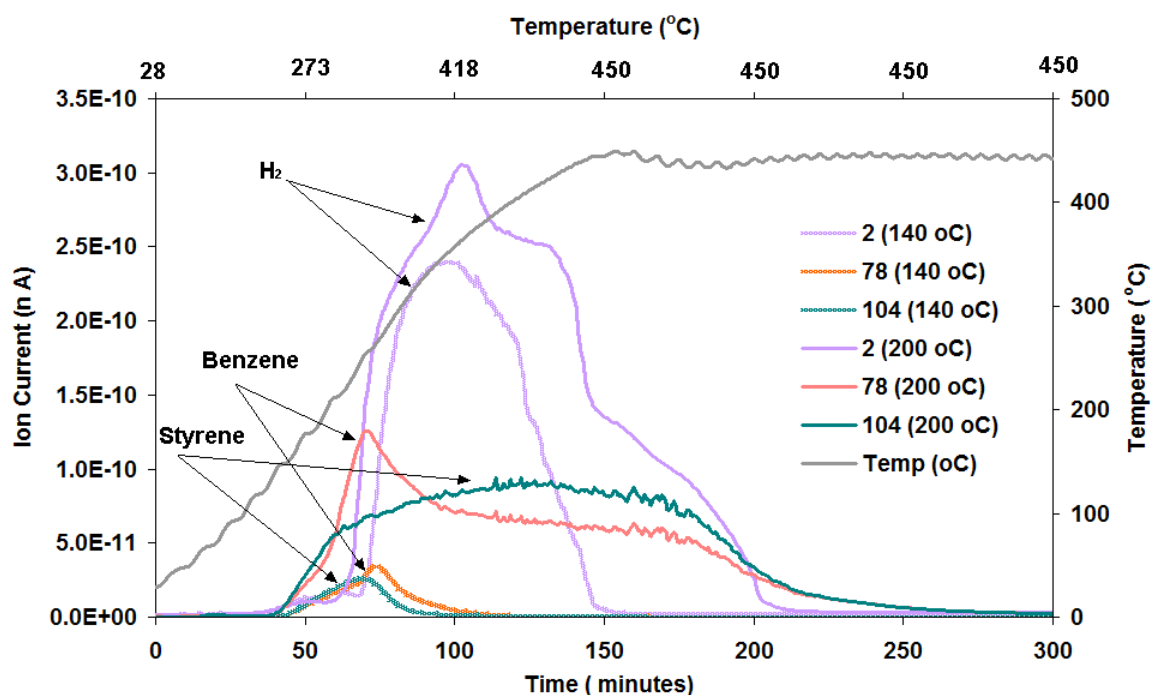
Figure 4.26 Comparison of aromatic species and H_2 evolution during *in-situ* TPO of Ni/Al$_2$O$_3$ at reaction temperature 140°C and 200°C [WHSV$_{PyGas}$ = 4 h^{-1}, P$_{H2}$ = 20 barg]

The significant increase in the amounts of aromatic species (styrene and benzene) evolved in the TPO suggests that the formation of condensed polyaromatic (hard type) coke increased with a higher reaction temperature, which is in close agreement with previous studies [93, 99].

A distinct difference was also noted in the mode of H_2 evolution in the TPO with an increase in reaction temperature. Evolution of H_2 was observed with the evolution of CO_2/CO in the TPO of the catalyst used in the reaction temperature at 140°C. However, the evolution of H_2 in the TPO of the catalyst used at 200°C showed a stepwise decrease until finally no hydrogen was evolved while the evolution of CO_2/CO was still observed, as shown in Figures 4.25-26. This

indicates the presence of various types of carbonaceous residues on the catalyst used at the higher reaction temperature.

These results illustrate that the combustion of hydrogen rich coke (soft coke) occurred at lower temperatures and produced CO_2/CO and H_2O. Subsequently, the combustion of hydrogen deficient type coke took place and mainly produced CO_2/CO and H_2. Finally the evolution of CO_2/CO with no evolution of H_2 at higher temperature shows the combustion of hard coke took place during TPO of the catalyst used at $200^\circ C$.

The amount of oxygen consumed during the TPO is directly proportional to amount of coke deposited on the catalyst. Although the amount of oxygen consumed can not give an accurate value of coke deposition due to the number of possible reactions of coke with oxygen as explained earlier in this section. However, reasonable estimates can be obtained by measuring oxygen consumption during the TPO. Therefore, the amount of oxygen consumed during the *in-situ* TPOs was calculated as described in section 2.5.5 and shown in Figure 4.27. These results show a linear increase in coke deposition with an increase in reaction temperature.
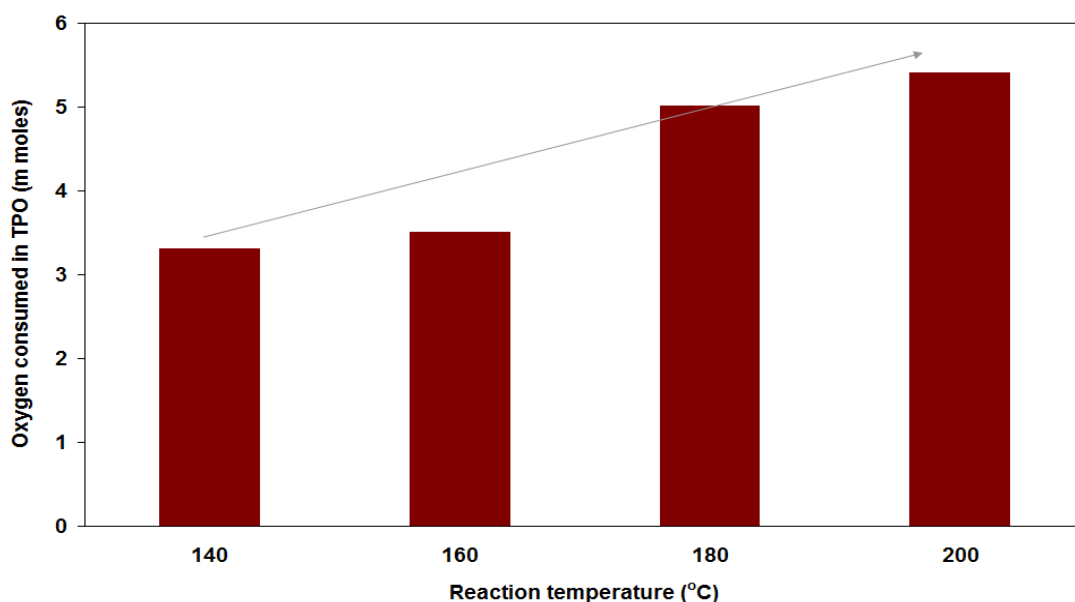
Figure 4.27 Oxygen consumption during *in-situ* TPO of Ni/Al$_2$O$_3$ catalysts, [T = 140-200°C, P$_{H2}$ = 20 barg, WHSV$_{PyGas}$ = 4 h^{-1}]

The carbon balance of each species was determined at each reaction temperature to investigate the main precursors of coke formation and are shown

in Figure 4.28. Styrene was observed to be the main precursor of coke formation, which is in close agreement with previous studies [11, 12]. However the olefins also contribute a reasonable amount to coke deposition. The carbon balance of styrene significantly decreased with an increase in the reaction temperature which suggests a higher amount of styrene polymerisation to coke deposition at the higher reaction temperature.
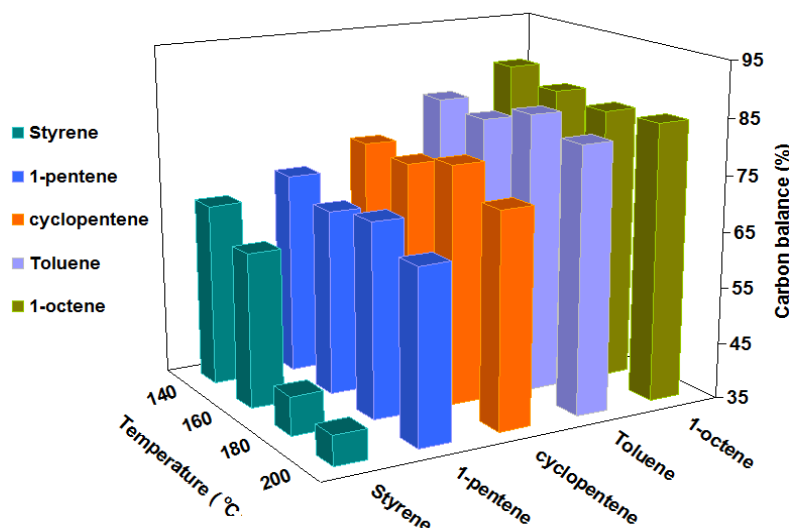
Figure 4.28 Carbon balance of PyGas components [T = 140-200°C, P$_{H2}$ = 20 barg, WHSV$_{PyGas}$ = 4 h^{-1}]

These results illustrate that an increase in the reaction temperature of PyGas hydrogenation not only increases the amount of coke deposition on the catalyst but also the nature of coke changes to a condensed polyaromatic type with a higher C/H ratio.

4.3.1.2 Effect of hydrogen partial pressure on coke deposition

A high amount of coke precursor polymerisation to coke takes place, when a small amount of hydrogen is available on the surface of the catalyst. Conversely, the polymerisation to coke can be depressed when a high level of hydrogen is present on the surface of the catalyst. Therefore, coke deposition on the catalysts increased with a decrease in the hydrogen partial pressure during PyGas hydrogenation. The effect of hydrogen partial pressure on coke deposition was investigated on the nickel catalyst and the results are shown in section 3.2.2.2. The results of the TPOs of the catalysts used in the reactions at 1 barg and 20 barg hydrogen partial pressure in 20 barg total reaction pressure are compared in this section, which is shown in Figure 4.29.
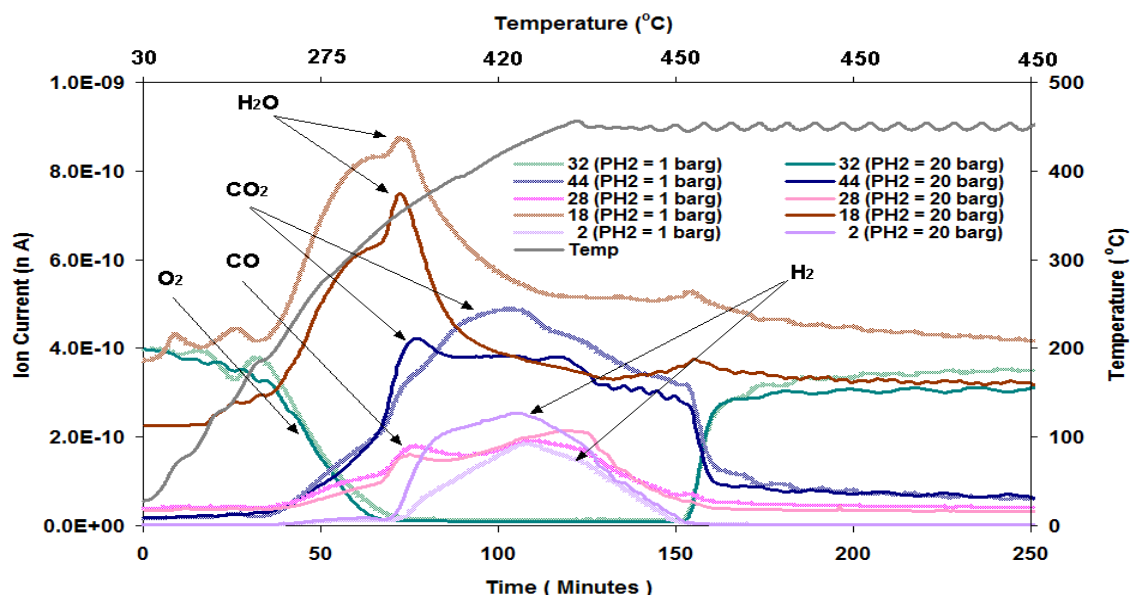
Figure 4.29 Comparison of *in-situ* TPO of Ni/Al$_2$O$_3$ at 1 barg and 20 barg hydrogen partial pressure [WHSV$_{PyGas}$ = 4 h^{-1}, T = 140°C, P$_T$ = 20 barg]

The results show that a higher amount of CO$_2$ and a lower amount of H$_2$ evolution was observed when the reaction was performed with 1 barg hydrogen partial pressure. This suggests that a higher amount of coke deposition with a comparatively higher C/H ratio occurred at a lower hydrogen partial pressure. However, no considerable difference was noted in the consumption of O$_2$ in the TPOs. Moreover, the evolution of aromatic species like styrene, benzene and aliphatic hydrocarbons species were found to be similar in both TPOs.

The carbon balance results also showed a decrease in the carbon balance of PyGas components with a decrease in hydrogen partial pressure, as shown in Figure 4.30.
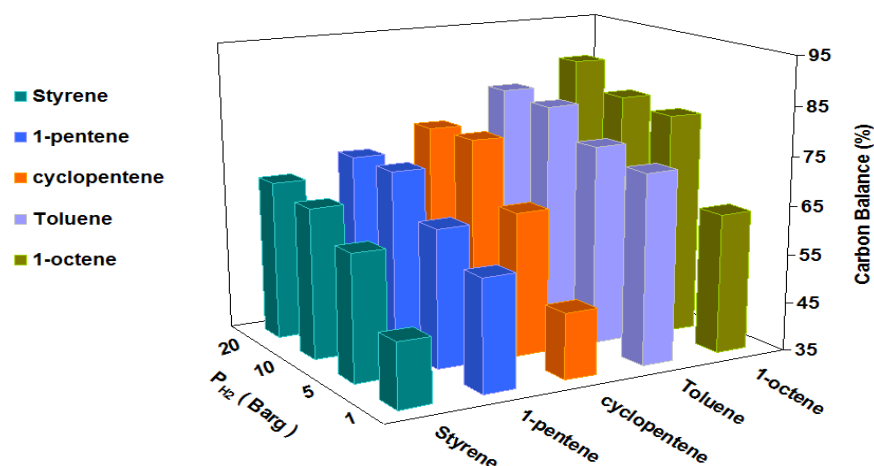
Figure 4.30 Carbon balance of PyGas components, [P$_{H2}$ = 1-20 barg, P$_T$ = 20 barg, T = 140°C, WHSV$_{PyGas}$ = 4 h^{-1}]

These results illustrate that coke deposition increased with a decrease in the hydrogen partial pressure, which is in close agreement with the literature [2, 11]. However, the effect was not as pronounced as that seen with an increase in the reaction temperature. The C/H ratio illustrates that the coke remained soft and did not convert to a very hard type coke with a decrease in hydrogen partial pressure at the lower reaction temperatures.

4.3.1.3 Effect of total reaction pressure on coke deposition

The coke deposition on the nickel catalyst was also investigated at different total reaction pressures (10 barg and 20 barg) during PyGas hydrogenation and the TPOs results are compared in Figure 4.31.
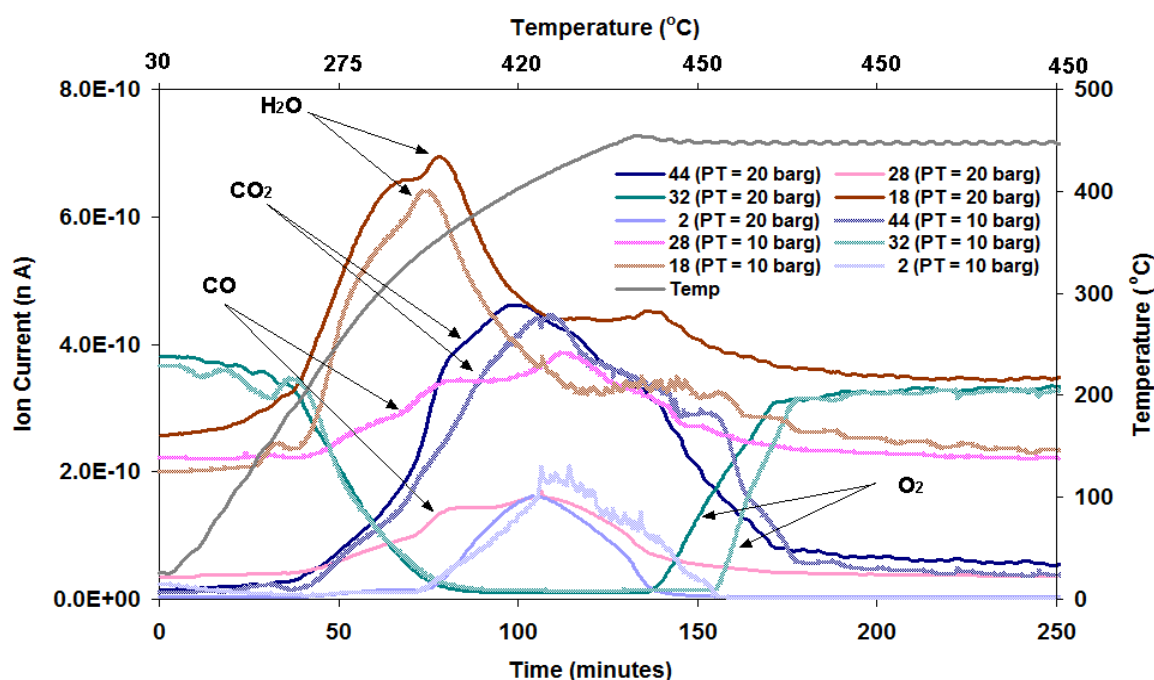
Figure 4.31 Comparison of *in-situ* TPO of Ni/Al$_2$O$_3$ at 10 barg and 20 barg total reaction pressure (50% hydrogen gas mixture) [WHSV$_{PyGas}$ = 4 h^{-1}, T = 140°C]

An increase was observed in the amount of oxygen consumption in the TPO when the reaction was performed at a lower total pressure (~10 barg). A small increase was observed in the evolution of CO$_2$ in the TPO of the catalyst that was used in the reaction at 10 barg total reaction pressure, however no considerable change was observed in the evolution of H$_2$O and H$_2$. Moreover, similar amounts of aromatic species *i.e.* benzene, styrene, toluene, methylcyclohexane, ethylcyclohexane and ethylbenzene, and aliphatic species *i.e.* cyclopentene, 1-pentene, pentane, 1-octene, and octane evolution were observed in the TPOs of the catalysts that were used in the reactions with 10 and 20 barg total reaction

pressure. These results illustrate that coke deposition on the catalyst increased with a decrease in total reaction pressure, which is in close agreement with previous studies [2]. However, no significant change was observed in the nature of coke.

4.3.1.4 Effect of PyGas feed flow rate (WHSV$_{PyGas}$) on coke deposition

The effect of increasing WHSV of PyGas from 4 h^{-1} to 8 h^{-1} on the coke deposition was also investigated with the other reaction conditions kept constant. The WHSV$_{PyGas}$ increased from 4 h^{-1} to 8 h^{-1} by doubling the feed flow rate of PyGas during the reaction, while the GHSV of the reaction increased only slightly from 1360 h^{-1} to 1415 h^{-1}. The TPOs of the post reaction catalysts carried out at WHSV$_{PyGas}$ 4 h^{-1} and 8 h^{-1} are compared in Figure 4.32.
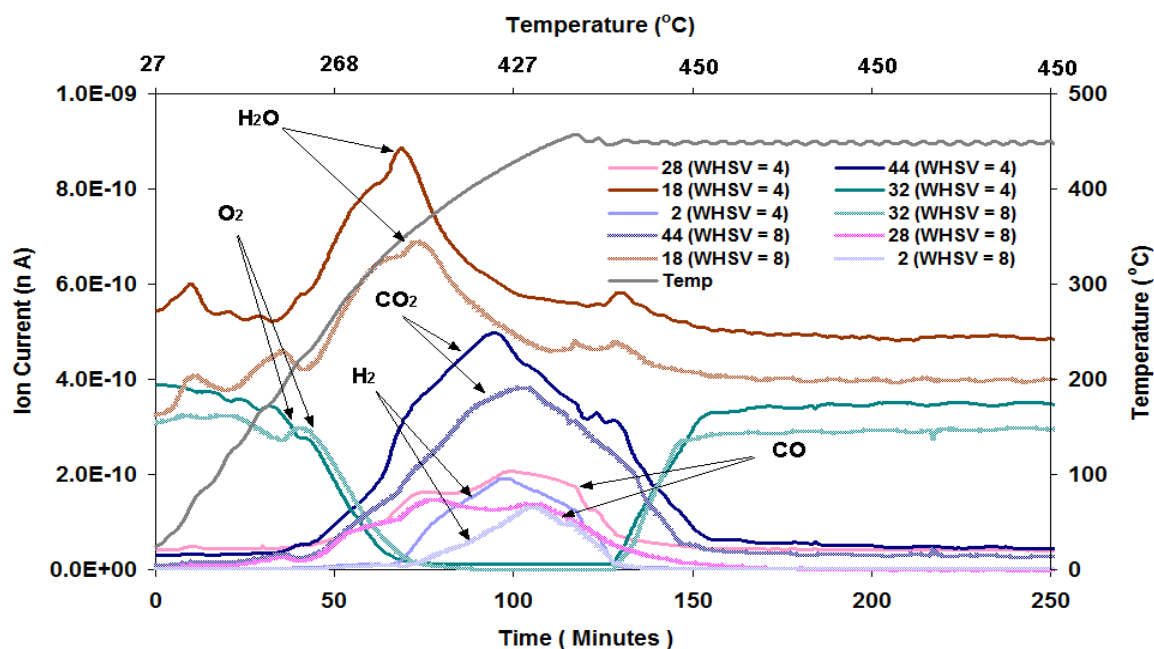
Figure 4.32 Comparison of *in-situ* TPO of Ni/Al$_2$O$_3$ at WHSV$_{PyGas}$ 4 h^{-1} and 8 h^{-1} [T = 140°C, P$_T$ = 20 barg, P$_{H2}$ = 5 barg]

The amount of oxygen consumed in both TPOs was practically the same, however a decrease was observed in the amount of CO$_2$ and CO produced when the WHSV of PyGas was 8 h^{-1}. A decrease in coke deposition was most likely due to a short residence period of the adsorbed species on the catalyst because the amount of reactant increased whilst the amount of catalyst and hence active sites remained constant. Figoli *et al*. [143] observed similar behaviour and a decrease was observed in the coke deposition with an increase in the naptha feed flow rate (WHSV$_{Naptha}$) during the naptha reforming over a alumina supported platinum catalyst.

The evolution of H_2O became slightly broader with an increase in $WHSV_{PyGas}$, which suggests that the coke deposited on the catalyst was comparitively soft type carbonaceous residues. A difference was also noted in the evolution of aromatic species (styrene and benzene), as shown in Figure 4.33. The amount of both styrene and benzene desorption increased below 250^oC while a decrease was found in evolution of styrene and benzene in the temperature range 250 and 400^oC, with an increase in WHSV of PyGas from 4 h^{-1} to 8 h^{-1}. This suggests that the extent of polymerisation of adsorbed species decreased with an increase in feed flow rate of PyGas ($WHSV_{PyGas}$) due to the shorter residence period over the catalyst. Consequently, a higher amount of adsorbed reactants and their oligomers and smaller amount of polyaromatic species (polystyrene /polyaromatic) were found on the catalyst.
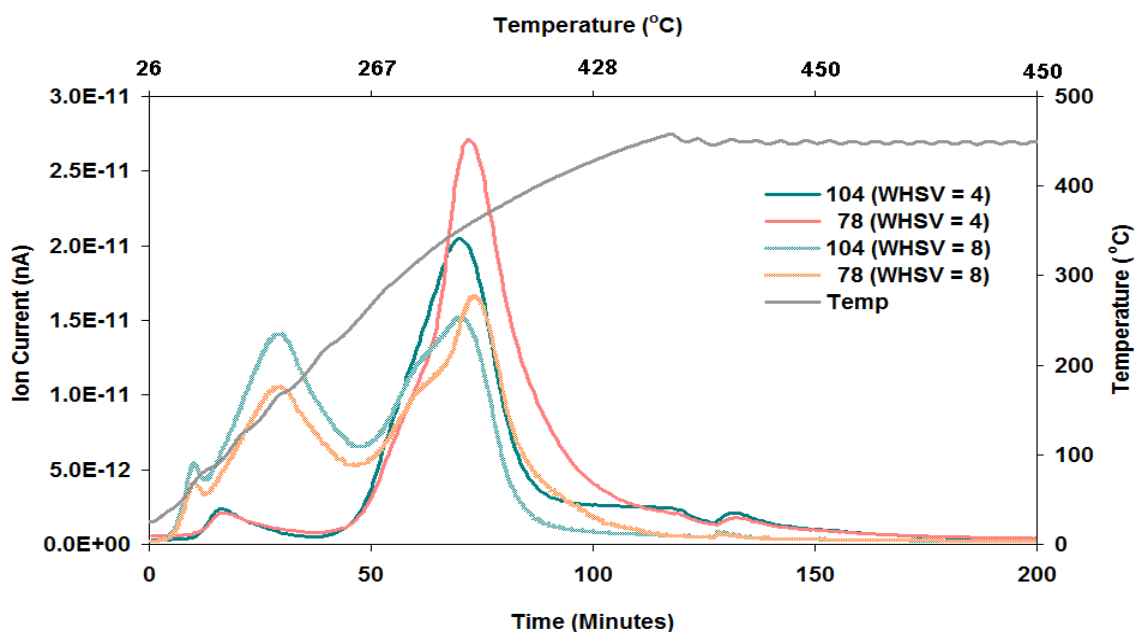
Figure 4.33 Comparison of aromatic species evolution during *in-situ* TPO of Ni/Al$_2$O$_3$ at WHSV$_{PyGas}$ 4 h^{-1} and 8 h^{-1} [T = 140°C, P$_T$ = 20 barg, P$_{H2}$ = 5 barg]

The amount of catalyst used in all the above reactions was 0.5 g, however the reaction was also performed with 0.25 g of catalyst, as discussed in the section 3.2.2.4.3. The post *in-situ* TPO was carried out in similar way and is shown in Figure 3.117. The amount of coke deposition was small because only 0.25 g catalyst was used in this reaction instead of 0.5 g. The combustion of coke mainly produced CO_2 and H_2O during the TPO. The broad evolution of H_2O suggested that soft type carbonaceous residues were present on the surface of the catalyst. Meanwhile, a reasonably small evolution of styrene and benzene and virtually no H_2 were observed in the TPO. This illustrates that the top half of

the catalyst bed had soft type coke deposited, while hard type coke deposition took place on the lower bed of the catalyst.

After the *in-situ* TPO, the regenerated catalysts were further analysed by BET, XRD and TGA/DSC to investigate any changes that may have occurred in the properties of the catalyst during the reaction or *in-situ* TPO. The surface areas and XRD patterns of regenerated catalysts were found to be similar to that of the fresh catalyst, which suggests that no significant support sintering or phase change occurred during reaction or TPO process. The TPOs of the regenerated catalysts were also performed up to a higher temperature (800°C) using the TGA/DSC to investigate any further coke that might still be present on the surface of the catalyst. However, no significant coke was observed on the surface on the regenerated catalysts. This suggests that the catalysts were successfully regenerated by *in-situ* TPO without losing any significant catalytic properties.

4.3.2 Coke deposition during PyGas hydrogenation and subsequent regeneration of Pd/Al$_2$O$_3$

Coke deposition took place over the Pd/Al$_2$O$_3$ during the PyGas hydrogenation which blocked the catalyst pores and consequently reduced the surface area of the post reaction catalyst, as shown in the Table 4.18.

Catalyst	Surface Area (m^{2}g^{-1})	Pore Volume (cm^{3}g^{-1})	Average Pore diameter (Å)
Pd/Al$_2$O$_3$	99	0.51	208
Pd/Al$_2$O$_3$ (Reduced)	104	0.50	197
Pd/Al$_2$O$_3$ (Post reaction)	70	0.32	185
Pd/Al$_2$O$_3$ (Regenerated)	93	0.45	196

Table 4.18 BET analysis of Pd/Al$_2$O$_3$ (fresh, reduced, post reaction and regenerated catalyst), [Reaction conditions: T = 140°C, WHSV$_{PyGas}$ = 4 h^{-1}, P$_{H2}$ = 20 barg]

The amounts and nature of coke deposition on the post-reaction palladium catalysts were investigated and the catalysts were regenerated by *in-situ* TPO. The detailed results are shown in Section 3.2.3. Figure 4.34 is an example of the *in-situ* TPO of Pd/Al$_2$O$_3$.
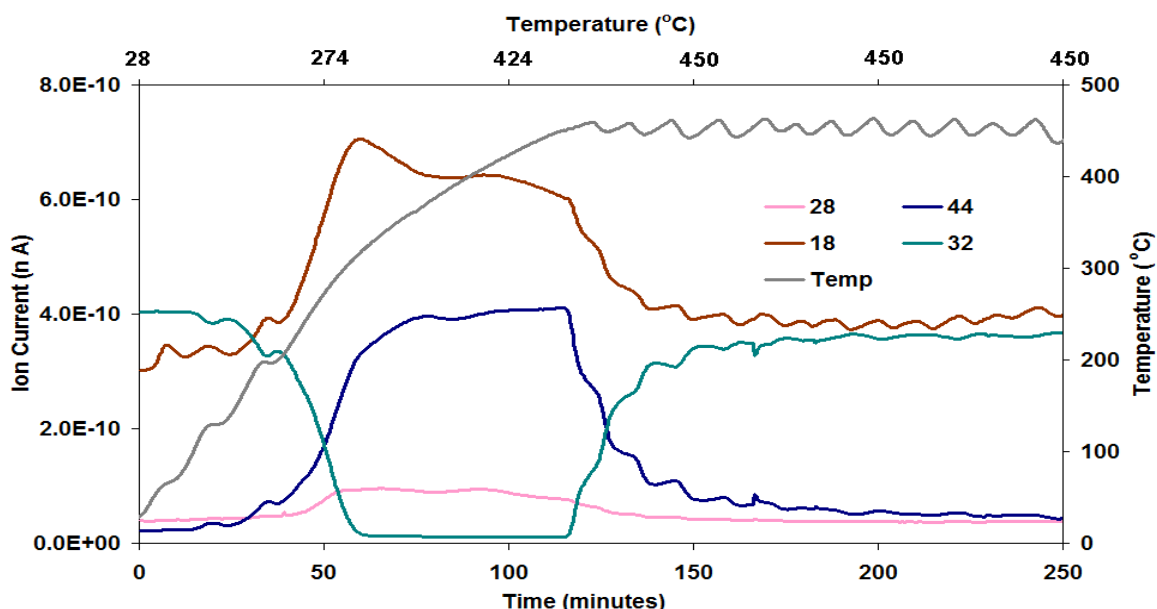
Figure 4.34 Post reaction *in-situ* TPO of Pd/Al$_2$O$_3$ catalyst [Reaction conditions: T = 140°C, WHSV$_{PyGas}$ = 4 h^{-1}, P$_T$ = 20 barg, P$_{H2}$ = 10 barg]

CO$_2$, CO and H$_2$O were the main species produced by coke combustion during *in-situ* TPO of the post reaction catalysts. The combustion of coke on the post reaction palladium catalyst started at 180°C and mainly produced CO$_2$ and H$_2$O with a small amount of CO. The higher amount of CO$_2$ and the negligible amount of CO suggests that the complete combustion of coke took place and mainly followed the reaction below;

$$CH_x \; + \; (1 + x/4)\, O_2 \longrightarrow CO_2 + x/2\; H_2O$$
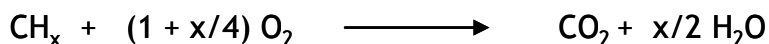
Small evolutions of H$_2$O occurred at temperatures below 180°C which can be ascribed to physisorbed H$_2$O, while the evolution of H$_2$O produced by the combustion of coke during the TPO occurred above 180°C. The broad evolution of H$_2$O suggests that soft type coke (high H/C ratio) was deposited over the palladium catalyst, when compared to the coke deposited over nickel catalyst under identical conditions.

The evolution of the following m/z fragments were also recorded during the *in-situ* TPO: 68 (cyclopentene), 70 (1-pentene), 72 (pentane), 78 (benzene), 92 (toluene), 98 (methylcyclohexane), 104 (styrene), 106 (ethyl benzene), 112 (1-octene/ethylcyclohexane), 114 (octane) and 2 (H$_2$), for a detailed analysis of the deposited coke. Figure 4.35 shows that reasonable amounts of styrene, benzene and H$_2$ with small amounts of 1-pentene, 1-octene, cyclopentene, toluene and

ethylbenzene were evolved during the TPO of the post reaction palladium catalyst.
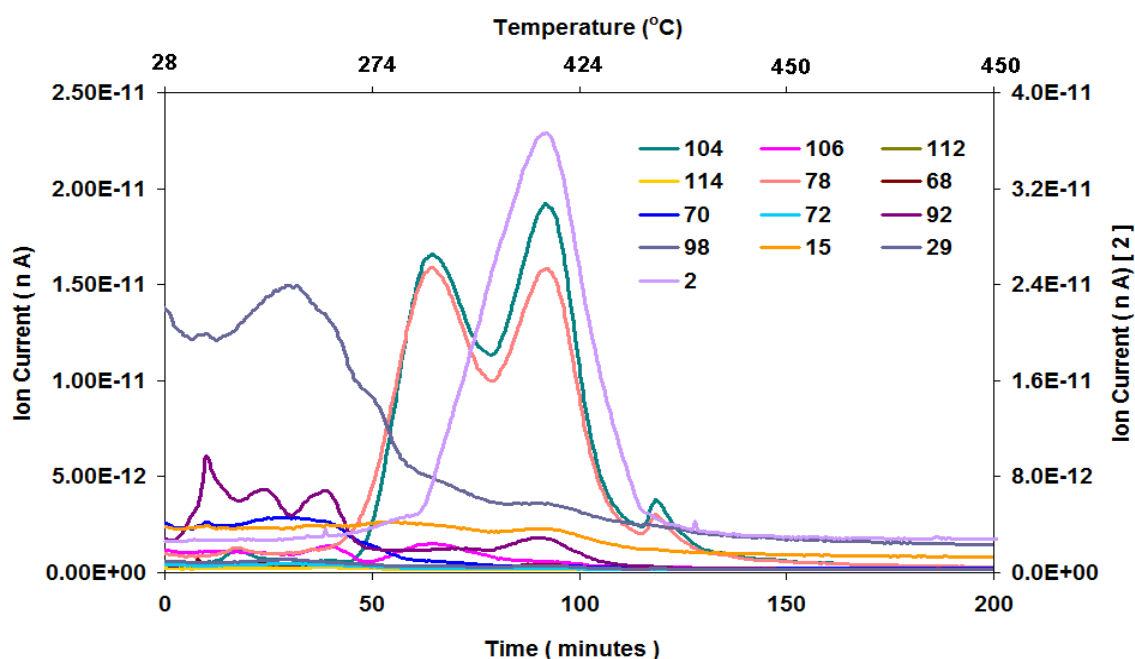
Figure 4.35 Evolution of other species during *in-situ* TPO of Pd/Al$_2$O$_3$ catalyst [Reaction conditions: T = 140°C, WHSV$_{PyGas}$ = 4 h^{-1}, P$_T$ = 20 barg, P$_{H2}$ = 10 barg]

Similar to the nickel catalyst, no considerable amount of saturated hydrocarbons *i.e.* reaction products, were found on the palladium catalyst during the *in-situ* TPO analysis. This suggests that hydrogenated products formed in the reaction are weakly adsorbed onto the catalyst and therefore desorb very easily. Consequently no noticeable amounts of hydrogenated hydrocarbons remained on the surface of catalyst. Whereas, small levels of 1-pentene, cyclopentene, 1-octene and toluene desorption illustrates that small amounts of the reactant species remained on the surface of the palladium catalyst.

Considerable amounts of styrene and benzene desorption during the TPO indicate that reasonable amounts of polyaromatics were present on the surface of the palladium catalyst. The evolution of styrene and benzene below 250°C were mainly from adsorbed aromatic compounds or their oligomers, while desorption at higher temperatures above 250°C are most likely from polymerised aromatic species (polystyrene/polyaromatic). A very small amount of styrene and benzene desorption occurred below 250°C and considerable amount of evolution of both occurred above 250°C, suggesting that a large amount of coke precursors polymerisation took place and formed polyaromatic species (polystyrene/polyaromatics). The two main evolutions of both styrene and

benzene, at about 320°C and 410°C, are most likely due to different polyaromatic species (polymers) present on the surface of catalyst.

As already revealed in the TPO analysis of the post reaction nickel catalyst, the combustion of soft coke occurred first, followed by the combustion of condensed coke and finally hard coke combustion. Meanwhile, reasonable amounts of styrene and benzene desorption also occurred during TPO. However over the nickel catalyst, no styrene and benzene evolution was observed in the final stages of the TPO in which the combustion of hard coke is likely to take place. In contrast, the evolution of styrene and benzene was observed until the complete removal of coke during the TPO of the post reaction palladium catalyst. This suggests that the coke deposited on the palladium was predominantly (poly) aromatics residues and the further conversion of (poly)aromatics to hard coke had not taken place. This is most likely due to the higher tendency of palladium to stabilise π-complexes of hydrocarbons and smaller tendency to form the σ-bonded complexes with unsaturated hydrocarbons than nickel [131, 133]. Therefore a low extent of dissociation of π-bond of the aromatics/polyaromatics took place over the palladium. Consequently, a small amount of polyaromatics were converted to hard type coke and the coke predominately remained in form of polyaromatic residues. Whereas nickel has a high tendency to make σ-bonds with unsaturated hydrocarbons and therefore a high extent of π-bond dissociation of aromatics/ polyaromatics could take place over nickel [144]. Therefore high levels of the polyaromatics were converted to hard coke over the nickel catalyst.

Moreover, only a small evolution of H$_2$ took place during the *in-situ* TPO of the palladium when compared to the evolution of H$_2$ from the nickel catalyst, because the combustion of soft type coke with a high content of hydrogen instantly produced CO_2/CO and H_2O. The high amount of H_2O evolution and the small amount of H$_2$ formation also suggests that the coke deposited on the palladium catalyst was a comparatively soft type coke and the further conversion to hard type coke had not occurred.

The formation of coke is mainly due to the polymerisation of coke precursors present in PyGas such as styrene, olefins and aromatic compounds [7, 11, 17, 53,

95]. Styrene was found to be the main precursor of coke formation over the palladium catalyst, as discussed in sections 4.3.2.1 and 4.3.2.2. The deposited species converts to polyaromatic hydrocarbons which then further convert to highly condensed polyaromatic residues and hard coke with the passage of time [53, 95], as shown in Figure 4.24.

The BET analysis of regenerated palladium showed that the surface area lost due to coke deposition was successfully recovered during the regeneration of the catalyst by *in-situ* TPO. This shows that no significant support sintering occurred in the catalyst, either during the reaction or in the regeneration process. Both the fresh and regenerated palladium catalyst samples showed similar XRD patterns, which suggests that no phase change had occurred during the reaction or the regeneration process. This illustrates that coke deposition is the main cause of catalyst deactivation during PyGas hydrogenation, which is in close agreement with previous studies [11-13].

4.3.2.1 Effect of reaction temperature on coke deposition

The TPO results of the catalysts used in the reactions preformed at $140^{\circ}C$ and $200^{\circ}C$ are compared below in Figure 4.36.
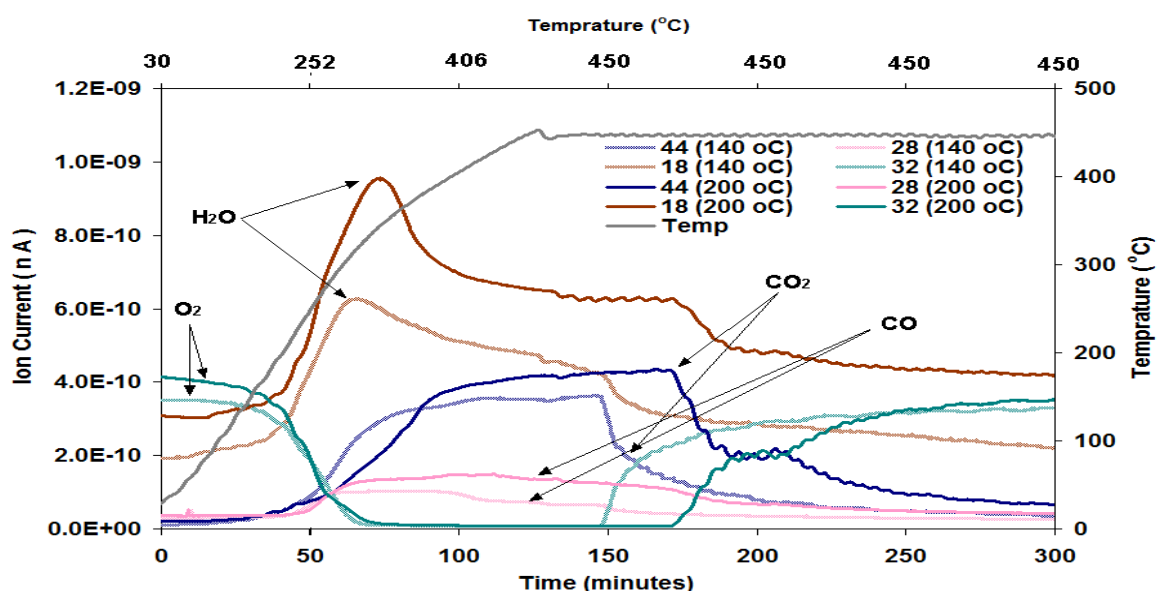
Figure 4.36 Comparison of *in-situ* TPO of Pd/Al$_2$O$_3$ at reaction temperature $140^{\circ}C$ and $200^{\circ}C$ [WHSV$_{PyGas}$ = 4 h^{-1}, P$_{H2}$ = 20 barg]

These results show that a higher amount of coke deposition was observed with an increase in reaction temperature. The increase in reaction temperature of PyGas hydrogenation not only increased the amount of coke deposition but also

produced a more condensed hydrogen deficient type coke. However, a small increase was observed in the coke deposition with an increase in reaction temperature over the palladium catalyst when compared to the nickel catalyst. A higher ratio of CO_2/H_2O was observed in the coke formed at the higher reaction temperature, which shows that the C/H ratio of the coke increased with an increase in the reaction temperature. This suggests that a condensed type of coke formation took place at the higher reaction temperatures, which is in close agreement with the literature [93, 99]. However the C/H ratio observed for the coke deposited over the Pd/Al_2O_3 was lower than the coke formed on the Ni/Al_2O_3. This illustrates that the coke deposited over the palladium was soft type when compared to the coke formed over the nickel.

The coke deposition increased with an increase in reaction temperature because a higher level of polymerisation took place to form coke at the higher reaction temperatures. The amount of oxygen consumed in the TPO analysis is presented in Figure 4.37.
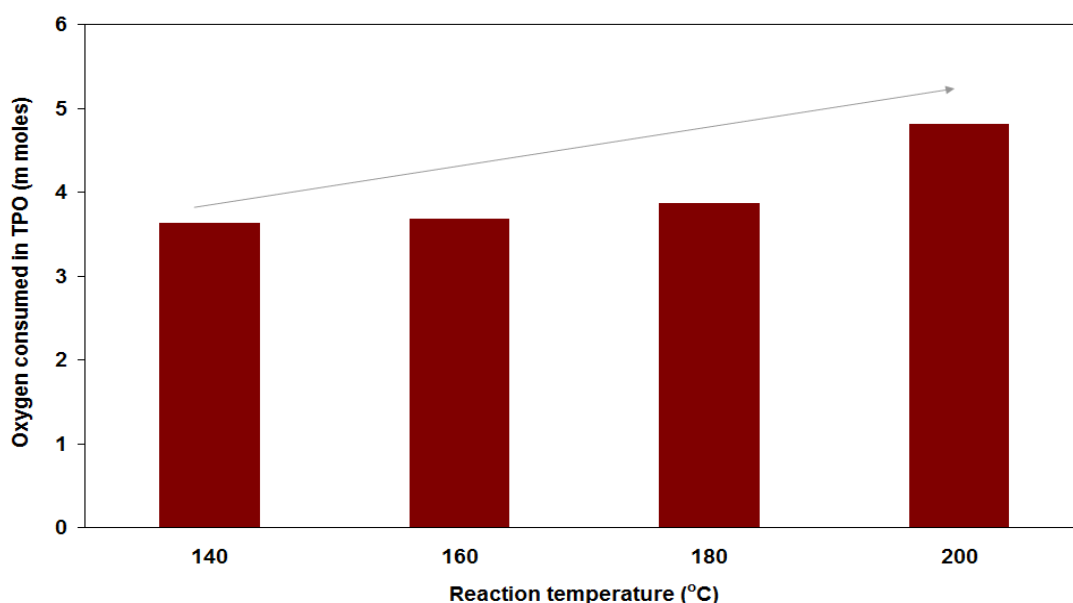
Figure 4.37 Oxygen consumption during *in-situ* TPO of Pd/Al_2O_3 catalysts, [T= 140-200°C, P_{H2} = 20 barg, $WHSV_{PyGas}$ = 4 h^{-1}]

The carbon balances of the PyGas components at different reaction temperatures were investigated and are shown in Figure 4.38. The carbon balance results show that styrene was the main precursor of coke formation, which is in close agreement with the literature [11, 12].
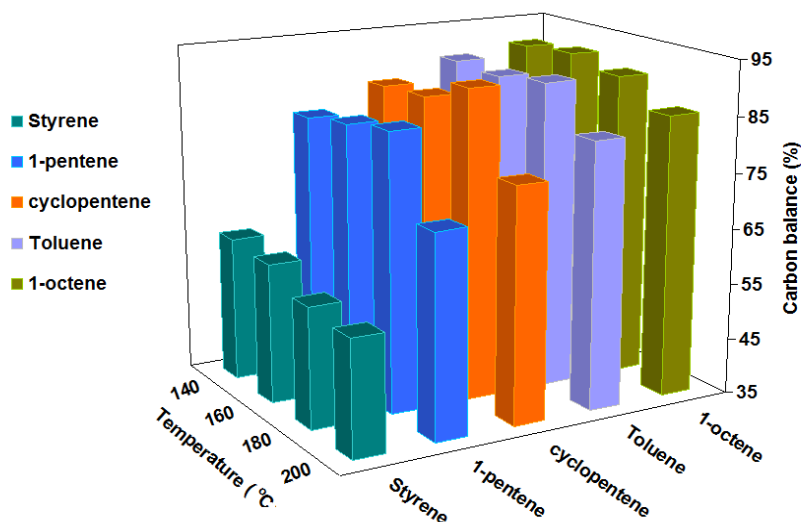
Figure 4.38 Carbon balance of PyGas components, [T = 140-200°C, P_{H2} = 20 barg, $WHSV_{PyGas}$ = 4 h^{-1}]

4.3.2.2 Effect of hydrogen partial pressure on coke deposition

Similar to the nickel catalyst, the coke deposition over the palladium increased with a decrease in the hydrogen partial pressure during PyGas hydrogenation, because a high degree of polymerisation takes place when a small amount of hydrogen is present on the surface of the catalyst. The coke deposition on the palladium catalyst was investigated during the PyGas hydrogenation at different hydrogen partial pressures and the results were shown in section 3.2.3.2. The results of the TPOs of the catalysts used in the reactions with 1 barg and 10 barg hydrogen partial pressure in 20 barg total reaction pressure are compared in this section, which is shown in Figure 4.39.
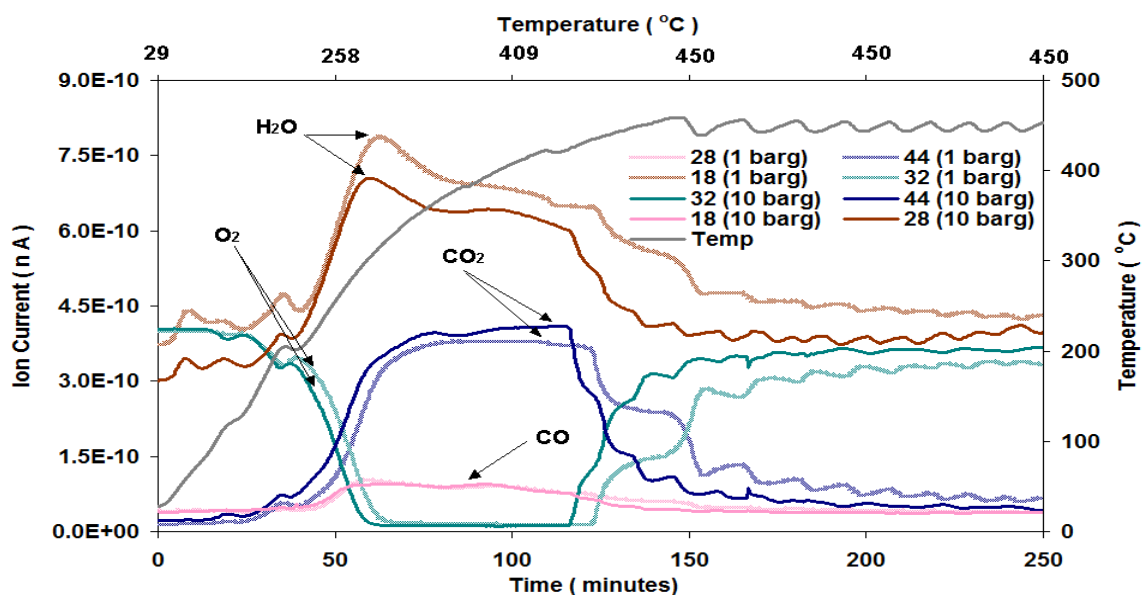
Figure 4.39 Comparison of *in-situ* TPO of Pd/Al₂O₃ at 1 barg and 10 barg hydrogen partial pressure [T = 140°C, $WHSV_{PyGas}$ = 4 h^{-1}, P_T = 20 barg]

The results show that a small increase was observed in the coke deposition with a decrease in the hydrogen partial pressure of the reaction. However, the increase in the coke deposition was not as prominent as observed with an increase in reaction temperature.

Furthermore, a small decrease was observed in the amount of H_2 evolution with the decrease in reaction hydrogen partial pressure, as shown in Figure 4.40. This shows that a slight increase occurred in the ratio of C/H of the coke. However, no significant difference was noted in the evolution of aromatic species (styrene and benzene).
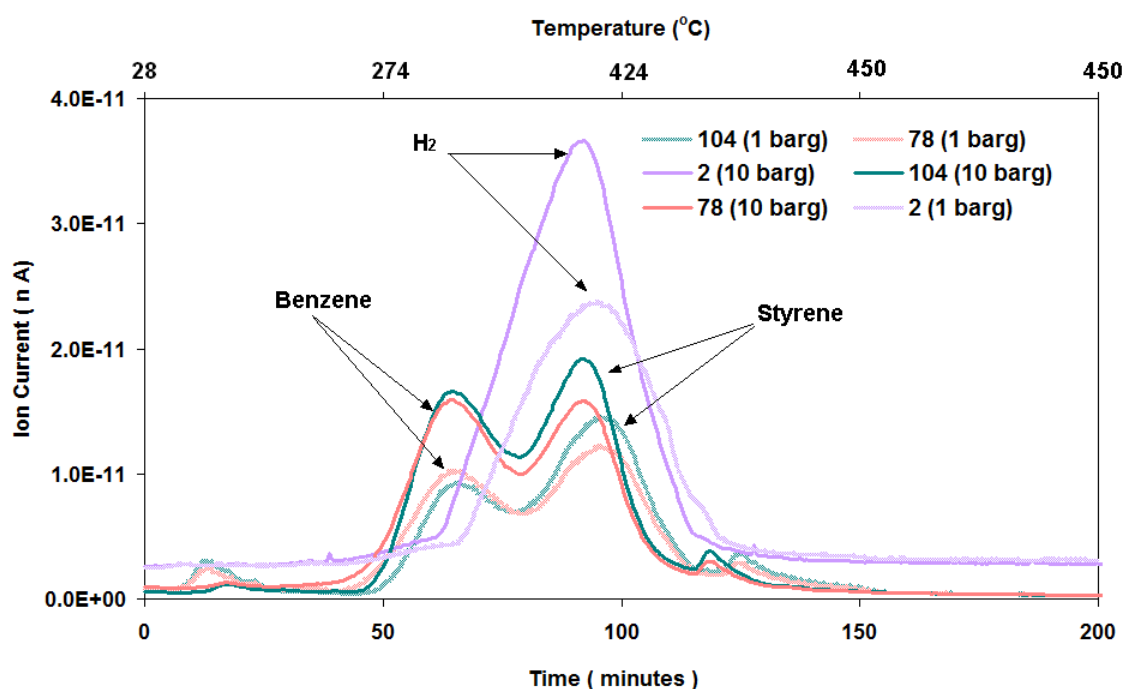
Figure 4.40 Comparison of aromatic species and H_2 evolution during *in-situ* TPO of Pd/Al$_2$O$_3$ at 1 bar and 10 bar hydrogen partial pressure [T = 140°C, WHSV$_{PyGas}$ = 4 h^{-1}, P$_T$ = 20 barg]

The results suggest that more reactive species polymerised to form coke when small amounts of hydrogen were present on the surface of catalyst, which is in close agreement with the literature [2, 11].

The carbon balance results also showed a decrease in carbon balance with a decrease in the hydrogen partial pressure, as shown in Figure 4.41.
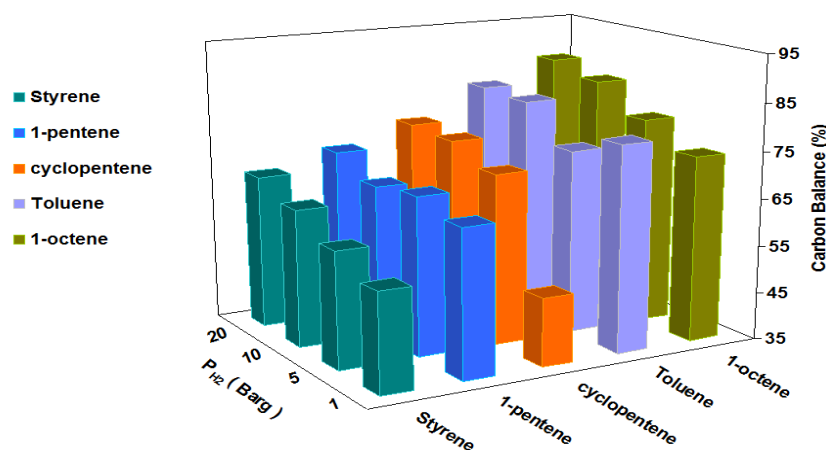
Figure 4.41 Carbon balance of PyGas components, [P_{H2} = 1-20 barg, P_T = 20 barg, T = 140°C, WHSV$_{PyGas}$ = 4 h^{-1}]

These results illustrate that the amount of coke deposition over palladium during PyGas hydrogenation increased with decreasing hydrogen partial pressure. However, the ratio of H_2O to CO_2 observed was virtually the same during TPO analysis of the palladium catalysts used in the reactions with different hydrogen partial pressures (1-20 barg). This suggests that the coke still remained in the soft type and was not converted into highly condensed coke at the lower temperature (140°C) with a decrease in hydrogen partial pressure.

4.3.2.3 Effect of total reaction pressure on coke deposition

The coke deposition on the palladium catalyst was also investigated at different total reaction pressures (10 barg and 20 barg) during PyGas hydrogenation and the TPO results are compared in Figure 4.42.
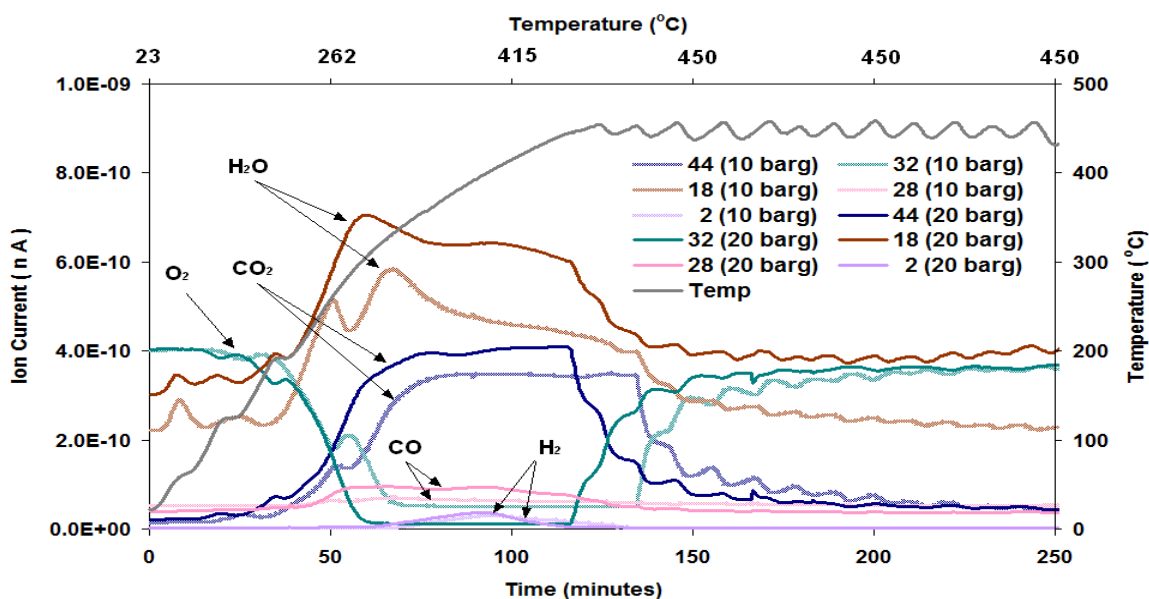
Figure 4.42 Comparison of *in-situ* TPO of Pd/Al$_2$O$_3$ at 10 barg and 20 barg total reaction pressure (50% hydrogen gas) [WHSV$_{PyGas}$ = 4 h^{-1}, T = 140°C]

The amount of CO_2 evolved and the amount of O_2 consumed increased with a decrease in the total reaction pressure from 20 barg to 10 barg. However, no considerable difference was noted in the evolution of the other species *i.e.* styrene, benzene, toluene, cyclopentene, pentane, 1-octene, octane, 1-pentene, methylcyclohexane, ethylbenzene, ethylcyclohexane, and H_2. This was found to be a similar mode of change in the coke deposition with a decrease in total reaction pressure, as was observed with the nickel catalyst. This shows that that coke deposition on the palladium also increased with a decrease in total reaction pressure, which is in close agreement with previous studies [2]. However, no significant change was observed in the nature of coke.

4.3.2.4 Effect of PyGas feed flow rate (WHSV$_{PyGas}$) on coke deposition

The effect of increasing WHSV of PyGas from 4 h^{-1} to 8 h^{-1} on the coke deposition was also investigated with the other reaction conditions kept constant. The WHSV$_{PyGas}$ increased from 4 h^{-1} to 8 h^{-1} by doubling the feed flow rate of PyGas during the reaction, however the GHSV of the reaction only slightly increased from 1175 h^{-1} to 1225 h^{-1}. The TPOs of the post reaction catalysts carried out at WHSV$_{PyGas}$ 4 h^{-1} and 8 h^{-1} are compared in Figure 4.43.
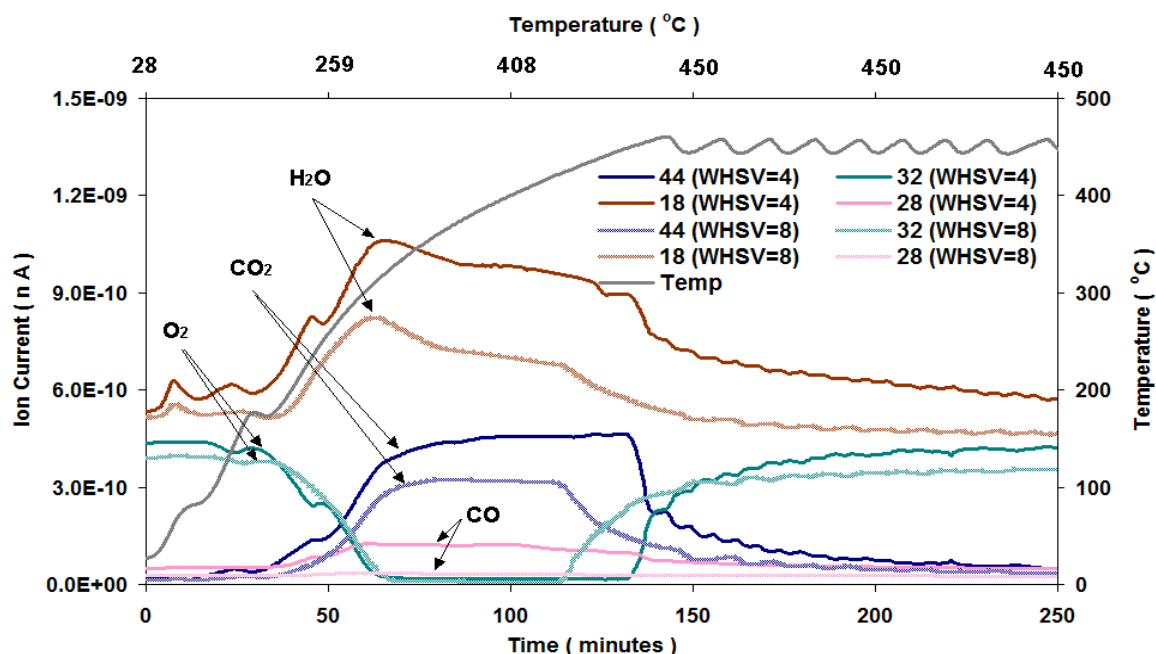
Figure 4.43 Comparison of *in-situ* TPO of Pd/Al$_2$O$_3$ at WHSV$_{PyGas}$ 4 h^{-1} and 8 h^{-1} [T = 140°C, P$_T$ = 20 barg, P$_{H2}$ = 5 barg]

Similar to the nickel system, the amount of coke deposition decreased with an increase in the WHSV of PyGas from 4 h^{-1} to 8 h^{-1}. The decrease in coke

deposition was most likely due to the shorter residence time of the adsorbed species on the catalyst as the amount of reactant increased while the amount of catalyst and hence active sites remained constant.

Moreover, higher levels of aromatic species (styrene and benzene) desorption were observed in the temperature range 250-350°C, while small amounts of styrene and benzene evolution occurred at 400°C with an increase in the WHSV of PyGas from 4 h^{-1} to 8 h^{-1}, as shown in Figure 4.44. These results illustrate that a higher amount of adsorbed reactants and their oligomers remained on the catalyst and a small amount was further converted to polyaromatic residues (polystyrene/polyaromatic) due to the shorter residence period with an increase in the PyGas feed flow rate (WHSV$_{PyGas}$).
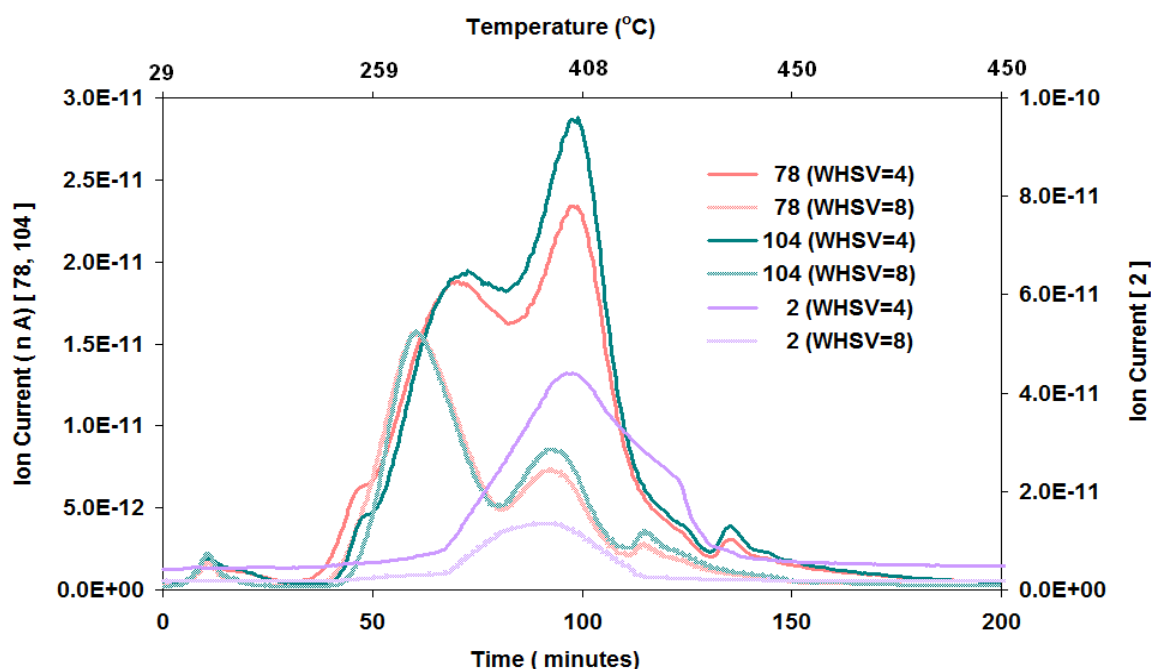
Figure 4.44 Comparison of aromatic species and H$_2$ evolution during *in-situ* TPO of Pd/Al$_2$O$_3$ at WHSV$_{PyGas}$ 4 h^{-1} and 8 h^{-1} [T = 140°C, P$_T$ = 20 barg, P$_{H2}$ = 5 barg]

PyGas hydrogenation was also performed with 0.25 g of the palladium catalyst, as discussed in the Section 3.2.3.4.3. A small amount of coke deposition was observed because the palladium catalyst used in the reaction was half the amount used in the previous reactions. An *in-situ* TPO of the post reaction palladium catalyst was carried out and is shown in Figure 3.217. The main species observed during the TPO were CO$_2$ and H$_2$O with very small amounts of styrene and benzene. No significant amounts of other species were noted. This

suggests that complete combustion of coke took place and produced CO_2 and H_2O and mainly followed the reaction below;

$$CH_x + (1 + x/4)\ O_2 \longrightarrow CO_2 + x/2\ H_2O$$
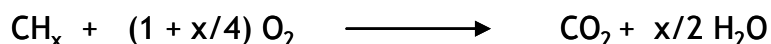
A broad evolution of H_2O was observed, which suggests that soft type coke deposition took place on the top half of the catalyst bed, while hard type coke deposition occurred on lower half of the catalyst bed. The results were comparable to the nickel system.

The regenerated palladium catalysts were further analysed by BET, XRD and TGA/DSC to investigate any changes that may have occurred in the properties of the catalyst during reaction or *in-situ* TPO. The surface areas and XRD patterns of regenerated catalysts were found to be similar to that of the fresh palladium catalyst. This shows that no significant support sintering or phase change occurred during the reaction or the regeneration process (*in-situ* TPO). The TPOs of the regenerated palladium catalysts were also performed up to a higher temperature (800°C) using TGA/DSC to investigate any further coke that might still be present on the surface of the catalyst. However, no significant amount of coke deposition was observed on the surface on regenerated catalysts. This suggests that the palladium catalysts were also effectively regenerated by the *in-situ* TPO, without losing significant catalytic properties.

5. Conclusion

Various reaction parameters such as hydrogen partial pressure (1-20 barg), reaction temperature (140-200°C), total reaction pressure (10-20 barg) and WHSV of PyGas (4-8 h^{-1}) were used to investigate the hydrogenation of PyGas over alumina supported nickel and palladium catalysts. Hydrogenation of PyGas increased over both the nickel and palladium catalysts with increase in hydrogen partial pressure. However, the selectivity of PyGas hydrogenation towards a high octane gasoline mixture decreased at very high hydrogen partial pressures. Conversely, PyGas hydrogenation was considerably decreased at very low hydrogen partial pressure and fast catalyst deactivation took place due to high amounts of coke deposition on the catalyst. Consequently, optimised hydrogen partial pressures are required to obtain the desired products and to maintain economical viability.

The reaction temperature is another important reaction parameter for optimising the PyGas hydrogenation process. Hydrogenation of PyGas increased and a higher degree of saturation of the PyGas components occurred with an increase in reaction temperature. Therefore, a low reaction temperature is favourable for a high octane gasoline mixture. However, a higher reaction temperature is required to hydrogenate the surplus aromatics present in PyGas. Higher quantities of aromatic hydrogenation were observed over the nickel catalyst during PyGas hydrogenation at reaction temperature of 140°C and no noticeable change was noted in the hydrogenation of aromatics with increasing the reaction temperature up to 200°C. Conversely, no significant hydrogenation of aromatics was observed over the palladium catalyst during PyGas hydrogenation at 140°C. However, the hydrogenation of aromatic compounds over the palladium catalyst increased with an increase in reaction temperature.

The hydrogenation of PyGas decreased with a decrease in total reaction pressure and high amounts of coke deposition occurred on the surface of the catalyst with a decrease in total reaction pressure. Consequently, a high total reaction pressure was found to be favourable for the hydrogenation of PyGas.

The hydrogenation of PyGas decreased with an increase in PyGas feed flow rate (WHSV$_{PyGas}$). However, the selectivity increased towards a high octane gasoline

mixture due to an increase in olefin isomerisation to internal olefins and a decrease in the hydrogenation of aromatics took place. The decrease in PyGas hydrogenation with an increase in PyGas feed flow rate (WHSV$_{PyGas}$) can be restored by an increase in hydrogen partial pressure, if desired.

Hydrogenation of PyGas was carried out by optimising these reaction conditions to obtain the desired product distribution. The hydrogenated PyGas (H-PyGas) obtained over both nickel and palladium catalysts with different reaction conditions can be divided in three main types, as shown in Figure 5.1.
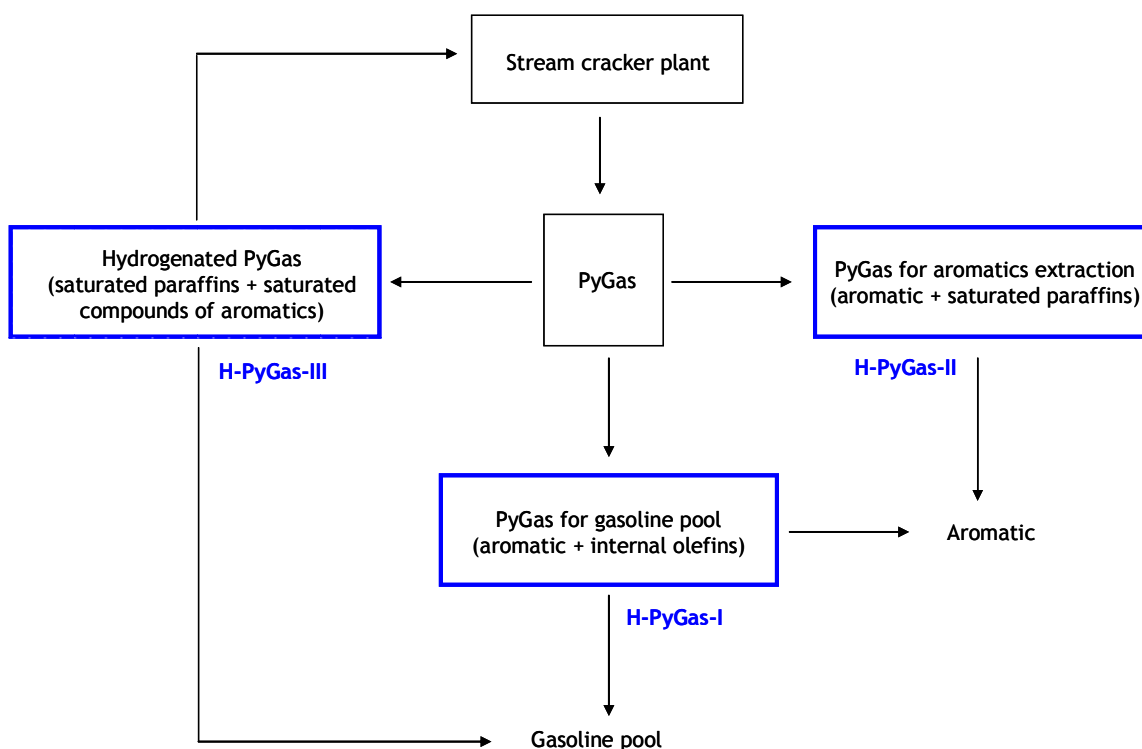
Figure 5.1 Hydrogenation of PyGas over Ni/Al$_2$O$_3$ and Pd/Al$_2$O$_3$ catalysts

H-PyGas-I is a high octane mixture which can be obtained by the selective hydrogenation of PyGas, without considerable loss in the octane number under mild reaction parameters [T ≈ 140°C, P$_T$ ≈ 20 barg, P$_{H2}$ ≈ 1-5 barg, WHSV$_{PyGas}$ ≈ 4-8 h^{-1}]. Under these conditions, reactive species like styrene were selectively hydrogenated. Moreover, significant amounts of the internal olefin formation took place by the isomerisation of olefin and no significant hydrogenation of the aromatic compounds occurred. Therefore, this mixture can be utilised as a gasoline blending mixture.

However, with the introduction of strict fuel regulations the reduction of aromatics in gasoline has become essential. This makes the consumption of PyGas more difficult as a gasoline blending mixture and so, an alternative useful avenue is required. The utilisation of PyGas as an aromatic source is an attractive substitute option. However, the olefins present in PyGas must also be hydrogenated because they generate gum and create problems in the aromatic extraction process. For this purpose, H-PyGas-II can be obtained by using moderate reaction conditions [T $\approx$ 140°C, $P_T \approx$ 20 barg, $WHSV_{PyGas} \approx$ 4 h^{-1}, $P_{H2} \approx$ 5-20 barg]. The selective hydrogenation of styrene and olefins was achieved without hydrogenating the aromatic compounds of PyGas and therefore can be readily utilised for aromatic extraction. The saturated paraffins fraction can be recycled to an ethylene and propylene plant.

As an alternative to aromatic extraction, aromatic hydrogenation and hydrocracking is an important route for the utilisation of surplus aromatics present in PyGas. Accordingly, the aromatics present in PyGas are generally first hydrogenated to saturated compounds. Subsequently, the saturated compounds can be converted to valuable products by ring opening/hydrocracking. H-PyGas-III can be obtained by using extensive hydrogenation reaction conditions [$P_{H2} \approx$ 20 barg, $P_T \approx$ 20 barg, $WHSV_{PyGas} \approx$ 4 h^{-1} T $\approx$ 140-200°C]. The high amount of aromatics present in the PyGas was converted to their respective saturated compounds. H-PyGas-III can be utilised as a gasoline pool mixture, with or without ring opening treatment, to reduce the amounts of aromatics present in gasoline to meet the fuel regulations. Furthermore, the ring opening treatment can be carried out with H-PyGas-III for the production of the high-octane components (iso-alkanes) for the gasoline pool mixture, and/or high quality synthetic stream cracker feed.

Both the nickel and the palladium catalysts were found to be suitable for PyGas hydrogenation. However, the palladium catalyst was found to be preferable for selective hydrogenation of PyGas without hydrogenating aromatics at mild reaction temperatures. However, aromatics hydrogenation can be achieved over the palladium catalyst with an increase in reaction temperature. Conversely, higher amounts of aromatics saturation were observed over the nickel catalyst during PyGas hydrogenation. Therefore, the nickel catalyst is considered preferable when aromatic ring saturation is desired during PyGas hydrogenation.

The selective hydrogenation of PyGas without aromatic saturation can be achieved over a nickel catalyst when using a low hydrogen partial pressure or sulfur promoted catalyst.

Coke deposition was believed to be the main reason for both the nickel and palladium catalyst deactivation. Coke formation on the surface of the catalyst was mainly due to the polymerisation of coke precursors present in the PyGas. Styrene was found to be the main precursor of coke deposition over both the nickel and the palladium catalyst. Coke deposition on the surface of the catalyst blocked the access of reactants to active sites and thus decreased the rate of the reaction. The deposited residues were converted into polyaromatic hydrocarbons, which were then further converted to highly condensed polyaromatics and finally to hard coke with the passage of time. Coke formation during PyGas hydrogenation on the surface of catalyst is summarised in Figure 4.24.

The amount of coke deposition on the surface of the catalyst increased with an increase in reaction temperature due to the greater polymerisation of PyGas components to coke. The coke was converted into a more condensed polyaromatic residue (with a higher C/H ratio) with increasing reaction temperature. Coke deposition also increased with a decrease in hydrogen partial pressure because a greater extent of polymerisation takes place when hydrogen is less abundant on the surface of the catalyst. However, the coke remained as soft type residues (with a lower C/H ratio) at lower reaction temperatures.

Higher amounts of coke deposition occurred on the nickel catalyst than the palladium catalyst under identical reaction conditions. Moreover, soft type coke (with a lower C/H ratio) deposition occurred over the palladium catalyst, while a comparatively hard type coke (with a higher C/H ratio) on the nickel catalyst.

The catalyst surface area lost due to coke deposition during the reaction was successfully recovered following regeneration of the catalysts by *in-situ* TPO. Therefore, no support sintering took place in either the reaction or the regeneration process. The similar powder XRD patterns of both the fresh and the regenerated catalysts showed that no noticeable catalyst phase change occurred during the reaction and the regeneration. Accordingly, coke deposition was

believed to be the main cause of catalyst deactivation during the PyGas hydrogenation and both the nickel and the palladium catalysts were effectively regenerated by *in-situ* TPO without significant loss to their catalytic properties.

6. Future Work

Although the present study has made significant in-roads into understanding PyGas hydrogenation there are always questions that remain unanswered at the end of any project. Therefore the following studies could be carried out to further develop our knowledge of the PyGas hydrogenation process.

- Hydrogenation of PyGas in the liquid phase. The present study was limited to the gas phase, however it would be useful to undertake a similar study in the liquid phase.

- The effect of poisons during the hydrogenation of PyGas. As with any system the catalyst used for PyGas hydrogenation is sensitive to poisons and this are has not been explored.

- The hydrogenation of PyGas over a sulfur-promoted catalyst. Industrially a sulphur-promoted nickel catalyst is often used to obtain the required selectivity. Examining the role of the sulphur promotion would be a useful further project.

7. References

[1] K.M. Reddy, S.K. Pokhriyal, P. Ratnasamy, S. Sivasanker, Applied Catalysis A: General, 83 (1992) 1-13.

[2] Y. M. Cheng, J. R. Chang, J. C. Wu, Applied Catalysis, 24 (1986) 273-285.

[3] A.I. Feinstein, (Wheaton, IL), Im, Un K. (Naperville, IL), Process for converting pyrolysis gasoline to benzene and ethylbenzene-lean xylenes, Standard Oil Company (Indiana) (Chicago, IL), United States, 1979.

[4] J. L. de. Medeiros, O. Q. F . Araujao, A. B. Gaspar, M. A. P. Silva, J.M. Britto, Brazilian Journal of Chemical Engineering, 24 (2007) 119 - 133.

[5] S. Babash, G. Amelichkina, T. Mukhina, Chemistry and Technology of Fuels and Oils, 47 (2011) 247-253.

[6] C.S. Hsu, P.R. Robinson, Practical advances in petroleum processing, Springer, USA, 2006.

[7] J. Weitkamp, A. Raichle, Y. Traa, Applied Catalysis A: General, 222 (2001) 277-297.

[8] H. Zimmermann, R. Walzl, Ethylene: Ullmann's Encyclopedia of Industrial Chemistry, Wiley-VCH Verlag GmbH & Co. KGaA, 2000.

[9] J.S. Plotkin, Catalysis Today, 106 (2005) 10-14.

[10] Plastemart, Technical articles and reports on plastic Industry,"Emerging imbalance between ethylene and propylene growth rates creates a propylene supply" http://www.plastemart.com/upload/literature/demand_of.asp (accessed 15 Dec 2011)

[11] J.F. Le Page, J.Cosyns, E.F. P. Courty, C. Marcilly, J.M. G. Martino, R. Montarnal, A. Sugier, H.V. Landeghem, Applied heterogeneous catalysis: desigm, manufacture, use of solid catalyst, Editions Technip, Paris, France, 1987.

[12] L. Lloyd, Handbook of Industrial Catalysts, Springer, London, UK, 2008.

[13] P. Castaño, B. Pawelec, J.L.G. Fierro, J.M. Arandes, J. Bilbao, Fuel, 86 (2007) 2262-2274.

[14] M.P. Kaminsky, Pyrolysis gasoline stabilization, in, USA, 2005.

[15] Z. Zhou, Z. Cheng, D. Yang, X. Zhou, W. Yuan, Journal of Chemical & Engineering Data, 51 (2006) 972-976.

[16] N. Mostoufi, R. Sotudeh-Gharebagh, M. Ahmadpour, J. Eyvani, Chemical Engineering & Technology, 28 (2005) 174-181.

[17] T.A. Nijhuis, M.T. Kreutzer, A.C.J. Romijn, F. Kapteijn, J.A. Moulijn, Catalysis Today, 66 (2001) 157-165.

[18] T.A. Nijhuis, F.M. Dautzenberg, J.A. Moulijn, Chemical Engineering Science, 58 (2003) 1113-1124.

[19] T. R. Boger, B. Camberg, S. Roy, J. C. M. Sorensen, System and Process for pyrolysis gasoline hydrotreatment, Corning Incorporated, USA, 2004.

[20] G.R. Gildert, Integrated pyrolysis gasoline treatment process, in, USA, 2000.

[21] W. V.Bauer, Hydrotreating of pyrolysis gasoline, The Lummus Company, Bloomfield, N.J., 1979.

[22] J.G. Christy, J.B. Wijffels, Process for selective hydrogenation of dienes in pyrolysis gasoline, Shell international research, Maatschappij B.V, UK, 1983.

[23] D. Yang, Z. M. Cheng, Z. M. Zhou, J. C. Zhang, W. K. Yuan, Ind Eng Chem Res, 47 (2008) 1051-1057.

[24] F. L. Lempert, E. Solomon, E.F. Schwarzenbek, HYDROTREATING PYROLYSIS GASOLINE, 492220, United States, 1970.

[25] A. Louloudi, N. Papayannakos, Applied Catalysis A: General, 175 (1998) 21-31.

[26] M. Wallstrom, Official J. Eur. Commun.L287, 2000, pp. 46-50. http://eur-lex.europa.eu/LexUriServ/LexUriServ.do?uri=OJ:L:2000:287:0046:0050:EN:PDF (accessed 23 Nov 2011)

[27] P. Greening, Topics in Catalysis, 16-17 (2001) 5-13.

[28] T.G. Kaufmann, A. Kaldor, G.F. Stuntz, M.C. Kerby, L.L. Ansell, Catalysis Today, 62 (2000) 77-90.

[29] P. Castaño, B. Pawelec, J.L.G. Fierro, J.M. Arandes, J. Bilbao, Applied Catalysis A: General, 315 (2006) 101-113.

[30] P. Castaño, A. Gutiérrez, B. Pawelec, J.L.G. Fierro, A.T. Aguayo, J.M. Arandes, Applied Catalysis A: General, 333 (2007) 161-171.

[31] C. Ringelhan, G. Burgfels, J.G. Neumayr, W. Seuffert, J. Klose, V. Kurth, Catalysis Today, 97 (2004) 277-282.

[32] A. Raichle, S. Moser, Y. Traa, M. Hunger, J. Weitkamp, Catalysis Communications, 2 (2001) 23-29.

[33] A. Raichle, M. Ramin, D. Singer, M. Hunger, Y. Traa, J. Weitkamp, Catalysis Communications, 2 (2001) 69-74.

[34] L.M. Kustov, T.V. Vasina, O.V. Masloboishchikova, E.G. Khelkovskaya-Sergeeva, P. Zeuthen, Cyclohexane ring opening on metal-oxide catalysts: F.V.M.S.M. Avelino Corma, G.F. José Luis (Eds.) Studies in Surface Science and Catalysis, Elsevier, 2000, pp. 227-232.

[35] P. Zeuthen, Catalysts and process for ring opening of cyclic compounds, in, EP 0 875 288, 1998.

[36] A. Raichle, Y. Traa, J. Weitkamp, Catalysis Today, 75 (2002) 133-139.

[37] Y. Qian, S. Liang, T. Wang, Z. Wang, W. Xie, X. Xu, Catalysis Communications, 12 (2011) 851-853.

[38] B.W. Hoffer, A. Dick van Langeveld, J.-P. Janssens, R.L.C. Bonné, C.M. Lok, J.A. Moulijn, Journal of Catalysis, 192 (2000) 432-440.

[39] B.W. Hoffer, F. Devred, P.J. Kooyman, A.D. van Langeveld, R.L.C. Bonné, C. Griffiths, C.M. Lok, J.A. Moulijn, Journal of Catalysis, 209 (2002) 245-255.

[40] B.W. Hoffer, R.L.C. Bonné, A.D. van Langeveld, C. Griffiths, C.M. Lok, J.A. Moulijn, Fuel, 83 (2004) 1-8.

[41] D.I. Enache, P. Landon, C.M. Lok, S.D. Pollington, E.H. Stitt, Industrial & Engineering Chemistry Research, 44 (2005) 9431-9439.

[42] W. B. Su, W. R. Chen, J. R. Chang, Industrial & Engineering Chemistry Research, 39 (2000) 4063-4069.

[43] T. B. Lin, T. C. Chou, Industrial & Engineering Chemistry Research, 34 (1995) 128-134.

[44] A.B. Gaspar, G.R. dos Santos, R. de Souza Costa, M.A.P. da Silva, Catalysis Today, 133-135 (2008) 400-405.

[45] V. Ragaini, C. Tine, Applied Catalysis, 10 (1984) 43-51.

[46] G.C. Bond, Metal-catalysed reaction of hydrocarbon, Springer, USA, 2005.

[47] P.N. Rylander, Hydrogenation methods, Academic press London, UK., 1985.

[48] W. V.Bauer, Hydrotreating of pyrolysis gasoline, The lummus Company, Bloomfield, N.J, 1977.

[49] W. V.Bauer, Two stage hydrotreating of pyrolysis gasoline to remove mercaptan and diene, The Lummus Company, Bloomfield, N.J, 1978.

[50] E. Goossens, R. Donker, F. van den Brink, Reactor runaway in pyrolysis gasoline hydrogenation: B.D. G.F. Froment, P. Grange (Eds.) Studies in Surface Science and Catalysis, Elsevier, 1997, pp. 245-254.

[51] K.R. Westerterp, A.E. Kronberg, Chemical Engineering & Technology, 25 (2002) 595-601.

[52] M. Fadoni, L. Lucarelli, Temperature programmed desorption, reduction, oxidation and flow chemisorption for the characterisation of heterogeneous

catalysts. Theoretical aspects, instrumentation and applications: A. Dąbrowski (Ed.) Studies in Surface Science and Catalysis, Elsevier, 1999, pp. 177-225.

[53] J. Hagen, Industrial Catalysis: A Practical Approach, Second Edition ed., Wiley-VCH, Mannheim, Germany, 2006.

[54] J. M. Thomas, W.J. Thomas, Principles and practice of heterogeneous catalysis, Wiley-VCH, New York, USA, 1997.

[55] P. W. Atkins, J.D. Paula, Physical chemistry 8th ed., Oxford University Press 2010.

[56] R. J. Baxter, P. Hu, Journal of Chemical Physics, 116 (2002) 4379-4381.

[57] H. Pines, The Chemistry of Catalytic Hydrocarbon Conversions'', Academic Press, London, UK., 1981.

[58] A.S. Canning, S.D. Jackson, A. Monaghan, T. Wright, Catalysis Today, 116 (2006) 22-29.

[59] J. Krupka, Z. Severa, J. Pasek, Reaction Kinetics and Catalysis Letters, 89 (2006) 359-368.

[60] Z. Dobrovolná, P. Kačer, L. Červený, Journal of Molecular Catalysis A: Chemical, 130 (1998) 279-284.

[61] C.N. Scatterfield, Heterogeneous Catalysis in Industrial Practice, Second Edition ed., Krieger Publishing Company, Florida, 1996.

[62] G. A. Ollah, A. Mohnar, Hydrocarbon Chemistry'', Second Edition ed., Wiley-Interscience, Canada, 2003.

[63] A. Stanislaus, B.H. Cooper, Catalysis Reviews, 36 (1994) 75-123.

[64] B.H. Cooper, B.B.L. Donnis, Applied Catalysis A: General, 137 (1996) 203-223.

[65] M.A. Keane, P.M. Patterson, Journal of the Chemical Society, Faraday Transactions, 92 (1996) 1413-1421.

[66] L.P. Lindfors, T. Salmi, Industrial & Engineering Chemistry Research, 32 (1993) 34-42.

[67] L.P. Lindfors, T. Salmi, S. Smeds, Chemical Engineering Science, 48 (1993) 3813-3828.

[68] C. Mirodatos, J.A. Dalmon, G.A. Martin, Journal of Catalysis, 105 (1987) 405-415.

[69] J.M. Orozco, G. Webb, Applied Catalysis, 6 (1983) 67-84.

[70] P.J. Van Der Steen, J.J.F. Scholten, Applied Catalysis, 58 (1990) 291-304.

[71] M.C. Schoenmaker-Stolk, J.W. Verwijs, J.A. Don, J.J.F. Scholten, Applied Catalysis, 29 (1987) 73-90.

[72] H.A. Franco, M.J. Phillips, Journal of Catalysis, 63 (1980) 346-354.

[73] J.K. Marangozis, B.G. Mantzouranls, A.N. Sophos, Industrial & Engineering Chemistry Product Research and Development, 18 (1979) 61-63.

[74] P. Chou, M.A. Vannice, Journal of Catalysis, 107 (1987) 140-153.

[75] N.G. Karanth, R. Hughes, Journal of Applied Chemistry and Biotechnology, 23 (1973) 817-827.

[76] M.A. Keane, P.M. Patterson, Industrial & Engineering Chemistry Research, 38 (1999) 1295-1305.

[77] R.Z.C. van Meerten, J.W.E. Coenen, Journal of Catalysis, 37 (1975) 37-43.

[78] G.M. Dixon, K. Singh, Transactions of the Faraday Society, 65 (1969) 1128-1137.

[79] J.P.G. Kehoe, J.B. Butt, Journal of Applied Chemistry and Biotechnology, 22 (1972) 23-30.

[80] A. B. Gaspar, L. Salvatore, K. S. Alves, M.A.P.d. Silva, Study of nickel catalyst in the styrene hydrogenation in: 2nd Mercosur Congress on Chemical Engineering, 4th Mercosur Congress on Process Systems Engineering, Rio de Janeiro. Brasil., 2005, pp. 1-10.

[81] Paˆrvulescu, Vasile I., G. Filoti, V. Paˆrvulescu, N. Grecu, E. Angelescu, I.V. Nicolescu, Journal of Molecular Catalysis, 89 (1994) 267-282.

[82] Z.M. Zhou, Z.M. Cheng, Y.N. Cao, J.C. Zhang, D. Yang, W.K. Yuan, Chemical Engineering & Technology, 30 (2007) 105-111.

[83] H.A. Smits, A. Stankiewicz, W.C. Glasz, T.H.A. Fogl, J.A. Moulijn, Chemical Engineering Science, 51 (1996) 3019-3025.

[84] J. Hanika, J. Lederer, Chemi. Listy, 93 (1999) 428-431.

[85] Z. Zhou, T. Zeng, Z. Cheng, W. Yuan, Industrial & Engineering Chemistry Research, 49 (2010) 11112-11118.

[86] A.A. Minkkinen, Hydrotreating of pyrolysis gasoline, in, The Lummus Company, Bloomfield, N.J., 1978.

[87] J.T. Richardson, Principles of catalyst development, Plenum Press, New York, USA, 1989.

[88] Z. Zhou, T. Zeng, Z. Cheng, W. Yuan, Industrial & Engineering Chemistry Research, 50 (2011) 883-890.

[89] T. Y. Zeng, Z. M. Zhou, J. Zhu, Z. M. Cheng, P. Q. Yuan, W. K. Yuan, Catalysis Today, 147, Supplement (2009) S41-S45.

[90] Axens', portfolio selective hydrogenation catalysts, Axens IFP Group Technologies(2003). http://www.axens.net/pdf/products/Axens%20Portfolio%20of%20Selective%20Hydrogenation%20Catalysts_imp_recto.pdf (accessed 19 Feb 2010)

[91] P.C. L'Argentiere, D.A. Liprandi, N.S. Figoli, Industrial & Engineering Chemistry Research, 34 (1995) 3713-3717.

[92] C.H. Bartholomew, R.J. Farrauto, Journal of Catalysis, 45 (1976) 41-53.

[93] C.H. Bartholomew, R.J.Farrauto, Fundamentals of industrial catalytic process, Second Edition ed., Wiley, USA, 2005.

[94] J.A. Moulijn, A.E. van Diepen, F. Kapteijn, Applied Catalysis A: General, 212 (2001) 3-16.

[95] C.H. Bartholomew, Applied Catalysis A: General, 212 (2001) 17-60.

[96] T. R. Boger, S. Roy, J. C. M. Sorensen, Systems and processes for the pyrolysis gasoline hydrotreatment, Corning Incorporated, USA, 2006.

[97] R. N. Jens R, Journal of Catalysis, 21 (1971) 171-178.

[98] A. Aguinaga, M. Montes, Applied Catalysis A: General, 90 (1992) 131-144.

[99] J. Barbier, E. Churin, J.M. Parera, J. Riviere, Reaction Kinetics and Catalysis Letters, 29 (1985) 323-330.

[100] J. Barbier, Applied Catalysis, 23 (1986) 225-243.

[101] J. A. Anderson, M.F. Garcia, Supported Metals in Catalysis Imperial College Press, London, UK, 2005.

[102] F. Porta, M. Rossi, Journal of Molecular Catalysis A: Chemical, 204-205 (2003) 553-559.

[103] ICDD's PDF-4 database. International Center for Diffraction Data: Newton Square,USA,2006.

[104] A.J. Akande, R.O. Idem, A.K. Dalai, Applied Catalysis A: General, 287 (2005) 159-175.

[105] J.T. Richardson, M. Lei, B. Turk, K. Forster, M.V. Twigg, Applied Catalysis A: General, 110 (1994) 217-237.

[106] J. Juan-Juan, M.C. Román-Martínez, M.J. Illán-Gómez, Applied Catalysis A: General, 264 (2004) 169-174.

[107] Z. Hao, Q. Zhu, Z. Lei, H. Li, Powder Technology, 182 (2008) 474-479.

[108] F.J. Mariño, E.G. Cerrella, S. Duhalde, M. Jobbagy, M.A. Laborde, International Journal of Hydrogen Energy, 23 (1998) 1095-1101.

[109] J. H. Lee, E. G. Lee, O. S. Joo, K. D. Jung, Applied Catalysis A: General, 269 (2004) 1-6.

[110] S. Y. Chin, F. J. Lin, A. N. Ko, Catalysis Letters, 132 (2009) 389-394.

[111] J. Zhang, H. Xu, X. Jin, Q. Ge, W. Li, Applied Catalysis A: General, 290 (2005) 87-96.

[112] C. B. Wang, G. Y. Gau, S. J. Gau, C. W. Tang, J. L. Bi, Catalysis Letters, 101 (2005) 241-247.

[113] Y. Choi, W. Lee, Catalysis Letters, 67 (2000) 155-161.

[114] H.P. Aytam, V. Akula, K. Janmanchi, S.R.R. Kamaraju, K.R. Panja, K. Gurram, J.W. Niemantsverdriet, The Journal of Physical Chemistry B, 106 (2002) 1024-1031.

[115] M. Skotak, Z. Karpiński, W. Juszczyk, J. Pielaszek, L. Kępiński, D.V. Kazachkin, V.I. Kovalchuk, J.L. d'Itri, Journal of Catalysis, 227 (2004) 11-25.

[116] G. Chen, W. T. Chou, C. t. Yeh, Applied Catalysis, 8 (1983) 389-397.

[117] S.A. Nikolaev, L.N. Zanaveskin, V.V. Smirnov, V.A. Averyanov, K.L. Zanaveskin, Russian Chemical Reviews, 78 (2009) 231-247.

[118] G.A. Martin, J.A. Dalmon, Journal of Catalysis, 75 (1982) 233-242.

[119] B. Coughlan, M.A. Keane, Zeolites, 11 (1991) 12-17.

[120] D.Y. Murzin, S. Smeds, T. Salmi, Reaction Kinetics and Catalysis Letters, 71 (2000) 47-54.

[121] S.D. Lin, M.A. Vannice, Journal of Catalysis, 143 (1993) 563-572.

[122] P. H. Jen, Y. H. Hsu, S.D. Lin, Catalysis Today, 123 (2007) 133-141.

[123] J.L. Garnett†, Catalysis Reviews, 5 (1972) 229-267.

[124] G.C. Bond, J.M. Winterbottom, Transactions of the Faraday Society, 65 (1969) 2779-2793.

[125] J. Silvestre-Albero, G. Rupprechter, H.-J. Freund, Journal of Catalysis, 235 (2005) 52-59.

[126] S.D. Jackson, A. Monaghan, Catalysis Today, 128 (2007) 47-51.

[127] E. Opara, D.T. Lundie, T. Lear, I.W. Sutherland, S.F. Parker, D. Lennon, Physical Chemistry Chemical Physics, 6 (2004) 5588-5595.

[128] P.B. Wells, G.R. Wilson, Journal of the Chemical Society A: Inorganic, Physical, Theoretical, (1970).

[129] W. J. Wang, M. H. Qiao, J. Yang, S. H. Xie, J. F. Deng, Applied Catalysis A: General, 163 (1997) 101-109.

[130] P.C. Aben, J.C. Platteeuw, B. Stouthamer, Recueil des Travaux Chimiques des Pays-Bas, 89 (1970) 449-459.

[131] R.L. Augustine, F. Yaghmaie, J.F. Van Peppen, The Journal of Organic Chemistry, 49 (1984) 1865-1870.

[132] J.P. Boitiaux, J. Cosyns, E. Robert, Applied Catalysis, 35 (1987) 193-209.

[133] F.G. Gault, J.J. Rooney, C. Kemball, Journal of Catalysis, 1 (1962) 255-274.

[134] P. Chou, M.A. Vannice, Journal of Catalysis, 107 (1987) 129-139.

[135] J. E. Demuth, Surface Science, 65 (1977) 369-375.

[136] K. Kishi, F. Kikui, S. Ikeda, Surface Science, 99 (1980) 405-418.

[137] R. Ding, Y. Hu, Z. Gui, R. Zong, Z. Chen, W. Fan, Polymer Degradation and Stability, 81 (2003) 473-476.

[138] SII application brief, T. No.78, Evolved Gas Analysis of Polystyrene using Simultaneous TG/DTA-MS or FTIR, SII NanoTechnology Inc. , Tokyo, Japan, 2007. http://www.siint.com/en/documents/technology/thermal_analysis/application_TA_078e.pdf (accessed 16 May 2011)

[139] M.A. Uguina, D.P. Serrano, R. Sanz, J.L.G. Fierro, M. López-Granados, R. Mariscal, Catalysis Today, 61 (2000) 263-270.

[140] M.M. Fares, T. Yalcin, J. Hacaloglu, A. Gungor, S. Suzer, Analyst, 119 (1994).

[141] A. Marcilla, M. Beltrán, Polymer Degradation and Stability, 50 (1995) 117-124.

[142] Application note, Double-Shot Pyrolyzer, Analysis of Residual Oligomers in Polystyrene (PS): Thermal Extraction in Evolved Gas Analysis (EGA, in, Frontier Laboratories Ltd, Fukushima, Japan.

http://www.youngin.com/application/0504-0021EN-E.pdf (accessed 09 Jan 2012)

[143] N.S. Figoli, J.N. Beltramini, E.E. Marinelli, M.R. Sad, J.M. Parera, Applied Catalysis, 5 (1983) 19-32.

[144] J.A. Silvent, P.W. Selwood, Journal of the American Chemical Society, 83 (1961) 1033-1035.